NBS SPECIAL PUBLICATION 614

U.S. DEPARTMENT OF COMMERCE / National Bureau of Standards

Sixth International Conference on Noise in Physical Systems

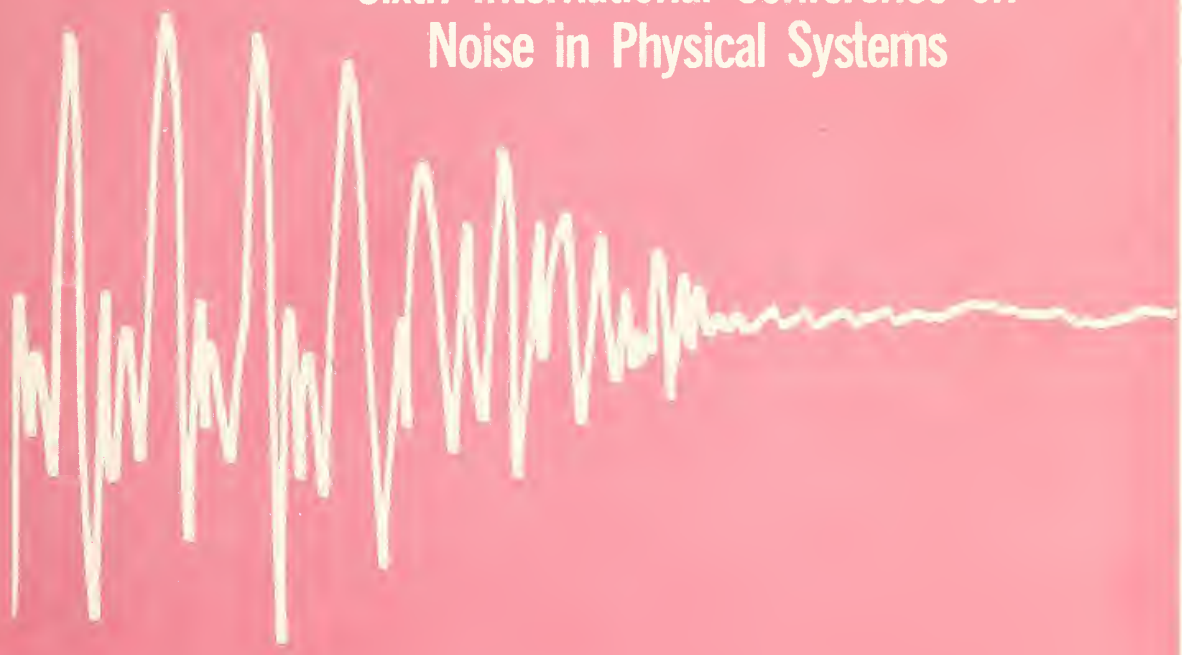

NATIONAL BUREAU OF STANDARDS

The National Bureau of Standards[1] was established by an act of Congress on March 3, 1901. The Bureau's overall goal is to strengthen and advance the Nation's science and technology and facilitate their effective application for public benefit. To this end, the Bureau conducts research and provides: (1) a basis for the Nation's physical measurement system, (2) scientific and technological services for industry and government, (3) a technical basis for equity in trade, and (4) technical services to promote public safety. The Bureau's technical work is performed by the National Measurement Laboratory, the National Engineering Laboratory, and the Institute for Computer Sciences and Technology.

THE NATIONAL MEASUREMENT LABORATORY provides the national system of physical and chemical and materials measurement; coordinates the system with measurement systems of other nations and furnishes essential services leading to accurate and uniform physical and chemical measurement throughout the Nation's scientific community, industry, and commerce; conducts materials research leading to improved methods of measurement, standards, and data on the properties of materials needed by industry, commerce, educational institutions, and Government; provides advisory and research services to other Government agencies; develops, produces, and distributes Standard Reference Materials; and provides calibration services. The Laboratory consists of the following centers:

Absolute Physical Quantities[2] — Radiation Research — Thermodynamics and Molecular Science — Analytical Chemistry — Materials Science.

THE NATIONAL ENGINEERING LABORATORY provides technology and technical services to the public and private sectors to address national needs and to solve national problems; conducts research in engineering and applied science in support of these efforts; builds and maintains competence in the necessary disciplines required to carry out this research and technical service; develops engineering data and measurement capabilities; provides engineering measurement traceability services; develops test methods and proposes engineering standards and code changes; develops and proposes new engineering practices; and develops and improves mechanisms to transfer results of its research to the ultimate user. The Laboratory consists of the following centers:

Applied Mathematics — Electronics and Electrical Engineering[2] — Mechanical Engineering and Process Technology[2] — Building Technology — Fire Research — Consumer Product Technology — Field Methods.

THE INSTITUTE FOR COMPUTER SCIENCES AND TECHNOLOGY conducts research and provides scientific and technical services to aid Federal agencies in the selection, acquisition, application, and use of computer technology to improve effectiveness and economy in Government operations in accordance with Public Law 89-306 (40 U.S.C. 759), relevant Executive Orders, and other directives; carries out this mission by managing the Federal Information Processing Standards Program, developing Federal ADP standards guidelines, and managing Federal participation in ADP voluntary standardization activities; provides scientific and technological advisory services and assistance to Federal agencies; and provides the technical foundation for computer-related policies of the Federal Government. The Institute consists of the following centers:

Programming Science and Technology — Computer Systems Engineering.

[1]Headquarters and Laboratories at Gaithersburg, MD, unless otherwise noted; mailing address Washington, DC 20234.
[2]Some divisions within the center are located at Boulder, CO 80303.

Sixth International Conference on Noise in Physical Systems

Proceedings of a conference held
at the National Bureau of Standards,
Gaithersburg, MD, April 6-10, 1981

Edited by:
P.H.E. Meijer
R.D. Mountain
R.J. Soulen, Jr.

National Measurement Laboratory
National Bureau of Standards
Washington, DC 20234

Sponsored by:

National Bureau of Standards
Washington, DC 20234

and

The Catholic University of America
Washington, DC 20064

and

National Science Foundation
Washington, DC 20550

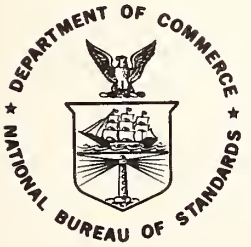

U.S. DEPARTMENT OF COMMERCE, Malcolm Baldrige, Secretary

NATIONAL BUREAU OF STANDARDS, Ernest Ambler, Director

Issued September 1981

Library of Congress Catalog Card Number: 81-600084

National Bureau of Standards Special Publication 614
Nat. Bur. Stand. (U.S.), Spec. Publ. 614, 419 pages (Sept. 1981)
CODEN: XNBSAV

U.S. GOVERNMENT PRINTING OFFICE
WASHINGTON : 1980

For sale by the Superintendent of Documents, U.S. Government Printing Office, Washington, D.C. 20402
Price $8.50
(Add 25 percent for other than U.S. mailing).

FOREWORD

The study of fluctuations (or noise) in a physical system provides insights, not available by any other technique, into the microscopic dynamic behavior of that system. Besides being a source of information, noise can also be a source of irritation, in that it limits the performance of numerous devices. The study of noise is of prime importance for the testing of physical theories as well as for the development of improved physical measurements and improved performance of devices. Therefore, the Conference has as one of its goals an improved understanding of noise in devices and its influence on the error budget of a measurement. Indeed, progress in relieving or minimizing noise in some devices was reported (e.g., the relationship of "burst noise" to the metallurgical condition of the sample).

Strong emphasis was given in this Conference to new topics for which the noise spectra proved to be particularly helpful in characterizing the underlying system dynamics. Papers discussed, for example, the transition from periodic to chaotic behavior in chemical systems and turbulent fluid flow, entropy generation in the computer process, the existence and implications of quantum mechanical noise, and noise spectra occurring in electrochemical processes.

Judging from the number of contributions and the intensity of the discussions following their presentations, the topic of 1/f noise remains as a very interesting one. It has resisted most, if not all theoretical attempts to explain it. An invited paper by T. Musha gave even more evidence to its ubiquity in nature. One of the most interesting developments here has been the connection between 1/f noise and human comfort. Extending beyond the observation that noise exhibiting a 1/f spectrum is pleasing to the listener, clinical evidence now suggests that electronic alleviation of pain in humans is improved when the electrical shocks are given a 1/f component.

We have to come to appreciate that studies of 1/f noise may benefit from techniques found useful in several other activities at NBS. That is, controversies have often been resolved in metrology by round robin exchanges among several laboratories of well-characterized samples. We suggest that a similar program (i.e., exchange of samples exhibiting 1/f noise) might help establish the level of accuracy of the magnitude of the observed noise, the precise exponent, and other sample parameters (e.g., number of surface states).

The Conference was held at the National Bureau of Standards, Gaithersburg, MD, from April 6-10, 1981. It was sponsored by the National Measurement Laboratory of NBS, The Catholic University of America, and the National Science Foundation. The NBS Conference was the sixth in a sequence of conferences previously held in Bad Nauheim, F.R. Germany (1978), Noordwijkerhout, Netherlands (1975), Gainesville, FL, USA (1973), Toulouse, France (1971), and Nottingham, England (1968).

An International Advisory Board, the members of which are listed herein, assisted in the program selection and organization. We thank them for their generous contributions and cooperation. We would also like to thank the NBS staff for their assistance in the smooth operation of the Conference.

April 1981

P. H. E. Meijer P.H.E. Meijer

R. D. Mountain R.D. Mountain

R. J. Soulen R.J. Soulen

Sixth International Conference on Noise in Physical Systems

International Advisory Board

A B S T R A C T

This document contains the full text of papers submitted to the Sixth International Conference on Noise in Physical Systems. There are six categories of papers: THEORY; DEVICES; 1/f NOISE; APPLICATIONS AND MEASUREMENT TECHNIQUES; QUANTUM NOISE; HOT CARRIER NOISE.

Key Words: Hot carrier noise; noise; noise in devices; noise measurement; quantum noise; 1/f noise.

TABLE OF CONTENTS

TABLE OF CONTENTS (Continued)

I. THEORY

CLASSIFICATION OF NOISE PHENOMENA

K. M. van Vliet

Department of Electrical Engineering
University of Florida, Gainesville, FL 32611

and

Centre de Recherches Mathematiques
University of Montreal, Canada

I. INTRODUCTION

The purpose of this paper is to give some broad guidelines on how to classify noise phenomena. In many respects this looks like an impossible task. First of all: Should we classify noise causes or noise manifestations? The more dogmatic oriented researcher would opt for noise causes, while the morphologist would seek to classify the various phenomena as they occur. The latter easily leads to a chaos; what, e.g., to make of 1/f noise (formerly often called current noise) observed in the Nyquist noise of a resistor by Clarke and Voss? But a classification solely in terms of noise causes is equally ubiquitous; for many phenomena we do not know the proper causes yet, and for others we may have the wrong causes in mind--as will perhaps be borne out by future research. So, I believe a systematic classification of all observed noise phenomena is impossible. All we can hope to do is to clarify certain principles, on account of which we can divide the phenomena in broad groups. First, in Section II of this paper I will present four such principles. They are:

(1) The principle of thermal equilibrium. This allows noise to be characterized as thermal or nonthermal.

(2) The principle of microscopic versus mesoscopic fluctuations. The term "mesoscopic" is due to van Kampen. It is used for quantities which are governed by the master equation for coarse-grained variables, these quantities being themselves fluctuations of macroscopic variables.

(3) The principle of lumped versus distributed representation. While we borrow these terms from the electrical engineer, the more mathematical-oriented researcher may want to speak of discrete and continuous random processes or of finite dimensional and infinite dimensional (Markovian) random processes.

(4) The principle of classical versus quantum nature of the noise. Of course, this writer adheres to the view that only quantum processes exist in nature. However, some allow for a classical description and others do not. However, in quantum statistical mechanics there is both statistical and quantum mechanical uncertainty. If both occur, we speak of quantum noise.

The elaboration of these principles will be set forth in Section II. It is to be understood that the various divisions are by no means mutually exclusive. Thus, on account of these principles there are not $2^4=16$ classes of noise; rather, a given noise phenomenon is to be classified in four different ways. If we call A the first part of each principle and B its antithesis, then shot noise in tunnel diodes is (1)B-(2)A-(3)A-(4)B.

Secondly, I must introduce a super distinction which occurs over and above the principle just mentioned. It has only recently become clear to me that not all noise phenomena can be reduced to manifestations of noise *sources* which describe the effects of *elementary events*. In more specific terms, there are not always Langevin sources, there need not be a Campbell-Carson elementary event, and there may not be characteristic time constants associated with such events. In this respect I should like to introduce the name CHARACTERISTIC

NOISE PHENOMENA for all phenomena which are reducible to noise sources and which thereby have characteristic time constants due to these sources, while I propose the name NON-CHARACTERISTIC NOISE PHENOMENA for those fluctuation processes which are not reducible to noise sources in the sense of Langevin, Campbell-Carson, or other elementary event pictures. Examples of characteristic noise are g-r noise and flux-flow noise in super conductors; examples of non-characteristic noise are wave interaction noise in photon statistics and quantum 1/f noise according to Handel.

In Section III we will describe some of the tenets of characteristic noise. In particular we will urge that these noise phenomena are named according to the nature of the source of the noise and not in view of the response behavior of the system. In Section IV we point out some aspects of non-characteristic noise.

II. VARIOUS PRINCIPLES OF CLASSIFICATION

The earliest noise phenomena discovered were thermal noise (Einstein 1906, de Haas Lorentz 1913, Johnson 1925, Nyquist 1928) and shot noise (Schottky 1918, 1922). In our opinion, these two noise processes are still the prototypes of all observed characteristic noise phenomena in and out of thermal equilibrium. Thermal noise in resistors is due to the thermal motion of the constituent electron and phonon gases; shot noise is due to the corpuscular nature of transport.

A. Thermal Equilibrium versus the Steady State

In a closed system thermal equilibrium prevails if the extensive thermodynamic parameters do not depend on the time explicitly, i.e., other than through the p's and q's on which they depend. In an open system--subject to interaction with an energy or particle reservoir--thermal equilibrium entails that there is no net transport of particles or energy across its boundaries; both definitions can be shown to be equivalent.

We define generalized thermal noise as fluctuations in any dissipative medium, i.e., any fluctuations associated with entropy production. For extensive variables in a lumped system the variance is given by

$$\langle \Delta a_i \Delta a_j \rangle = k \left(\frac{\partial^2 S}{\partial a_i \partial a_j} \right)^{-1}_{eq} \tag{1}$$

The spectral density of $\langle \Delta a_i \Delta a_j \rangle$ is now given by the generalized Nyquist relation or fluctuation-dissipation theorem (Callen and Welton 1951, Callen and Greene 1952, Kubo 1967, van Vliet 1978):

$$S_{\dot{a}_i \dot{a}_j} = 4 \mathcal{E}(\omega,T) \quad [L'_{ij}(\omega)]^s + i[L''_{ij}(\omega)]^a \tag{2}$$

where $\dot{a}_i \equiv J_a$ is the flow associated with the extensive thermodynamic variable a, $L = L' + iL''$ is the generalized conductivity tensor, the superscripts s and a denote symmetric and antisymmetric combinations of L_{ij}, whereas $\mathcal{E}(\omega,T)$ is the energy of a harmonic oscillator of frequency ω,

$$\mathcal{E}(\omega,T) = (\hbar\omega/2) \cosh (\hbar\omega/2kT). \tag{3}$$

One also writes $\mathcal{E}(\omega,T) = kTp(\omega)$; then $p(\omega)$ is the "quantum correction factor;" if a = Q, (2) reduces to the ordinary Nyquist relation for electrical current fluctuation, J = dQ/dt.

Many examples of generalized thermal noise exist, the most important ones being Brownian motion noise (Uhlenbeck and Ornstein 1930, M. C. Wang and Uhlenbeck 1945), generation-recombination noise (van Vliet 1958), temperature noise (Milatz and van der Velden 1943), and blackbody radiation or thermal photon noise (R. C. Jones 1953). Two remarks on the thermal nature of these phenomena are to be made.

First, these phenomena may have an "analytical continuation" outside thermal equilibrium proper. The nonequilibrium state may or may not affect the nature and magnitude of

the noise. For example, generation-recombination noise, which is due to the thermal fluctuations in the transition rates and the associated Nyquist noise of the quasi Fermi levels, usually requires the passage of electrical current in order to detect the conductivity fluctuations due to g-r noise. When this current is small, we still have a quasi-equilibrium state and the noise is thermal noise. (Since this current does not produce the noise, we once more emphasize that g-r noise is not a form of shot noise as thought in the early fifties.) The deviation from thermal equilibrium may also be large as in hot electron noise or in photo-induced g-r noise. In this case the physical phenomena may still be similar as in thermal equilibrium, but the noise should not be called generalized thermal noise (a term we reserved for the noise as in eq (2)); the phenomenon should be called nonthermal g-r noise or photo-induced g-r noise as we mentioned above. Noise in resistors outside thermal equilibrium should be called hot carrier noise, nonthermal Johnson noise, or nonthermal diffusion noise (see Section III).

Secondly, we note that shot noise methods may apply to thermal noise sources, but this does not make the noise shot noise. In this regard we note that all thermal equilibria are maintained by opposing flows of particles or heat according to the principle of detailed balance. Quite often the right thermal noise source is obtained by attributing full shot noise to these opposing flows. Thus it is well-known that in a diode at thermal equilibrium we have

$$S_i(\omega) = 4eI_0 = 4kTg \tag{4}$$

since the differential conductance is given by

$$g = \frac{d}{dV}\left[I_0(e^{eV/kT} - 1)\right]_{V=0} = eI_0/kT \ . \tag{5}$$

This argument was first given as a derivation of thermal noise by Weiszkopf (1943). Sometimes, however, this argument is phony and only by luck one obtains the right result. For the sources of g-r noise one often writes the Langevin equation

$$\frac{dn}{dt} = g(n) - r(n) + \xi_g - \xi_r \ . \tag{6}$$

Attributing full shot noise to the transition rates ξ_g and ξ_r, we have

$$S_{\xi_g} + S_{\xi_r} = 2\langle g\rangle + 2\langle r\rangle = 4\langle g\rangle \ . \tag{7}$$

Fourier analysis of (6) now shows

$$\langle \Delta n^2\rangle = \left(S_{\xi_g} + S_{\xi_r}\right)\tau = \langle g\rangle\tau = \langle g\rangle \Big/ \left[\frac{dr}{dn} - \frac{dg}{dn}\right]_{n=\langle n\rangle} , \tag{8}$$

which is Burgess' g-r theorem (1954). However, a correct corpuscular treatment involving phonon or photon emission or absorption easily shows that $S_{\xi_r} \neq 2\langle g\rangle$, $S_{\xi_r} \neq 2\langle r\rangle$, and $S_{\xi_g,\xi_r} \neq 0$ (van Vliet and Zijlstra 1977, van Vliet, Zijlstra and van Kampen 1978). Thus, although the detailed balance picture plus shot noise argument often gives the right thermal noise source, we emphasize that the result is often fortuitous.

Shot noise correctly is associated with a situation in which there is no detailed balance, but in which net transport occurs. Similarly, as in our distinction of thermal noise proper (Nyquist) and generalized thermal noise (fluct. diss. theorem), we can distinguish between shot noise proper (noise in electrical current flows) and generalized shot noise (noise in energy flow, entropy flow, etc.). In all cases shot noise is proportional to the average flow under consideration, $\langle J\rangle$ --if it is not, it is not shot noise. The noise also possesses quantum attributes. Though the quantum noise correction factor was reported as early as 1955 by Epstein and Rostoker (Epstein and Rostoker 1955), and also at one of the Armour Research Foundation meetings organized by J. J. Brophy, no correct detailed publication of this quantum effect appeared until 1979 (Tucker 1979). For tunnel junctions

Tucker finds

$$S_I(\omega) = e\left\{\coth\left[(eV_0+\hbar\omega)/2kT\right] I(V_0+\hbar\omega/e) + \coth\left[(eV_0-\hbar\omega)/2kT\right] I(V_0-\hbar\omega/e)\right\}. \quad (9)$$

Here I(V) is the current-voltage characteristic. For $V_0 >> \hbar\omega/e$ and $eV_0 >> kT$ one finds 2eI. For $V_0 \to 0$ one obtains thermal noise, $4g\,\mathcal{E}(\omega,T)$ with $\mathcal{E}$ as in (3), noticing that the quantum conductance is given by

$$g(\omega) = \frac{I(V_0+\hbar\omega/e) - I(V_0-\hbar\omega/e)}{2\hbar\omega/e} . \quad (10)$$

These equations apply to tunnel diodes and metal-oxide-metal diodes. For Schottky barrier, p n diodes and vacuum diodes, they may need modification.

Generalized shot noise finds, as examples, particle flow noise, heat flow noise, and photon noise (van Vliet 1976). Thus, if $\bar{m}$ is the number of emitted photons per second, and if the line shape is Lorentzian,

$$S_m(\omega) = 2\bar{m}\left[1 + \frac{2\bar{m}\eta(\tau_c/2)}{1+\omega^2(\tau_c/2)^2}\right] , \quad (11)$$

where τ_c is the coherence time and η is the detection efficiency; the last factor is due to wave-interaction noise (Section V). For noise due to an incoherent thermal source of radiative temperature T_s, filtered with a monochromator of slit width $\Delta\nu$:

$$S_m(\omega) = 2\bar{m}\left[1 + \eta B(\nu_0)\,(1 - \omega/2\pi\Delta\nu)\right], (0 \le \omega \le 2\pi\Delta\nu) , \quad (12)$$

where

$$B(\nu_0) = 1 / \left[e^{(h\nu_0/kT_s)} - 1\right] , \quad (13)$$

is the Boson factor.

Still, a word is in order about noise which is proportional to the square of the current, as is the case for 1/f noise and g-r noise. In the early days (Bernamont 1937) these phenomena were called current noise. It is appropriate that this name has been abandoned. It should not be used for phenomena in which the current is only a vehicle to detect conductivity fluctuations, as with g-r noise. For 1/f noise the situation is dubious. Granted, also here one can write $S_I/\langle I\rangle^2 = S_g/\langle g\rangle^2$, where S_g denotes conductivity fluctuations. If the fluctuations are number fluctuations, then $S_g/\langle g\rangle^2 = S_n/\langle n\rangle^2$, and the current flow is nonessential. If, however, we have mobility fluctuations $S_g/\langle g\rangle^2 = S_\mu/\langle\mu\rangle^2$, then one may argue that the existence of a drift field is essential; yet the mobility itself is a thermal equilibrium quantity. In Handel's theory the noise is due to fluctuations in scattering cross section: $S_\mu/\langle\mu\rangle^2 = S_\sigma/\langle\sigma\rangle^2$, and the presence of a current is essential for the description.

The name excess noise is often used to denote all noise above proper thermal noise. It serves no useful purpose.

B. Microscopic versus Mesoscopic Fluctuations

It is often said that noise involves the microscopic description of electronic or other processes. However, this is usually not the case. The microscopic description in classical statistical mechanics refers to the motion in terms of particle positions and momenta; in quantum statistical mechanics it involves the occupancies of many body or one particle quantum states, e.g., Bloch states or momentum states in solids. Statistical mechanics has a great deal to say about the microscopic fluctuations. The two particle correlation function $\langle\Delta n(p_1 q_1 t_1)\Delta n(p_2 q_2 t_2)\rangle$ can be obtained from the BBGKY hierarchy; in quantum statistical mechanics $\langle\Delta n_\zeta(t)\Delta n_{\zeta'}\rangle$, where (ζ) is a one particle state, can be obtained from the Pauli-van Hove quantum master equation (Charbonneau, van Vliet, Vasilopoulos 1981; van Vliet 1978).

Usually, however, in noise problems we do not deal with the microscopic fluctuations. On the contrary, the fluctuations involve coarse graining over a volume in phase space or over a range of quantum states. Thus, pressure fluctuations in a microphone involve the momenta of a large number of particles in a certain subvolume of the phase space; in g-r noise we are interested in the occupancy of a large number of states in the conduction or valence band; etc. Such fluctuations, being themselves still small with respect to the corresponding macroscopic variables, are called mesoscopic. Markovian mesoscopic variables are governed by a master equation for $P(a,t\,|\,a';t_0)$ in a-space (van Vliet and Fassett 1965). Though this master equation is easily derived from the Smoluchowski or Chapman-Kolmogoroff equation, this constitutes no physical proof. In our opinion, this equation should be derived from the Pauli-van Hove master equation; a satisfactory proof has not yet been given in our opinion. However, fruitful applications to Brownian motion, g-r noise, laser noise, nonlinear processes, etc., abound.

C. Lumped versus Distributed Noise

Irreversible thermodynamics these days is divided in the theory for discrete thermodynamic variables pertaining to homogeneous systems and the theory for continuous variables involving, e.g., particle densities in inhomogeneous systems (De Groot and Mazur 1962). Likewise, in noise we can distinguish processes involving a discrete set $a_1 \ldots a_m$ of (Markovian) variables, and those involving densities in $(\underset{\sim}{k},\underset{\sim}{r})$-space (microscopic continuous processes) or in r-space (mesoscopic continuous processes). Examples for these cases are g-r noise in bulk solids, spontaneous emission noise in lasers and masers (discrete), and density fluctuations in inhomogeneous solids or devices, such as semiconductor samples with surface recombination or noise in bipolar transistors (continuous). From a mathematical statistical point of view such processes are finite dimensional processes or infinite-dimensional Markov processes. The theory for discrete processes is well-known (van Vliet and Fassett 1965); they can often be represented by a lumped equivalent network (Champlin 1960,a). The continuous processes form the domain of transport noise. They can often be represented by a transmission line model (van der Ziel 1955,1957; Champlin 1960,b). The master equation level description for these processes is too cumbersome, since it involves the functional $P[a(\underset{\sim}{r},t)\,|\,\bar{a}(\underset{\sim}{r},t_0)]$. One therefore uses a Langevin description, i.e., one supplements the phenomenological transport equation with Langevin sources. The general form for a mesoscopic transport process is

$$\left(\frac{\partial}{\partial t} + \Lambda\right) a(\underset{\sim}{r},t) = \xi(\underset{\sim}{r},t) \tag{14}$$

where Λ is a spatial integral or differential operator. In case of diffusion, $\Lambda = -D\nabla^2$, eq (14) has to be supplemented with deterministic or stochastic boundary conditions. For a recent survey paper, see van Vliet and Mehta (1981). The noise solution of (14) requires eigenfunction expansions or Green's function procedures.

The name transport noise denotes a category of noise processes, but individual processes have their own designation. See Section III for proposed nomenclature.

D. Classical versus Quantum Noise

The name quantum noise has come into use in recent years for a number of processes in which the quantum mechanical nature is imperative. Thus we have quantum thermal noise, eq (2); quantum shot noise, eq (9); quantum 1/f noise (Section IV). Further, the name seems to be specifically used for noise in lasers, masers, Josephson junctions (see Wednesday p.m. section of the Conference). However, all g-r noise is also quantum noise. On the contrary, for Brownian motion of a colloidal suspension, purely classical methods suffice; so this is an example of classical noise.

III. CHARACTERISTIC NOISE

All noise processes which are governed by a master equation allow a Langevin description, which means that the phenomenological equations are amended by noise sources: $\xi_i(t)$ (discrete case), $\xi_i(\underset{\sim}{r},t)$ (mesoscopic distributed case). The problem now involves two parts. First, the noise source spectra must be known. Secondly, one must solve the

Langevin equation for the response of the system. If the noise source spectra are white, the response will result in a sum of Lorentzians,

$$S_a(\omega) = \sum_k A_k \tau_k / (1 + j\omega\tau_k). \tag{15}$$

For lumped processes the number of modes and the number of relaxation times τ_k is finite; for distributed processes this number is infinite. For finite physical systems (however large) this will always result in a constant spectrum for $\omega \to 0$ and an $\omega^{-\alpha}$ ($\alpha > 1$) spectrum for $\omega \to \infty$. Thus 1/f noise for very low and very high frequencies cannot arise as characteristic noise.

In naming the noise phenomenon, one has now the choice of characterizing it by the source function or by the response operator Λ. This leads to conflicting statements. In nonhomogeneous solids the source is due to g-r fluctuations, while the response is due to diffusion; in single injection diodes, the source is due to diffusion fluctuations, while the response represents mainly drift; in bipolar transistors the source is due to g-r and diffusion fluctuations and the response represents recombination and diffusion. We recommend that the process be characterized by its sources. Or, one can describe the process by names like "diffusion-aided g-r noise," drift-aided diffusion noise, etc. In particular, we would like to reserve the name "diffusion noise" for processes which have the source spectra

$$S_\eta = 4e^2 D n(\underset{\sim}{r}) \delta(\underset{\sim}{r} - \underset{\sim}{r}') \tag{16}$$

which in thermal equilibrium gives the thermal noise source $4kT\sigma(\underset{\sim}{r})\delta(\underset{\sim}{r}-\underset{\sim}{r}')$ by Einstein's relation. Hot electron noise generally is diffusion noise. The name diffusion noise should not be used for transport noise in which $\Lambda = -D\nabla^2$ but the source is g-r.

We still mention that in the case of characteristic noise, often the noise can also be treated with the Campbell-Carson method of elementary events. Clearly, these events are what make up the noise source. However, one incorporates the response in terms of the Fourier transform of these events, rather than on the collective level. Discrete Markov processes can be shown to be equivalent with the Campbell-Carson method applied to multistable random telegraph signals. For a two-level process the equivalence with a bistable random telegraph signal is clear from the work of Machlup and Onsager (1954).

IV. NONCHARACTERISTIC NOISE

When no noise sounds can be indicated (and also no response part to the problem can be separated off), we propose the classification "noncharacteristic noise." Such processes lack a Master-, Langevin-, or Campbell-Carson description. Since there are no "elementary events," the noise basically is a collective phenomenon. Examples are afforded by wave interaction noise and quantum 1/f noise (Handel 1975; 1980). Recently, 1/f noise has also been described in terms of a wave self-interference phenomenon, similar to wave interaction noise (van Vliet, Handel, and van der Ziel 1981). We will here briefly describe both effects.

The emission of photons is governed by compound Poisson statistics for emission of M photons in time $\mathcal{T}$:

$$W(M,\mathcal{T}) = \int_0^\infty \frac{(\gamma U)^M}{M!} e^{-\gamma U} W(U)\,dU \tag{17}$$

where $U = \int_t^{t+\mathcal{T}} I(t')dt'$ is the fluctuating light intensity. The fluctuations of I(t), which affect the mean emission rate, are collective as is clear. (Formerly (van Vliet 1958b) we labeled such fluctuations as "modulation noise.") Finding the covariance $\langle \Delta M_{\mathcal{T}}^2 \rangle$ and using MacDonald's theorem, (17) yields for the spectrum of the rate $m = M/\mathcal{T}$:

$$S_m(\omega) = 2\bar{m}\,[1 + \tfrac{1}{2}\,\bar{m}\,\hat{S}_{\Delta I}(\omega)] \tag{18}$$

where $\hat{S}$ is the normalized light-intensity noise. If $S_{E^+}(\nu)$ is the distribution of the spectral line width, one has by convolution

$$\hat{S}_{\Delta I}(\omega) = \int_{-\infty}^{\infty} \hat{S}_{E^+}(\nu)\, S_{E^+}(f-\nu)\, d\nu \ , \tag{19}$$

where $\omega = 2\pi f$ is the frequency of the beats, i.e., of the noise. For a Lorentzian line width

$$S_{E^+}(\nu) = \frac{2\,\Gamma}{4\pi^2(\nu-\nu_0)^2 + \Gamma^2} \ , \quad \Gamma \approxeq 1/\tau_c \ , \tag{20}$$

eq (11) is easily obtained; τ_c is the coherence time. This coherence time is, however, not the characteristic time constant of an elementary event, as is clear since Γ is the line width due to photon bunching (corpuscular picture) or due to collision and Doppler broadening of the light signal (wave picture); thus Γ represents a collective feature of the photons or of the light wave packet.

We now describe 1/f noise in terms of self-interference. Equations (18) and (19) are still valid, but the analytic signal $S_{E^+}(\nu)$ must be replaced by the Schrodinger field S_{ψ^+}. Hence,

$$\hat{S}_{\Delta I} = \int_{-\infty}^{\infty} S_{\psi^+}(\nu)\, S_{\psi^+}(f-\nu)\, d\nu \tag{21}$$

where ψ^+ is the local creation operator of the quantized field; $I = \psi^+\psi$ is the particle density of the scattered field, which yields the cross section fluctuations. We assume that ψ^+ represents both elastic (or rather "subthreshold inelastic" in Handel's terminology) and inelastic scattering (with the lattice as occurring in mobility fluctuations) due to the emission of infraquanta. Then (Handel 1980),

$$\hat{S}_{\psi^+}(\varepsilon) = C\,[\delta(\varepsilon) + \alpha A\ (\varepsilon/\varepsilon_0)^{\alpha A}\ \varepsilon^{-1}] \tag{22}$$

where αA is the infrared exponent, α is the fine structure constant if the infraquanta are photons, and C is a normalization constant; $\varepsilon = h\nu$ and ε_0 is determined by the low frequency detection limit allowed in the system (as indicated above, the elastic contribution "$\delta(\varepsilon)$" incorporates all $\varepsilon \leq \varepsilon_0$). From (21) and (22) one obtains for the spectrum of the beats

$$\hat{S}_{\Delta I} \approxeq \delta(f) + 2\alpha A(f/f_0)^{\alpha A}\ f^{-1}\ \Theta(f-f_0) \tag{23}$$

where Θ is the unit step function. Note, however, that f_0 can be taken arbitrarily low, there being no lower limit. Since $2\alpha A$ is Hooge's constant $<<1$, $(f/f_0)^{\alpha A} \sim 1$. The current noise, taking into account incoherence of N_c contributions is by (18) and (23)--noting $i = em$,

$$S_i = 2\langle i\rangle^2 \alpha A/N_c f \ , \tag{24}$$

which is Hooge's law if $N_c = N$, the number of carriers involved in the scattering process, (Hooge 1969, 1972).

The problem with this version of quantum 1/f noise is not with the mathematical derivation (a fuller account of (23) and the ensuing mobility fluctuations both for lattice and impurity scattering will be presented elsewhere). The main obstacle is the physical interpretation of αA. Handel has presented a number of processes which lead to emission of infraquanta. The values of $2\alpha A$ seem, however, to be below Hooge's constant. However, it is not clear whether the coherence factor N_c represents all carriers as in Hooge's formula. If $N_c << N$, the results could well be reconciled. The fact that there are no characteristic time constants in the theory of quantum 1/f noise, and consequently no lower limit appears in the theory, is the attractive feature of this theory. Lack of space prevents us from presenting other theories of this nature, like Ngai's theory of collective states (Ngai 1980).

CONCLUSIONS

We have presented a number of principles to distinguish fluctuation phenomena. Various names and concepts have been introduced which will hopefully lead to a sharper classification of noise processes.

REFERENCES

J. Bernamont (1937), *Ann. de Physique* 7, 71.

R. E. Burgess (1954), *Physica* 20, 1007.

H. B. Callen and T. A. Welton (1951), *Phys. Rev.* 83, 34.

H. B. Callen and R. F. Greene (1952), *Phys. Rev.* 86, 702.

K. S. Champlin (1960a), *Physica* 26, 751.

K. S. Champlin (1960b), *IRE Trans. E-D* 7, 29.

M. Charbonneau, K. M. van Vliet and P. Vasilopoulos, "*Linear Response Theory Revisited III*," submitted to *J. Math. Phys.*

S. R. deGroot and P. Mazur (1962), *Non-Equilibrium Thermodynamics* (North Holland, Amsterdam).

G. H. de Haas-Lorentz (1913), *Die Brownsche Bewegung und einige verwandte Erscheinungen* (Vieweg Braunschweig).

A. Einstein (1906), *Ann. der Physik* 19, 371.

H. Ekstein and N. Rostoker (1955), *Phys. Rev.* 100, 1023.

P. H. Handel (1975), *Phys. Rev. Letters* 34, 1492.

P. H. Handel (1980), *Phys. Rev.* A22, 745.

F. N. Hooge (1969), *Phys. Letters* 29A, 139.

F. N. Hooge (1972), *Physica* 60, 130.

J. B. Johnson (1925), *Phys. Rev.* 26, 70.

R. C. Jones (1953), in *Advances in Electronics*, Vol. V, Ed. L. Martin (Acad. Press, N. Y.).

R. Kubo (1957), *J. Phys. Soc. Japan* 12, 570.

S. Machlup (1954), *J. Appl. Physics* 25, 341.

J. M. W. Milatz and H. A. van der Velden (1943), *Physica* 10, 369.

K. L. Ngai (1980), in *Proc. 2nd Intern. Symp. 1/f Noise*, Ed. K. M. van Vliet, p. 445.

H. Nyquist (1928), *Phys. Rev.* 32, 110.

W. Schottky (1918), *Ann. der Physik* 57, 541.

W. Schottky (1922), *Ann. der Physik* 68, 157.

J. R. Tucker (1979), *IEEE J. Quantum Electr.* 15, 1234.

G. E. Uhlenbeck and L. S. Ornstein (1930), *Phys. Rev.* 36, 823.

A. van der Ziel (1955), *Proc. IRE* 43, 1639.

A. van der Ziel (1957), *Proc. IRE* 45, 1011.

K. M. van Vliet (1958a), *Phys. Rev.* 110, 50.

K. M. van Vliet (1958b), *Proc. IRE* 46, 1004.

K. M. van Vliet and J. R. Fassett (1965), in *Fluctuation Phenomena in Solids*, Ed. R. E. Burgess (Acad. Press, New York), p. 267.

K. M. van Vliet (1976), *Physica* 83 B & C, 52.

K. M. van Vliet and R. J. J. Zijlstra (1977), *Physica* 89A, 353.

K. M. van Vliet (1978), *J. Math. Phys.* 19, 1345.

K. M. van Vliet, R. J. J. Zijlstra, and N. G. van Kampen (1978), in *Noise in Physical Systems*, Ed. D. Wolf (Springer), p.309.

K. M. van Vliet and H. Mehta (1981), "*Theory of Transport Noise*," *Physica Status Solidi* (b), in press.

K. M. van Vliet, P. H. Handel and A. van der Ziel (1981), "*Super Statistical Emission Noise*," submitted to *Physica*.

M. C. Wang and G. E. Uhlenbeck (1945), *Rev. Mod. Phys.* 17, 323.

V. Weiskopf (1943), *Nat. Defense Research Council Report.*

POSTSCRIPT

1. Altogether, it seems to us that there are four broad classes of noise phenomena, viz.:

(i) noise due to thermal statistical uncertainty, as described by equilibrium statistical mechanics, and labeled here as generalized thermal noise;

(ii) similar processes outside thermal equilibrium, as described by nonequilibrium statistical mechanics, labeled here as "analytical continuations" of generalized thermal noise;

(iii) noise due to the corpuscular nature of transport, labeled generalized shot noise, being either of a classical nature (tubes) or of a quantum mechanical nature (photon noise, shot noise in tunnel diodes);

(iv) noise due to quantum mechanical uncertainty, labeled "quantum mechanical noise" (this noise does not contain kT in contrast to quantum statistical noise); quantum 1/f noise (Handel-Ngai) is an example.

2. All noise phenomena can further be classified according to the four principles of Section II and in addition as characteristic or noncharacteristic noise. In response to some papers of the Conference, to the distinction "microscopic-mesoscopic," we would like to add "macroscopic." The coupled oscillator noise reported by Gollup et al. is a macroscopic noise manifestation; in this category also comes noise due to turbulence.

FUNDAMENTAL PHYSICAL LIMITATIONS OF THE COMPUTATIONAL PROCESS

Rolf Landauer

IBM Thomas J. Watson Research Center
P. O. Box 218, Yorktown Heights, New York 10598

INTRODUCTION

Thermodynamics arose out of attempts to understand the limits on the efficiency of steam engines. Information theory arose out of the effort to understand channel capacity limitations. These models have motivated an attempt to do the same thing for the computer. A first conference on the subject follows this noise conference by a few weeks, and the proceedings of the later conference will be published in the *International Journal of Theoretical Physics* [1]. It is easier to ask questions about computer limitations than to answer them, and we can claim only very modest progress.

There has been enough progress, however, so that within the severe space limitation imposed by this conference we can only allude, in a very general way, to what has been done, and provide a road map of sorts. At the outset, let me emphasize the distinction between this field, and more well known areas.

Information theory deals with the behavior of linear channels where we hopefully take out information just as we put it in. A computer is clearly different, the logic process creates a nonlinear interaction between two or more information streams. The one part of a computer that is very much like a communications channel is the memory, where one hopes to find things unchanged.

The attempt to do scaling calculations, in which we ask how a computer changes as we reduce the components in size, including both active components and transmission lines, is another well established field. Our concern differs; we are attempting to describe the computer in phase space, without invoking a particular set of devices. A recent review paper by Keyes [2] discusses both fundamental limitations and scaling theories for the computer.

In contrast to our historical models, information theory and thermodynamics, the fundamental limitations of the computer, to the extent they are understood today, are far too many powers of ten away from the technological limits, to be a guide for further technological progress. Then why is the subject important or interesting? We are attempting to provide a physical basis for mathematics. The mathematician has given us the impression that it makes sense to talk about an arbitrarily long sequence of information handling steps, with each step guaranteed to be unquestionably correct. Now we come back and ask whether nature really allows that.

The kind of questions we are tempted to ask:

1. How many degrees of freedom are there available in the universe, to handle information? How many of these can really be brought together, to interact effectively, in a computer?

2. What is the minimum energy consumption required by the computational process?

3. How immune to noise can the computational process be made?

4. The preceding question refers to degradation of information, by noise, in a fixed physical structure. We can also ask how much can be done to offset the inevitable physical degradation arising from diffusion, corrosion, electromigration, etc. Does this structural deterioration establish a limit to the number of computational steps?

5. How many photons, or more generally signal quanta, are required to bring a bit into a logic stage?

Of these questions, only 2 and 3 have been answered, to some reasonable extent. It is often hard to understand the difference between fundamental limits, and those that are less fundamental and circumventable. Take the question about noise immunity as an example. We normally think of thermal equilibrium noise, i.e. Nyquist noise, as an inevitable minimum. It is determined by the temperature. Is there a minimum achievable temperature? Can additional sources of noise, e.g. 1/f noise, be reduced to an arbitrary extent? (The answer, for 1/f noise, is likely to be affirmative since, as we will show, computing can be carried out arbitrarily close to thermal equilibrium.) In recent years we have become very conscious of the fact that secondary electrons, produced by particle radiation, can act as a source of noise [3], and destroy information stored in the form of electrical charge. Does this radiation have an unavoidable minimum level? Even if it does, information does not need to be handled in the form of charges. We can use superconducting currents, magnetization, hydraulic flow, or many other degrees of freedom. But while some of these may interact less strongly with particle radiation, they undoubtedly all still interact with it to some extent.

THE UNIVERSE HAS A FINITE MEMORY CAPACITY

One of the earliest and most perceptive treatments of memory limitations is due to Swanson [4] and is summarized in a later review paper [5]. Swanson asks how finely should we subdivide a given amount of memory material, to obtain the maximum storage capacity, given a period T over which we want to preserve information. If we make our elements too small, they are too susceptible to noise, and lose their information too quickly. If we make the elements very large they become immune to noise, but we don't have much capacity, either. In between these extremes there must be a maximum, and Swanson utilized information theory, i.e. the possibility of redundancy to protect information, to find the optimum element size. Swanson's considerations are not completely general and model independent, but have a broad degree of applicability. The result: The individual elements must be large enough to be relatively reliable. We lose if we depend too much on redundancy. Swanson's considerations do not allow, explicitly, for readout, after time intervals short compared to T, and then utilizing the information protection provided by redundancy, to restore all the bits to their initial state. To do this sensibly, we must understand the probability of error in the readout and restoration process, and thus we become even more model dependent.

Information is sent into storage, and retrieved from it, via a channel. Therefore one can invoke channel capacity theory to describe storage limitations, without regard to the physical storage mechanism. If we invoke classical channel capacity theory [6], a minimal energy of $kT\ln 2$ is required per transmitted bit. I do not know what value of T characterizes the universe in some average way, but 3°K is (certainly within a few powers of ten) a reasonable guess. We can then divide the energy of the universe by $kT\ln 2$ to get an upper limit on the amount of information that can be sent into a memory [6]. Alternatively, we can invoke quantum channel capacity theory [7].

While the aforementioned channel capacity considerations yield a quick and easy way to point to the existence of physical limitations, unfortunately, we believe they are wrong. One could apply the above reasoning equally to all interconnections between successive logic stages in a computer, and thus determine channel capacity energy requirements for each of these *channels*. As we shall see in the next section, however, we have hypothetical computers whose energy requirements are far lower. The answer to this apparent paradox: The energies required by channel capacity considerations represent energy *dissipation* only if the message is destroyed at the receiving end, and a computer need not do that. Consider, for example, a high density reel of storage tape sent physically through space, at high velocity. Motion of the reel can be controlled through a few degrees of freedom, related to the tape's position and orientation, and unrelated to the huge number of information bits. The required dissipation is at most a few kT, or perhaps, even zero, since the kinetic energy of tape motion need not be dissipated. Shipment of the tape does, however, constitute transmission of information. Alternatively we could receive a message in electromagnetic form and store it between reflecting mirrors, for eventual later controlled release. Similar confusion underlies many discussions of the measurement process [8]. Szilard's pioneering analysis [9] of the measurement process taught us that measurement requires energy expenditure. But it does not seem to be adequately recognized that coupling a meter to an object to be measured, and letting the object thus influence the meter does not require dissipation. The dissipation arises from the need to reset the meter after subsequent decoupling, in order to prepare the meter for further use. Again it is the *destruction* of information which is associated with the real need for

energy dissipation. This relationship to information destruction has been emphasized only in our own field, and not equally in the related analyses of the measurement process and of channel capacity requirements.

Finally we make a different point, related to the fact that infomation can be stored in bistable dissipative systems, e.g. active circuits, not only in dissipationless systems, such as ferromagnets. Since 1962 there has been analysis [10] to see how small such structures can be, and still preserve information in the presence of fluctuations. We do not discuss this subject, here, in further detail, for two reasons. First of all, no very fundamental model independent conclusions have been reached. Furthermore, analyses of that sort have become very fashionable. This author has, in fact, taken the liberty in one recent publication [11] of poking fun at the proliferation, and at some of the new labels, e.g. *multiplicative noise* that have been produced. Another paper [12] points to the unnecessary complexity of some recent discussions of the noise activated escape from a metastable state.

REVERSIBLE COMPUTATION

The fact that an elementary logic event is, in some vague sense, *associated* with a minimal energy of the order of kT, was a widespread supposition in the 1950's, but not generally articulated in print [13]. Subsequently it became clear [14] that only logical processes which throw away information require energy dissipation. This viewpoint has, since then, been elaborated on a number of occasions, and we cite only one of the more recent discussions [15]. It was, initially, unclear whether loss of information was essential to the computational process, but the obvious supposition was that intermediate scrap results had to be discarded. Ref. 14 pointed out that individual logic operations could be made logically reversible by the addition of unnecessary outputs to each logic stage. Consider a particular three-input, three-output device. Let p, q, and r be the input variables. The truth function under consideration is one which replaces r by $p \bullet q$ if $r = 0$, and replaces r by $\overline{p \bullet q}$ if $r = 1$. The variables p and q are fed through the device unchanged. All logic can be performed by iterations of this logically reversible operation [16]. To perform a simple negation $\bar{p}$, for example, we would feed fixed bias variables $q = 1$ and $r = 1$ into the device. r would be replaced by the desired output, $\bar{p}$. To duplicate a variable, i.e. generate *fan-out,* we feed in the variable p, and fixed inputs $q = 1$, $r = 0$, thus obtaining the variable p in two of the output positions. The unnecessary outputs would then be saved, for example, by feeding into a shift register; otherwise their destruction would require energy loss. It was originally presumed that this was a useless complication: We avoided the need to discard information by the addition of many shift registers, whose content would eventually have to be erased anyway. Bennett, in 1973 [17], finally pointed out that this erasure was not necessary. If the logical reversibility is properly utilized in a physical device, then erasure is not needed; we clean out the shift registers by running the machine backwards. *Properly utilized* in the preceding sentence means that the device can be pushed in the reverse direction to perform the inverse of the original logical operation. We do not require the device to be *strictly* physically reversible, i.e. lossless, but only as reversible as automobiles or locomotives, which can back up along their path. We also assume that the frictional forces are proportional to velocity and, thus, the accompanying energy losses, per logic step, can be made as small as desired, by sufficiently slow computation. The reader is referred to other discussions [8,15,17] for further details.

A logic device which provides one-to-one mapping, and is logically reversible, does not necessarily have the physical reversibility specified above. A number of *Gedanken* model computers have been devised to show that physical reversibility can actually be achieved. Note that the reversibility, at a local level, insures total reversibility: every initial state is mapped into a unique final state, if the computation comes to a termination. That does not mean such computers are simply table look-up devices where the designer has to anticipate all possible computations. The design of these computers can be simpler and more straightforward than that. We list some of the proposed models, without attempting a real description, and also briefly comment on their relative advantages and disadvantages.

1. Bennett's springless clockwork [8] Turing machine. In many ways the most satisfactory and most developed model. Does not assume perfect parts, or the absence of backlash. Does assume hard components whose shape and size is not subject to fluctuation.

2. Bennett's enzyme controlled DNA type Turing machine [8]. As a result of the molecular scale of the parts thermally induced errors in the information content, as well as in the basic structure of the machinery, will occur.

3. Toffoli's meshed gear computer [18]. A rigid linkage in which the information has to propagate from one stage to the next, instantaneously. This is not without further elaboration, a Turing machine capable of computations of arbitrary length. This is also a proposal in which, at least without further modification, errors accumulate through successive stages. To avoid that, logic devices must continually restandardize signals, i.e. push the signal level back toward favored states [19].

4. Fredkin's ballistic colliding billiard ball computer [20]. Information is represented by the presence or absence of particles which have a hard-core repulsion, no internal degrees of freedom, and are guided by reflecting mirrors. Logic is accomplished through the deflection produced by particle collisions. This scheme, in unmodified form, requires perfect mirror placement and exact initial velocities. Consider, instead, a modified version in which the particles move along guiding tracks and have a short range repulsion. The tracks are viscous, and also expose the particles to thermal agitation. The tracks have branches where there is a fork between a straightforward continuation of the original track and a branching track, off at some angle. (There are also compensating inverse branches, bringing tracks together, just as in the unmodified scheme [20].) We also invoke (as Fredkin does, in some versions of this model) moving potential wells, i.e. time dependent fields, which pace the particles in their motion along the tracks. Let two adjoining tracks have forks at adjoining positions, along their lengths. Then if a particle arrives along only one of the tracks it will continue undisturbed. If two particles arrive simultaneously, they will repel and move into their respective branching tracks. The strength of the repulsive force between particles will determine the probability that particles will take the desired branching tracks. For any given repulsive force there will be a nonvanishing residual error probability determined by thermal agitation. To insure that particles, in the absence of the interacting repulsive force, stay on the straightforward continuation, we need a static bias field near the bifurcation point, which, in turn, will be overcome by the repulsive interaction, when that is present. Additionally, of course, this system requires some elaboration to describe how the information bearing particles can move in and out of storage in a memory, or Turing machine tape.

5. I have described a Turing machine [15,21] whose active logic elements were proposed by Fredkin and whose overall organization follows Bennett's ideas [17], and have called this the Bennett-Fredkin-Turing (BFT) machine. It resembles Bennett's springless clockwork Turing machine in its characteristics. But it has the disadvantage that it invokes springs with a function closely related to that of the bias fields discussed above, in connection with the interacting charged particle scheme. Thus the BFT machine has an error probability, per step, which can be made arbitrarily small by a suitable choice of parameters. But for any given *design* there will be a maximal length of relatively error free computation.

NOISE IMMUNITY

Computers of the type described above consist of a series of one-to-one logical mappings. Thus the computation is a progression through a sequence of states, with only one antecedent state, and one consequent state, for each intermediate state of the computation. If the computation is driven forward, with a very small force, then fluctuations along that path, whether they are thermal equilibrium noise or some other form of noise, do not induce errors. In the presence of noise and a small driving force, a computation will proceed diffusively, going backwards almost as often as forwards. That, however, is irrelevant as long as it proceeds forward on the average. When the computation reaches its final state a modest one time energy loss is required to trap it there, and to prevent diffusion back toward earlier states.

If we want a machine which, at each step of the computation, proceeds forward rather than backward, then we must drive the mechanism sufficiently strongly to dissipate a few kT per step. Note, however, that one of these steps can involve a great many logic operations in parallel, and can be far less than a dissipation of kT per elementary logic operation. This dissipation, of only a few kT per machine cycle, requires that all of the machine's logic operations are coupled together rigidly, and that we are not dealing with many relatively independent degrees of freedom.

The discussion in the preceding paragraph assumes that the computation is constrained to follow the desired one dimensional path, and that noise can only affect motion along that path. Noise, in principle, can do more than that. First of all, fluctuations can have an effect on the actual physical computer structure, not just on its information content. (Point 4, Introduction). If the structure is massive enough, this can be made small, but once again, any given design will leave a nonvanishing probability, per unit time, for computer failure. Additionally, we must ask whether it is reasonable to invoke an unlimited structure (as in a Turing

machine) of arbitrarily massive elements. We must also ask whether there are fluctuations which do not ruin the structure, but take us from the track corresponding to one program, to that of another, e.g. by changing one bit in the program. If the information bearing degrees of freedom are massive, e.g. if information is denoted by massive balls, or their absence, as in the BFT machine, this will be very improbable, but can happen. The probability for fluctuations which mess up the machinery, e.g. a change of the ball into a shape which cannot move along the tracks intended for it, will be very much larger. If, however, the information bearing degree of freedom is very easily altered by fluctuations, as in Bennett's DNA model of a Turing machine, then the unintentionally induced transitions from one track to another become a genuine possibility.

The key point: It is easy to find models where, if the probability of permanent machine failure is negligible, then the probability of track jumping is even more negligible, and thus the results of the computation becomes immune to fluctuations along the allowed track. This is independent of the computational velocity; slow computation is not necessarily more reliable. Indeed a slow computation affords a greater opportunity for fluctuations which deteriorate the physical machinery. The availability of almost perfect noise immunity, for computations which are not extremely slow, may be somewhat counterintuitive. It is certainly in contradiction to some of the more easily analyzed models, including one discussed by this author [22]. On the other hand, the availability of computing which can be as free of thermally induced errors, as desired, at slow enough computing rates, was known before the existence of reversible computing was clearly understood [23].

QUANTUM EFFECTS

Several authors have casually invoked the uncertainty principle, $\Delta E \Delta t \sim \hbar$, to yield an energy dissipation for fast switching. Δt is typically equated with the duration of a switching event. While we cannot *guarantee* that this is an incorrect conclusion, it is certainly an unsubstantiated conclusion. The uncertainty principle refers to a spread in energy measurements, not to an energy dissipation. Futhermore, a fast event does not require an energy spread; an electron can pass an atomic nucleus in a crystal, or an interface between two crystals, very rapidly, and still be in an eigenstate. Only if we try to measure the time when the fast event occurred, do we meet the energy spread. Other authors have invoked quantum channel capacity considerations, instead of appealing directly to the uncertainty principle. But if a classical computer does not have to expend of the order of kT per bit, between successive logic stages, why should we expect channel capacity considerations to apply to a quantum computer? The thoughts on quantum effects, presented here, are discussed in more detail elsewhere [21].

RELATION TO REAL COMPUTERS

Real systems require an energy dissipation, per elementary logic step, many powers of ten above kT. Why are they so far from our limits? There are a number of reasons for this, probably not all of them understood. A key contribution, however, comes from the fact that our simplified models treat the machine's internal coupling mechanisms as structures whose own degrees of freedom do not have to be taken into account. Genuinely practical machines, however, are not periodic structures in which interaction is limited to neighboring elements. Real machines require *long* transmission lines [15], and lines which differ greatly from each other in their length. These lines have to be energized to voltages which are tied to the scale of the nonlinearities available in transistors [2], and cannot be made smaller than that, by going to very slow computation. We have not yet seen a way to save and reutilize that transmission line energy.

REFERENCES

[1] Proceedings of the Conference on *Physics of Computation,* MIT, Cambridge, Massachusetts (May 6-8, 1981), to be published in *Int. J. Theor. Phys.*

[2] R. W. Keyes, *Proc. IEEE* 69, 267 (1981).

[3] J. F. Ziegler, and W. A. Lanford, *Science* 206, 776 (1979).

[4] J. A. Swanson, *IBM J. Res. Dev.* 4, 305 (1960).

[5] R. Landauer, and J. W. F. Woo, in *Synergetics,* Ed. H. Haken (Teubner, Stuttgart, 1973).

[6] H. Marko, *Kybernetik* 2, 274 (1965).

[7] H. J. Bremermann, in *The Encyclopaedia of Ignorance,* Eds. R. Duncan, and M. Weston-Smith (Pergamon, New York, 1977) p. 167; J. D. Bekenstein, *Phys. Rev. Lett.* 46, 623 (1981); See also Ref. 6.

[8] C. H. Bennett, in Ref. 1.

[9] L. Szilard, *Z. Phys.* 53, 840 (1929).

[10] R. Landauer, *J. Appl. Phys.* 33, 2209 (1962).

[11] R. Landauer, in *Self-Organizing Systems: The Emergence of Order,* Eds. F. E. Yates, D. O. Walter, G. B. Yates (Plenum, New York, 1981).

[12] M. Büttiker, and R. Landauer, in *Nonlinear Phenomena at Phase Transitions and Instabilities,* Ed. T. Riste (Plenum, New York, to be published) see Appendix.

[13] J. von Neumann, *Theory of Self-Reproducing Automata* (Univ. of Illinois Press, Urbana, 1966).

[14] R. Landauer, *IBM J. Res. Dev.* 5, 183 (1961).

[15] R. Landauer, *Ber. Bunsenges* 80, 1048 (1976).

[16] T. Toffoli, Techn. Memo MIT/LCS/TM-151, Lab. for Comp. Sci., MIT (1980); T. Toffoli, in *Automata, Languages, and Programming,* Eds. J. W. deBakker and J. van Leeuwen (Springer, Berlin, 1980) p. 632.

[17] C. H. Bennett, *IBM J. Res. Dev.* 17, 525 (1973).

[18] T. Toffoli, *Math. Syst. Theory* 14, 13 (1981).

[19] A. W. Lo, in *Microwave Electronics,* Ed. E. Koenjian (Macmillan, New York, 1961) p. 19.

[20] E. Fredkin in Ref. 1.

[21] R. Landauer in Ref. 1.

[22] R. Landauer, and J. W. F. Woo, *J. Appl. Phys.* 42, 2301 (1971).

[23] R. W. Keyes, and R. Landauer, *IBM J. Res. Dev.* 14, 152 (1970).

FRACTAL RANDOM WALKS

Michael F. Shlesinger, Barry D. Hughes and Elliott W. Montroll

Institute for Physical Science and Technology
University of Maryland
College Park, MD 20742

INTRODUCTION

Mandelbrot [1] has discussed properties of the Weierstrass function

$$W(\omega,\gamma,t) = \sum_{n=0}^{\infty} \omega^n \exp(2\pi i \gamma^n t), \tag{1}$$

where $0 < \omega < 1$, $\gamma > 0$ and $-\infty < t < \infty$. Although the series is uniformly convergent for $-\infty < t < \infty$ and therefore represents a continuous function of t, it is nowhere differentiable if $\omega\gamma \geq 1$. For the frequency $f = \gamma^n$ ($n = ln f/ln\gamma$) there is a spectral line with energy ω^{2n}. The total energy in the set of frequencies exceeding $f = \gamma^n$ is $\omega^{2n}(1-\omega^2)^{-1} = f^{-2H}(1-\omega^2)^{-1}$, where $H = ln(\omega^{-1})/ln\gamma$ and $0 < H \leq 1$ in the non-differentiable regime. This form of the cumulative noise spectrum is similar to that of many physical noise processes.

THE WEIERSTRASS RANDOM WALK (WRW)

To gain further insight into the nature of the Weierstrass function, we use it to generate a random walk on a perfect one-dimensional lattice [2]. Our walk starts at the origin and makes jumps of ℓ sites according to the probability distribution

$$p(\ell) = \frac{a-1}{2a} \sum_{n=0}^{\infty} a^{-n}[\delta_{\ell,b^n} + \delta_{\ell,-b^n}], \tag{2}$$

where $a > 1$, $b > 1$ and b is integral. The walker makes about "a" jumps of unit length in a region, forming a cluster of points visited, before jumping a distance "b" to begin a new cluster. After about a^2 jumps occur, a jump of distance b^2 occurs, etc. While this argument is not precise, it shows that we have built a self-similar clustering property into $p(\ell)$, so that for a walk of a modest number of steps, a clustering of the sites visited may be expected. If $0 < ln a/ln b < 1$, then the walk is transient and distinguishable clusters remain as the number of steps taken tends to infinity, giving non-Gaussian behaviour.

We first note that

$$\hat{p}(k) \equiv \sum_{\ell} \exp(ik\ell)p(\ell) = \frac{a-1}{a} \sum_{n=0}^{\infty} a^{-n}\cos(b^n k) \tag{3}$$

is a multiple of the Weierstrass function, with $\omega = a^{-1}$ and $\gamma = b$. It is also related to the lacunary Taylor series [3]

$$S(z) = \sum_{n=0}^{\infty} c^n z^{b^n} \qquad (c > 0,\ b \text{ an integer} > 1). \tag{4}$$

We should expect interesting behaviour from eq (3) since S(z) cannot be analytically

continued beyond its circle of convergence $|z| = 1$ because it has a dense set of singular points on $|z| = 1$ at $z = \exp(2\pi ih/b^m)$, for all integers h and m.

Except for the initial position, $\hat{p}(k)$ contains all the information about the random walk, since

$$P_{n+1}(\ell) = \sum_{\ell'} P_n(\ell')p(\ell-\ell') \tag{5}$$

implies that

$$\hat{P}_n(k) = [\hat{p}(k)]^n \hat{P}_0(k), \tag{6}$$

where $P_n(\ell)$ is the probability of reaching site ℓ at the n-th step. If the mean squared displacement per step $\langle\ell^2\rangle = \Sigma\ell^2 p(\ell)$ is finite, then

$$\hat{p}(k) = 1 - \frac{1}{2}\langle\ell^2\rangle k^2 + o(k^2) \tag{7}$$

and (for large n) $P_n(\ell)$ will be a Gaussian centered around $\ell = 0$, with variance $n\langle\ell^2\rangle$, i.e. no clustering occurs.

For the WRW

$$\langle\ell^2\rangle = \frac{a-1}{a} \sum_{n=0}^{\infty} (b^2/a)^n = \infty \qquad \text{if } b^2 \geq a \tag{8}$$

and eq (7) no longer holds. The small k behaviour may be found using a Mellin transform technique or Poisson's summation formula [2] to be

$$\hat{p}(k) = 1 - |k|^H Q(|k|) + O(k^2) \tag{9}$$

if $0 < H = \ln a/\ln b < 2$, where $Q(|k|)$ is a periodic function of $\ln|k|$ with period $\ln b$. We note that H corresponds to the fractal dimension of the self-similar clusters ("a" sub-clusters per cluster, scaled down by a factor "b"). The smaller H is, the more separated will be the clusters.

A similar expression for $\hat{p}(k)$ without self-similar clustering may be obtained by combining two incommensurate WRW's, i.e.

$$\hat{p}(k) = \sum_{n=0}^{\infty} [\frac{a-1}{2a} a^{-n} \cos(b^n k) + \frac{\alpha-1}{2\alpha} \alpha^{-n} \cos(\beta^n k)], \tag{10}$$

with $H = \ln a/\ln b = \ln\alpha/\ln\beta$, but a and α and b and β incommensurate. The fractal dimension H does not contain sufficient information to characterize the clusters completely. We conjecture that for a higher dimensional generalization of eq (10) an infinite percolating cluster may exist.

If the WRW is generalized to continuous space [2], with allowed steps $\pm\Delta b^n$ (Δ a length scale and b no longer restricted to integral values), and the time interval between steps is τ, then a Lévy (stable) distribution of order H is obtained in the continuum limit $\Delta, \tau \to 0$ if $a-1 \sim \alpha\Delta$, $b-1 \sim \beta\Delta$ ($0 < \alpha < 2$) and $\Delta^H/\tau \sim$ constant. The WRW is a discrete analog of a Lévy flight [1]. An effective dimension for the WRW may be defined in terms of the small k behaviour of $\hat{p}(k)$ [2]. In one dimension,

$1 <$ effective dimension $= 3-H < 3$.

If the effective dimension exceeds 2, the walk is transient.

RENORMALIZATION GROUP TRANSFORMATIONS

Under a (real space) renormalization group transformation for the interaction parameters of a system $K' = K'(K)$, the free energy F satisfies the scaling equation [4]

$$F(K) = \ell^{-d}F(K') + G(K), \tag{11}$$

where d is the dimension, ℓ a decimation length and G an analytic function. In terms of a scaling field u, eq (11) becomes

$$F(u) = \ell^{-d}F(\lambda u) + G(u) \tag{12}$$

$$= \lim_{n\to\infty} [\ell^{-nd}F(\lambda^n u) + \sum_{j=0}^{n-1} \ell^{-jd}G(\lambda^j u)]. \tag{13}$$

It is usually assumed as a boundary condition that the first term in brackets on the right hand side of eq (13) vanishes and all singular behaviour resides in the sum involving G. Eq (12) admits singular behaviour of the form

$$F_{sing}(u) = A(u)|u|^{d/y}, \tag{14}$$

with

$$y = \ell n\lambda/\ell n\ell, \tag{15}$$

where

$$A(u) = A(\lambda u) = \sum_n A_n \exp(2\pi i n \ell nu/\ell n\lambda). \tag{16}$$

The eigenvalue λ is chosen to depend on ℓ so that the critical exponent will not. Only the $n = 0$ term in eq (16) is kept, since otherwise the free energy would depend on ℓ through $\lambda(\ell)$.

For the Weierstrass random walk

$$\hat{p}(k) = a^{-m}\hat{p}(b^m k) + \frac{a-1}{a}\sum_{j=0}^{m-1} a^{-j}\cos(b^j k), \tag{17}$$

in analogy with eq (13). When $m\to\infty$ the boundary condition in eq (13) holds. We have

$$\hat{p}_{sing}(k) = k^H Q(k), \tag{18}$$

where $Q(k) = Q(bk)$, in analogy with eqs (14) - (16), implying a geometrical interpretation for critical exponents. These matters will be discussed more fully elsewhere.

REFERENCES

[1] B. B. Mandelbrot, *Fractals: Form, Chance and Dimension* (W. H. Freeman, San Francisco,1977) p. 327.

[2] B. D. Hughes, M. F. Shlesinger, and E. W. Montroll, *Proc. Nat. Acad. Sci. USA* (in press).

[3] P. Dienes, *The Taylor Series*(Clarendon Press, Oxford, 1931) p. 227.

[4] Th. Niemeijer and J. M. J. van Leeuwen, in *Phase Transitions and Critical Phenomena*, vol. 6, Ed. C. Domb and M. S. Green (Academic Press, London, 1976).

TRANSPORT FLUCTUATIONS AROUND NON-EQUILIBRIUM STEADY STATES IN DISCRETE SYSTEMS.

Eckart Frehland

Universität Konstanz,
Fakultät für Physik,
Postfach 5560,
D-7750 Konstanz, FRG

We recently have developed a general theoretical approach to transport fluctuations around steady states in discrete transport systems [1,2]. The discrete description of transport seems to be adequate for systems with discontinuous structures and coupling between transport and other processes as e.g. chemical reactions. It has been especially successful for the theoretical description of complex ion transport mechanisms through biological membranes, e.g. carrier mediated transport [3] or hopping diffusion through narrow channels [4,5] (single-file transport), which additionally may assume different conductivity states (e.g. open and closed). Especially in those systems, where the transport process takes place in microscopic dimensions, the discrete description is more appropriate than continuous models. Applications to modern technological microstructures as e.g. highly integrated electronic circuits, might also be possible.

TRANSPORT IN DISCRETE SYSTEMS

The basic idea leading to the concept of transport in discrete systems is that the state of the system can be described by a discrete set of variables, each of which stands for a certain state. The time dependent probabilistic behaviour is given by a master equation for the probabilities of the different states

$$\frac{\partial P_\mu}{\partial t} = \sum_{\nu,\mu\neq\nu} (M_{\mu\nu} P_\nu - M_{\nu\mu} P_\mu) \qquad (1)$$

$M_{\mu\nu}$ $(\mu\neq\nu)$: transition rate per unit time.

The description of transport observables (e.g. of electric current J) is based on the transitions (fluxes) between different states of the system. Transport observables are defined as a linear mapping of the fluxes $\phi_{\mu\nu}$ between states μ and ν

$$T = \sum_{\substack{\mu,\nu \\ \mu\neq\nu}} \gamma_{\mu\nu}\, \phi_{\mu\nu} \qquad (2)$$

Equilibrium and nonequilibrium stationary states are distinguished by the validity or nonvalidity of detailed balance

$$\phi_{\mu\nu}^{\,s} = \phi_{\nu\mu}^{\,s} \quad \text{for all } \nu,\mu \quad (\phi_{\mu\nu}^{\,s}\text{: stationary fluxes}).$$

The underlying idea is that transport is determined by changes of the state of the system and a special transition $\nu \to \mu$ is coupled with a special, well defined contribution to T. Obviously, in principle there are no difficulties concerning the approximation of continuum models by discrete models. In an appropriate limit to an infinite number of states, the discrete systems go over into continuum systems. As a consequence the general results e.g. for the nonequilibrium transport fluctuations, can be applied also for continuum transport processes.

STEADY STATE TRANSPORT FLUCTUATIONS

By studying the time correlations between individual fluxes the autocorrelation function and spectral density $G_{\Delta T}(\omega)$ characterizing the steady state fluctuations of T can be derived [1], [2], [7]

$$G_{\Delta T}(\omega) = 2 \sum_{\mu,\nu=1}^{n} \gamma_{\mu\nu}^{\ 2} \ \phi_{\mu\nu}^{\ 2}$$

$$+ 4 \sum_{\kappa,\mu,\nu,\rho} \gamma_{\mu\nu} \ \gamma_{\kappa\rho} \ \phi_{\mu\nu}^{\ s} \ M_{\kappa\rho} \int_0^\infty \Omega_{\rho\mu}(t) \cos \omega t \, dt \qquad (3)$$

with the fundamental solutions $\Omega_{\rho\mu}(t)$ of (1)

$$\Omega_{\rho\mu}(t) = (P_\rho - P_\rho^{\ s}) \mid (P_\nu(t=0) = \delta_{\nu\mu}) \, .$$

Our general approach to transport noise has been used in order to investigate general properties of nonequilibrium fluctuations. It can be shown that the Nyquist or fluctuations dissipation theorem, by which at equilibrium the macroscopic admittance $Y(\omega)$ can be expressed in terms of fluctuation properties of the system, breaks down at nonequilibrium. The spectral density of steady state transport noise may be decomposed into one term containing the macroscopic admittance $Y(\omega)$ and a second term bilinear in the fluxes:

$$G_{\Delta T}(\omega) = 4 \, k_B T_a \, \mathrm{Re} \, Y(\omega)$$

$$+ 4 \sum_{\kappa,\nu,\mu,\rho} \gamma_{\mu\nu} \ \gamma_{\kappa\rho} \ \frac{1}{2} (\phi_{\mu\nu}^{\ s} - \phi_{\nu\mu}^{\ s}) \ M_{\kappa\rho} \int_0^\infty \Omega_{\rho\mu}(t) \cos \omega t \, dt \, . \qquad (5)$$

The second term is decisive for the occurrence of "excess noise". In the case of electric current fluctuations this typical nonequilibrium noise (1/f noise (?), $1/f^2$ noise, carrier noise) has been measured in different systems in agreement with the theory (e.g. [3]).

DIFFERENT BEHAVIOUR OF SCALAR AND VECTORIAL FLUXES

An apparent discrepancy between our result and a number of classical papers (e.g. [6]) showing possibilities of generalization of the Nyquist theorem to nonequilibrium states can be clarified in the following way: These papers are concerned with fluctuations of scalar fluxes, i.e. the time derivatives of the state variables, while the treatment of (directed) transport must be based on vectorial fluxes. It can be proven [7] that transport observables defined by (2) can be represented by (a linear combination of) the time derivatives of the state variables only in cases where the stationary value T^s of the transport observable vanishes, i.e. in equilibrium situations. Thus a main result of our contribution is the essentially different noise behaviour of scalar and vectorial quantities at nonequilibrium.

APPLICATIONS

Apart from these general aspects of nonequilibrium fluctuations, we have performed a number of model calculations in order to investigate the influence of the internal structure of transport systems (e.g. the potential profile for ionic hopping diffusion in membrane channels) on the properties of current noise. We mention the following two aspects:

a) the influence of nonequilibrium oscillatory transport on the current noise [5] and
b) the dependence of the intensity of transport noise on the transport parameters, e.g. special interactions.

In the latter case we have been able to show that under special conditions this dependence may be very strong. At the example of single-file transport through narrow pores we could demonstrate that the (low frequency) current noise is drastically reduced as a consequence of the ionic interactions within the channels in comparison with situations, where the ionic interactions may be neglected.

As one example numerical results are given in Fig. 1

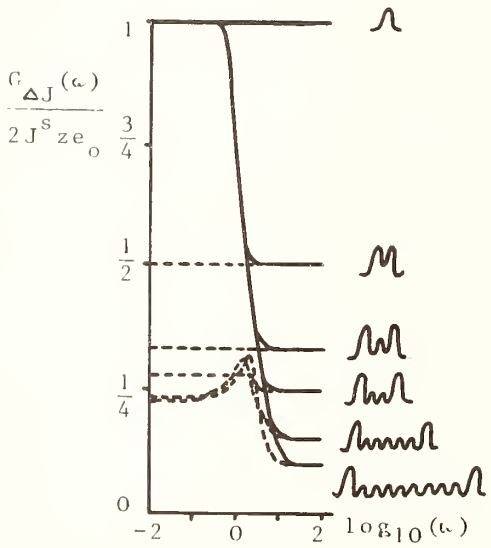

Fig. 1:

Current noise in ionic channels for high applied voltage. Dependence of noise intensity on ionic interactions and on the number of ionic binding sites within the channels.—: interactions neglected, ---:single file transport. At each line the assumed potential profiles within the channels are indicated. The minima indicate the number of ionic binding sites (0,1,2,3,6, and 9). The spectral density is given in units of $2J\,ze_o$, i.e. the expected low frequency shot noise. Frequency is given in arbitrary units.

It is assumed that a high voltage is applied to the membrane, so that ionic jumps mainly occur in one direction. In the low frequency region, i.e. for times long compared with the characteristic ion passage times through the channels, the resulting current noise is usual shot noise $2J\,ze_o$ (z: valency, e_o: elementary charge) in those cases where interactions can be neglected. This occurrence of shot noise at low frequencies for systems with negligible interactions can quite generally be derived from eq (3). In the single-file transport through narrow channels ionic interactions within the channels are taken into account in so far as each ionic binding site within the channel can be occupied by only one ion [5]. The results in Fig. 1 clearly show a dependence of (low frequency) noise intensity on the interactions and on the number of binding sites within the channels. Furthermore in the single-file case, a peaking of spectral density (resonance) comes in as a consequence of the damped oscillatory behaviour of transport (cf. [5]).

The possibilities of minimization of nonequilibrium transport noise should be further investigated. It will be interesting to see if and how biological transport systems during their evolution have reached states of minimum fluctuations. Furthermore technological application should be discussed.

REFERENCES

[1] E. Frehland, Biophysical Chemistry 8 (1978), 255; 10 (1979) 128.
[2] E. Frehland, Biophysical Chemistry 12 (1980); 63.
[3] H.-A. Kolb, E. Frehland, Biophysical Chemistry 12 (1980); 21.
[4] E. Frehland, Biophys. Struct. Mechanism 5 (1979); 91.
[5] E. Frehland, W. Stephan, Biochim. Biophys. Acta 553 (1979); 326.
[6] M. Lax, Rev. Mod. Phys. 32 (1960); 25.
[7] E. Frehland (1981, in preparation).

MULTIPLICATIVE NOISE IN STOCHASTIC DIFFERENTIAL EQUATIONS: A NUMERICAL STUDY

J. M. Sancho and M. San Miguel

Departamento Fisica Teorica, Universidad de Barcelona
Diagonal 647, Barcelona 28, Spain

S. Katz and J. D. Gunton

Physics Department, Temple University
Philadelphia, Pa. 19122 U.S.A.

Stochastic differential equations of the Langevin type for a finite set of variables are a common tool to study a variety of physical, chemical, and biological systems. Interest in these types of equations has recently increased because of their success in describing nonequilibrium situations and in particular nonequilibrium steady states. From a mathematical point of view, remarkable novel features appear when considering the case in which the random term depends on the variables of the equation ("multiplicative noise"). There are at least two main sources of such multiplicative noise. The first one is the usual procedure of adiabatic elimination of the fast variables of a system. The second one is modelling a fluctuating environment or a superimposed external fluctuation by letting a parameter in a phenomenological equation of motion become a random variable with prescribed statistics. This external noise situation has been considered experimentally in illuminated chemical reactions [1] , electrical circuits [2] , and liquid crystals [3] . The theoretical analysis of these situations predicts [4] a kind of nonequilibrium phase transition in which the external parameters governing the transition are the noise parameters.

In this paper we present some preliminary results of a numerical study of the effects of external multiplicative noise on such nonequilibrium phase transitions. The full details of our work will be presented elsewhere [5] . We consider a prototype equation of motion for a single variable q of the form

$$\dot{q} = q - q^3 + q\,\xi(t). \tag{1}$$

We have chosen dimensionless units such that the usual coefficients of the linear and cubic terms in this Ginzburg-Landau like model have been included in the noise term of (1). The random variable $\xi(t)$ is assumed to be Gaussian distributed with a zero mean value. We have considered two different models for the correlation $\langle \xi(t)\,\xi(t') \rangle$, the first being the so-called "colored noise" case in which

$$\langle \xi(t)\,\xi(t') \rangle = \frac{D}{\tau}\, e^{-|t-t'|/\tau}, \tag{2}$$

with two independent noise parameters, the correlation time τ and the intensity D. The second model is the conventional white noise limit of (2) in which $\tau \to 0$ with D finite so that the correlation becomes $2D\,\delta(t - t')$. We have investigated the dependence of the stationary state solution of (1) on the parameters D and τ. In particular, we have computed the stationary state probability distribution function $P_s(q)$ which would correspond to the steady state solution of the Fokker-Planck equation associated with (1). We have also computed the first and second moments, $\langle q \rangle$ and $\langle q^2 \rangle$, in this steady state. In addition to these time independent properties we have studied the time dependent correlation function in the steady state and its relaxation time T defined as

$$T = \int_0^\infty dt' \{\langle q_s(t+t')q_s(t)\rangle_s - \langle q_s(t)\rangle_s^2\} / \{\langle q_s^2(t)\rangle_s - \langle q_s(t)\rangle_s^2\}. \qquad (3)$$

This relaxation time is usually used to characterize "critical slowing down" in the dynamics of second order equilibrium phase transitions and is also of interest for nonequilibrium phase transitions.

Our results for the time independent properties for the white noise model are in very good agreement with the available exact analytical results, which gives us confidence in the algorithm used in our study. Our results for $\langle q \rangle$, $\langle q^2 \rangle$, $P_s(q)$, and T for the colored noise case show an interesting dependence on D and τ and are in qualitative agreement with an approximate analytical theory. We now turn to an explicit discussion of our investigation, beginning with the white noise model.

We first summarize the existing theory for the white noise model. The time independent properties in the stationary state are completely known, since the stationary solution $P_s(q)$ of the Markovian Fokker-Planck equation associated with (1) is exactly known [6]. Of particular interest to us is the position of the most probable value q_0 (the maximum of P_s) which is zero if $D \geq 1$ and is equal to $(1-D)^{\frac{1}{2}}$ if $D \leq 1$. Thus, although the moments of P_s show no significant change as a function D, P_s itself is qualitatively different for $D > 1$ and $D < 1$, since for $D < 1$ the most probable value q_0 becomes different from zero. If we identify q_0 as the macroscopic state [7], and define a transition point (or threshold value of D) as one for which the most probable value becomes different from zero [2, 7, 8, 9], then D = 1 is a transition point. There is no divergence of fluctuations in q at this point, however, since the moments of P_s remain finite.

The dynamical properties of (1) for the white noise case can be analyzed in terms of the eigenvalue problem associated with the Fokker-Planck equation for this model. The eigenvalue spectrum has been discussed in references [8] and [9] and has been shown to contain a continuous as well as a discrete part, with the discrete spectrum given by $\lambda_n = 4\ n\ D(1/2D - n)$, for $n \leq n_0$. Although there is a disagreement about the actual value of n_0, no discrete spectrum exists for $D > 1/2$. This means that the transition point D = 1 lies in the region where only the continuous spectrum exists. The description of the time dependence of the correlation function is therefore quite complicated near this threshold value. Thus we have studied this function in our computer simulation for both the white and colored noise models. Another important aspect of the discrete spectrum given above is that well below threshold, in the region where this discrete spectrum exists, the damping constants of the system decrease linearly with increasing noise intensity D. Hence the approach of the system to equilibrium should be slowed down by increasing D. Our numerical results for the relaxation time T, shown below in Figure 1, support this conclusion.

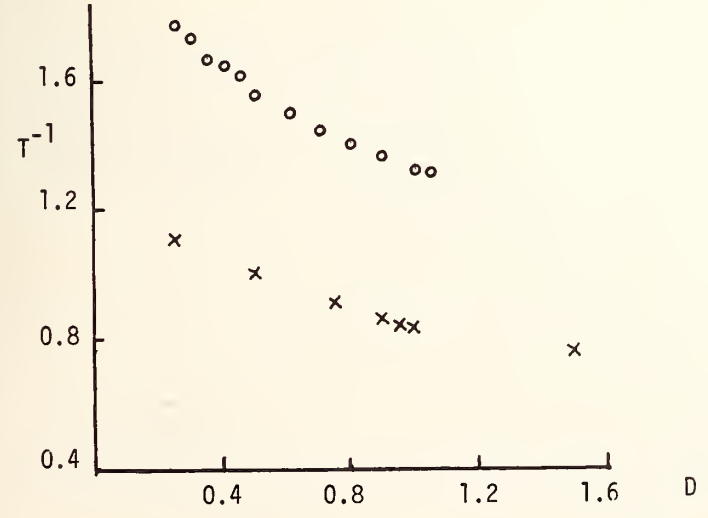

Fig. 1 Numerical results for the inverse relaxation time T^{-1} as a function of noise intensity D. The open circles correspond to white noise. The crosses correspond to a colored noise with $\tau = 1/3$.

It is clear that for the white noise case T increases monotonically with D, so that there is indeed a slowing down with increasing D in the entire range of values we have explored. This is in agreement with the results for the discrete spectrum. Our analysis shows, however, that the slowing down persists in the domain in which only a continuous spectrum exists. It should also be noted that it appears that T^{-1} decreases more slowly than as a linear function of D for larger D. If so, this would be qualitatively different from the linear behavior obtained from the discrete spectrum for small D. Finally we note that we observe no "critical slowing down" ($T \to \infty$) as $D \to 1$.

One issue which we leave for future discussion [5] is the relationship between our computer studies of (1) and the closely related experimental studies by Kabashima et al. [2] on a parametric oscillator under the influence of a wide band external noise.

We now turn to the more difficult theoretical problem of colored noise. Here there is an approximate theory [5],[10] to compare with, which is based on a first order expansion in the correlation time τ. We begin by displaying our results for the mean values, $\langle q \rangle$ and $\langle q^2 \rangle$ in Table 1.

Table 1

D	τ	$\langle q \rangle$	$\langle q^2 \rangle$	$(\langle q \rangle - \langle q \rangle_0)/q$	$\frac{\langle q^2 \rangle - \langle q^2 \rangle_0}{\langle q^2 \rangle_0}$	$\frac{D\tau}{2}$	$\frac{D\tau_R}{2}$
0.25	1/18	0.9458	-	0.0063	-	0.0069	0.0062
1.5	1/18	0.7545	-	0.035	-	0.042	0.038
0.5	1/3	0.9280	1.005	0.0472	0.0047	0.083	0.05
0.75	1/3	0.8946	1.003	0.066	0.0028	0.125	0.075
0.90	1/3	0.8734	0.9988	0.095	-0.0012	0.15	0.09
1.5	1/3	0.8113	1.011	0.113	0.011	0.25	0.15
0.90	1/2.5	0.8836	1.006	0.0856	0.006	0.18	0.100
1.50	1/2.5	0.8232	1.007	0.129	0.007	0.30	0.167
2.00	1/2.5	0.7869	1.0147	0.164	0.0147	0.40	0.222

Here $\langle q^n \rangle_0$ denotes the white noise value. The last two columns show two theoretical predictions based on the first order τ analysis for the value of $\{\langle q \rangle - \langle q \rangle_0\}/\langle q \rangle_0$. As can be seen, the better fit with our data is obtained using a phenomenological "renormalized" correlation time $\tau_R = \tau/(1+2\tau)$. Figure 2 shows the dependence of $\langle q \rangle$ on D for fixed $\tau = 1/3$. There is a clear difference between the white and colored noise results. In addition the first order theory for the colored noise (solid line) seems to qualitatively explain our results, although there is clearly a need for a more accurate theory.

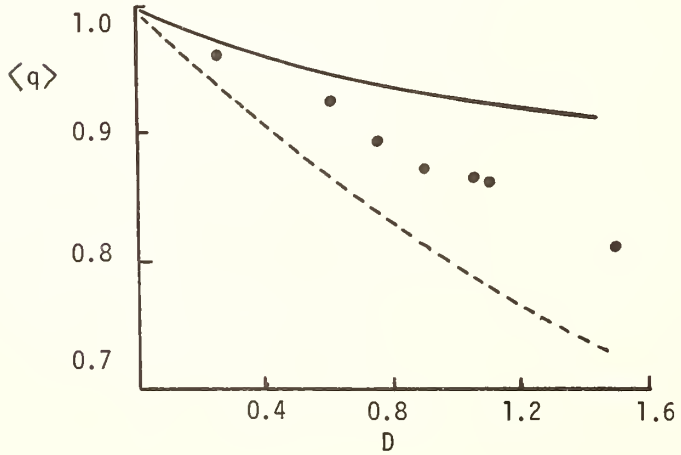

Fig. 2 The first moment q as a function of D for $\tau = 1/3$. The full circles are the numerical results. The solid and dashed lines are the theoretical and white noise predictions, respectively.

Another prediction of the existing theory is that $\langle q^2 \rangle - \langle q^2 \rangle_o$ should be independent of both D and τ. As can be seen from Table 1, this seems to be confirmed by our results.

An interesting qualitative feature that emerges from our study is the development of a new "phase transition" due to the colored noise. This can be seen from our results for $P_s(q)$ obtained for different values of D and τ. In Figure 3 below we show a typical curve for $P_s(q)$. This shows a distinct and interesting difference between the white noise and colored case for D = 1.5. The "colored noise" model for this value of τ = (1/2.1) shows a new phase transition not seen in the white noise case, at least in the sense of a qualitatively different $P_s(q)$ vis-a-vis two extrema. The significance of this transition is not completely clear, but it is in qualitative agreement with the first order τ theory, as discussed in [5]. The effect of τ is less significant in other regions of the (D,τ) domain, with the results for $P_s(q)$ being very similar to the white noise distribution function. Finally, we note that the effect of colored noise can also be seen in dynamical properties such as the relaxation time. In Figure 1 we see that there is a slowing down associated with increasing noise intensity D for fixed τ. In addition our preliminary results indicate that T increases with τ for fixed D, although more extensive investigation is needed of this particular point.

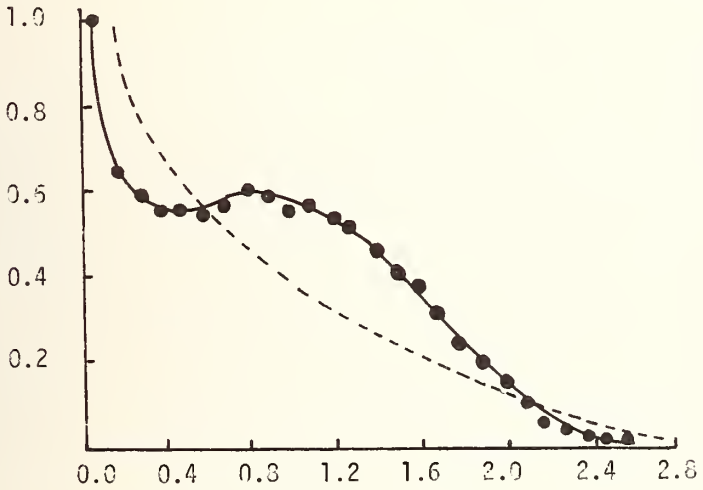

Fig. 3 The steady state distribution function $P_s(q)$,(full circles) as a function of q, for D = 1.5, τ = 1/2.1. The dashed line shows $P_s(q)$ for the white noise model for D = 1.5

References

1. P. deKepper and W. Horsthemke, C. R. Acad. Sci. Ser. C287, 251 (1978)
2. S. Kabashima, S. Kogure, T. Kawakubo and T. Okada, J. Appl. Phys. 50, 6296 (1979)
3. S. Kai, T. Kai, M. Takata and K. Hirakawa, J. Phys. Soc. (Japan) 47, 1379 (1979)
4. W. Horsthemke in Dynamics of Synergetic Systems, p 67, ed. H. Haken, Springer Verlag (Berlin, Heidelberg, New York 1980)
5. J. M. Sancho, M. San Miguel, S. Katz and J. D. Gunton (unpublished)
6. R. L. Stratonovich, Topics in the Theory of Random Noise, Vol. 2, Gordon and Breach (New York 1967)
7. W. Horsthemke in Stochastic Nonlinear Systems in Physics, Chemistry and Biology, Synergetic Series, Springer Verlag (Berlin 1981)
8. A. Schenzle and H. Brand, Phys. Rev. A20, 1628 (1979)
9. M. Suzuki, "Fluctuations and Relaxation in Stochastic Systems" preprint (1980)
10. J. M. Sancho and M. San Miguel, Z. Phys. B36, 357 (1980)

Acknowledgements

Work supported by grants from the National Science Foundation, the U.S.-Spanish Committee for Scientific Cooperation and the Research Corporation.

LEVEL-CROSSING INTERVALS OF A GAUSSIAN NOISE

Tadashi Mimaki and Hiroshi Sato

University of Electro-Communications
Chofu, Tokyo, Japan 182

Masami Tanabe

Kumamoto Radio Technical College
Kikuchi-Gun, Kumamoto, Japan 861-11

INTRODUCTION

The present paper treats the distribution density $P_{n+}(\tau,I)$ of the sum of (n+1) successive level-crossing interval lengths of a Gaussian process, where τ and I denote time length and crossing level, respectively. The suffix "+" means that the intervals start at an upcrossing, i.e. crossing with positive slope. This density is not determined yet in analytical form. Therefore, considerable effort has been directed in the past toward the numerical determination of it both theoretically and empirically [1-9]. It was found that for Gaussian process having eighth order Butterworth spectrum the densities $P_{0+}(\tau,I)$, $P_{1+}(\tau,I)$ and $P_{2+}(\tau,I)$ show a plural number of peaks if the crossing level I is negative [10]. The number and height of the peaks depend on the spectrum bandwidth and on the crossing level I. The first peak is not necessarily the highest peak. Occasionally even $P_{3+}(\tau,I)$, $P_{4+}(\tau,I)$, and $P_{5+}(\tau,I)$ show several peaks, too. The dependence of this property, called multi-peak property, on the spectrum bandwidth is not as strong as that of the correlation property between the level-crossing intervals, which changes remarkably with the spectra of low-pass, broad and narrow band-pass types. The multi-peak property appears for all of the spectrum bandwidths.

In order to explain the multi-peak property we introduced the random excursion model, which was originally proposed by Sato et al. [11] to interpret the behaviour of the variance of the number of the upcrossings in a long fixed period. Since the model treats only upcrossings, we restrict ourselves to the density $P_{n+}(\tau,I)$ with odd n in the present paper. It is found that the distribution density $P_{1+}(\tau,I)$ of arbitrary crossing level I itself can approximately be expressed in terms of $P_{n+}(\tau,I_0)$ at a reference level I_0 by utilizing this model. The expression is compared with the experimental data. Although the model is very simple, the agreement is surprisingly good and the multi-peak property of the level-crossing intervals is explained excellently at least for the low-pass case.

INTERVAL DISTRIBUTION

At first we introduce the notion of random excursion model: If only the part of the waveform of a random process that lies above an arbitrary reference level I_0 is observed, that part is seen to consist of a succession of excursions, where an excursion means a part of the sample function that starts from the level I_0 and stays above it until it finally returns to the original level I_0. Now the following assumptions will be made:
(a) A Gaussian process consists of a succession of random excursions, each

of which hasn't any minimum; (b) For any level I ($>I_0$) an excursion is said to be in state zero or one, according to whether the excursion attains the level I or not. The change of the state of the successive excursion obeys a simple Markov law. Let q and r be the transition probabilities from zero to one and from one to zero, respectively. Let p be the probability that an excursion reaches the level I. Then we have a relation, pq=r(1-p). If the heights of the successive excursions are mutually independent, q=1-p and r=p. For a Gaussian process and $I_0=0$, then $p=\exp(-I^2/2)$; (c) The interval distribution at reference level I_0 is independent of the distribution of the heights of excursions.

Let $f_n(\tau)$ be the distribution density of the sum of the lengths of successive n intervals of level I_0 defined only by upcrossings. Since the distribution density $f_n(\tau)$ of n intervals contributes to the distribution density $P_{1+}(\tau,I)$ of level I, only when the intermediate (n-1) excursions don't attain the level I and finally n-th excursion attains the level I, we obtain,

$$P_{1+}(\tau,I)=(1-q)f_1(\tau)+qr\sum_{n=2}^{\infty}(1-r)^{n-2}f_n(\tau). \tag{1}$$

This expression indicates that the distribution density $P_{1+}(\tau,I)$ of arbitrary level I can be given by the distribution densities $f_1(\tau)$, $f_2(\tau)$, $f_3(\tau)$,...at reference level I_0. The closeness of the approximation depends on the validity of the above assumptions. Let $C(\xi)$ and $F_n(\xi)$ be the characteristic functions of $P_{1+}(\tau,I)$ and $f_n(\tau)$, respectively. We have from eq (1),

$$C(\xi)=E[e^{i\xi\tau}]=(1-q)F_1(\xi)+qr\sum_{n=2}^{\infty}(1-r)^{n-2}F_n(\xi), \tag{2}$$

where E indicates the expectation. If the crossing intervals at reference level I_0 are mutually independent, we obtain,

$$f_n(\tau)=f_1(\tau)*f_1(\tau)*\ldots*f_1(\tau) \text{ or } F_n(\xi)=F_1^n(\xi),$$

where "*" means the convolution process. Thus, eq (2) is reduced to

$$C(\xi)=F_1(\xi)[1-q+qrF_1(\xi)\{1-\bar{r}F_1(\xi)\}^{-1}], \tag{3}$$

where $\bar{r}=1-r$. Furthermore, if the heights of the excursions are mutually independent, we obtain q=1-p and r=p, with the result that

$$P_{1+}(\tau,I)=\sum_{n=1}^{\infty}p(1-p)^{n-1}f_n(\tau), \tag{4}$$

and correspondingly

$$C(\xi)=\sum_{n=1}^{\infty}p(1-p)^{n-1}F_1(\xi)=pF_1(\xi)[1-\bar{p}F_1(\xi)]^{-1}, \tag{5}$$

where $\bar{p}=1-p$. According to above expression, the distribution density $P_{1+}(\tau,I)$ of arbitrary level I is given only by the distribution density $f_1(\tau)$ of the single interval at reference level I_0.

Heretofore, three independence assumptions, that is, interval independence, excursion independence, and independence between interval and excursion sequences, are individually treated. However, in the actual situation they may appear in a mutually related way. The present paper mainly concerns itself with the case where they are simultaneously valid. should be noted that the above expressions can be applied not only to the Gaussian process, but also to most of the general continuous stationary random processes.

VARIANCE OF LEVEL-CROSSING INTERVALS

Let μ_0, σ_0^2 and κ_i^0 be the expected length, variance of intervals and correlation coefficient between zeroth and i-th crossing intervals at reference level I_0, respectively. Also, let μ, σ^2 and κ_i be the corresponding quantities at level I. Now, we expand $F_n(\xi)$ in power series in ξ, substitute it into eqs (2), (3), and (5), and then compare it term by term with an expression,

$$C(\xi)=1+iE(\tau)\xi-E(\tau^2)\xi^2/2+\cdots\cdots\cdots$$

From term of ξ, we obtain

$$E(\tau)=\mu=\mu_0/p \ . \tag{6}$$

From term of ξ^2, we obtain the following expressions:

From eq (2);
$$E(\tau^2)=\left(\frac{1}{p}+\frac{2q}{r^2}\right)\mu_0^2+\left(\frac{1}{p}+\frac{2\bar{p}}{p}\sum_{i=1}^{\infty}\kappa_i^0 r^{i-1}\right)\sigma_0^2. \tag{7}$$

$$\sigma^2=E(\tau^2)-E^2(\tau)=\frac{1}{p}\left[\bar{p}\left(\frac{2}{r}-\frac{1}{p}\right)\mu_0^2+\left\{1+2\bar{p}\sum_{i=1}^{\infty}\kappa_i^0 r^{i-1}\right\}\sigma_0^2\right]. \tag{8}$$

From eq (3);
$$E(\tau^2)=\left(\frac{1}{p}+\frac{2q}{r^2}\right)\mu_0^2+\frac{1}{p}\sigma_0^2. \tag{9}$$

$$\sigma^2=\frac{1}{p}\left[\bar{p}\left(\frac{2}{r}-\frac{1}{p}\right)\mu_0^2+\sigma_0^2\right]. \tag{10}$$

From eq (5);
$$E(\tau^2)=\frac{1}{p}\left[\frac{2-p}{p}\mu_0^2+\sigma_0^2\right]. \tag{11}$$

$$\sigma^2=\frac{1}{p}\left[\frac{\bar{p}}{p}\mu_0^2+\sigma_0^2\right]. \tag{12}$$

The equation (12) shows that the quntity $p^2\sigma^2$ is linear in p. The equation (10) can also be obtained from the expression of the variance of the number of the upcrossing points during constant time period.

COMPARISON WITH EXPERIMENT

Figures 1(a) and (b) show the examples of the calculated results based on eq (4) together with the experimental densities $P_{1+}(\tau,I)$, where only three densities $f_1(\tau)$, $f_2(\tau)$, and $f_3(\tau)$ experimentally determined at zero level are used. The power spectrum of the original Gaussian process is 8-th order Butterworth low-pass. The crossing levels I are 1.0 in Fig. 1(a) and 2.23 in Fig. 1(b), respectively. Although the model is very simple, the agreement is surprisingly good and the multi-peak property of the level-crossing intervals is explained excellently at least for the low-pass case.

The following table shows the comparison of the calculated result based on eq (12) with the experimental data for the Gaussian processes having 8-th order Butterworth low-pass and band-pass spectra. Since the

coincidence between theoretical and experimental values is excellent for low-pass spectrum, the level-crossing intervals deem to be mutually independent for this spectrum. For band-pass spectrum, the coincidence is poor, except for the high crossing level.

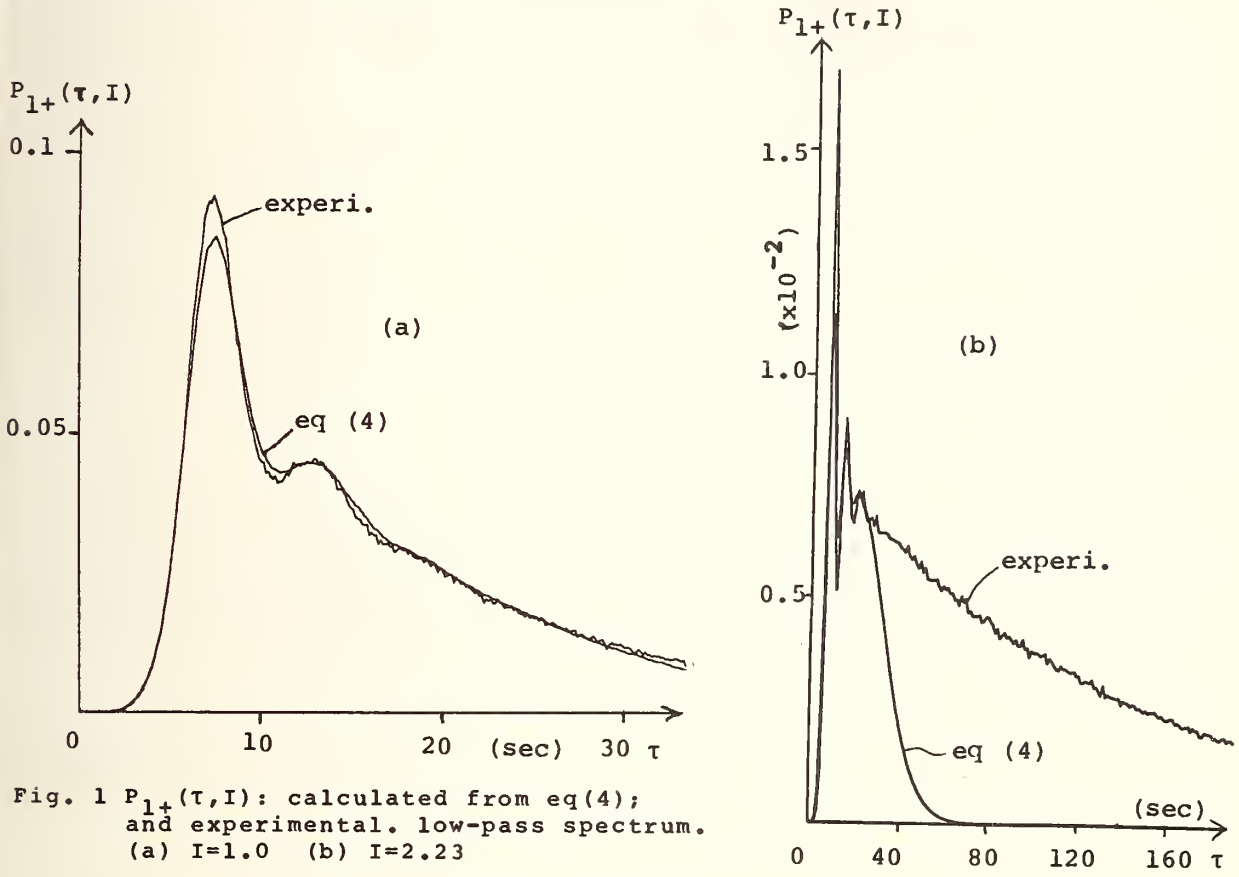

Fig. 1 $P_{1+}(\tau,I)$: calculated from eq(4); and experimental. low-pass spectrum. (a) I=1.0 (b) I=2.23

f_1/f_2	I	p	μ theo.	μ experi.	σ^2 eq (12)	σ^2 experi.
0.0	1.0	0.606	17.5	17.7	168	165
	2.0	0.135	78.3	77.5	5690	5641
	3.0	0.011	954	970	9.40×10^5	9.33×10^5
0.1	1.0	0.606	16.6	16.8	146	105
	2.0	0.135	74.4	75.8	5108	4387
	3.0	0.011	905	930	8.48×10^5	8.37×10^5

Table 1

Comparison of σ^2 calculated from eq (12) with experimental σ^2.

REFERENCES

[1] S. O. Rice, BSTJ 23, 282 (1944); 24, 46 (1945).
[2] M. S. Longuet-Higgins, Phil. Trans. Roy. Soc. A254, 557 (1962).
[3] J. A. McFadden, IRE Trans. IT IT-2, 146 (1956); IT-4, 14 (1958).
[4] D. Wolf and H. Brehm, AEU 27, 477 (1973).
[5] A. J. Rainal, IRE Trans. IT IT-8, 372 (1962).
[6] T. Mimaki, JAP 44, 477 (1973).
[7] S. O. Rice, BSTJ 37, 581 (1958).
[8] H. Brehm and D. Wolf, AEU 29, 415 (1975).
[9] T. Mimaki and T. Munakata, IEEE Trans. IT IT-24, 515 (1978).
[10] T. Mimaki, M. Tanabe and D. Wolf, to appear on IEEE Trans. on IT (1981).
[11] H. Sato and M. Tanabe, IEEE Trans. on IT IT-25, 127 (1979).

STUDY OF DISORDERED STRUCTURES AS A SPATIAL NOISE PROBLEM

M. Celasco*, P. Mazzetti** and A. Stepanescu

Istituto Elettrotecnico Nazionale Galileo Ferraris
Gruppo Nazionale Struttura della Materia - U.R. 24 - Torino (Italy)

INTRODUCTION

The technique used to characterize noises can be conveniently applied to the study of disordered structures constituted by the superposition of spatially distributed elementary events, representing some local property of a physical system.

In the case of three-dimensional structures of atoms or molecules, the type of order (long-range or short-range order, type of crystallographic order, range of directional order etc.) is essential in determining many properties of the system, like electrical and magnetic properties, X-rays, and neutron scattering, etc. In many cases a direct physical meaning can be associated to the three-dimensional power spectrum. For instance, if in an atomic structure the elementary events considered are the atomic form factors, then the power spectrum $\phi(\vec{k})$ describes the scattered intensity with wave vector $\vec{k}'=\vec{k}_0+\vec{k}$ when an electromagnetic radiation with wave vector $\vec{k}_0$ incides on the structure. Another important case is the one where the elementary events are localized fields or currents, like fluxons in superconductors or local eddy currents due to Barkhausen jumps in ferromagnets: the power spectrum can then be used to describe the excess energy or power loss in the system in relation to the spatial distribution of such events.

More generally, the whole electronic structure of a condensed body may be visualized in terms of the scattering properties towards the plane wave components of the electronic wave function in a very similar way as for X-ray scattering. In the following, to make the language easier, we shall make reference to a system whose elementary events are simply called "atoms" and shall use the same terminology found in X-ray scattering problems from atomic systems.

The description of a partially disordered three-dimensional structure is in general a difficult problem, which involves the introduction of the local type of crystallographic order (b.c.c., f.c.c., h.c.p. ...), its range, the range of the directional order, and the distribution functions describing the displacements of the neighbours of each particular atom or elementary event in the structure. Two different types of approach to the problem are found in literature. The first one [1,2] makes use of computer simulated structures, on which relevant statistical quantities as the autocorrelation function and the structure factor, are numerically calculated. This approach is particularly suitable to explain the experimental results about X-ray scattering for amorphous substances, but has the big disadvantage that it does not allow to obtain analytical expression describing these quantities in terms of the elements characterizing the structure from the statistical point of view. The second type of approach starts from a perfectly ordered structure and introduces the disorder through an external perturbation of the atom positions characterized by a given fluctuation spectrum [3]. This type of approach is suitable to describe, for instance, defects like dislocations, vacancies and interstitials in real crystals, but does not allow to represent the structure from a microscopic point of view introducing atom pairs correlations effects.

The present approach has the advantage that the results are expressed in terms of very general analytical expressions which can be used to describe the scattering properties of structures having any type of local crystallographic order. Further, the range of local order is described in terms of distribution functions taking into account the interactions between nearest neighbour pairs, and thus they can be given some clear physical meaning.

---

* Permanent address: Istituto di Fisica Generale dell'Università di Torino.

** Permanent address: Istituto di Fisica Sperimentale del Politecnico di Torino.

MODEL DESCRIPTION AND POWER SPECTRUM CALCULATION

The starting point is a perfectly ordered lattice having the crystallographic type of order characterizing the short-range order of the system under study.

The disorder is introduced by displacing the atoms from their crystallographic positions through three distribution functions, which give the probability for the position of the nearest neighbour atoms of each atom along the three axes of a primitive reference system. The whole structure is self-consistently described, from the statistical point of view, by a convolution technique, which allows to obtain the probability distribution for the relative position of any atom in the structure with respect to any other atom chosen as the origin of a reference system bound to the local crystallographic order.

Thus, choosing any atom A in the structure and introducing a local primitive reference system with origin in A and consistent with the local crystallographic type of order, the probability distribution for the position vector $\vec{r}_B$ of any other atom B, which in a perfectly ordered structure would have crystallographic indexes l, m, n, is given by

$$p(\vec{r}_B) = \underbrace{p_a(\vec{r}) * p_a(\vec{r}) * \ldots * p_a(\vec{r})}_{l \text{ terms}} * \underbrace{p_b(\vec{r}) * p_b(\vec{r}) * \ldots * p_b(\vec{r})}_{m \text{ terms}} * \underbrace{p_c(\vec{r}) * p_c(\vec{r}) * \ldots * p_c(\vec{r})}_{n \text{ terms}} \qquad (1)$$

where * means convolution product:

$$p_a(\vec{r}) * p_a(\vec{r}) \equiv \int p_a(\vec{r})\, p_a(\vec{r}-\vec{r}_B)\, d\vec{r} \qquad (2)$$

and $p_a(\vec{r})$, $p_b(\vec{r})$, $p_c(\vec{r})$ are the three distribution functions representing the probability for the position vectors of the nearest neighbour atoms of A which, in a perfectly ordered lattice, would be displaced with respect to A of the primitive vectors $\vec{a}$, $\vec{b}$, $\vec{c}$ respectively.

Starting from eq.(1) it is possible to represent in terms of these local distribution functions the autocorrelation function $\Psi(\vec{\tau})$ of the whole structure. Details of calculations are given in another paper [4]. It is important to note here that upon Fourier transform of $\Psi(\vec{\tau})$, the convolution products become ordinary products, and thus the expression of the power spectrum $\phi(\vec{r})$ assumes a rather simple analytical form:

$$\phi(\vec{r}) = \frac{N}{8\pi^3} \left\{ \left[\langle |S(\vec{k})|^2 \rangle - |\langle S(\vec{k}) \rangle|^2 \right] + |\langle S(\vec{k}) \rangle|^2 \left[(1+2\theta_a)\cdot(1+2\theta_b)\cdot(1+2\theta_c) \right] \right\}, \qquad (3)$$

where N represents the average number of atoms per unit volume and

$$\theta_i(\vec{k}) = R_e \left(\frac{Z_i(\vec{k})}{1-Z_i(\vec{k})} \right) \; ; \quad Z_i(\vec{k}) = \int p_i(\vec{r}) \exp(i\, \vec{k}\cdot\vec{r})\, d\vec{r} \qquad [i = a, b, c] \, . \qquad (4)$$

In eq.(4) R_e means the real part of the expression within brackets.

Equation (2) has singular points when one, two, or all of the three distribution functions $p_i(r)$ are Dirac δ-functions. This corresponds to the case where there is long range order in one, two, or three dimensions respectively, and consequently the power spectrum $\phi(\vec{k})$ has a line component as well as a continuous one. The line positions are given by the equations

$$Z_i(\vec{k}) = 1 \qquad [i = a, b, c] \, , \qquad (5)$$

while the line intensities can be calculated by using the mathematical technique described in paper [5], and are simply given by

$$A_{l,m,n} = N \, |\langle S(k_{l,m,n}) \rangle| , \qquad (6)$$

where $\vec{k}_{l,m,n}$ is a k-vector satisfying eq.(5). Obviously, when all three $p_i(\vec{r})$ distribution functions are Dirac δ-functions and all the atomic form factors are identical, the well known Bragg result for X-ray scattering from crystals is obtained.

When the primitive axes are not an orthogonal set, it is convenient to use contravariant coordinates for r-vectors and covariant coordinates for k-vectors (*). In this case

---

(*) This is equivalent, but more convenient, than the introduction of a reciprocal space for k-vectors, as is usually done in X-ray scattering textbooks.

eq. (4) simplifies to

$$Z_a(\vec{k}) = \exp(k_a\, a)\, Q_a(\vec{k}) . \qquad (7)$$

Similar equations are true for $Z_b(\vec{k})$ and $Z_c(\vec{k})$.

In eq.(7) k_a is the covariant coordinate of $\vec{k}$ along the a-axis of the reference system, a the length of the primitive vector $\vec{a}$ and $Q_a(\vec{k})$ the three-dimensional Fourier transform of the distribution function $q_a(\vec{r})$, defined in terms of $p_a(\vec{r})$ by the equations:

$$q_i(\vec{r}') = p_i(\vec{a}+\vec{r}') \qquad [i = a, b, c] . \qquad (8)$$

These functions give the probability density for the displacements $\vec{r}'$, of the nearest neighbours of each atom with respect to the positions they should have in a perfectly ordered lattice having the chosen atom in one of its reticular points.

Equation (3) gives the power spectrum for a structure which may have short-range as well as long-range crystallographic order, but on which a long-range directional order is always assumed. This means that the crystallographic axes associated with the local type of order are the same in every point of the structure instead of being randomly rotated, as it is expected in isotropic disordered structures. To describe such types of structures it is thus necessary to perform a spectrum averaging over a sphere S of a radius k:

$$\phi_0(k) = \frac{1}{4\pi k^2} \iint_S \phi(\vec{k})\, d\vec{k} . \qquad (9)$$

For atomic systems, the three-dimensional Fourier transform of $\phi_0(k)$ is directly related to the pair distribution function (P.D.F.). This quantity represents the three-dimensional autocorrelation function of the system in the case where the atomic form factor is a Dirac δ-function.

In the case where some sort of anisotropy concerning the directional order exists in the structure, as is the case for many disordered structures, averaging should be made by introducing a suitable distribution function in eq.(9). Simplified expression for power spectrum and autocorrelation function calculations in the case of directional isotropy, when the distribution fractions $q_i(\vec{r}')$ are spherical gaussians, are given in [4]. In the same paper some extensions and generalizations of eq.(3), taking into account the symmetry of the autocorrelation function, are also given. There we report few typical results concerning the pair distribution function of amorphous structures with b.c.c. and f.c.c. short-range order. The parameter H represents the inverse of the "correlation length" characterizing the local order in terms of the side a of the conventional cells of the b.c.c. and f.c.c. lattices (see figure 1). For comparison, some results obtained by Ichikawa [6] by using numerical calculations in a microcrystallite model, are reported in figure 2. It is seen that what he calls "heavily distorted structure" corresponds closely to a short-range order having a "correlation length" of the order of 6-7 times the interatomic distance a. Figure 3 shows the reduced interference function $I(k) = \phi_0(k) / |\langle S_0(k) \rangle|^2 \cdot N$ for a f.c.c. structure with H=0.05. An interesting aspect of this quantity is its typical behaviour in the low k range. In the case of a completely disordered structure with point-like atoms, I(k) is a constant equal to 1, while in a perfectly ordered structure it should be zero until the appearance of the first peak. In the case of short-range order it is seen that I(k) remains lower than 1 (i.e. the structure scatters less than a completely disordered one) from k = 0 up to the first peak, but for very small k values there is also a peak which a direct analysis through eq.(3) and eq.(9) shows to be of the type $I(k) \propto k^{-2}$.

This aspect of I(k), which is generally not found in other types of calculations where a large but finite number of atoms are considered, is very important both for what concerns the scattering of long wavelength radiations from atomic systems and, in the case of other types of physical systems, like ferromagnetics and superconductors, for the computation of the excess power loss during cycling. It is worth noting that such a behaviour of I(k) is identical with the one expected for systems undergoing an order-disorder phase transition.

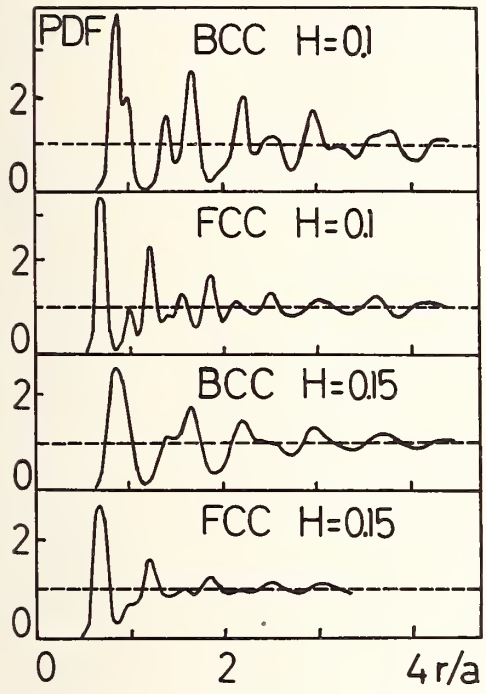

Figure 1 - Pair distribution function for isotropically disordered structures having a B.C.C. and F.C.C. short-range order. H represents the inverse of the correlation length expressed in terms of the conventional cell side a.

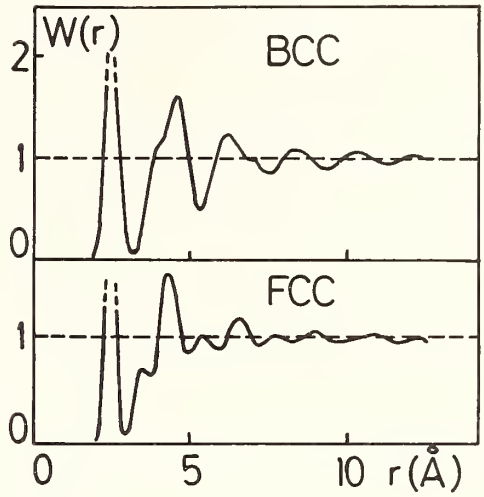

Figure 2 - Some results obtained by Ichikawa [6] for heavily distorted structures having a B.C.C. and a F.C.C. local order (Microcrystallite model).

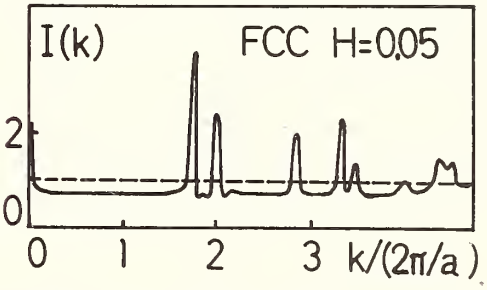

Figure 3 - Reduced interference function for a isotropically disordered structure having a F.C.C. short-range order, computed through eq.(3) H=.05 corresponds to a correlation length of 20 a.

REFERENCES

[1] G. S. Cargill III, *Solid State Phys.*, 30, 227 (1975).

[2] J. Graczyk and P. Chaudhari, *Phys. Stat. Sol. B.*, 58, 501 (1973), J. Non-Crist. Solids 17, 299 (1975).

[3] M. A. Krivoglas, *"Theorie de la diffusion des rayons X et des neutrons thermiques par les cristaux reels"*, Maddon et Cie (1969).

[4] M. Celasco, P. Mazzetti, A. Stepanescu, *"Power spectrum and scattering properties of three-dimensional disordered systems having a variable degree of short-range order"* (to be published).

[5] P. Mazzetti, C. Oldano, *J. Appl. Phys.*, 49, 5357 (1978).

[6] I. Ichikawa, *Phys. Stat. Sol. A*, 19, 707 (1973).

ON THE THEORY OF AMBIENT ACOUSTIC NOISE IN THE SHALLOW OCEAN

Michael J. Buckingham

Radio and Navigation Department
Royal Aircraft Establishment
Farnborough, Hampshire GU14 6TD
England

INTRODUCTION

In the present context, 'shallow' water is defined as that part of the ocean which overlies the continental shelf and shows a depth of 200 m or less. In general, acoustic propagation in shallow-water channels is a complicated phenomenon due to the proximity of the boundaries, the nature of the bottom, and the variation of the speed of sound with depth. The usual approach is to treat the channel as a waveguide in which the sound field is a sum of normal modes. Considerable simplification is achieved if isovelocity (*ie* sound-speed independent of depth) water is assumed, and if the boundaries are treated as plane and parallel. Then the Fourier transform of the velocity potential at depth z due to a source at range r and depth z_0 is

$$\psi(z,z_0 r) \simeq \frac{A \exp(jkr)}{r^{\frac{1}{2}}} \sum_{m=1}^{M} \sin\left(\frac{m\pi z_0}{h}\right) \sin\left(\frac{m\pi z}{h}\right) , \qquad (1)$$

where A is a constant independent of r, z and z_0, h is the depth of the channel, m is the mode number, M is the total number of modes the channel can support at angular frequency ω, and $k = \omega/c$ is the wave number (c = speed of sound in the channel). For simplicity, bottom losses have been ignored in this expression, the bottom interface has been treated as a pressure-release boundary, and a factor (equal to the reciprocal of the square root of the horizontal wave number), which is essentially constant over the grazing angles of interest, has been omitted. The total number of modes in the channel is

$$M = \left(\frac{\omega h}{\pi c}\right) \sin \alpha_c , \qquad (2)$$

where α_c is the critical grazing angle of the bottom.

Equations (1) and (2) are the basis for the model of wind-generated noise in the shallow ocean described below. A full analysis of the problem is given in Ref [1]. The model is valid for frequencies up to about 1 kHz. At higher frequencies, the acoustic wavelength is comparable with the surface wave height, surface scattering is then important and eq (1) is no longer a reasonable approximation.

THE NOISE MODEL

The source of wind-generated noise in the ocean can be modelled as a very large number of independent, impulsive monopoles located in a plane immediately below the surface [1,2]. These sources give rise to a continuous noise field and a modal noise field. The former is

associated with near-field sources, and the latter with the very large number of far field sources. Assuming low losses in the bottom, the modal field will dominate and the continuous-radiation component of the noise field can be safely neglected. Only the modal contribution is discussed here.

The cross-spectral density of the noise field at two vertically separated sensors due to those sources in an annulus on the surface of radius r and thickness dr , centred on the vertical axis of the sensors, is obtained from eq (1) in conjunction with an extension of Carson's theorem. On integrating over the surface, the vertical cross-spectral density of the noise field due to all the sources is obtained.

The result for the cross-spectral density can be expressed as the sum of two terms, one of which depends on the *difference* in depth between the two sensors and another which depends on the *sum* of the depths of the sensors. If either sensor is on a boundary, these two terms sum to zero, in accord with the pressure-release boundary conditions. But away from the boundaries, in the centre portion of the water column, the term containing the sensor separation predominates. Thus, to a good approximation, the cross-spectral density in this region of the channel is independent of the mean depth of the sensors and depends only on their separation. This establishes the noise field as essentially spatially homogeneous away from the boundaries of the channel. The region of quasi-homogeneity is indicated in figure 1, which shows the power spectral density of the noise as a function of depth for two different

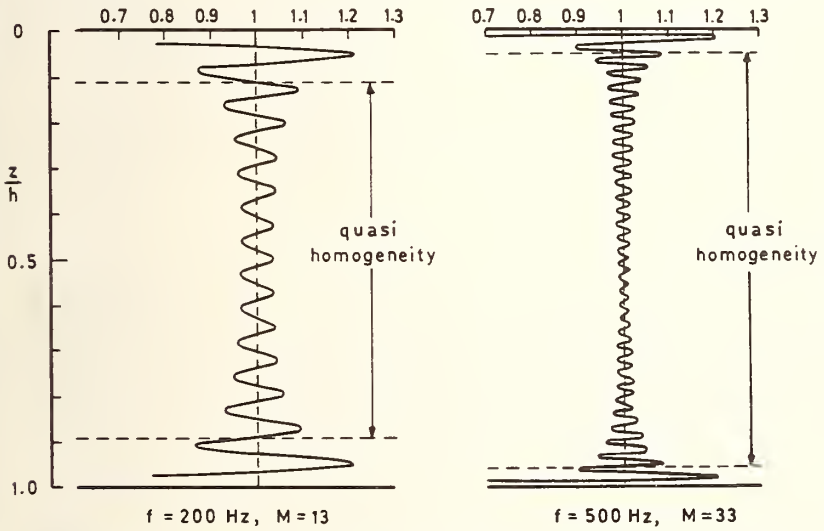

Fig 1 The power spectral density of the noise as a function of depth, at two different frequencies, in a water column 100 m deep.

frequencies. The expression for the power spectral density in figure 1 is

$$\bar{S} = \left\{ 1 - \frac{\sin\left[(2M + 1)\pi z/h\right]}{(2M + 1)\sin(\pi z/h)} \right\} . \qquad (3)$$

Note that the oscillatory component of the power spectral density, representing the non-homogeneous component of the noise field, is less than 10% of the depth-independent component over the quasi-homogeneous region.

If the noise in the quasi-homogeneous region is treated as truly homogeneous, a considerable simplification can be achieved in representing the spatial properties of the noise field: the concept of a unique directional density function can be introduced to describe the noise power incident at a point in the field from a given direction. The directional density function of a homogeneous noise field is uniquely related to the cross-spectral density through a Fourier transform relationship. (The Fourier variables are the sensor separation and the angle of incidence of the radiation.) The directional density function for the shallow water noise field is

$$F(\theta) = \left(\frac{1}{M}\right)\left[\sum_{s=-M}^{M} \delta\left(\cos\theta - \frac{\pi s c}{\omega h}\right) - \delta(\cos\theta)\right] \qquad (4)$$

where θ is the vertical angle measured from the zenith and $\delta(\cos\theta)$ is the Dirac delta function. A sketch of $F(\theta)$ is shown in figure 2.

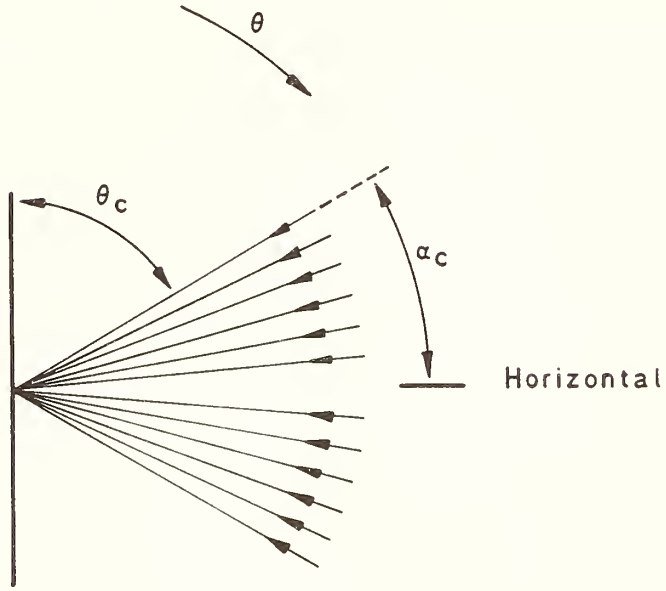

Fig. 2 Sketch of the directional density function, $F(\theta)$, in eq (3). $\theta_c = (\pi/2 - \alpha_c)$ is the critical angle.

$F(\theta)$ shows some interesting features. It varies discretely with vertical angle, showing 'rays' in the directions of the eigenrays associated with the modes in the channel. There is no horizontal noise 'ray' because the pressure-release boundary condition precludes the existence of a zeroth-order mode. At grazing angles greater than the critical grazing angle there is no modal noise because, at these relatively high grazing angles, total internal reflection at the bottom boundary no longer occurs and the modes cannot propagate. The noise 'rays' all have the same intensity, as indicated in the figure by their equal length. At first sight this is perhaps an unexpected result, since the outer 'rays', associated with the higher-order modes, undergo more encounters with the (lossy) bottom per unit distance than those 'rays' closer to the horizontal. Thus, if this 'mode stripping' phenomenon were the only mechanism acting, the outer 'rays' should be attenuated relative to the inner 'rays'. However, this effect is exactly compensated by the generation mechanism: the sources lie in a plane immediately below the surface and, as can be seen from eq (1), excite the higher-order modes more strongly than the lower-order modes. This accounts for the uniformity of the noise 'rays' in figure 2.

The angular separation between the noise 'rays' in figure 2 depends on frequency. At 100 Hz, for example, it is about 4°. In order to resolve the 'rays', an array of acoustic sensors with an angular resolution better than the angular distance between the 'rays' is required. A *vertical* line array would seem to be the obvious choice for an experimental investigation of the vertical directionality of the noise field; but such an array is unlikely to have sufficient angular resolution because its aperture is limited in extent to the depth of the channel.

An alternative approach would be to use a *horizontal* line array, which could be made as long as necessary in order to achieve the required angular resolution. The (theoretical) response [3] of a limiting form of such an array, in which the aperture is infinite and the beam is of infinitesimal angular width, to the discrete noise field represented in figure 2, is shown in figure 3. The figure shows the noise gain, G_{∞}, versus the steering angle, β,

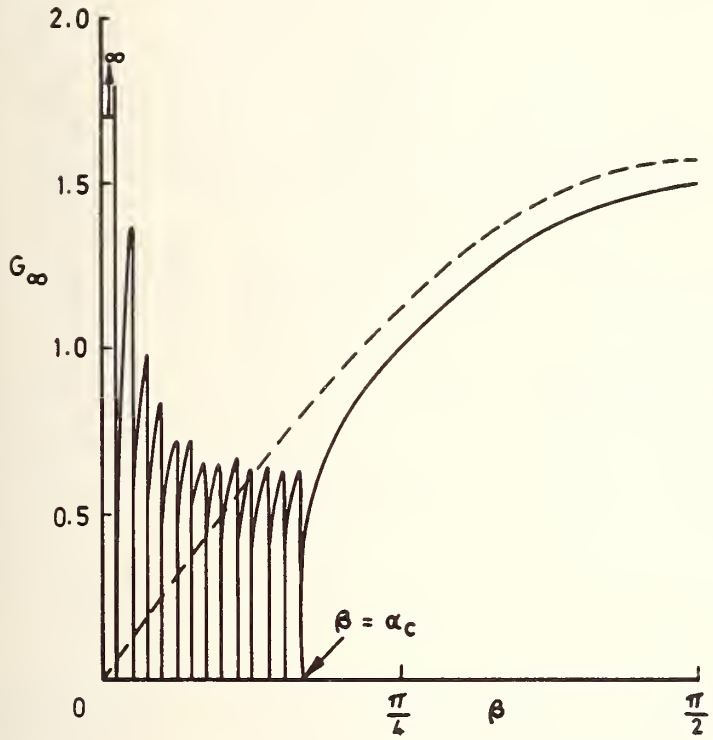

Fig. 3 The theoretical noise gain versus steering angle for a very long horizontal line array in shallow water

measured from the axis of the array. Note that for steering angles less than the critical grazing angle, the noise gain goes through a series of zeros, occurring when the beam is pointing directly at a noise 'ray'. Thus, this 'fine structure' on the curve is ascribed to the modal nature of the noise. When the steering angle is greater than α_c , the noise gain is monotonic increasing up to a steering angle of $\pi/2$, corresponding to the broadside condition. The fine structure around endfire in figure 3 could provide the means whereby the modal character of the ambient noise in shallow water is experimentally detected.

REFERENCES

[1] M. J. Buckingham, *J. Acoust. Soc. Am.* 67(4), 1186 (1980)

[2] W. A. Kuperman and F. Ingenito, *J. Acoust. Soc. Am.* 67(6), 1988 (1980)

[3] M. J. Buckingham, submitted to the J. Acoust. Soc. Am.

MATHEMATICAL FORMULATION OF THE IMPEDANCE FIELD METHOD. APPLICATION TO THE NOISE OF THE CHANNEL OF FIELD EFFECT TRANSISTORS

J.P. Nougier, J.C. Vaissière, D. Gasquet

Centre d'Etudes d'Electronique des Solides [1)2)], Université des Sciences et Techniques du Languedoc, 34060 Montpellier Cédex, France.

1. MATHEMATICAL FORMULATION OF THE IMPEDANCE FIELD :

The impedance field method of Shockley et al. [1], for one dimensional devices, gives the noise voltage spectral density S_V at the terminals of the device, as a sum of the weighted contributions of the noise sources $K(x)$ of the different slices at point x, of cross section $A(x)$:

$$S_V = \int_0^L A(x')\ K(x')\ |\nabla Z(x')|^2\ dx' \qquad (1)$$

$K(x')$ being supposed to be known, the critical step is the calculation of the impedance field $\nabla Z(x')$. One method for determining it, suitable when the basic parameter is the local electric field $E(x)$, is the transfer impedance method [2]. The purpose of this paper is to develop a method suitable when the basic parameter is the local voltage $V(x)$, and to apply it for modelling the noise of field effect transistors (FET).

Let us consider a device (Fig. 1) with a d.c. bias applied to the electrodes M and N. The noise is studied between the electrodes (or probes) M' and N', which may be identical with, or different from, M and N. Let us apply, between M' and N', a small a.c. voltage, at frequency ω, superimposed to the d.c. one between M and N. This results in a set of a.c. equipotential surfaces, and a.c. current lines orthogonal to them (see Fig. 1). Let us consider such a line, labelled P, of total length L between M' and N', and an equipotential surface S crossing P at point of abscissa x along P. The value $\delta V(x) \exp i\omega t$ of the a.c. potential at point x is related to the a.c. current $\delta I(x) \exp i\omega t$ across S through a relation obtained by linearizing the conduction equations around the bias point. One thus gets

$$\hat{\mathcal{L}}\, \delta V(x) = \delta I(x) \qquad (2)$$

where $\hat{\mathcal{L}}$ is a linear operator. Let $\mathcal{Z}(x,x',\omega)$ be the Green function of $\hat{\mathcal{L}}$, defined as :

$$\hat{\mathcal{L}}\, \mathcal{Z}(x,x',\omega) = \delta(x - x') \qquad (3)$$

where $\delta(x-x')$ is the Dirac function. The a.c. voltages $\delta V(x)$ at x and $\delta V(L)$ between M' and N' are :

$$\delta V(x) \int_0^L \mathcal{Z}(x,x',\omega)\ \delta I(x')\ dx' \qquad (4)$$

$$\delta V(L) \int_0^L \mathcal{Z}(L,x',\omega)\ \delta I(x')\ dx' \qquad (5)$$

---

1) Laboratoire associé au C.N.R.S. LA 21 and Greco Microondes.

2) This work was partially supported by D.G.R.S.T. (contract n° 79.7.0726) and G.CIS.

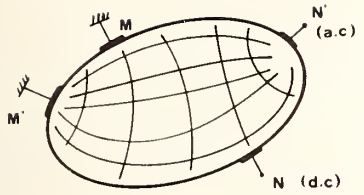

Fig. 1 : a.c. equipotential surfaces and current lines

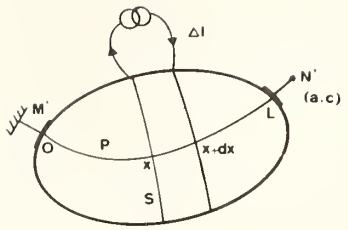

Fig. 2 : Impedance field method

Let us introduce (Fig. 2) a current $\delta I(x')$ null everywhere except in the slice Δx where its value is ΔI : this results in a voltage ΔV at the probes M' and N', and the impedance field [1] is $\nabla Z(x,\omega)$ given by $\nabla Z(x,\omega)\,\Delta x = \Delta V/\Delta I$, eq. (5) shows that

$$\nabla Z(x',\omega) = \mathcal{Z}(L,\ x',\omega) \tag{6}$$

Of course the impedance of the device between M' and N' is given by :

$$Z(\omega) = \int_0^L \mathcal{Z}(L,\ x',\omega)\ dx' \tag{7}$$

The device can be considered as being one dimensional between M' and N', when the curvature radius of the a.c. equipotential surfaces is large compared with the transverse dimensions of the device, that is when the areas of the equipotential surfaces are approximately equal to the cross sections of the device. Then the noise source term is constant everywhere in the slice dx, thus depends only on x, so that eq. (1) can be used.

2. IMPEDANCE FIELD OF FIELD EFFECT TRANSISTORS :

The noise of the channel of FETs was recently calculated by Van Vliet [3], using the transfer impedance method [2], at low drain bias when the mobility μ is constant. However, at higher drain bias, hot carriers are involved and $\mu = \mu(E)$. The theory of section 1 will be used in order to get the impedance field. Here M' = M is the source electrode, and N' = N is the drain electrode. We suppose that the frequency is low enough so that no leakage drain current occurs through the gate-channel capacitance. Furthermore the free electron density will be supposed to be constant, equal to the impurity concentration N_D (this is no more true in the saturation region of the $I\text{-}V_D$ characteristics). The conduction equation then writes :

$$I = q\,N_D\,v(E)\,A\left[V(x)\right] . \tag{8}$$

This gives, for a.c. values (the subscript 0 means the d.c. values), using $\delta E = -d\delta V/dx$:

$$-q\,N_D\,A(V_o)(dv/dE)_o\,d\delta V/dx + q\,N_D\,v(E_o)\,(dA/dV)_o\,\delta V = \delta I . \tag{9}$$

The Green function $\mathcal{Z}(x,x')$ is readily obtained (the integration constant vanishes since $\delta V(x=0) \equiv 0$ implies through eq. (4) that $\mathcal{Z}(x=0,\ x') = 0$) :

$$\mathcal{Z}(x,x') = -\frac{H(x-x')}{q\,N_D\,A\left[V_o(x')\right](dv/dE)_{o,x'}}\ \exp\int_{x'}^{x}\frac{v\left[E_o(u)\right](dA/dV)_{o,u}\,du}{(dv/dE)_{o,u}\,A\left[(V_o(u)\right]} \tag{10}$$

$H(x-x')$ is the step function. By setting $x=L$ in eq. (10), one gets $\nabla Z(x') = \mathcal{Z}(x=L,x')$. Generally speaking, v(E) has no analytical form, so that $\nabla Z(x')$ is obtained numerically, thus getting the impedance and the noise of the FET (provided the source term is known). In the ohmic range (low drain bias), when $v(E) = \mu_o E$, eq. (10) gives the expression obtained by Van Vliet [3] : $\nabla Z(x') = \{q\,N_D\mu_o\,A\left[V(L)\right]\}^{-1}$.

3. NOISE OF THE CHANNEL OF FETs :

In order to get further information on the noise of FETs, we approximate v(E) using an hyperbolic law [4] :

$$v(E) = - \mu_o E / [1 - (E/E_c)] \qquad (11)$$

The signs choosen in eqs. (8) and (11) correspond to a n-type channel FET, with the source at $x = 0$, the drain at $x = L > 0$, $q > 0$, $V(x) > 0$, $E(x) < 0$, $v[E(x)] > 0$ and $I > 0$, $E_c > 0$. Equation (11), carried into eq. (8), gives then, for the d.c. and a.c. values:

$$I_o(1 - E_o/E_c) = - q N_D \mu_o E_o A_o \qquad (12)$$

$$- \frac{q N_D \mu_o E_o(x)}{1 - E_o(x)/E_c} \left(\frac{dA}{dV}\right)_{o,x} \delta V(x) + \frac{q N_D \mu_o A_o[V_o(x)] - I_o/E_c}{1 - E_o(x)/E_c} \frac{d\,\delta V(x)}{dx} = \delta I(x) \qquad (13)$$

In the same way as in section 2, one gets the Green function.

$$\mathcal{Z}(x,x') = \frac{[1 - E_o(x')/E_c] H(x-x')}{q N_D \mu_o A[V_o(x')] - I_o/E_c} \exp \int_{x'}^{x} \frac{q N_D \mu_o E_o(u) (dA/dV)_{o,u}}{q N_D \mu_o A[V_o(u)] - I_o/E_c} du \qquad ,$$

The integral in eq. (14) can be carried out using V_o as a new variable: $E_o = - d V_o/dx$:

$$\mathcal{Z}(x,x') = \frac{1 - E_o(x')/E_c}{q N_D \mu_o A[V_o(x)] - I_o/E_c} H(x - x') \quad .$$

Finally, by setting $x = L$, and taking into account eq. (12), one gets :

$$\nabla Z(x') = [E_o(L)/I_o][1 - E_o(x')/E_c] \quad . \qquad (15)$$

The impedance Z is readily obtained. Carrying eq. (15) into eq. (1) and dividing by $|Z|^2$ gives the noise current S_I, which is more meaningful than S_V because $E_o(L)$ is not well known for actual geometries. This gives, where V(L) is the drain voltage :

$$S_I = L^{-2} \left[1 + \frac{V_o(L)}{E_c L}\right]^{-2} \int_o^L K(x') \left[1 - \frac{E_o(x')}{E_c}\right]^2 A(x')\, dx' \qquad (16)$$

When E_c tends towards infinity, eq. (16) gives back the result of Van Vliet [3]. Equation (16) shows that the noise current is the sum of the contributions of the different slides of the FET, the contribution of the slice at abscissa x' being proportional to its volume A(x')dx', to the noise source in it K(x'), and depending on the field through the quantity $[1 - E_o(x')/E_c]^2$. Note that this theory includes the channel as well as then regions between the source and the gate and between the drain and the gate.

The noise can also be expressed using the local noise temperature $T_n(x')$, related to K(x') through the following equation [5], where the minus sign takes into account the opposite directions of v and E, and k_B is the Boltzmann constant :

$$K(x') = - 4 k_B q N_D T_n(x') (dv/dE) = 4 k_B q N_D \mu_o T_n(x') / [1 - E_o(x')/E_c]^2$$

This relation carried into eq. (16) gives

$$S_I = \frac{4 k_B q N_D \mu_o}{L^2 [1 + V(L)/E_c L]^2} \int_o^L T_n(x')\, A(x')\, dx' \qquad (17)$$

This formula shows that, at low drain bias, the contribution, to the noise, of the channel itself gives, since $A(x') = A =$ constant, $T_n(x') \to T$ and $V(L) \to 0$: $S_I = 4 k_B T\, I/V$.

a) Diffusion noise :

For diffusion noise, T_n increases, more or less linearly with increasing E [6], and

therefore is maximum at the end of the channel, but the cross section A(x') is then minimum. As a consequence, it can be expected that the contributions of all the slices of the FET are of comparable importance. It has been noticed that $S_I \propto I/V$ at low bias, that is $S_I \simeq$ constant; at higher bias the increase of the noise in the channel versus V(L) in eq. (17) is counter balanced by the factor $V(L)/E_c L$, so that S_I does not vary much.

b) Hot carrier generation-recombination (G-R) noise : in some devices, at low temperature, all the impurities are not thermally ionized. Under the effect of high field, the neutral impurities are ionized, via Poole Frenkel [7] or impact ionization effect, thus leading to an additionnal noise of G-R type, the parameters of which depend on E. Then, at the end of the channel, T_n increases steeply, so that the noise is mainly due to the contribution of this part of the FET, the total noise thus being much higher (40 to 100 times) than expected [6].

c) Thermal G.R. noise : For G.R. noise involving the conduction band and one impurity level, one has $K(x') = 4\, q^2\, n(x')\, v^2(x')\, \alpha\tau/(1+\omega^2\tau^2)$. This expression, carried into eq. (16) gives, taking into account eq. (11).

$$S_{IGR} = \frac{4\, q^2\, N_D\, \mu_o^2}{L^2\,[1 + V(L)/E_c L]^2} \int_o^L \frac{\alpha\,\tau}{1+\omega^2\tau^2}\, E^2(x')\, A(x')\, dx' \qquad (18)$$

Now the quasi one dimensional Poisson's equation writes :

$$\partial[E(x)\, A(x)]/\,\partial x = q\, A(x)\, [N_D - n(x)]/\varepsilon\ . \qquad (19)$$

The hypothesis $n(x) = N_D$ implies $E(x)\, A(x) = \text{constant} = E(o)\, A(o)$. Since the electric field at the source electrode is weak, eq. (12) gives $- I_o = q N_D \mu_o E(o) A(o) = q N_D \mu_o E(x) A(x)$. This relation carried into eq. (18) gives :

$$S_{IGR} = \frac{-\,4\, q\, \mu_o\, I_o}{L^2[1 + V(L)/E_c L]^2} \int_o^L \frac{\alpha\,\tau}{1+\omega^2\tau^2}\, E(x')\, dx' \qquad (20)$$

For hot carrier G.R. noise, α and τ depend on E, thus on x' (see section 3b above). As a consequence, the frequency spectrum is a sum of weighted $1/(1+\omega^2\tau^2)$ curves, and thus does not vary as $1/(1+\omega^2\tau^2)$: the noise spectrum, even for a single impurity level, behaves as the G.R noise of an infinite set of uncorrelated levels lying in a sub-band with a distribution of relaxation times.
For thermal G.R noise, α and τ are constants, and eq. (20) writes :

$$S_{IGR} = \frac{4\, q\, \mu_o}{L^2[1 + V(L)/E_c L]^2} \frac{\alpha\,\tau}{(1+\omega^2\tau^2)}\, I_o\, V(L) \qquad (21)$$

Therefore, at low bias, such as $V(L)/E_c L \ll 1$, the thermal G.R noise is proportional to the d.c. power $I_o V(L)$ displayed in the FET. This holds until saturation for long FETs, but for very short FETs one would expect a decrease of S_{IGR} at high drain bias.

d) 1/f bulk noise : Then, $K(x') = \alpha_H\, n(x')\, q^2 v^2(x')/f$, where α_H is the Hooge constant. Carried into eq. (16) in the same way as previously, one gets

$$S_{I\ Bulk\ 1/f} = \frac{q\, \mu_o\, \alpha_H}{L^2[1 + V(L)/E_c L]^2} \frac{I_o\, V(L)}{f} \qquad (22)$$

One gets 1/f noise, proportional to $I_o V(L)$ at least at low bias. This is also the case in MES FETs for 1/f noise due to interface states between the epitaxial layer and the wafer, but with a constant different from α_H (provided that this constant is actually independent on the electric field).

e) 1/f contact noise : when the 1/f noise takes place at the interface at the source electrode, one may write $K(x') = \lambda n(x')\, q^2\, v^2(x')\delta(x')/f$ where $\delta(x')$ is the Dirac function. This gives, carried into eq. (16) :

$$S_I = \frac{\lambda\, N_D\, q^2\, \mu_o^2}{L^2[1 + V(L)/E_c L]^2} \frac{E^2(o)\, A(o)}{f} = \frac{\lambda}{N_D\, A(o)\, L^2[1 + V(L)/E_c L]^2} \frac{I_o^2}{f}$$

This noise behaves differently from the bulk 1/f noise, since the numerator involves I_o^2 instead of $I_o V(L)$. Hence the measurement of the 1/f noise current versus the drain bias allows one to localize the 1/f noise source.

4. CONCLUSION :

In this paper, we have settled a new formulation of the impedance field method, particularly well suited for the cases when the main parameter is the local potential. This method has been applied to the theoretical determination of the noise of field effect transistors, which may be JG FETs, MOS FETs or MES FETs. A general formula has been given[eq. (10)] and, under some simplifying hypotheses, complete results have been carried out, leading to expressions very simple to use, and providing quite general features of the noise in a wide range of operating conditions.

REFERENCES

[1] W. Shockley, J.A. Copeland and R.P. James, in "Quantum theory of Atoms, Molecules and the Solid State, P. Lowdin ed., Acad. Press, New York, 1966.

[2] K.M. Van Vliet, A. Friedmann, R.J.J. Zijlstra, A. Gisolf and A. Van der Ziel, J. Appl. Phys. 46, 1804 (1975) and J. Appl. Phys. 46, 1814 (1975).

[3] K.M. Van Vliet, Sol. State Electron. 29, 233 (1979).

[4] F.N. Trofimenkoff, Proc. IEEE 53, 1765 (1965)

[5] J.P. Nougier, J. Appl. Phys., to be published.

[6] J.P. Nougier, in Physics of nonlinear transport in semiconductors, ed. by D.K.Ferry, J.R. Barker, C. Jacoboni, Plenum Publi. Corp. (1980), p. 415-465.

[7] A. Van der Ziel, R. Jindal, S.K. Kim, H. Park, J.P. Nougier, Solid State Electron. 22, 177 (1979).

TIME DOMAIN LARGE SIGNAL NOISE MODELLING IN MICROWAVE OSCILLATORS

J.F. Sautereau - J. Graffeuil - J.C. Martin

Laboratoire d'Automatique et d'Analyse des Systèmes
Universite Paul Sabatier
Greco microondes - Centre National de la Recherche Scientifique
7 Ave. Roche, 31400 Toulouse, France

I INTRODUCTION

Noise in microwave oscillators has in the past been investigated mainly in the frequency domain and the oscillator represented by an equivalent lumped circuit with the voltage or current noise source in the appropriate section of the circuit. The variations of all the elements of the circuit versus frequency and ac voltage or current was then needed to derive the phase or amplitude noise performances of the oscillator.

Such a goal may be impossible to reach when many non linear elements are involved in the equivalent circuit, such as in oscillators built with two-port devices.

We report here an alternative approach based in a time domain large signal analysis which allows the obtaining of the up converted amplitude modulation (AM) and frequency modulation (FM) noise as well as the frequency and output power. Consequences for the design of low noise oscillators are outlined.

II LARGE SIGNAL TIME DOMAIN APPROACH IN MICROWAVE OSCILLATOR NOISE

The active device is described by an appropriate network involving frequency and instantaneous voltage dependent elements, frequency dependent and voltage independent elements. This equivalent circuit is implemented into a time domain analysis program IMAG III. A feedback circuit is then added to provide oscillations. The theoretical output wave of the oscillator is consequently available versus time (figure 1). In the present work two identical oscillators were simulated at the same time ; The only difference consists of a low frequency (LF) source (frequency f_{AN}) being added in one of the two equivalent networks. Consequently the two oscillators deliver two output waves :

The first called V_{10} is noise free and corresponds to an noiseless oscillator. The other, called V11, is noisy and corresponds to an oscillator with a low frequency noise source added. The LF noise source may be introduced anywhere in the oscillator network. V10 and V11 can be expressed in the following way :

$$V_{10} = A \cdot \sin (2\pi f_0 t).$$

$$V_{11} = (A + \delta A(t)) \sin (2\pi f_0 t + \delta\varphi(t)).$$

Where A is the carrier amplitude fo is the oscillation frequency, $\delta A(t)$ is the amplitude fluctuation (AM noise) and $\delta\varphi(t)$ is the phase fluctuation which is linked to frequency fluctuation (FM noise).

In most solid state oscillators FM noise near the carrier is many orders of magnitude higher than AM noise. Then, it may be assumed that the difference between the two output

voltages (V10 noiseless, V11 noisy) is only due to a phase fluctuation induced by an LF noise source.

Thus :

$$V_{10} = A \cdot \sin(2\pi f_0 t)$$

$$V_{11} = A \cdot \sin(2\pi f_0 t + \delta\varphi(t))$$

the phase fluctuation $\delta\varphi(t)$ is given by

$$\delta\varphi(t) = \text{Arc}\sin\left(\frac{V_{11}}{A}\right) - \text{Arc}\sin\left(\frac{V_{10}}{A}\right)$$

A is the amplitude maximum value of the noiseless output wave. In a strip of bandwith Δf located at a frequency fAN,

$\delta\varphi(t)$ may be written : $\delta\varphi(t) = \varphi_m \cdot \sin(2\pi f_{AN} t)$

and FM noise (SSB) is given by : $\Delta f_{rms} = \sqrt{2} \cdot f_{AN} \cdot \varphi_m$

As to calculate φ_m a supplementary network was included in the model to suppress the D.C component and to remove the small parasitic amplitude modulation of the output waves.

The circuit used is shown in Fig (2) ; it is made up of a DC suppression network and a diode limiter.

III RESULTS

Typical theoretical result for FM noise obtained with an X band GaAs FET oscillator is given in Figure (3). fo is 10 GHz , f_{AN} is 1 GHz and the amplitude of the low frequency ac generator located in the active region of the device is 10^{-4} A. This curve shows that there is an up conversion of the LF signal to FM fluctuations.

We deduced from the noise measurements the ratio k_1 between the FM noise of several X band GaAs FET oscillators in the 1 Hz bandwith at 10^3 Hz off the carrier and the spectral intensity of the input noise generator measured at a frequency equal to 1 KHz.

Results are given in table 1 ; it must be concluded that the larger the low frequency noise of the device, the noisier the oscillator.

In order to better understand this phenomenon we measured the increase between a c LF fluctuations of the gate voltage of an oscillator and the FM fluctuation resulting when an a c LF signal of frequency f_{AN} was applied in conjunction with the DC supply on the

FET gate.

Frequency deviations were measured by a carrier null method on a microwave spectrum analyzer. Aratio k between the a c LF signal amplitude and FM fluctuations was then deduced; this ratio k was compared both to the theoretical one k_{th} deduced from the large signal time domain simulation and tc the experimental one kl deduced from the noise measurements. Results are given in table 2 for an x band GaAs FET oscillator using a RAYTHEON LNC 832 D device in chip presentation. Oscillation frequency is 10.2 GHz . Theoretical time-domain simulation was limited by computation time to frequencies higher than 100 MHz, and the experimental procedure did not allow operations at frequencies greater than 30 MHz off the carrier.

However, an extrapolation of the measurements to 100 MHz gives a good agreement between the three coefficients. This extrapolation is possible because the amplitude and the frequency of the oscillator output wave settle the value of the network elements. It was verified that ratios k and kl were constant for frequencies near the carrier ($f_{AN} < 30$ MHz).

CONCLUSION

It was found that the FM noise of a FET oscillator depends both on the low frequency input noise resistance of the device and on the up conversion of this low frequency noise. The up conversion coefficient was measured and also theoretically investigated using a new large signal time-domain approach. We believe that the up conversion coefficient could be decreased with a proper choice of the oscillator feedback circuit and of the device biasing conditions. We also found that checking the low frequency noise and rejecting noisier LF devices is an important condition in obtaining good FM noise performances.

This work was supported by DAII-France.

1 J.F. SAUTERFAU - J. GRAFFEUIL - K. TANTRARONGROJ - P. ROSSEL. High efficiency GaAs schottky-barrier gate FET oscillator.
Electronics letters 19 th june 1980 volb n° 13 p 490-491

2 J.F. SAUTEREAU - J. GRAFFEUIL - K. TANTRARONGROJ - P. ROSSEL. X Band GaAs FET oscillator large signal Design. 10 th European Microwave conference. (8-11 th) Sept 80. VARSAW.

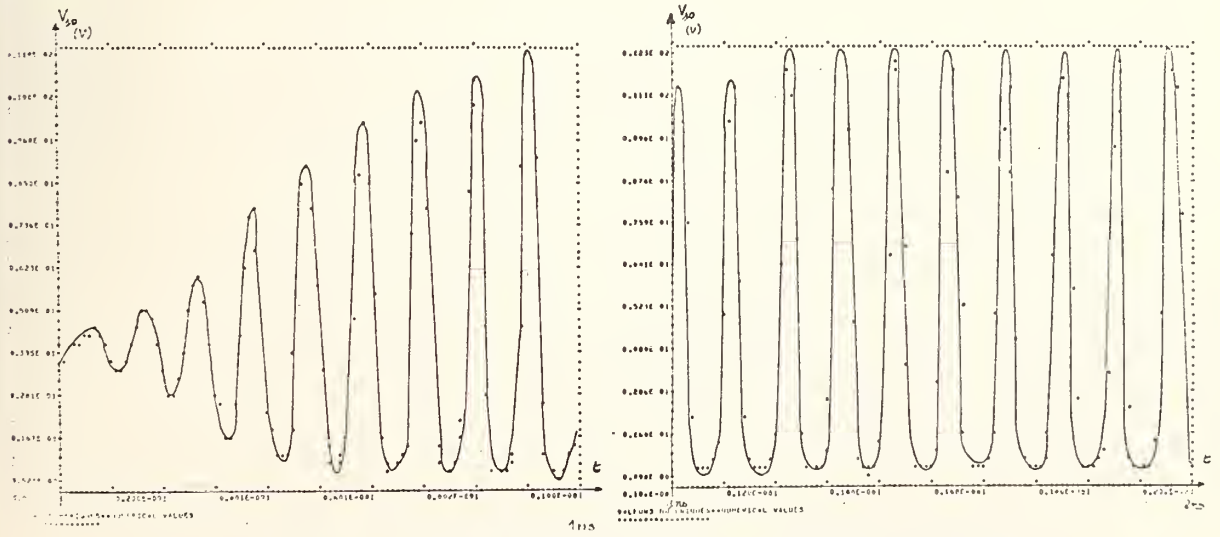

FIGURE 1 : MICROWAVE OSCILLATOR LARGE SIGNAL OUTPUT WAVE.

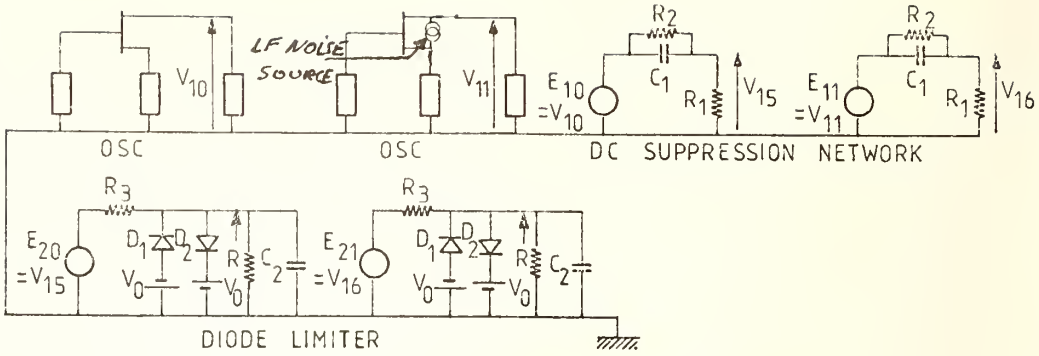

FIGURE 2 : OSCILLATOR NOISE ANALYSIS NETWORK

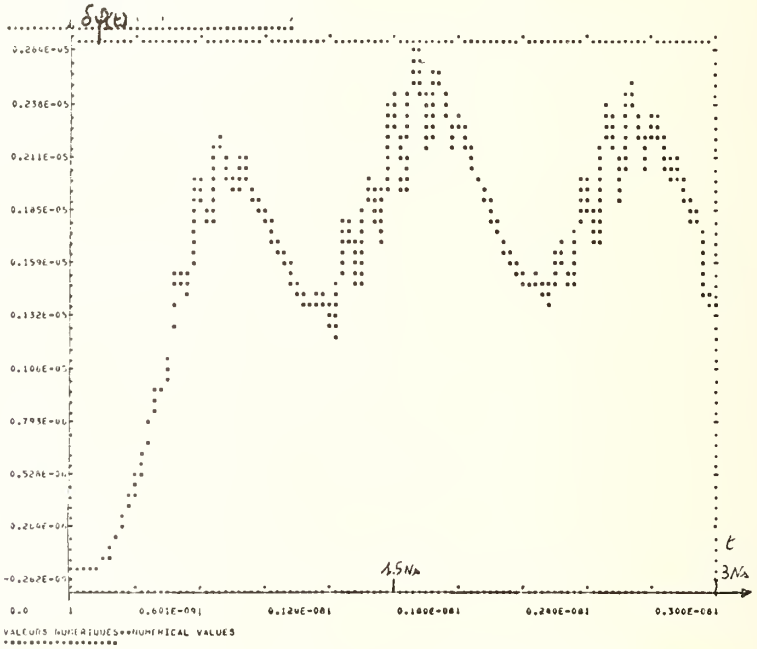

FIGURE 3 : THEORETICAL PM NOISE OF X BAND GaAs FET OSCILLATOR.

(1) k	k_{Th}	k1
$Hz/_V$	$Hz/_V$	$Hz/_V$
$3.5\ 10^7$	$2\ 10^7$	$3.5\ 10^7$

TABLE 2 :
COMPARISON OF THE UP-CONVERSION COEFFICIENT (k_{th}: theoretical, k1 : from noise measurements, k: from carrier null method) FOR AN X-BAND RAYTHEON 832D GaAs FET OSCILLATOR

(2) Device	$(S_{vg})^{1/2}$ in 1 HzBw $(V/\sqrt{Hz})$ $L_{L.F\ NOISE}$	$\Delta frms_{in\ 1\ HzBw}$ $(Hz/\sqrt{Hz})$ FM NOISE	k1 $(Hz/_V)$ Up-conversion coefficient
G	$7.\ 10^{-7}$	25	$3.\ 5\ 10^7$
A	$4.5\ 10^{-7}$	45	$10\ .10^7$
D	$1.5\ 10^{-6}$	170	$11.\ 3.10^7$
C	$5.5\ 10^{-6}$	100	$3.\ 6.10^7$
D	$1.\ 10^{-6}$	160	$16\ .10^7$
F	$2.\ 10^{-6}$	80	$4.\ 10^7$

TABLE1: COMPARISON OF THE UP-CONVERSION COEFFICIENT DEDUCED FROM L.F AND F.M NOISE MEASUREMENTS ON SEVERAL X-BAND GaAs FET OSCILLATORS

SPECTRAL SUPERPOSITION AND IRREVERSIBILITY

Alle A.Walma

Centre d'Etudes d'Electronique des Solides,associé au CNRS,
Université des Sciences et Techniques du Languedoc,
34060 Montpellier-Cedex,France.

INTRODUCTION

Irreversibility is deeply rooted in daily experience since work can only be done whenever two systems are not in thermal equilibrium with each other.The reestablishment of equilibrium is closely related to fluctuations on a microscopic level.For a more general theory of non-equilibrium Statistical Mechanics there are two lines of attack; (i)The Boltzmann and Pauli equation in classical and quantum mechanical dynamics respectively,and (ii)The time-correlation method or linear response theory.Their range of validity remains unclear however.

Generally speaking,satisfactory theories exist only in those cases where a macroscopic characterisation is sufficient (Optics,Classical Thermodynamics,Hydrodynamics etc.).When this is not allowed,our knowledge is not satisfactory (Quantum Mechanics,Nuclear Physics,Solid State Physics etc.).It would then be interesting to know at what degree of coarse graining of the state variables and time the superposition of Lorentzian spectra is allowed ($1/\tau$ idea). The least we can do is to recognise certain strong concepts such as the Einstein relation or the Fluctuation Dissipation theorem.In this case a conceptional difficulty arises with respect to existing 1/f treatments.

It is suggested that in the single variable case the Fluctuation Dissipation theorem excludes the existence of 1/f noise in the thermodynamic limit.A rigorous proof is still lacking,but some evidence in favour of this goes as follows.The Equipartition Theorem requires Ergodicity and Einstein's interpretation of the Boltzmann principle shows the effectiveness of the central limit theorem.Since it can be linearised in the thermodynamic limit,the relevant variable can be modelled by an Ornstein-Uhlenbeck process |1| and therefore does not yield 1/f noise (exponential relaxation).Going a step further,one might ask whether Kolmogorov's axiomatic description of an experiment can explain 1/f noise in the one dimensional case for homogeneous processes,or equivalently,whether an isolated and weakly interacting (van Hove limit) system does incorporate 1/f noise.We think that it does not,since a Master Equation expansion |2| yields in the thermodynamic limit a (non)homogeneous Ornstein-Uhlenbeck process. Markov systems tend to propagate their equilibrium distribution in time and converge to some Fokker-Planck description.This becomes easily a representative Ornstein-Uhlenbeck process for times that are relevant to a 1/f spectrum.

The 1/f theories in physical devices all incorporate the Fluctuation-Dissipation idea. This means that on their way to the desired spectrum some "nonthermodynamic trick"must have been used.This is to our opinion the superposition,averaging,or integration of the basic spectra ($1/\tau$ idea).It is therefore unrealistic since:
(i)The spectrum as a function of a random variable implies a fluctuating variance,which is incompatible with the ergodicity requirement of the Fluctuation-Dissipation theorem.
(ii)It has been shown in |3| that the variable under concern becomes non-Markovian and therefore does not satisfy the Onsager-Machlup theory of Irreversible Thermodynamics.

Roughly speaking,noise theory in physical devices as it stands today is based upon the Ornstein-Uhlenbeck process and therefore of a phenomenological character.The more microscopic theories for irreversibility (Boltzmann,BBGKY hierarchy,linear response and generalised Langevin,Prigogine-Glansdorff and van Hove's theory) all have problems with the stochastics at an atomic scale.In this contribution it is therefore started with a macroscopic characterisation.An attempt is made to explain the superposition idea within the context of the Onsager-Machlup theory by adding enough variables in order to make the process Markovian. This coarse grained framework includes necessarily (i)Seperation of timescales (ii)Molecular Chaos (Boltzmann) (iii)Random Phase Approximation (Pauli) (iiii)Ergodicity (Liouville) (iiiii) Locality (Prigogine) (iiiiii)Timereversibility (Onsager).It remains to be seen whether these approximations are allowed for a real explanation of 1/f noise.As for surface related theories this can be listed as follows (i)Adiabacy of the free density (ii)Boltzmann Approximation (iii)Linearisation (iiii)Detailed Balance.They are a direct consequence of the superposition principle |3| and of the abovementioned assumptions from Irreversible Thermodynamics.

THEORY

A large literature exists about the n-dimensional Ornstein-Uhlenbeck process.For physical devices the standard texts are | 4 || 5 |.Assuming detailed balance,the spectrum can be written as:

$$S(f) = 4\ \mathrm{Re}\{\, M + j\omega I \,\}^{-1}\ C \qquad (1)$$

where M is the relaxation,I the identity and C the covariance matrix.From the two and three variable case onwards,the expressions become hopelessly complicated and usually the spectra are therefore computed numerically.The simple $1/\tau$ structure appearently does not exist.This maybe the reason why 1/f theories use so oft ad-hoc assumptions as a distribution of relaxation times and independent trapping centers for instance.It is shown in |3| that the covariance matrix can be calculated explicitly.The variance of the i-th subsystem,denoted by $\overline{\Delta n_i^2}$,can be expressed into the grandcanonical variances of the other systems:

$$\overline{\Delta n_i^2} = \frac{\sigma_i \sigma_{rest}}{\sigma_i + \sigma_{rest}} = \frac{\sigma_i(\sigma_1+\ldots\sigma_{i-1}+\sigma_{i+1}+\ldots\sigma_k+\sigma)}{(\sigma_1+\ldots\sigma_{i-1}+\sigma_i+\sigma_{i+1}+\ldots\sigma_k+\sigma)} \quad , \quad \sigma_k = f_k(1-f_k)N_k \qquad (2)$$

where σ is the grandcanonical variance of the system of interest (which is the free density in our case) and f_k the occupation of the k-th subsystem with N_k being the total number of states.On the basis of the particle constraint,the covariances are:

$$\overline{\Delta n_i \Delta n_j} = \frac{-\sigma_i \sigma_j}{\sigma_1+\ldots\sigma_{i-1}+\sigma_i+\sigma_{i+1}+\ldots\sigma_k+\sigma} \qquad (3)$$

Applying the adiabatic assumption $\sigma \gg \sigma_i$ ("G-R linearisation of SHR statistics") and working with identical subsystems ("Uniform traps") with $\sigma_1=\sigma_2=\ldots=\sigma_o$:

$$\overline{\Delta n_i^2} \simeq \sigma_o \quad , \quad \overline{\Delta n_i \Delta n_j} \simeq -\frac{\sigma_o^2}{\sigma} \quad , \quad \overline{\Delta n^2} \simeq k\sigma_o \qquad (4)$$

The covariance matrix can now be written as:

$$C = \begin{vmatrix} \sigma_o, 0, 0, \ldots\ldots\ldots, 0, -\sigma_o \\ 0, \sigma_o, 0, \ldots\ldots\ldots, 0, -\sigma_o \\ 0, 0, \sigma_o, \ldots\ldots\ldots, 0, -\sigma_o \\ \vdots \\ 0, 0, 0, \ldots\ldots, \sigma_o, 0, -\sigma_o \\ 0, 0, 0, \ldots\ldots, 0, -\sigma_o, -\sigma_o \\ -\sigma_o, -\sigma_o, -\sigma_o, \ldots\ldots, -\sigma_o, -\sigma_o, k\sigma_o \end{vmatrix} \qquad (5)$$

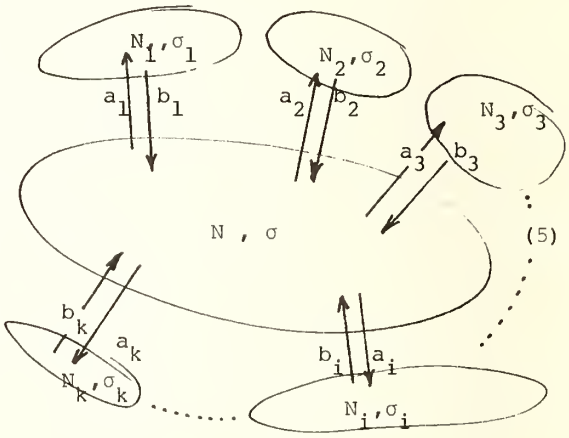

The Phenomenological Relaxation Matrix is obtained in the usual way |4| |5| ,and is based upon the configuration which is shown on the right:

$$M = \begin{vmatrix} a_1N & , & 0 & , & 0 & ,\ldots\ldots, & 0 & , -a_1N_t \\ 0 & , & a_2N & , & 0 & ,\ldots\ldots, & 0 & , -a_2N_t \\ 0 & , & 0 & , & a_3N & ,\ldots\ldots, & 0 & , -a_3N_t \\ \vdots & & & & & & \vdots & \\ 0 & , & 0 & ,\ldots, & a_{k-2}N & , & 0 & , -a_{k-2}N_t \\ 0 & , & 0 & ,\ldots, & 0 & , & a_{k-1}N & , -a_{k-1}N_t \\ (a_k-a_1)N, & & (a_k-a_2)N, & \ldots, & (a_k-a_{k-2})N, & & (a_k-a_{k-1})N, & \sum_k a_kN_t+(a_kN) \end{vmatrix} \qquad (6)$$

where a_k is the rate of transitions per particle from the k-th subsystem to the heatbath and where $N_1^k=N_2=\ldots=N_t$ implies identical subsystems.The interactions take place at the same energy ("Direct communication of conduction band with the oxide").This assumption can be relaxed,which will be shown elsewhere.It is the diagonal character of the covariance matrix that allows an explicit result.The spectral density of the particles in the heatbath becomes |3|:

$$S_{nn}(f) = 4\,\sigma_o \sum_{\ell=1}^{k} \frac{a_\ell N}{a_\ell^2 N^2 + \omega^2} \qquad (7)$$

It will be clear that numerous subsystems and a suitable choice of a_ℓ can account for the desired 1/f type of spectrum.For an exponential rate dependency a pure 1/f spectrum is obtained |3|,where the thermodynamically unrealistic $1/\tau$ idea is avoided.

CONCLUSION

More important than the final result are the underlying conditions.They are often not satisfied in surface related theories,which will be shown elsewhere.Concerning the origins of 1/f noise,the classification of the superposition idea in terms of well established theories of Irreversible Thermodynamics maybe helpfull.It shows that this principle has a phenomenological character and implies (i)A seperation of timescales (ii)Macroscopic linearity (iii)Microscopic additivity,and (iiii)Adiabacy.The theories based upon this idea offer an explanation in the coarse grained sense on the basis of averaged quantities and cannot be considered as microscopic.

REFERENCES

|1| L.Onsager,S.Machlup,Phys.Rev.91,1505 (1953).

|2| N.G.v.Kampen,In:Stochastic processes in Nonequilibrium Systems,Springer Verlag,1978.

|3| A.A.Walma,Revue Phys.Appl.16,(1981).

|4| K.M.v.Vliet,J.R.Fasset,In:Fluctuation Phenomena in Solids,Ch.7,Ac.Press,1965.

|5| M.Lax,Rev.Mod.Phys.32,25 (1960).

CLASSICAL NOISE AND NON-LINEARITY

Alle A.Walma

Centre d'Etudes d'Electronique des Solides,associe´au CNRS.
Universite´des Sciences et Techniques du Languedoc
34060 MONTPELLIER CEDEX,FRANCE

INTRODUCTION

Noise theory in Physical Devices |1||2| relies upon the Ornstein-Uhlenbeck process |3| . This includes Rice's method,the simple Langevin procedure,Burgess'variance theorem,G-R theory and the use of Greens' functions.It affords (i)Additive microscopic processes (ii)A separation of timescales (iii)Processes that are linear in their state variables or that can be linearised,and (iiii)Time homogeneous phenomena in the majority of cases.The analysis is of a phenomenological character.

As far as the fluctuations are concerned,the nearest one can get to the axiomatic propositions of Kolmogorov |4| is by means of his differential equations,usually referred to as the Master Equation.No complete solution is known yet of these equations and one generally introduces a locality assumption.The latter enables a complete solution of linear processes. In the non-linear case an infinite hierarchy of moment equations arises,which has not been solved yet.It is therefore looked for a suitable parameter that allows an expansion,by means of which the hierarchy can be closed effectively.In this contribution the closure is carried out through the large system assumption.A quasi exact solution is compared with the linearised version of a simple non-linear problem.

THEORY

Our macrovariable is the free density in a uniform semiconductor.The recombination process can then be modelled by:

$$\frac{dn}{dt} = a - bn^2 \tag{1}$$

where the rate a is a function of temperature and lattice properties and b of the thermal velocity and recombination crossection.The linear noise procedures yield for the autocovariance |1|| 2| :

$$C(t) = \overline{\Delta n^2}\, e^{-\frac{t}{\tau}} \quad , \tau^{-1} = 2\sqrt{ab} \quad , \quad \overline{\Delta n^2} = \frac{1}{2}\sqrt{\frac{a}{b}} \tag{2}$$

The question is now whether these linearised results are correct.The following assumption is made:The macroscopic differential equation yields the evolution with respect to time of the mean of the process in the thermodynamic limit.

We have in mind a homogeneous and stable Markov process that is stationary and not far from equilibrium.At first sight,the above assumption seems to be unrealistic in view of eq (1) It is quite strong however in equilibrium statistical mechanics and phenomenological thermodynamics.Not only can it be seen as an Onsager relation,but it also constitutes the basis of thermostatics.It enables definite statements about thermodynamic variables because the mean values can be identified with the deterministic ones.It also legalizes the molecular chaos and random phase approximation in classical and quantum mechanical dynamics respectively. This independent particle idea is possible on a macroscopic scale where the large system assumption can be made.It is suggested in our case that the obtained result is exact in the thermodynamic limit.Our confidence is based upon the systematic expansion of the Master Equation from |5| where it is shown that in the limit the most probable path is determined by the deterministic law of evolution(pathological processes that do not satisfy the central limit theorem are excluded).

The exact equilibrium statistics of our problem can be obtained from the general equation of Markov processes |6| (see also for further references).The generating function of the random variable n:

$$P(s,t) = \sum_{n=o}^{\infty} p_n(t)\, s^n \tag{3}$$

satisfies:

$$\frac{\partial P}{\partial t} = a(s-1)P + b(1-s)\{\frac{\partial P}{\partial s} + s\frac{\partial^2 P}{\partial s^2}\} \quad , \quad P = P(s,t) \tag{4}$$

In equilibrium:

$$bsP'' + bP' - aP = 0 \tag{5}$$

This yields:

$$P(s,\infty) = \frac{I_o(z\sqrt{s})}{I_1(z)} \quad , \quad z = 2\sqrt{\frac{a}{b}} \tag{6}$$

with I_o and I_1 being modified bessel functions |7| :

$$I_\nu(z) = (\frac{1}{2}z)^\nu \sum_{k=o}^{\infty} \frac{(\frac{1}{4}z^2)^k}{k!\ \Gamma(\nu+k+1)} \tag{7}$$

Transforming back:

$$p_n(\infty) = \frac{(\frac{a}{b})^n}{(n!)^2 I_o(z)} \tag{8}$$

This shows that the normal assumption of linear noise theories does not hold.With (2) it becomes highly accurate however in the thermodynamic limit.This follows straightforwardly from Stirling's approximation for n! and by means of the following expansions |7| :

$$I_o(z) = \frac{e^z}{\sqrt{2\pi z}}\{1 + \frac{1}{8z} + \frac{9}{2!(8z)^2} + \ldots.\} \tag{9}$$

$$I_1(z) = \frac{e^z}{\sqrt{2z\pi}}\{1 - \frac{3}{8z} - \frac{15}{2!(8z)^2} - \ldots.\} \tag{10}$$

The exact mean is obtained from (6) :

$$\bar{n} = P'(1) = \sqrt{\frac{a}{b}}\frac{I_1(z)}{I_o(z)} \tag{11}$$

and the variance:

$$\overline{\Delta n}^2 = P''(1) + P'(1) - P'^2(1) = \frac{a}{b}\{1 - \frac{I_1^2(z)}{I_o^2(z)}\} \tag{12}$$

These values reduce in the limit to those from eq (2).

For the timedependency the solution of eq (1) is identified with the average regression upon the initial value n(o):

$$\overline{n(t)}^{n(o)} = \sqrt{\frac{a}{b}}\,\frac{n(o) + \sqrt{\frac{a}{b}}\,\mathrm{tgh}\sqrt{abt}}{\sqrt{\frac{a}{b}} + n(o)\,\mathrm{tgh}\sqrt{abt}} \tag{13}$$

For obtaining the autocovariance, this conditional mean is averaged over the exact equilibrium distribution given by eq (8). Denoting n(o) by x, one is thus interested in $\overline{xf(x)}$, which can be written as:

$$C_x(t) = \overline{xf(x)} = \bar{x}f(\bar{x}) + \frac{1}{2}\mu_2\{xf(x)\}''_{x=\bar{x}} + \frac{1}{6}\mu_3\{xf(x)\}'''_{x=\bar{x}} + \ldots. \tag{14}$$

where it is expanded around the equilibrium value. The moments μ_k, k=2,3,..., are taken from (6). The third term on the right can be neglected. This follows from a straightforward calculation of $\{xf(x)\}_{x=\bar{x}}$ and because:

$$\mu_3 = 2\bar{n}^3 - 3\bar{n}\overline{n^2} + \overline{n^3} \tag{15}$$

The autocovariance becomes finally:

$$C_x(t) = p^2\,\frac{I_1}{I_o}\,\frac{I_1+I_oA}{I_o+I_1A} + p^2\,\frac{I_o(1-A^2)}{(I_o+I_1A)^3}\,(I_o-I_1)(I_o+I_1) \tag{16}$$

with $I_1=I_1(z)$, $I_o=I_o(z)$, $z=2\sqrt{\frac{a}{b}}$, and $A=\mathrm{tgh}\sqrt{abt}$. In the limit ($z\to\infty$):

$$C_n(t) = \frac{a}{b} + \frac{1}{4}\sqrt{\frac{a}{b}}\left(e^{-2\sqrt{abt}} + e^{-4\sqrt{abt}}\right) \tag{17}$$

where x is replaced by n. This should be compared with the result from linear noise theory, as is given by eq (2):

$$C(t) = \frac{a}{b} + \frac{1}{2}\sqrt{\frac{a}{b}}\,e^{-2\sqrt{abt}} \tag{18}$$

Note that eq (2) represents $\overline{\Delta n(t)\Delta n(t+\tau)}$, whereas eq (17) equals $\overline{n(t)n(t+\tau)}$. For t=o, both (17) and (18) yield the same equilibrium value.

CONCLUSION

A diffusion limit of a stochastic process (as is given by G-R theory for instance) may be accurate in the thermodynamic limit for a nonlinear process as far as its equilibrium properties are concerned, but difficulties arise with respect to the timedependency. The rapid vanishing of the influence of the higher moments means that a nonlinear stationary and homogeneous Markov process is not a suitable candidate for 1/f noise. The appearance of a second relaxation in our quadratic case suggests a reinterpretation of SHR statistics in physical devices.

REFERENCES

|1| M.Lax, Rev.Mod.Phys. 32, 25 (1960).

|2| K.M.v.Vliet, J.R.Fasset, In: Fluctuation Phenomena in Solids, Acad.Press, 1965.

|3| A.A.Walma, Revue Phys.Appl. 15, 1435 (1980).

|4| A.Kolmogorov, Math.Ann. 104, 451 (1931).

|5| N.G.v.Kampen, Can.J.Phys. 39, 551 (1961).

|6| A.A.Walma, In: Noise in Physical Systems, Springer Verlag, 1978.

|7| M.Abramowitz, J.A.Stegun, Handbook of Mathematical Functions, Dover Publ., 1965.

FLUCTUATIONS AND TRANSITION RATES IN TIME DEPENDENT DISSIPATIVE STEADY STATES

David J. Bergman* and Eshel Ben-Jacob*.

Department of Physics and Astronomy
Tel-Aviv University, 69978 Tel-Aviv, Israel

Zeev Schuss**

Department of Applied Mathematics,
School of Mathematics, Tel-Aviv University 69978 Tel-Aviv Israel

1. INTRODUCTION

It is well known that a particle moving in a potential well under the influence of random forces exhibits fluctuations in its position x and velocity $\dot{x}$. Moreover, if the well is finite, the particle will have a finite probability per unit time for leaving the well. An old paper by Kramers[1] discusses the one dimensional version of this problem in detail for the case where the distribution function in phase space $\rho(x,\dot{x},t)$ satisfies a Fokker-Planck equation, and derives simple expressions for the transition rate in various limits. (The fluctuations about the equilibrium state are given, as usual, by the Boltzmann distribution.) The calculation is achieved by first transforming to a Smoluchowski-type diffusion equation, for which a stationary diffusion solution is then sought. This approach, which is very useful for discussing transitions between two equilibrium states, cannot be applied to the equally interesting probelm of transitions involving one or more nonequilibrium steady states. Moreover, in the case of steady states with low dissipation, there has not existed, until now, a general prescription even for calculating the spontaneous fluctuations about the steady state. In Section 2 we propose a rather general approach to such problems that enables us to obtain very simple expressions for both the fluctuations and the transition rates of nonequilibrium steady states. In Section 3 we apply our method to the case of a hysteretic Josephson junction[2]. In Section 4 we present a general formal approach to the problem based on the results of ref.3. An extension of this approach can be used to discuss potential wells in higher dimensions.

2. THE METHOD OF EFFECTIVE ACTION-ANGLE VARIABLES

We start from the usual Fokker-Planck equation for a particle of unit mass

$$\frac{\partial \rho}{\partial t} = -\frac{\partial \dot{x}\rho}{\partial x} - \frac{\partial F\rho}{\partial \dot{x}} + G\frac{\partial}{\partial \dot{x}}\left(\dot{x}\rho + T\frac{\partial \rho}{\partial \dot{x}}\right) \qquad (1)$$

where G is the dissipation coefficient and T is the temperature in energy units. The force F_0 acting on the particle may depend explicitly on time. We will focus our attention on the cases where, in the absence of noise, the equations of motion have a time-dependent, steady state solution in which at least $\dot{x}$ is periodic. Examples of motion of this type are: a) A particle moving in a potential well with a barrier of finite height, under the influence of friction as well as a periodic driving force[4]. b) A hysteretic Josephson junction with a constant driving current[2] (see fig.1).

The main idea of our approach is to find a family of steady-state trajectories in phase space and use a trajectory index A as the appropriate slow variable of the problem. The fast variable η is taken to be the position along such a trajectory, measured in units that are proportional to the time. One way to define such a trajectory index is by

$$A \equiv \int \dot{X}(t)\, dX(t) \qquad (2)$$

where the integration is over one period of $\dot{x}$. Although this definition appears identical to the action variable used by Kramers in his discussion of low dissipation equilibrium states, we stress that in our case the variable A has a completely different meaning. We now assume, following Kramers, that when ρ is defined in terms of A,η, it is independent of η. In order to do away with the streaming terms in eq.(1), we first rewrite it as follows

$$\frac{\partial \rho}{\partial t} = -\frac{\partial}{\partial x}(\dot{x}\rho) - \frac{\partial}{\partial \dot{x}}\left[\left(F_0+\Delta F - G\dot{x}\right)\rho\right] + \qquad (3)$$

$$+ \frac{\partial}{\partial \dot{x}}\left(\Delta F\rho + GT\frac{\partial \rho}{\partial \dot{x}}\right)$$

where $\Delta F=\Delta F(x,\dot{x},t)$ is chosen so that the point $x,\dot{x}$ lies upon the steady state trajectory corresponding to the force $F_0+\Delta F$. If this equation is now averaged over x and $\dot{x}$ for a fixed trajectory, i.e., for a fixed value of A, the streaming terms (i.e., the first two terms on the r.h.s. of eq.(3)) vanish. If we know the steady state solutions of the noise-free equation of motion, we can in principle calculate $A(x,\dot{x})$ as well as ΔF, and use these results to calculate the average of the last two terms on the r.h.s. of eq.(3) over a

fixed trajectory. The final result is then a Smoluchowski-type equation for $\rho(A,t)$, from which both the fluctuations and the transition rates in the steady state can be deduced. The example of a particle moving in a potential well in the presence of an external oscillating force is discussed in ref.4, in the next section we discuss the example of a hysteretic Josephson junction.

3. HYSTERETIC JOSEPHSON JUNCTION

Assuming the RSJ model[5,6] for the junction, the equation of motion in the absence of noise is

$$\ddot{\theta} + G\dot{\theta} + \sin\theta = I$$

$$G \equiv (\omega_J RC)^{-1} \equiv \beta_c^{-1/2} \quad ; \quad \omega_J^2 \equiv 2eI_J/\hbar C \tag{4}$$

Here θ is the phase difference across the junction, R and C are the resistance and capacitance of the junction, I is the externally driven current in units of the critical current I_J, and time is measured in units of ω_J^{-1}, the reciprocal Josephson plasma frequency. In the underdamped regime G<1, the junction is hysteretic. The I-V characteristic consists of two overlapping branches as shown in fig.2.

The typical motion in phase space for $I_{min}<I<1$ is shown in Fig.1(I_{min} is defined in fig.2): There is a non-equilibrium, time-dependent, dissipative, steady-state trajectory corresponding to the finite voltage branch, as well as a set of metastable equilibrium states that correspond to the zero voltage branch and that are time independent and the different domains of attraction are separated by separatrices[7] (see fig.1). At nonzero temperature, thermal noise will cause transitions from the steady state to one of the equilibrium states and vice versa.

By contrast, when $I<I_{min}$ only the equilibrium states are possible, and thermal transitions take place between neighboring states. Finally, when I>1 only the steady state is possible, and thermal noise will only cause fluctuations about that state, without any transitions to a different, long lived state.

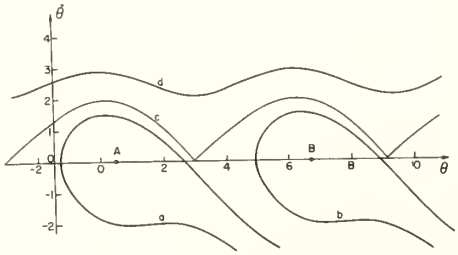

Fig. 1. States and trajectories in phase space for G=0.2, I_o=0.5. The points A and B represent equilibrium (V=0) states. The line d represents the steady-state.
The lines a and b are the separatrices of the states A and B, respectively. The line c is both the steady-state trajectory and part of the separatrix corresponding to the current $I_{min}\cong 0.26$, (see fig.2). Below that line there are no steady-state trajectories.

The Fokker-Planck equation for this problem has the following form

$$\frac{\partial\rho(\theta,\dot{\theta},t)}{\partial t} = -\dot{\theta}\frac{\partial\rho}{\partial\theta} - (I_o - \sin\theta)\frac{\partial\rho}{\partial\dot{\theta}} + \tag{5}$$

$$+ G\frac{\partial}{\partial\dot{\theta}}\left(\dot{\theta}\rho + T\frac{\partial\rho}{\partial\dot{\theta}}\right)$$

Restricting our discussion to the case G<<I, we use the approximate form of the steady-state trajectory,

$$\dot{\theta} \cong \frac{I}{G} + \frac{G}{I}\cos(\theta + \theta_o) \tag{6}$$

in order to get

$$A \equiv \frac{1}{2\pi}\int_0^{2\pi}\dot{\theta}\,d\theta \cong \frac{I}{G} \tag{7}$$

We can therefore choose I to be the slow variable, while the fast variable is the position along the trajectory, which is roughly the same thing as the phase θ. Rewriting the Fokker-Planck equation as follows

$$\frac{\partial\rho(\theta,\dot{\theta},t)}{\partial t} = -\frac{\partial}{\partial\theta}(\dot{\theta}\rho) - \frac{\partial}{\partial\dot{\theta}}\Big[\big(I_o + \Delta I - \sin\theta - \tag{8}$$

$$- G\dot{\theta}\big)\rho\Big] + \frac{\partial}{\partial\dot{\theta}}(\Delta I\rho) + GT\frac{\partial^2\rho}{\partial\dot{\theta}^2}$$

We average over θ for fixed $I=I_o+\Delta I$, assuming that ρ depends only on I. In this way we get

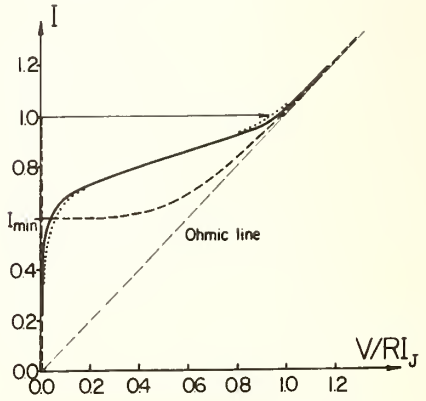

Fig. 2. The I-V characteristics with (solid line) and without (dashed line) thermal noise for G=0.5, Γ=0.1. For comparison, we plot also the I-V characteristic calculated in Ref. 9 from numerical solutions of the Langevin equation (dotted line).

the following equation

$$\frac{\partial \rho(I,t)}{\partial t} = G\frac{\partial}{\partial I}\left(\Delta I \rho + G^2 T \frac{\partial \rho}{\partial I}\right) \qquad (9)$$

which is just the Smoluchowski equation for a particle moving in a harmonic oscillator potential $\frac{1}{2}(\Delta I)^2$, with a friction coefficient $1/G$, at a temperature G^2T.

This description is valid in the region of phase space that includes the I_o steady state trajectory, but does not extend all the way to the separatrices (see fig.1). Since Eq.(9) is valid in the vicinity of the I_o trajectory, we can obtain from it the probability distribution ρ_{ss} for thermal fluctuations about the steady state.

$$\rho_{ss} = (const.)\, e^{-\frac{\Delta I^2}{2G^2T}} \qquad (10)$$

The fluctuations in the voltage ΔV across the junction are related to ΔI according to

$$\Delta V \approx R_D I_J \Delta I \qquad (11)$$

where R_D is the dynamic resistance of the junction ($R_D \simeq R$ for $I \gg G$).[8] Thus the distribution function of Eq.(10) can be compared with a measurable quantity. The transition rate from the steady state to points on the I_{min} trajectory can be calculated by following the procedure of Kramers, and this can be shown to yield a good approximation to the transition rate $1/\tau_{ss}$ out of the steady state provided the I_{min} trajectory is close enough to the separatrix[2]. The result is

$$1/\tau_{ss} \approx G\left(\frac{\Delta U}{T}\right)^{1/2} e^{-\frac{\Delta U}{T}} \qquad (12)$$

where ΔU is an effective potential barrier height given by

$$\Delta U \approx (I_{min} - I_o)^2 / 2G^2 \qquad (13)$$

With the aid of the lifetime τ_{ss} and the lifetime of the static solution, which can also be calculated using Kramers approach, we can predict the average voltage across the junction.[2] In Fig.2 we show a typical computed I-V characteristic in the presence of noise, which is in excellent quantitative agreement with the numerical simulations of ref.9.

4. EFFECTIVE ENERGY APPROACH

As mentioned earlier there are cases where a more general approach to the problem is needed. This, for example, is the case of the Josephson junction in which the distance in phase space between the I_{min} trajectory and the separatrix is large.

The method we present in this section is based on a generalization of the form of the Boltzmann distribution about equilibrium states, which is given by

$$\rho = \rho_o e^{-\frac{E}{T}} \qquad (14)$$

In this approach, we define an effective energy E_e such that the stationary distribution about the steady state is given by an infinite series

$$\rho_{ss} = e^{-\frac{E_e}{T}} \sum_{n=0}^{\infty} \rho_n T^n \qquad (15)$$

Using the Fokker-Planck equation, we obtain, at low temperatures, the following equations for E_e and ρ_o,

$$G\left(\frac{\partial E_e}{\partial \dot{x}}\right)^2 + \dot{x}\frac{\partial E_e}{\partial x} + (F_o - G\dot{x})\frac{\partial E_e}{\partial \dot{x}} = 0 \qquad (16a)$$

$$\dot{x}\frac{\partial \rho_o}{\partial x} + G\frac{\partial E_e}{\partial \dot{x}}\frac{\partial \rho_o}{\partial \dot{x}} + \left[G\frac{\partial^2 E_e}{\partial \dot{x}^2} + \frac{\partial}{\partial \dot{x}}(F_o - G\dot{x})\right]\rho_o = 0 \qquad (16b)$$

We require $E_e = 0$ on the trajectory of the steady state solution and $E_e > 0$ away from it. On this trajectory we define ρ_o to be the non trivial periodic solution of eq.(16b) with the periodicity of the trajectory.

It can be shown[10] that the transition rate is given by

$$1/\tau_{ss} = \Omega_e e^{-\frac{\Delta E_e}{T}} \qquad (17)$$

where ΔE_e is the minimum of E_e on the separatrix at the lowest saddlepoint, and the effective frequency Ω_e is given by $\Omega_e=\omega_N<\omega>/2\pi\omega_T$, where $<\omega>$ is the frequency of the oscillations in E_e normal to the steady state trajectory, averaged with respect to ρ_o over this trajectory. The quantities ω_N and ω_T are the frequencies of the normal modes of E_e at the lowest saddlepoint in the directions perpendicular and parallel to the separatrix, respectively. (A more general case is discussed in refs. 3,10.)

It can be shown that when $I/G >> 1$ in the Josephson junction problem, E_e is given approximately by $\Delta I^2/2G^2$. This is consistent with the results obtained in section 3. If G is large then $E_e \cong E$, the energy. This is consistent with the usual Smoluchowski approximation , which is the right one for this limit.

REFERENCES

* Partially supported by the US-Israel Binational Science Foundation BSF.

** Partially supported by A.F.O.S.R. AFOSR78-3620A.

[1] H.A.Kramers, Physica 7, 284 (1940).

[2] E.Ben-Jacob, D.J.Bergman, Z.Schuss, Submitted to Phys.Rev.Lett.

[3] B.J.Mathkowsky, Z.Schuss, SIAM J.Appl. Math. (in press)

[4] E.Ben-Jacob, D.J.Bergman, B.Carmely, A.Nitzan. This proceedings

[5] D.E.McCumber, J.Appl.Phys. 39, 3113 (1968).

[6] W.C.Stewart, Appl.Phys.Lett. 12, 277 (1968).

[7] M.Levi, F.C.Hoppensteadt, W.L.Miranker, Quart. Appl.Math, 36, 167 (1978).

[8] A.J.Dahm, A.Dennenstein, D.N.Langenberg, W.H.Parker, D.Rgovin, D.J.Scalapino, Phys.Rev. Lett. 22, 1416 (1969).

[9] J.Kurkijarvi, V.Ambegaokar, Phys.Lett. 31A, 314 (1970).

[10] "Theory and Applications of Stochastic Differential Equations" by Z.Schuss, John Wiley and Sons NY (1980).

II. DEVICES

A NEW APPROACH TO MODEL CHANNEL "THERMAL" NOISE OF THE JG.FET CONSIDERED AS AN ACTIVE R-C LINE

D. Sodini, D. Rigaud

Centre d'Etudes d'Electronique des Solides, associé au C.N.R.S.
Université des Sciences et Techniques du Languedoc
34060 MONTPELLIER CEDEX, FRANCE

1. INTRODUCTION

The theory of the "thermal" noise in the channel of JG.FET was first developed by A. Van der Ziel | 1 | assuming that ohmic conditions hold inside the channel and that the hypotheses of Shockley are valid. Later, introducing hot carrier phenomena, new noise expressions have been carried out |2,3| but till now, in particular at 77 K, no satisfactory theory for the device noise calculation has been convincing.

The purpose of this paper is not to determine if the origin of the increase of noise at low temperature is due to hot carrier phenomena or can be produced by other noise sources such as generation-recombination | 4 | but to show how it is possible to introduce in a computed model the experimental Si bulk data for the noise calculation of an active device as JG.FET's.

2. ANALYSIS OF THE NOISE MODEL

The channel noise of an epitaxial channel and diffused gate FET has been calculated from a quasi-unidimensional numerical analysis.

The model takes into account the electrical data (mobility and diffusion laws versus electric field | 5 || 6 |) obtained on Si bulk material and the technological data given by the manufacturer (Thomson-Sescosem, France) such as geometry, resistivity, diffusions...

This computer simulation is carried out by sampling in slice the whole channel of the FET in common gate configuration from the source to the drain contacts which first allows us to obtain the static and dynamic behaviour of the device | 7 |. The equivalent circuit of each slice considered as an elementary transistor is given on Fig. 1.

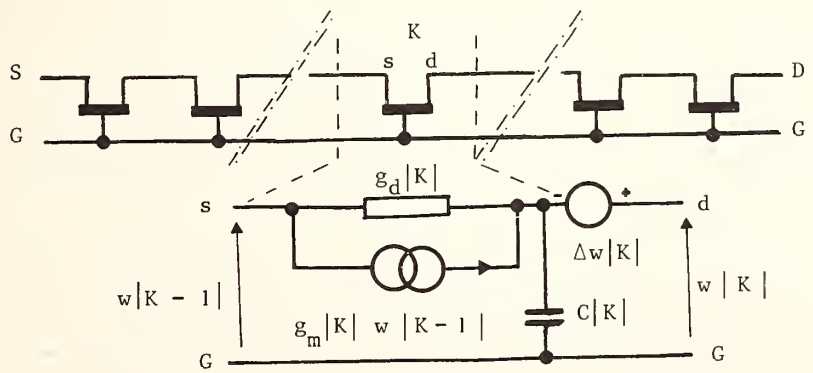

Figure 1

The noise of this elementary transistor is represented by the generator $\Delta W \mid K \mid$. (The equivalent circuit needs one generator since only $g_d \mid K \mid$ is noisy). With the aid of the transfer matrix of the elementary transistors located between the $K+1^{th}$ cell and the drain contact we obtain the output noise contribution of the K^{th} slice : $\Delta W_D \mid K \mid$ and $\Delta J_D \mid K \mid$. Assuming that all the elementary generators $\Delta W \mid K \mid$ are decorrelated, the output noise of the whole transistor is :

$$\Sigma_K \Delta W_D \mid K \mid \text{ and } \Sigma_K \Delta J_D \mid K \mid \quad \text{(Fig.2.a)}$$

Then the input noise generators E_n and I_n can be obtained in the common source configuration (see (Fig. 2.b)) and we deduce with the admittance matrix the channel noise i_c and the induced gate noise i_g (see (Fig.2.c)) :

$$i_c = - y_{21} E_n$$

$$i_g = y_{11} E_n + I_n$$

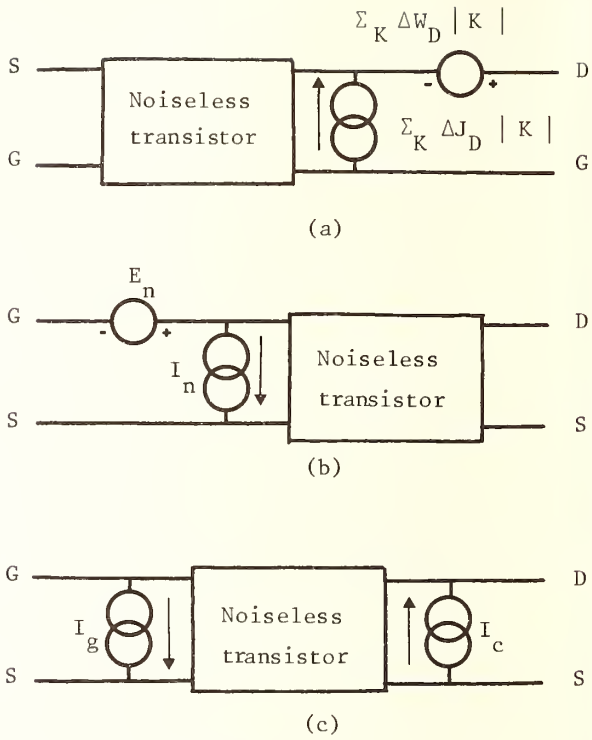

Figure 2

3. EXPRESSION FOR THE ELEMENTARY NOISE VOLTAGE GENERATOR

The noise voltage spectral density $\Delta S_V \mid K \mid$ of the K^{th} slice must be expressed as [3] :

$$\Delta S_V \mid K \mid = 4\, k\, \frac{T_n \mid K \mid}{g_d \mid K \mid}$$

where $g_d \mid K \mid = \left(\frac{\partial I_D}{\partial V_{ds}} \right)_{V_{gs}=cte}$ and $T_n \mid K \mid = T_n(E \mid K \mid)$ is the noise temperature which is different from the lattice temperature T_o, since electric field is high.

This expression differs from the one used by Van der Ziel in that :
i) the lattice temperature T_o is replaced by the noise temperature T_n.
ii) we use the differential conductance instead of the d.c. conductance.
iii) we include in the g_d calculation the mobility law given by Jacoboni et al. [5].

The noise temperature $T_n(E)$ of hot carriers in n-Si has been measured on homogeneous bars at 300 K and 77 K [3] [8]. From these measurements we have deduced two empirical laws :

$$T_n(E) = T_o \, (1 + 1.72\ 10^{-6} \mid E \mid^{1.02}) \text{ for 300 K}$$

and

$$T_n(E) = T_o \, (1 + 3.66\ 10^{-6} \mid E \mid^{1.43}) \text{ for 77 K.}$$

4. RESULTS

The thermal channel noise has been measured at 100 kHz using a pulse technique (pulses of 5 ms duration at repetition rate of 0.1 s) in order to avoid heating effects of the device.

Figure 3 shows a comparison between the experimental and computed data at 300 K and 77 K.

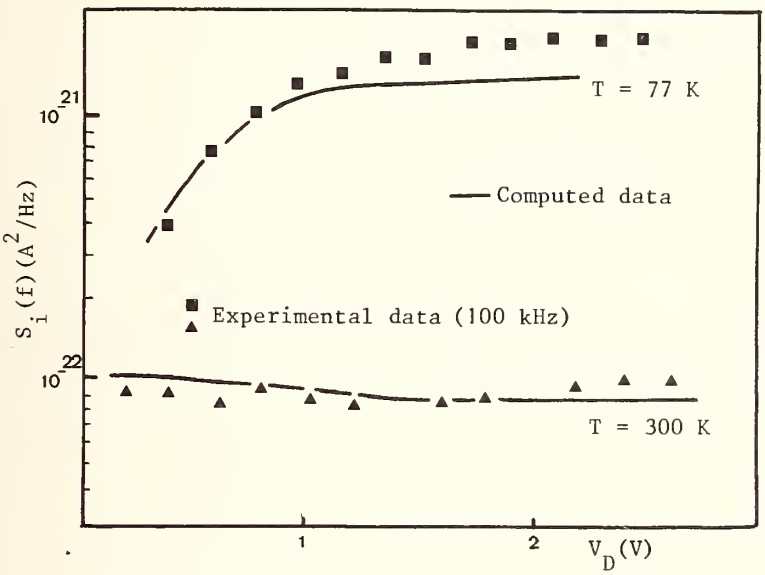

Figure 3

In the saturation range, the discrepancy with the experimental data may be due to the failure of the unidimensional approach for modelling (gradual channel hypothesis). Furthermore at 77 K because of the ionization effect of phosphorus impurities, the characteristics modelling is less accurate [4] and it must be remembered that the excess noise temperature can increase by a factor of two according to the direction of measurement so that the agreement of the computed curve is quite satisfactory.

This model allowed us also to compute the behaviour at high frequencies of the channel noise, the induced gate noise, their correlation and the noise figure.

CONCLUSION

In spite of the roughness of the approximations used for modelling the I.V. characteristics and the noise temperature the agreement between experimental and computed data is satisfactory. Especially at 77 K, the present theory gives results 30 % lower than the experimental curve but compared with other noise calculations [3] this result is better. To improve this model we need experimental data for the mobility and the noise temperature at very high electric field for usual doping levels. Nevertheless this paper gives a way for

modelling every one dimensional device where hot carriers play an important part.

ACKNOWLEDGMENT

The authors wish to thank SESCOSEM France for supplying the devices used in this study and Prof. J.P. Nougier for many helpful suggestions.

REFERENCES

| 1 | A. Van der Ziel, Proc. I.R.E. 50 p. 1808-1812 (1962)

| 2 | A. Van der Ziel, S.S.E. 14, p. 347-350 (1971)

| 3 | J.P. Nougier et al., S.S.E. 21, 133-138 (1978)

| 4 | A. Van der Ziel et al., S.S.E. 22, 177-179 (1979)

| 5 | C. Jacoboni et al., S.S.E. 20, 77-89 (1977)

| 6 | J.P. Nougier et al., Physical Review B, 11, 1497-1502 (1975)

| 7 | D. Sodini, S.S.E. to be published

| 8 | M. Rolland, J.P. Nougier, Proc. 13th Int. Conf. Phys. Semicond., Roma, p.1227 (1976).

NOISE AND SCALING PROPERTIES OF SUBTHRESHOLD MOSFETS

S.T. Liu

Honeywell Corporate Technology Center
Bloomington, MN 55420

J.S.T. Huang
Honeywell Solid State Division
Plymouth, MN 55441

INTRODUCTION

The high frequency noise in subthreshold (weakly inverted) MOSFET was recently reported to be thermal noise given by Liu and van der Ziel [1]

$$S_v = 4kTR_n = 4kT \frac{n^*\alpha}{\beta I} \tag{1}$$

where $\alpha = 2/3$, n^* and β are parameters defined in the subthreshold drain current equation. The drain current of an n-channel MOSFET in subthreshold region has been given by van Overstraeten, et.al.[2]

$$I = \frac{W}{L} \mu C_D^* \frac{n^*}{m^*} \frac{1}{\beta^2} \exp\left(\frac{-\beta\phi_F}{2}\right) \exp\left(\frac{\beta(V_G - V_G^*)}{n^*}\right) X \left[1-\exp\left(-\frac{m^*\beta V_D}{n^*}\right)\right], \quad V_G < V_T \tag{2}$$

and C_D^* is the depletion capacitance per unit area at $\phi_s = 3\phi_F/2$ and $\beta = q/kT$. The constants n^* and m^* are capacitance ratios evaluated at the surface potential $\phi_s = 3\phi_F/2$ and defined as $n^* = (1 + C_D^*/C_{ox} + qN_{ss}/C_{ox})$ and $m^* = (1 + C_D^*/C_{ox})$, where C_{ox} is the oxide capacitance per unit area and N_{ss} the surface state density. The constant V_G^* is the gate voltage at $\phi_s = 3\phi_F/2$ and V_T is the threshold voltage.

In this paper, we present both low frequency and high frequency noise data and correlate the results with the parameters n^* and m^* defined in the current equation. We also assess the scaling parameters which affect the performance of these subthreshold MOSFETS.

EXPERIMENTAL RESULTS AND DISCUSSIONS

Figure 1 shows the I-V characteristics of an n-channel MOSFET in subthreshold regions. This device has an oxide thickness of 1100 Å, gate area of $2.56 \times 10^{-6}cm^2$ and threshold doping density of $0.8 \times 10^{16}cm^{-3}$. The source and drain regions are formed using Arsenic implantation and the junction depths are about 0.35μm. This device has a threshold voltage of 0.95 V. In the exponential region, the parameter n^* was evaluated to be 2.5 from the slope of the I-V characteristics.

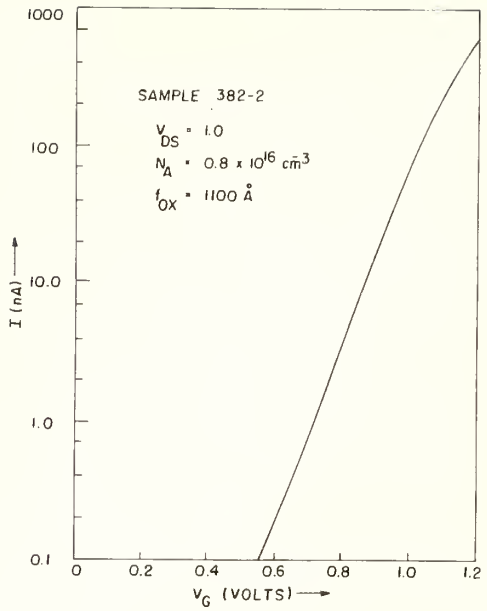

Fig. 1 I-V_G of a subthreshold MOSFET

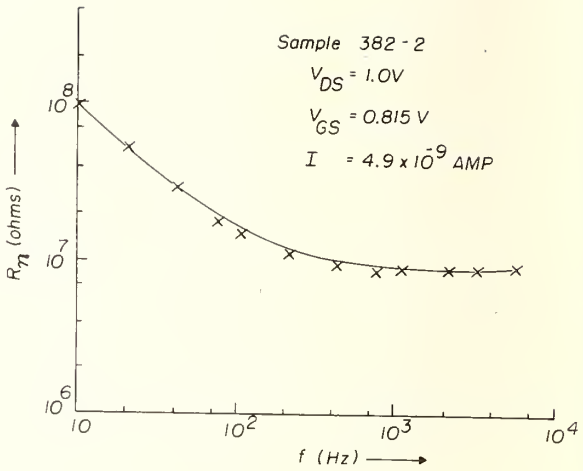

Fig. 2 Noise resistance of a subthreshold MOSFET

Figure 2 shows the noise resistance R_n as a function of frequency for this device at a subthreshold current of 4.9 X 10^{-9} Ampere and a drain bias of 1 V. The result is fitted to

$$R_n = \frac{8.75 \text{ X } 10^8}{f} + 9.06 \text{ X } 10^6 \text{ ohms.} \tag{3}$$

From eq (1) the high frequency noise resistance is

$$R_n = \frac{2}{3} \frac{n^*}{\beta I} = 8.8 \text{ X } 10^6 \text{ ohms}$$

which is close to the observed value of 9.06 X 10^6.

According to van der Ziel, the limiting 1/f noise is set by the dielectric loss in the oxide and is given by [3]

$$R_n = \frac{\tan \delta}{\omega C} \tag{4}$$

where C is the gate capacitance and tan δ is the loss tangent of the oxide. If we take C and tan δ as the effective gate capacitance and the effective loss tangent, we have

$$\frac{1}{C} = \frac{1}{C_{ox} WL} + \frac{1}{C_D^* WL} \tag{5}$$

where WL is the gate area. For this device, WL = 256 $(\mu m)^2$, C_{ox} = 3.13 X 10^{-8} F cm^{-2}, C_D^* = 3.6 X 10^{-8} F cm^{-2}. From 1/f noise data, we evaluate tan δ_{ox} to be 2.4 X 10^{-4}. The loss tangent of 2.4 X 10^{-4} is not unreasonable because the value of tan δ is 0.7 X 10^{-4} for quartz [4]. Equation (4) can be rewritten in terms of m* as:

$$R_n = \tan\delta \left(\frac{m^*}{m^* - 1}\right) \left(\frac{1}{\omega\varepsilon_{ox}\varepsilon_o}\right) \left(\frac{t_{ox}}{WL}\right) \qquad (4a)$$

where $\varepsilon_{ox} = 3.9$ is the dielectric constant of SiO_2. We see from eq (4a) that the limiting 1/f noise is proportional to t_{ox} and inversely proportional to the gate area WL, which is seen in samples with tan $\delta < 10^{-4}$. Further, it is related to the parameter m* as m*/(m*-1). It should be pointed out that m* may be frequency dependent since the low frequency noise data varies slower than 1/f in some devices. Another point is that the N_{ss} contribution is absorbed in the tan δ term. It means the trapping and detrapping in the interface would give rise to the ac loss.

The dependence of the noise on gate area is shown in Fig. 3 for two sets of devices at f = 40 Hz. One set of devices has an oxide thickness of 1100 Å and the other 540 Å. It is clear from the figure that the noise spectrum is inversely proportional to the gate area as expected, except for devices with small channel length. The noise in short channel devices is observed to be higher than the long channel devices. This may be due to the high field effect which was not investigated here. It is clear also from the figure that the noise in thinner oxide devices is smaller than those devices with thicker oxide for the same gate area.

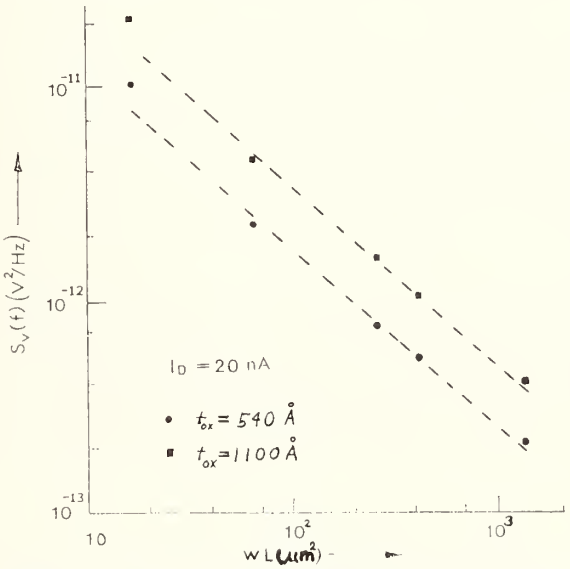

Fig. 3 Gate area dependence of 1/f noise

The effect of oxide thickness scaling on I-V characteristics is further examined in Figure 4. In the exponential region the parameter n* is evaluated to be 2.5 for t_{ox} = 1100 Å and 1.9 for t_{ox} = 540 Å for the same threshold doping density. It is clear that scaling down t_{ox} improves the parameter n*. We do not scale upward the doping density N_A, because n* and m* would increase through C_D^*, which scales slower than the square root of N_A ratio. Scaling up N_A would certainly degrade the I-V (eq (2)) and the noise as given by eq (1) and (4a). It is often necessary to scale up N_A as channel length L is scaled down in order to avoid punch through [5]. From the figures, the parameters V_G^* are V_G^* = 0.584 V for t_{ox} = 1100 Å and V_G^* = 0.152 V for t_{ox} = 540 Å. The threshold voltages are respectively 0.95 V and 0.55 V. Therefore, we see $(V_G^* - V_G'^*) \simeq (V_T - V_T')$. We can therefore maintain the operating voltage by letting $(V_G - V_G') \simeq (V_T - V_T')$ while maintaining the same subthreshold current level.

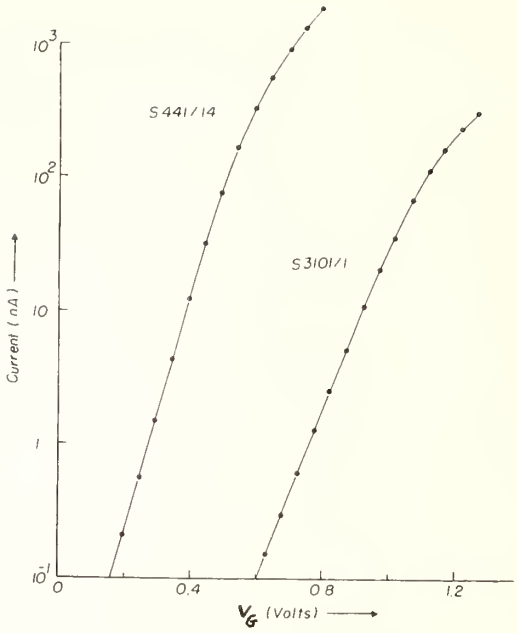

Fig. 4 Effect of gate oxide thickness on I-V (S441/14 t_{ox} = 540 Å, S3101/1 t_{ox} = 1100 Å)

CONCLUSION

It is clear from the 1/f noise results discussed that we should not scale down the gate area or scale up doping density for linear circuit application where noise is an important consideration. We can, however, scale down the oxide thickness to improve the noise performance. In so doing we maintain the operating voltage difference as the difference of the threshold voltages between the unscaled and scaled devices. Further, we have related the high frequency noise to the parameter n* and the low frequency noise to the parameter m*.

ACKNOWLEDGEMENT

We would like to thank Prof. A. van der Ziel of the University of Minnesota for a fruitful discussion and Mr. M. Vogt for the measurement.

REFERENCES

[1] S.T. Liu and A. van der Ziel, Appl. phys. Lett. 37, 950 (1980).

[2] R.J. van Overstraeten, G.J. Declerck, and P.A. Muls, IEEE Trans. Electron. Devices ED-22, 282 (1975).

[3] A van der Ziel, Solid St. Electron. 18, 1031 (1975).

[4] W. Espe, Werkstoffkunde der Hochvakuumtechnik, Band II, p463, VEB Deutscher Verlag der Wissenshaften, Berlin (1960).

[5] R.W. Keyes, Proceedings of the IEEE 63, 740 (1975).

THE DEPENDENCE OF THE LOW FREQUENCY NOISE OF JFETs ON DEVICE PARAMETERS AND OPERATING CONDITIONS

C.E. Cox and K. Kandiah

U.K. Atomic Energy Authority
Harwell, Didcot, Oxon

1. INTRODUCTION

The important physical mechanisms which generate noise in the drain current of JFETs are fluctuations of carrier velocity and density in the channel and modulation of the current by charge state fluctuations at defects situated in the depletion or Debye regions adjoining the channel. The power spectrum of the noise is dependent on temperature and device parameters. Papers on noise generally deal with individual mechanisms and sometimes fall short of practical information relating to device parameters.

Recent work *[1,2]* on low frequency noise in JFETs has given a better understanding of the responsible mechanisms. In this paper we expand those studies to cover variable operating conditions. The emphasis is on the performance of 4-terminal silicon JFETs at frequencies below a few MHz. In section 2 we briefly review current understanding of the major noise sources. In the later sections we study the dependence of noise on temperature, bias conditions and device gate width for a fixed manufacturing technology.

2. MAJOR NOISE SOURCES

Noise due to thermal agitation of the carriers in the channel is always present and is well understood. It has a white noise spectrum and the equivalent noise resistance R_n in series with the gate for a three terminal device is inversely proportional to the mutual conductance g. In 4-terminal JFETs it will be more convenient to consider the drain current noise I_n since the signal is applied only to one gate. We have

$$(I_{nt})^2 = 4kTg\Gamma \qquad (1)$$

where I_{nt} is the thermal drain noise current, T is the temperature, k is Boltzmann's constant and Γ is a constant.

Fluctuations of carrier density due to incomplete ionisation of the dopant atoms in the channel *[3]* cause an increase in the noise at lower temperatures. In the case of phosphorous doped silicon the effect is observable at temperatures below 125K and is independent of frequency for temperatures greater than 75K.

Low frequency noise due to defects present in the Debye region adjacent to the channel gives noise peaks in certain temperature bands depending on the energy level of the defect. This is usually the most significant source of low frequency noise. At temperatures greater than about 220K low frequency noise can be generated by defects with near midband energy levels even when they are situated in the fully depleted region between the gate and the channel *[4]*. I_{nd} is the total drain noise current due to defects.

3. TEMPERATURE AND SUBSTRATE BIAS DEPENDENCE AT CONSTANT DRAIN CURRENT

Figure 1 shows I_n at 100kHz as a function of temperature at fixed drain current for three very different substrate voltages. It is seen that above 125K, where I_{nt} is the major component at this frequency, the noise is independent of substrate bias and temperature. This behaviour is consistent with eq (1) since g is approximately inversely proportional to temperature and independent of substrate voltage. If the noise had been expressed as R_n it

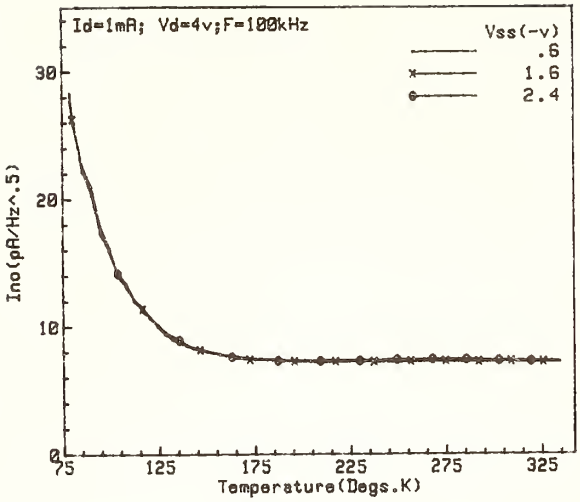

Fig 1 The dependence of noise current on temperature and substrate bias measured at 100kHz. Device XS01. 620μm gate width

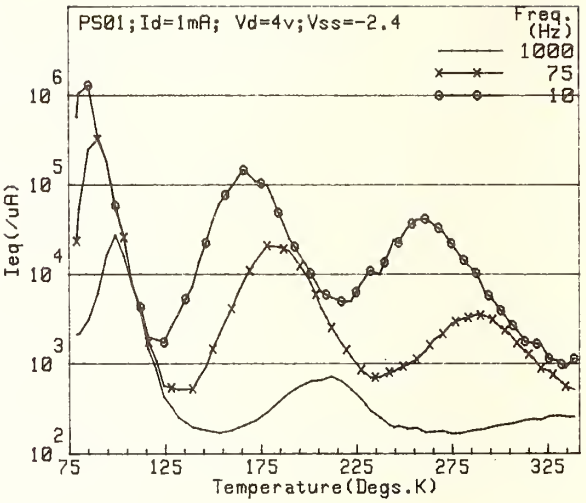

Fig 2 The dependence of low frequency noise on temperature. Device PS01. 620μm gate width

would have shown both a temperature and substrate bias dependence. Below 125K the predicted increase in noise due to carrier density fluctuations *[3]* is observed.

In figure 2 I_{nd} is seen to exhibit peaks as a function of temperature at the lower frequencies, the temperature for peak noise varying with frequency. In most devices studied three temperatures corresponding to noise peaks at 10Hz are seen at about 85K, 170K and 270K. The magnitude of the two higher temperature peaks has been shown to be strongly dependent on the substrate bias *[2]*. The degree of substrate bias dependence of the peak at 85K varies widely with the device. The magnitude of the noise in the valley regions falls at bias voltages at which the noise at the peaks is very low. However the valley noise does not fall below a level I_{np}, called the plateau noise level, which consists of a component with a 1/f spectrum adding to the thermal noise. I_{np} increases smoothly by a few percent from 100K to 300K but is seen to decrease at temperatures above 300K.

Figure 3 illustrates the dependence of I_{nd} on substrate bias at a fixed temperature for a device of 620μm gate width and shows the generation of noise peaks when a point defect is positioned in the Debye region. For any given defect at a fixed drain current the magnitude of the noise peak at the optimum activation temperature for each frequency has a 1/f spectrum.

4. DRAIN CURRENT AND DRAIN VOLTAGE DEPENDENCE

The movement of a low frequency noise peak with respect to substrate bias as the drain current is varied at constant temperature and drain voltage is shown in figure 3. The defect generating this peak is situated in the Debye region nearest the top gate electrode thus making the position of the peak dependent upon drain current. As expected, no such movement with drain current is observed for a defect positioned in the other Debye region nearest the substrate.

The magnitudes of I_{nt}, I_{nd} and I_{np} are all dependent upon drain current for fixed temperature and drain voltage. It can be seen in figure 3 that the magnitude of I_{nd} at 10Hz saturates at some drain current. A similar saturation effect is observed for I_{np}, but not for I_{nt} which continues to increase very slowly at high drain currents.

It is well known that I_{nt} is invariant at drain voltages at and above the pinch-off voltage. Little or no dependence of I_{nd} on drain voltage is observed, as the movement of the Debye region on the source side of the pinch-down region with drain voltage is negligible.

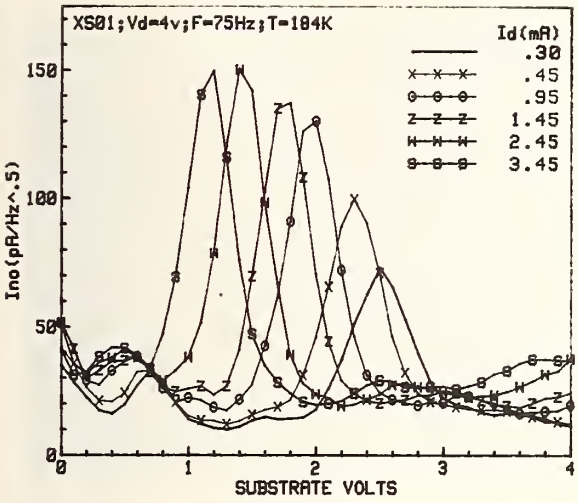

Fig 3 The dependence of low frequency noise on substrate bias and drain current. Device XS01. 620μm gate width

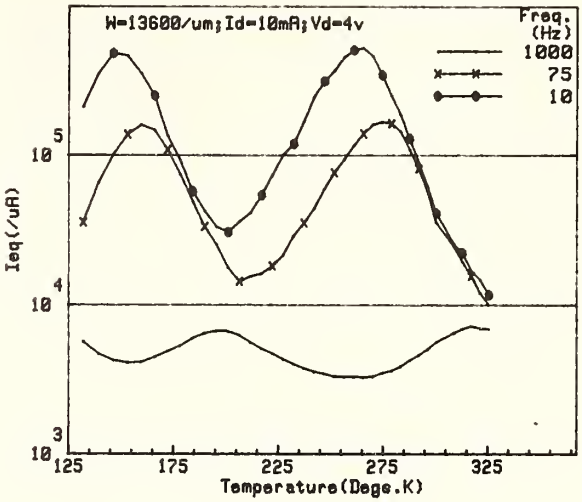

Fig 4 Dependence of low frequency noise on temperature for a large gate width device. Device YHA84. 13600μm gate width

5. DISCUSSION OF THE OBSERVED BEHAVIOUR AND DEPENDENCE UPON GATE WIDTH

Preliminary calculations *[5]* indicate that the effective modulation of the drain current by a point defect in the Debye region is approximately proportional to the local mean drift velocity u. It is believed that noise peaks are only observed from defects near the pinch-down region. A statistical analysis of the noise peak magnitudes in a large number of devices at 10Hz and 167K shows similar distributions for devices of 620μm and 1800μm gate width when operated with the same channel current density. It is found that the number of peaks observed per unit noise magnitude interval is independent of the magnitude of the peak (expressed as I_n) up to about $200pA(Hz)^{-\frac{1}{2}}$. A very small number of peaks are observed at higher magnitudes and are probably the result of the chance coincidence at some substrate bias of two or more peaks.

At sufficiently small drain currents and fixed frequency and temperature the magnitude of a noise peak generated by a defect near the pinch-down region is seen to decrease with decreasing drain current (figure 2). It is believed that at very low drain currents the width of the channel is so small that insufficient charge is available in the adjacent region of the channel for maximum modulation of the drain current to take place. A saturation of the peak magnitude is seen at higher drain currents as more than adequate charge is available. This effect is also observed for I_{np}.

The noise mechanism responsible for the generation of I_{np} is not fully understood but is thought to be connected with surface states near the pinch-down region. When devices are operated at similar channel current densities it is found that the maximum magnitude of I_{nd} due to a single defect near the pinch-down region is independent of gate width, and that I_{nt} and I_{np} (when expressed as an equivalent saturated diode current) are approximately proportional to the gate width. A statistical analysis of noise peaks shows that the number of defects observed per device (which is about six for a device of 620μm gate width) is also approximately proportional to the gate width. Figure 4 illustrates the dependence of I_{nd} on temperature at low frequencies for a device of 13600μm gate width. Assuming a defect density independent of device size many defects are expected to be present in the Debye region in this device at any one substrate bias and the summation of noise peaks at the peak temperatures can be seen.

We have measured the noise in a number of three-terminal JFETs as a function of drain current and temperature. At any measurement frequency the peaks of noise occurred at the same temperatures as in the four terminal devices. The magnitude of the noise peaks varied randomly by large amounts between samples of the same type and as a function of drain current for the same device. This is consistent with the present model *[2]*.

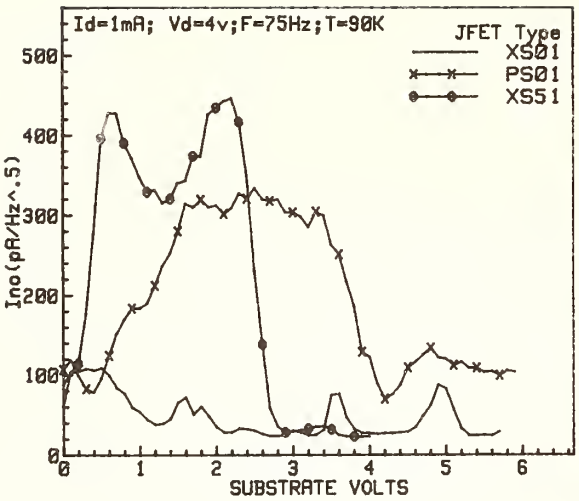

Fig 5 Dependence of low frequency noise on substrate bias at very low temperatures for 3 typical devices of 620μm gate width

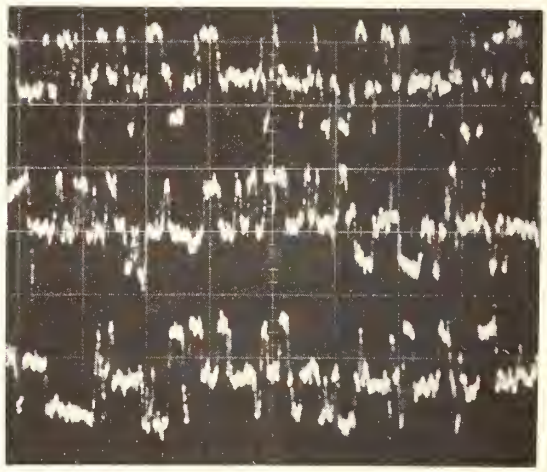

Fig 6 Waveform of drain current modulation at very low temperatures. Device PS01, T = 90K, Vertical 10nA/cm, Horizontal 10ms/cm

6. EFFECT AT TEMPERATURES BELOW 120K

The noise at 75Hz and 85K for three devices of 620μm gate width is shown in figure 5. Note that in some devices one large, broad peak is observed rather than many individual peaks. It is seen in figure 2 that there are characteristic temperatures at which the noise has a maximum at each frequency. An analysis of these peaks suggests the existence of a shallow defect with an energy level of about 190meV below the conduction band. If the increase in noise below 120K was entirely due to carrier density fluctuations the noise would be independent of frequency below a few MHz.

In many devices studied a three-level random telegraph signal drain current waveform has been observed directly as shown in figure 6 especially when the temperature and bias conditions correspond to the broad peaks in figure 5. An adequate explanation of this behaviour has not been found.

ACKNOWLEDGEMENTS

The authors are indebted to M.O. Deighton for discussions on the mechanism of drain current modulation in a JFET and F.B. Whiting and D. Lloyd for assistance with the measurements. Some of the devices used in our work were produced under a programme funded by M.O.D.(DCVD).

REFERENCES

[1] K. Kandiah and F.B. Whiting, *Solid State Electronics*, 21, pp 1079-1088, April 1978

[2] K. Kandiah, M.O. Deighton and F.B. Whiting, this conference

[3] A. Van der Ziel, *Proc. IEEE*, 51, p.1670, November 1963

[4] C.T. Sah, *Proc. IEEE*, 52, pp 795-814, July 1964

[5] M.O. Deighton, private communication

THE CHARACTERISTICS OF NOISE DUE TO INDIVIDUAL DEFECTS IN JFETs

K. Kandiah, M.O. Deighton and F.B. Whiting

U.K. Atomic Energy Authority
Harwell, Didcot, Oxon

1. INTRODUCTION

Low-frequency noise in JFETs has been attributed *[1]* to charge fluctuations at electrically active centres (defects) situated in the gate-to-channel depletion region. The spectrum of this component of noise is strongly dependent on temperature and frequency *[2,3]*, varying as f^{-n} over a large part of the spectrum where f is the frequency and n lies between 1 and 2. Sah's model *[1]* accounts for the noise due to defects with an energy level near midband at temperatures above about 220K. Experimental confirmation of this model comes from noise measurements in which a high density of defects with a deep level, such as gold impurities, were introduced into the device. Most of the published work on low-frequency noise deals with defects with energy levels near midband owing to the interest in the use of the devices at room temperature. Measurements on some neutron irradiated JFETs *[4]* and normal devices *[2,3]* showed the presence of shallower level defects but no model describing the mechanism in detail has been published.

This paper discusses noise in JFETs caused by point defects with arbitrary energy levels and physical location in the device as a function of temperature and frequency. In section 2 we present some noise measurements on low noise 4-terminal JFETs and introduce the principles of a model which explains these results. In section 3 we examine charge transitions at point defects. Finally the drain current noise as a function of temperature and carrier density at the defect is discussed in section 4.

2. NOISE IN 4-TERMINAL JFETs

The JFETs used in our experiments were silicon n-channel 4-terminal types in which separate connections are available to the gates on either side of the channel. The channel is in an epitaxial layer with a dopant concentration of about $10^{16}cm^{-3}$ on a p+ substrate which acts as one gate. The other gate (top gate) is formed with a p+ diffusion into the top of the epitaxial layer giving a gate length of about 2.5μm. All the results reported in this paper are on JFETs with gate widths of 620μm but devices with a range of gate widths are discussed in another paper *[5]*.

In each set of measurements the drain voltage V_d and current I_d were maintained at predetermined values and the drain current noise was measured as functions of substrate bias voltage V_{ss} and temperature. When the V_{ss} is varied the measurement system automatically adjusts the top gate bias voltage to maintain the desired constant V_d and I_d. This variation of V_{ss} therefore shifts the position of the channel in a direction normal to the substrate. Each noise current reading was calibrated measuring the response to a current from a pseudo-random telegraph signal generator, with an accurately known amplitude and clock frequency, injected into the drain. The filters used for noise measurements had about 20% bandwidth with centre frequencies in the range 10Hz to 100kHz. A servo system was used to maintain the device temperature within ±0.5K of any temperature in the range 79K to 335K.

Typical results showing the variation of noise with temperature for fixed bias conditions are shown in figure 1. These results indicate the presence of 3 types of defects which generate noise in three (overlapping) temperature ranges. Referring to the noise at 10Hz the ranges are A (<70K to 130K), B (110K to 230K) and C (200K to 350K). We have observed that the heights of the noise peaks in the temperature ranges B and C vary independently with bias.

The variation of noise with substrate bias in two different JFETs, at various fixed temperatures in regions B and C, is shown in figure 2 and figure 3. In general the positions of the peaks (in terms of substrate voltage) in the different temperature ranges do not correspond for the same drain current and drain voltage. The peaks are wider (expressed in substrate volts) for the larger values of substrate voltage but are of nearly constant width when expressed in terms of the distance moved by the channel. The peak shapes are not dependent on device type when there is no overlap between peaks.

The interpretation of these results is that each noise peak in figure 2 and figure 3 is generated by a point defect when it is situated in the Debye region between the neutral channel and the fully depleted region. The term 'Debye region' is used in preference to 'transition region' in order to avoid confusion, since we often refer to charge transitions. The significance of the peak positions in figure 2 and figure 3 is that the noise is maximum at a given frequency when the substrate bias places the defect at a position in the Debye region, where the carrier capture rate and the emission rate match the frequency. A typical waveform of drain current modulation in this case is seen in figure 4.

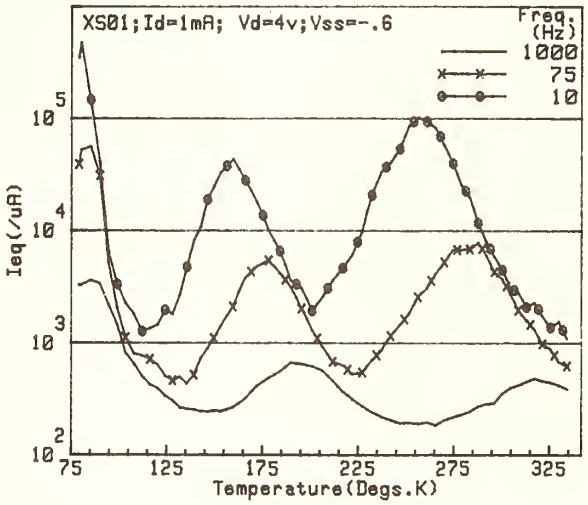

Fig 1 Drain current noise vs temperature for fixed bias at 1000Hz, 75Hz and 10Hz

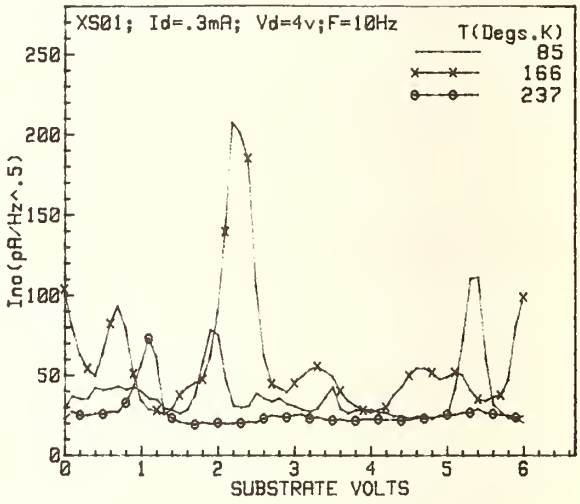

Fig 2 Drain current noise vs substrate bias in JFET type XS01

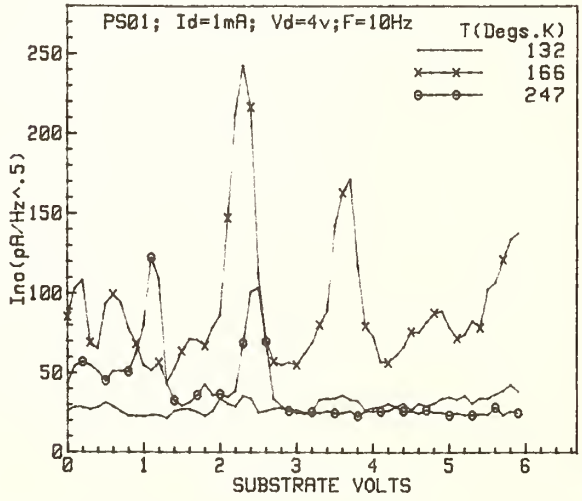

Fig 3 Drain current noise vs substrate bias in JFET type PS01

Fig 4 Waveform of drain current modulation vertical 5nA/cm, horizontal 5ms/cm

3. CHARGE TRANSITIONS AT POINT DEFECTS

Charge transitions due to electron capture and emission take place with a characteristic capture time τ_1 and emission time τ_2 given by

$$\tau_1 = 1/nv_{th}\sigma \quad (1)$$

$$\tau_2 = (1/N_c\, v_{th}\sigma)\, \exp\,(E/kT) \quad (2)$$

where v_{th} is the mean thermal velocity and n the density of free electrons, σ is the capture cross-section of the defect, N_c is the density of states in the conduction band, E the defect energy level, T the temperature and k Boltzmann's constant. Similar expressions apply for the capture and emission of holes with appropriate values for the parameters. In uncompensated n-channel JFETs hole capture can only take place when holes are generated by avalanche multiplication in high-field regions of the channel. We ignore this possibility, leaving electron emission as the only possible route for a charge transition to the more positive state. A defect in the depletion region can acquire an electron only by hole emission, owing to a virtual absence of any carriers in this region. On the other hand, a defect in the channel or Debye regions can undergo such a transition either by hole emission or electron capture. We therefore consider a Markov chain in which electron emission is followed either by electron capture or hole emission.

In general, acquisition of an electron by a defect is governed by two characteristic times, τ_{1c} and τ_{1e} representing the respective probabilities of the two competing processes. τ_{1c} is given by eq (1), while τ_{1e} is a version of eq (2) modified for holes. The two probabilities are simply additive and we have a net electron acquisition time τ_1, where

$$1/\tau_1 = 1/\tau_{1c} + 1/\tau_{1e} \quad (3)$$

Thus, τ_1 tends to a finite upper limit (τ_{1e}) as the defect moves into the fully depleted region where τ_{1c} is nearly infinite.

4. DRAIN CURRENT NOISE AS A FUNCTION OF TEMPERATURE AND BIAS

The two distinct aspects of the present theory of drain current noise i_n (f) are:

(i) the mechanism by which a charge increment $\pm q$ (the electron charge) at a defect causes a change $\pm\Delta I_D$ in drain current of a JFET (this is the subject of a separate study)

and (ii) the influence of the independent time parameters τ_1 and τ_2 on the frequency spectrum of the noise, and hence on the amount passing through the measurement filter.

In this paper we are chiefly concerned with (ii). The noise current waveform at the drain consists of alternate positive and negative steps ΔI_D, assumed to be constant and separated by randomly variable intervals having mean values τ_1 at one level and τ_2 at the other. Such an asymmetric random telegraph signal has been shown by Machlup *[6]* to have a well-known spectrum shape $1/(1 + \omega^2\tau^2_c)$ with a corner frequency (or time constant τ_c) given by:

$$1/\tau_c = 1/\tau_1 + 1/\tau_2 \quad (4)$$

If this noise is passed through a narrow-band filter, centred at frequency f (= $1/2\pi\tau$) and of bandwidth Δf, the resulting output noise can conveniently be written in terms of the normalised parameters x(= τ_1/τ) and y(= τ_2/τ):

$$I_n^2 = i_n^2(f)\,\Delta f = \tau(\Delta I_D)^2\,\Delta f \cdot \frac{4x^2y^2}{(x+y)^3 + x^2y^2(x+y)} \qquad (5)$$

The last fraction has maximum possible value 0.5 when x = y = 2. If either x or y is held constant at a value other than 2, while the other is varied, then the filtered noise plotted as a function of this variable shows a smaller peak displaced to one side or the other of the main peak. Since τ_1 is related to local electron density i.e. to substrate bias, while τ_2 depends mainly on temperature and defect energy level, one can interpret many features of the measurements directly as properties of the function of x, y above.

The observed behaviour of the peaks of noise is in line with this model. The measured widths and shapes of the noise peaks as a function of substrate bias agree with changes in carrier concentration at the defect estimated from the movement of channel position. The expected asymmetry of the peaks and the higher level of noise on one side due to hole emission (at T > 250K), as discussed in section 3, are also observed as in the noise at 247K in figure 3. The movement of the position of the highest peaks (when x = y = 2), found to be about 0.35v for a change in frequency from 1000Hz to 100Hz for the temperature range C, also agrees with the predictions.

In our theoretical model we have assumed that ΔI_D is independent of τ_1 and τ_2 over the limited range where the defect is most active. We have observed that the magnitude of the step in the drain current waveform, as seen in figure 4, does not change significantly as the substrate bias and temperature are varied although the mean dwell times τ_1 and τ_2 in the two states behave as predicted.

Measurements of the temperatures at which the noise is a maximum for various values of τ will yield activation energies for the defects. We have found a scatter in these measured energy levels which cannot be attributed to experimental error. Possible explanations could be the variation in τ_2 due to the large varying electric fields around the pinched down region of the channel or the dependence of τ_1 on the crystal orientation in relation to the direction of maximum gradient of carrier velocity and density at the defect. The three energy levels for the temperatures ranges A, B and C are .15 ± .04eV, .28 ± .02eV and 0.56 ± .03eV respectively with σ having values in the range 10^{-14}cm^2 to 10^{-17}cm^2.

5. ACKNOWLEDGEMENTS

The JFETs used in our work were produced as part of a programme funded by M.O.D.(DCVD). We are also indebted to Mr. D. Colman for valuable discussions during the earlier measurements.

REFERENCES

[1] C.T. Sah, *Proc. IEEE*, 52, pp 795-814, July 1964

[2] J.W. Haslett and E.J.M. Kendall, *IEEE Trans Electron Devices*, ED-19, pp 943-950, August 1971

[3] J. Llacer and D.F. Meier, *IEEE Trans. Nucl. Sci*, NS-24, pp 317-326, February 1977

[4] K.K. Wang, A. Van der Ziel and E. Chennette, *IEEE Trans. Electron Devices*, ED-22, pp 591-593, August 1975

[5] C.E. Cox and K. Kandiah, this conference

[6] S. Machlup, *Jnl. App. Phys.*, 25, pp 341-343, March 1954

NOISE DUE TO FAST SURFACE STATES IN MOSFETs

H. Mehta and K. M. van Vliet

Department of Electrical Engineering
University of Florida
Gainesville, Florida 32611

INTRODUCTION

McWhorter's theory of 1/f noise due to tunneling of conduction carriers (say electrons in an n-type channel) via interface states to oxide traps is very suitable for explaining low-frequency 1/f noise in MOSFETs [1]. A detailed investigation of the applicability of this theory to MOSFETs has recently been made by van der Ziel [2]. Though basically this theory involves density fluctuations, the fluctuating trap occupancy also causes surface mobility fluctuations due to ionized impurity scattering. The combined effect is accounted for by a modulation factor $[1+(N/\mu)(d\mu/dN)]$. In order to obtain 1/f noise, one invokes the well-known distribution of time constants $g(\tau)\propto 1/\tau$, which results from a uniform distribution in tunneling widths. However, there is a limit to the lowest possible relaxation time, set by the interaction of the channel carriers with the fast surface states at the oxide channel interface, since no recombination can be faster than this interaction, even if the tunneling time becomes very small. Also, the bulk lifetime plays a role. If the bulk lifetime is smaller than the time to recombine via fast surface states, then this sets an upper limit to the occurring of 1/f noise due to the McWhorter-van der Ziel model. Yet, experimentally the 1/f noise may occur over several decades beyond this limit.

In this paper we will show that, where the McWhorter-van der Ziel spectrum ends, a new 1/f noise regime occurs due to the stochastic generation-recombination of carriers via the fast surface states, and the associated carrier diffusion to these states. In this respect we point out that all older theories involving surface generation-recombination are incomplete (Champlin [3], Hyde [4], van Vliet-Fassett [5], Lax-Mengert [6]). These theories have correctly dealt with the effect of the *response* modification of transport noise due to the surface generation-recombination path; usually the response changes from $1/\omega^2$ to $1/\omega^{3/2}$, typical for the carrier diffusion to the surface states; however, these theories have not considered the noise *source* associated with this surface generation-recombination process. This was for the first time considered by Mehta and van Vliet [7,8].

We basically consider three models: (1) We formulate the equations for a bulk semiconductor with surface recombination at both sides and with a stochastic surface source. We set the bulk noise source equal to zero. Thus this noise must be *added* to the spectra due to references [3 to 6] stemming from the volume noise source--modified by the boundary conditions involving surface recombination as explained above. (2) We consider a MOSFET with an inversion layer serving as the channel, with surface recombination both on the oxide side and at the bulk semiconductor side. The noise concerns here the carrier population in the carrier enriched channel only; we take the mobility and lifetime to be uniform over the entire channel-semiconductor region. (3) Finally, we consider a MOSFET model with surface recombination at the oxice side and reflection of the current at the semiconductor side, with the mobility and carrier lifetime in the channel being different from those in the bulk semiconductor.

COMPUTATION OF THE NOISE

The transport problem is described by the following equation:

$$\frac{\partial \Delta n(x,t)}{\partial t} - D\frac{\partial^2 \Delta n(x,t)}{\partial x^2} + \frac{\Delta n(x,t)}{\tau_b} = \xi(x,t) \quad , \tag{1}$$

where τ_b is the bulk lifetime and ξ is the sum of volume g-r source and diffusion source, x is the coordinate perpendicular to the oxide surface interface. The boundary conditions are taken to be

$$D \frac{\partial \Delta n}{\partial x}\Big|_{x=0} - \sigma \Delta n\Big|_{x=0} = \zeta(t) \tag{2a}$$

$$D \frac{\partial \Delta n}{\partial x}\Big|_{x=W} + \sigma \Delta n\Big|_{x=W} = \zeta(t) \tag{2b}$$

where D is the diffusion constant and σ is the surface recombination velocity; ζ is the surface Langevin noise source. Since we are interested in the noise due to the surface noise source, we set $\xi = 0$. The surface noise source ζ has the spectrum

$$S_\zeta = 4M\alpha N_o \sigma / A \tag{3}$$

where N_o is the number of surface carriers and where M is a modulation factor, which accounts for the fact that the noise is enhanced due to the effect of band bending caused by the surface charge on the recombination velocity σ (see also McWhorter's theory), $\alpha = \langle \Delta n^2 \rangle / n_o$.

The noise is calculated using the Green's function procedure. The response of $\Delta n(x)$ due to the surface source is characterized by the Fourier-Laplace transformed surface Green's function [10] $H(x,0,i\omega)$; then for the carrier density fluctuation spectrum of $\langle \Delta n(x,t) \Delta n(x',t) \rangle$ we have

$$S_{\Delta n}(x,x',\omega) = H(x,0,i\omega)\, H(x',0,-i\omega)\, S_\zeta \,. \tag{4}$$

For the first problem the carrier density fluctuations in the whole sample are of importance. Thus, if $\bar{n}$ is the average number of carriers in the sample, then from (4)

$$S_{\Delta \bar{n}}(\omega) = \frac{S_\zeta}{\sigma^2} \left| \frac{\sigma}{W} \int_o^W H(x,0,i\omega)\, dx \right|^2 , \tag{5}$$

where W is the thickness of the sample. Thus for the noise spectrum we must compute the response function

$$f(i\omega) = \frac{\sigma}{W} \int_o^W H(x,0,i\omega) \quad . \tag{6}$$

With the b.c. (2a) one easily shows that $H(x,0,i\omega) = (\alpha/D)\, G(x,0,i\omega)$, where

$$\alpha = \frac{Di\omega}{i\omega + 1/\tau} \tag{7}$$

and where G is the volume Green's function defined as in [5]. Explicitly, we obtained

$$f(i\omega) = \frac{-L[1-\cosh W/L - (D/\sigma L)\sinh W/L]}{W[1+(D^2/\sigma^2 L^2)]\sinh W/L + 2(DW/\sigma L)\cosh W/L} . \tag{8}$$

The normalized spectrum $\bar{S}(\omega)$ is $|f(i\omega)|^2$; $L = \sqrt{\alpha/i\omega}$. At sufficiently low frequencies we find

$$\bar{S}(\omega) \underset{\omega\to 0}{\approx} \left(\frac{1}{\sqrt{\frac{\tau_d \tau}{\tau_s^2}} + 2} \right)^2 \longrightarrow \text{constant} \tag{9}$$

Here $\tau_d = W^2/D$ is the diffusion time and $\tau_s = W/\sigma$ is the surface lifetime. At high frequencies we obtain

$$\bar{S}(\omega) \underset{\omega\to\infty}{\sim} \frac{1}{(\omega\tau_s)^2} \tag{10}$$

The spectrum closely resembles a Lorentzian.

Next we consider a MOSFET with inversion layer. For our purpose we shall approximate the carrier distribution such that

$$n = n_s, \quad 0 \le x \le W_1 \quad \text{(surface region)}$$

$$n = n_b, \quad W_1 \le x \le W \quad \text{(bulk region)} \tag{11}$$

where $n_s >> n_b$ and where $W = W_1 + W_2$, W_2 being the width of the bulk region. Though the carrier density in the bulk n_s is much less than the channel density n_s, carriers diffuse into the bulk and undergo bulk recombination and surface recombination at the other end. For simplicity we assume that the surface recombination velocity in the oxide and at the free surface of the semiconductor are the same. Thus the b.c. are again eqs (2a) and (2b). Also, we assume μ, D, and τ to be the same in the channel as in the bulk. The normalized spectrum is now obtained by integrating $H(x,0,i\omega)$ up to W_1 (instead of up to W as in eq (6); hence, we obtain

$$\bar{S}(\omega) = \frac{1}{W_1^2} \left| \frac{2L\left[\sinh\left(\frac{W_2}{L} + \frac{W_1}{2L}\right)\sinh\frac{W_1}{2L} + \frac{D}{\sigma L}\cosh\left(\frac{W_2}{L} + \frac{W_1}{2L}\right)\sinh\frac{W_1}{2L}\right]}{\left(1 + \frac{D^2}{\sigma^2 L^2}\right)\left[\sinh\frac{W_1}{L}\cosh\frac{W_2}{L} + \cosh\frac{W_1}{L}\sinh\frac{W_2}{L}\right] + \frac{2D}{\sigma L}(R)} \right|^2 \tag{12}$$

where

$$R = \left(\cosh\frac{W_1}{L}\cosh\frac{W_2}{L} + \sinh\frac{W_1}{L}\sinh\frac{W_2}{L}\right). \tag{12a}$$

At sufficiently low frequencies we find

$$\bar{S}(\omega) \underset{\omega\to 0}{\approx} \frac{\text{constant}}{\left(1 + \frac{\tau_s^2}{\tau_d \tau_b}\right)^2} \tag{13}$$

At intermediate frequencies we set $|W_1/L| << 1$ and $|W_2/L| >> 1$. In a straightforward manner we obtain

$$S(\omega) \approx \left| \frac{1 + \sqrt{D\sigma^{-2}(i\omega+1/\tau)}}{1 + D\sigma^{-2}(i\omega+1/\tau) + 2\sqrt{D\sigma^{-2}(i\omega+1\tau)}} \right|^2 . \qquad (14)$$

If in addition $\omega > 1/\tau$, we have

$$S(\omega) \underset{\omega\to\text{int}}{\approx} \frac{\tau'_d}{\tau'^2_s \omega} \qquad (15)$$

where now $\tau'_d = W_1^2/D$ and $\tau'_s = W_1/\sigma$. The spectrum shows 1/f behavior in this frequency range. For very high frequencies ($W_1/L >> 1$, $W_2/L >> 1$) we find

$$\bar{S}(\omega) \underset{\omega\to\infty}{\sim} \frac{\sigma^2}{W_1^2 \omega^2} \qquad (16)$$

The high frequency range is in practice never realized for we find that the 1/f and $1/f^2$ region meet at $\omega_o = D/W_1^2$. With D = 25 cm^2/sec and W_1 = 400A°, this yields $\omega_o = 1.6 \times 10^{12}$ rad/sec or f_o $25^o \times 10^{10}$hz. If $\tau_b = 10^{-4}$ sec, then the spectrum goes as 1/f for $2 \times 10^3 < f < 25 \times 10^{10}$, i.e., over eight decades!. Likely, however, the noise drowns in the white thermal noise at a much lower frequency. A computer plot of the full equation (12) is given in figure 1.

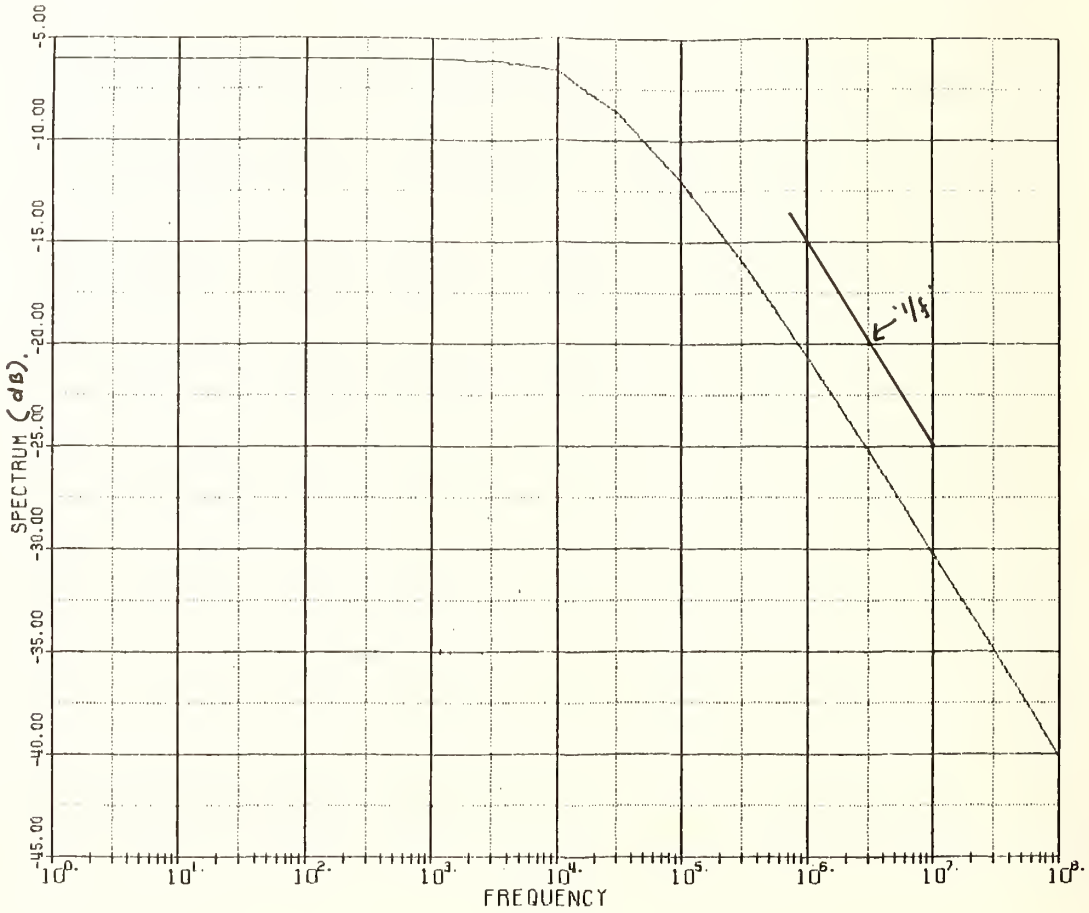

Finally, we consider a model in which D, μ, and τ are different in the channel and for the bulk, and we take the b.c. at x = W to be $D\nabla n = 0$. In this form the results are mathematically very close to the results for temperature fluctuations in a thin film supported by a substrate, published recently [11]. The 1/f noise range is again found to be as in (15), with τ_d' now being $W_1^2/D_{channel}$. Since $D_{channel} \sim (1/5)D_{bulk}$, the noise is enhanced by a factor five. Also, the noise is apparently insensitive to the b.c. at the far end of the bulk (x = W). Further, we note that, in contrast to the case of temperature fluctuations [11], it is likely that the surface noise contribution (due to S_ζ) as computed here dominates the volume noise contribution (due to S_ζ), since as a rule M>>1, particularly for strong inversion. Altogether, the models presented here for MOSFETs give a very realistic model for 1/f noise over many decades above the reciprocal lifetime $1/\tau_b$. This explains that the 1/f noise in some MOSFETs extends up to many megahertz. Since the noise source S_ζ is essentially the same as in McWhorter's model (but not in van der Ziel's model which misses the modulation factor M), the noise spectra from slow and fast surface states should be continuous, though possibly there is a small 'wiggle' in the spectrum near $\omega = 1/\tau$, which should be searched for experimentally.

Finally, we note that the carrier density fluctuations in the channel are coupled to the gate in the same way as the low frequency 1/f noise. Thus one has for near zero drain bias

$$S_{V_{eq_o}} = \frac{e^2}{C_{ox}^2 dL} S_{\bar{n}}(f) \tag{17}$$

where d and L are the breadth and length of the channel, C_{ox} is the capacitance per unit length of channel. Since $S_{\bar{n}}(f)$ is proportional to $\bar{n}$, with $\bar{n} = e^{-1}C_{ox}(V_g - V_T)$, we find as for Klaassen's result [12],

$$S_{V_{eq}}(f) = \frac{\text{constant}}{f} W_1 (V_G - V_T). \tag{18}$$

The dependence on drain bias is the same as that calculated by van der Ziel [2].

REFERENCES

[1] A. L. McWhorter, *1/f Noise and Related Surface Effects in Germanium*, M.I.T. Lincoln Lab Report No. 80 (1955).

[2] A. van der Ziel, in *Advances in Electronics and Electron Physics*, Eds. L. Martin and C. Martin (Academic Press, New York, 1979) Vol. 49, 225-297.

[3] K. S. Champlin, *Physica* 26, 751 (1960).

[4] F. J. Hyde, *Rept. Conf. Phys. Soc. on Semiconductors*, Rugby, England (1956), 57.

[5] K. M. van Vliet and J. R. Fassett, in *Fluctuation Phenomena in Solids*, Ed. R. E. Burgess (Academic Press, New York, 1965) 267, Sections V and VI.

[6] M. Lax and P. Mengert, *Phys. Chem. Solids* 14, 248 (1960).

[7] H. Mehta, *Transport Noise Arising from Diffusion and Bulk or Surface Generation-Recombination in Semiconductors*, Ph.D. thesis, University of Florida (1981).

[8] H. Mehta and K. M. van Vliet, *Phys. Stat. Solidi* (to be published).

[9] K. M. van Vliet, *Solid State Electronics* 15, 1033, Appendix C (1972).

[10] P. Morse and H. Feshbach, *Methods of Theoretical Physics* (McGraw-Hill, New York, 1953), Vol. 1, Chapter 7.

[11] K. M. van Vliet, A. van der Ziel, and R.R. Schmidt, *J. Appl. Phys.* 51 (6), 2947 (1980).

[12] F. M. Klaassen, *IEEE Trans. El. Dev.*, ED-18, 887 (1971).

LOW FREQUENCY NOISE IN GaAs FET's AT LOW DRAIN VOLTAGES

J. GRAFFEUIL, J.F. SAUTEREAU, K. TANTRARONGROJ

Laboratoire d'Automatique et d'Analyse des Systèmes
Toulouse, France

Université Paul Sabatier, Toulouse, France

I - INTRODUCTION

Low frequency noise sources in field effect transistors have already been extensively investigated mainly on silicon J. FET. The dominant low frequency noise sources in these devices were found to be charge fluctuation of generation centers in the depletion region (1). Subsequently it was reported that carrier density fluctuations in the channel may also contribute to the overall low frequency noise(2).Low frequency noise in GaAs MESFETs was attributed to trapping in the channel (3,4), 1/f noise sources in the semi-conductor-oxyde interface (5) and to a process governed by a distribution in time constant (6).

The aim of this paper is first to theoretically investigate carrier density fluctuation noise and charge density fluctuation noise in GaAs MESFETs at low drain voltages in the one dimensionnal FET model. Secondly, it will be shown that the experimentally observed noise is the consequence of these two physical mechanisms previously investigated. Finally, an original technique to derive noise coefficients which depend only on the material used for processing the device is proposed.

II - CARRIER DENSITY FLUCTUATION NOISE

Carrier density fluctuation may arise in the transistor's channel from generation and recombination on trapping. Let us assume that only single time constant processes are involved. According to Van Der Ziel's theory (2) the spectral intensity of the short circuit channel noise current (nonsaturated) is given by :

$$S_i(f) = \frac{4 I_D W_{DS} q \mu \delta_c \tau_c}{L^2 (1 + \omega^2 \tau_c^2)} \qquad 1$$

where W_{DS} is the potentiel between source and drain ends of the active channel, μ the low field mobility, L the gate length, τ_c the carrier density fluctuation time constant, ω is equal to $2\pi f$ where f is the frequency and δ_c a constant given by

$$\overline{\Delta N^2} = \delta_c N$$

where N is the number of free carriers in the channel and $\overline{\Delta N^2}$ the variance.

The output conductance in the one-dimensionnal model is given by :

$$\frac{I_D}{V_{DS}} = g_d = G_o(1-\sqrt{X}) \quad \text{with} \quad X = \frac{V_{bi} - V_G}{W_{oo}} \qquad 2$$

where I_D is the drain D.C. current, G_o the conductance of the open channel, V_{bi} the gate junction built-in voltage, V_G the gate voltage and W_{oo} the pinch-off potential. The spectral intensity of the open circuit channel noise voltage is :

$$S_{vo}(f) = S_i(f)/g_d^2 = \frac{4 I_D^2 q \mu \delta_c \tau_c}{L^2 G_o^3 (1-\sqrt{X})^3 (1+\omega^2 \tau_c^2)} \qquad 3$$

In GaAs FETs the influence of regions between source and gate (length L_{SG}) and gate and drain (length L_{GD}) may be important. Let us assume that epilayer thickness is constant between source and drain and that noise sources are uniformly distributed in it : the lateral regions will also contribute to the overall low frequency noise. The spectral intensity of the open circuit lateral regions voltage noise is found from 1 and 2 where L_{SG} and L_{GD} are substituted from L and $g_{dSG} = \frac{G_o L}{L_{SG}}$, $g_{dGD} = \frac{G_o L}{L_{GD}}$ are substituted from g_d. Let the two lateral regions noise sources and the channel noise source been uncorrelated so that the three spectral intensities add together, and let the total output conductance be $g'_d = I_D / V_D$ where V_D is the drain voltage, the total short circuit noise current contributed by carrier density fluctuation is

$$S_{i_d}(f) = 4 \frac{I_D^4}{V_D^2} \frac{q\mu L}{(G_o L)^3} \frac{\gamma_c \tau_c}{1+\omega^2\tau^2} \left[\frac{1}{(1-\sqrt{X})^3} + \frac{L_{SG}+L_{GD}}{L} \right] \qquad 4$$

As a consequence the plot of the product of the spectral intensity at a given frequency by V_D^2 / I_D^4 against $\frac{1}{(1-\sqrt{X})^3}$ should be a straight line. The slope of this line should provide the noise coefficient $\gamma_c \tau_c / (1+\omega^2\tau_c^2)$ and the linear extrapolation of the plot to the ordinate should give the ratio $(L_{SG}+L_{GD})/L$

III - CHARGE FLUCTUATION NOISE

According to SAH's theory (7), the random generation of electrons and holes from N_t centers in the transition region of the gate induces a charge fluctuation on the gate contact. Subsequently an equivalent voltage fluctuation on the gate is derived using the relationship between voltage, charge and gate-to channel capacitance (7). The spectral intensity ot this fluctuation is given by :

$$S_{v_g}(f) = 4 \frac{\gamma_t \tau_t}{1+\omega^2\tau^2} \cdot \frac{4}{3} \cdot \frac{W_{oo}^2 q\mu}{G_o L^2} (\sqrt{X})^3 \qquad 5$$

where the time constant τ_t is given in (7), and where γ_t is equal to $N_t f_t (1-f_t)/N_D$ if f_t is the fraction of filled traps. The total transconductance g_m including series resistances is given (one-dimensionally) by :

$$g'_m = \frac{1}{2} \cdot \frac{I_D^2}{V_D} \cdot \frac{1}{G_o W_{oo} \sqrt{X} (1-\sqrt{X})^2} \qquad 6$$

and the spectral intensity of the short circuit channel noise current contributed by charge fluctuations is :

$$S_{i_g}(f) = g'^2_m S_{v_g}(f) = \frac{4}{3} \cdot \frac{q\mu L}{(G_o L)^3} \cdot \frac{I_D^4}{V_D^2} \cdot \frac{\gamma_t \tau_t}{1+\omega^2\tau^2} \cdot \frac{\sqrt{X}}{(1-\sqrt{X})^4} \qquad 7$$

The plot of the product of the spectral intensity at a given frequency by V_D^2 / I_D^4 against $\sqrt{X}/(1-\sqrt{X})^4$ should also be a straight line. The slope should provide the noise coefficient $\gamma_t \tau_t / (1+\omega^2\tau_t^2)$ and the intercept point with the axis should be at the origin.

IV - EXPERIMENTS

The equivalent short circuit noise current was measured on about ten short gate length devices (0.5 μm to 1 μm) available from most of the major manufacturers. For a given gate voltage these measurements were performed between 10^2 Hz and 10^5 Hz for different drain currents and drain voltages selected so that the one dimensionnal model holds, i.e. I_D and V_D must satisfy (8) :

$$\frac{V_D}{I_D} = \frac{1}{G_o} \cdot \frac{1}{1-\sqrt{X}} + R_S + R_D \qquad 8$$

where R_S and R_D are source and drain series resistances.

From the plot of Si (f) versus f (figure 1) we can observe spectra of various forms which may be attributed to either a process governed by a distribution in time constants (6) or to the superposition of a few single time processes (4). So as to generalize the previous theoretical analysis we must substitute frequency dependent noise coefficients $N_c(f)$ and $N_g(f)$ for the coefficients $\gamma_c \tau_c / (1+\omega^2\tau_c^2)$ and $\gamma_g \tau_g / (1+\omega^2\tau_g^2)$ previously introduced.

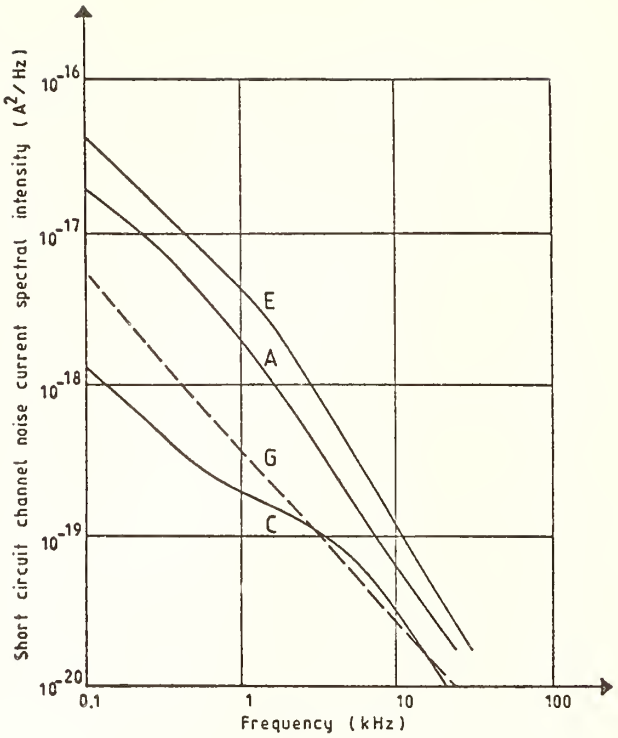

Fig. 1 : Noise spectra of for different devices at low drain voltages (V_D = 100 mV, V_G = o)

The experimental results from all the samples indicate that the product of $S_i(f)$ by V_D^2/I_D^4 is a constant at a given gate voltage and a given frequency as long as equality 8 holds. Furthermore, once the pinch-off voltage has been carefully determined (9), $S_i(f) \cdot V_D^2/I_D^4$ was plotted versus $(1-\sqrt{x})^{-3}$. Two typical plots of devices A and G are given in Figure 2.

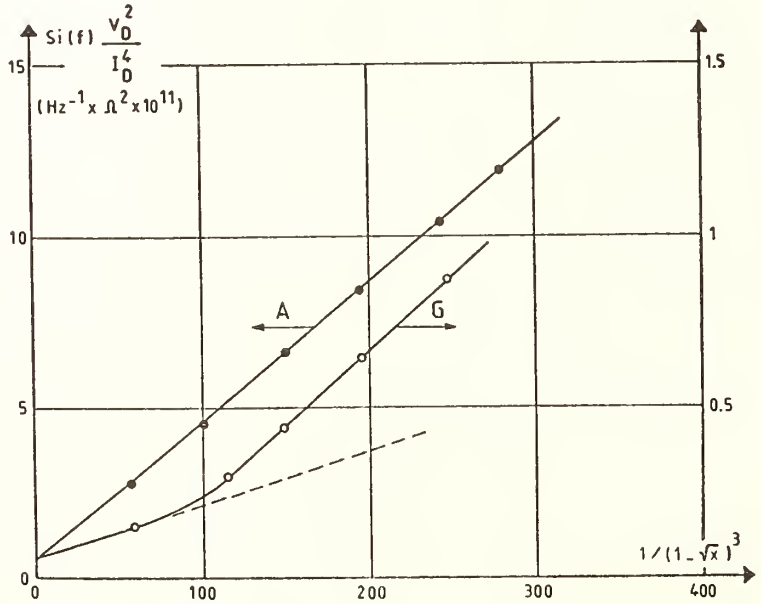

Fig. 2 : Observed dependance of the product of the open circuit output spectral current intensity by V_D^2/I_D^4 on $(1-\sqrt{x})^{-3}$ with $x = (V_i - V_G)/W_{oo}$ ($30 \leq V_{D(mV)} \leq 100$ and $f = 10^3$ Hz)

Plot A clearly shows following 4 , that carrier density fluctuation is the major source of noise in device A. Moreover values of N_C at 10^3 Hz and of $(L_{SG}+L_{GD})/L$ evaluated from this plot are $1.7 \cdot 10^{-7}$ s. and 2.5 . The latter value compares well with the one found by microscopic observation of the device.

Plot G is a two sections plot : the first section is a straight line and shows that the carrier density fluctuation noise predominates at low gate voltages ($N_C = 8 \cdot 10^{-8}$ S. and $(L_{SG}+L_{GD})/L \simeq 4$). The difference between the second section and the linear extrapolation of the first section to high V_G was plotted versus $\sqrt{X}/(1-\sqrt{X})^4$. We obtained a straight line, which fairly matches relationship 7 with $N_g = 4 \cdot 10^{-8}$ S . It must therefore be concluded that both carrier density fluctuation and charge fluctuation will contribute to the overall noise - The major contribution is carrier density fluctuation at low gate voltages and charge fluctuations at large gate voltages - We believe that this conclusion is valid for most of the devices, but in some cases(for example, device A), the carrier density fluctuation noise is too large so that charge density fluctuation noise cannot be detected.

Moreover since the spectrum of device G exhibits a quite perfect 1/f behaviour, the open channel noise current spectral intensitycalculated from Hoodge's formula should have been :

$$S_i(f) = \frac{I_D^2 \alpha_H}{nVf}$$

where α_H is Hoodge's constant, V the epilayer volume and $n = N_D$ the mean free carrier density in the epilayer. From the extrapolated plot G at $X = 0$ it can be deduced that α_H should be approximately two orders of magnitude smaller than α_H measured in bulk materials.

V - CONCLUSION

A new method was used to distinguish between carrier density fluctuation noise and charge density fluctuation noise in GaAs MESFETs at low frequencies and low drain voltages. This technique provides noise coefficients independent of bias conditions and other parameters of the devices. The technique appears to be useful as a means of monitoring material used for devices. For example we found that the carrier density fluctuation noise coefficient at 10^3 Hz is usually lower in LPE devices than in VPE ones (10). Finally, since the low frequency of the FET under normal operating conditions is closely related to the low bias noise coefficients N_C and N_g (10), the technique could also provide an efficient means of evaluating devices for microwave low noise large signals applications as oscillators or mixers (10).

This work was supported by a DAII-CNET contract. We wish to thank Dr BLASQUEZ for his useful comments.

(1) P.O. LAURITZEN - Solid State Electron. 8, 41 (1965)

(2) C.F. HIATT, A. VAN DER ZIEL, K.M. VAN VLIET IEEE trans ED 614 (1955)

(3) J. GRAFFEUIL, J. CAMINADE - EL. Letters 10-13 (1974)

(4) D. SODINI, A. TOUBOUL, G. LECOY, M. SAVELLI EL. Letters 12-2 (1976)

(5) K. TAKAGI, A. VAN DER ZIEL Solid State Electron22-285 22-285 (1979)

(6) C.H. SUH, A. VAN DER ZIEL Appl. Phys. Lett 37-565 (1980)

(7) C.T. SAH Proc IEEE 52-795 (1964)

(8) J. GRAFFEUIL - Thèse Université Paul Sabatier (1974)

(9) H. FUKUI Bell Syst. Tech. J. 771 (1979)

(10) J. GRAFFEUIL (....) to be published.

THERMAL NOISE IN THE SEMICONDUCTOR REGIME OF DOUBLE-INJECTION DIODES

A. van der Ziel

Electrical Engineering Department
University of Minnesota
Minneapolis, MN 55455

SUMMARY

In an earlier paper Huang and van der Ziel could not fully evaluate the thermal noise in the semiconductor regime of a double-injection diode. By a careful application of the boundary conditions and by making the approximation for the semiconductor regime only at the end of the calculation this problem has now been solved. The final result consists of thermal noise of the d.c. resistance V_a/I_a at all frequencies plus a g-r like noise term that disappears at high frequencies and is small for long diodes.

In their calculation of the noise in double injection diodes operating in the semiconductor regime Huang and van der Ziel[1] ran into difficulties because the approximation for the semiconductor regime was introduced early in the calculation. This removed one of the boundary conditions, which, in turn, made a solution impossible. By applying the approximation at the end of the calculation these difficulties can be avoided.

The basic equations for the double-injection diode are [1]

$$J_p = e\mu_p(p+p_T)E - eD_p\partial p/\partial x + eh_p \tag{1}$$

$$J_n = e\mu_n(n+n_T)E + eD_n\partial n/\partial x - eh_n \tag{2}$$

$$\partial p/\partial t = -R - (1/e)\partial J_p/\partial x - r \tag{3}$$

$$\partial n/\partial t = -R + (1/e)\partial J_n/\partial x - r \tag{4}$$

$$\partial E/\partial x = (e/\varepsilon\varepsilon_o)(p-n) \tag{5}$$

Here J_p and J_n are the hole and electron current densities, n and p the injected hole and electron densities, n_T and p_T the equilibrium electron and hole densities, $R = n/\tau$ the recombination rate per unit volume and τ the lifetime of the injected carriers, E the field strength, h_p and h_n the particle current densities for holes and electrons describing the diffusion noise sources and r the generation-recombination noise source.

If we now manipulate eqs. (3) and (4) properly, neglect the diffusion terms except h_p and h_n and ignore r, we obtain

$$-\frac{\varepsilon\varepsilon_o}{e}\frac{\partial}{\partial x}\left(E\frac{\partial E}{\partial x}\right) + (n_T-p_T)\frac{\partial E}{\partial x} - \frac{\mu_p+\mu_n}{\mu_p\mu_n}\left(\frac{\partial n}{\partial t}+\frac{n}{\tau}\right) = \frac{\partial}{\partial x}\left(\frac{h_p(x)}{\mu_p}+\frac{h_n(x)}{\mu_n}\right) \tag{6}$$

If the small terms with p_T and n_T are neglected, and if also the diffusion terms except h_p and h_n are neglected, and if furthermore the approximate space charge neutrality condition $n \simeq p$ is introduced, the total current density J(t) is

$$J(t) = J_p + J_n = e(\mu_p + \mu_n)nE + e[h_p(x) - h_n(x)] \tag{7}$$

We now put $J = J_o + J_1$, $n = n_o + n_1$, $E = E_o + E_1$, $V = V_o + V_1$, where V is the potential; the subscripts o denote d.c. quantities and the subscripts 1 denote small signal a.c. quantities. We next make a Fourier analysis for the a.c. quantities for $0 \leq t \leq T$, where T is sufficiently large, and introduce the Fourier coefficients $E_{1n}, n_{1n}, V_{1n}, J_{1n}, h_{pn}$ and h_{nn}. We make the assumption that the device is open-circuited for a.c., i.e., $J_{1n} = 0$. This yields the equations

$$-\frac{\varepsilon\varepsilon_o}{e}\frac{d}{dx}\left(E_o\frac{dE_o}{dx}\right) + (n_T - p_T)\frac{dE_o}{dx} = \frac{\mu_p+\mu_n}{\mu_p\mu_n\tau}n_o \tag{8}$$

$$J_o = e(\mu_p+\mu_n)n_oE_o \tag{9}$$

$$-\frac{\varepsilon\varepsilon_o}{e}\frac{d^2}{dx^2}(E_oE_{1n}) + (n_T-p_T)\frac{dE_{1n}}{dx} - \frac{\mu_p+\mu_n}{\mu_p\mu_n\tau}(1+j\omega\tau)n_{1n} = \frac{d}{dx}\left(\frac{h_{pn}}{\mu_p}+\frac{h_{nn}}{\mu_n}\right) \tag{10}$$

$$0 = e(\mu_p+\mu_n)(n_{1n}E_o+n_oE_{1n}) + e(h_{pn}-h_{nn}) \tag{11}$$

Eliminating n_o in (8) with the help of (9) yields

$$\frac{J_o}{e\mu_p\mu_n\tau} = -\frac{\varepsilon\varepsilon_o}{e}E_o\frac{d}{dx}\left(E_o\frac{dE_o}{dx}\right) + (n_T-p_T)E_o\frac{dE_o}{dx} \tag{12}$$

Equation (11) may be written

$$\frac{n_{1n}}{n_o} = -\frac{E_{1n}}{E_o} - \frac{e(h_{pn}-h_{nn})}{J_o} \tag{13}$$

Substituting for n_{1n}/n_o with the help of (13) and for n_o with the help of (9) yields

$$-\frac{\varepsilon\varepsilon_o}{e}E_o^2\frac{d^2}{dx^2}(E_oE_{1n}) + (n_T-p_T)E_o^2\frac{dE_{1n}}{dx} + \frac{J_o(1+j\omega\tau)}{e\mu_p\mu_n\tau}E_{in}$$

$$= -\frac{(1+j\omega\tau)}{\mu_p\mu_n\tau}E_o(h_{pn}-h_{nn}) + E_o^2\frac{d}{dx}\left(\frac{h_{pn}}{\mu_p}+\frac{h_{nn}}{\mu_n}\right) \tag{14}$$

which must be solved with the boundary conditions $E_o = 0$ at $x = 0$ and $x = d$.

We now introduce the spectra

$$S_{hp}(x,x',f) = \lim_{T\to\infty}\overline{2T\,h_{pn}h_{pn}^*} = 4D_pn_o(x')\delta(x'-x)/A \tag{15}$$

$$S_{hn}(x,x',f) = \lim_{T\to\infty} 2T\, \overline{h_{nn} h_{nn}^{*}} = 4D_n n_o(x')\delta(x'-x)/A \tag{16}$$

where A is the cross-sectional area of the device. We also bear in mind that $[h_{pn}(x) - h_{nn}(x)]$ and $[h_{pn}(x')/\mu_p + h_{nn}(x')/\mu_n]$ have a zero cross-correlation spectrum, as is found by applying (15) and (16) and the Einstein relation $D_p/\mu_p = D_n/\mu_n = kT/e$.

Up to here we have not yet discriminated between the semiconductor regime and the insulator regime. We do so by introducing[2]

$$J_o = J_{oi}(x) + J_{os}(x) \tag{17}$$

where

$$\frac{J_{oi}(x)}{e\mu_p\mu_n\tau} = -\frac{\varepsilon\varepsilon_o}{e} E_o \frac{d}{dx}\left(E_o \frac{dE_o}{dx}\right) \tag{17a}$$

and

$$\frac{J_{os}(x)}{e\mu_p\mu_n\tau} = (n_T - p_T) E_o \frac{dE_o}{dx} \tag{17b}$$

Here $J_{oi}(x)$ and $J_{os}(x)$ refer to the insulator term and the semiconductor term in (12), respectively. In addition there is a diffusion current density, here neglected, which is small everywhere except near the points x = 0 and x = d. In the semiconductor regime $J_{oi}(x) \ll J_o$ for most of the region $0 \leq x \leq d$, whereas for the insulator regime $J_{os}(x) \ll J_o$ for most of the region $0 \leq x \leq d$. The important point to make, however, is that these approximations are made at the <u>end</u> of the calculation. The reason is that in the approximation for the semiconductor regime one of the boundary conditions $E_o = 0$ at x = 0, $E_o = 0$ at x = d is violated [3].

We now multiply Eq. (14) on both sides by dx, integrate by parts from 0 to d and apply the boundary conditions at x = 0 and x = d. This yields [4]

$$\int_o^d E_o^2 \frac{d^2}{dx^2}(E_o E_{1n})\, dx = 2\int_o^d E_o \frac{d}{dx}\left(E_o \frac{dE_o}{dx}\right) E_{1n}\, dx \tag{18}$$

$$\int_o^d E_o^2 \frac{dE_{1n}}{dx}\, dx = -2\int_o^d E_o \frac{dE_o}{dx} E_{1n}\, dx \tag{19}$$

$$\int_o^d E_o^2 \frac{d}{dx}\left(\frac{h_{pn}}{\mu_p} + \frac{h_{nn}}{\mu_n}\right) dx = -2\int_o^d E_o \frac{dE_o}{dx}\left(\frac{h_{pn}}{\mu_p} + \frac{h_{nn}}{\mu_n}\right) dx \tag{20}$$

Substituting all this into the integral of (14) yields

$$\int_o^d \frac{J_{oi}(x)(3+j\omega\tau)-J_{os}(x)(1-j\omega\tau)}{e\mu_p\mu_n\tau} E_{1n}dx = \frac{1+j\omega\tau}{\mu_n\mu_p\tau}\int_o^d E_o(h_{pn}-h_{nn})dx$$

$$-2\int_o^d \frac{J_{os}(x)(h_{pn}/\mu_p+h_{nn}/\mu_n)}{e\mu_p\mu_n\tau(n_T-p_T)}dx \qquad (21)$$

We now apply this to the semiconductor regime by putting $J_{oi}(x) = 0$ and $J_{os}(x) = J_o$ and bearing in mind that

$$\int_o^d E_{1n}dx = - v_{1n}(d) \qquad (21a)$$

where $v_{1n}(d)$ is the Fourier coefficient of the open-circuit voltage at d. This yields

$$v_{1n}(d) = -\frac{e}{J_o}\left(\frac{1+j\omega\tau}{1-j\omega\tau}\right)\int_o^d E_o(h_{pn}-h_{nn})dx - \frac{2}{(n_T-p_T)(1-j\omega\tau)}\int_o^d \left(\frac{h_{pn}}{\mu_p}+\frac{h_{nn}}{\mu_n}\right)dx \qquad (22)$$

Defining

$$S_{V_a}(f) = \lim_{T\to\infty} 2T\,\overline{v_{1n}(d)v_{1n}^*(d)} \qquad (23)$$

yields after some manipulations

$$S_{V_a}(f) = 4kT\frac{V_a}{I_a} + 4kT\frac{V_a}{I_a}\left[\frac{12\tau^2/(\tau_{dn}\tau_{dp})}{1+\omega^2\tau^2}\right] \qquad (24)$$

where the anode current $I_a = -J_oA$ is taken positive (J_o flows from cathode to anode and hence is negative). Here

$$\tau_{dp} = 4d^2/(3\mu_pV_a) \text{ and } \tau_{dn} = 4d^2/(3\mu_nV_a) \qquad (24a)$$

are the drift times for holes and electrons, respectively.

In the evaluation of the integrals use was made of the fact that in the semiconductor regime [3]

$$V_o(x) = V_a[d^{3/2} - (d-x)^{3/2}]/d^{3/2} \qquad (25)$$

when $n_T > p_T$. Note that here the condition $dV_o/dx = 0$ is violated at $x = 0$. Since this was done only in the last step of the calculation, the error thus introduced is small.

REFERENCES

[1] C. H. Huang and A. van der Ziel, Physica, 78 (1974) 220.

[2] R. J. J. Zijlstra and A. Gisolf, Solid State Electron. 15 (1972) 877.

[3] A. van der Ziel, in Semiconductors and Semimetals, Vol. 14 (1979) 195-247.

[4] A. van der Ziel, Physics (1981) in the press.

PHOTOCURRENT NOISE CAUSED BY IMPACT IONIZATION OF NEUTRAL DONORS, AND FREE AND BOUND EXCITONS IN n-GaAs

K. Aoki, K. Miyamae, T. Kobayashi and K. Yamamoto

Department of Electrical and Electronic Engineering, Faculty of Engineering, Kobe University, Rokko, Nada, Kobe, Japan

Abstract

In this paper, we have investigated in detail the photocurrent noise or current-filament instability caused by impact ionization of shallow neutral donors, and free and bound excitons in n-GaAs at 4.2 K. From the power spectra of the observed photocurrent noise, it was found that the current-filament instability can be described by the bifurcation theory based on the first-order phase transition.

1. Introduction

Electrical breakdown of the low temperature freeze-out of shallow neutral donors in the compensated materials of semiconductors [1-3] causes the current-controled negative resistance or the current-filament instability. Many works have been reported concerning the impact ionization mechanisms [4] and the energy relaxation mechanisms of hot electrons [5], while little attention has been made on the characterization of the current-filament instability based upon the phase transition regime. The purpose of this paper is to investigate the photocurrent noise (i.e., the current-filament instability under the weak photoexcitation) caused by impact ionization of shallow neutral donors, and free and bound excitons at 4.2 K in n-GaAs. Our final goal is to characterize the current-filament instability based upon the phase transition regime of the current noise and to speculate the microscopic origin of the fluctuating force.

2. Experimental Procedure

Samples used were epitaxial n-GaAs ($n = 2\times10^{14}/cm^2$ at 300 K) grown on Cr-doped substrate. Thickness of the epitaxial layer was about 12 μm. Planar-type ohmic contacts were formed by alloying Sn on the sample surfaces. Typical dimensions of the sample surfaces were 5.5 mm in length and 4 mm in width, respectively. The light sources used were a 20 mW He-Ne laser, and also a standard halogen lamp for the illumination of monochromatic light around band gap energy of GaAs. All measurements were done at 4.2 K.

3. Experimental Results and Discussions

3.1 Power spectra

The electrical breakdown of the shallow neutral donors occurs at around the critical electric field of 4 ∿ 6 V/cm under the dark and the illumination. The critical electric field differs slightly from sample to sample. Figure 1 shows a typical current-voltage characteristics under the dark. Above the onset voltage of the electrical breakdown with dc-applied electric field (E > 4 V/cm), the spiky noise with the duration of 10 ∿40 ms was observed, and was randomly distributed in time.

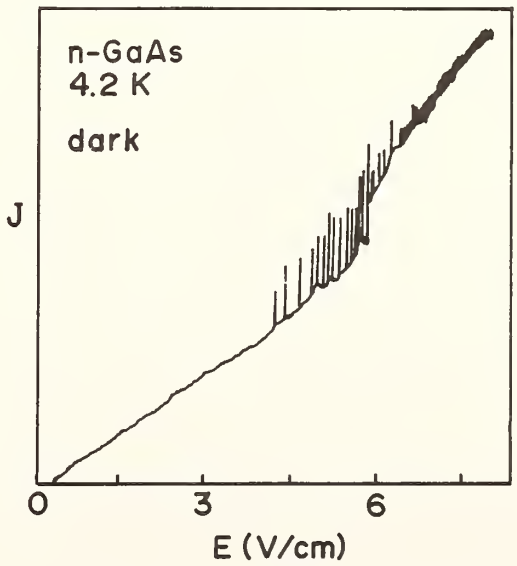

Fig.1 Typical current-voltage characteristics under the dark, obtained by the continuous motor-drive. Speed of the motor-drive was about 30 mV/s.

Each spike contains superimposed oscillations [6] and was explained well by the current-filament instability, as is discussed below. Under the weak photoexcitation, the breakdown voltage shifts to lower electric field, and the number of spikes per unit time increases with increasing the photoexcitation density J_p.

Figure 2 shows the power spectrum around 0 Hz observed by He-Ne laser excitation, with J_p= 3.2 mW/cm^2 and E= 4.5 V/cm, respectively. The spectrum in the low frequency range is very similar with those of the dielectric relaxation in various semiconductors [7] and also with that of random telegraph signals. Assuming the Lorentzian shape (broken line in Fig. 2), the effective relaxation time was obtained to be 2 ms. The behaviors of the current-filament correspond to the soft-mode excitation in the first-order phase transition, and are rather a static property of the hysterysis loop in the S-shape of J-E curve with the frequency around 0 Hz.

Furthermore, the photocurrent noise contains a discrete line spectrum in the higher frequency range (0 $\sim$ 1 MHz), which corresponds to the noise structures superimposed on each current-filament. The number of discrete lines increases at the same frequency range when the electric field and/or photoexcitation density is increased. Figure 3 shows the discrete line spectra as a function of photoexcitation density with E= 4.5 V/cm, indicating existence of many periodic states of the current filament. From the detailed analysis, it was found that the observed line spectrum seems to be incommensurate [8],i.e., containing several discrete lines expressed by sum and difference of the higher harmonics of two frequencies f_1 and f_2. Above the critical photoexcitation density of J_p= 40 mW/cm^2, the discrete line spectrum changes abruptly into the continuous spectrum, as is shown in Fig.3 (c). All of the results mentioned above greatly suggest that both the soft- and hard-modes' excitations occur at the same time and that the continuous bifurcation occurs as a function of photoexcitation density and/or electric field.

Qualitatively, the current-filament instability can be explained by the feedback mechanism of the impact ionization of neutral donors. At the onset of the electrical breakdown, the impact ionization of the neutral donors enhances the impact ionization rate and thus increases the carrier density due to the carrier heating, while the excess energy of the hot electrons is relaxed into acoustic phonon system due to the heat balance, and in a little while the carrier density begins to decrease with a short time lag. Again, the impact ionization takes place due to the applied electric field as soon as the cooling of the carrier gas facilitate the current filament to disappear.

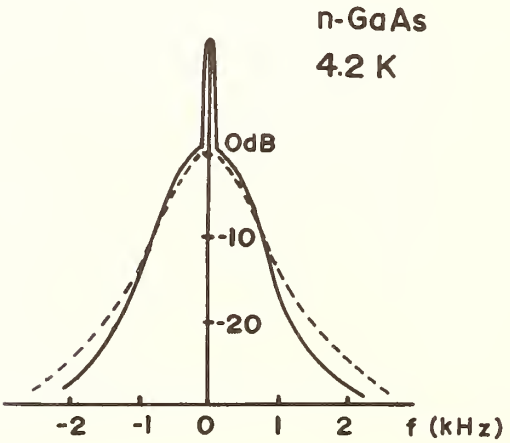

Fig.2 Power spectrum of the photocurrent noise observed with J_p= 3.2 mW/cm^2 and E= 4.5 V/cm, respectively. The broken line is calculated Lorentzian shape with τ=2ms.

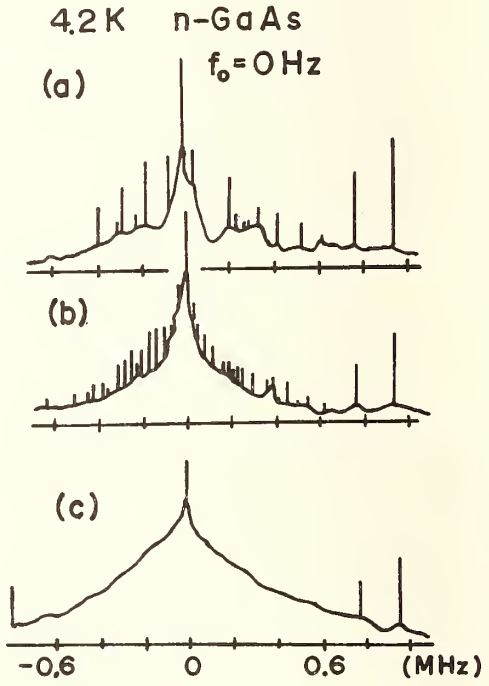

Fig.3 Change of the power spectra as a function of photoexcitation density; J_p=3.2 mW/cm^2 in (a), 32 mW/cm^2 in (b), and 80 mW/cm^2 in (c), respectively. The electric field was fixed to be 4.5 V/cm. The line spectra around 1 MHz are stray signals from radio frequencies.

A couple of nonlinear differential equations can be obtained as follows,

$$C\frac{\partial T_e}{\partial t} = \frac{\partial}{\partial x}(\kappa \frac{\partial T_e}{\partial x}) - n\frac{T_e - T_L}{\tau_\varepsilon} + ne\mu E^2 + P(J_p) + P_{e\text{-}e} + f_1(J_p,t) \qquad (1)$$

$$\frac{\partial n}{\partial t} = D\frac{\partial^2 n}{\partial x^2} + n(N_D - N_A - n)B_I + (N_D - N_A - n)B_T - nA_T(N_A + n) + f_2(J_p,t) \qquad (2)$$

where one dimensional diffusion is assumed for simplicity, and the x-direction is perpendicular to the current flow. In eq.(1), T_e and T_L are the electron temperature of the current filament and the lattice temperature, respectively, C is the heat capacity, κ is the thermal conductivity, τ_ε is the energy relaxation time, n is the carrier density, μ is the electron mobility, E is applied electric field, $P(J_p)$ is the energy added to the carrier gas by the photoexcitation, $P_{e\text{-}e}$ is the energy gain due to electron-electron scattering if it is important, and $f_1(J_p,t)$ is the random fluctuating force or small agitation for the heating process, respectively. In eq.(2), D is the diffusion constant of the majority carriers in the filament, B_I and B_T are the impact ionization rate per carrier and the thermal ionization rate of the neutral donors, respectively, A_T is the thermal recombination rate of the majority carriers, N_D and N_A are the densities of the shallow donors and acceptors, respectively, and $f_2(J_p,t)$ is also the random fluctuating force. A couple of nonlinear equations (1) and (2) are very similar with those in the fluid system and the chemical-reaction system [8], and suggest that the diffusions of the electron temperature and the carrier gas play important roles for the current-filament instability (diffusion-induced instability). If we assume that the solution for the current filamentation has mode patterns in space and time, the linear stability analysis can be easily investigated. The necessary condition for the soft-mode excitation must be satisfied as follows,

$$D_{T_e} \equiv \frac{\kappa}{C} > D \qquad (3)$$

The relation describes that the diffusion constant of the electron temperature or the heat flow defined by eq.(3) should be larger than the diffusion constant of the majority carriers for the soft-mode excitation. At low temperature where the heat capacity changes by the T^{-3} rule, the mean-free path is very long and competitive with the sample size. Therefore, eq.(3) seems to be fully satisfied at the temperatures as low as 4.2 K.

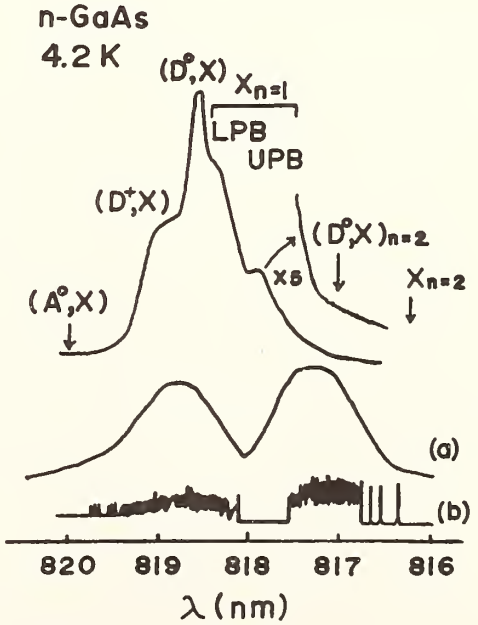

Fig.4 Photocurrent noise (PCN) spectra as a function of the excitation wavelength, with $J_p \sim 2\ \mu W/cm^2$ and E= 4 V/cm. Spectrum (a) was obtained by applying the pulse voltage with the width of 500 ns and the repetition of 100 kHz, and was detected by a lock-in amplifier. Spectrum (b) was obtained by dc voltage, and was directly recorded on the recorder. The scanning speed of the monochromator was 10 A/min. For comparison, photoluminescence spectrum observed by He-Ne laser excitation with J_p = 80 mW/cm^2 is also shown.

3.2 Fluctuating Force

In order to obtain a clear evidence for the microscopic origin of the fluctuating force for the trigger of the current filamentation, we investigated the excitation-wavelength dependence of the photocurrent noise (PCN spectrum) with using resonant photoexcitation around band gap energy. Figure 4 shows the PCN spectra observed with $J_p \approx 2$ μW/cm^2 and E= 4 V/cm. It is clear that the current-filament can be selectively generated at the excitation wavelength of the bound excitons and the excited donor state for the resonant formation of the bound excitons (we denote as $(D^0,X)_{n=2}$). Figure 5 shows the PCN spectra as a function of electric field. The results in Figs.4 and 5 are very suggestive of the microscopic origin of the fluctuating force; (a) the current filamentation originates from the localized donor sites in the microscopic region and (b) some preferential dissociation-process of bound excitons acts as a trigger of the current filamentation [9]. The number of spikes or density of the current filament per unit time greatly depends upon the photo-excitation density. The generation mechanism was found to be the Poisson process, which gives a clear evidence that the photon noise and the chance process of the bound-exciton formation and dissociation in the microscopic region act as a seed for the trigger of the current filamentation. Concerning the preferential dissociation of the bound excitons, Auger recombination process is inferred to be very effective for the trigger mechanism, since Auger recombination is autoionization process releasing the majority carrier energetically into conduction band.

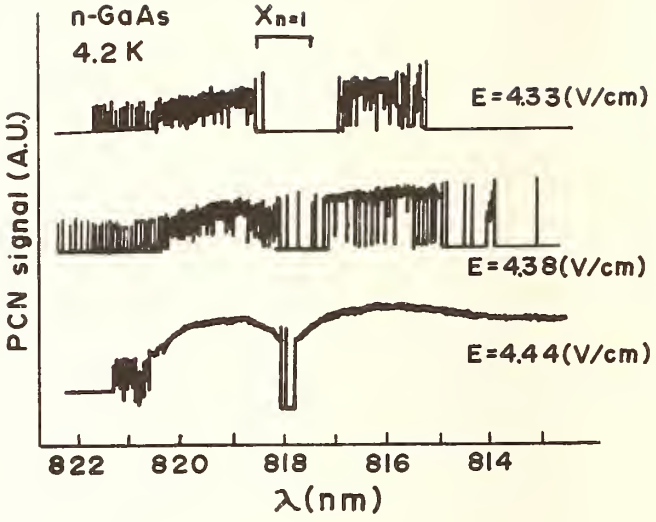

Fig.5 PCN spectra as a function of electric field. Photoexcitation density is ≈ 1 μW/cm^2.

The current-filament instability discussed here is very analogous with the oscillatory chemical reaction [8] and the turbulence in the fluid system [10], revealing an unique problem of the "turbulence" in semiconductors.

References

[1] W. Schairer and N. Stath, J. Appl. Phys. 43, 447 (1972)

[2] T. Yao, K. Inagaki, and S. Maekawa, Solid State Commun. 13, 533 (1973)

[3] W. Bludau and E. Wagner, Phys. Rev. B13, 5410 (1976)

[4] R. P. Khosla, J.R. Fischer and B.C. Burkey, Phys. Rev. B7, 2551 (1973)

[5] T. Kurosawa, J. Phys. Soc. Japan 20, 1405 (1965)

[6] K. Aoki, K. Miyamae, T. Kobayashi and K. Yamamoto, Jpn. J. Appl. Phys. 19, L657(1980)

[7] M. Buttiker and H. Thomas, Noise in Physical Systems ed. D. Wolf (Springer-Verlag, Berlin, Heidelberg and New York, 1978) p.115

[8] H. Thomas, ibid ref.[7] p.278

[9] K. Aoki, K. Miyamae, T. Kobayashi and K. Yamamoto, J. Phys. Soc. Japan 50, 357 (1981)

[10] G. Ahlers and R.P. Behringer, Phys. Rev. Letters 40, 712 (1978)

LOW ENERGY ELECTRON BEAM INVESTIGATION OF PLANAR TRANSISTORS USING SCANNING ELECTRON MICROSCOPY WITH PARTICULAR REFERENCE TO BURST NOISE

Kenneth F. Knott

Department of Electrical Engineering
University of Salford, England M5 4WT

INTRODUCTION

Several workers [1] have attempted to correlate burst noise and dislocations on a statistical basis whilst others [2] have studied the effect on burst noise of gate voltage in tetrode transistors. In the work to be presently described an attempt has been made to obtain 100% correlation between burst noise and a specific dislocation or dislocation network in the transistor. In order to do this the operation of the transistor needs to be influenced on a microscopic scale. One way of doing this is to subject the transistor to an electron beam either in the form of a spot or in the form of a small raster in a scanning electron microscope (SEM). At low incident energy (2-6 keV) the effect of the beam is to charge up positively the S_i-S_iO_2 interface with results similar to the application of gate potential in a tetrode structure but on a much smaller geometric scale. At higher energies the beam can be used to generate hole-electron pairs in the bulk of the transistor and hence artificially increase the leakage current in specific parts of the device. If this induced current is monitored the SEM is said to be operating in the Electron-Beam Induced Current (EBIC) mode.

EXPERIMENTAL PROCEDURE

In all experiments the transistor was connected in the circuit shown in Fig. 1, with V_{BE} zero if unbiassed operation was being studied, e.g. in the EBIC mode.

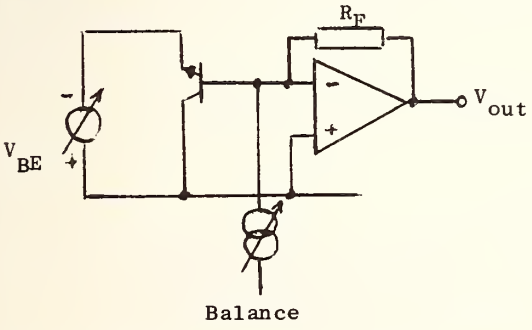

Figure 1. Test circuit.

Before carrying out detailed investigations of particular devices several transistors were 'sacrificed' to demonstrate the general feasibility of the experimental method. Firstly, the effect of the beam on base current, I_B was tested by subjecting transistors to successive scans of the whole of their base and emitter areas. Some results are shown in Fig. 2 where the ratio of final value of I_B to initial value of I_B is plotted against estimated aggregate electron dose. These effects were long-term, the changes in I_B persisting for periods ranging from several days to several weeks.

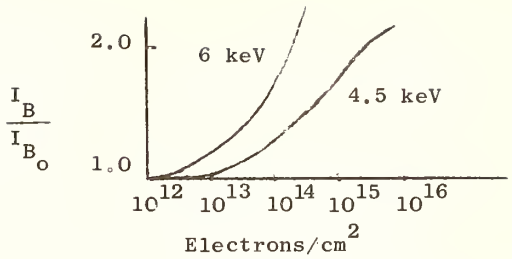

Figure 2. Change in I_B with electron dose for CA2018 transistors.

Secondly, ten transistors exhibiting burst noise were subjected to scanning of their complete base and emitter areas. Three of these showed changes in burst noise characteristics at low incident energy. Five showed no change in burst noise even when scanned at 20 keV, an energy high enough to increase I_B by 50 times. In the remaining two, burst noise disappeared completely after scanning at 20 keV.

Having demonstrated the possibility of altering burst noise with the electron beam a more rigorous and detailed investigation was initiated. Two approaches were adopted for the next steps in the study. Firstly, the SEM raster was reduced in size so that the exposed area on the specimen was small compared with the emitter area. The raster was then stepped around the region where the emitter-base junction intersected the surface. Each time a new area was exposed the beam was shut off and the burst noise observed. By controlling the time of exposure and incident energy known increments in I_B could be impressed. Secondly, the SEM was set to 'spot' scan and the noise of the EBIC signal was observed as the spot was moved over the specimen.

RESULTS - ELECTRICAL

Results have been obtained with three transistors up to date. These transistors have been subsequently etched and re-examined in the SEM.

The first transistor was examined with a small raster whilst maintaining V_{BE} constant at 510 mV, the initial value of I_B being 40 nA. At 5 keV a particular area of the transistor was showing signs of modifying the burst noise. This area was then scanned at 10 keV with a marked effect on the burst noise as I_B went through the range 250-300 nA. The change in form of the noise is indicated in Figs. 3a and b. When allowed to drift back the original form of the noise reappeared at I_B = 265 nA.

The second and third transistors were examined with a spot scan. Burst noise was induced in both devices at sites on the collector-base junction perimeters.

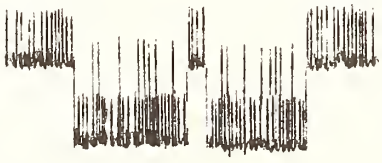

Figure 3a. Burst noise, I_B < 250 nA.

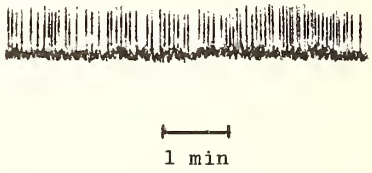

Figure 3b. Burst noise, I_B > 300 nA.

RESULTS - ETCH PIT STUDY

Having noted the positions where burst noise was either affected or induced in the electrical tests the devices were then etched with Dash solution. In all three devices etch pits were found at these positions, indicating the presence of dislocations. Fig. 4 is a micrograph of one of the etched devices. The bright line running across the centre is the intersection of the c-b junction with the surface. Many etch pits are in evidence but the group arranged in a triangular pattern near the centre of the figure are in a

position where burst noise was induced.

Figure 4. Micrograph of an etched CA3018 transistor.

4 μm

CONCLUSIONS

It has been demonstrated that areas of a transistor associated with burst noise activity have crystallographic damage although the converse is not necessarily true. More work needs to be done in the future on the effects of parameters such as incident energy and electron dose on the burst noise characteristics since induced burst appears to be a transitory phenomenon.

ACKNOWLEDGEMENTS

Thanks are expressed to T.J. Brady and J.R. Hunter who carried out some of the experiments described here as part of their final year project at Salford University.

REFERENCES

|1| G. Blasquez and J. Caminade, 5th Int. Conf. Noise in Physical Systems, Bad Nauheim, (1978).

|2| R. Radenheber, M. Stoisiek and D. Wolf, 4th Int. Conf. Noise in Physical Systems, Noordwijkerhout, (1975).

BURST NOISE IN DIODES

J.Šikula, M.Šikulová, P.Vašina and B.Koktavý

Department of Physics
Technical University of Brno, Barvičova 85
Czechoslovakia

INTRODUCTION

According to S.T.Hsu, R.J.Whittier and C.A.Maed [1], the burst noise is a random process caused by the generation-recombination (g-r) process of capture and emission of a carrier by a trap controlling the current through the defect. The experimental results cannot, however, be explained satis - factorily by their model, even if the modification of K.B.Cook and A.J.Brodersen [2] is taken into account. Remarkable discrepancies are observed in the voltage and temperature dependencies of the mean impulse duration as well as the capture cross section. The heart of the problem is in the as - sumption that the set is "pure" and thus the probability density of the i-th state occupation time is a single exponential function.

We have studied the burst noise of LED´s, transistors, Schottky diodes and we found out that the mentioned assumption is fulfilled only in some particular cases. The occupation time probability density is, in general, expressed as a sum of two exponential distributions.

THEORY

In the present paper we assume that the X(t) process of the trap occupation by a carrier is a three-state one. The state of the system is determined by the number of carriers in the band, on the trap, or at the g-r center. The following table gives the system states for an acceptor-like g-r center. The X-state denotes the X(t) process state.

Table 1.

X-state	cond.band	g-r center	valence b.	Y-state
0	n - 1	1	p	α
1	n	0	p	β
2	n - 1	0	p - 1	β

The X(t) primary process of the trap occupation induces the Y(t) secondary process of the current modulation. This process is a two-state g-r process. The single zeroth state of the X(t) process is transformed into the α-state of the secondary process, while the two states, i.e., 1 and 2 of the X(t) process are transformed into one state of the Y(t) process, which is denoted β .

To find the absolute probability distribution we assume that the primary process states can be projected on the set I=(0,1,2). We suppose that X(t) is stationary with constant transition probability intensities μ_{ij} (i,j=0,1,2) defined by

$$\mu_{ij} = \lim_{t \to s} \frac{p_{ij}(s,t)}{t - s} \qquad (1)$$

where p_{ij} is the transition probability at the time s from the i-state to the j-state at the time t. If Y(t) process is such a function of the primary process that it holds

$$Y(t) = \alpha \text{ for } X(t) = 0 \; ; \quad Y(t) = \beta \text{ for } X(t) = 1 \text{ or } 2 \; ; \qquad (2)$$

the we can find out the distribution function of the Y(t) process as well as its other characteristics. The absolute probability distribution of the X(t) process, i.e., $\Pi_i(t) = P\{X(t) = i\}$ $i \in I$, can be determined by solving the Kolmogorov's differential equations

$$\frac{d\Pi_i(t)}{dt} = \sum_{j \in I} \Pi_j(t) \mu_{ji} \qquad (3)$$

With respect to the stationarity of the primary process we have $d\Pi_i/dt = 0$; $\Pi_i(t) = \Pi_i(0) = \Pi_i$. Then we obtain the absolute probability distribution in the i-state:

$$\Pi_0 = M_{00} / \sum_i M_{ii} \; ; \quad \Pi_1 = M_{11} / \sum_i M_{ii} \; ; \quad \Pi_2 = M_{22} / \sum_i M_{ii} \qquad (4)$$

where M_{ij} is minor of the μ_{ij} term in the probability intensity matrix. It holds

$$\mu_{ii} = -\mu_i = -\sum \mu_{ij} \qquad \text{for } j \in I, \; j \neq i \qquad (5)$$

The absolute probability distribution of the Y(t) process, i.e., $\Pi_i(t) = P\{Y(t) = i\}$ for $i \in I$, $I = (\alpha, \beta)$, is then

$$\Pi_\alpha = \Pi_0 \; ; \quad \Pi_\beta = \Pi_1 + \Pi_2 = 1 - \Pi_\alpha \qquad (6)$$

The Y(t) process is stationary. It is not, however, identical with a homogeneous markovian two-state process, even though it has the same absolute distribution of probability. The Y(t) process differs from the homogeneous markovian process by the distribution of the β-state occupation time.

Now we find the matrix of the transition probability intensities for a two-charge acceptor-like center through which the excess carriers recombine. The intensity of the system transition from the i-state into the j-state is determined by means the probability intensity of quantum transitions from the center to the allowed energy bands and vice versa. In the Shockley-Read model terms we get the matrix of probability intensities of transition of the system from the i-state into the j-state

$$\mu_{ij} = \begin{Vmatrix} c_n n_1 + c_p p & c_n n_1 & c_p p \\ c_n n & c_n n & 0 \\ c_p p_1 & 0 & c_p p_1 \end{Vmatrix} \qquad (8)$$

where c_p, c_n are the capture coefficients of the hole and electron, respectively, p_1, n_1 are the hole and electron concentrations corresponding to the Fermi energy equal to the trap level.

The absolute probability distribution in the α-state is then

$$\Pi_\alpha = (1 + n_1/n + p/p_1)^{-1} \qquad (9)$$

In conditions of the thermodynamical equilibrium it is $n_1/n = \exp[(E_t - E_f)/kT]$ and $n_1/n = p/p_1$, so that

$$\Pi_\alpha = \{1 + 2 \exp[(E_t - E_f)/kT]\}^{-1} . \qquad (10)$$

The distribution of the α state occupation time is

$$g_\alpha(t) = \mu_0 \exp(-\mu_0 t) = \frac{1}{\tau_\alpha} \exp(-t/\tau_\alpha), \qquad (11)$$

where $$\tau_\alpha = (c_n n_1 + c_p p)^{-1} . \qquad (12)$$

The distribution of the β-state occupation time (for detailed derivation see [3]) is

$$g_\beta(t) = \frac{a_1}{\tau_1} \exp(-t/\tau_1) + \frac{a_2}{\tau_2} \exp(-t/\tau_2) , \qquad (13)$$

where $$a_1 = (1 + c_p p/c_n n_1)^{-1} \; ; \; a_2 = 1 - a_1 . \qquad (14)$$

$$\tau_1 = 1/c_n n \; ; \; \tau_2 = 1/c_p p_1 . \qquad (15)$$

The mean occupation time of the α state is $E\{T_\alpha\} = \langle\tau_\alpha\rangle = \tau_\alpha$, and that of the β state is $E\{T_\beta\} = a_1\tau_1 + a_2\tau_2 = \langle\tau_\beta\rangle$ (16)

From eq. (14)-(16) we get

$$\tau_\beta = \langle\tau_\alpha\rangle \exp\{(E_t - E_{fn})/kT\} + \exp\{(E_t - E_{fp})/kT\} \qquad (17)$$

The mean occupation time of the β-state differs substantially from that derived in [1] and [2]. The expected value of the β-state occupation time is determined by the electron capture as well as the hole emission. The coef-

ficients a_1 and a_2 express the relative participation of the two mentioned processes.

If the capture probability intensity of a hole is lower than the probability intensity of emission of an electron from a g-r center to the conductivity band, than $\tau_\alpha = 1/c_n n_1$; $a_1 \approx 1$. The mean occupation time of the β-state is given by the probability intensity of an electron capture only in the case that it simultaneously holds $p_1 \gg p$. This g-r center makes a trap and the equations for τ_α and τ_β are identical with those derived in [1] (see eqs (9),(10)). When increasing the injection the hole concentration grows up and the condition $p_1 \gg p$ is no longer satisfied. Then τ_α drops with increasing the forward voltage and the mean β-state occupation time is determined also by the process of hole capture and emission.

EXPERIMENT AND DISCUSSION

We measured the burst noise on p-n juction diodes and on Schottky diodes. The noise voltage was amplified by means of a wide-band amplifier and fed to a low-pass filter to reject other noise components than those of the burst noise. The durations of the pulses τ_α, τ_β were measured directly by a universal counter. The pulse duration distributions g_α, g_β were evaluated by a computer.

The probability density of the occupation of the α-state is represented in fig.1. The mean pulse length pertinent to the α -state $\langle\tau\rangle$ was found as aritmetic average of all pulse lenghts. This average value $\langle\tau_\alpha\rangle$ is an estimate of the τ_α, which determines according to (11) the theoretical distribution of the α state occupation time. The teoretical distribution $g_\alpha(t)$ is represented by the heavy line in fig.1. and is in a good agreement with the measured distribution.

The β-state distribution consists of two components which both correspond to exponential distributions with different time constants τ_1, τ_2 (fig. 2 and 4). The time constants τ_1, and τ_2 cannot be determined from the mean pulse durations in the β-state. To estimate them the second and third momentum of the pulse durations is to be determined. The estimate method will be published in the next paper.

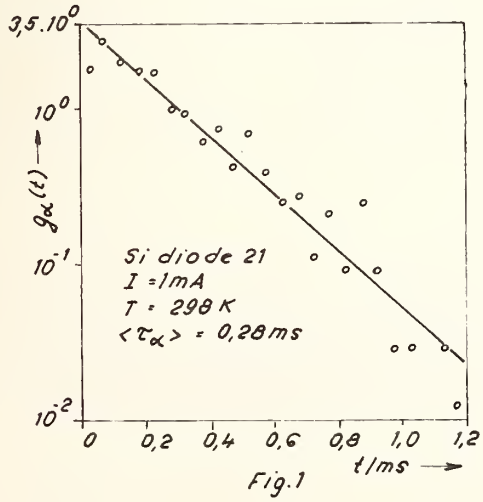

Fig.1

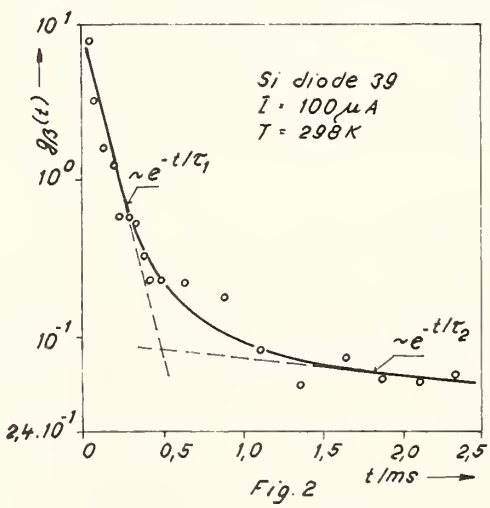

Fig. 2

The frequency dependence of the current fluctuation-spectral density (Fig.3) is a superposition of the 1/f-type noise and the g-r noise. The experimental dependence S_i can be approximated by a g-r noise spectral density with a single relaxation time $\tau_r = 156\mu s$. This value is near the time constant τ_1 value found from the probability of the β-state occupation time. The components of the spectral density S_i corresponding to the time constants τ_2 and $\langle\tau_\alpha\rangle$ should be within the frequency range f<500 Hz and probably are masked by the 1/f-noise.

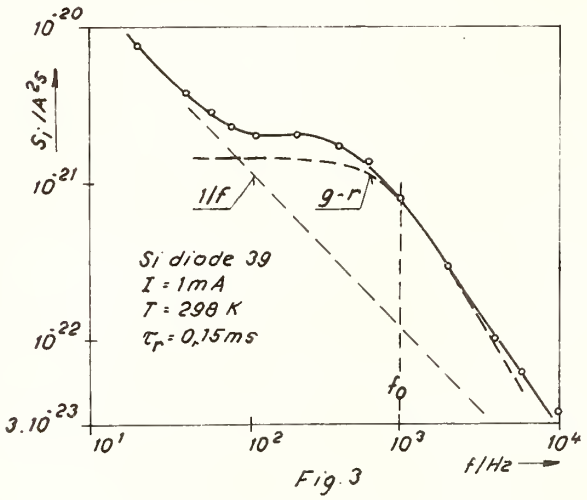

Fig.3

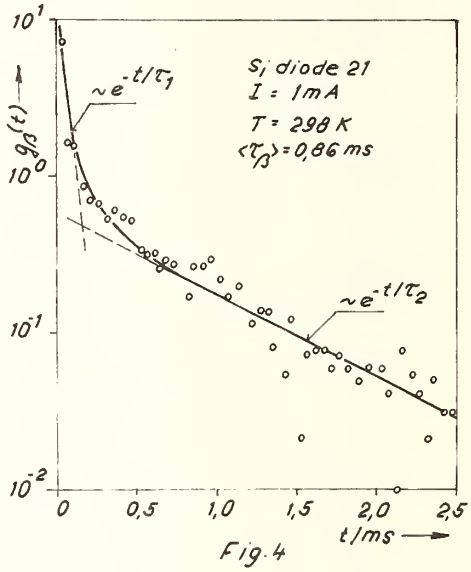

Fig.4

CONCLUSION

The generation-recombination process through the traps which have two charge states makes a three-state primary process. The secondary process representing the current modulation is a two-state process which, unlike the models presented up to now [1,2], features two states of the primary process projected into one state of the secondary process. Owing to this fact the system cannot be desribed by a markovian process. Experimental study of the α and β state occupation time distribution on p-n juction and Schottky diodes indicate that the β state occupation time set is not pure and consists of at least two subsets. These subsets are observed on the g_β distribution only in the case that the transition intensities of the primary process from the 0 state to the 1 and 2 state are not too different.

REFERENCES

1. S.T.Hsu, R.J.Whittier and C.A.Mead, Solid-State Electronics 13, 1055(1970)
2. K.B.Cook and A.J.Brodersen, Solid-State Electronics 14, 1237 (1971)
3. J.Šikula, M.Šikulová, B.Koktavý, P.Vašina, Burst Noise in LED's, in the Proc. of the International Conf.Radiative Recombination and Related Phenomena in III-V Compound Semiconductors, Prague Sept. 4-7 (1979).

NON-WHITE MULTIPLICATION NOISE IN THE DARK CURRENT REGIME OF A $P^+\Pi P\Pi N^+$ AVALANCHE DIODE

R. Alabedra, A.A. Walma, C. Maille, G. Lecoy

Centre d'Etudes d'Electronique des Solides, associé au C.N.R.S.
Université des Sciences et Techniques du Languedoc
34060 Montpellier Cédex, France

The object of this communication is to give experimental evidence of non-white noise appearing in the multiplication regime of avalanche photodiodes (R.A.P.D.) for frequencies lower than transit time effects. The darkness behaviour of the device was used to show this effect.

1. DEVICE UNDER ILLUMINATION CONDITION

In figure 1 is represented a crossection view of the device under test[1]

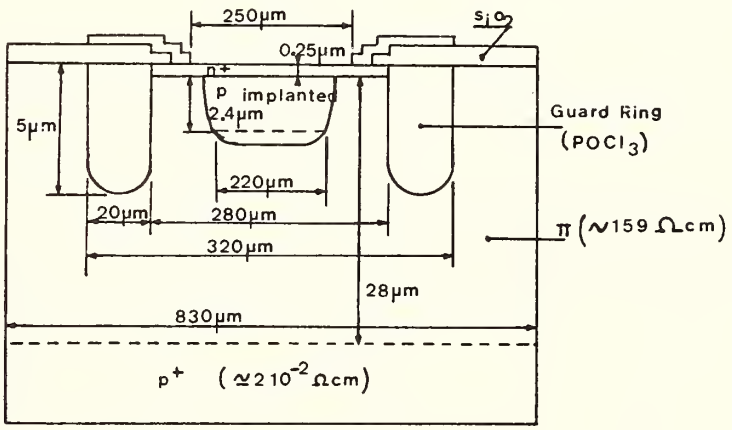

Fig. 1 Crossection view of the $n^+\pi p\pi p^+$ diode.

When illuminated on the n^+ side at λ = 827 nm, the multiplication regime is initiated by three current components | 1 | which are :

- The diffusion current of holes created in the n^+ region.
- The primary current of electrons created in the outside active multiplication region.
- The primary photocurrent of carriers generated in this active region.

---

(1) Devices provided by C.G.E. Marcoussis, France.

Without any multiplication, shot noise 2 q I_{ph} is associated to this photocurrent I_{ph} (see figure 2).

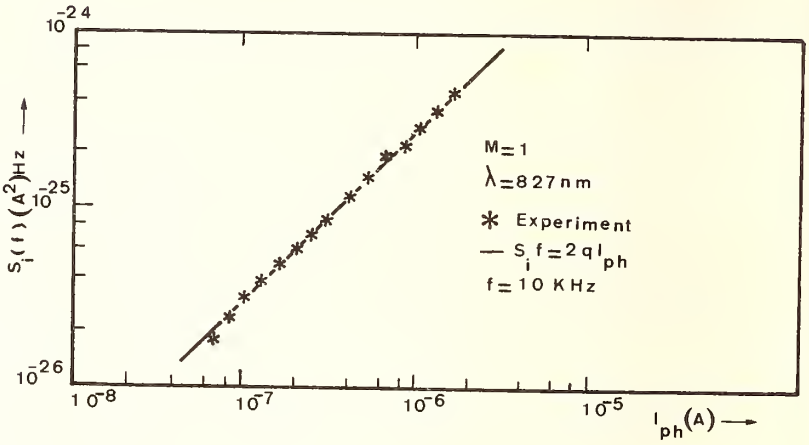

Fig. 2 Shot noise of the photocurrent without multiplication.

The statistics of the avalanche process amplifies the shot noise without any modification of its frequency dependence | 2 || 3 |. This result is represented in Fig. 3.

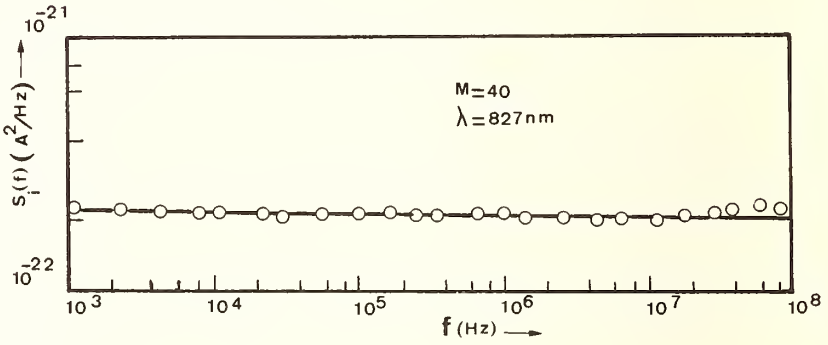

Fig. 3 Current spectral density as a function of frequency at M = 40.

The law describing the multiplication noise can be experimentally derived as :

$$S_i(f) = 2\ q\ I_{inj}\ M^x \qquad \text{with } 2 < x < 4 \qquad (1)$$

where I_{inj} is the macroscopic incident current.

M the macroscopic multiplication coefficient due to the three components of I_{inj} | 1 |.

Equation 1 can be written as :

$$S_i(f) = 2\ q\ I_{inj}^{1-x}\ I^x \qquad (2)$$

where $M = \frac{I}{I_{inj}}$

Measurements of the parameter x are performed for important bias current in order to avoid space charge spreading [4]. Fig. 4 gives the plot of $S_i(f)$ versus the bias current I. The deduced value of x is 2.25, which leads to an excess noise factor of 0.25 (this result is in good agreement with those published by J.J. Goedbloed and al. [5]).

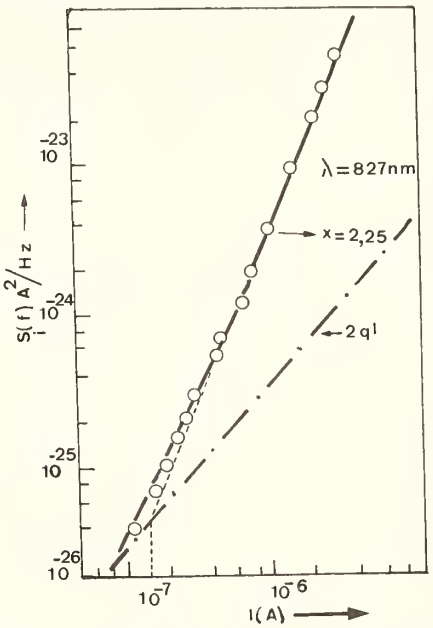

Fig. 4 Current spectral density as a function of the bias current at λ = 827 nm.

2. DEVICE UNDER DARKNESS CONDITION

Without illumination, experimental difficulties arise with respect to the extremely high impedance of the diode, the input capacity of the amplifier and low noise level. The nearest we can get for the moment with respect to the real dark current regime is by allowing a multiplication of about 40.

In the obscurity condition the incident current is not controlled, nevertheless a similar noise variation was expected. Noise spectra represented in Fig. 5 are not white whereas the experimental variation of $S_i(f)$ versus bias current follow nearly the same law given by equation 2 (see figure 6).

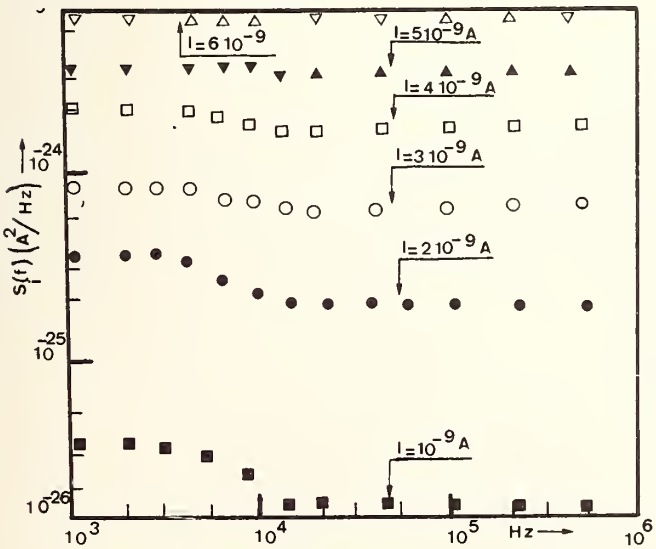

Fig. 5 : $S_i(f)$ versus frequency.

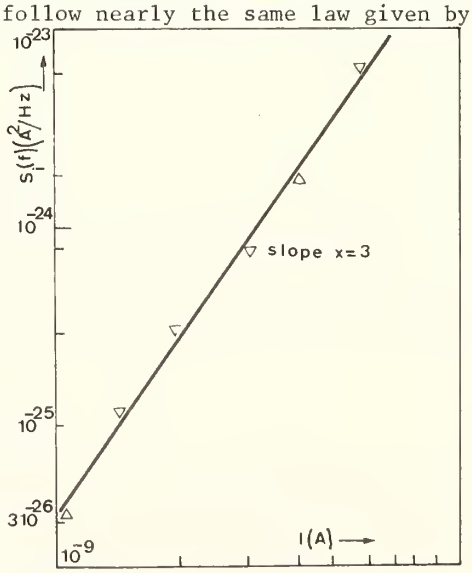

Fig. 6 Current spectral density versus bias current.

These experimental results without any attempt of physical interpretation confirm the remark of Van Vliet and al. | 3 | stating that it is not necessary to commit oneself to Poisson statistics of the primary particles.

One can notice in Fig. 5 that noise spectra are white when the bias current increases. This fact can be explained because the conduction regime is near of the avalanche process in which the incident current does not play any part . This behaviour starts for values of the bias current as low as 6.10^{-9} A. We propose an interpretation which consists of associating to the incident current a G-R noise instead of shot noise. The impurities can be identified as Au. This non-white noise is found but for weak darkness current ($I < 4.10^{-9}$ A). As soon as a photocurrent is injected in the device the results of the first paragraph are obtained again.

REFERENCES

| 1 | R. Alabedra, C. Maille, D. Ratsira et G. Lecoy, Revue de Physique Appliquée, 15, pp. 1201-1208, Juillet 1980.

| 2 | R.J. Mc Intyre, IEEE Trans. El. Dev. 13, 164 (1966).

| 3 | K. Van Vliet, A. Friedman, Z. Rucher, Part I and II, IEEE Trans. El. Dev. 26, pp. 746-764, May 1979.

| 4 | G. Lecoy, C. Maille, D. Ratsira, R. Alabedra, V^{th} International Conference on Noise in Physical Systems, Bad-Nauheim (1978).

| 5 | J.J. Goedbloed and E.T.J.M. Smeets, Elect. Lett. Vol. 14, pp. 67-69, (1978).

THEORY AND EXPERIMENT OF AVALANCHE NOISE IN THE WEAK MULTIPLICATION REGIME

C. Maille, R. Alabedra, G. Lecoy, M. Savelli

Centre d'Etudes d'Electronique des Solides, associé au C.N.R.S.
Université des Sciences et Techniques du Languedoc
34060 Montpellier Cédex, France.

INTRODUCTION

The purpose of this work is to verify the noise theories presented successively by Mc Intyre | 1 | and Van Vliet | 2 | on the basis of experimental results obtained on R.A.P.D. photodiodes (silicon diodes $n^+\pi p\pi p^+$ described in a previous work by R. Alabedra and al. | 3 |).

The interpretation of these results will be carried out with the help of the real structure modeling leading to the determination of the different currents created in the device and of the spectral intensity of the related noise currents.

MODELING

From the experimental capacity-voltage characteristics and values of the technological data given by the manufacturer, it has been possible to determine the doping profile of the carriers (ionic implantation) and the distribution of the electric field and the potential in the device | 4 |.

The exact profile being known it is then easy with the help of Poisson, transport and continuity equations to compute the different primary currents flowing through the device under illumination.

In the avalanche photodiode, the primary photocurrent is the sum of three components : the injected electron and hole currents (I_{on} and I_{op}) and the generated current in the high field region.

$$I_o = I_{on} + I_{op} + I_{ow} \qquad (1)$$

Using numerical data from Sze | 5 | for the calculation of the electron and hole ionization coefficients α and β, we have computed the electron and the hole multiplication factors M_n and M_p as M(x) which is related to the electron-hole pairs generated in the strong electric field region as a function of the x direction. The last parameter M(x) was computed on the basis of relations derived by Mc Intyre | 1 |. The knowledge of M(x) allows the definition of a multiplication factor M_w associated to the primary current I_{on} generated in the multiplication zone.

The expression of the multiplied total current is then :

$$I = M_n I_{on} + M_p I_{op} + M_w I_{ow} = M I_o \qquad (2)$$

where M is the overall multiplication.

Figure 1 gives the variations of the three multiplication factors as a function of M.

In Figure 2 are represented the related contributions to the total photocurrent I of the components $I_n = M_n I_{on}$ and $I_w = M_w I_{ow}$ for an illumination on the n^+ side at λ = 827 nm and a primary photocurrent I_o of 10^{-7} Amperes.

The contribution of $M_p I_{op}$ was found negligible ($\sim 10^{-9}$ Ampere).

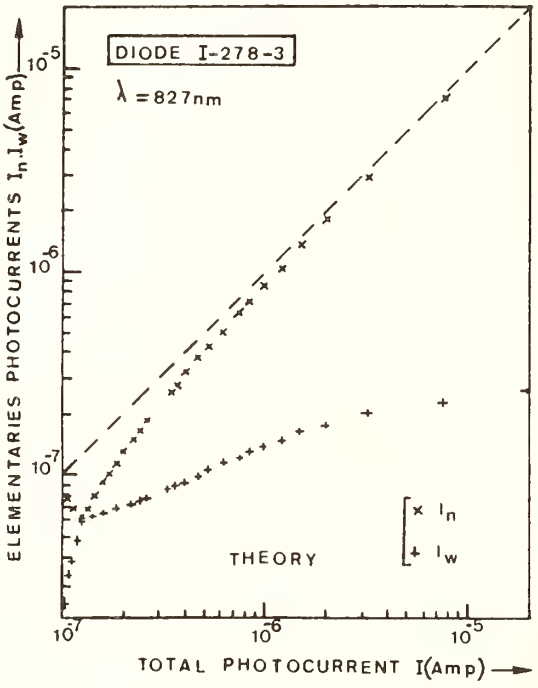

Figure 2 : Elementaries photocurrent components versus total photocurrent.

The good agreement of the experimental current-voltage characteristics under different illumination conditions (at λ = 827 nm) with the data given by the described model is verified in Figure 3.

The effects of the dark current can be non negligible if the injected photocurrent is low (i.e. for $I_o = 10^{-9}$ Ampere it is possible to observe an increase of the current in the I-V characteristic).

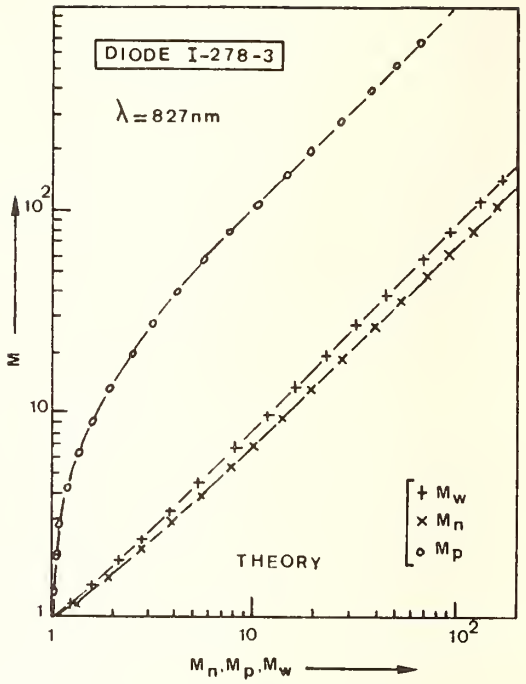

Figure 1 : Macroscopic multiplication factor M versus microscopic multiplication factor M_n , M_p , M_w .

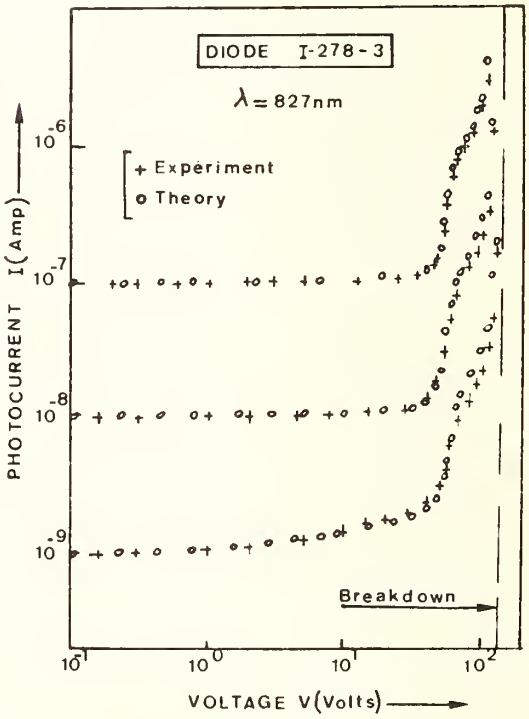

Figure 3 : Photocurrent-voltage characteristic.

NOISE

With the three current components I_n, I_p and I_w are associated uncorrelated noise components defined by their current spectral intensity $S_{in}(f)$, $S_{ip}(f)$ and $S_{iw}(f)$ such as :

$$S_i(f) = S_{in}(f) + S_{ip}(f) + S_{iw}(f) \qquad (5)$$

On the basis of the relations proposed by Mc Intyre | 1 |, it is possible to determine these three components and the total spectral intensity $S_i(f)$. The above mentioned spectral intensities are plotted versus the bias photocurrent in Figure 4.

If they are compared to the experimental results, we must point out the following remarks :

1) From both theoretical and experimental point of view, $S_i(f)$ can but be expressed in an empiric way by the relation $2 q I_o M^x$ in a restricted range of the multiplication factor.

2) The contribution of $S_{ip}(f)$ to the total noise is negligible.

3) On the other hand the contribution of $S_{iw}(f)$ cannot be neglected because it takes into account the simultaneous fluctuations of electrons and holes.

4) The theoretical results deduced from Mc Intyre's model | 1 | are greater than the experimental data.

Van Vliet | 2 | has theoreticaly shown yet that as soon as the possible number of ionizations by primary carrier transit was small ($N < 8$), Mc Intyre's results were overestimated.

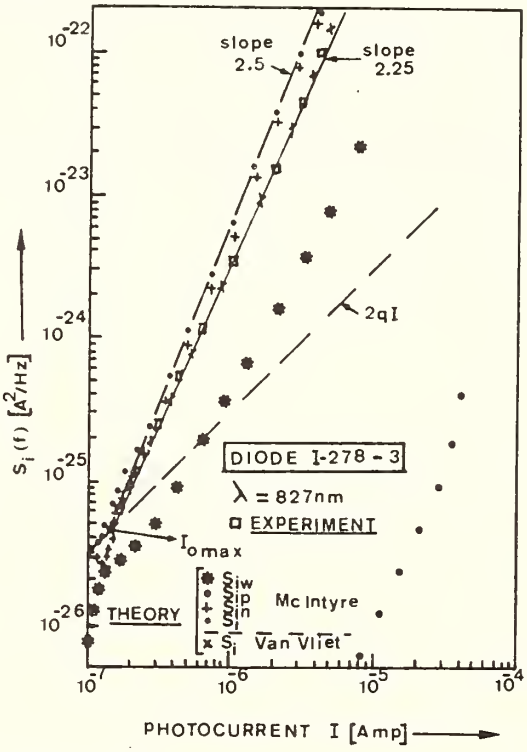

Figure 4 : Noise versus photocurrent.

We have then applied Van Vliet's variance method in which the constant values of k_{ef} (0.028 for silicon) has been replaced by its computed values as a function of M (see Figure 5) | 4 |.

In Figure 4 are reported the corresponding results. They show a good agreement with experimental datas. Goedbloed and Smeets | 6 | have obtained the same results on the basis of noise measurements performed in similar structures. This confirms that in $n^+ \Pi p \Pi p^+$ type photodiode, the number of ionizations per primary carrier transit is small as soon as M <100.

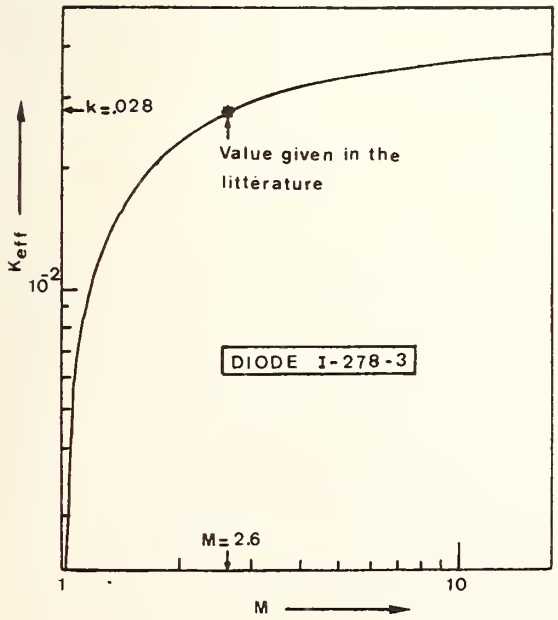

Figure 5 : Computed value of k_{eff} versus multiplication factor M.

REFERENCES

| 1 | R.J. Mc Intyre, IEEE Trans. Electron. Devices, Vol. ED-13, 164, (1966).

R.J. Mc Intyre, IEEE Trans. Electron. Devices, Vol. ED-19, 703, (1972).

R.J. Mc Intyre, IEEE Trans. Electron. Devices, Vol. 20, 637, (1973).

| 2 | K. Van Vliet, A. Friedman, Z. Rucher, Part. I and II, IEEE Trans. Electron. Devices, Vol. ED-26, 746, (1979).

| 3 | R. Alabedra, A.A. Walma, C. Maille, G. Lecoy, This issue.

| 4 | C. Maille, Thèse de Doctorat d'Etat, Montpellier, Juillet (1980).

| 5 | G.M. Sze, Phys. of Semiconductor Devices, Wiley, (1969).

| 6 | Goedbloed and J.M. Smeets, Electronic Letters, Vol. 14, 67, (1978).

NOISE MEASUREMENTS ON PHOTO AVALANCHE DIODES

Jeng Gong and K. M. van Vliet

Department of Electrical Engineering
University of Florida
Gainesville, Florida 32611

I. INTRODUCTION

A new theory based on "discrete device physics" was presented recently by van Vliet et al. [1], [2]. The salient features of this theory were: (1) The noise, when plotted as a function of the mean multiplication factor or gain M, shows breakpoints when the regime changes from N possible ionizations per carrier transit to N+1 possible ionizations per carrier transit; (2) the noise is always lower than the McIntyre limit, the latter being approached to within 5% for gains of the order of 100 or higher.

In this paper we present data on three types of diodes; RCA, Philips, and Nippon Electric, which closely confirm the new theory.

II. RESULTS OF THE THEORY

The main results of the theory for discrete ionization processes [2], obtained with the "method of recurrent generating functions," devised in that paper, are contained in the following two formulas [eqs (2-1) and (2-2)]. The gain or mean multiplication factor, $M \equiv \langle X \rangle$, for the regime in which N ionizations can take place in the path length W of the high field region, is given by:

$$M = \frac{(1+\lambda)^N (1-k)}{(1+k\lambda)^{N+1} - k(1+\lambda)^{N+1}} , \qquad (2\text{-}1)$$

where λ is the a priori probability for ionization by an electron after the length ℓ, necessary to gain sufficient energy to ionize, has been covered; μ is similarly the a priori probability for ionization by a hole and $k=\mu/\lambda$. The variance of the multiplication process was found to be, $\text{var } X_N \equiv \langle \Delta X_N^2 \rangle$:

$$\text{var } X_N = \frac{M(M-1)(1-k)}{2+\lambda+k\lambda} \left\{ -\lambda + 2 \frac{1-k\lambda^2}{1+k\lambda} \left[M k \frac{1+\lambda}{1-k} + \frac{1}{1+\lambda} \right] \right\} . \qquad (2\text{-}2)$$

We now consider the results (2-1) and (2-2) in more detail. At the onset of ionization the field is just high enough to sustain one possible ionization in the avalanche region W; thus N=1. With increasing field, the value of the probability, denoted as $\lambda(1)$, increases and so the gain increases according to eq. (2-1). The length ℓ_1 necessary to gain the ionizing energy simultaneously decreases, until two ionizations per carrier transit are possible. The value of $\lambda(1)$ just prior to this is denoted as $\lambda(1)_{max}$. When two ionizations per carrier transit are possible, the diode switches over from the regime N=1 to the regime N=2. To realize the gain M of that operating point, the value of λ for the new regime, denoted as $\lambda(2)$, is considerably less than the value of $\lambda(1)_{max}$ prior to the switchover, as is found by inverting eq (2-1) for λ with M fixed, taking N=1 and N=2 respectively. We also illustrate this behavior in Figure 1.

Equation (2-2) indicates that the decrease in λ causes var X to make a positive jump at this fixed M, which is called a break-point value. Figure 2 shows an overall curve of var X versus M.

III. NOISE REPRESENTATION

According to the variance theorem the total noise, spectral intensity S_{I_d}, due to primary current noise and multiplication noise, is given by

$$S_{I_d} = M^2 S_{I_{pr}} + 2qI_{pr}\,\text{var } X \approx 2qI_{pr}(M^2 + \text{var } X) \tag{3-1}$$

where we have assumed full shot noise for the primary current noise. For the equivalent saturated diode current of the noise we have

$$I_{eq} = I_{pr}(M^2 + \text{var } X) = I_{pr}\langle X^2 \rangle \ . \tag{3-2}$$

The excess noise factor is described by $I_{eq} = I_{pr}M^2F$ so that

$$F = 1 + (\text{var } X)/M^2 \ . \tag{3-3}$$

Instead of F we are interested in FM^2. The variance theorem result (3-2) is written as

$$I_{eq}/I_{pr} = M^2 + \text{var } X = FM^2$$

$$I_d/I_{pr} = M \ . \tag{3-4}$$

Theoretically, we have plotted log $(M^2 + \text{var } X)$ versus M (see figure 3). *If we now plot from the experimental data log (I_{eq}) versus log (I_d), then by eq (3-4) this plot must be identical with the theoretical curve of log $(M^2 + \text{var } X)$ versus log (M), the origin of the two curves being displaced along a locus at an angle of 45° with respect to the axes, the x-axis and the y-axis displacements being log (I_{pr}).* Thus, one simply needs to superimpose the experimental curve over the theoretical one, displacing the origin of the former along a 45° line from that of the latter, until the two curves superimpose. The horizontal (and vertical) displacement required yields I_{pr}. Once I_{pr} has been found, we then plot I_{eq}/I_{pr} versus I_d/I_{pr} on linear paper, and we compare it with the theoretical curves. From the magnitude as well as the break points in the curve, k is obtained for the best fit. Here we only give one log (I_{eq}) versus log (I_d) curve (see figure 4). The curve is very close to that of figure 3. The displacement of the origin gives I_{pr} = 96 nA.

IV. EXPERIMENTAL RESULTS

In the data to be presented we show the noise as expressed in equivalent saturated diode current $I_{eq} \equiv S_{Id}/2q$, as a function of diode current I_d. Figure 5 shows I_{eq} versus I_d for an RCA 3393 diode labeled RCA-3. The noise I_{eq} shows distinct breaks (vertical inflection points) indicated by arrows in the graph, corresponding to the transitions N→N+1.

Data for Philips diode (labeled PH1) are shown in figure 6; the regimes N=1 to 9 are clearly discernible.

The I_{eq} versus I_d curve for Nippon Electric diode (labeled N63) yielded similar results, as shown in Figure 7. The break points are somewhat less pronounced than for the previous diodes.

V. DISCUSSION OF THE RESULTS

A. RCA DIODES

For the diode RCA-3 the plot of log (I_{eq}) versus log (I_d), corresponding to figure 5, is given in figure 8; this yielded I_{pr} = 96 nA.

We will now make a rough estimate of the ionization coefficient α, where $\alpha=\lambda/\ell$ and $\ell=W/N$. We then compute α for the various break points. The λ's are inferred from the M break-point values and (2-1). For simplicity, we replace the triangular top of the field profile, see figure 9, by a rectangle of width W = 1.2μ and a field E = 3.5×10^5V/cm. Now we have the values of ℓ and α. Also, we calculate αs, where s is the phonon scattering mean free path (63Å at room temperature [3]) and E_I/eEs, where E_I is the ionization energy (1.6 ev) and E is proportional to applied bias V_b, with E being 3.5×10^5 at V_b = 100 volts. The results are plotted in figure 10. Also plotted is the theoretical Baraff curve [4] for the parameters E_R/E_I = 0.04 where E_R is the optical phonon energy of 0.063 eV [5] and r = 0.4. (Baraff's r is equivalent to the mean λ for the curve.)

We note that the data are of the right order of magnitude, which lends strong support to our interpretation of the break points and the small N-numbers involved. The results also compare favorably with the data of Lee et al. [6]. For E = 3.4×10^5V/cm, they give $\alpha = 2 \times 10^4$ cm^{-1} (their figure 12). We have (V = 97 volts), $\alpha = 1.3 \times 10^4$ cm^{-1}.

B. OTHER DIODES

For the Philips data of figure 6, the primary current was found to be I_{pr} = 10 nA. Converting the data of figure 6 to a plot of M^2 + var X versus M, the curve of figure 11 is obtained. The results are in excellent agreement with the theoretical plot for k=0.018.

The Nippon Electric diode data of figure 7 also fit the theory quite well, as shown in figure 12, with a primary current of I_{pr} = 5.1 nA, and for k=0.028.

REFERENCES

[1] K. M. van Vliet and L. M. Rucker, *IEEE Trans. Electron Devices* ED-26, 746 (1979).

[2] K. M. van Vliet and L. M. Rucker, *IEEE Trans. Electron Devices* ED-26, 752 (1979).

[3] J. Conradi, *Solid State Electr.* 17, 1145 (1967).

[4] G. A. Baraff, *Phys. Review* 128, 2507 (1962).

[5] C. R. Crowell and S. M. Sze, *Appl. Phys. Letters* 9, 242 (1966).

[6] C. A. Lee R. A. Logan, R. L. Batdorf, J. J. Kleimach, and W. Wiegmann, *Phys. Review* 34, A761 (1964).

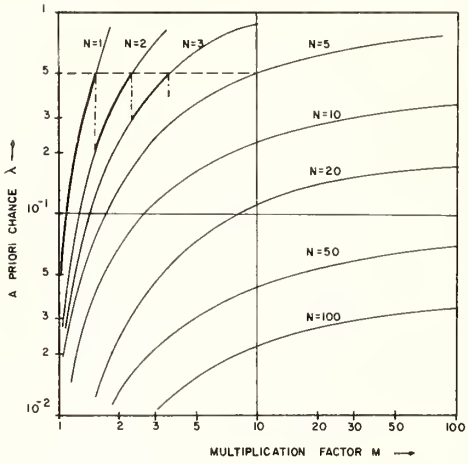

Fig. 1 λ vs. M.

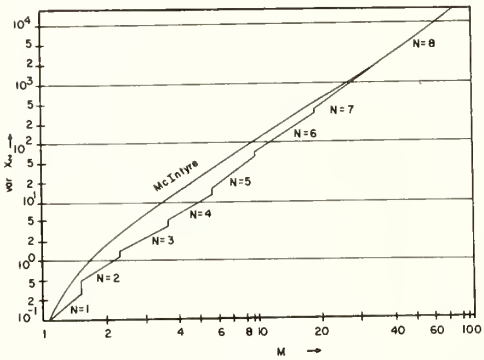

Fig. 2 var X_N vs. M.

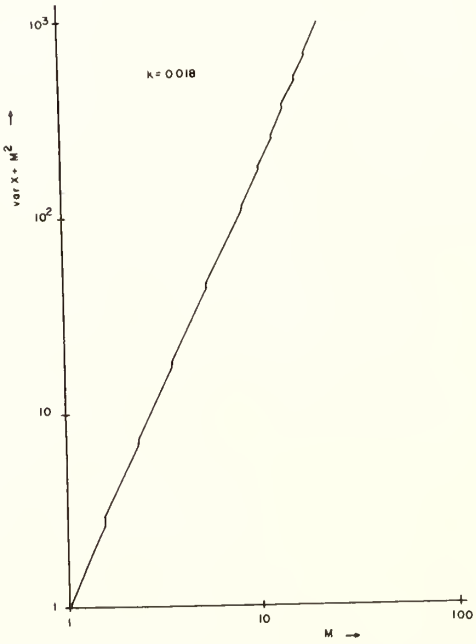

Fig. 3 var X + M^2 vs. M for k = 0.018.

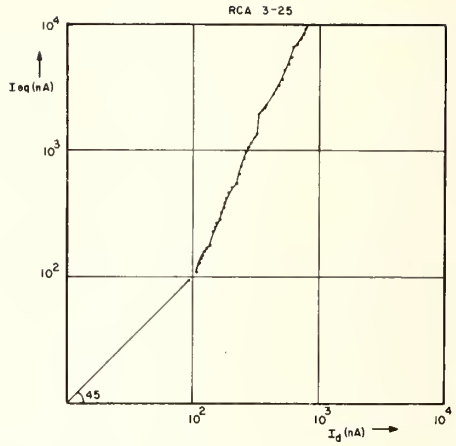

Fig. 4 RCA 3 I_{eq} vs. I_d in log-log scale.

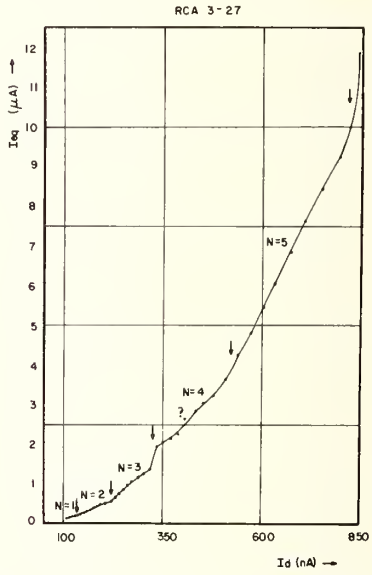

Fig. 5 RCA 3 I_{eq} vs. I_d in linear scale

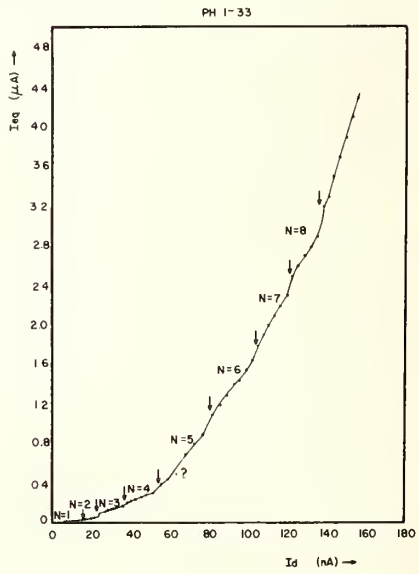

Fig. 6 PH 1 I_{eq} vs. I_d in linear scale.

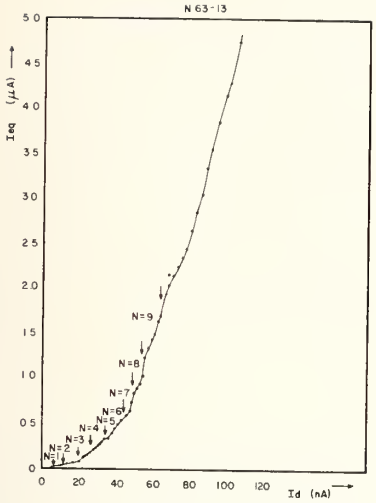

Fig. 7 N63 I_{eq} vs. I_d in linear scale.

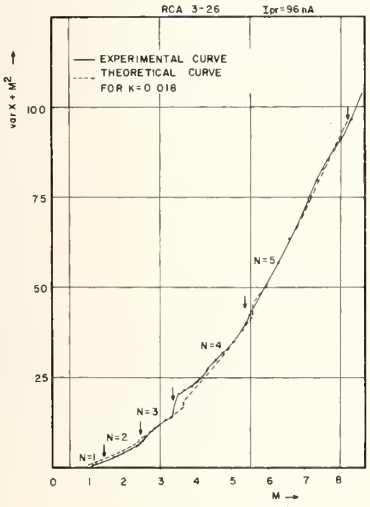

Fig. 8 RCA 3 var X + M^2 vs. M.

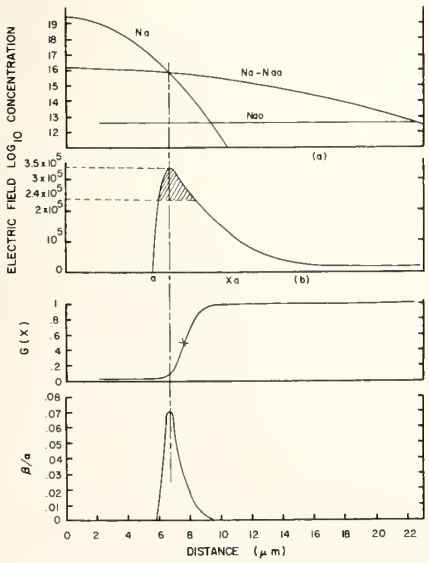

Fig. 9 RCA diode structure.
Courtesy of RCA Ltd., Quebec, Canada.

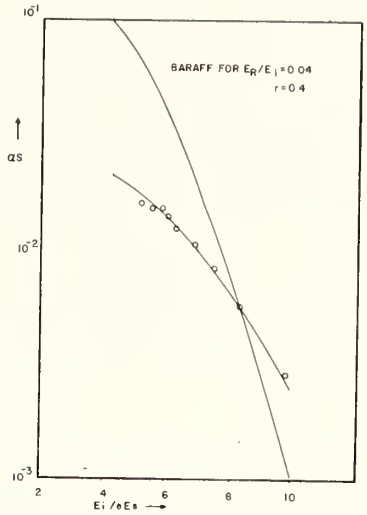

Fig. 10 Comparison of experimental values with Baraff curve.

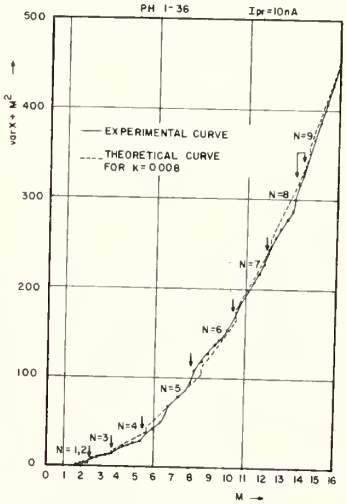

Fig. 11 PH 1 var X + M^2 vs. M.

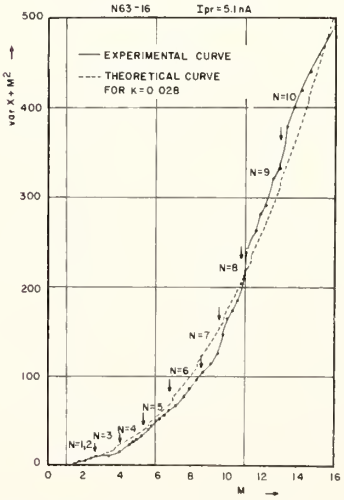

Fig. 12 N63 var X + M^2 vs. M.

NOISE IN HETEROJUNCTION TRANSISTORS

G. Blasquez, F. Lavernhe, A. Marty and J.P. Bailbe

Laboratoire d'Automatique et d'Analyse des Systèmes
Centre National de la Recherche Scientifique
7 Ave. Roche, 31400 Toulouse, France

THEORETICAL MODEL

In the majority of studies of hetero junctions it is considered that carrier transport can be carried out by diffusion, by tunneling and by thermoionic effect. The noise associated with these three mechanisms is fundamentally shot noise. If in addition, recombination centres exist in the hetero junction space charge, some of the carriers recombine by creating an extra noise source. Since the mean squared value of this noise is hardly different to that of the shot noise, the total noise associated with the sum of the current components is described, as a first approximation, by the Schottky relationship. Consequently the noise behavior of a heterojunction transistor (H.T.) must be analogous to that of a junction transistor (J.T.).

EXPERIMENTAL RESULTS

In order to investigate the real behaviour of these devices a mesa-type transistor has been processed by liquid-phase epitaxy in our laboratory [1] . The growth procedure starts first with a substrate etching by a nondoped unsaturated melt ; the substrate material used is $<100>$ oriented and tellurium doped n^+ - Ga As. Next comes the deposition of an n - type collector layer from the same melt subject to a temperature decrease. The following p - Ga As type base layer has a thickness ranging between 0. 5 and 1 μm and is strongly Ge doped (N_{AB} of about 10^{19} cm $^{-3}$). Finally the emitter region, which is Sn-doped GaAlAs, consists of two layers : the first one with an Al concentration $x \simeq 0.4$ is weakly doped, the second with a smaller aluminium content ($x \simeq 0.2$) but with a much more higher doping level. This last layer is intended to facilitate the deposition of good quality ohmic contacts.

A study of D.C. and A.C. behavior showed that the h_{FE} gain varied from ten or more to some hundreds, that the breakdown voltage BV_{ceo} was equal to or higher than 25 volts and that the gain bandwidth product was of the order of some GHz [1] , [2].

The noise study consisted of measuring the input equivalent voltage e_n and the current i_n noise generators. Measurements were made by the direct method described in [3] .Biasing conditions were $0.3\,\mu A \leq I_c \leq 3\,mA$, $3V \leq V_{CE} \leq 10V$. The frequency range analyzed was from 10Hz to 1MHz. The accuracy of the measurements was estimated at about 10 %. At low frequency 1/f excess noise has been observed. In the present state of our technology its value is dispersed. In the frequency range where this excess noise did not predominate (typically f >10 kHz) the spectra are white and independent of the collector base voltage. In such conditions, and for a collector current $I_c \leq 30\ \mu A$, an examination of Figs. 1 and 2 shows that the behaviour of the H.T. is analogous to that of the J.T. for $I_c \geq 30\ \mu A$ the generator e_n has a mean squared value. Which goes through a minimum and then slowly increases. Correlatively the generator i_n has its m.s.v. which increases more rapidly than $2\ q\ I_B\ \Delta f$.

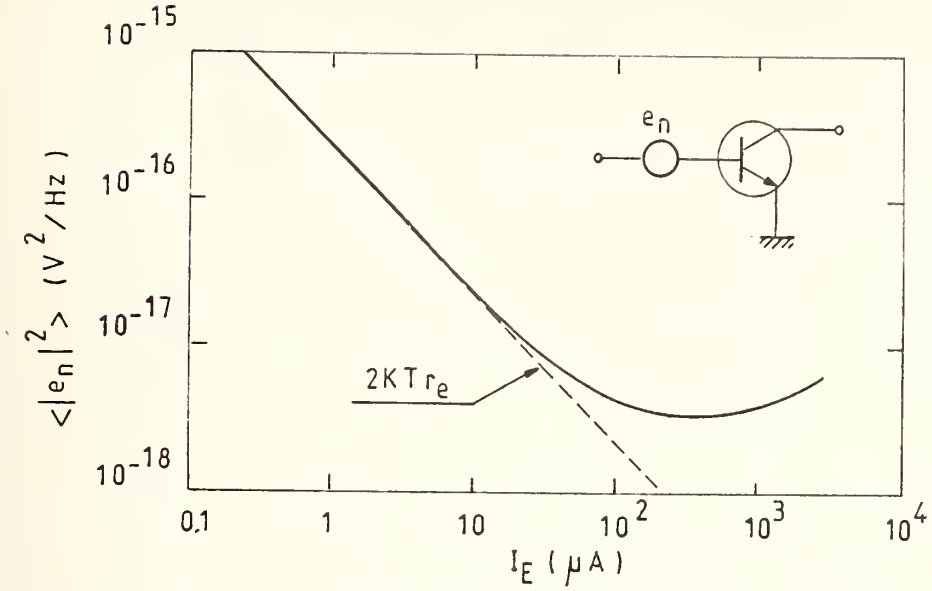

Fig. 1 : Equivalent input voltage noise generator vs emitter current.
Experimental conditions : T = 20°C, V_{CE} = 3 V, f = 30 kHz.

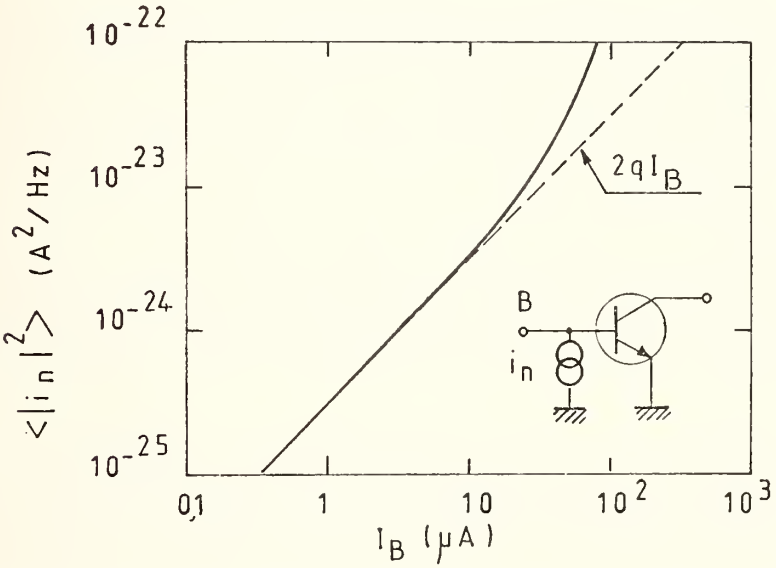

Fig. 2 : Equivalent input current noise generator vs base current.
Experimental conditions : T = 20°C, V_{CE} = 3 V, f = 30 kHz.

Figure 3 gives the equivalent input current noise generator in the common base configuration when the input is short-circuited.

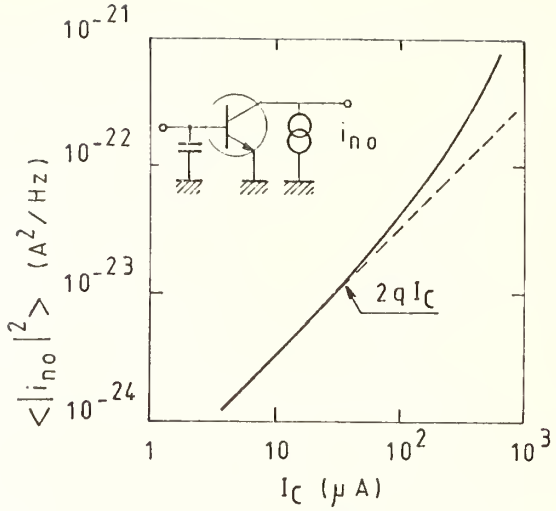

Fig. 3 : Equivalent output current noise generator vs. collector current. Experimental conditions : T = 20°C, V_{cB} = 2 V, f = 30 kHz.

For $I_c \leq 30\,\mu A$ we have $\langle |i_{no}|^2 \rangle \simeq 2qI_c\Delta f$ as expected. For $I_c > 30\,\mu A$ an excess noise is again observed. By substituting $\langle |i_{no}|^2 \rangle$ into the theoretical expressions of $\langle |e_n|^2 \rangle$ and $\langle |i_n|^2 \rangle$ it appears that the excess noise is essentially due to that of $\langle |i_{no}|^2 \rangle$. With the aim of localizing the origin of this excess, a study of i_{no} as a function of the collector base voltage was carried out. The results obtained show that $\langle |i_{no}|^2 \rangle$ is independent of V_{cE}. This suggests that the origin of the excess noise is due to a generation recombination mechanism.

CONCLUSION

To summarize : simple theoretical considerations suggest that heterojunction bipolar transistor noise is described by the same expressions as those for junction transistors. An experimental study of GaAlAs/GaAs heterojunction transistors confirmed this analysis for low biasing levels.

We thank the technology center of LAAS for fabrication of the experimental transistors ; more specially, Mr G. Pierrel, Mr Pham Huu Hiep, Mrs J. Chevalier, G. Lacoste, C. Solano and P. Fadel for their assistance.

REFERENCES

[1] J.P. Bailbe, A. Marty, Pham Huu Hiep and G. Rey, IEEE Trans. on Electron. Dev ED27, 6, 1160 (1980).

[2] A. Marty, G. Rey and J.P. Bailbe, Solid State Electronics 22, 549 (1979).

[3] G. Blasquez, Comptes Rendus à l'Académie des Sciences, Paris, t 289, Série B, 219 (1979).

DIGITAL ANALYSIS OF SUPERIMPOSED FLUCTUATIONS ON A PULSE TRAIN

A. Touboul, A.A. Walma, G. Lecoy

Centre d'Etudes d'Electronique des Solides, associé au C.N.R.S.
Université des Sciences et Techniques du Languedoc
34060 Montpellier Cédex, France

INTRODUCTION

The output signal of a Charge-Coupled Device (Surface and Buried Channel) consists of pulses determined by the clock pulses frequency with superimposed fluctuations due to the non-ideal behaviour of the transfer and the storage of the charge packet. These devices play an important role in signal processing and imaging applications. Noise measurements can be used as a means of electrical characterization. A well-known figure of merit for a C.C.D. is the r.m.s. number of fluctuating carriers associated to the charge packet. We propose a digital method of noise measurements. Results obtained on surface-channel C.C.D.'s will be discussed.

COMMENTS ABOUT THE ANALOG METHOD

The usual procedure is described widely in literature [1],[2],[3]. It consists of filtering out the clock pulses (at half the clock frequency) and performing a spectral density analysis. For this purpose, the output signal is supposed to be stationary and the fluctuations should follow a gaussian law. The weaknesses of this method are the following.

This analog method multiplies the measured spectral density at half the clock frequency with the relevant bandwidth in order to obtain the variance of the number of fluctuating carriers in the well. An important error arises from the fact that the measured noise is not white. Moreover, the output signal consists of pulses the amplitudes of which are related to a reference (or "reset") level. During the read-out and the reset phases, the output amplifier is biased under different conditions. So the output amplifier gives an "average" of the noise from which informations about the C.C.D. operation should be extracted.Another limitation of this method could be mentioned if the "sampling effect" of the C.C.D. operation is considered. Indeed for a 3-phase C.C.D., a numerical factor has to be determined according to calculations given in reference [4].

DIGITAL ANALYSIS OF THE NOISE

In order to overcome all the above-mentioned difficulties, we propose a different method described in figure 1. The output signal is sampled and A/D converted after amplifying the superimposed fluctuations by using an artificial threshold as a reference. The latter avoids any saturation of the amplifier by the clock pulses. The data acquisition is performed at the clock frequency, but any sequence of data acquisition can be realized.

This procedure is no longer limited by the filter-response and by the noise standard precision. Moreover it is unsensitive to drifts of the C.C.D. bias system. (For a 50 kHz clock frequency data are stored in 20 m sec).

Before calculating the fluctuations parameters, the following tests are performed on the data considered as time series :

- The stationarity is checked by means of a "rank test" giving the "Kendall's τ" [5].
- The randomness of the data is verified by using the "turning-point" method [5] .

- Trend analysis can be performed to suppress a possible parasitic signal present in the data by means of averaging the data.

Then, the following statistical parameters are calculated for each file of 1024 data : the mean value M, the variance V, the skewness S and the kurtosis K of the amplitude distribution, the autocorrelation factor C.

The spectral intensity of the noise voltage is obtained by a F.F.T. program including a Hamming-window to avoid aliasing effects.

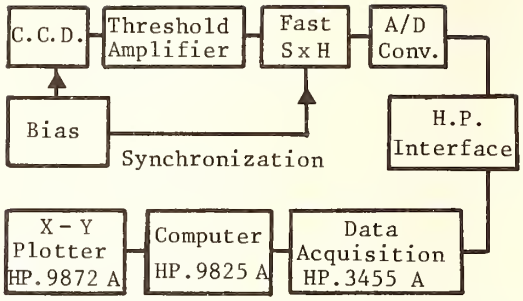

Fig.1: Block diagram of the experimental set-up.

The calculated variance is easily converted into a r.m.s. number of carriers with the help of a numerical factor including the amplifier gain and the total output capacitance of the on-chip read-out circuit.

RESULTS ON SURFACE-CHANNEL C.C.D.'s[1]

3-phase C.C.D.'s with one level of Al gates have been tested. The rather large gate areas allow the processing of charge packets in the order of 3×10^7 carriers.

The stationary and random properties of the C.C.D. noise have been verified through the parameters described in the previous section. The r.m.s. number of noise carriers are in the range 4400 → 5600 for a standard delay line operation. They confirm the low noise properties of C.C.D.'s and lead to S/N ratios better than 75 dB's. As a comparison, the fluctuations measured on a clock pulse necessary to drive the C.C.D.'s under test have given an equivalent number of noise carriers of 120.

To eliminate the effect of a possible pick-up (50 Hz and its harmonics) or of a deterministic trend in the noise, the data can be "smoothed" by realizing an averaging over at least 10 files (10 x 1024 samples). So, parasitic signals vanish as their phase is random.

Thornber's calculations [6],[7] on the transfer have shown the existence of correlations between neighbouring charge packets. The calculations of the autocorrelation coefficient did not point out such a mechanism (see figure 2).

The frequency dependence of the output noise is represented in figure 3 ; at lower frequencies, the noise follows a 1/f law and reaches a constant level till the Nyquist frequency ($f_c/2$). The ($1 - \cos 2\pi f/f_c$) behaviour is not observed. This result could be expected on the basis of the correlation coefficient represented in figure 2.

Carnes et al. [7] had derived a general expression of the charge variance by considering an "incomplete transfer" noise source :

$$\overline{N^2} = 2\, n\, \varepsilon\, N_s \qquad (1)$$

where n is the number of transfers, ε the transfer inefficiency and N_s the number of carriers in the well. This expression can also be obtained by assuming that the trapping on Fast Interface States [8] dominates the noise.

The measured noise is in good agreement with values given by eq. 1 as long as N_s is less than 75 to 80 % of the full well. For greater values of the charge packet, the measured noise decreases (see figure 4). This same variation has been found for ε measurements versus the packet size.

---

[1] Devices provided by LETI/MEA - CENG - FRANCE.

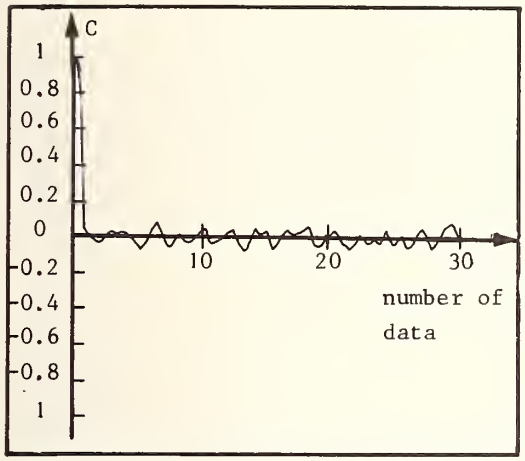

Fig.2 : Autocorrelation coefficient vs. the number of data.

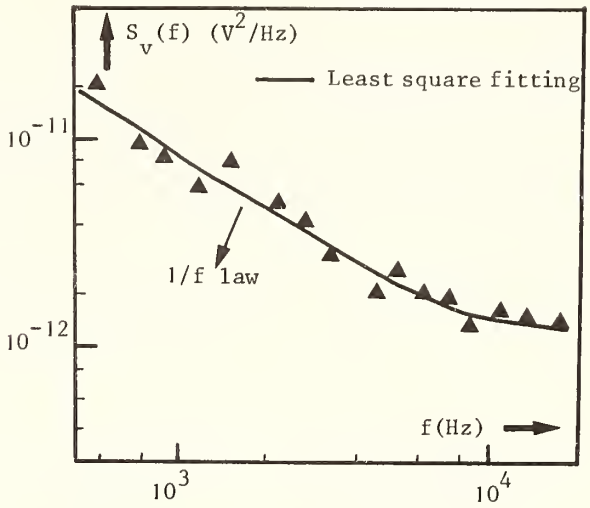

Fig.3 : Spectral intensity of the noise voltage (by F.F.T.).

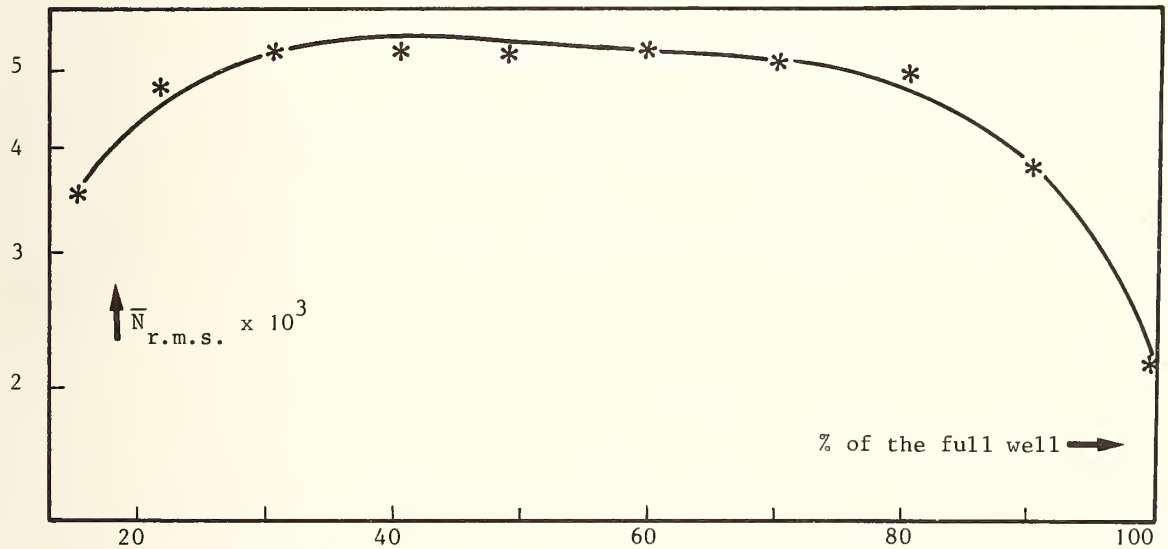

Fig. 4 : Variation of the rms number of noise carriers vs. the packet size.

This last behaviour can be explained within the F.I.S. and the S.H.R. statistics context. Indeed the minimum value of the fluctuations of the number of trapped carriers occurs for a full well when the product $f_t(1-f_t)$ becomes null. So the value of $\overline{N}_{r.m.s.}$ obtained for a full well is mainly due to the extrinsic noise sources (charge injection, output amplifier...). The calculated value of the number of noise carriers due to trapping mechanisms is compared to the product result $f_t(1-f_t)$. A good agreement with the theoretical law is obtained (see figure 5).

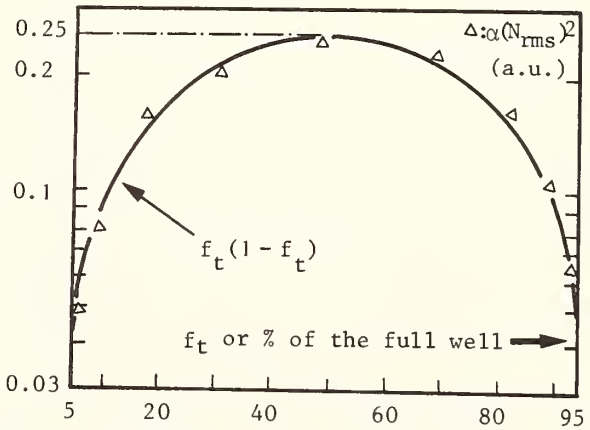

Fig. 5 : Comparison of $f_t(1-f_t)$ and calculated values of $(N_{rms})^2$.

CONCLUSION

The flexibility of this method of measuring fluctuations in C.C.D.'s has been checked by applying it to various kinds of devices. These means of electrical characterization represent a powerful tool to predict the performances of devices with reduced geometry gates (and small packet sizes). They can give information on the lower limit of the storage cell dimension when considering the V.L.S.I. development of C.C.D.'s. However their low noise properties are such that other limitations as hot electrons effects may be more restrictive.

REFERENCES

[1] J.E. Carnes, W.F. Kosonocky, RCA Rev. 33, 327 (1972)

[2] A.M. Mohsen, M.F. Tompsett et al., IEEE Trans. on Electron Dev. ED-22, 209 (1975)

[3] R.W. Brodersen, S.P. Emmons et al., IEEE Trans. on Electron Dev.ED-23, 215 (1976)

[4] D. Middleton in "An Introd. to Stat. Comm. Theory" Ed. Mc Graw-Hill (New-York, 1960) Chap. 4.

[5] S.M. Kendall in "Time-Series" Ed. C. Griffin (London, 1976), Chap. 3→7.

[6] K.K. Thornber, Proc. IEEE 60, 1113 (1972)

[7] K.K. Thornber, B.S.T.J. 53, 1211 (1974)

[8] M.F. Tompsett, IEEE Trans. on Electron. Dev. ED-21, 701 (1974)

NOISE IN DIELECTRIC MATERIALS

J.Šikula, A.Čermáková, M.Čermák, P.Vašina

Department of Physics
Technical University of Brno, Barvičova 85.
Czechoslovakia

INTRODUCTION

During the process of the dielectric polarization, the time fluctuation of the polarization vector $\vec{P}$ takes place. Consequently, there appears a noise current in the circuit. We studied the current fluctuations in a dielectric produced by a) a steady electric field, b) varying electric field.

In a capacitor in the thermal equilibrium there is a noise the origin of which is in the stochastic nature of the interaction among the electric dipoles and the phonon field. This is the steady state thermal noise [1,2]. In the second case, i.e., when a varying electric field is applied a non-stationary noise is produced due to the stochastic process of dipole orientation in the external electrical field and in the case of ferroelectric materials due to the domain nucleation, decay and their motion.

In the short circuit the polarization vector fluctuation can be measured[1]. The current fluctuations are due to the polarization fluctuations and it holds

$$i = \frac{d}{dt}\int \vec{P}.d\vec{A} \qquad (1)$$

where i_P is the polarization current, A-the area, $\vec{P}$-the polarization vector.

Simultaneously with the polarization current there flows also a conductivity current both due to the DC sample conductivity and due to the carrier injection from the electrode. Along with spectral density of the current noise we measured the U-I curve and the time dependence of the DC component of sample current.

EXPERIMENT

We studied samples of three industrially important insulating materials, namely the paper base laminated sheets whose thickness was 0.6 mm and the electrode diameter was 3 cm; the polyethylene terephtalate (40 μm thichness) and softened PVC coaxial cable with a cylindrical internal electrode of a diameter 0.8 mm and external dielectric diameter 1.6mm. The electrical parameters of PVC were as follows: the relative permittivity ε_r = 3.5; tgδ = 0.08 at 800 Hz and the breakdown electral field strength 4.10 V/m. The heat resistance of this material is 70° after Martens. The U-I curves and the time dependence of the DC current were measured by conventional methods. Fig.1 shows the U-I curve of the PVC-1 sample and the aging effect (the time cycle 28 days, the temperature 80°C). The original state is represented by the curve 1.1. The current can approximated by the function

$$I = I_0 \exp(a\sqrt{U}), \qquad (2)$$

where for the PVC-1.1 sample we have $I = 3.10$ A, $a = 5.5 \cdot 10$ $V^{-1/2}$. The U-I curve of the polyethylene terephtalate sample has not been measured owing

to a very high sample resistance (more than 10^{15} ohms). The U-I curve of the paper base laminated sheets can be expressed in the form $I \sim U^n$, where the Ohm's law region (n = 1) passes into the square law (n = 2) region at the electric field intensity of about 5.10^5 V/m.

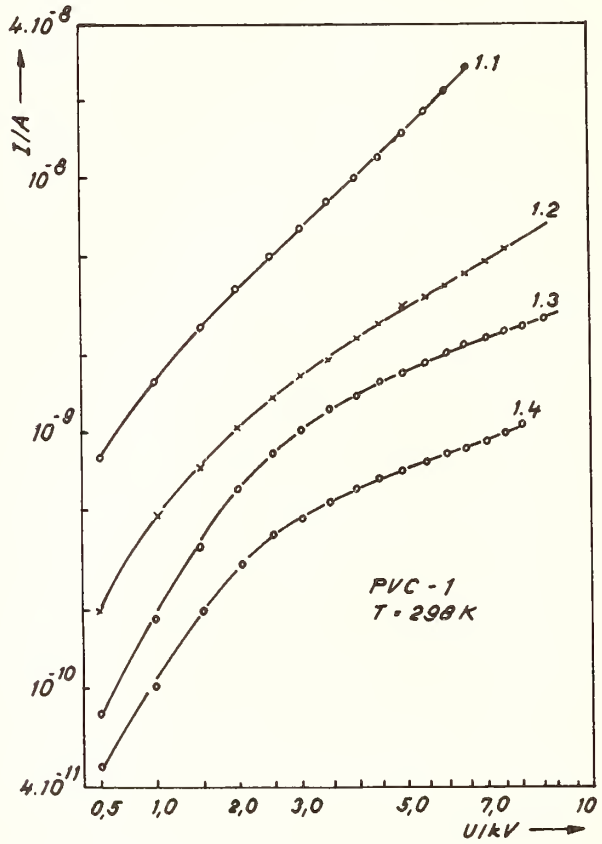

Fig.1. The U-I curve of the PVC-1 sample

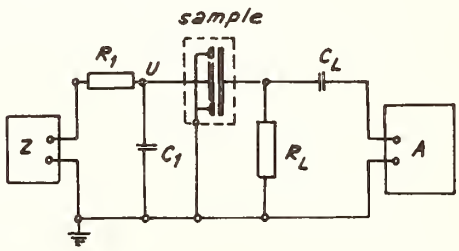

Fig.2. Apparatus for the measurement of the dielectric noise

If we neglect the transient effect of the capacitor charging (the time constant is less than 1 ms) then the time dependence of the DC component is due to the polarization relaxation current and it holds

$$I = I_o + I_r \exp(-t/\tau), \qquad (3)$$

where we have for the paper base laminated sheet τ_1 = 3.6 s, for PVC τ_2 = 30 ms at U = 1 kV and τ_2 = 16 ms at 6 kV. The time necessary for reaching the steady state decreases when the applied voltage increases.

The experimental study of the dielectric noise was carried out as follows. The sample with the measured dielectric was connected in the circuit drawn in Fig.2., where A is the statistical analyzer, Z-the supply, C_1 R_1-the filter, R_L-the load resistor, and C_L the coupling capacitor. The sample was shielded and the electrode connected to the supply was protected by means of a guard ring. The resistance of R_L was more then 100 times as less as the real component of the impedance of the measured capacitor, so that for the AC component the sample was short circuited.

The spectral density S_i of the current fluctuations depends on the time dependence of the electrical field strength. In Fig.3 the time dependence of the spectral density S at f = 800 Hz is shown for the PVC-1.4 sample for the step voltage of 8 kV. If we neglect the transients in the measuring apparatus, the spectral density of the current fluctuation decreases to its steady state value with a time constant of about 42s . For the polyethylene terephtalate the time constant is of the same order, while for the paper base laminated sheets the speed of reaching the steady state value is by more than one order of magnitude higher.

For the paper base laminated sheets, the steady state spectral density vs. voltage plot at f = 800 Hz is in Fig.4. Within the limits of the measuring error, this result is in agreement with the value of S_i obtained in the conditions of the ramp voltage, the slope of which is less than 10 V/s.

The spectral density S_i of the PVC and the polyethylene terephtalate de-

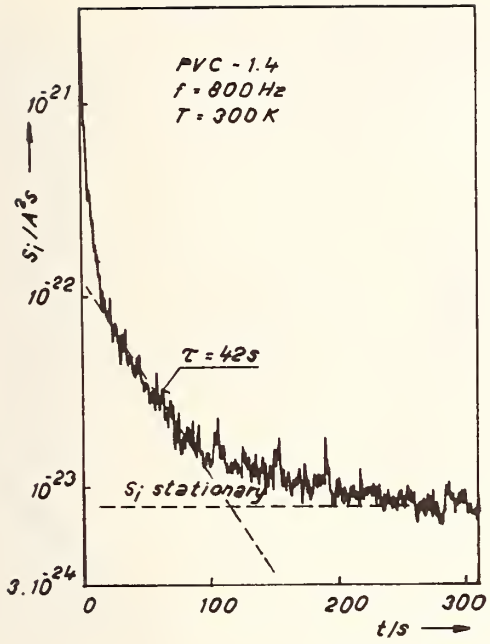

Fig.3. Time dependence of the spectral density of the PVC-1.4 sample

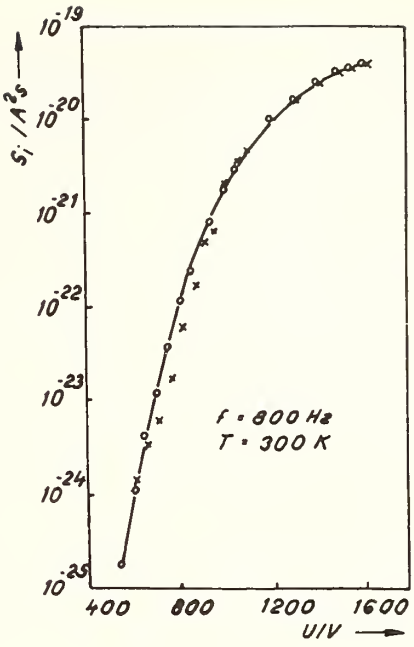

Fig.4. The steady state spectral density of the paper base laminated sheet

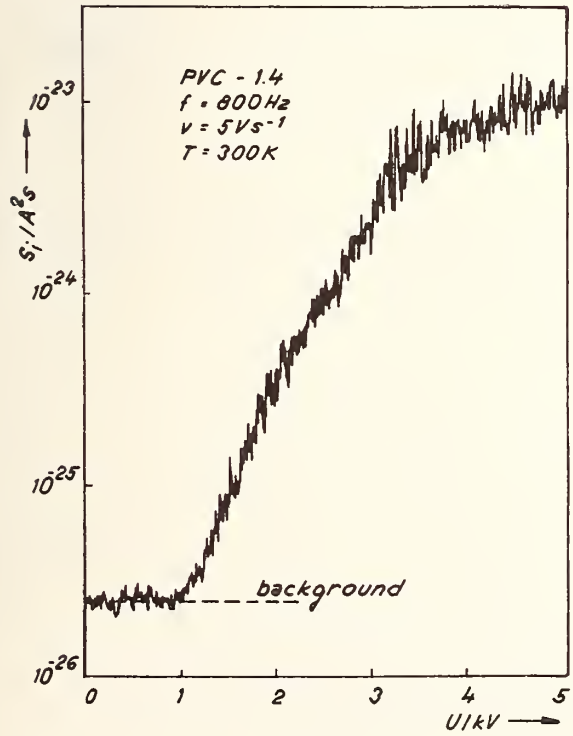

Fig.5. The S_i vs. U plot.

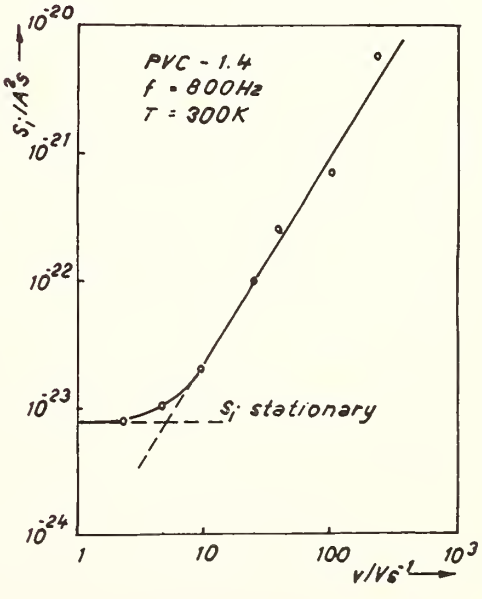

Fig.6. The spectral density vs. the ramp voltage time rate diagram.

pends on the ramp voltage slope. Fig.5 shows the spectral density S_i ; for the PVC-1.4 sample at f = 800 Hz and the ramp voltage slope 5 V/s. In Fig.6 we bring the spectral densities at U = 8 kV for various slopes v of the ramp voltage ($2.5 \leq v \leq 250$ V/s). The steady state value of the spectral density is indicated by the dotted line.

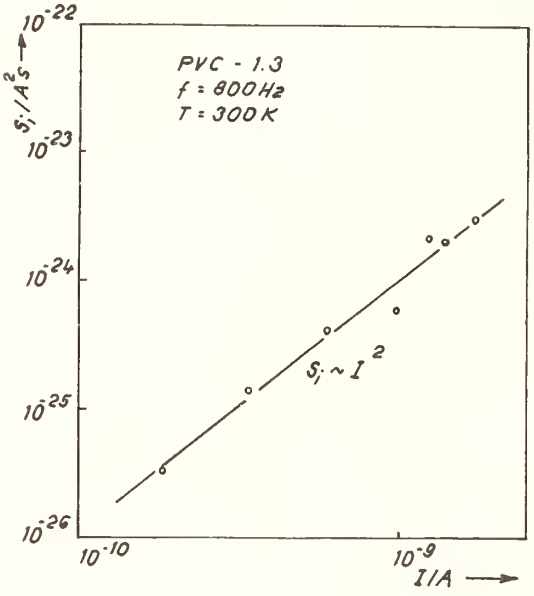

Fig.7. The spectral vs.current plot for the PVC-1.3 sample

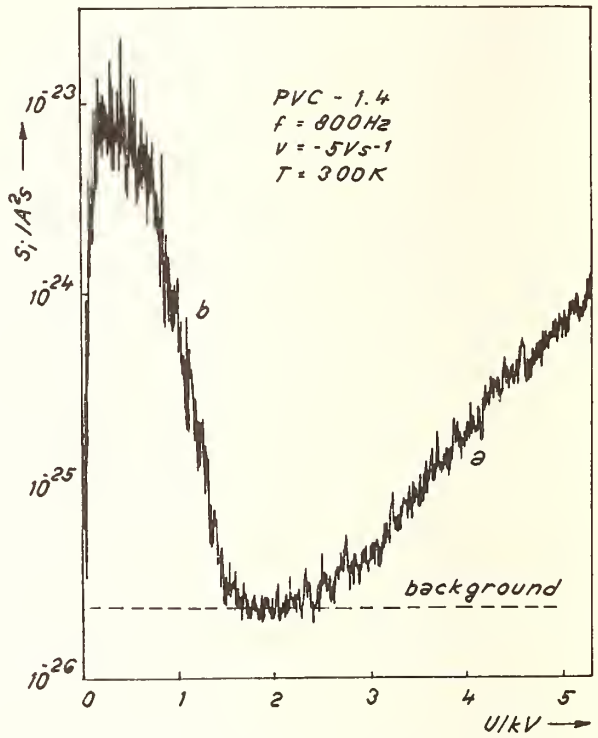

Fig.8. The spectral density vs. voltage plot for linearly decreasing sample voltage

In Fig.7 is the dependence of the current fluctuation steady state spectral density on the current for PVC-1.3 at f = 800 Hz. From this experiment it follows that the spectral density is proportional to the square of the current.

The spectral density vs. voltage plot when linearly decreasing the sample field strength for PVC-1.4 is in Fig.8.

DISCUSSION

For our experiments we chose insulating materials with a wide range of the electrical resistivity. The lower value of resistance was exhibited by the paper base laminated sheets (the sample resistance being of the order of $10^{11}\,\Omega$), while the resistance of the PVC samples was about $10^{13}\,\Omega$ and that of the polyethylene terephtalate was higher than $10^{15}\,\Omega$.

The S_i vs.voltage plots show a saturation both for the steady state and the linearly increasing voltage (Figs. 4 and 5). The spectral density S_i is an exponential function of the voltage (see Figs. 5,8). At lower values of the voltage, the noise of the sample is lower than the apparatus backround which is $2.4 \cdot 10^{-26}\,A^2s$.

On samples which have lower resistivity (paper base laminated sheets)we observed that increasing the electric field time rate up to 10 V/s does not influence substantially the measured value of the spectral density which is

the same as in the steady state conditions (see Fig.4).

Samples of PVC and polyethylene terephtalate have their spectral density pronouncedly dependent on the electrical field strength time rate. This is illustrated by Fig.6. It is seen that the spectral density vs.electric field strength time rate v plot follows the power law, $S_i \sim v^{1,6}$.

We suppose that this effect is due to the process of orientation of the dipole quasi-domains, similarly to domains in crystallic materials. When an external electric field is applied the probability of the quasi-domain to set into a new position with a lower energy follows the exponential law.The energy of the quasi-domains drops when the external electric field is applied which gives rise to an electric impulse in the circuit. When all quasi-domains are oriented into the external field direction the noise saturation takes place. To make sure that the measured noise is not due to breakdown (which is the case supposed by Pender and Wintle [3]) we loaded same PVC samples until the breakdown occurred which happened at voltage 40-50 kV, so that in all our measurements we were far below the breakdown voltage.

The only means to pick up the polarization vector fluctuation is the current in the circuit. This is why the spectral density for the PVC-1.3(Fig.7) is proportional to the square of the conductivity current and for PVC-14 (Fig.6) approximately to the square of the polarization current $I_P = v.C$, where C is the capacitance.

When reversing the polarization current at a given voltage the spectral density for PVC and polyethylene terephtalate decreases substantially(Fig.8, curve a). For example, for the PVC-1.4 , at the voltage 5 kV reversing the sense of the voltage time rate, the magnitude remaining unchanged, i.e., 5 V/s, makes the spectral density decrease by one order. The same procedure applied to the polyethylene terephtalate makes the noise decrease under the apparatus background. Removing the external electric field from the oriented quasi-domains gives rise to a random orientation of the dipole quasi-domains, thus producing noise and discharching the surface charge in the case of the polyethylene terphalate. This case is represented by the curve b in Fig.8.

CONCLUSION

The noise of dielectric materials of reasonably low resistivity is measurable both in the steady state and in the conditions of the time varying electric field strength, while in the case of dielectrics with high resistivity only the time varying field strength method can be used.

The spectral density vs. voltage dependence shows saturation and is proportional to the square of the total current. From the point of view of noise the PVC and terephtalate samples behave as if they had a domain structure. To reach the ferroelectric-like properties of these materials a certain threshold value of the field strength must be applied.

REFERENCES

[1] J.Brophy in: Fluctuation Phenomena in Solids, ed. by R.E.Burges, Ac.Press, N.Y.(1965) p.1.

[2] H.Bittel, Physica 83 B, 6, (1976)

[3] L.F.Pender, H.J.Wintle, J.Appl.Phys., 50 (1), 361, (1979)

III. 1/f NOISE

SURVEY OF RECENT 1/f NOISE THEORIES

M. B. Weissman

Department of Physics
University of Illinois at Urbana-Champaign
1110 West Green Street
Urbana, IL 61801

INTRODUCTION

When current flows in many types of resistors, an excess voltage noise appears which has a power spectrum, S(f), inversely proportional to frequency, f, or to f^{α} with $\alpha \approx 1$. Typically this scaling holds up to frequencies at which the excess noise is lost in Johnson noise and down to frequencies limited by the time available for an experiment. This phenomenon, 1/f noise, has been known for over fifty years, and such progress as there has been in explaining it has been reviewed several times [1,2,3,4,5]. In this review I shall emphasize recent theories and those experiments which are needed for their evaluation. Due to space limitations, I shall concentrate on relatively simple devices operating near equilibrium. For a good review including much fascinating work in more complicated systems, see Van der Ziel [4].

With rare exceptions [6] the voltage noise appears to result directly from resistance fluctuations which are present without current. Van der Ziel has reviewed the evidence for this conclusion [4], of which the most elegant remains the detection of fluctuations in the Johnson noise envelope [7,8]. Since the value of a resistance is given by $((\sum_{i^{th}} n_i q_i \mu_i)c)^{-1}$, where n_i, μ_i, and q_i are the concentration mean mobility, and charge of the i^{th} carrier species, and c depends on the size and shape of the resistor. Most models of 1/f noise involve fluctuations in n or μ, although for some surface effects c fluctuations may also be involved.

NUMBER FLUCTUATIONS

The effective carrier concentration can fluctuate by two general mechanisms — exchange with an external bath or exchange with immobile internal states. For materials with carriers of only one sign of charge, such as metals and extrinsic semiconductors, charge neutrality essentially eliminates the first mechanism, so that significant carrier number fluctuations require trapping states.

In many metal film and semiconductor samples, resistance fluctuations have been found to be roughly described by Hooge's relation [3]:

$$S_R(f)/R^2 = \alpha_H/Nf \qquad (1)$$

with $\alpha_H \approx 2 \cdot 10^{-3}$, where N is the total number of carriers. Integrating this expression over ten decades (a reasonably conservative estimate of the 1/f range) gives $\langle(\delta R)^2/R^2\rangle \approx 1/(20\ N)$. This large magnitude would require that the number of traps be comparable with the number of carriers, which is out of the question for metals. Therefore carrier number fluctuations cannot account for the 1/f noise in metal films [7,9,10] and whiskers [11,12]. Kleinpenning [13] has oberved noise in space-charge limited diodes for which magnitude arguments also appear to rule out carrier number fluctuations.

In semiconductors the number of carriers is not comparable to the number of atoms, so that one cannot immediately exclude the possibility that the 1/f noise results from trap occupation fluctuations. Each independent trap contributes an amount p(1-p) to the mean square fluctuations, where p is the occupation probability, as for the variance in any two state system. The ordinary donors in an extrinsic bulk material have a very small p at room temperature, and it is very temperature sensitive. Neither the magnitude nor temperature spectrum of 1/f noise can be accounted for by trapping by such shallow donors. What

would be required is a range of trapping depths (to produce approximately temperature-independent noise) and a range of characteristic trapping times for each energy (to account for the 1/f spectrum). Partially occupied traps imply temperature dependent carrier concentrations. An approximate relation may be shown [14]:

$$\left(\frac{\partial \ell n N}{\partial \ell n T}\right) \gtrsim \left(\frac{\kappa}{1+\kappa}\right) \left[\ell n \left(\frac{n_q}{n}\right) + \frac{3}{2}\right] \qquad (2)$$

where N is the number of carriers, n_q is the quantum concentration and $\kappa = \langle(\delta N)^2\rangle/N^2 \approx \alpha_H \ell n(\tau_2/\tau_1)$, where α_H is the numerical factor in equation (1) and τ_2/τ_1 gives the range of timescales for which equation (1) applies. If we use $\alpha_H = 2 \cdot 10^{-3}$, $\ell n\, \tau_2/\tau_1 \approx 25$, and $\ell n(n_q/n) \approx 6$ (this analysis only applies for non-degenerate semiconductors), we find $\partial \ell n N/\partial \ell n T \approx 0.4$. So far as I know, no such large temperature dependences of the number of carriers are ordinarily found in noisy samples, although there seems to have been little effort to find them. Thus it is unlikely that samples obeying equation (1) or having more noise are showing simple number fluctuations. This restriction applies regardless of whether the traps are in the bulk or near the surface. Smaller noise magnitudes may of course be due to simple number fluctuations.

Pelligrini [15] has recently suggested that the trapping and release of charge carriers by defect clusters may be a process with a natural spread of relaxation times and trap depths due to random variations in cluster sizes and shapes. As with any number fluctuation theory, the island trap theory cannot quantitatively account for the noise in metals and in many semiconductors.

P. H. Handel and coworkers have set forth one of the most intriguing general theories of 1/f noise, which was recently summarized [6]. The 1/f noise phenomenom is attributed to the infrared divergence found in cross-sections for inelastic scattering [bremsstrahlung]. Semi-classical calculations indicate that interference terms between elastically scattered and inelastically scattered waves can cause 1/f fluctuations in the current density. Ngai [7] has proposed that the same effect may arise when the energy lost in the inelastic scattering goes into certain "correlated states" of the system rather than into photons. Tremblay, however, has made a fully quantum-mechanical version of Handel's calculations without finding a predicted 1/f noise [18].

Regardless of the resolution of that dispute, it is clear that actual 1/f noise does not result from the infrared divergence mechanism. In that theory, one may easily show that the square of the wave function itself exhibits the same 1/f fluctuations as the current density. Thus I consider these theories to be number fluctuation theories. This is not surprising, since the theory explicitly neglects any momentum difference between the elastic and inelastic wave. However, the integral over the entire wave packet of the square of the wave function is a constant, so that, if present, the local 1/f fluctuations would integrate to zero over the wave packet.

MOBILITY FLUCTUATIONS

Hooge and coworkers [3] have proposed that equation (1) applies to all homogeneous materials, with the conductivity fluctuations resulting from independent fluctuations of the mobility of each carrier. This formulation has since been modified to include only fluctuations in lattice scattering [19], not impurity scattering, so that the numerical prefactor is material dependent. In ionic solutions it has been proposed [20] that this factor is proportional to ionic concentration; in effect this leaves a formula in which the noise is inversely proportional to volume, with no direct dependence on the number of carriers.

One obvious objection to any mobility fluctuation description of 1/f noise in semiconductors is that the Hall coefficient has been found to fluctuate by about as much as the resistance [21,22], while for mobility fluctuations equally affecting all carriers no Hall coefficient fluctuations would result. Kleinpenning and Bell [23] have pointed out, however, that if the noise is inversely proportional to the number of carriers the carriers would experience independent mobility fluctuations. If, as in a non-degenerate semicon-

ductor, there are a range of mobilities Hall coefficient fluctuations would be predicted [22,23]. However, attempts to show that the magnitude of the Hall effect noise fits such a model even better than a simple number fluctuation model [22] have been brought into question [24].

Kleinpenning has found that the relative magnitudes of ordinary resistance fluctuations and noise in the thermoelectric effects in intrinsic and extrinsic semiconductors can be well described by the independent carrier fluctuation description, but not by simple number fluctuations [25]. More importantly, he found a rather low coherence between thermoelectric and resistance noises. Since the spatial weighting functions [26] for both heat flow and current flow follow the same pattern in a homogeneous material, this observation is inconsistent with any model, including number fluctuations, in which the fluctuations are locally describable by a single parameter, which would give a coherence of one or minus one. However, since this experiment used point-contact resistors one cannot completely exclude the possibility that surface effects were involved, in which case different spatial weighting patterns for heat flow and electrical current could give a relatively uninteresting explanation of the lack of coherence.

Despite its popularity the independent carrier mobility fluctuation model must be rejected on simple physical grounds. The explanations of the Hall effect and thermoelectric noise observations [23,25] would require the fluctuations to remain associated with carriers of a particular kinetic energy for times on the order of a fluctuation lifetime -- at least a second. Since the carrier scattering time is about a picosecond this would be impossible if each carrier fluctuated independently [27]. Furthermore, 1/f noise in samples with carrier transit times in the microsecond to millisecond range looks no different from that in the relatively rare samples with longer transit times. Obviously low frequency fluctuations are not tied to individual carriers which hang around for less than a millisecond.

If Hooge's relation held in many types of materials, it would be difficult to explain the 1/N behavior except by independent carrier fluctuations. However, very great deviations of the numerical prefactor α_H both toward larger and smaller values may be found, as summarized by Van der Ziel [4]. The recent results of VandeVoorde et al. [28] on InSb crystals are a particularly good example, since the sample was apparently quite well characterized. With some surface treatments, the noise was more than two orders of magnitude smaller than relation (1) would predict. In one of the best known measurements of very low frequency excess noise in Ge, the frequency dependence was $f^{-1.3}$, which obviously cannot agree with equation (1) [29].

Hooge and Vandamme [19] found that in semiconductor samples so heavily doped as to give significant impurity scattering, α_H, decreased as the inverse square of the mobility. This effect was interpreted to mean that only phonon scattering cross-sections fluctuated. It was subsequently shown [27] that their data did not fit the independent carrier model, and thus they remain unexplained.

The results of Hooge and Gaal [20] who obtained 1/f noise of about the same magnitude in the resistance and concentration-gradient voltage of ionic cells remain to be explained, if the unphysical hypothesis of independent long-lived mobility fluctuations is abandoned. Van der Ziel [30] has suggested that surface trapping of ions could account for independent fluctuations in the number of mobile anions and cations, which would produce comparable magnitudes of resistance and concentration-gradient noise. However, the observed magnitude of the noise could only be accounted for by assuming strong positive cooperativity in the binding for each sign of ion separately, with little cooperativity between the anion and cation binding [30]. This would of course be exactly the opposite of what would be expected from thermodynamics for ordinary binding processes, given the electrostatic interactions.

There is one well-known mechanism, loosely referred to as temperature fluctuations, which does cause mobility fluctuations. Voss and Clarke [7] obtained evidence that the 1/f noise in metal films results from temperature fluctuations. The principal evidence was a similarity of noise magnitudes in various films except for manganin, which has a low temperature coefficient of resistivity; and a strong positive correlation between the low

frequency noise in adjacent portions of a strip of Bi. The noise was attributed to equilibrium temperature fluctuations, although the spectral shape could not be explained [7].

The expected magnitude of equilibrium temperature fluctuations is determined by thermodynamics [31]. So long as the heat capacity and thermal coefficient of resistivity are uniform throughout a conductor, regardless of the function describing the space-time evolution of temperature fluctuations, a simple relation exists between the autocorrelation function of the resistance fluctuations due to equilibrium temperature fluctuations and the Green's function for the resistance charge produced by Joule heating [32,33,34]. This relation has been confirmed experimentally in two disparate systems with high temperature coefficients of resistivity — an ionic resistor [34] and (with a somewhat adjustable magnitude) metal films at the superconducting transition [35]. The low frequency limit of the thermodynamic prediction is particularly simple [33]:

$$\frac{S_v(0)}{4kTR} = \frac{\Delta R}{R}\,\frac{\partial \ell nR}{\partial \ell nT} \qquad (3)$$

where S_v is the spectrum due to temperature fluctuations and ΔR is the change in resistance due to Joule heating. Except for materials with exceptionally large values of $\partial \ell nR/\partial \ell nT$, spontaneous temperature fluctuation noise is always small compared with Nyquist noise. In those systems where spontaneous temperature fluctuations have been observed, it has not had a 1/f form. Very low frequency temperature fluctuations associated with the thermostat rather than the sample have also been observed [28,36], but these are neither 1/f noise nor of much theoretical interest.

We have not yet accounted for the Voss and Clarke data. The absence of noise in manganin has been disputed [37], although the contrary data were obtained in a point-contact sample which might exhibit surface effects. Manganin might also be distinguished by its relatively small fraction of phonon scattering. Horn's group has shown that the temperature dependence of the noise magnitude does not resemble that predicted for spontaneous temperature fluctuations [10]. The spatial cross-correlation experiments are most crucial. Recent work in my lab [38] on Cr films of dimensions similar to those of the original Bi samples, except with the distance between the two observed regions reduced by a factor of ~ 6 has revealed no cross-correlations. Work in Webb's lab on Au films in good thermal but not electrical contact has also revealed no cross-correlations [39]. J. Clarke has suggested that the possibility of some artifactually correlated signal resulting from instability of the Bi samples cannot be eliminated [40]. Therefore we conclude that there is no longer any reason to suspect any role for equilibrium temperature fluctuations in metal films.

Several theoretical papers have appeared to explain why spontaneous temperature fluctuations can be important for low frequency excess noise [41,42,43,44]. One [41] has been shown to be inconsistent [45], while the others are not altogether convincing. In view of the experimental situation, I shall not discuss them.

Min [46] has argued that mobility fluctuations in nondegenerate semiconductors can only be found in systems not in quasi-equilibriium. The argument is essentially that Fermi-level fluctuations do not change the average mobility [46]. However, spontaneous occupation number fluctuations of different momentum states will give mobility fluctuations, but on a picosecond time scale.

To avoid these difficulties while retaining a 1/f noise model in which only electronic, not lattice, properties fluctuate, Min postulates [47] that the presence of traps may disturb the quasi-equilibrium distribution of electrons. In order to obtain slow fluctuations, Min makes two additional claims. First, that free electron ↔ trapped electron processes are fast compared with intraband scattering; and second, that the rate of these trapping processes scales as a power of the energy above the band minimum. The result is that there is a range of trapping times caused not by a range of trap parameters but by the inevitable spread of carrier momenta. By adjusting the rate-energy scaling parameter one may obtain a 1/f prediction [47]. (A somewhat simlar model was once put forth by Burgess [48] and criticized by McWhorter [1].)

The assumption that intraband scattering may be neglected, however, can apply only in the momentum range for which the trapping process is very fast. The low frequency noise in the model comes from low-energy electrons, for which intraband scattering would still dominate. The characteristic rate for occupation number fluctuations of these low-energy states is not slowed by adding a parallel trapping pathway. No 1/f noise would actually be predicted if the intraband scattering were not neglected. In view of this, I shall not consider other difficulties with the model.

SURFACE EFFECTS

A very substantial amount of experimental evidence, well summarized by Van der Ziel, indicates that surface effects are responsible for much of the 1/f noise in semiconductors [4]. The situation in thick metal films is less clear because most experiments involve similar surfaces and surface to volume ratios.

McWhorter proposed that number fluctuations due to trapping in surface oxide states could cause 1/f noise [1]. The 1/f spectrum may be predicted as a natural consequence of a tunneling rate distribution resulting from a uniform distribution of traps in a thick oxide layer [1]. Part of the appeal of this proposal is that the spectrum thus appears from simple, almost first-principles considerations rather than from ad-hoc constructions. Unfortunately, experimental data generally indicate that almost any surface treatment affects the magnitude of the 1/f noise without changing its spectrum [1,34]. That is, each layer appears to contribute a 1/f spectrum itself, so that the spectral shape may even for surface effects require some ad hoc assumptions. One piece of experimental data shows signs of preferential removal of low frequency noise sources by surface cleaning, but the spectra are still not consistent with the original McWhorter explanation [28].

Van der Ziel and others [4] have pointed out that in thin-channel devices such as MOSFET's the fluctuating surface trap occupancy can have a greater effect on carrier mobility than on carrier concentration. One may also view such fluctuations as noise in the boundary-condition parameter. It would be of great interest to investigate whether, in simple semiconductor and metal resistors, fluctuating net surface charges or fluctuating patterns of surface charge could produce significant mobility fluctuations. A fluctuating pattern of surface charges would produce fluctuating interference terms in the Coulomb scattering, analogous to the flicker pattern seen in laser light-scattering off solutions. In addition such a fluctuating pattern can cause percolation-like effects [50].

The fluctuating scattering cross section is inherently wave vector dependent and hence could give some of the experimental results which require multiparameter fluctuations. A simple dependence of mobility on total occupied trap concentration in a region, such a Van der Ziel has suggested [4] can produce Hall effect fluctuations due to the energy-dependent proportional contribution of lattice scattering, but remainas a locally single-parameter model. Contrary to Van der Ziel's speculation [51] no plausible mobility fluctuation model not based on independent carriers can fully reproduce Kleinpenning's model. I have discussed some of the experimental implications elsewhere [27].

McWhorter [1] also considered the effect of trap occupation on the band gap near the surface. In near-intrinsic materials this effect can be large, but it cannot be important in strongly extrinsic materials and of course plays no role in metals. Such net carrier number fluctuations are electrophoretically transported with the minority carriers — this effect was observed experimentally [49].

DEFECT DIFFUSION

Horn's group has extensively studied the temperature dependence of the noise magnitude in several types of metal films on several types of substrate [10,5]. Although they have not set forth a specific model, they have pointed to some likely features of one. The most striking result [52] was the correspondence noted between the temperature dependence of the noise magnitude in a particular frequency range and deviations from an f^{-1} spectral shape in the same range. If one assumes that the net fractional resistance fluctuations are temperature independent but that their rate (spectral distribution) does depend on temperature, one finds that the flat, low frequency part of the spectrum drops as the temperature is raised. The sharp, high frequency part increases.

Dutta et al. [52] assume that the noise is expressible as the sum of many Lorentzians with characteristic times given by the same Arrhenius prefactor τ_o with a range of activation energies. They obtain the experimentally checkable result

$$\alpha(\omega,T) = 1 - \frac{1}{\ell n(\omega\tau_o)} \left(\frac{\partial \ell nS(\omega,T)}{\partial \ell nT} - 1\right) \qquad (4)$$

where $\partial \ell nS(\omega,T)/\partial \ell n\omega \equiv -\alpha(\omega,T)$. This prediction qualitatively fits their data, except for a feature in the noise magnitude near 550°C. A roughly comparable fit could be obtained by assuming a constant activation energy with a range of prefactors [14]. The peak magnitude of the noise occurred at a temperature that was a monotonically increasing function of the lattice cohesive energy [52].

The strong implication is that defect diffusion is involved in generating the noise. (Arguments against such mechanisms in semiconductors [1] do not apply to these metal films.) Reproducibility of the noise magnitudes by different labs [7,9,10,38] suggests that impurities are not necessary. However, defect creation and annihilation would show far too great a temperature dependence, so a non-equilibrium defect concentration is likely to be involved. The question arises — why should the resistivity depend on the positions of defects?

Macroscopic inhomogeneities in the current density due to sample geometry are unlikely to supply the answer, because diffusion is too slow to give noise in the right frequency range. Diffusion very close to surface irregularities is also not likely to explain the effect, because the defects which can diffuse near the surface reach an equilibrium concentration. The explanation may lie in the dependence of the conductivity on the relative positions of defects [53]. One such dependence arises from interference terms in the scattering. Yakota [54] has calculated the magnitude of this effect, finding that it is not necessarily tiny. The relevant distance for diffusion to affect conductance in this mechanism is an inverse Fermi wave vector,, about one lattice spacing [14], not the typical nearest-neighbor defect spacing assumed by Yakota, so that essentially all the defects are mobile in the time-temperature range of interest. The range of activation energies might itself be due to defect-defect interactions.

A major difficulty with Yakota's explanation is that if the noise was due to residual non-phonon scattering, one would expect its net magnitude to decrease rather sharply as the temperature increased. Perhaps the alteration of the phonon dispersion relation by the presence of the defects causes the phonon scattering rates themselves to fluctuate. Likewise the carriers see a modified lattice which will affect their dispersion relation. These effects have not been calculated, so far as I know.

It is interesting to note that all of these effects, as well as some surface effcts, predict tensor, not scalar, fluctuations in the conductivity. Although one may have a cubic lattice with scalar conductivity and even have equal mean-square fluctuations along any projection, the instantaneous conductivity will not be a scalar. Techniques for measuring this effect have been proposed [24]. This property contrasts sharply with the inherently scalar nature of any fluctuations resulting from simple number fluctuation processes.

Lest it seem that 1/f noise in metals is nearly understood, I should point out that two groups have now reported 1/f noise in metal whiskers about 2-3 orders of magnitude larger than in metal films of similar volume [11,12]. Equations (1,2,3 and 4) were not obeyed. Reasonable, if not airtight, precautions against contact noise were taken. The whiskers have less surface area and many less defects than the films. No theory appears to begin to explain these results.

WEIGHTING FUNCTION SINGULARITIES

It has long been known [55] that diffusion does not produce 1/f noise in any variable, B, which affects resistance through an equation of the form

$$\delta R(t) = \int \delta B(\vec{r},t) W(\vec{r}) d^n\vec{r} \qquad (5)$$

so long as $W(\vec{r})$ is non-singular. For the ordinarily considered $W(\vec{r})$'s, which have a delta function singularity in the gradient, an $f^{-3/2}$ high frequency limmit of S(f) is found -- the "universal" three-halves power law for diffusion.

In an idealized contact resistor a singularity occurs in the electric field [56]. This singularity gives a predicted 1/f noise spectrum, with a low frequency cutoff determined by the size of the contact and a high frequency cutoff determined by the smallest distance over which the macroscopic idealizations hold [57,58]. For diffusion, frequency scales as the inverse square of distance, so a distance scale range of a factor of 10^3 would give about six decades of 1/f noise. Very few plausible geometries could give more than about eight decades by such a mechanism.

The singularity theory predicts that the $W(\vec{r})$ singularities which give 1/f noise for diffusion will also do so for other fluctuation transport mechanisms [58]. The theory has been confirmed in a somewhat contrived experimental arrangement in which light scatterers were flowed past a cylindrically focussed beam [59].

In the ionic contact resistors studied by Hooge and Gaal [20], the 1/f law was only approximately obeyed over a frequency range of one or two decades. Simple carrier number fluctuations would give 1/f resistance fluctuation in about the right frequency range, but with a magnitude slightly lower than the smallest found. They would not give noise in concentration-cell voltage. However, electrophoresis or diffusion of small charged contaminant particles could give noise in about the right frequency range. As in Van der Ziel's model [30] it would appear as largely uncorrelated fluctuations in the anion and cation mobility, but with the large, concentration independent, somewhat irreproducible magnitude appearing naturally. The absence (reduction by at least two orders of magnitude from the prediction of [20]) of 1/f noise in long pores filled with meticulously filtered solutions [60] supports this interpretation. So does the wide range of amplitudes found by another group [61].

In lipid bilayers conductance usually occurs in discrete channels which are free to diffuse in two dimensions. The conductance of a pair of channels is reduced as they approach each other, due to field-line overlap, with the effect scaling inversely with distance. As a result one may predict 1/f noise over about eight decades centered around one Hz, with a magnitude determined by the single-channel conductance [53]. The observed magnitudes are larger than predicted by this effect, being apparently dominated by gating mechanisms with a range of activation energies [62,63]. Nevertheless, this case remains interesting because the 1/f prediction follows directly from well known fundamental features of the system, with no ad hoc assumptions and with no adjustable parameters in the magnitude.

It is tempting to consider the possibility that defect diffusion in metals might give 1/f noise directly through singular defect-defect interaction terms. However, in three dimensions the required singularity would have an $r^{-3/2}$ functional form, which does not correspond to anything I know of. A 1/r dependence for point like objects diffusing on a surface could produce a limited range of 1/f noise. So could a 1/r dependence for point-like defects diffusing in the vicinity of stationary line-like defects [57]. Overall, however, a range of time constant logarithms as in tunneling or activated processes seems much more likely to account for very broad 1/f spectra, as found in semiconductors, than does a natural distance scaling.

STATISTICAL CONSIDERATIONS

The simplicity of the 1/f spectrum encourages speculation (e.g. [2]) that some general statistical considerations may account for it. The central limit theorem predicts that when an activation energy, barrier height, or tunneling distance appearing in an expression for the logarithm of the characteristic frequency is affected by many random parameters, its distribution function will approach a Gaussian shape. Since near the maximum such a distribution is flat, a range of 1/f noise is expected. However, the wings of the Gaussian

also give power-law spectra. In fact, if the homogeneous lineshape is Lorentzian, there are fewer decades approximating 1/f than any other power law between f^0 and f^{-2}. It appears that the prevalence of 1/f noise is nearly equivalent to the assertion that distribution functions for logarithms of rates tend not only to be broad but to have wings that fall off much less sharply than Gaussians. Except in special cases this remains unexplained.

CONCLUSIONS

Despite the progress that has been made in accounting for the 1/f noise in some devices, particularly MOSFETS, the substantial noise very nearly following the 1/f law that appears in such simple materials as metal films, metal whiskers, semiconductor filaments, and liquid metals [64,65] has not been satisfactorily explained. Even the relative roles of surface vs volume effects or of mobility vs carrier number fluctuations are not well established. Much of the theoretical work has been wrong, some merely irrelevant. McWhorter's words still apply [1]: "The similarity of the 1/f noise from the various devices mentioned earlier certainly leads one to look for a common mechanism, but so far it has been difficult to get a satisfactory explanation for even one device.".

Nevertheless, we may make some tentative judgements. Some variant of the McWhorter model including mobility fluctuations at internal noise sources at grain boundaries [66] seems to be the most likely explanation for the noise in semiconductors. The dominant mechanism in metal films may involve a rate-limiting defect diffusion step. Metal whiskers and liquid metals are very poorly understood although it is possible that in the liquid metal experiments a fluctuating charge on the oxide surface of the contacts produced the noise.

Recently there has been a renewed emphasis on studying the relations between resistance fluctuations and other fluctuating electrical properties such as the Hall coefficient and thermoelectric EMF's. While the initial results have not been as clear cut as one might hope, this type of experiment, closely tied to theory, appears to offer the best road toward understanding 1/f noise.

This work was supported by NSF grant DMR 80-07057 and, through the Materials Research Laboratory by DMR 77-23999. I think J. Clarke, P. M. Horn, A. M. Tremblay, G. Feher and W. W. Webb for helpful conversations at one stage or another of my work in this field. None, of course, bears any responsibility for the controversial views expressed here.

REFERENCES

[1] A. L. McWhorter, in Semiconductor Surface Physics, Ed. R. H. Kingston (Univ. of Penn., Philadelphia, 1957) p. 207.

[2] D. A. Bell, Electrical Noise (Van Nostrand, London, 1960) p. 140.

[3] F. N. Hooge, Physica 83B, 14 (1976).

[4] A. Van der Ziel, in Adv. in Elect. and Elect. Phys., V. 49, Ed. L. Marton and C. Marton (Academic Press, New York, 1979) p. 225.

[5] D. A. Bell, Proc. 2nd Int. Conf. on 1/f Noise (1980) p. 19 (unpublished).

[6] S. Lifson, B. Gavish and S. Reich, Biophys. Struct. Mechanism 4, 53 (1978)

[7] R. F. Voss and J. Clarke, Phys. Rev. B13, 556 (1976).

[8] H. G. E. Beck and W. P. Spruitt, J. Appl. Phys. 49, 3384 (1978).

[9] F. N. Hooge and A. M. H. Hoppenbrouwers, Physica 45, 386 (1969).

[10] J. W. Eberhard and P. M. Horn, Phys. Rev. B18, 6681 (1978).

[11] P. Dutta, J. W. Eberhard and P. M. Horn, Sol. St. Comm. 21, 679 (1977).

[12] C. Leemann, M. J. Skove and E. P. Stillwell, Sol. St. Comm. 35, 97 (1980).

[13] T. G. M. Kleinpenning, Physica 94B, 458 (1978).

[14] M. B. Weissman, unpublished.

[15] B. Pellegrini, Phys. Rev. B22, 4684 (1980).

[16] P. H. Handel, Phys. Rev. A22, 745 (1980).

[17] K. L. Ngai, Phys. Rev. B22, 2066 (1980).

[18] A. M. Tremblay, Thesis, M.I.T. (1978).

[19] F. N. Hooge and L. K. J. Vandamme, Phys. Lett. 66A, 315 (1978).

[20] F. N. Hooge and J. L. M. Gaal, Philips Res. Repts. 26, 77 (1971).

[21] J. J. Brophy, Phys. Rev. 106, 675 (1957).

[22] T. G. M. Kleinpenning, J. Appl. Phys. 51, 3438 (1980).

[23] T. G. M. Kleinpenning and D. A. Bell, Physica 81B, 301 (1976).

[24] M. B. Weissman, J. Appl. Phys. 51, 5872 (1980).

[25] T. G. M. Kleinpenning, Physica 77, 78 (1974).

[26] J. M. Richardson, Bell. Syst. Tech. J. 29, 117 (1950).

[27] M. B. Weissman, Physica 100B, 157 (1980).

[28] P. VandeVoorde, C. K. Iddings, W. F. Love and D. Halford, Phys. Rev. B19, 4121 (1979)

[29] M. A. Caloyannides, J. Appl. Phys. 45, 307 (1974).

[30] A. Van der Ziel, Physica 96B, 81 (1979).

[31] J. W. Gibbs, Elementary Principles in Statistical Mechanics (Yale, New Haven, 1902) pp. 68-86.

[32] M. B. Weissman, Appl. Phys. Lett. 32, 193 (1978).

[33] M. B. Weissman, Phys. Rev. Lett. 41, 1 (1979).

[34] M. B. Weissman and G. D. Dollinger, J. Appl. Phys. (in press).

[35] M. B. Ketchen and J. Clarke, Phys. Rev. B17, 114 (1978).

[36] J. Clarke and T. Hsiang, Phys. Rev. B13, 4790 (1976).

[37] T. G. M. Kleinpenning, reported in Ref. 3.

[38] R. D. Black, F. Fliegle and M. B. Weissman, in these Proceedings.

[39] W. W. Webb,, private communication.

[40] J. Clarke, private communication.

[41] S. H. Liu, Phys. Rev. B16, 4218 (1977).

[42] S. Putterman, Phys. Rev. Lett. 39, 585 (1977).

[43] I. Pavlin and S. Englesberg, 2nd Int. Symp. on 1/f Noise (1980) (unpublished).

[44] M. Mikulinsky and S. Starobinets, Phys. Rev. B21, 5558 (1980).

[45] M. B. Weissman, Phys. Rev. B18, 4538 (1978).

[46] H. S. Min, J. Appl. Phys. 50, 4461 (1979).

[47] H. S. Min, J. Appl. Phys. 51, 1637 (1980).

[48] R. E. Burgess, Brit. J. Appl. Phys. 6, 185 (1955).

[49] H. C. Montgomery, Bell Syst. Tech. J. 31, 950 (1952).

[50] M. Aoki, H. Katto, E. Yamado, J. Appl. Phys. 48, 5135 (1977).

[51] A. Van der Ziel, Appl. Phys. Lett. 33, 883 (1978).

[52] P. Dutta, P. Dimon and P. J. Horn, Phys. Rev. Lett. 43, 646 (1979).

[53] M. B. Weissman, Biophys. J. 21, 87 (1978).

[54] M. Yakota, Proc. 2nd Int. Conf. on 1/f Noise, (1980) p. 484 (unpublished).

[55] K. M. Van Vliet and J. R. Fassett, in Fluctuation Phenomena in Solids, Ed. R. E. Burgess (Academic Press, New York, 1975) pp. 267-354.

[56] J. C. Maxwell, A Treatise on Electricity and Magnetism (Clarendon, Oxford, 1904) Vol. I, p. 328-329.

[57] M. B. Weissman, Phys. Rev. Lett. 35, 689 (1975).

[58] M. B. Weissman, J. Appl. Phys. 48, 1705 (1977).

[59] M. B. Weissman, R. A. Isaacson and G. Feher, Phys. Rev. Lett. 43, 733, (1979).

[60] G. Feher and M. Weissman, Proc. Nat. Acad. Sci. USA 70, 870 (1973).

[61] D. L. Dorset and H. M. Fishman, J. Memb. Biol. 21, 291 (1975).

[62] R. Sauvé, , private communication.

[63] S. M. Bezrukov, G. M. Drabkin, L. A. Fonina, A. I. Irkhin, E. I. Meluik and A. I. Sibilev, preprint 598 of the Acad. of Sci. USSR, Leningrad Nuc. Phys. Inst. (1980).

[64] J. T. M. Stroeken and T. G. M. Kleinpenning, J. Appl. Phys. 47, 4691 (1976).

[65] J. Kedzia and L. K. J. Vandamme, Phys. Lett A66, 313 (1978).

[66] H. I. Hanafi and A. Van der Ziel, Sol. State Elect. 21, 1019 (1978).

1/f Fluctuations in Biological Systems

Toshimitsu Musha

Department of Applied Electronics
Tokyo Institute of Technology
Nagatsuta, Midoriku, Yokohama 227, JAPAN

INTRODUCTION

Since Johnson reported in 1925 the first observation of enhancement of a low-frequency tail of the spectral density of shot noise passing a vacuum tube, a number of papers have been published that report dc electric current through (or dc voltage across) an electric resistor have the so-called 1/f spectral density regardless of the kind of material composing the resistor. At the moment it is believed that 1/f noise is a result of conductivity fluctuations[1 - 5]. The mechanism for 1/f fluctuations is not fully understood as yet. On the other hand, 1/f fluctuations have also been found in various other fields; typical examples are frequency fluctuations of well-regulated quartz oscillators and of atomic clocks [6 - 8], and cellular membrane potential fluctuations[9 - 12]. The present paper aims at suggesting some relationship of human perception to 1/f-like fluctuations. Firstly, some examples will be mentioned that show bodily 1/f-like fluctuations and then external stimuli of 1/f spectral densities that are accepted by the human body are described; finally 1/f-like noise that appears in biological information transmission will be discussed.

BODILY FLUCTUATIONS

EEG alpha wave: The electroencephalogram (EEG) is a potential fluctuation observed across electrodes placed on the specified locations on the head, which reflects mental activities. The EEG is divided in four components according to the frequency. The alpha wave is a component between 8 and 13 Hz and its amplitude is large as compared with other components. Suzuki et al. [13] counted the number of zero crossings of the alpha wave in 1 sec to estimate the spectral density of frequency fluctuations. 15 Subjects were examined. Figure 1a refers to a subject placed in a dark, quiet room, and figure 1b refers to a subject who was hearing audio impulses at 1 kHz at large sound levels. The subject in a quiet environment extends the 1/f spectrum down to 0.02 Hz but the subject in a noisy environments limits the 1/f spectrum above 0.1 Hz. When a patient comes round from narcosis after a surgical operation, spectral density of the alpha wave is almost white. After taking a pain killer, however, the 1/f spectrum is gradually recovered [14]. Extension of the 1/f spectrum toward lower frequencies is an evidence of pleasing.

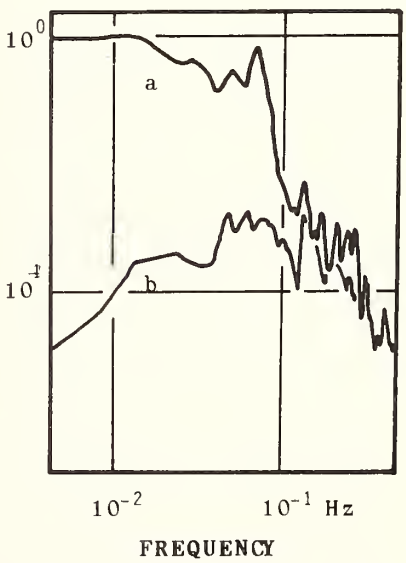

Fig. 1 Spectral densities of the alpha wave of a subject in a quiet (a) and noisy (b) environment. The vertical axis is arbitrary scale.

Heart beat period: The cardiac sinus has pace-making cells that make spontaneous electric oscillations. We measured the heart beat period fluctuations of a normal subject. The beat period was defined as a time interval between the R peaks of the electrocardiogram and a spectral density estimated is shown in figure 2. A peak at 0.3 Hz was caused by breathing; for lower frequencies the spectral density is approximately proportional to 1/f. The body temperature was measured simultaneously with the heart beat period, and a coherence function was estimated. It was 0.3 to 0.5 and hence their correlation is very weak.

Body sway: When one stands upright, the body sways laterally and back and forth. The horizontal position of the center-of-gravity of the body was measured with GRAVICORDER that has three strain guages on a trangle supporting a metallic plate on which one stands. The spectral density of its lateral fluctuation when one stood on a single foot is plotted in figure; this is proportional to 1/f below 1 Hz. If eyes are closed the fluctuation amplitude would be larger but the shape of the spectrum would remain the same. We have found two types of the spectrum; the other has a wavy structure above 1 Hz; we tentatively call them types A and B. The spectral shape is suggesting mechanism of controlling the posture of the body.

EXTERNAL STMULI

Music: The spectral density of fluctuations in the loudness of (especially classic) music is found to be 1/f type down to 5×10^{-4} Hz, and the frequency fluctuations of music also have the 1/f spectrum down to the inverse of the length of the piece of music [15]. Character of the composer is hidden in the phase relations between sinusoidal vibrations with audio frequencies. Voss [15] presented three pieces of music composed of random numbers that were sampled from fluctuations with white, 1/f, and $1/f^2$ spectral densities. They were performed at the 1st Symposium on 1/f Fluctuations in Tokyo; the white music was irritating, the $1/f^2$ music was boresome, and the 1/f music sounded nice.

Picture: We enjoy good paintings and photos. What kind of stochastic characters do they have in common as is the case in music? Kosugi and I evaluated spectral densities of pictures with respect to space frequency, in which original pictures were reformed as black-and-white photos of the size 10 cm wide and 15 cm long, and darkness of the picture elements was measured along horizontal and vertical lines with a line-scanning camera. Literalistic paintings and ordinary photos are of $1/f^2$ type and cartoons are of 1/f type. All the pictures we examined were between these. Three typical examples are shown in figure 4.

Pain-relieving stimuli: Various kinds of chronic, intractable pain can be relieved by transcutaneous electrical nerve stimulation (TENS) through transcutaneous electrodes or acupuncture needles. It was reported that TENS was effective approximately 25 to 45% of patients [16 - 19]. Takakura et al. [20] applied rectangular electric current impulses of 0.1 ms in width to patients. The impulse repetition frequerncy f_i and the duration t_i were determined by random numbers that were generated by 1/f fluctuations. Furthermore, they used fluctuations of frequency and audio power of music to determine the values of f_i and t_i, respectively, and gave patients music performance in synchronism with the transcutaneous stimuli. They examined 220 patients and found that TENS was effective for 35% of 60 patients treated with constant pulse repetition rates, 70% of 91 patients treated by 1/f stimulations without music, and 74% of 69 patients treated by 1/f stimulations with synchronized music performance. Effectiveness was judged by the degree of recovery of the 1/f spectral density of the frequency fluctuation of the EEG alpha wave.

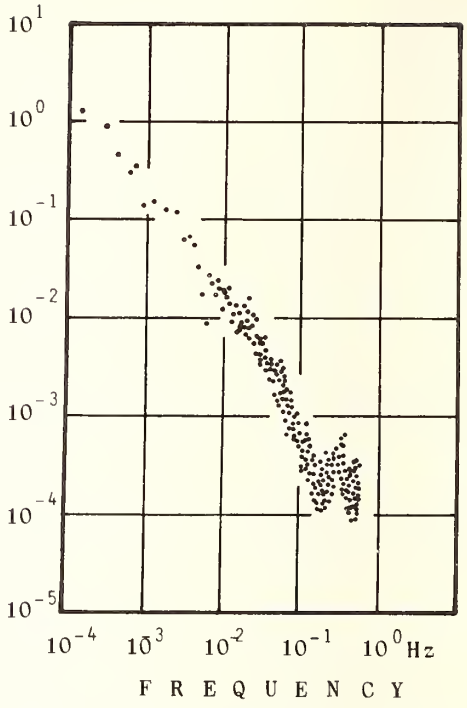

Fig. 2 Spectral density of heart beat period of a normal subject. The period is normalized to the mean value, and the unit in the vertical axis is /Hz.

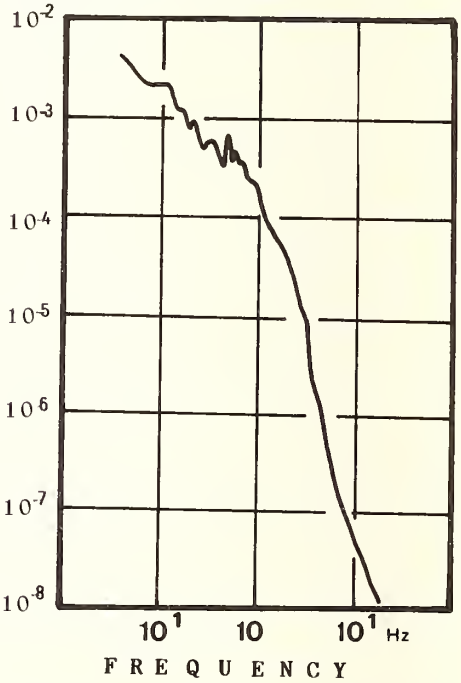

Fig. 3 Spectral density of body sway in the lateral direction when one stands on single foot. The vertical scale is arbitrary.

DENSITY MODULATION OF ACTION POTENTIALS ON NERVE AXON

Biological information is carried by impulses of the action potential that propagate on a nerve axon. The action potential takes the same shape under a given environmental condition regardless of the stimulus waveform, and, therefore, biological information must be coded in the time relation of the action potential [21,22]. It is naturally expected that biological information will be distorted or acquire noise if the time relation of the action potentials is modulated or distorted stochastically during their propagation on the axon. There are three possible origins for the distortion and noise. Propagation speed of the action potential on a nerve axon is functions of ionic concentrations outside and inside the axon, the environmental temperature, and the time relations to the foregoing action potentials. The former two would cause very little effect on the speed of the action potential under well-regulated experimental conditions as compared with the last one. Modulation of the time relations of the action potentials was experimentally examined and the following results have been obtained.

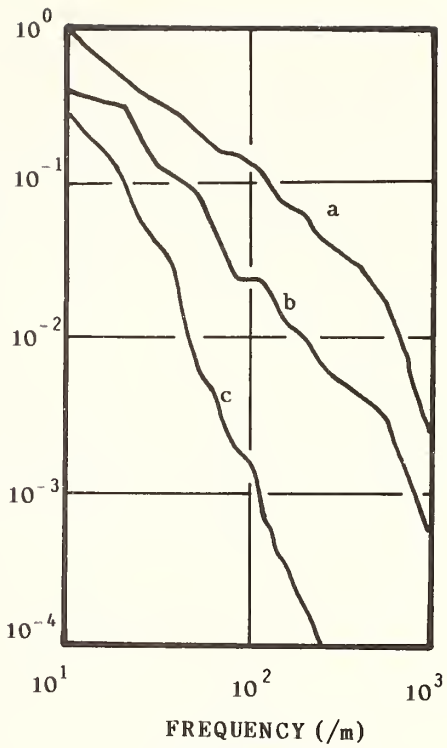

Fig. 4 Spectral densities of a catoon 'Yasuda'(a), Picasso's 'Le trois femmes'(b), and Renoir's 'Femme au chapeau'(c).

Speed of the action potential: Giant axons of squid (doryteuthis bleekeri) were used in the experiment. An axon was placed in a nerve chamber filled with natural sea water at about 10°C. The axon about 6 to 7 cm long was tied at the ends with threads, the diameter being 0.5 to 0.7 mm. A silver wire electrode, 0.025 mm in diameter, bare for 7 mm length and the other portion coated with enamel, was inserted into the axon near the end and used as intracellular electrode for stimulation. The stimulation current was received by a wire electrode placed outside the axon near the intracellular electrode. The action potential was excited with a rectangular electric current impulse of 0.1 ms wide that was twice as high as the threshold level. The four action potentials were successively excited and their propagation speeds were measured. The result is plotted in figure 5. The first action potential travels at 25 m/s, but the following three action potentials travel at slower speeds because the axon gets into a refractory state right after an action potential is excited. This effect is equivalent to existence of some kind of repulsive interactions between the action potentials, where it acts only onto the following ones.

Impulse interval distributions: Sequences of random impulses were generated by a computer whose time intervals were in Gaussian distributions. The propagation length was 44 mm, and the output impulses were reformed in 0.1-ms rectangular impulses, which were again applied to the stimulation electrode; thus four runs were tried. Figure 6 shows interval distributions; the bottom refers to the computer-generated impulses that are Gaussian with a mean of 3 ms and a standard deviation of 1 ms. Intervals shorter than 4 ms were cut off because of the absolute refractory period of the axon.

Spectral densities of the impulse trains: Spectral densities of fluctuations of the impulse density were plotted in figure 7, where the bottom refers to the computer-generated impulses that is 'white' except for a peak at 300 Hz that has been caused by a mean interval of 3 ms. The repulsive interactions of the impulses gave rise to modulation of the impulse density that results in the 1/f rise in the spectrum. The four sepctral densities have almost the same shape, suggesting that the time relations of the impulses have reached a stable state after a single run on the axon. Cross-correlations between the input and output impulse trains, where action potentials were reformed in 0.1-ms rectagular impulses, has a peak at a lag of 4 ms, and its width agreed with spread of the speed of the action potential.

Resemblance to automobile current fluctuations: This density modulation of the action potentials that is acquired during propagation on the axon[23] resembles that of automobiles which was first observed by Musha and Higuchi [24]. The spectral density consists of shot

noise and a 1/f part that is associated with bunching of the cars. This spectrum was derived by a hydrodynamical model with an assumption that the car speed is a linearly decreasing function of the car concentration 25 . The observed speed-concentration relations of the action potential as shown in figure 5 is well approximated by the same model. Therefore, the density modulation of the action potentials on the axon has the same mathematical background as that of the cars on the expressway.

CONCLUSIONS

The 1/f spectrum is often found in fluctuations in biological control and biological oscillations. It seems that the 1/f fluctuation is accepted as a pleasing sensation. Biological information has been found to acquire the 1/f fluctuation as a result of the refractory nature of the nerve axon.

REFERENCES

[1] F. N. Hooge, Physica, 60, 130 (1972).

[2] T. G. M. Kleinpenning, Physica 77, 78 (1978).

[3] H. M. J. Vaes and T. G. M. Kleinpenning, J. Appl. Phys. 48, 5131 (1977).

[4] T. G. M. Kleinpenning, J. Appl. Phys. 51, 3438 (1980).

[5] F. N. Hooge and L. K. J. Vandamme, Phys. Letters 66A, 315 (1978).

[6] D.W.Allan, Proc. 1st Symp. 1/f (1977), p.158.
[7] J.J.Gagnepain and J.Uebersfeld, ibid. p.173
[8] J.J.Gagnepain, P.Handel, and J.Uebersfeld Proc. 2nd Symp. 1/f (1980), p.550.
[9] R.J.van den Berg, E.Siebenga, J.de Goede, W.H.Moolenaar and A.A.Verveen, Proc. 1st Symp. 1/f (1977), p.97.
[10] L.DeFelice, Proc. 2nd Symp. 1/f (1980), p.112.
[11] H.M.Fushman, ibid., p.132.
[12] F.F.Offner, ibid., p.140.
[13] M.Suzuki, et al., Tech. Rep. IECE Japan, MBE 80-59.
[14] M.Suzuki, Master's thesis, Tokyo Inst. Tech. (1981).
[15] R.F.Voss, Proc. 1st Symp. 1/f (1977), p.199.
[16] J.D.Loeser, et al., J. Neurosurgery 42 March (1975).
[17] D.Burton, Postgraduate Medicine 59, June (1976).
[18] C.N.Shealey, Clin. Neurosurgery 21, 269 (1974).
[19] L.Augustinson, et al., Lakartid 73, 4205 (1976).
[20] K.Takakura, K.Sano, Y.Kosugi, and J.Ikebe, Appl. Neurophysiology 42, 314 (1979).
[21] Y.Lass and M.Abeles, Biological Cybernetics 19, 61 (1975).
[22] M.Abeles and Y.Lass, Biological Cybernetics 19, 121 (1975).
[23] T. Musha, Y. Kosugi, and G. Matsumoto, Proc. 2nd Symp. 1/f (1980), p.176.
[24] T. Musha and H. Higuchi, Jap. J. Appl. Phys. 15, 1271 (1976).
[25] T. Musha and H. Higuchi, Jap. J. Appl. Phys. 17 811 (1978).

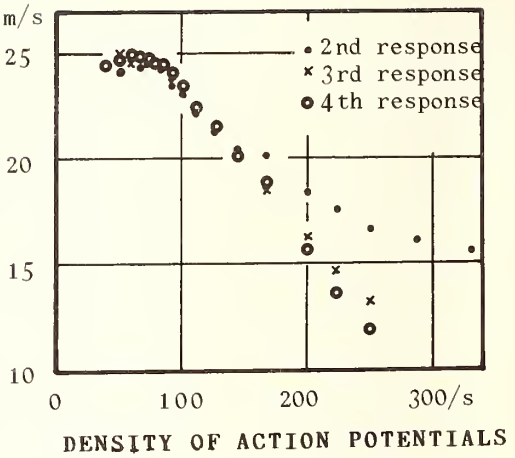

Fig. 5 Speed of action potential vs. density of action potential when 4 action potentials are excited.

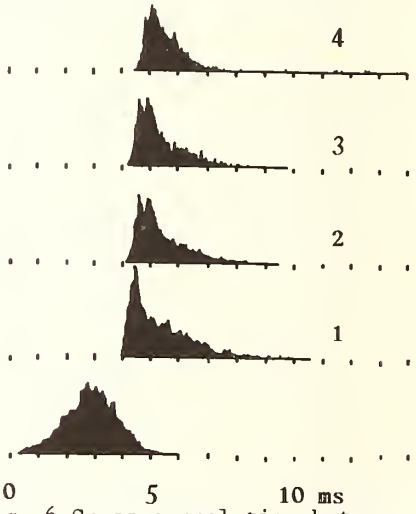

Fig. 6 Cross-correlation between stimuli and responses.

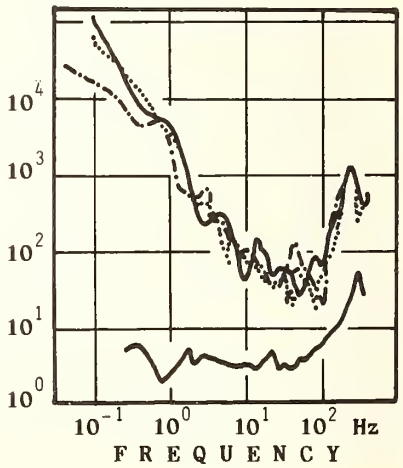

Fig. 7 Spectral density of density modulation of action potentials as they travel down the axon. The bottom refers to the random stimuli.

1/F NOISE IN CONTINUOUS METAL FILMS IS NOT DUE TO TEMPERATURE FLUCTUATIONS[1]

J. H. Scofield, D. H. Darling[2] and W. W. Webb

Applied Physics
Cornell University
Ithaca, New York 14853

The possibility that 1/f conductance noise (also referred to as "excess", or "1/f" noise) in thin continuous metal films is caused by temperature fluctuations has been considered by several authors [1-6]. The power spectral density (PSD) of the voltage fluctuations $S_V(f)$, if generated by temperature fluctuations is supposed to be $S_V(f)=\beta^2\bar{V}^2S_T(f)$, where $S_T(f)$ is the PSD of the fluctuations of the average temperature of the film, $\bar{V}$ is the mean voltage across the film, and $\beta = (1/R)(dR/dT)$ is the film's temperature coefficient of resistance. Whatever the origin of temperature fluctuations, their propagation is governed by the diffusion equation so that the resulting excess noise would exhibit a frequency dependent correlation length characteristic of a diffusion process, $\lambda(f) = \{D/\pi f\}^{1/2}$, where D is the thermal diffusivity of the material. Spatial correlations of the excess noise along metal films have been observed [1,2].

Equilibrium temperature fluctuations do account for the magnitude and spectrum of measured conductance noise in freely suspended tin films near their superconducting transition temperature (where $\beta T>1000$) [3]. However, for substrate supported metal films various theoretical temperature fluctuation models predict spectra with a low frequency cut off, a limited 1/f range, if any, and a monotonic temperature dependence. In contrast, experiments reveal a wide range of 1/f spectrum and complex temperature dependence [1,4]. Thus, equilibrium temperature fluctuations do not appear to account for most observed 1/f noise in metal films. Voss and Clarke have proposed a thermal fluctuation model with a 1/f regime [1]. Such alternative temperature fluctuations of yet unrecognized origin might generate the observed 1/f noise [1,5]. Van Vliet, et al. have calculated that the spectrum of the fluctuations of the average temperature of a metal film on an insulating substrate with a uniform surface noise source having a white spectrum spatially coherent across the top of the substrate would yield a 1/f spectrum [6]. However, they find that the magnitude of the resulting temperature fluctuations would be negligible for thermal radiation fluctuations. Nevertheless, temperature fluctuations in conducting metal films near room temperature has remained in contention as a seductively simple mechanism to account for 1/f conductance noise.

We have designed an experiment to detect the possible existence of temperature fluctuations large enough to account for excess noise in thin metal films. Calculations and experiments showed that the temperatures of superimposed films separated by a thin electrically insulating layer are closely coupled over the relevant frequency range. Thus temperature fluctuations in one film will be correlated with the temperature fluctuations of the other. Therefore, if the 1/f noise in a film were due to temperature fluctuations this noise would be correlated with the 1/f noise in the neighboring film. We have fabricated suitable superimposed gold films, confirmed the calculated thermal coupling by modulated heat input experiments, and have looked for a correlation in their 1/f noise. Our experiments show that the coherence (defined below) between the excess noise of the two films is less than 1/100th the value anticipated were the measured 1/f noise in each film due to temperature fluctuations.

---

1 This research was supported primarily by the NSF through the Materials Science Center at Cornell

2 Present address: Lawrence Livermore National Laboratory, Livermore, CA 94550

The superimposed electrically insulated film bridges were prepared by evaporating a 600 Å layer of gold onto a 0.6 mm thick single crystal sapphire substrate and photo-etching it to a 1 mm long, 80 μm wide bridge. Next, a 6000 Å layer of SiO was evaporated on top of the gold bridge and surrounding sapphire substrate, and a second bridge similar to the first was evaporated and formed on top of the SiO layer. Finally, a thicker gold 4-probe electrical contact super-structure was evaporated onto the sample for electrical connections. Noise free contacts of negligible resistance were made using either pressed indium wire or gold wire soldered with indium. The substrate was then mounted onto a large copper heat sink. Bridge resistances ranged between 11Ω and 19Ω due to differences in geometry. Calculated resistivities were typically 6 μΩ·cm (about twice the bulk value) and the measured thermal coefficients of resistance were about $\beta = 0.003°C^{-1}$ (similar to the bulk value).

Conductance and Nyquist noise were measured with a constant current I < 40 mA derived from lead-acid batteries in series with a 1 KΩ wire wound ballast resistor. Due to the large thermal conductivity (K=0.1 cal/C s cm) of the single crystal sapphire substrate, the relatively large current densities (10^6 $A \cdot cm^{-2}$) generated less than a 1°C film temperature rise as measured by I-V characteristics and confirmed by heat flow calculations.

Voltages across each sample were amplified with either an Ithaco 1201 or a PAR 113 low-noise preamplifier, impedance matched to the films with a PAR 190 low-noise transformer, and fed into an HP 5420A spectrum analyzer. The PSD of the excess noise for each film was obtained by measuring the PSD of its voltage fluctuations $S_E(f)$ and subtracting from this the PSD of the background (mostly Nyquist) noise $S_B(f)$, obtained by replacing the film with an equivalent wire-wound resistor. For frequencies between 1 Hz and 5 Hz it was necessary to correct up to 8 dB for the transfer characteristics of the instrumentation. Within the frequency range measured, 1 Hz <f< 100Hz, both films showed excess noise roughly consistent with Hooge's empirical formula, $S_v(f)/\bar{V}^2 = a/\{N_c f^b\}$, with 1.0 <b< 1.1 and 0.005 <a< 0.014, where N_c is the number of carriers [7].

We have modeled the three-dimensional thermal coupling problem by considering diffusion into the substrate. Our model calculations indicate that the average temperatures of those portions of each of the two films that are directly superimposed upon one another are virtually identical for frequencies $f << 1/\tau_{SiO}$, where $\tau_{SiO} = \pi s^2/D_{SiO}$, s is the thickness, and D_{SiO} the diffusivity of the SiO layer [8]. Since $\tau_{SiO} < 1$ μs this result holds true for all frequencies of interest. In order to confirm the validity of our model and to test for possible thermal barriers at the interfaces we have calculated the amplitude of the sin (2πft) component of the average temperature of the lower film that results when the top film dissipates a power $P_1 \sin(2\pi ft)$. We measured this same quantity by passing a current $i_1 \sin(\pi ft + \theta)$ through the top film and a steady current I through the bottom film. The amplitude of the sin (2πft) component of the voltage across the bottom film is then a measure of its average temperature modulation amplitude. Measurements of the ratio of the modulation amplitude of the average temperature of the bottom film $\Delta T_2(f)$ to the amplitude of the power dissipated in the top film P_1, for frequencies 0.2 Hz <f< 24 KHz are plotted in figure 1. The modulation amplitude was proportional to Ii_1^2 as expected for thermal coupling. Measurements taken with the roles of the two bridges reversed gave identical results. The calculated values of $\Delta T_2(f)/P_1$ are plotted as the solid curve in figure 1. Theory and experiment agree at all frequencies within the factor of two uncertainty due to β, the temperature coefficient of resistance of the film, K, the thermal conductivity of the substrate, and the transfer function calibration at low frequency. The excellent agreement without adjustable parameters indicates that the model incorporates the important features of the system, and gives us confidence in its prediction for strong thermal coupling between the two films.

The correlation between fluctuations of the average temperatures of the two films can be expressed by the coherence function, $\gamma_T^2(f) = |S_{T12}(f)|^2/\{S_{T1}(f) \cdot S_{T2}(f)\}$, where S_{T12} is the cross-PSD between the average temperatures of the two films, and S_{T1} and S_{T2} are their individual PSD's [9]. The thermal coupling calculation indicates that if the two films were perfectly superimposed the coherence between fluctuations of their average temperatures would be unity for $f << 1/\tau_{SiO}$. However, since they are not perfectly aligned $\gamma_T^2(f)$ is slightly reduced by a factor that depends on the fraction of the area of one film which overlaps the other film. For our film geometry we expect $0.9 < \gamma_T^2(f) < 1.0$.

Consequently, if temperature fluctuations were the cause of the 1/f noise, essentially

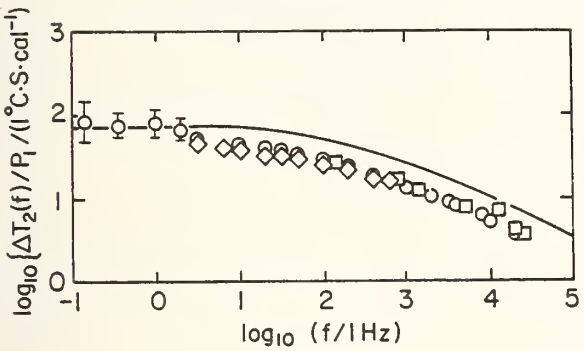

Fig. 1 Thermal response $\Delta T_2(f)/P_1$. Data points are representative of several different runs; omitted points superimpose; ○ and ◇ observed with power into top film, □ with power into bottom film. Error bars represent low frequency uncertainties in the transfer function. Solid line is the calculated value of the thermal response $\Delta T_2(f)/P_1$.

the same temperature fluctuations would appear in both films and the 1/f noise would be correlated. In this case we expect $\gamma_v^2(f) = \gamma_T^2(f)$, where $\gamma_v^2(f)$ is the coherence between the 1/f noise of the two films. Since the measured voltage fluctuations across a film include both the 1/f noise and (mostly incoherent) background noise, the coherence $\gamma_E^2(f)$ of the measured voltage fluctuations of the two films is not in general equal to $\gamma_v^2(f)$. Instead, $\gamma_v^2(f)$ and $\gamma_E^2(f)$ are related by

$$\gamma_E^2(f) = \gamma_v^2(f)/\{[1+S_{B1}(f)/S_{v1}(f)][1+S_{B2}(f)/S_{v2}(f)\}, \qquad (1)$$

where S_{v1} and S_{v2} are the PSD's of the excess noise of each film and S_{B1} and S_{B2} are the PSD's of their background noise. Using measured values of S_{v1}, S_{v2}, S_{B1}, and S_{B2}, $\gamma_E^2(f)$ has been calculated and is plotted as curve a in figure 2 assuming that temperature fluctuations are completely responsible for the observed 1/f noise of a single film (i.e. $\gamma_v^2 = \gamma_T^2$).

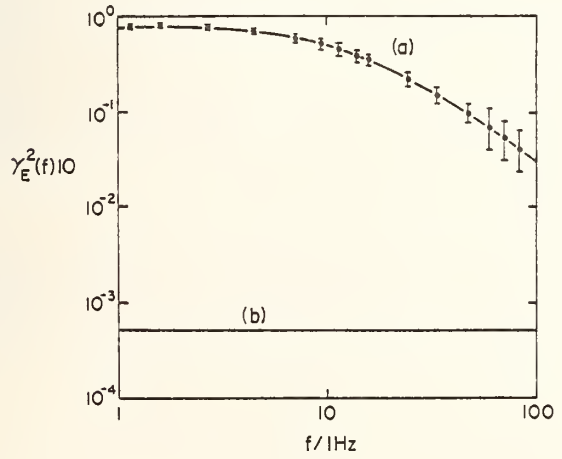

Fig. 2 (a) Calculated $\gamma_E^2(f)$ assuming $\gamma_v^2(f) = \gamma_T^2(f)$ from measured S_{v1}, S_{v2}, S_{B1}, and S_{B2}. (b) Upper limit of experimental coherence $\gamma_E^2(f)$.

Measurements of $\gamma_E^2(f)$ for frequencies 1 Hz <f< 100 Hz discovered no coherence above the instrumental sensitivity indicated by curve b in figure 2. In this frequency range $0 < \gamma_E^2(f) < 5 \times 10^{-4}$. At the low frequency the coherence is more than a factor of 10^3 lower than would be expected if the 1/f noise were due to temperature fluctuations. At higher frequencies the Johnson noise reduces $\gamma_E^2(f)$, but the discrepancy is still large. Since the correlation length for temperature fluctuations $\lambda(f) = \{D/\pi f\}^{1/2}$ at 1Hz is already very much longer than the separation between the two films, and increases with decreasing frequency, this result should extend to lower frequencies. Therefore, we must conclude that the 1/f noise in these gold films is not due to temperature fluctuations.

Voss and Clarke [1] and Zhigal'skiy, et al. [2] have previously reported the observations of frequency dependent spacial correlations in the room temperature 1/f noise along metal films, as would be expected if the noise were due to thermal fluctuations. However, elsewhere in this conference Weissman reports similar experiments in which spacial correlations were not observed. Van Vliet and Chenette also report in private communication the lack of correlation of the 1/f noise between two thermally coupled semiconductor junctions.

In summary, we have measured the coherence between the 1/f conductance noise of two substrate mounted thin gold films that have been demonstrated to be in strong thermal contact, and have calculated the coherence between the 1/f noise that would be expected if temperature fluctuations were responsible for the observed 1/f noise. The measured coherence is several orders of magnitude lower than predicted for temperature fluctuations. Therefore, we conclude that the 1/f noise is not caused by temperature fluctuations.

We would like to thank Joe Mantese and Dr. Mark Nelkin for helpful discussions.

REFERENCES

[1] R. F. Voss and J. Clarke, *Phys. Rev. B* 13, 556 (1976); *Phys. Rev. Lett.* 33, 24 (1974).

[2] G. P. Zhigal'skiy and A. V. Karev, *Radio Engin. and Electr. Phys. (USA)* 22(12), 112 (1979).

[3] M. B. Ketchen and J. Clarke, *Phys. Rev. B* 17, 114 (1978).

[4] J. W. Eberhard and P. M. Horn, *Phys. Rev. B* 18, 6681 (1978); see also P. Dutta, P. Dimon, and P. M. Horn, *Phys. Rev. Lett.* 43, 646 (1979).

[5] M. B. Weissman, *Phys. Rev. Lett.* 41, 1 (1978).

[6] K. M. Van Vliet, A. Van der Ziel, and R. R. Schmidt, *J. Appl. Phys.* 51, 2947 (1980).

[7] F. N. Hooge and A. M. H. Hoppenbrouwers, *Physica* 45, 386 (1969).

[8] J. H. Scofield, D. H. Darling, and W. W. Webb, to be published.

[9] J. S. Bendat and G. Piersol, *Random Data: Analysis and Measurement Procedures* (John Wiley and Sons, Inc., 1971), p. 141.

TEMPERATURE RESPONSE AND CORRELATION OF 1/f NOISE IN TRANSISTORS

J. Kilmer, K. M. van Vliet, E. R. Chenette,
and P. H. Handel

Electrical Engineering Department
University of Florida
Gainesville, Florida 32611

In order to investigate the possibility of temperature fluctuations as the origin of 1/f noise in thin films and in devices, we examined the thermal coupling properties of several bipolar transistors on an integrated circuit chip (CA3018NPN). The transistors chosen for investigation were thermally coupled by the substrate but electrically isolated; they were 10 to 200 microns apart. One transistor was used as a "heater" and another one nearby as a "sensor." The heater power frequency was varied between a few hertz and about 20 kilohertz. The response of the other transistor was measured by monitoring V_{BE}, which is a sensitive function of temperature. The thermal response was quite well observable. The transfer function was nearly flat below 100 hertz, and above this varied as $1/\sqrt{f}$, in accord with the solution of the one dimensional heat diffusion equation. In order to rule out capacitive coupling effects, the response was also determined by using two frequencies for the heater input signal, and by measuring the response for the sum or difference frequencies; the latter only can occur due to the quadratic function of the Joule heating. Thus the occurrence of a strong thermal coupling was ascertained.

Next, we measured the noise of both isolated transistors in the range 5 millihertz to 25 kilohertz; in most of this range the noise was pure 1/f. Using a Hewlett Packard fast Fourier spectrum analyzer in this frequency range, we then determined the cross-correlation noise of the two transistors. Within experimental error this yielded zero for the coherence coefficient in the entire frequency range.

From the measured heat transfer response we could in principle calculate how strong the noise correlation should be, if the noise were due to spontaneous temperature fluctuations. However, this requires knowledge of the heat coupling sensitivity factors, like $V_{BE}(T)$, etc., the determination of which may involve relatively large errors. Therefore, we modified the heat transfer experiment as follows. We selected three electrically isolated transistors on the integrated circuit chip, and used one transistor as the "heater" and two others as "sensors." A good heat transfer response between heater and sensors was obtained. We then measured the correlation between the two sensors when an a.c. signal was fed into the heater.

For a heater frequency of 12.5 hz the coherence coefficient, $\rho = \overline{v_1 v_2} / \sqrt{\overline{v_1^2}\,\overline{v_2^2}}$, was found to be 0.6, and at 40 hz the coherence coefficient was found to be 0.4. This experiment allows a direct comparison with the measured coherence of the noise, which was 0 ± 0.02. We thus conclude that the measured 1/f noise in these transistors could not have been due to temperature fluctuations of the transistors or the substrate.

LACK OF SPATIAL CROSS-CORRELATION IN 1/f NOISE IN CHROME FILMS

R. D. Black*, M. B. Weissman* and F. M. Fliegle†
*Department of Physics, †Electrical Engineering Department
University of Illinois at Urbana-Champaign
Urbana, IL 61801

Several years ago Voss and Clarke [1] observed correlations in the low frequency components of the excess noise in two adjacent lengths of a strip of bismuth film. From the characteristic frequency of the effect and from the center-to-center spacing of the regions, a diffusion coefficient was calculated which seemed too large to be associated with most variables affecting the resistance except for temperature. As a result, much theoretical effort has gone into explaining the connection between temperature fluctuations and 1/f noise. We have performed similar experiments on chrome films and have found no spatial cross-correlations in the 1/f noise.

The films were obtained from Basic Microelectronics Industries. The specified thickness was 1000 ± 100 Å on a soda-lime glass substrate. Assay by emitted-photon spectroscopy using an SEM showed no significant contaminants. Patterns were etched using optical lithography. The observed stretches were ~ 10 μm wide and 500 μm long, each. A seven probe contact method was used, with separate pairs of current-carrying contacts on each region. One voltage-sensing contact was shared by the two regions, but no current flowed through the shared path. Three similarly prepared samples showed resistances and noise magnitudes matched to within ~ 20%. One sample was observed in an SEM; it showed shallow (~ 1 μm) scallops on the edges of the film and some shadowing of the edges, indicating a bit of edge-thinning during etching.

The resistance of the film was larger than expected for pure Cr by about an order of magnitude, and the temperature coefficient of resistivity was about $-3 \cdot 10^{-4}/^{\circ}C$. Although this indicates significant disorder, we observed no grains at a resolution of several hundred angstroms.

Leads were attached by compressing blobs of indium very tightly onto the contact pads using steel screws. The standard checks for battery and contact noise were run, revealing none above one Herz. Below one Herz there were intermittent current fluctuations much smaller than sample noise. We used a PAR 114-185 amplifier for one channel and two series PAR 113's for the other. Spectra were taken with a PAR 4520 dual channel FFT analyzer.

The 1/f noise magnitude was within the range found in other metal film and semimetal film samples of comparable volume [1]. No spatially correlated 1/f noise components were found, to an accuracy of ~ ±.05 of the sample 1/f noise in the one to ten Herz range and ~ ±0.1 in the one-eighth to one Herz range. A slight correlated Johnson noise component due to the shared part of the two voltage lead paths was detectable at higher frequencies. In our samples, there is no reason to suspect any fast-diffusing variable, whether associated with the lattice or the carriers, of playing a role in the 1/f noise.

We have also made measurements in which only one current source was used, connected to the outer current pads. Some intermittent low-frequency coherence (~ 10% below 0.5 Hz) appeared, but a similar correlated noise component could also be found with one region replaced by a wire-wound resistor, so this small correlation was due to current fluctuations. Since the time for carriers to move from one stretch to the other was less than 10 msec, fluctuations transported with the carriers would be fully correlated below ~ 15 Hz. We believe such fluctuations can be ruled out. Data on one non-annealed bismuth sample using independent current paths also show no cross-spectra down to 0.12 Hz.

This work was supported by NSF grant DMR 80-07057 and, through the Materials Research Laboratory, by NSF DMR 77-23999.

REFERENCES

[1] R. F. Voss and J. Clarke, Phys. Rev. B13, 556 (1976).

TEMPERATURE FLUCTUATIONS IN A STEADY STATE

Igor Pavlin

Department of Physics and Astronomy
University of Massachusetts
Amherst, MA 01003, USA
and
Institute "Boris Kidrič"
Belgrade, Yugoslavia

Stanley Engelsberg

Department of Physics and Astronomy
University of Massachusetts
Amherst, MA 01003, USA

INTRODUCTION

Are temperature fluctuations responsible for the 1/f noise of voltage fluctuations in thin metal films? This problem, posed by experiments of Voss and Clarke [1], is still not resolved. The authors assume that temperature fluctuations are spatially correlated and use equilibrium statistical mechanics in order to obtain satisfactory theoretical explanation. Due to the large currents used in experiments, one might suggest that temperature fluctuations in a steady state cause 1/f noise. One of the arguments might be that steady state fluctuations would lead to 1/f noise without the additional assumption of correlated fluctuations. However, we argue that the assumption of spatially uncorrelated temperature fluctuations in a steady state cannot be responsible for 1/f noise. It is a spatial correlation either in the equilibrium or in a non-equilibrium which could be the cause of 1/f noise.

Our results should provide an excellent opportunity for experimental verification of some questions related to temperature fluctuations. First, they can check indirectly whether or not temperature fluctuations cause the voltage noise seen in thin metal films. Second, the applicability of microscopic reversibility, Onsager [2], to temperature fluctuations in a steady state could be verified. Third, one can test the concept of local equilibrium for temperature fluctuations (see, for example, Balescu [3]).

In the next section we outline our theoretical predictions. Than we give two one-dimensional examples. One example is of a thin rod of length l, whose lateral sides are thermally isolated. The ends of the rod are maintained at different temperatures. Fluctuations around the steady state are examined. The exact solution for the spectrum is found. In the second case we consider an infinite homogeneous rod. A steady state with a smooth spatial dependence in the rod is considered. The spectrum of temperature fluctuations coming from a small part of length 2l is found. In both cases we conclude that spatial dependence of the steady state temperature distribution cannot be the cause of correlated temperature fluctuations.

TEMPERATURE FLUCTUATIONS AROUND A STEADY STATE

The formalism for temperature fluctuations around a steady state temperature distribution is derived on the assumptions of the linearity and microscopic reversibility of the system. The probability of a temperature deviation δT from some mean temperature in a steady state $T_0(\vec{r})$

$$Pr\{\delta T\} \propto \exp\left\{-\frac{C_V}{2k_B}\int_{\Omega} d\Omega\left[\frac{\delta T(\vec{r},t)}{T_0(\vec{r})}\right]^2\right\} \qquad (1)$$

is given by Prigogine [4]. Let us interpret eq (1). A fluctuation δT as a whole is composed of many independent deviations of temperature from the mean temperature $T_0(\vec{r})$. In a very small volume $\Delta\Omega$ containing the point $\vec{r}$ we assume that the system behaves as if it is in equilibrium at temperature $T_0=T_0(\vec{r})$. The distribution of a deviation from the mean temperature at that particular point $\vec{r}$ is Gaussian

$$p_r\{\delta T(\vec{r},t)\} \propto \exp\left\{-\frac{C_v}{2k_B}\left[\frac{\delta T(\vec{r},t)}{T_0(\vec{r})}\right]^2 \Delta\Omega\right\}. \tag{2}$$

The probability of a deviation at some other point $\vec{r}'$ would be as in eq (2) with $\vec{r}$ replaced by $\vec{r}'$. When equal-time temperature fluctuations are assumed to be independent, the joint probability distribution of $\delta T(\vec{r},t)$ and $\delta T(\vec{r}',t)$ is the product of their distributions. The probability of a fluctuation δT as a whole in a system is then the product of the individu al probabilities for any small volume $\Delta\Omega$ contained in Ω. The change to the continuum results in the integral over the considered volume Ω.

The expected value of $|\delta T(\vec{r},t)|^2$ at the point $\vec{r}$ can be obtained in a similar way as in the case of the equilibrium. It is the variance of the random variable $\delta T(\vec{r},t)$ having the Gaussian distribution and the mean zero. Using the assumption of uncorrelated temperature fluctuations, the equal-time two-point correlation function, $\Gamma(\vec{r},\vec{r}')$, is than assumed to be

$$\Gamma(\vec{r},\vec{r}') \equiv \langle \delta T(\vec{r},t)^* \delta T(\vec{r}',t)\rangle = \frac{k_B |T_0(\vec{r})|^2}{C_v}\delta(\vec{r}-\vec{r}'). \tag{3}$$

In the case of $T_0(\vec{r})=T_0$ we get the standard equilibrium result. Similar considerations are given to the case of density fluctuations in a nonhomogeneous gas, Cohen [6].

Using the Green's function formalism, van Vliet [5], and the correlation functions $\Gamma(\vec{r},\vec{r}')$ we find the spectrum $S_T(\omega)$ of temperature fluctuations around a steady state $T_0(\vec{r})$

$$S_T(\omega) = \frac{4Dk_B}{C_v}\sum_{m=1}^{\infty}\sum_{n=1}^{\infty}\frac{\lambda_n^2 B_m^* B_n}{\omega^2 + D^2\lambda_n^4}\cdot A_{mn} \tag{4}$$

where

$$A_{mn} \equiv \int_\Omega d^3\vec{r}\, \varphi_m(\vec{r})\varphi_n(\vec{r})|T_0(\vec{r})|^2, \qquad B_m \equiv \frac{1}{\Omega}\int_\Omega d^3\vec{r}\,\varphi_m(\vec{r}). \tag{5}$$

The noise spectrum $S_T(\omega)$ originates from the volume Ω. D is the diffusion constant. φ_m, λ_m

are the eigenfunctions and eigenvalues of the related Sturm-Liouville problem, which satisfy the relevant boundary conditions. C_v is the heat capacity per unit volume of the sample.

When $T_o(\vec{r})=T_o$ we obtain the coefficients $A^{eq}_{mn}(T_o)$ for uncorrelated temperature fluctuations in the equilibrium at T_o. The coefficients A_{mn} are in many cases bounded between $A^{eq}_{mn}(Tmin) \leq A_{mn} \leq A^{eq}_{mn}(Tmax)$ where $Tmin \leq T(r) \leq Tmax$. The spectrum of any steady state temperature distribution which is contained between Tmin and Tmax is bounded above and below by the spectra of uncorrelated equilibrium fluctuations taken at Tmax and Tmin. Since the spectra of uncorrelated equilibrium temperature fluctuations do not contain a 1/f part in its spectrum, the spectra of fluctuations around steady state, assuming uncorrelated random flows, do not contain it either.

TWO ONE-DIMENSIONAL EXAMPLES

Thin rod. We denote the temperatures at the ends of a rod of length l, T_o, T_1. The eigenfunctions are $\varphi_m = \sqrt{2/l}\,\sin(\lambda_m x)$, with the corresponding eigenvalues $\lambda_m = m\pi/l$; m=1,2,3... The stationary temperature distribution is $T_o(x)=T_o+(T_1-T_o)x/l$. Using eq (4) and (5) we find that the spectrum is

$$S_T(\omega) = \frac{32\,k_B\,l}{\pi^4 C_v D}\left\{\frac{T_o^2+T_1^2}{2}\sum_{m=1}^{\infty}{}' \frac{1}{m^4+\Theta^4} - \frac{2}{\pi^4}(T_1-T_o)^2\sum_{m=1}^{\infty}{}' \frac{1}{m^2}\cdot\frac{1}{m^4+\Theta^4}\right\} \qquad (6)$$

(' denotes summation over odd integers, $\Theta=(\omega/\omega_l)^{1/2}$, $\omega_l = D\pi^2/4l^2$). The spectrum (6) reduces as $T_1 \to T_o$ to that obtained by Ketchen and Clarke [7] for uncorrelated temperature fluctuations in equilibrium. Using complex analysis we find the analytic form of the spectrum (6). The spectrum (6) retains the shape of the spectrum of uncorrelated equilibrium temperature fluctuations and no significant change is introduced by the spatial dependence of the steady state temperature distribution $T_o(x)$, as long as the linearity of the system is maintained. The results are plotted in figure 1.

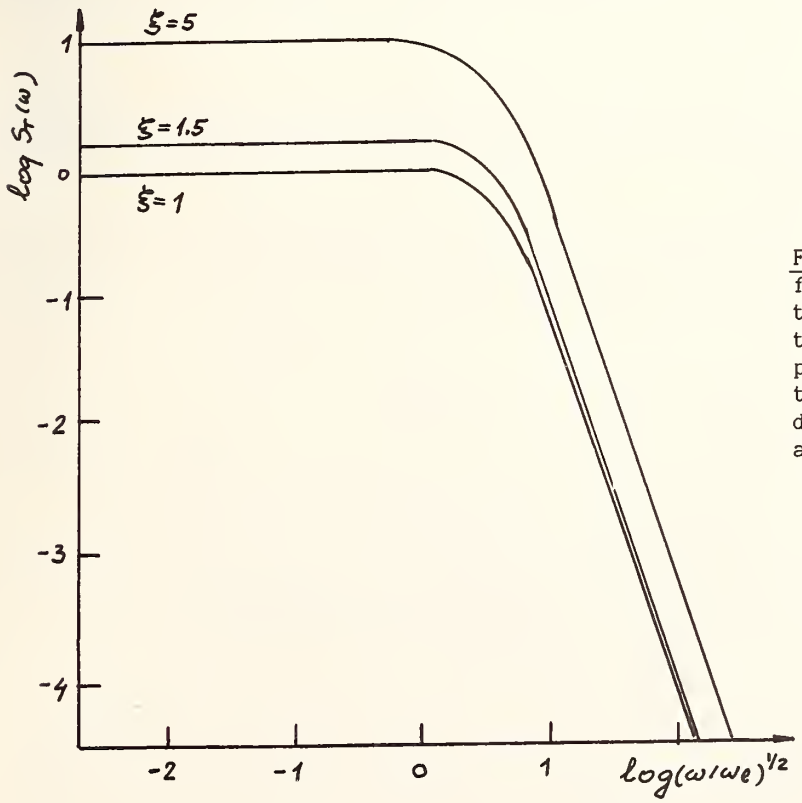

Fig. 1 Spectrum of uncorrelated fluctuations for a thin rod in the steady state. Temperatures of the rod's end are T_o and T_1. The parameter $\xi = T_1/T_o$ is a measure of the steady state temperature gradient. The spectra are obtained according to eq (6) in the text.

Smooth steady state temperature distribution. We consider a slowly varying spatial distribution of temperature over a length much longer than the length 2l of a rod. The rod itself is a part of an infinite homogeneous system. To simplify, we write

$$[T_0(x)]^2 = T_0^2 + \frac{(\Delta T)^2}{1 + (\frac{x}{a})^2} \qquad (7)$$

where $\xi \equiv \Delta T/T_0 \ll 1$ and $a \gg l$. The eigensolutions will be plane waves.

If the assumption $a \gg l$ is used, the spectrum is approximated using Taylor expansion

$$S_T(\omega) = \frac{k_B T_0^2}{2\pi C_v} \cdot \left\{ \left[1 + \xi^2 \left(1 - \frac{l^2}{a^2}\right)\right] \int_{-\infty}^{\infty} \frac{dk \cdot k^2 j_0^2(kl)}{\omega^2 + D^2 k^4} + \frac{\xi^2}{a^2} \int_{-\infty}^{\infty} \frac{dk \sin(kl) j_1(kl)}{\omega^2 + D^2 k^4} \right\}. \qquad (8)$$

j_0 and j_1 are spherical Bessel functions. The integrals can be evaluated using a contour integration. After that, asymptotic expansion of the spectrum gives

$$S_T(\omega) \sim \begin{cases} \left[1 - \left(\frac{l}{a}\right)^2\right]\left(\frac{\omega_l}{\omega}\right)^{3/2} + 2\left(\frac{l}{a}\right)^2\left(\frac{\omega_l}{\omega}\right)^2 + \cdots \sim \frac{1}{\omega^{3/2}}, & \omega \gg \omega_l \\ \left[1 - \frac{2}{3}\left(\frac{l}{a}\right)^2\right]\left(\frac{\omega_l}{\omega}\right)^{1/2} - \frac{2}{3} + \frac{7}{5}\left(\frac{l}{a}\right)^2 + \cdots \sim \frac{1}{\omega^{1/2}}, & \omega \ll \omega_l. \end{cases} \qquad (9)$$

For $a \gg l$, the results in eq (9) are only a slight modification of spectra for uncorrelated temperature fluctuations in a part of the homogeneous rod which is in thermal equilibrium with its surroundings.

CONCLUSIONS

Non-equilibrium fluctuations in a system with spatially uncorrelated temperature fluctuations cannot be responsible for a 1/f spectrum. Thus, theoretical support is given to the intuitive assumption of experimentalists that the introduction of a steady state does not enhance spectrum significantly.

Derived expressions for temperature fluctuations in a thin rod having different end temperatures are suitable for experimental verification of our theory. The verification of the theory would imply the applicability of Onsager's hypothesis of microscopic reversibility to temperature fluctuations in non-equilibrium.

REFERENCES

[1] Voss, R. F. and Clarke, J. Phys. Rev. B 13, 556-573 (1976).
[2] Onsager, L. Phys. Rev. 38, 2265-2279 (1931).
[3] Balescu, R. Equilibrium and nonequilibrium statistical mechanics. New York: John Wiley & So., 1975.
[4] Prigogine, I. Introduction to thermodynamics of irreversible processes. Third edition. New York: John Wiley & Sons, Inc., 1967.
[5] Van Vliet, K. M. J. Math. Phys. 12, 1981-1998 (1971).
[6] Cohen, E. G. D. The Boltzmann equation and fluctuations. In Fundamental Problems in Statistical Mechanics V. Ed. E.G.D. Cohen, North Holland, 1980.
[7] Ketchen, M.B. and Clarke, J. Phys. Rev. B 17, 114-121 (1978).

EARTHQUAKES, THUNDERSTORMS, AND OTHER 1/F NOISES

Stefan Machlup

Department of Physics
Case Institute of Technology
Case Western Reserve University
Cleveland, OH 44106

ABSTRACT

Improving an experiment may mean getting better signal-to-noise ratio, perhaps by filtering out a specific source of noise. Each such noise source is likely to have a characteristic frequency or time scale. The noises most difficult to filter are the catastrophic events, fortunately rare, whatever their cause. The ensemble of such events has no characteristic time scale[1]. There are as many repeat times in the interval between 1 and 2 seconds as between 1 and 2 minutes, etc. The distribution is scale-invariant, i.e. logarithmic. Differentiating a logarithmic cumulative distribution results in a 1/f spectral density. Filtering the noise out in any frequency band means the 1/f shape obtains only for frequencies below that band. If you have not found the 1/f spectrum, it is because you have not waited long enough. You have not looked at low enough frequencies.

In designing experiments, one tries to foresee the possible sources of noise and, of course, to eliminate them. Johnson (thermal) noise and shot noise set a floor, a minimum below which noise can not be reduced. Thermal noise and shot noise both have white spectra, i.e. they are flat up to very high frequencies -- what I like to call quantum frequencies -- where the spectra bend down in a Lorentz shape. In this gathering I don't have to demonstrate what white noise sounds like. It is the shshsh sound of rushing water. What characterizes white noise is that, for any given frequency, there is more noise power in the frequency bands above the given frequency than in the bands below the given frequency.

Here I also don't have to demonstrate what flicker noise sounds like. Flicker noise is also called pink noise, because its spectrum is proportional to 1/frequency. There is more noise power at low frequencies than at high. There is twice as much noise power in a 1-Hz band near 1 kHz as in a 1Hz band near 2kHz. Well, I'll do it anyway. In a transistor, the 1/f noise sounds like pshsh, ktshsh, pdk, kshsh... You can hear the individual events. Big events are less frequent than little events. Twice as big occurs half as often. That is the meaning of 1/f spectrum.

UNLIKELY EVENTS

Mandelbrot[1] uses the term Joseph Effect for unlikely events having low characteristic frequencies. The name refers to the biblical Joseph, who predicted the 7 years of plenty followed by 7 years of famine. Clearly the remarkable feature was not the existence of a world-shaking phenomenon with a 14-year period (a frequency of 2×10^{-9} Hz). The remarkable feature was the accuracy of Joseph's prediction.

1/f spectra are so common that there is a large literature exploring noise mechanisms having such a spectral shape over many decades. This paper is not intended to be a contribution to that literature. It takes the opposite point of view. It asks the question: What can the ubiquity of 1/f spectra in widely different situations tell us about unexpected events? The answer is that the ensemble of unforeseen events has characteristic repetition times which have a scale-invariant distribution.

SCALE-INVARIANCE

This is not arcane mathematics. It is elementary. A 1/f spectral shape is the only shape that has no characteristic time, or, if you prefer, no characteristic frequency. If all frequencies are multiplied by a constant, the spectrum does not change: df/f is independent of the units of f. That means that the statistical distribution governing the events that produce that spectrum also has to be scale-invariant. You may find the argument more convincing if we talk about the integrated power spectrum. For a 1/f spectrum the total power in a frequency interval (f_1, f_2) is proportional to $\log(f_2/f_1)$ -- the integral $\int df/f$. The only function of f that is dimensionless is log f. Only this spectral shape has the property that there is the same amount of power between 1 Hz and 2 Hz as between 10 Hz and 20 Hz...

Readers of the Scientific American know by now that the height of the floods of the Nile has a 1/f spectrum[2]. They have read that the music[3] of Bach and Mozart and even jazz is 1/f. Designers of experiments know that the banging of doors is 1/f, and they design their measuring devices to block out such interruptions. By this I don't mean that the spectrum of one bang is 1/f. Indeed, one bang has a lot of high-frequency components. What the 1/f shape of door-banging noise says is that hard slams are scarcer than soft slams and the whole phenomenon does not have a characteristic repetition time. If the soft slams are not recorded, all that remains is the lower-frequency hard slams. Some noises are too big and/or too infrequent to discriminate against. These catastrophic events get through our filters, our vibration-free mountings, our isolation transformers. The term "earthquakes and thunderstorms" in the title is a euphemism for the rare, unforeseen and cataclysmic events that constitute low-frequency noise you just can't block out. They would include the truck crashing into your lab. The better you are at eliminating noise, the more nearly the spectrum of the remaining noise is likely to be 1/f, i.e. scale-invariant.

You conclude that a badly designed experiment may have a 1/f noise spectrum simply because there is a large ensemble of sources of big noise, so large an ensemble that the statistical distribution of characteristic times is scale-invariant. As these noises are removed by better design, what noise remains is likely to be dominated by one or two mechanisms, and to have a characteristic time -- a Lorentzian spectrum. When the predictable noise source has been removed, what remains are the unpredictable cataclysmic events -- the earthquakes and thunderstorms. They are likely to have myriad causes, so again, to have a scale-invariant distribution of characteristic times. Both the very raw experiment and the very mature experiments are likely to have 1/f noise spectra -- at different levels, to be sure.

HIGH AND LOW-FREQUENCY BENDPOINTS

Back in 1952 I was assigned the 1/f noise problem in transistors by William Shockley, who headed my research group at Bell Telephone Laboratories. One of my early worries was the infinities, the divergences at both high and low frequencies. I resolved the high-frequency-divergence worry quickly. Scale-invariance breaks down at high frequencies because Planck's constant determines a scale. The high characteristic frequencies that cause 1/f spectra to curve down to $1/f^2$ shapes I have called quantum frequencies. The existence of atoms determines both a length scale and a time scale on the short end. The low frequency divergence of a 1/f spectrum was resolved by Mandelbrot[4] for the theorists. The experimenters were never bothered by it. They know intuitively that to measure noise at 10^{-1} Hz they have to measure for at least 10 seconds; to measure at 10^{-3} Hz the measuring time has to be at least 10^3 seconds; etc. They know the bandwidth theorem.

I was always looking for a low-frequency cut-off. In other words, I thought there ought to exist a very low frequency below which the flicker noise would be white. I was looking for a time scale on the long-time end. If such a characteristic time were to exist, i.e., if there were a longest characteristic repeat time for random events, then the 1/f spectra would have that shape for only a limited number of decades in frequency. That would imply the existence of a pure number characteristic of the universe, giving the ratio of the quantum frequency bendpoint to that low-frequency bendpoint. The persistence of 1/f spectra to ever lower frequencies can be taken as evidence that nature does not possess such a ratio. If, for example, the age of the universe turns out to

set a low-frequency bound, then 1/f spectra might span as much as 34 decades in frequency. We would be talking about a pure number somewhere around 10^{34}. There are, of course, some big dimensionless numbers in nature. For example, the ratio of the electrical repulsion to the gravitational attraction of two electrons is 4×10^{42}. To have a 1/f noise spectrum covering 42 decades seems almost mindboggling.

No attempt is made here at a model for a low-frequency bendpoint. The question at issue is whether scale-invariance might be one of the approximate symmetries of nature. We know it breaks down at the short-time end. We do not know how far into the long-time region it might extend. The ubiquity of 1/f noise spectra is our evidence for conjecturing this symmetry property.

What kinds of experimental evidence would support or contradict this conjecture? To be sure, no matter how many decades long an observed 1/f spectrum might be, not even dozens of such spectra would constitute proof. But if a universal low-frequency bendpoint were to be found, with no 1/f noise at lower frequencies, that would be sufficient to disprove the conjecture.

ENSEMBLE OF PURELY RANDOM PROCESSES

It might be useful to write down the connection between the power spectrum and the statistical distribution of repeat times for purely random processes. A purely random process is one with an autocorrelation function of the form $e^{-t/\tau}$. The power spectrum of such a process has a Lorentz (also called Debye) shape[5]:

$$\begin{aligned} S(\omega) &\propto \text{Fourier Transform of } e^{-t/\tau} \\ &\propto \tau/(1 + \omega^2\tau^2) \end{aligned} \tag{1}$$

If we have a large collection of different random processes, each with its own correlation time τ, then the power spectrum of the whole ensemble depends on the statistical distribution $\rho(\tau)$ of thesecorrelation times. If these processes have not been filtered, then our conjecture is that the weighting function is scale-invariant:

$$\rho(\tau)\, d\tau \propto d\tau/\tau \tag{2}$$

This gives a power spectrum

$$\begin{aligned} \int_{\tau_1}^{\tau_2} S_\tau(\omega)\rho(\tau)d\tau &\propto \int_{\tau_1}^{\tau_2} \frac{\tau}{1 + \omega^2\tau^2} \frac{d\tau}{\tau} \\ &= \frac{\tan^{-1}\omega\tau}{\omega} \Bigg|_{\tau_1}^{\tau_2} . \end{aligned} \tag{3}$$

If the scale-invariance extends over many orders of magnitude, i.e. if τ_2/τ_1 is a large ratio, then the spectrum is $1/\omega$ over a correspondingly large range[6]. For many years we have been scratching our heads to find special mechanisms that would have that special distribution of time constants over many decades. But we do not need special mechanisms. We need simply a large ensemble of mechanisms with no prejudice about scale. The conjecture is that nature is sufficiently chaotic to possess this lack of prejudice.

Some of my friends refuse to call this sort of thing physical theory. They feel it belongs more properly in the realm of philosophy, metaphysics perhaps. It is important to note that whatever the status of this approximate symmetry principle, it does not detract in any way from the work of those who have explored individual noise mechanisms with 1/f spectra.

ACKNOWLEDGEMENTS

This paper grew out of conversations with my colleague Professor T. Hoshiko of the Case Western Reserve University School of Medicine. Our work is partially supported by the National Institutes of Health under Grant AM-05865-13.

REFERENCES

[1] Benoit Mandelbrot, Fractals: Form, Chance, and Dimension (W. H. Freeman and Co., San Francisco, 1977)

[2] Martin Gardner, Scientific American 238, No. 4, 16 (April 1978).

[3] R. F. Voss and J. Clarke, J. Acoust. Soc. Am. 63, 258 (1978).

[4] Benoit Mandelbrot, I.E.E.E. Transactions on Information Theory 13, 289 (1967).

[5] S. Machlup, Journal of Applied Physics 25, 341 (1953).

[6] A. Van der Ziel, Fluctuation Phenomena in Semiconductors (Academic Press, New York 1958) p. 56.

1/f DIFFUSION NOISE*

K. L. Ngai

Naval Research Laboratory
Washington, D. C. 20375

Fu-sui Liu

Department of Physics
Beijing University, Beijing, China

A physical description of low frequency fluctuation, dissipation, and relaxation properties of condensed matter that departs from the conventional ideas has recently been proposed by one of us [1-7]. In this model we have explored and found the nature and some universal features of excitations in condensed matter when the excitation energy $h\omega$ can be arbitrarily small. This new class of states and associated excitations between them have been discussed in detail [4]. To distinguish them from well known elementary excitations in solid state physics which offer no help to an arbitrary low-energy regime, these states are called correlated states (CS) and the excitations between them correlated-state excitations (CSE). By nature a CS involves for its description a large number of coordinates which, dependent on the particular material, can be nuclear, bonding, ionic, electronic, etc., or their composite in origin. These coordinates are themselves engaged in complex interactions and their number that is required to describe a CS increases as the excitation energy for the CSE it gives rise to decreases. This complex situation makes a conventional Hamiltonian or Lagrangian modeling approach to CS properties, if not impossible, at least so cumbersome that it would be futile to try to extract from the results any well-defined behaviors. Fortunately, Wigner's statistical approach [8] to quantum mechanics comes to the rescue [4] and enables us to deduce some general properties of CS and CSE. One of these invariant properties is that the density $N(E)$ of CSE with energy E will be linear in E provided E is small enough. In any low frequency fluctuation-dissipation (F-D) phenomenon, a primary species responsible for it can be identified. They can be dipolar groups, charged particles, etc. F-D is caused by transition of the primary species [4] that has a characteristic time τ_o. The primary species is coupled to the CS. Its transition, considered as sudden for times $t>>\tau_o$, will switch on a new potential V that induces excitation and deexcitation of correlated states, and the corresponding matrix element of V is uncorrelated with and independent of the CSE energy E. Thus E - dependence of $|V|^2N(E)$ comes from $N(E)$ alone and is hence linear in E. Written as $|V|^2N(E) = nE$, this condition guarantees that the CS excitations and deexcitations that trail the primary transition will be infrared divergent. That is, there is increasingly high probability of exciting (deexciting) decreasingly small energy $h\omega$ CSE. This causes a power law $\omega^{n-1}(t^{-n})$ dependence of the response in the frequency (time) domain at low frequencies (long times). Here $0\leq n<1$, and n will be referred to as the infrared divergence exponent. Explicitly, the transition rate of the primary species τ_o^{-1} is modified to be time dependent as $\tau_o^{-1}\exp(-n\gamma)\ (E_c t)^{-n}$ where $\gamma=0.577$ and E_c the upper cutoff energy for CSE such that, for $E>E_c$, $N(E)$ is no longer linear in E. It is important to note that we are interested in low frequencies $\nu<10^{10}$ Hz and ambient temperatures T such that $h\omega/kT<<1$. Unlike electron-hole pairs in the X-ray edge problem where the infrared divergence is removed for $h\omega\lesssim kT$ by thermal factors, such a problem does not arise in the case of correlated state excitations with $h\omega/kT<<1$ and infrared divergence continue to arbitrary low $h\omega$.

When addressing any specific F-D properties, a physical quantity Q pertaining to the primary species is considered [4]. For dielectric relaxation, Q is the electric polarization of dipoles or charges; and for particle hopping transport and diffusion, Q is the probability density that the particle remain on a particular site. The transition rate equation for Q is modified from $dQ/dt=-Q/\tau_o$ to

$$dQ/dt = -\tau_o^{-1} e^{-n\gamma} (E_c t)^{-n} Q \qquad (1)$$

by the infrared divergence. Of central importance is the function $\psi(t) \equiv -dQ/dt$ which, from eq (1), is

$$\psi_n(t) = (1-n)\, a_n t^{-n} \exp(-a_n t^{1-n}); \quad a_n = e^{-n\gamma}/(1-n)\tau_o E_c^n \qquad (2)$$

In dipolar dielectric relaxation the polarization correlation function $-\langle P_i(t)\, \dot{P}_i(t-\tau)\rangle_o$ is simply $p_o^2 \psi_n(t)$ with p_o being the dipolar polarization. In particle hopping transport and diffusion, $\psi_n(t)$ is the hopping time probability density (distribution function). That is, the particle if initially at a site will hop between t and t+δt with probability $\psi_n(t)\delta t$. The fundamental process of infrared divergent excitations (deexcitations) of CS that is proposed to occur in all condensed matter always introduces a distribution of event time "constants" and stochasticity in a natural and well-defined manner according to eq (2). The distribution is characterized mainly by one parameter n, the infrared divergence exponent. The limit as $n \to o$ of eq (2) recaptures the classical Markov process.

Predictions of our model based on $\psi_n(t)$ in a number of areas including dielectric relaxation, mechanical and viscoelastic relaxations, internal friction, voltage noise, g-r noise, 1/f noise from mobility fluctuations, NMR spin-lattice relaxation, transient electrical transport, and transient capacitance have been worked out [4]. We have then a unified theory [4]. Good agreement of the predictions with experimental data is achieved for these diverse low frequency responses and for materials of different physical and chemical structures. The most accurate and direct observation of our $\psi_n(t)$ are in mechanical relaxations by photon-correlation spectroscopy [9]. Over a great number of decades of t, the data are in excellent agreement with $\psi_n(t)$ of eq (2). The unified theory offers predictions on quantities such as activation energies [4] as well as dispersion.

In this work we have extended the unified theory to the study of non-Markovian diffusion transport and noise caused by $\psi_n(t)$. For non-Markovian processes the starting point is the generalized master equation. We use the form given by Kenkre, et al. [10]:

$$d\bar{P}(\ell,t)/dt = \int_o^t \phi_n(t-\tau) \Sigma_{\ell'} [p(\ell,\ell')\bar{P}(\ell',\tau) - p(\ell',\ell)\bar{P}(\ell,\tau)]\, d\tau \qquad (3)$$

where $\bar{P}(\ell,t)$ is the probability that the primary species is in a state ℓ at time t, $p(\ell,\ell')$ is the probability of the transition's being from ℓ' to ℓ and $\phi_n(t)$ is the memory or relaxation function that is derived from dynamics specified by $\psi_n(t)$. The Laplace transform (LT) $\phi_n^*(u)$ of $\phi_n(t)$ is given in terms of $\psi_n^*(u)$ the LT of $\psi_n(t)$ by[10]

$$\phi_n^*(u) = u\psi_n^*(u)/[1-\psi_n^*(u)] \qquad (4)$$

One can easily check from eqs (2) and (4) for the limiting case n=0, $\phi_o(t) = 2a_o\delta(t)$ and the non-Markovian master eq (3) becomes the Markovian master equation. We now specialize eq (3) to hopping in a lattice network (where ℓ is lattice site) with the possible presence of a constant electric field E in the x-direction. In the limit of small jump distance Δ_o, a continuum form of eq (3) useful for further discussion is[11]

$$\partial\rho(x,t)/\partial t = \Delta_o^2/6 \int_o^t \phi_n(t-\tau)\, [\partial^2\rho(x,\tau)/\partial x^2]\, d\tau - 2\Delta_o bE \int_o^t \phi_n(t-\tau)\, [\partial\rho(x,\tau)/\partial x]\, d\tau \qquad (5)$$

where b is a constant such that bE is the increment of the probability p for hopping in the direction of the field. The first term on the right hand side of eq (5) is due to diffusion, and the second term is the drift by the electric field when present.

The noise spectrum resulting from spatially-dependent stochastic processes such as diffusion has been a subject of great interest in the past three decades. The motivation behind these activities in diffusion noise is the hope of deriving a 1/f spectrum over a wide frequency range and of explaining the ubiquitous 1/f noise which accompanies all transport and

diffusion processes. Earlier works that employed specific models have claimed to derive a 1/f spectrum from classical Markovian diffusion transport [12](n=0 case of eq (5)). However, it has been convincingly proved that infinite systems classical Markovian transport by diffusion or by drift will in general not have a 1/f noise spectrum [13]. Specifically for diffusion, one always finds a high frequency $\omega^{-3/2}$ behavior, and for sufficiently low frequencies one finds $\omega^{-1/2}$, log ω and ω^0 behavior for one, two and three dimensional diffusion systems [14,15]. In a recent work through the assumption of a volume noise called the "P-source," it is possible to obtain a 1/f spectrum [16] over a frequency range. However, the "P-source" implies long-range spatial correlations, which is unphysical [17]. Thus classical Markovian diffusion will not give rise to 1/f noise. The physical picture in our model is that diffusion in condensed matter in general is non-Markovian ($0 \leq n < 1$) in a well-defined way [eqs (2), (4) and (5)]. The question that naturally arises is: will a 1/f noise spectrum emerge from diffusion transport with $n \neq 0$? We proceed to answer this.

We calculate the diffusion noise spectra by the Green's function procedure [14]. The Green's function $G(\underset{\sim}{r}, \underset{\sim}{r}', t)$ is the probability that a carrier will be found at $\underset{\sim}{r}$ at time t if it is at r' at time 0. For diffusion transport in one-dimension described by the 1-dim. counterpart of eq (5), G satisfies $\partial G(x,t)/2t = \Delta_o^2/2 \int_o^t \phi_n(t-\tau)[\partial^2 G(x,\tau)/\partial x^2]d\tau + \delta(t)\delta(x)$. Taking the LT in t (denoted by *) and Fourier transform in x (denoted by $\sim$), the transform $\tilde{G}^*(k,u)$ can be solved as $\tilde{G}^*(k,u) = [u + \Delta_o^2 k^2 \phi^*(u)/2]^{-1}$. The noise spectrum $S_N(\omega)$ of number fluctuation is given by $S_N(\omega) = 4\langle \Delta N^2 \rangle \ \Omega^{-1} \ \mathrm{Re} \int_\Omega \int_\Omega G^*(x,x',i\omega)dvdv'$, where Ω is the volume of the domain in which one-dimensional diffusion occurs in a sample of length 2ℓ, N(t) the total number of carriers in Ω, and $\langle \Delta N^2 \rangle$ the variance of N. $G^*(x,x',i\omega)$ is the LT in t of G(x,x',t) with $u=i\omega$. In terms of Laplace-Fourier transform $\tilde{G}^*(k,u)$, $S_N(\omega) = 4\langle \Delta N^2 \rangle \Omega^{-1} \ \mathrm{Re} \int_\Omega dv \int_\Omega dv' \ (1/2\pi) \int dk e^{ik(x-x')} \tilde{G}^*(k,i\omega)$. Examine first the high frequency behavior of the noise spectrum. High frequencies or equivalently earlier times behavior is governed by the earlier time dependence of $\psi(t)$ of eq (2) which is $\psi_n(t) = (1-n)a_n t^{-n}$ for $t \ll a_n^{-1/(1-n)}$ with LT given by $\psi_n^*(u) = (1-n)a_n \Gamma(1-n) u^{n-1} \equiv \lambda_n u^{n-1}$ where $\Gamma(z)$ is the Gamma function. From eq (4) we have $\phi_n^*(u) = \lambda_n u^n [1 - \lambda_n u^{-1+n}]^{-1}$. Substituting this into $S_N(\omega)$ gives $S_N(\omega) = 4(\langle \Delta N^2 \rangle / \Omega) \ \mathrm{Re} \int dk/2\pi \left| \int_{-\ell}^{\ell} e^{ikx} dx \right|^2 \{ i\omega + (\lambda_n \Delta_o^2/2)k^2 (i\omega)^n / [1 - \lambda_n (i\omega)^{n-1}] \}$. For high frequencies such that $\lambda_n i\omega^{n-1} \ll 1$, it can be simplified to $S_N(\omega) = (8\langle \Delta N^2 \rangle / \pi\Omega) \ \mathrm{Re} \int dk (\sin^2 k\ell / k^2) [i\omega + (\lambda_n \Delta_o^2/2) k^2 (i\omega)^n]^{-1}$. The integral is evaluated by contour integration in the complex k-plane. On introduction of a natural frequency $\omega_n = (\lambda_n \Delta_o^2 / 4\ell^2)^{1-n}$, the noise spectrum is given explicitly by $S_N(\omega) = (\langle \Delta N^2 \rangle / \Omega) \ (2\lambda_n \Delta_o^2)^{1/2} \cos(n\pi/2) / \cos\phi \{ [1 - \cos\phi \sin((\omega/\omega_n)^{(1-n)/2} \sin\phi) + \cos((\omega/\omega_n)^{(1-n)/2} \sin\phi)] \cdot \exp[-(\omega/\omega_n)^{(1-n)/2} \cos\phi] \} \ \omega^{(-3+n)/2}$ where $\phi = \pi(1-n)/4$. This expression is evaluated for several representative values of n and the results can be seen in Fig. 1.

When n=0, we recapture the results of Markovian 1-dimensional diffusion: the $\omega^{-3/2}$ low at $\omega >> \omega_o$, and the $\omega^{-1/2}$ low at $\omega << \omega_o$, and $\omega_o = D_o/2\ell^2$ with D_o, the 1-dimensional diffusion constant, equals $\lambda_o \Delta_o^2/2$.

For $n \neq 0$ both the high frequency $\omega^{-3/2}$ law and the low frequency $\omega^{-1/2}$ law are modified as evident from Fig. (1). Analytically those modified asymptotic behaviors for $S_N(\omega)$ are

$$S_N(\omega) = \begin{cases} \Omega_n (\omega/\omega_n)^{-(3-n)/2} & ; \ \omega >> \omega_n \\ (\Omega_n/2) \ (\omega/\omega_n)^{-(1+n)/2} & ; \ \omega << \omega_n \end{cases}$$

where $\Omega_n = 2(\lambda_n \Delta_o^2/2)^{1/2} \cos(n\pi/2) \langle \Delta N^2 \rangle / \Omega \cos\phi$. As n increases continuously from zero to unity, both (3-n)/2 and (1+n)/2 approaches one. Thus we have found 1/f spectra of many decades in our model. These predictions now await detailed comparisons with experimental data.

It is worthwhile to emphasize that the present dispersive diffusion model is just one extension among many of our unified theory of low frequency fluctuation-dissipation properties of condensed matter [1-7]. In earlier works we have shown that the unified theory enjoys remarkable success in its application to other areas [4] including dielectric relaxation, mechanical and viscoelastic relaxation, NMR spin-lattice relaxations, voltage noise, 1/f mobility fluctuations and dispersive transient transport. Non-zero value of n for the description of these phenomena in laboratory condensed matter systems is found to be the rule rather than the exception. Hence the general occurrence of diffusion-associated 1/f noise in condensed matter can be understood in our present model that is based on the unified theory [4]. Most intimately related to dispersive diffusion is dispersive transient transport [4]. Their relationship can be seen through eq (5) which gives both phenomena

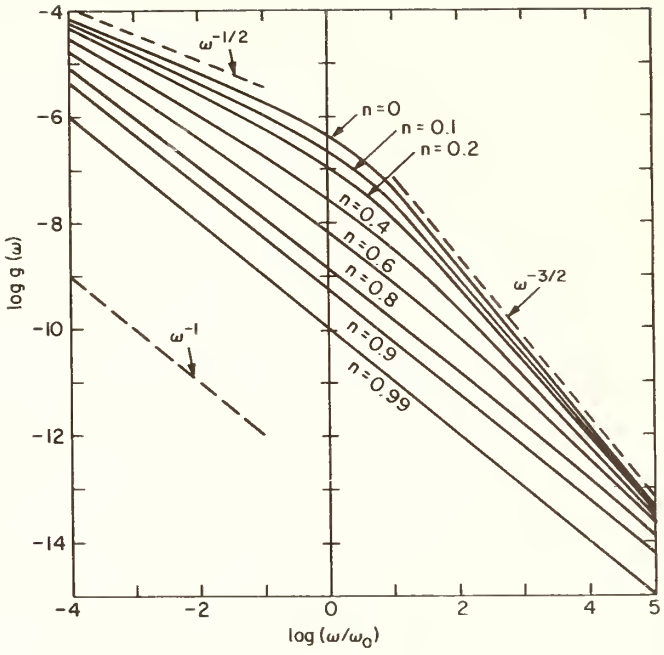

Fig. 1. The noise spectra $g(\omega)$ for several representative values of n between zero and one. Except for the multiplicative constant $\Omega\tau_o^{\frac{1}{2}}/\langle\Delta N^2\rangle 2^{\frac{1}{2}}\Delta_o$, $g(\omega)$ is essentially $S_N(\omega)$ given by eq (16). We have chosen $E_c = 10^9$Hz and $\omega_o = 10^4$Hz when evaluating $g(\omega)$.

with a common memory function $\phi_n(t)$. Experimental data of dispersive transient transport gives direct evidence for non-zero values of n. In SiO_2, the value of n for hole hopping [4] is 0.7 to 0.8. In a-As_2Se_3 n has the value [4] of 0.46. These independent measurements in related phenomena should enhance the credibility of our model of diffusion noise.

REFERENCES

* Work supported in part by ONR.

[1] K.L. Ngai, Bull. Am. Phys. Soc. 24B, 284 (1979).
[2] K.L. Ngai, A.K. Jonscher and C.T. White, Nature, 277, 185 (1979).
[3] K.L. Ngai and C.T. White, Phys. Rev. 20B, 2475 (1979).
[4] K.L. Ngai, Comments Solid State Phys. 9, 127 (1979) Part I; 9, 141 (1980) Part II.
[5] K.L. Ngai, in Fast Ion Transport in Solids, ed. Vashista, Mundy and Shenoy (Elsevier, North Holland, 1979), p. 203.
[6] S.T. Liu, K.L. Ngai and S. Teitler, Ferroelectric 28, 369 (1980).
[7] K.L. Ngai, Naval Research Laboratory, Memorandum Report #3917, Jan., 1979; Phys. Rev., B22, 2066 (1980).
[8] E.P. Wigner, Gatlinberg Conf. on Neutron Physics, Oak Ridge National Lab Report No. ORNL-2309, p. 59; M.L. Mehta, Random Matrices, Academic Press, N.Y. (1967).
[9] C.C. Lai, P.B. Macedo and C.J. Montrose, J. Am. Ceram. Soc. 58, 120 (1975); J.A. Bucaro, H.D. Dardy and R.D. Corsaro, J. Appl. Phys. 47, 741 (1975); and C.P. Lindsey, G.D. Patterson and J.R. Stevens, J. Polymer Sci. PPE.
[10] V.M. Kenkre, E.W. Montroll and M.F. Shlesinger, J. Stat. Phys. 9, 45 (1973).
[11] G.F. Leal Ferreira, Phys. Rev. B 16, 4719 (1977); G.F. Leal Ferreira and L.E. Carrano de Almeida, Phys. Rev. B 19, 6601 (1979).
[12] J.R. Richardson, Bell Syst. Techn. J., 29, 117 (1950); C.G. MacFarlane, Proc. Phys. Soc. (London, B63, 807 (1950)).
[13] K.M. van Vliet and A. van der Ziel, Physica, 24, 415, 556 (1958).
[14] K.M. van Vliet and J.R. Fassett, Fluctuation Phenomena in Solids, ed. R.E. Burgess (Acad. Press. N.Y., 1965), p. 267.
[15] M. Lax, Rev. Mod. Phys. 32, 25 (1960).
[16] R.F. Voss and J. Clarke, Phys. Rev. B 13, 556 (1976).
[17] K.M. van Vliet, Proceedings of Second International Symposium on 1/f Noise, Orlando, Florida (1980), p. 305.

TEMPERATURE DEPENDENCE OF THE EXCESS 1/f NOISE IN METALS

K. L. Ngai

Naval Research Laboratory
Washington, D. C. 20375

INTRODUCTION

The temperature dependence of the excess (1/f) noise is a subject of some interest since the discovery of Eberhard and Horn [1] of a strong temperature dependence of the excess (1/f) voltage noise in thin films of the group IB transition metals and in Ni. This strong temperature dependence of the matnigude of 1/f noise is accompanied also by the appearance of a high temperature peak in Ag and Cu. These behaviors for thin metal films should be contrasted with the rather weak temperature dependences of 1/f noise observed in semiconductors and carbon resistors. Any of the current models of 1/f noise in their respective present forms either do not predict or have not yet made a connection with this strong temperature dependence. Dutta, Dimon and Horn [2] have nevertheless made progress in the understanding of the temperature dependence of the magnitude and of the frequency spectrum of the 1/f noise in metal films by postulating a distribution of activation energies D(E) centered in the vicinity of 1 eV. They envisage an activated process with activation energy E has a characteristic time $\tau = \tau_o \exp(E/kT)$ will contribute to resistance fluctuations and voltage noise $S_V(\omega)$: $\tau/(\omega^2\tau^2+1)$. Then the distribution of activation energies will give rise to a total voltage noise of

$$S_V(\omega,T) \propto \int [\tau/(\omega^2\tau^2 + 1)]\, D(E)\, dE \qquad (1)$$

Proceeding from eq (1) and assuming the width of D(E) is much larger than kT, Dutta et al. then demonstrated that a given D(E) can explain both the strong dependence of S_V on T and the variation of the exponent α with $0.8<\alpha<1.4$ in the $1/f^{\alpha}$ frequency spectrum of the excess noise. These results do follow from some key assumptions that have to be made. To this author's mind the important question that has not yet been addressed to in Dutta et al.'s model is how the noise of resistance fluctuations comes from the fluctuating quantity the characteristic time of which is thermally activated and its activation energy is distributed according to D(E). Dutta and coworker [2] certainly are aware of this problem but, in order to proceed along the lines of their model, they simply assume that the resistance is linearly coupled to the fluctuating quantity. In this short note I would like to propose a specific mechanism for resistance fluctuation noise as caused by the fluctuating quantity. The fluctuating quantity can be diffusing vacancies as suggested by Dutta et al. or diffusing impurity atoms. Both possibilities will collectively be referred to as diffusing species.

MODEL

We consider excess 1/f noise contribution in metal films that is caused by electron scattering from hopping and/or diffusing species. Hopping/diffusion of vacancies or impurities in metal films are generally thermally activated. The autocorrelation function C(t) of the current fluctuation associated with electron scattering is to be calculated. Electrons are scattered by static impurities, phonons and imperfections of the metallic film as well as from the hopping/diffusing species on which we focus our attention in this paper. In a unified model approach [3,4], I have shown in an earlier published work on 1/f noise that electron scattering from the static impurities, phonons and imperfections will give rise to resistance fluctuations that have the power spectral function with the frequency dependence of

$$S(f) \propto 1/f^{1-n} \qquad (2)$$

and its magnitude is weakly temperature dependent. The quantity n, called the infrared divergence exponent, is a positive number that is expected to be small compared with unity for metal films. The mechanism for the mobility fluctuations from electron scattering is from infrared divergent excitation and deexcitation of correlated states. The name "correlated states" was coined [5-7] to describe the states of any condensed matter that excitations and deexcitations between any two of them are of arbitrary low energy. It is worth emphasizing that for the correlated states, the infrared divergence condition holds down to arbitrary low frequencies for any ambient temperature. This follows from the properties of the correlated states.

The unified theory emerges from an inquiry into the nature and properties of excitations of low energy (say below 10^9 Hz) and the corresponding states that, through transitions between them, give rise to these excitations and deexcitations. For an excitation of low energy, the two states that define it must each involve for its description a very large number of coordinates (atomic, bonding, electronic or their composite). In fact the number of coordinates that must be included to describe the states must increase as the excitation energy decreases towards zero. This can be proved by reduction to absurdum. Let us assume on the contrary that the number of coordinates that describe the states do not increase as the excitation energy decreases towards zero. Then for the finite number of coordinates, there are only a finite number of admissible states and their excitation spectrum will have a lower cut-off in energy, contradicting the assumption that the excitation energy decreases towards zero. Returning to our discussion, the Hamiltonian relevant for the description of the states cannot be specified due to complex interactions and the increasing large number of coordinates. However, there is a way out of this apparently hopeless situation by adopting the statistical approach to quantum mechanics of Wigner, also known as random matrices, to our problem. Wigner's approach enables us to deduce some very general properties of the low energy excitations that hold for any material. Among these is one that the density of excitation N(E) with energy E is linear in E provided E is smaller than a characteristic energy E_c, i.e. $N(E) = \kappa E$ for $E<E_c$. The physics behind this is level repulsion. The proportionality constant κ and E_c are material dependent however. For crystalline solid state material both κ and E_c are expected to be small. This is also the case for liquids which are simple, such as water, non-glass-forming liquids or even non-polymeric glass-forming liquids such as B_2O_3 at temperatures far above the glass transition. Proceeding from crystalline to disordered, amorphous or glassy solid state materials the Wigner analogue states (referred to from now on as correlated states) as well as their low energy excitations increase in density, hence both κ and E_c increase. For the same reason for liquids on going from simple to more complex molecular ones including glass-forming polymeric liquids and supercooled non-polymeric liquids, both κ and E_c will increase.

In most if not all considerations of the low frequency responses, a primary species can be identified to be responsible for any particular response. There can be dipolar groups of atoms or molecules, chain segment, charged and uncharged particles. Response and fluctuations are triggered by transitions of the primary species. The primary species does interact with the correlated states however, and its sudden transition will switch on a new potential V which causes both excitations and deexcitations of correlated states. The matrix element of V_i for excitation or deexcitation of energy E connecting two correlated states are uncorrelated with and independent of E itself if E is low enough. This follows from the local extent of the primary species limiting its interaction with only a small fraction of the totality of large numbers of coordinates that define the two correlation states and determine their energy separation E. Recalling that $N(E) = \kappa E$, the independence of V_i on E then implies that $|V|^2 N(E) = nE$. Here n is a dimensionless constant and $|V|^2$ is the average of the matrix elements $|V_i|^2$ and independent of E. The last equation turns out to be the condition for infrared divergence and n is called the infrared divergence exponent. "Infrared" carries the meaning of low frequency and has nothing to do in our case with the infrared optical spectrum. Its usage in infrared divergence comes from the first known example of such phenomena in Cerenkov radiation or Bremstrahlung where there is an increasingly high probability of exciting low energy (infrared) photons emitted after a charged particle impacts on a target. In our case, the primary species transition will be trailed by an infrared divergent excitation and deexcitations of the correlated states. That is there is an increasingly high probability of exciting (or deexciting) decreasingly small energy correlated state excitations, and this causes a power law ω^{n-1} divergence at small ω of the response in the frequency domain and the algebraic t^{-n} time dependence of

the response function at large times with $0 \leq n < 1$. This is the fundamental result that comes out of an adaptation of Wigner's formulation of complex quantum systems and the infrared divergence principle.

TEMPERATURE DEPENDENCE OF EXCESS NOISE

For electron scattering from the species that is hopping/diffusing in the metallic film, the autocorrelation function $C(t)$ of the current fluctuation is now a convolution of $C_1(t)$, the autocorrelation function of the electron current fluctuation due to scattering of electrons from the species, with $C_2(t)$ the correlation function of the hopping/diffusive motion of the species. We have seen in the last paragraphs $C_1(t)$ will contribute a $S_1(f) \propto 1/f^{\alpha}$ resistance fluctuation noise with $\alpha = 1-n_1$, and n_1 is small compared with unity. $C_2(t)$ can be calculated also from the unified model of low frequency fluctuation, dissipation and relaxation properties of condensed matter [7]. Consider hopping motion of the species with a jump time $\tau = \tau_o \exp(E_A/kT)$. Again infrared divergent excitation and deexcitation of correlated states by the hopping species modifies the correlation function from the familiar form $C_2(t) = \exp(-t/\tau)$ to the form of

$$C_2(t) = \exp[-e^{-n_2\gamma}\, t^{1-n_2}/(1-n_2)\tau E_c^{n_2}] \qquad (3)$$

where n_2 with $0 \leq n_2 < 1$ is the infrared divergence exponent for the hopping motion of the species; γ is the Euler's constant and E_c is the upper cut-off energy for the correlated state excitations [7]. Note that for $n_2 = 0$, the expression for $C_2(t)$ that appears on the right hand side of eq (3) reduces to $\exp(-t/\tau)$. The correlation function $C_2(t)$ of eq (3) alone will give rise to a noise $S_2(f)$ which has a peak at a certain temperature T_{max}. This can be readily seen from the similar results on the spin-lattice relaxation time T_1 in nuclear magnetic resonance as discussed in Ref. (7). The noise power spectrum $S_2(f)$, except for a constant, has the same temperature and frequency dependence as the inverse of T_1. It has no frequency dependence for $T \geq T_{max}$ and a frequency dependence $1/f^{\beta}$ for $T < T_{max}$ (Fig. 1). Note that β increases monotonically from $\beta=0$ at $T=T_{max}$ to the value of $\beta=2-n_2$ at

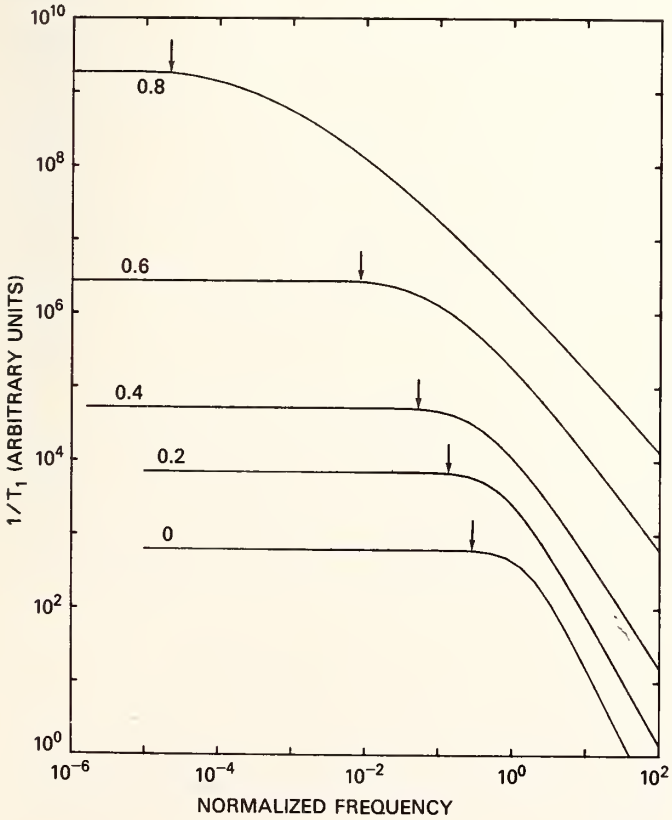

Fig. 1. Frequency dependence of $S_2(f)$ for several values of n_2 = 0, 0.2, 0.4, 0.6 and 0.8. The ordinate as labelled in the figure is $1/T_1$ which has the same functional dependence on f as $S_2(f)$.

$T<<T_{max}$. Here n_2 is expected for a significant fraction of unity. Since C(t) is a convolution of $C_1(t)$ and $C_2(t)$, the voltage or current noise spectrum S(f) is the product $S_1(f)$ $S_2(f)$. The result we find are then consistent with several striking features of the excess (1/f) noise observed by Eberhard and Horn [1]. These include: (1) the strong temperature dependence and the appearance of high-temperature peak in S(f) for a fix f due to $S_2(f)$; (2) the predicted $1/f^{\gamma}$ spectrum with $\gamma = \alpha+\beta$ which decreases continuously from a value larger than unity at $T<T_{max}$ to $\gamma=\alpha=1-n_1<1$ as T approaches T_{max} and beyond; and (3) the shape of the calculated peak structure is approximately the same as was observed by Eberhard and Horn [1] for some chosen value of n_2. Although we have discussed only the hopping motion, the results are similar for diffusive motion. Thus the contribution to resistance fluctuation from electron scattering by hopping/diffusing species when taken together with the weakly temperature dependent $1/f^{\alpha}$ noise caused by electron scattering from other static potentials and from phonons etc., can explain the data of Eberhard and Horn on metal thin films. Nevertheless the overall mechanisms involved in the noise observed in metal thin films can be much more complicated than the simple specific model proposed here. In spite of the limited success of the present model, this work should be viewed as a first step in incorporating a fundamental process of 1/f noise into a model that attributes the strong temperature dependence of the noise magnitude to fluctuating quantities that have characteristic times which are thermally activated.

REFERENCES

[1] J. W. Eberhard and P. M. Horn, Phys. Rev. B18, 6681 (1978).

[2] P. Dutta, P. Dimon and P. M. Horn, Phys. Rev. Lett. 43, 646 (1979).

[3] K. L. Ngai, Bull. Am. Phys. Soc. 24, 235 (1979); 284 (1979); K. L. Ngai and C.T. White, NRL Memo Report 3863 (1978).

[4] K. L. Ngai, NRL Memo Report 3917 (1978); Phys. Rev. B22, 2066 (1980).

[5] K. L. Ngai, A. K. Jonscher and C. T. White, Nature 277, 185 (1979); K. L. Ngai, Bull. Am. Phys. Soc. 24, 465 (1979).

[6] K. L. Ngai and C. T. White, Phys. Rev. B20, 2475 (1979).

[7] K. L. Ngai, Comments Solid State Phys. 9, 127 (1979); 9, 141 (1980).

THE ROLE OF MOBILITY IN 1/f NOISE

D. A. Bell

Professor Emeritus of Electronic Engineering
University of Hull
Hull HU6 7RX, U.K.

THE NUMBER OR MOBILITY QUESTION

The usual characteristic of 1/f noise, a mean-square voltage proportional to the square of steady current, suggests a fluctuation in conductance; and this has been confirmed by several tests, notably the correlation experiment of Jones and Francis [1]. Since conductance is proportional to the product of number and mobility of carriers, the next question to be asked was whether the 1/f noise represented a fluctuation in number or in mobility of the charge carriers. Early work favoured a fluctuation in number [2], but there has been accumulating evidence that it is the mobility which is involved. The elegant experiments of Kleinpenning [3] on 1/f fluctuations in thermo-e.m.f. seem to have established that 1/f noise is associated with fluctuations in mobility rather than in number of charge carriers.

Meanwhile Hooge had proposed [4], and demonstrated for a metal [5], the attractive hypothesis that 1/f noise can be described by the formula

$$\frac{\Delta R^2}{R} = \frac{\alpha}{N} \cdot \frac{\Delta f}{f} \qquad (1)$$

where N is the total number of charge carriers taking part in the conduction. Hooge originally suggested that α would be a universal constant, but this has since been found unsatisfactory, e.g. for the results of Hooge and Gaal on electrolytic conductors [6]. Equation (1) is not necessarily in conflict with the finding that fluctuations in conductance, the left-hand side of eq (1), are due to fluctuations in mobility. If each charge carrier or group of carriers makes an independent contribution to the total fluctuation, then usual statistical principles indicate that the mean-square relative fluctuation in the combined effect may be expected to be inversely proportional to the number of individual contributions, i.e. inversely proportional to N. On the other hand the spatial correlation of 1/f noise in semiconductors is found to be limited to a distance of less than 1 μm which is even less than the mean free path of electrons in some materials [7].

MOBILITY OR DIFFUSION ?

The electrons in a conductor have always a random (thermal) motion, but a directed drift velocity only when a field is applied; and usually the random motion involves much higher velocities, of the order of 10^5 m/sec, than the drift velocity. Now "mobility"[1] normally refers to drift velocity, by means of which it may most directly be measured. "Diffusion," on the other hand, normally implies a concentration gradient and rate of transport of particles down this gradient. Mobility and diffusion are difficult to distinguish because the coefficient or diffusion is proportional to the mobility according to the equation.

$$D = \mu_{abs} kT/e$$

[1] In semiconductors one often uses Hall mobility, which may be determined by comparing Hall coefficient with conductivity. Both terms in the comparison involve drift velocities.

Here μ_{abs} is the absolute mobility, with the applied field measured in absolute e.s.u. It is clearly a constant multiple of the "conventional" mobility expressed in $cm^2V^{-1}sec^{-1}$. But now suppose there is neither applied field nor concentration gradient: a particle will still move from an initial position, and given long enough time will move through any given distance, however large. Since it depends on the random motion of thermal agitation, this movement is akin to diffusion and in this paper will be regarded as diffusion, in spite of the absence of a concentration gradient. It is in this sense that it is queried whether 1/f noise is a diffusion rather than mobility phenomenon, since it is most probably related to the random motions of individual charge carriers. (This is entirely different from the diffusion theories of the 1950's, in which it was supposed that the conductance of a semiconductor was modulated by the diffusion through it of some "foreign" particle, probably in the neighbourhood of the terminal contacts.)

THE ZERO-CURRENT EVIDENCE

It has been questioned whether 1/f noise is caused or revealed by the passage of current. Hooge and Gaal [8] observed 1/f noise in a closed circuit at zero current, this being obtained by balancing a thermo-e.m.f. against an e.m.f. of opposite sign from an external source. There was then no obvious drift velocity and the 1/f noise appears to have been associated with the random motions of electrons, which can be regarded as diffusion. There is, however, a serious difficulty about this interpretation: when there is a current the addition of a small drift velocity to a large random velocity will make little difference to the mean-square velocity. The excitation of 1/f noise by a steady current is of a different order of magnitude than "hot electron" effects. Alternatively one can say that the observations of Hooge and Gaal were made at zero net current, but there were two equal currents of oppositely charged particles. In the end one cannot say definitely that 1/f noise has been observed in the absence of current. Min [9] deduced that in non-degenerate semiconductors the 1/f noise could not be due to scattering. Experimentally there is 1/f noise in highly conducting metals, which are certainly degenerate. No indication has been recorded of the state of degeneracy of semiconductors used for 1/f experiments; but most of them, of small or moderate degree of doping, are probably non-degenerate at room temperature. There does not seem to be any clear distinction between degenerate and non-degenerate conductors as generators of 1/f noise.

EXPERIMENTAL EVIDENCE ON MOBILITY

Taking a very broad sweep, from the measurements of Van de Voorde et al. [10] on indium antimonide through the Hooge average for silicon to the results of Hooge and Gaal for electrolytes, the data are consistent (within the variability of observations) with a simple hypothesis that α is inversely proportional to the 2/3 power of mobility, as shown in figure 1. The noise coefficients for metals are based on the work of Hoppenbrouwers and Hooge [11] but with the following reservations:

(i) Only the hemispherical samples of the "good" metals have been considered.

(ii) The numbers of conduction electrons per atom have been taken from Ehrenberg [12]. These are based on Hall coefficients, not valency.

(iii) Values of α have been estimated by drawing a line of appropriate slope and good fit through the experimental points and noting its displacement from the line for $\alpha = 2 \times 10^{-3}$. It may be a coincidence that a good fit to the 2/3 power law for α is only obtained for silver, the one of the three metals which is uniquely monovalent.

But the relationship breaks down when one examines a particular limited group, for example the metals in figure 1. Hooge's first publication of his hypothesis [4] included a diagram showing noise versus total number of carriers for various previously published experiments. This shows both n-InSb (his reference 3) and p-InSb (his reference 10) near the line established for n-Si, although the n-InSb had an electron mobility between 100 and 350 times as great as that in silicon and the hole mobility in InSb, which should be relevant to the p-InSb of Hooge's reference 10, is about half that of electrons in silicon. Some dispersion is to be expected on account of the powerful influence of the surface state, but one can only say that the data collected by Hooge in 1969 give no positive evidence in support of a hypothesis relating 1/f noise to mobility.

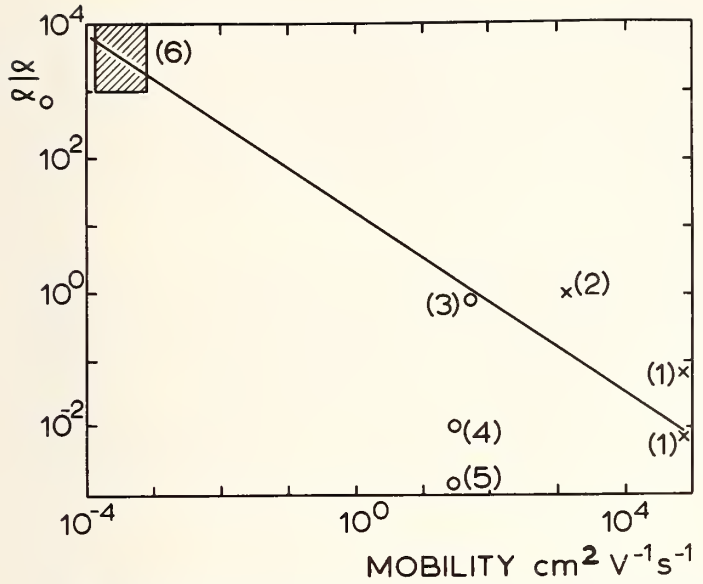

Fig. 1. Mobility and relative noise coefficients for various materials: (1) InSb; (2) n-Si; (3) Ag; (4) Au; (5) Cu; (6) hatched area, electrolytes.

$\alpha_o = 2\times10^{-3}$. The line is of slope $\alpha \propto \mu^{-2/3}$.

The hypothesis that α is inversely proportional to mobility appears to be clearly contradicted by the results of Hooge and Gaal on electrolytes [6], where they found α to be linearly proportional to the molar concentration. But the variation of mobility with concentration is small and far from linear. A further difficulty is that the mobility of protons (hydrogen ions) is some seven times greater than that of most other ions in water [13] and this would be expected to make the behaviour of HCl significantly different from that of salts: yet no significant difference appears in figure 6 of [6]. A complicating factor, however, is that the transport of protons through an aqueous solution is not by drift but by exchange between neighbouring water molecules, so it might not make the same contribution to 1/f noise. The results for electrolytes also cast doubt on the usual assumption that 1/f noise is the resultant of numerous current pulses corresponding to the movement of individual particles, because the contribution of each to the mean-square fluctuation would be proportional to the square of the charge which it carries. Thus $AgNO_3 \rightarrow Ag^+ + NO_3^-$ would make a relative contribution of $1^2 + 1^2 = 2$ while $Cu(NO_3)_2 \rightarrow Cu^{++} + 2(NO_3)$ would give $2^2 + 2\times1^2 = 6$. There is no indication of such a distinction by valency in [6]. This leads to the suggestion that 1/f noise may be a collective phenomenon, i.e. a modulation of mobility rather than a diffusion effect. Some clue to the distinction between mobility and diffusion might come from the effect of temperature, since eq (2) shows that for constant mobility the diffusion coefficient is proportional to temperature. But temperature also changes the number of charge carriers in a semiconductor, and may in fact have some effect on mobility.

LATTICE SCATTERING

It has been suggested [14] that 1/f noise is produced only by lattice scattering and that α in eq (1) ought to be given the value $(\mu/\mu_{latt})^2 \times 2.10^{-3}$ where the effective mobility μ is a combination of lattice mobility and the component μ_i due to impurity scattering according to the formula.

$$\frac{1}{\mu} = \frac{1}{\mu_{latt}} + \frac{1}{\mu_i} \qquad (3)$$

This was supported by measurements with ohmic metallic point contacts on specimens of germanium and gallium arsenside having low resistivities in the range 3×10^{-2} to 4.5×10^{-4} ohn-cm and later by measurements on films of bismuth having thicknesses between 0.08 and 8 times the electron free path [15]. The major difficulty with this hypothesis is that it predicts only a decrease in α below its standard value, whereas the data originally collected

by Hooge [4] had 11 examples of α substantially higher, against 6 substantially lower. The position of some metals in figure 1 causes difficulty since one would expect only lattice scattering and therefore α of standard value in bulk metals. Presumably electrolytes can be excluded from the argument by qualifying the hypothesis as applicable only to homogeneous solid or electronic conductors, other mechanisms being present elsewhere. (It would be interesting to know whether 1/f noise is generated in solid electrolytes, and if so, how it compares with that in aqueous electrolytes.)

CONCLUSION

It does appear that 1/f noise depends in a very general way on the number of charge carriers involved and on their mobility. But when one limits investigation to a particular type of conductor and assumes an inverse proportionality to the number of charge carriers, there is no clear relationship between noise and mobility. The attribution of 1/f noise solely to lattice scattering has so far been confirmed for a few specimens only: there is not sufficient evidence that 1/f noise in general can be so attributed. Whatever the role of mobility and of scattering there is still no general mechanism for the 1/f shape of spectrum and there still seems to be a need for different mechanisms in different types of conductor.

REFERENCES

[1] B. K. Jones and J. D. Francis, *J. Phys. D*, 8, 1172 (1975).

[2] J. J. Brophy and N. Rostoker, *Phys. Rev* 100, 745 (1955).

[3] T. G. M. Kleinpenning, *Physica* 7, 78 (1974).

[4] F. N. Hooge, *Phys. Lett. A.* 29, 139 (1969).

[5] F. N. Hooge and A. M. H. Hoppenbrouwers, *Physica* 45, 386 (1969).

[6] F. N. Hooge and J. L. M. Gaal, *Philips Res. Repts.* 26, 77 (1971).

[7] T. G. M. Kleinpenning, *J. Appl. Phys.* 48, 2946 (1977).

[8] F. N. Hooge and J. L. M. Gaal, *Philips Res. Repts.* 26, 77 (1971).

[9] H. S. Min, *Journ. Appl. Phys.* 50, 4461 (1979).

[10] P. Van de Voorde, C. K. Iddings, W. F. Love and D. Halford, *Phys. Rev. B* 19, 4121 (1979).

[11] A. M. H. Hoppenbrouwers and F. N. Hooge, *Philips Res. Repts.* 25, 69 (1970).

[12] W. Ehrenberg, *Electric Conduction in Semiconductors and Metals* (Clarendon Press, Oxford, 1958).

[13] J. O'M. Bockris and A. K. N. Reddy, *Modern Electrochemistry: Volume 1* (Plenum Press, New York, 1970).

[14] F. N. Hooge and L. K. J. Vandamme, *Phys. Lett.* 66A, 315 (1978).

[15] F. N. Hooge, J. Kedziah and L. K. J. Vandamme, *Journ. Appl. Phys.* 50, 8087 (1979).

A MODEL FOR 1/f MOBILITY FLUCTUATIONS IN ELEMENTAL SEMICONDUCTORS

R. P. Jindal and A. Van der Ziel*
Electrical Engineering Department
University of Minnesota
Minneapolis, Minnesota 55455

INTRODUCTION

$1/f$ noise in semiconductor devices has been explained using the number fluctuation model [1-3] as well as the mobility fluctuation formula [4,5]. The first experimental hint towards a connection between lattice scattering and mobility fluctuation was by Hooge and Vandamme [6]. Using the idea of phonon population fluctuations [7,8] we shall establish this connection in detail. Also, the effect of a finite electric field will be examined.

ESTABLISHMENT OF g-r SPECTRUM FOR PHONON POPULATION FLUCTUATIONS

Consider phonons with wave vector q. The number of such phonons $= n_q$. From statistical considerations, we have

$$\overline{n_q} = 1/[(\exp(\hbar\omega_q/KT) - 1]. \tag{1}$$

Also we have

$$\overline{\Delta n_q^2} = \overline{n_q}(1 + \overline{n_q}). \tag{2}$$

Both eqs (1) and (2) do not refer to any specific mechanism for this phonon population fluctuation. In general, there are a number of mechanisms which can give rise to phonon scattering and hence population fluctuations. From the experimental data [9,10], for germanium and silicon, it can be inferred that thermal conductivity, above 30K is dominated by isotope scattering for fairly pure samples. For samples with higher doping, phonon scattering from chemical impurities lowers the thermal conductivity further. However, whatever be the mechanism, the existence of time constant τ_q gives,

$$S_{\Delta n_q}(f) = \overline{\Delta n_q^2}\,\frac{4\tau_q}{1+\omega^2\tau_q^2} \tag{3}$$

ESTIMATION OF τ_q FOR ISOTOPE SCATTERING

From [9], we get

$$\tau_q = \frac{4\pi}{sq^4}\,\frac{M^2}{\overline{\Delta M^2}}\left(\frac{\rho}{m}\right) \tag{4}$$

m = atomic mass, $\overline{\Delta M^2} = \sum_j x_j(\Delta M_j)^2$

where x_j is the fraction of isotopes with mass M_j and ρ = density of crystal.

Substituting typical numbers for silicon, i.e., $\overline{\Delta M^2} = 0.209$, $M = 28$, $\rho = 2.33$ g/cm^3, $s = 8\times10^3$ m/sec, $m = 28$ atomic mass units we get

* Now with Bell Laboratories, Murray Hill, N. J. 07974.

$$\tau_q = (\lambda_{cm} \times 3.7 \times 10^4)^4 \quad \text{sec.} \tag{5}$$

Then for $\tau_q = 10^{-6}$ sec, $\lambda = 86$Å, and for $\tau_q = 10^6$ sec, $\lambda = 8.6\ \mu$m. Thus for a range of 12 decades, the corresponding phonon wave lengths are quite meaningful.

ABSOLUTE LIMITS FOR 1/f SPECTRUM

The limits of τ_q are the limits of the $1/f$ spectrum. An upper bound can be derived by taking $\lambda =$ lattice spacing.

$\therefore$ for $\lambda = 5$Å, $f_{max} = 1.4 \times 10^{10}$ Hz

Also, since the $q = 0$ mode always exists (if not for the sample then for the noise cage as a whole), it would seem that there is no lower limit for the $1/f$ spectrum. However, bounds more restrictive than those derived above, might exist, from other considerations.

PHONON MEAN-FREE PATH AND SAMPLE LENGTH

Note that even for $\tau_q = 10^{-6}$ sec, the phonon has a mean-free path of 0.8 cm. It therefore seems likely that for a sample whose dimensions are smaller than 0.8 cm, boundary scattering [11] should become important.

However, one should note that this is true only for "perfectly rough" surfaces. From [12,13], it is clear, that the roughness of the surface depends upon the phonon wave length. Thus for surface roughness $<<86$Å (corresponding to $\tau_q = 10^{-6}$ sec), we will have specular reflection which does not give rise to scattering. Hence the estimate of mean-free path ℓ_q and relaxation time τ_q are valid.

MEAN-FREE PATH FORMULATION FOR CARRIERS

In order to determine the momentum relaxation time, we shall evaluate the collision term in Boltzmann Transport Equation.

From time dependent perturbation theory, we get

$$\left(\frac{\partial f}{\partial t}\right)_{coll} = \frac{\epsilon_{ac}^2}{(2\pi)^2} \frac{1}{\rho} \int \frac{q^2}{\omega_q} \Big[(n_q+1) f(\underline{k}) \Big(1 - f(\underline{k}')\Big) - n_q f(\underline{k}') \Big(1 - f(\underline{k})\Big)\Big] \delta\Big(\epsilon(\underline{k}) - \epsilon(\underline{k}')\Big) d^3k' \tag{6}$$

To be able to extract momentum relaxation time under low electric field conditions, we have to assume

$$\frac{\overline{n_q} - n_q}{\overline{n_q} + 1} < 1$$

or for $\overline{n_q} >> 1$, we have

$$\Delta n_q < \overline{n_q} \tag{7}$$

Now

$$\overline{\Delta n_q^2}\Big|_{actual} = \overline{n_q}(1+\overline{n_q})$$

Therefore, let

$$\overline{\Delta n_q^2}\Big|_{allowed} = \overline{\Delta n_q^2}\Big|_{actual} \alpha_a^2$$

$$= \overline{n_q}(1 + \overline{n_q})\alpha_a^2, \quad 0 < \alpha_a < 1. \tag{8}$$

We shall refer to this as the small fluctuation approximation. Then under the small fluctuation approximation and assuming elastic collisions $[f_0(\underline{k}) = f_0(\underline{k}')]$, we get after some manipulation

$$\frac{1}{\ell} = \frac{1}{v\tau} = \frac{1}{4\pi} \int\int \frac{1}{\ell(\theta,\phi)} (1 - \cos\theta)\sin\theta \, d\theta \, d\phi \tag{9}$$

$\ell(\theta,\phi)$ = average distance travelled by carriers before they are scattered in (θ,ϕ) direction. In this case, it is independent of the electron energy.

FLUCTUATIONS IN CARRIER MEAN-FREE PATH

$$\frac{1}{\ell(\theta,\phi)} = \frac{m^2\epsilon_{ac}^2}{\pi\hbar^4 C_1} \hbar\omega_q n_q. \tag{10}$$

Using (3) and (8), we get

$$\therefore \quad S_\ell(\theta,\phi)(f) = \overline{\ell(\theta,\phi)}^2 \frac{4\tau_q}{1+\omega^2\tau_q^2} \alpha_a^2. \tag{11}$$

We shall now *average* this over electrons travelling along the z axis with different *speeds* (Fig. 1).

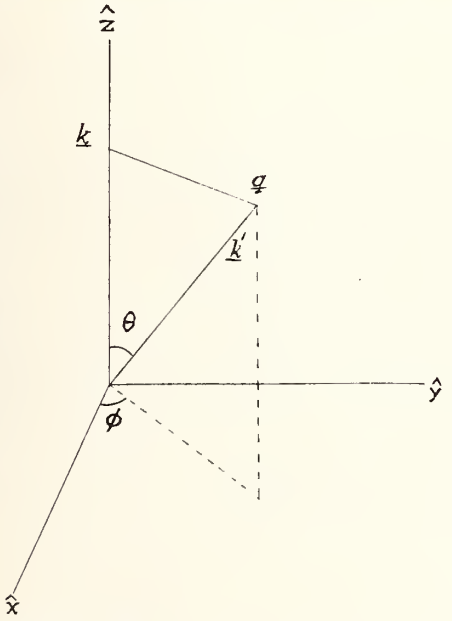

Fig. 1 Coordinate axes showing the direction of motion of the carrier along the vector $\underline{k}$ before scattering and along $\underline{k}'$ after scattering.

Now $\sin\frac{\theta}{2} = \frac{q}{2k}$.

Hence, as we vary k, keeping θ and $\hat{q}$ constant, we are in effect varying the magnitude q. However, q is related to τ. Thus averaging over energy is effectively an average over a time constant distribution. We shall presently show that,

$$g(\tau)d\tau = \frac{d\tau}{\tau} \frac{1}{ln(\tau_1/\tau_0)}. \tag{12}$$

Now

$$\overline{\ell(\theta,\phi)} = \frac{m^2\epsilon_{ac}^2\hbar\omega_q}{h^4\pi C_1} \overline{n_q} = \frac{m^2\epsilon_{ac}^2}{\hbar^4\pi C_1} KT. \tag{13}$$

This is independent of q. Therefore, averaging over energy and dropping the subscript q, we get from (11)

$$S_{\ell(\theta,\phi)}(f) = \frac{\overline{\ell(\theta,\phi)}^2}{ln(\tau_1/\tau_0)} \frac{\alpha_a^2}{f} \quad \text{for} \quad \frac{1}{\tau_0} \ll \omega \ll \frac{1}{\tau_1} \tag{14}$$

From (9) and (14) we get

$$\frac{S_\ell(f)}{\ell^2} = \frac{\alpha_a^2}{ln(\tau_1/\tau_0)} \frac{1}{f} . \tag{15}$$

Now $\mu = \left(\frac{e}{m^*}\right) \left\langle \frac{1}{\nu} \right\rangle \ell$

$$\therefore \quad \frac{S_\mu(f)}{\mu^2} = \frac{\alpha_a^2}{\ln(\tau_1/\tau_0)} \frac{1}{f} . \tag{17}$$

Since ℓ for different carriers fluctuate independently, we get for N carriers

$$\frac{S_\mu(f)}{\mu^2} = \frac{\alpha_a^2}{\ln(\tau_1/\tau_0)} \frac{1}{fN} = \frac{\alpha}{fN} \tag{18}$$

where

$$\alpha = \frac{\alpha_a^2}{\ln(\tau_1/\tau_0)} . \tag{19}$$

Note for $\frac{\tau_1}{\tau_0} = 10^{12}$ and $\alpha_a \simeq 0.2$ we get $\alpha = 1.4 \times 10^{-3}$ which is close to Hooge's parameter $\alpha_H = 2 \times 10^{-3}$. A detailed determination of α_a and its dependence on doping is still to be investigated.

DETERMINATION OF THE TIME CONSTANT DISTRIBUTION FUNCTION

The averaging over the magnitude of $\underline{q}$ is done for $\underline{q}$ pointing in a particular direction. Hence we are concerned with phonons with $\underline{q}$ pointing along a specific direction. Hence the phonon distribution can be treated to be one dimensional.

The number of states which are responsible for generating the modulation with time constant τ_q is proportional to the number of phonons with wave vector $\underline{q}$.

Number of phonons with wave vector $\underline{q}$

$$= \bar{n}_{\underline{q}} = \frac{KT}{\hbar\omega_q} \qquad (KT \gg \hbar\omega_q) \tag{20}$$

$$\therefore \quad g(\tau)d\tau \; \alpha \bar{n}_q d_q = \frac{KT}{\hbar s} \frac{dq}{q} . \tag{21}$$

Now, for point defect scattering in general, we have

$$\tau \propto \frac{1}{q^4} \tag{22}$$

This yields,

$$\frac{dq}{q} = -\frac{1}{4} \frac{d\tau}{\tau} .$$

Comparing with (21) and normalizing, we get

$$g(\tau)d\tau = \frac{1}{\ln(\tau_1/\tau_0)} \frac{d\tau}{\tau} . \tag{23}$$

as assumed in (12).

NOISE IN PRESENCE OF OTHER SCATTERING MECHANISMS

According to the model presented here, $1/f$ noise is generated by fluctuations in the population of acoustic phonons and hence in the zero electric field acoustic mobility μ_{aco}. In the presence of other noiseless scattering mechanisms, following Hooge and Vandamme [6], we get

$$\alpha = \alpha_{ac}\left(\frac{\mu}{\mu_{aco}}\right)^2 \tag{24}$$

ELECTRIC FIELD DEPENDENCE OF 1/f NOISE

Experimentally it has been shown [16] that

$$\alpha(E) = \alpha(0)/[1 + [E/E_C']^2]. \tag{25}$$

where $\mu_0 E_C' =$ speed of sound in the medium. This can be explained [17] in terms of the present model by considering the acoustic and optical mode scattering jointly and letting only μ_{aco} generate *1/f* noise. The field dependence for μ_{ac} that fits with the above analysis is given by

$$\mu_{ac} = \mu_{aco}[1 + (E/E_C')^2]. \tag{26}$$

REFERENCES

[1] A. van der Ziel, *Physica* **16,** 359 (1950).

[2] F. K. Du Pre', *Phys. Rev.* **78,** 615 (1950).

[3] A. L. McWhorter, M.I.T., Lincoln Laboratory Report, No. 80 (1955).

[4] F. N. Hooge, *Phys. Lett.* **29A,** 139 (1969).

[5] F. N. Hooge, *Physica* **60,** 130 (1972).

[6] F. N. Hooge and L. K. J. Vandamme, *Phys. Lett.*, **66A,**. 315 (1978).

[7] R. P. Jindal and A. van der Ziel, *Appl. Phys. Lett.* to be published.

[8] R. P. Jindal and A. van der Ziel, *Jour. Appl. Phys.*, to be published.

[9] R. Berman, E. L. Foster and J. M. Ziman, *Proc. Roy. Soc. A.* **237,** 344 (1956).

[10] J. A. Carruthers, T. H. Geballe, H. M. Rosenberg and J. M. Ziman, *Proc. Roy. Soc. A.* **238,** 501 (1956).

[11] H. B. G. Casimir, *Physica* **5,** 595 (1938).

[12] R. Berman, F. E. Simon and J. M. Ziman, *proc. Roy. Soc. A.*, **220,** 171 (1953).

[13] R. Berman, E. L. Foster and J. M. Ziman, *proc. Roy. Soc. A.* **231,** 130 (1955).

[14] See for example, J. Callaway, *Quantum Theory of Solid State,* part B, Chapter 7, Academic Press, New York and London (1974).

[15] See for example, K. Seager, *Semiconductor Physics,* Chapter 6, Springer-Verlag, New York (1973).

[16] G. Bosman, R. J. J. Zijlstra and A. van Rheenen, *Phys. lett.* **78A,** 385 (1980).

[17] R. P. Jindal and A. van der Ziel, in process with S.S.E.

COMMON MECHANISM OF 1/f NOISE AND BURST NOISE

A.M.Zaklikiewicz

Instytut Technologii Elektronowej CEMI, 02-668 Warszawa, Poland

1. INTRODUCTION

It is a known fact that 1/f noise generation is related to the grain boundaries in resistive materials and is dependent on the defects level in semiconductor materials and devices. One assumes that the local potential barriers on the metal precipitations are responsible for burst noise generation in semiconductor devices [1].

The author assumes that there exists a common source of 1/f noise and burst noise. This source is related to the potential barriers on a different defects and discontinuities in resistive and semiconductor materials.

It is obvious that if there exists a discharging mechanism of the local potential barriers, which explains burst noise generation, then with it a charging process should be associated. A charging relaxation processes of the local potential barriers can result in 1/f noise spectrum [3] in the limited low frequency range.

2. PHYSICAL MODEL

We assume that there exists a kind of random distribution of the local potential barriers in the considered element. The proposed equivalent circuit of such a single barrier is shown in Fig.1, where C is the capacity of the barrier, R_c - charging resistance, R_d - discharging resistance, ηR - resistance of that part of the element which is parallel to the barrier.

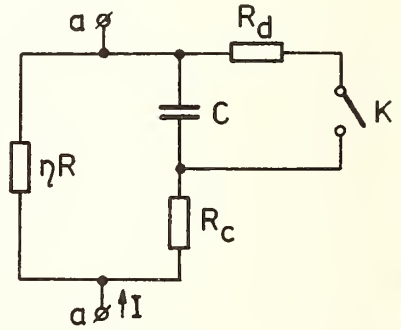

Fig.1. The equivalent circuit of the single potential barrier

We can surmise that key K is the generation-recombination center associated with the local potential barrier as it is done for the case of the

proposed burst noise mechanism [1] . Such a potential barrier is charged with the time constant CR_c when the external electrical field is applied.

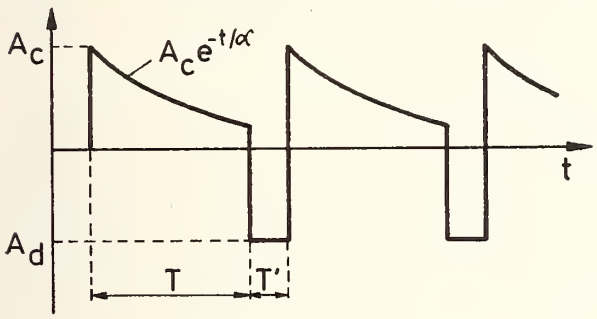

Fig.2. The processes at the external connections of the single potential barrier

The discharging process takes place in the C, R_d, K circuit when the switch K is closed. Some amount of discharging current flows in the C, ηR, R_c circuit and can give rectangular pulses at the external connections of the considered element. After the discharging current pulse is finished, the circuit is charged again - the cycle is repeated. As a result of this mechanism we receive a series of periodical rectangular and exponential pulses for any single barrier, as it is shown in Fig.2.

Similar model has been proposed previously [2] to explain 1/f noise phenomenon but discharging processes were disregarded at that time.

3. NOISE SPECTRUM

If we consider only charging process for the single potential barrier then the power spectrum is [2] :

$$|A(\omega)| = \frac{A_c^2}{\omega T} \qquad (1)$$

where angular frequency

$$\omega = 2\pi f = \frac{2\pi k}{T}, \quad k = 1, 2, 3, \ldots$$

A single relaxation process is periodical and cannot be named noise.

For random distribution of such relaxation processes coming from many local potential barriers located in the considered element we can apply the relation given by M.Agu [3]. For the limited low frequency range noise power spectrum is

$$|\overline{A(\omega)}| = \frac{\pi}{2} P(0) |\overline{A_c}|^2 \frac{1}{\omega} \qquad (2)$$

where: A_c - the initial value of each individual relaxation process,

P(0)- the density function of the random process P(C) for random variable $C \to 0$.

For a common case of the multilevel burst noise we have got the equation describing noise power spectrum [4],[5] :

$$|\overline{A(\omega)}| = \frac{4 \overline{U_{BNO}^2} \lambda}{\lambda^2 + \omega^2} \qquad (3)$$

where: $\overline{U_{BNO}^2}$ - the square mean value of bursts amplitude,

λ - the mean number of level changes in the unit of time

The relation given here [3] is valid also for two-level and three-level burst noise, which are particular cases of burst noise, most frequently observed in practice.

Burst noise can give some deviations in typical 1/f noise spectrum [4],[5] . It is impossible, however, to calculate the common spectrum for 1/f noise and burst noise without the knowledge of the elements of equivalent circuit shown in Fig.1.

4. DISCUSSION

The common mechanism of 1/f noise and burst noise, presented here, makes it possible to explain the fundamental difference between these kinds of noise, namely universal character of 1/f noise and limited presence of burst noise. Considering equivalent circuit of the 1/f noise and burst noise source /Fig.1/, we can notice that the exponential processes of the barrier charging are always present at the a-a connections and thus at the external connections of the considered element. To the contrary discharging processes take place mainly in the C, R_d, K circuit and they can be observed at the external connections over background noise level only for sufficient value of the $R_d / (\eta R + R_c)$ ratio.

In the conclusion we may state that burst noise should be recognized as the associated, side effect of 1/f noise.

REFERENCES

[1] S.T.Hsu, R.J.Whittier, C.A.Mead, Solid-State Electronics 13, 1055-1071, 1970.

[2] A.M.Zaklikiewicz in Proc. Colloque international sur le bruit de fond des composants active semiconducteurs, Toulouse, 1971, pp.27-29.

[3] M.Agu, Journal of the Physical Society of Japan 40, 1510-1511, 1976.

[4] A.M.Zaklikiewicz, Doctorate Thesis, Warszawa, 1978 /in Polish/.

[5] A.M.Zaklikiewicz, Solid-State Electronics 24, 1-3, 1981.

1/f VOLTAGE NOISE CAUSED BY SCATTERING OF ELECTRONS IN METALS

Leendert M. Bliek

Physikalisch-Technische Bundesanstalt
D 3300 Braunschweig, Fed. Rep. Germany

INTRODUCTION

The spectral intensity $S_U(f)$ of the voltage noise in current carrying electric conductors is often found to depend on the frequency f as 1/f. Experimentally, Hooge´s empirical relation

$$\frac{S_U(f)}{U^2} = \frac{\alpha}{N} f^{-1} \qquad (1)$$

where U is the average potential difference, N is the number of electrons or holes involved, and the constant α is normally close to $2.\ 10^{-3}$, holds in most cases, but it is found difficult to give a conclusive explanation for the effect [1].

In the following, thermo e.m.f.´s, due to temperature fluctuations, caused by scattering of the electrons, are considered as a possible mechanism for generating 1/f noise. For electrically conducting rectangular bars, thermally isolated from their surroundings, the noise power spectrum can be calculated analytically and is found to agree closely with eq (1) over a wide frequency range.

POWER SPECTRUM OF TEMPERATURE FLUCTUATIONS WHICH ARE DUE TO ELECTRON SCATTERING

As is well known from resistance theory, only electrons with energies, within a few kT from the Fermi energy ζ, take part in scattering processes. Let their number be N´ and let $kT \ll \zeta$, as in normal metals near room temperature. Before being scattered, the electrons are accelerated by the electric field and obtain an extra kinetic energy W and an extra momentum $\vec{p}$ in addition to the Fermi momentum $\vec{p}_\zeta$:

$$(\zeta + W) = \frac{1}{2m} (\vec{p}_\zeta + \vec{p}) \qquad (2)$$

By the scattering process, this energy W is transferred to the lattice as Joule heat and consequently one finds for the average value of W

$$\overline{W} = \frac{e^2 E^2 \tau_s^2 N}{m N'} \qquad (3)$$

Here e is the elementary charge, E is the applied electric field, m is the effective electron mass, τ_s is the mean free time between two scattering processes, and N is the total number of conduction electrons. Since the electrons move in all directions, $\sum_{N'} \vec{p}_\zeta \cdot \vec{p}$ is zero, apart from fluctuations, and hence

$$\overline{|p|} = e E \tau_s (2 N / N')^{1/2} \qquad (4)$$

Therefore, the amount of energy transferred in each scattering process fluctuates around the average value $\bar{W}$, given by eq (3), with an average amplitude

$$\Delta W = p_\zeta \cdot \frac{e\,E\,\tau_s}{m} \cdot (2\,N / N')^{1/2} \tag{5}$$

As a result, local temperature fluctuations around the average temperature T_o arise. The temperature equalization process being governed by the equation

$$\frac{\partial T}{\partial t} = a\,\nabla^2\,T \tag{6}$$

where a is the thermal diffusivity, these fluctuations will have the form

$$T - T_o = T_s \frac{V}{2\sqrt{a\,(t-t_o)^3}}\; e^{\frac{-(\vec{r}-\vec{r}_o)^2}{4a(t-t_o)}} \tag{7}$$

with an average value of $\Delta W/C$ for the amplitude T_s. Here, C and V are the heat capacity and the volume, respectively, of the conductor. The individual scattering process considered, is supposed to have taken place at $(\vec{r}_o, t_o)$. On the average, N'/τ_s such fluctuations will arise per second in the conductor; half of them negative and half of them positive.

A suitable method, to calculate the resulting power spectrum for thermally isolated conductors in the form of rectangular bars, has been published previously [2]. For the present purpose, one needs to know the power spectrum $S_{\Delta T}(f)$ of fluctuations in the temperature difference ΔT between two points of the sample which are a distance $\vec{l}$ apart, rather than the power spectrum for the temperature at a given point. Using eq (7) to calculate ΔT, $S_{\Delta T}(f)$ can be obtained in the same manner, described in reference [2], as $S_T(f)$. One finds:

$$S_{\Delta T}(f) = \frac{2\,N'\,\bar{T}_s^2}{\tau_s} \sum_{n_x=-\frac{L_x}{d}}^{\frac{L_x}{d}} \sum_{n_y=-\frac{L_y}{d}}^{\frac{L_y}{d}} \sum_{n_z=-\frac{L_z}{d}}^{\frac{L_z}{d}} \frac{1 - \cos 2\pi \left(\frac{n_x l_x}{L_x} + \frac{n_y l_y}{L_y} + \frac{n_z l_z}{L_z}\right)}{16\,\pi^2 a^2 \left(\frac{n_x^2}{L_x^2} + \frac{n_y^2}{L_y^2} + \frac{n_z^2}{L_z^2}\right)^2 + 4\pi^2 f^2} \tag{8}$$

where d is the lattice constant and $L_x \geq L_y \geq L_z$ are the dimensions of the conductor. Unlike $S_T(f)$, from which it differs by the additional cosine term, $S_{\Delta T}(f)$ remains finite for f=0, even, if the fluctuations are completely uncorrelated. As for $S_T(f)$, a correlation time τ of the kind discussed in [2], would introduce an additional factor $4\pi^2 f^2 \tau^2/(1+4\pi^2 f^2 \tau^2)$ on the left-hand side of eq (8).

Temperature fluctuations, of course, affect the distribution of the electrons. Energy equilibrium requires that a temperature difference ΔT should be accompanied by a difference in electrostatic potential U, such that

$$C_e \cdot \Delta T / N = e\,U \tag{9}$$

where C_e is the heat capacity of the N electrons (see, e. g., reference [3], p. 732 and p. 148). Hence,

$$S_U(f) = (C_e / e N)^2 S_{\Delta T}(f) \tag{10}$$

For the special case, where the electric field points in the $\vec{x}$ direction and $\vec{l}=(\frac{L_x}{2}, 0,0)$ one finds , upon inserting $U= L_x E / 2$ and $\overline{T_s} = \Delta W/C$:

$$\frac{S_U(f)}{U^2} = \frac{64\, C_e^2\, \tau_s}{N\, C^2\, L_x^2\, m} \sum_{n_x=-\frac{L_x}{2d}}^{n_x=\frac{L_x}{2d}} \sum_{n_y=-\frac{L_y}{d}}^{n_y=\frac{L_y}{d}} \sum_{n_z=-\frac{L_z}{d}}^{n_z=\frac{L_z}{d}} \frac{1}{16\pi^2 a^2 \left[\frac{(2n_x+1)^2}{L_x^2} + \frac{n_y^2}{L_y^2} + \frac{n_z^2}{L_z^2} \right]^2 + 4\pi^2 f^2} \tag{11}$$

If $2\pi a/L_x^2,\ 2\pi a/L_y^2 << f << 2\pi a/L_z^2,\ 2\pi a/d^2$, the sums over n_x and n_y can be replaced by integrals, and out of the sum over n_z only the term with $n_z=0$ has to be retained. This leads to a 1/f spectrum as given by eq (1), with

$$\alpha = \frac{2\, L_y\, \tau_s\, \zeta\, C_e^2}{\pi\, L_x\, m\, a\, C^2} \tag{12}$$

Depending on the dimensions of the conducting bar, eq (11) predicts up to four further regions with simple frequency dependencies of the form

$$S_U(f)/U^2 = \alpha_m\, f^m / N \tag{13}$$

If $f >> 2\pi a/d^2$, one finds $m = -2$ and $\alpha_{-2} = \alpha .16 a L_z/(\pi d^3)$.
If $2\pi a/L_x^2,\ 2\pi a/L_y^2,\ 2\pi a/L_z^2 << f << 2\pi a/d^2$, one finds $m = -1/2$ and $\alpha_{-1/2} = \alpha .2L_z/(\pi a)^{1/2}$.
If $2\pi a/L_x^2 << f << 2\pi a/L_y^2,\ 2\pi a/L_z^2$, one finds $m = -3/2$ and $\alpha_{-3/2} = \alpha .(2/L_y).(a/\pi)^{1/2}$.
If $f << 2\pi a/L_x^2,\ 2\pi a/L_y^2,\ 2\pi a/L_z^2$, one finds $m = 0$ and $\alpha_0 = \alpha .2L_x^3/(\pi^3 L_y\, a)$.

α FOR ROOM-TEMPERATURE METALS

For metals at room temperature, the thermal and electric conductivities are related by the Wiedemann-Franz law (see, e.g., [3], p.761) which leads to

$$a = 2\, \zeta\, \tau_s\, C_e / (3\, m\, C) \tag{14}$$

Inserting eq (14), $C = 3N_a k$, where N_a is the number of atoms in the conductor,

$$C_e = N\pi^2\, k^2\, T / (2\, \zeta) \tag{15}$$

(v., e.g., reference [3], p.148) and $\zeta = (\hbar^2/2m).(3\pi^2 N/V)^{2/3}$ into eq (12) leads to

$$\alpha = \frac{L_y\, d^2\, m\, k\, T}{L_x\, \pi\, \hbar^2} \cdot \left(\frac{\pi^2 N}{9 N_a}\right)^{1/3} \qquad (16)$$

As an example, figure 1 shows the calculated noise power spectrum for three gold samples with different dimensions. For this material, complete agreement in the 1/f region with Hooge´s empirical relation, i. e., a value of 0.002 for α, is obtained at 0 °C for $L_x/L_y = 7$. To facilitate comparison with the results presented in [2], an arbitrarily choosen correlation time of 100 s was assumed. Without it, the spectrum would have remained flat at low frequencies.

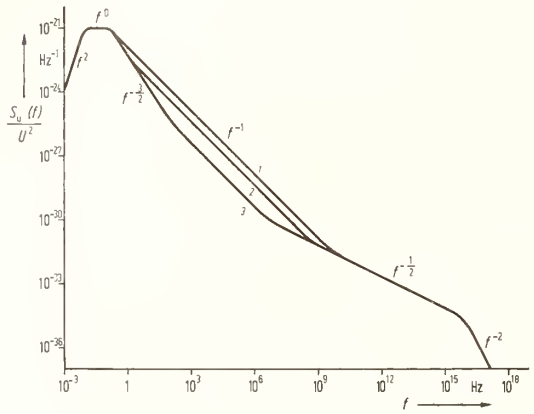

Fig. 1 Calculated noise power spectrum according to eq (11) and eq (16) for three gold samples, with different dimensions, at 0 °C.

curve 1: L_x = 15 cm, L_y = 6.325 cm and L_z = 0.316 µm

curve 2: L_x = 15 cm, L_y = 2 cm and L_z = 1 µm

curve 3: L_x = 15 cm, L_y = 2 mm and L_z = 10 µm

DISCUSSION

The calculations, presented above, show that scattering of the conduction electrons which is responsible for the electric resistance, can also generate 1/f noise. For thermally isolated metal bars, this 1/f noise has the experimentally observed magnitude. Further calculations, treating other boundary conditions, such as those, corresponding to thin metal or semiconductor layers on thermally conducting substrates, would be desirable.

The author is endebted to Prof. Dr. V. Kose (PTB, Braunschweig) for drawing his attention to the interesting phenomenon of 1/f noise and to him, to Prof. F. N. Hooge and his group (T U Eindhoven), to Prof. P. H. Handel (U. St. Louis) and to many of his colleagues at PTB for helpful discussions on the subject.

REFERENCES

[1] F. N. Hooge, *Physica 84B*, 14 (1976)

[2] L. Bliek, in *Proc. 2nd Int. Symposium on 1/f Noise*, Orlando and Gainesville, Fla. (USA) (1980). Ed. E. R. Chenette, Univ. of Florida, Gainesville, Fla. (USA), 1980, p.343.

[3] W. Jones and N. M. March, *Theoretical Solid State Physics* (John Wiley & Sons Ltd., London, New York, Sidney, Toronto, 1973)

COMPLEMENTS OF 1/f NOISE THEORY

Bruno Pellegrini

Istituto di Elettronica e Telecomunicazioni
Università di Pisa, Via Diotisalvi 2, 56100 Pisa, Italy

A new and general model of the flicker noise has been proposed in a recent paper [1]. The physical origin and mechanism of the phenomenon have been found in islands and microdefects, of any nature and size, of the conducting medium which are enclosed by an energy barrier or which contain an energy well for the carriers. The essential characteristic of these is that the relaxation time of their electric charge is an exponential function of a random variable energy and that, accordingly, it has a huge dispersion able to account for the flicker noise spectrum on many frequency decades and down to any, however low, frequency.

Some developments and new results of the theory are now presented. They are carried out by taking into account, other than the electric potential fluctuations, the ones of the quasi Fermi level both inside and outside the islands.

ISLAND OUTSIDE

- Conductance -

Let

$$n=N_C \exp\left[-(E_C-E_F)/kT\right] \quad , \tag{1}$$

$$\underline{J}=q(\mu n \underline{\mathcal{E}}+D\underline{\nabla}n) \quad , \tag{2}$$

be the electron concentration and the current density, respectively, in the conducting medium outside the island. The symbols have the usual meaning: N_C is the effective density of the states of the conduction band and E_C is its edge, E_F is the quasi Fermi level, k is the Boltzmann constant, T is the absolute temperature, q is the electron charge, μ is electron mobility, $D=kT\mu/q$ is the diffusion constant and

$$\underline{\mathcal{E}}=\underline{\nabla}E_C/q \quad , \tag{3}$$

is the electric field.

The fluctuations $\Delta E_C=-q\Delta v$ and $\Delta E_F=-q\Delta u$ of E_C and E_F, originated by whichever cause, produce, according to (1)-(3), the fluctuations

$$\Delta n=(q\bar{n}/kT)(\Delta v-\Delta u) \quad , \tag{4}$$

$$\Delta\underline{J}=(\underline{J}_o/\bar{n})\Delta n-\sigma\underline{\nabla}\Delta u \quad , \tag{5}$$

of n and $\underline{J}$, respectively. The symbols $\bar{y}$ ($\underline{Y}_o$) and Δy ($\Delta\underline{Y}$) represent the time average and the fluctuations, respectively, of the quantity y (vector Y) and $\sigma=q\mu\bar{n}$ is the conductivity; $\bar{n}$ is assumed to be constant in the island neighborhood.

On the other hand, for frequencies smaller than the reciprocal of the dielectric relaxation time τ_D, the current divergency is null, i.e. $\underline{\nabla}\cdot\underline{J}_o=0$ and $\underline{\nabla}\cdot\Delta\underline{J}=0$, so that, for $\underline{J}_o$ values which make $|\underline{J}_o\cdot\underline{\nabla}\Delta n/n| \ll |\sigma\underline{\nabla}^2 u|$, from (5) it follows that

$$\nabla^2\Delta u = 0 \quad . \tag{6}$$

For spherical islands of radius r_I, to which one refers for simplicity, and for $\Delta u=\Delta u_E$=constant on the island surface $A_I=4\pi r_I^2$, from (6) one has that

$$\Delta u=(r_I/r)\,\Delta u_E \quad , \tag{7}$$

where r is the distance from the island center.

According to $\underline{\nabla}\cdot\Delta\underline{J}=0$, the current $\Delta i=-\int_{A'_I} d\underline{A}\cdot\Delta\underline{J}$, entering any surface A'_I enclosing the island is independent of A'_I itself so that by chosing surfaces A''_I on which $\Delta n/\bar{n}$ is constant from (5), (7) and $\underline{\nabla}\cdot\underline{J}_o=0$ one obtains

$$\Delta i=-G_E\,\Delta u_E \quad , \qquad (8)$$

where $G_E=\sigma A_I/r_I$ is the conductance of the medium surrounding the island.

- *Capacitances* -

The Poisson equation for the fluctuations

$$\underline{\nabla}\cdot\Delta\underline{\mathscr{E}}=-(q/\varepsilon)\,\Delta n \quad , \qquad (9)$$

where ε is the dielectric constant, and the eqs (3), (4) and (6) give

$$\nabla^2(\Delta v-\Delta u)=(\Delta v-\Delta u)/\lambda \quad , \qquad (10)$$

where $\lambda=(\varepsilon kT/q^2\bar{n})^{1/2}$ is the Debye length.

For the boundary condition $(\Delta v-\Delta u)=(\Delta v_E-\Delta u_E)$=constant on the island surface, the solution of (10) becomes

$$(\Delta v-\Delta u)=(r_I/r)\exp\left[-(r-r_I)/\lambda\right](\Delta v_E-\Delta u_E) \quad . \qquad (11)$$

Then, according to (7), (11) and the Gauss theorem, the fluctuation ΔQ of the island charge becomes

$$\Delta Q=C_E\,\Delta v_E-C_F\,\Delta u_E \quad , \qquad (12)$$

where the capacitances are given by $C_F=\varepsilon A_I/\lambda$ and by

$$C_E=\varepsilon A_I(1/r_I+1/\lambda) \quad . \qquad (13)$$

- *Current Dipole Vector* -

The charge fluctuation ΔQ induce a current dipole vector $\Delta\underline{\dot{P}}=\int\Delta\underline{J}d^3x$ [1] which, according to (5), (7)-(9) and (11)-(13) and on the assumption that $\underline{J}_o/\bar{n}$ be constant in a zone a few λ large surrounding the island, becomes

$$\Delta\underline{\dot{P}}=(\underline{J}_o/q\bar{n})(\Delta Q-\tau_D\,\Delta i) \quad , \qquad (14)$$

where $\tau_D=\varepsilon/\sigma$ is the dielectric relaxation time.

Since in the following part it will be shown that $\Delta i=-\Delta Q/\tau$, where the island relaxation time τ is much greater than τ_D, from (14) one obtains the relationship

$$\Delta\underline{\dot{P}}=(\underline{J}_o/q\bar{n})\,\Delta Q \quad , \qquad (15)$$

which differs from the one obtained in the preceding analysis [1] for the fact that it holds for any current type $\underline{J}_o$.

ISLAND INSIDE

- *Islands Surrounded by an Energy Barrier* -

When the island sizes are much greater than the wavelength of the states localized in it, the current density which crosses the energy barrier surrounding the island itself becomes proportional to $[\exp(-\varphi_2/kT)-\exp(-\varphi_1/kT)]$ where φ_1 and φ_2 are the energy barrier heights evaluated from the Fermi levels inside and outside the island, respectively [1]. Therefore, since $(\varphi_2-\varphi_1)=-q(\Delta u_E-\Delta u_I)$ where $-q\,\Delta u_I$ is the Fermi level fluctuation inside the island, the fluctuation Δi_I of the current entering the island becomes

$$\Delta i_I=G(\Delta u_E-\Delta u_I) \quad , \qquad (16)$$

where the island conductance G is given by the eqs (6) and (13) of the Ref. [1].

The variation Δu_I and the one Δv_I of the mean electric potential inside the island produce a variation ΔQ of its charge $Q=-q\,\Omega_I n$ given by

$$\Delta Q=C_I(\Delta u_I-\Delta v_I) \quad , \qquad (17)$$

where, according to (1), the internal capacitance C_I is

$$C_I=q^2\bar{n}\,\Omega_I/kT \quad , \qquad (18)$$

Ω_I being the island volume.

On the other hand the electric field fluctuation $\Delta\mathscr{E}=(\Delta v_I-\Delta v_E)/w$ across the barrier, of width w, according to the Gauss theorem leads to

$$\Delta Q=C_W(\Delta v_I-\Delta v_E) \quad , \qquad (19)$$

where the barrier capacitance C_W, for $w\ll r_I$, is given by

$$C_W=\varepsilon\int_{A_I}(1/w)\,dA \quad . \qquad (20)$$

- *Islands Containing an Energy Well* -

When the sizes of the islands are comparable with the wavelength of the states loca-

lised in it, the current i_I entering the island itself may be computed by means of the theory of the generation-recombination processes. By taking into account the effects of the fluctuations of Fermi level and of the electric potential inside and outside the island on the flow of the electron emitted and captured by the island, since now it is $w=0$ and $\Delta v_E = \Delta v_I$, one obtains again eq (16) where the conductance G is given yet by eqs (14) and (16) of the preceding analysis [1], i.e.

$$G=(q^2/kT) \sum_j \bar{n} v_m \sigma_j N_j (1-\bar{f}_j) \quad , \qquad (21)$$

where v_m is the electron thermal velocity, σ_j and N_j are the capture cross section and the number of the states of energy E_j, respectively, and

$$\bar{f}_j = \left\{1+\exp\left[(\bar{E}_j-\bar{E}_I)/kT\right]\right\}^{-1} \quad , \qquad (22)$$

is their mean occupation factor, E_I being the Fermi level inside the island.

Also (17) and (19) continue to hold, where, however, now it is

$$C_I=(q^2/kT) \sum_j N_j \bar{f}_j (1-\bar{f}_j) \quad , \qquad (23)$$

and

$$C_W=\infty \quad . \qquad (24)$$

RELAXATION TIME AND NOISE

- *Relaxation time* -

From the current continuity $\Delta i = \Delta i_I$ on the island surface and from (8), (12), (16), (17) and (19) one obtains

$$\Delta i=-(C_I^{-1}+C_W^{-1}+C_E^{-1})(1+\tau_D G C_E^{-1})^{-1} G \Delta Q \quad , \qquad (25)$$

so that the island charge conservation leads to the stochastic equation $(d\Delta Q/dt)=-\Delta Q/\tau+\eta$ where η is the stochastic component of the current crossing the island surface and τ is the relaxation time which, according to (25) where normally it is $\tau_D \ll G^{-1} C_E \simeq \tau$, is given again by

$$\tau = C/G \quad , \qquad (26)$$

in which now, however, the island capacitance

$$C=(C_I^{-1}+C_W^{-1}+C_E^{-1})^{-1} \quad , \qquad (27)$$

is the series of the three capacitance C_I, C_W and C_E. τ, instead, according to (13) and (25) remains independent of the conductance $G_E=\sigma A_I/r_I$ of medium surrounding the island because $\tau_D \ll G^{-1} C_E \simeq \tau$.

- *Noise* -

The more general and detailed analysis, which takes into account the effects on the currents and the charges of the fluctuations of the electric potential and of the Fermi level, both inside and outside the island, leads to the new expression (27) of the island capacitance C which intervenes in the relaxation time and in the noise equations obtained in the preceding model [1]. In fact now C is the series of C_I, C_W and C_E, whereas in the previous case it was $C=C_W$ or $C=C_E$.

However, if one excludes the case of islands which contain energy wells and have sizes so small as to make

$$C_I \ll C_E \quad , \qquad (28)$$

one obtains again the results of the preceding approach [1] because C and G remain largely independent each other and G is the quantity which depends exponentially on a random variable energy Φ.

In particular, by taking into account also the more general expression (15) of the current dipole vector, the coefficient β of the noise spectrum $S_V=\beta \bar{V}^2/Nf^{\gamma}$ of a homogeneous device, according to (14) of the Ref. [1], may be written in the more simple form

$$\beta=(kT/q)^2 f^{*\delta} \bar{n}^{-1} \int CD(\Phi_F^*, C)\, dC \quad , \qquad (29)$$

where $\bar{V}$ is the average voltage across the device, N is the its carrier number, δ is a proper exponent (see (6.6) of the Ref. [1]), $\gamma=1+\delta$, f^* is a given reference value of the frequency f, $\Phi_F^*=-kT\ln(\tau_o f^*)$, D is the island density in the space $(\underline{r}, C, \Phi)$.

Instead when (28) is verified, according to (21), (23), (24) and (27), one has that G tightly depends on C through $\bar{f}_j$ so that, from also (1), (22) and (26), for $(\bar{E}_{jmax}-\bar{E}_{jmin}) \lesssim kT$ one gets

$$\tau=\frac{\bar{f}_j}{v_m \sigma_m \bar{n}}=\tau_o\left[\exp\left(\frac{\bar{E}_F-\bar{E}_C}{kT}\right)+\exp\left(\frac{E_m-\bar{E}_C}{kT}\right)\right]^{-1}, \qquad (30)$$

where $\tau_o=1/N_C v_m \sigma_m$, E_m and σ_m are mean values

of $\bar{E}_j$ and σ_j, respectively. According to (30), τ is an exponential function either of $(\bar{E}_C-\bar{E}_F)$ or of the random variable $(\bar{E}_C-E_m)$, according to $(\bar{E}_C-E_m) \gtrless (\bar{E}_C-\bar{E}_F)$. Therefore in both case τ may have a great dispersion only in the device depletion-regions, both on the surface and in the bulk, because only in them $(\bar{E}_C-\bar{E}_F)$ may reach great values.

However, since the island contribute

$$S_{VI}=|\underline{J}_o \cdot \underline{\nabla} z|^2 (4kTG)/(q\bar{n})^2 (\tau^{-2}+\omega^2) \quad , \quad (31)$$

to the noise spectrum [1], owing to the (21) and (30) and to the dependence on $\bar{n}$ of $\underline{J}_o$, τ and $\underline{\nabla} Z$, has not the form $S_{VI} \propto \tau/(1+\tau^2\omega^2)$, such an exponential dependence of τ on a random variable energy now leads to a total noise spectrum $S_V=\Gamma/f^\gamma$ with an exponent γ which may be rather different from 1 and may change appreciably with the frequency even on narrow bands.

- *Island Size* -

When $(\bar{E}_{j_{max}}-\bar{E}_{j_{min}}) \lesssim kT$ and the state number $\sum_j N_j \simeq \Omega_I/\Omega_s$ is proportional to the island volume Ω_I, form (23) one obtains

$$C_I \simeq q^2 \Omega_I/kT\,\Omega_e \quad (32)$$

where $\Omega_e=\Omega_s \exp|(\bar{E}_F-E_m)/kT|$ and Ω_I/Ω_e is the average number of electron or holes contained in the island. In this case, according to (13) and (32), the condition (28) is verfied for

$$r_I \ll r^*=(\Omega_e/2\lambda L)\left[1+(1+4L\lambda^2/\Omega_e)^{1/2}\right] \quad , \quad (33)$$

where $L=q^2/3\varepsilon kT \simeq 20nm$, for $T=300^\circ K$ and $\varepsilon = 10^{-10} F/m$.

For instance for $\Omega_s=1(nm)^3$ and $\bar{n}=10^{15}$ cm^{-3}, which leads to $\lambda = 130$ nm, from (33) one obtains $r^*=0.22$, 1.54 and 10.6 nm for $|\bar{E}_F-E_m|=0$, 0.1 and 0.2 eV, respectively.

Therefore, in any case, microdefects with sizes greater than a few nm generate flicker noise with a spectrum $S_V=\Gamma/f^\gamma$ characterised by γ value near one, whereas that does not happen for the point defects.

CONCLUSIONS

Same complements and new results, which generalize and strengthen the preceding flicker noise theory [1], have been carried out by taking into account the effects, on the carrier and current densities, of the electric potential and Fermi level fluctuations both inside and outside the islands.

A more accurate and general expression of the current dipole vector has been so obtained.

Above all a new expression of the island relaxation time has been achieved according to which it is proportional to the series of the internal external and barrier capacitances of the island itself.

Finally from such a result it has been deduced that the noise spectrum differs appreciably from the 1/f shape when the sizes of the islands are so small as to make its current depending on the capture-emission processes and the internal capacitance smaller than the external one.

REFERENCES

1 B.Pellegrini, Phys.Rev. B22, 4684 (1980).

FLUCTUATIONS OF THE RELAXATION TIME AS A SOURCE OF 1/f NOISE IN MACROSCOPIC PHYSICAL SYSTEMS

J. Uebersfeld

University of Paris VI "Pierre et Marie Curie"
75005 Paris, France

P. H. Handel

Physics Department
University of Missouri
St. Louis, MO 63121

J. J. Gagnepain

Laboratoire de Physique et Metrologie
des Oscillateurs du C.N.R.S.
25000 Besancon, France

As was pointed out in the theory of quantum 1/f noise, cross sections of many elementary processes are infrared quasi-divergent and consequently exhibit low frequency 1/f fluctuations.

In large systems, characterized by relaxation times τ, the fluctuations of the elementary cross sections are likely to produce 1/f fluctuations of τ.

In many cases, the system is characterized by a single, dominant, τ. This will be reflected in the behavior of the susceptibilities of the macroscopic system. If X is a force-field applied to the system, Y the causal and linear response of the system, and $W = XY$ the stored energy in the system caused by the X-field, any fluctuation of the loss rate of the system will produce a fluctuation in the stored energy. The quantitative connection between these two fluctuations is given by the Kramers-Kronig relations, applied to the complex susceptibility K, which expresses the causal and linear relation between X and Y.

This method has been applied to quartz crystal resonators and easily yields a theoretical interpretation of the experimental spectrum of the flicker of frequency noise

$$S_y(f) = \frac{\Lambda}{Q^4 f}, \qquad (0)$$

where y is the fractional frequency fluctuation, Q the quality factor of the resonator, and Λ a dimensionless constant of about 1 for quartz resonators.

It is known that the interaction between the sound wave and the thermal phonons in a dielectric crystal is at the origin of the attenuation of the wave. Such an interaction being a nonlinear process, the wave velocity, and therefore the resonator frequency, are also affected [1]. In a first approach three-phonon collisions are considered, involving a sound wave phonon and two thermal phonons. Three different types of collisions must be distinguished:

1) Normal processes (N), in which the total energy of the phonons and the total quasi-momentum are conserved.

2) Umklapp processes (U), in which only the total energy is conserved, but not the quasi-momentum.

3) Elastic scattering (E), corresponding to collisions of phonons with impurities, defects, etc. The scattering being elastic, the frequency does not change, but the wave vector and the polarisation can be altered. The total energy is conserved. However, the number of phonons of any particular frequency cannot change.

The phonon has a finite lifetime τ, which makes its energy uncertain by an amount $\hbar/\tau$. The effect on the attenuation and velocity will be more or less important if this uncertainty is larger or smaller than $\hbar\omega$, the energy of a sound wave phonon, of angular frequency ω.

At high temperature, i.e., $\omega\tau \ll 1$, the previous processes N, U and E and/or combinations like N with some U and E processes, or E with some N and U processes, lead to attenuations α and velocity changes $V-V_o$ which all take the general form [1]:

$$\alpha = \frac{CT\omega}{2\rho V_o^3} \gamma^2 \frac{\omega\tau}{1+\omega^2\tau^2} \tag{1}$$

$$V-V_o = \frac{CT}{2\rho V_o} \gamma^2 \frac{\omega^2\tau^2}{1+\omega^2\tau^2} , \tag{2}$$

where γ is an effective Grueneisen constant depending on the nature of the processes involved, C the specific heat, T the temperature, ρ the specific mass, and V_o the sound wave phase velocity.

Introducing the low frequency Young modulus $E_o = \rho V_o^2$, the quantity $\Delta E \equiv CT.\gamma^2$, and the relation between attenuation and Q-factor $\alpha = \omega/2QV_o$, one obtains:

$$\frac{1}{Q} = \frac{\Delta E}{E_o} \frac{\omega\tau}{1+\omega^2\tau^2} \tag{3}$$

$$\frac{V-V_o}{V_o} = \frac{\Delta E}{2E_o} \frac{\omega^2\tau^2}{1+\omega^2\tau^2} . \tag{4}$$

A fluctuation $\delta\tau$ in τ will produce a velocity fluctuation δV, and therefore a fractional fluctuation y of the resonator frequency ω_r

$$y = \frac{\delta\omega_r}{\omega_r} = \frac{\Delta E}{E_o} \frac{\omega_r^2\tau^2}{(1+\omega^2\tau^2)^2} \frac{\delta\tau}{\tau} . \tag{5}$$

Introducing the power spectral densities $S_y(f)$, and using in eq (5) the expression eq (3) for Q^{-1}, one obtains immediately

$$S_y(f) = \frac{1}{Q^4} \left(\frac{E_o}{\Delta E}\right)^2 S_{\delta\tau/\tau}(f) \tag{6}$$

which exhibits the Q^{-4}-law.

If it is now assumed that τ has a power spectral density $S_{\delta\tau/\tau}(f) = \Lambda'/f$ in the spirit of the quantum 1/f noise approach [2-3], eq (6) coincides with the experimental law (0).

A rough evaluation of the Grueneisen constant γ can be made either by means of its relation with the thermal expansion constant, or by means of the third order elastic constants. In both cases it is found that γ is of the order of 10, for quartz. Therefore $(\Delta E/E_o)^{-2} \simeq 10^5$. This means, since $\Lambda \approx 1$ in eq (0), that Λ' is approximately equal to 10^{-5}, which is a reasonable value if considering that $\delta\tau/\tau = -\delta Q/Q$.

A similar formula can be derived for electromagnetic resonators filled with a lossy dielectric material.

In each case, the constant Λ depends either on the mechanical, or the electrical properties of the material. The exact behavior of the mechanical (or the electrical) susceptibility is irrelevant, if the susceptibility depends on only one relaxation time τ, and if the condition $\omega_r\tau \ll 1$ is satisfied (ω_r being the resonance frequency of the electrical or mechanical resonator).

Although the method has been applied only to the electrical and mechanical case, it is anticipated that it would work for other systems.

Finally, we would like to discuss the experimental basis of the Q^{-4}-law. Measurements of 1/f frequency noise were performed on a large number of quartz resonators, at different frequencies, and with different quality factors. The measuring system is composed of a phase bridge, doubly balanced

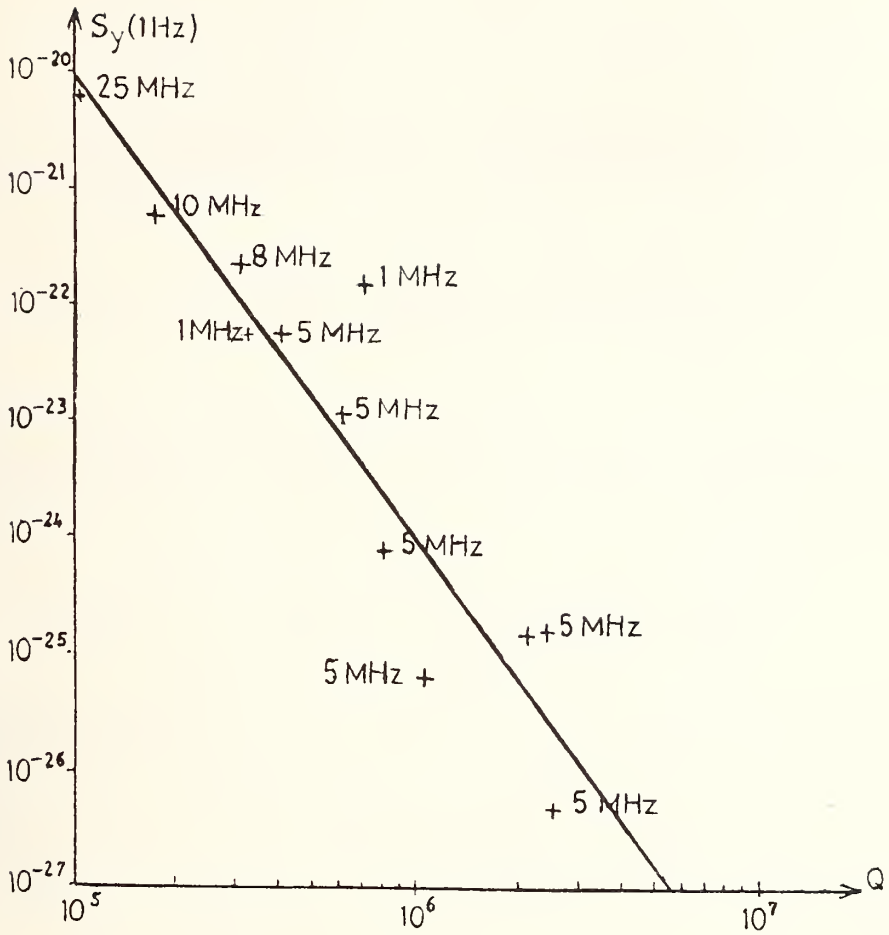

Fig. 1 Spectral density S of fractional frequency fluctuations y at 1 Hz Fourier frequency as a function of the quality factor Q for various quartz resonators. The resonance frequency of the quartz is indicated for each point. The solid line has a slope of -4.

in order to reject the frequency noise of the source itself. Fig. 1 gives the noise levels, measured at 1 Hz Fourier frequency, as a function of the unloaded Q-factor. It can be observed that the dependence of the noise power on Q is well described by a Q^{-4}-law.

We have some indications that the Q^{-4}-law is more general and can also be applied to frequency standards other than quartz.

REFERENCES

[1] H. J. Maris, *Physical Acoustics, Vol. VIII*, Eds. W. P. Mason and R. N. Thurston (Academic Press, New York, 1971).

[2] P. H. Handel, *Solid State Electronics* 22, 875 (1979).

[3] P. H. Handel, *Phys. Rev. Letters* 34, 1492,1495 (1975).

[4] P. H. Handel, *Phys. Rev.* 22A, 745 (1980).

$1/f^{\alpha}$ NOISES AND THE RIEMANN - LIOUVILLE FRACTIONAL INTEGRAL / DERIVATIVE OF THE BROWNIAN MOTION

Claudio Maccone

(Private address : Via Martorelli 43 -
- 10155 Torino (Turin) - Italy)

INTRODUCTION

Let $B(t)$ denote the Brownian motion. The present paper is devoted to the study of its Riemann - Liouville fractional integral / derivative of order $H-\frac{1}{2}$, which is formally defined

$$B_H(t) = \int_0^t \frac{(t-s)^{H-\frac{1}{2}}}{\Gamma\left(H+\frac{1}{2}\right)}\, dB(s) \qquad (t \geq 0)\,. \tag{1}$$

This process is a fractional integral of the Brownian motion for $H > \frac{1}{2}$, and a fractional derivative for $H < \frac{1}{2}$. Actually it is a one - parameter class of processes (the parameter being H), and will be called the fractional Brownian motions in the sequel. Its definition seems to go back to Paul Lévy [1]. Benoit B. Mandelbrot [2] provides a full list of the references to the subject up to 1977. It is evident from eq (1) that the Brownian motion can be regarded as the particular case $H = \frac{1}{2}$ of the fractional Brownian motions, since the initial condition $B_H(0) = 0$ holds good. Moreover, remembering the scaling property fulfilled by the Brownian motion

$$B(rt) = \sqrt{r}\; B(t) \qquad (r > 0) \tag{2}$$

it is easy to prove that the fractional Brownian motions fulfill the scaling property

$$B_H(rt) = r^H\; B_H(t) \tag{3}$$

sometimes called the H self - similarity property.

LINEAR SYSTEM WHITE NOISE - FRACTIONAL BROWNIAN MOTIONS AND CONSEQUENCES

The fractional Brownian motions can be regarded as the output of a suitable linear system of which the input is the (uniform) white noise : in fact eq (1) is already in a convolution form, so that it suffices to replace $dB(t)$ by $B'(t)\,dt$, where $B'(t)$ is the (uniform) white noise. Thus, we find at once the impulse response of the system

$$h(t) = \frac{t^{H-\frac{1}{2}}\; U(t)}{\Gamma\left(H+\frac{1}{2}\right)} \qquad \text{with} \quad U(t) = \begin{cases} 1 & t > 0 \\ 0 & t < 0 \end{cases} \tag{4}$$

and, by computing the latter's Fourier transform, the system function $H(i\omega)$

$$H(i\omega) = \frac{1}{(i\omega)^{H+\frac{1}{2}}} \qquad \text{whence} \qquad \left|H(i\omega)\right|^2 = \frac{1}{\omega^{2H+1}} . \tag{5}$$

Since the white noise autocorrelation is the delta function $\delta(t_1-t_2)$, use of eq (4) and of the standard formula $R_{B'B_H}(t_1,t_2) = \delta(t_1-t_2) * h(t_2)$ yields the cross-correlation $R_{B'B_H}(t_1,t_2)$ white noise - fractional Brownian motions

$$R_{B'B_H}(t_1,t_2) = \left\langle B'(t_1)\ B_H(t_2)\right\rangle = \frac{(t_2-t_1)^{H-\frac{1}{2}}\ U(t_2-t_1)}{\Gamma\left(H+\frac{1}{2}\right)} . \tag{6}$$

The autocorrelation $R_{B_HB_H}(t_1,t_2)$ of the fractional Brownian motions can then be found from eqs (4) and (6) by virtue of the standard formula $R_{B_HB_H}(t_1,t_2) = R_{B'B_H}(t_1,t_2) * * h(t_1)$, and reads (the symbol $t_1 \wedge t_2$ denoting the minimum among t_1 and t_2)

$$R_{B_HB_H}(t_1,t_2) = \left\langle B_H(t_1)\ B_H(t_2)\right\rangle = \frac{(t_1 \wedge t_2)^{2H}}{2H\left[\Gamma\left(H+\frac{1}{2}\right)\right]^2} . \tag{7}$$

Setting $t_1 = t_2 = t$, eq (7) yields the variance of the fractional Brownian motions (the mean being zero)

$$\sigma^2_{B_H(t)} = \frac{t^{2H}}{2H\left[\Gamma\left(H+\frac{1}{2}\right)\right]^2} \tag{8}$$

whence

$$\sigma_{B_H(t)} = \pm \frac{t^H}{\sqrt{2H}\ \Gamma\left(H+\frac{1}{2}\right)} \tag{9}$$

is the standard deviation of the fractional Brownian motions, and is evidently H self-similar. Also, eq (9) shows that H must be positive, and, by plotting the curves $\sigma_{B_H(t)}$ on the $t - B_H(t)$ plane, that H must be less than one (otherwise the curves would be "divergent"). In conclusion, the important restriction $0 < H < 1$ arises.

POWER SPECTRA OF THE FRACTIONAL BROWNIAN MOTIONS

From eq (5) the power spectra of the fractional Brownian motions follow upon resorting to the non-stationary spectral theory, as outlined, for instance, in [3]. The result is

$$S(f) = \begin{pmatrix}\text{normalization}\\ \text{constant}\end{pmatrix} \cdot f^{-2H-1} \tag{10}$$

Hence the fractional Brownian motions are an example of a rigorous mathematical theory leading to a spectral law of the type $1/f^x$, in which $1 < x < 3$. Though the $1/f$ noise is not covered by the theory, it can be approximated indefinitely from above. This fact seems to suggest that further investigations along these lines might lead to a model for the $1/f$ noise. From eq (10) it also appears that the fractional Brownian motions are necessarily a class of band-limited noises, a realistic feature for their usage.

It is not difficult to prove, by virtue of eqs (2) and (7), that the formula holds

$$\left\langle B\left(\frac{t_1^{2H}}{2H\left[\Gamma\left(H+\frac{1}{2}\right)\right]^2}\right)\ B\left(\frac{t_2^{2H}}{2H\left[\Gamma\left(H+\frac{1}{2}\right)\right]^2}\right)\right\rangle = \left\langle B_H(t_1)\ B_H(t_2)\right\rangle \tag{11}$$

that is, the autocorrelation of the process on the right equals that of the fractional Brownian motions. Since both processes have equal mean (zero), we conclude that

$$B_H(t) = B\left(\frac{t^{2H}}{2H\left[\Gamma\left(H+\frac{1}{2}\right)\right]^2}\right). \tag{12}$$

Thus, the fractional Brownian motions are just a rescaled form of the Brownian motion, and of course they are Gaussian processes. For $H>\frac{1}{2}$, that is for the fractional integral, the diffusion is faster than the Brownian diffusion, whereas for $H<\frac{1}{2}$, that is for the fractional derivative, the diffusion is slower. The density of $B_H(t)$ reads

$$f_{B_H(t)}(x) = \frac{\sqrt{H}\ \Gamma\left(H+\frac{1}{2}\right)}{\sqrt{\pi}\ t^H}\ \exp\left\{-H\left[\Gamma\left(H+\frac{1}{2}\right)\right]^2\frac{x^2}{t^{2H}}\right\} \tag{13}$$

and

$$\Phi_{B_H(t)}(z) = \exp\left\{-\frac{t^{2H}\ z^2}{4H\left[\Gamma\left(H+\frac{1}{2}\right)\right]^2}\right\} \tag{14}$$

is its characteristic function (that is, the Fourier transform of eq (13)). A number of results can be derived from eqs (13) and (14) by following up the procedures that are well-known from the theory of the Brownian motion, but we have little space here. For instance, the density of the first-passage time at any abscissa $a>0$ reads

$$\text{first-passage time density}\ (t) = \frac{2\,a\,H^{3/2}\ \Gamma\left(H+\frac{1}{2}\right)}{\sqrt{\pi}\ t^{H+1}}\ \exp\left\{-H\left[\Gamma\left(H+\frac{1}{2}\right)\right]^2\ \frac{a^2}{t^{2H}}\right\}. \tag{15}$$

Another interesting result is the diffusion partial differential equation

$$\frac{\left[\Gamma\left(H+\frac{1}{2}\right)\right]^2}{t^{2H-1}}\ \frac{\partial f_{B_H}(t,x)}{\partial t} = \frac{1}{2}\ \frac{\partial^2 f_{B_H}(t,x)}{\partial x^2} \tag{16}$$

fulfilled by the fractional Brownian motion density (13) with the initial condition $f_{B_H}(0,x)=\delta(x)$. The left side of eq (16) reflects the time rescaling, and its right side the Gaussian character of the density (13). Therefore it would be easy to consider higher-dimensional fractional Brownian motions simply by inserting the Laplacian on the right side of eq (16). If expressed in polar coordinates, only the radial part would be left, and the radial density would be found. These developments are left to the reader.

EIGENFUNCTION EXPANSION (KARHUNEN - LOEVE EXPANSION)

The present author proved in [4] the eigenfunction expansion of the fractional Brownian motions which will presently be stated without proof. The expansion reads

$$B_H(t) = t^H \sum_{n=1}^{\infty} Z_n N_n J_\nu\left(\gamma_n \frac{t^{H+\frac{1}{2}}}{T^{H+\frac{1}{2}}}\right) \tag{17}$$

Here : 1) The time t ranges from zero to a fixed positive instant T : $0 \leq t \leq T$.

2) The order ν of the Bessel functions of the first kind, $J_\nu(x)$, is a one - to - one function of H given by

$$\nu = \frac{2H}{2H+1} . \tag{18}$$

3) The constants γ_n are the real positive zeros of the Bessel function $J_{\nu-1}(x)$, arranged in ascending order of magnitude. These can be computed numerically as soon as a value of ν (that is, a value of H, by virtue of eq (18)) has been fixed.

4) The normalization constants N_n are given by

$$N_n = \frac{\gamma_n \sqrt{2H+1}}{T^{H+\frac{1}{2}} \sqrt{\gamma_n^2 \left[J'_\nu(\gamma_n)\right]^2 + \left(\gamma_n^2 - \nu^2\right)\left[J_\nu(\gamma_n)\right]^2}} . \tag{19}$$

5) And finally the Z_n are a set of orthogonal Gaussian random variables, having each zero mean and variance given by the eigenvalue λ_n, that is

$$\left\langle Z_m Z_n \right\rangle = \delta_{mn} \lambda_n = \delta_{mn} \frac{T^{2H+1}}{\gamma_n^2 \left[\Gamma\left(H+\frac{3}{2}\right)\right]^2} . \tag{20}$$

There is only one eigenfunction (given by the two last terms under the summation in eq (17)) corresponding to the eigenvalue λ_n, that is, there is no degeneracy. And, since the eigenvalues λ_n form a decreasing sequence as $n \to \infty$, the series (17) converges.

The author thanks Prof. J.G. Taylor of the University of London (England) King's College and Prof. P. Mazzetti of the Istituto Elettrotecnico Nazionale Galileo Ferraris, Torino, Italy, for their cooperation.

REFERENCES

[1] Paul Lévy, Univ. California Publ. Statis. 1, 357 (1953).

[2] Benoit B. Mandelbrot, in "Fractals: form, chance, and dimension" (Freeman, San Francisco, 1977).

[3] Athanasios Papoulis, in "Probability, random variables and stochastic processes" (McGraw-Hill, New York, 1965).

[4] Claudio Maccone, Il Nuovo Cimento B (to appear spring 1981).

NON-GAUSSIAN AMPLITUDE DISTRIBUTION OF THERMAL NOISE IN RESISTORS WITH 1/f NOISE

P. H. Handel

University of Missouri
St. Louis, MO 63121

D. Wolf

University of Frankfurt
Frankfurt a.M., F.R. Germany

K. M. van Vliet

University of Florida, Gainesville FL 32611
and
University of Montreal, Canada

It is well-known that resistors of any nature which contain a relatively small number of carriers are also characterized in general by the presence of resistance fluctuations with a 1/f spectrum. These, apparently fundamental, 1/f resistance fluctuations are not due to temperature fluctuations, but are present both in thermal equilibrium and in the presence of an applied voltage. From a theoretical point of view, a certain level of such fundamental 1/f fluctuations is to be expected as a consequence of quantum 1/f noise at the level of the scattering cross sections, from various systems of infraquanta, both in equilibrium and nonequilibrium. In general, the fundamental 1/f fluctuations of the resistance should cause fluctuations in the spectral power level N = 4kTG of thermal current fluctuations, and in the power level N' = 4kTR of voltage fluctuations:

$$\frac{\langle(\delta N)^2\rangle_f}{\langle N\rangle^2} = \frac{\langle(\delta N')^2\rangle_f}{\langle N'\rangle^2} = \frac{\langle(\delta G)^2\rangle_f}{\langle G\rangle^2} = \frac{C}{f}\ , \tag{1}$$

where C is the 1/f-coefficient observed also in the presence of an applied voltage. However, there should not be 1/f fluctuations in the available power level N" = kT

$$\langle(\delta N'')^2\rangle_f \simeq 0. \tag{2}$$

Experimentally, Clarke and Voss [1] have first observed the presence of the 1/f fluctuations (1), although they interpreted their results in terms of temperature fluctuations, rather than true 1/f noise. Beck and Spruit [2] have observed the Nyquist-level fluctuations subsequently in carbon resistors. It would be useful if Eq. (2) could also be verified experimentally.

The purpose of the present communication is to derive the amplitude distribution for the 1/f power-modulated thermal noise described by eqs (1) and (2).

Let us denote by x(t) the (unmodulated) Nyquist noise variable, and by ξ the resulting thermal noise variable. We interpret the resulting thermal noise by writing

$$\xi = x(G/G_o)^{1/2} = x(1 + \delta G/G_o)^{1/2} = x + xy\ , \tag{3}$$

where G_o is the average conductance, and

$$y \simeq \frac{\delta G}{2G_o} \tag{3}$$

is half the relative conductance fluctuation. (4)

Notice that ξ will have a white spectrum up to high frequencies, described by the Nyquist-Planck formula. Indeed, we know that x is white, and therefore has a δ-function autocorrelation. Since x and y are independent, the xy-term has an autocorrelation function which is the product of the corresponding autocorrelation functions, i.e., also a δ-function. This means that xy is white. Since x and xy are uncorrelated (although they are not independent) their autocorrelation functions and spectral densities must be additive. Consequently, ξ is white, as claimed.

In order to derive the amplitude distribution of $z = xy$, we introduce $\eta \equiv \ell n\, z$, $\alpha \equiv \ell n\, x$ and $\beta \equiv \ell n\, y$. From $\eta = \alpha + \beta$ we obtain the distribution

$$P''(\eta)d\eta = d\eta \int P_1'(\alpha)\, P_2'(\eta-\alpha)d\alpha = \frac{2d\eta}{2\pi\sigma_1\sigma_2}\int_{-\infty}^{\infty} \exp\left[-\frac{e^{2\alpha}}{2\sigma_1^2} + \alpha\right]\exp\left[-\frac{e^{2(\eta-\alpha)}}{2\sigma_2^2} + \eta - \alpha\right]d\alpha$$

$$= \frac{e^{\eta}d\eta}{2\pi\sigma_1\sigma_2}\int_{-\infty}^{\infty} \exp\left[-\frac{e^{\eta}}{\sigma_1\sigma_2}\cosh\varepsilon\right]d\varepsilon = \frac{e^{\eta}d\eta}{\pi\sigma_1\sigma_2} K_o\left(\frac{e^{\eta}}{\sigma_1\sigma_2}\right), \tag{5}$$

where $P_1'(\alpha)$ and $P_2'(\beta)$ are derived from Gaussians of dispersion σ_1 and σ_2 respectively, $\varepsilon \equiv 2\alpha - \eta + \ell n(\sigma_2/\sigma_1)$, and K_o is the modified zero-order Bessel function. Returning to the real variable z, we obtain from $P''(\eta)d\eta = P(z)dz$

$$P(z) = \frac{1}{\pi\sigma_1\sigma_2} K_o\left(\frac{z}{\sigma_1\sigma_2}\right). \tag{6}$$

The corresponding characteristic function is elementary:

$$\chi(v) = (1 + \sigma_1^2\sigma_2^2 v^2)^{-1/2}. \tag{7}$$

Due to the mutual dependence of x and z, the characteristic function of ξ differs from the product of the characteristic functions of x and z. We obtain instead the amplitude p.d.f.

$$I(\xi) = \int_{-\infty}^{\infty} P_1(x)P_2\left(\frac{\xi}{x} - 1\right)\frac{1}{|x|}dx = \frac{e^{-1/2\sigma_2^2}}{2\pi\sigma_1\sigma_2}\int_{-\infty}^{\infty} \exp\left[-\frac{x^2}{2\sigma_1^2} - \frac{\xi^2}{2x^2\sigma_2^2} + \frac{\xi}{x\sigma_2^2}\right]dx/|x|$$

$$\equiv \frac{e^{-1/2\sigma_2^2}}{\pi\sigma_1\sigma_2}\int_{0}^{\infty} \exp\left[-\frac{x^2}{2\sigma_1^2} - \frac{\xi^2}{2x^2\sigma_2^2}\right]\cosh\left(\frac{\xi}{x\sigma_2^2}\right)dx/x. \tag{8}$$

This distribution tends to a Gaussian in the limit $\sigma_2 \to 0$, but differs slightly from a Gaussian in general. The skewness is zero, but the kurtosis exhibits the small deviation

from the Gaussian amplitude p.d.f. The necessity of a non-Gaussian behavior of thermal noise has been mentioned recently by Tremblay and Nelkin [3].

Finally, we mention that for the current fluctuations ζ in the presence of an applied voltage V_o we can write the symmetrical expression

$$\zeta = x + \frac{xy'}{2G_o V_o} + y' ,$$

where $y' \equiv 2G_o V_o y$. The corresponding amplitude distribution will be closer to a Gaussian, and will not be discussed here.

The authors acknowledge support from Contract N00014-79-0405 and AFOSR.

REFFERENCES

[1] R. F. Voss and J. Clarke, *Phys. Rev.* B13, 556 (1976).

[2] H. G. E. Beck and W. P. Spruit, *J. Appl. Phys.* 49, 3384 (1978).

[3] M. Nelkin and A. M. Tremblay, *Proc. II Int. Conf. on 1/f Noise*, Orlando, 1980, p. 71.

$1/f^{\alpha}$ NOISE BEHAVIOR IN INFRARED PHOTOCONDUCTIVE POLYCRYSTALLINE THIN FILMS OF $Pb_xSn_{1-x}Te$

A. D'Amico, G. Cappuccio, G. Petrocco, C. Fotinos
Istituto di Elettronica dello Stato Solido del
Consiglio Nazionale delle Ricerche
Via Cineto Romano, 42
00156 Roma

G. Stochino
Laboratorio Circuiti Analogici FATME
Via Anagnina, Roma
Italy

We report experimental results concerning the $1/f^{\alpha}$ noise behavior [1-5] in semiconductor polycrystalline thin films of $Pb_xSn_{1-x}Te$ used as photoconductors in infrared applications. Such a noise has been seen in relation to the spread mosaic variation of the films due to suitable annealing processes.

These films have been obtained by the radio frequency sputtering technique using a mixed Ar- O_2 gaseous plasma with the following partial pressure: $p(A_2) = 3 \times 10^{-3}$ torr, $p(O_2) = 9 \times 10^{-5}$ torr. The surface substrate temperature during the deposition has been maintained close to 150°C.

BaF_2 [100], NaCl [100], CaF_2 [100] oriented samples with 1.6, 1.8, 1.4 degrees respectively of spread mosaic were used as substrates for the polycrystalline growth of $Pb_xSn_{1-x}Te$. Dimension of the deposited films were thickness about 8500 Å and contactless area equal to $(1x2)mm^2$.

The mosaic spread of the substrates and films was measured by X-ray diffraction techniques by using a Bragg-Breantano single-axis diffractometer. All the measurements were performed by the Θ-scan technique [6].

Here the X-ray source and the film are set up in a fixed position in order to select the Bragg angle of a specific reflection: the specimen turns around the goniometer axis, in order to bring the differently oriented grains toward reflection. The reflection intensity as a function of rotation angle Θ (rocking-curve) gives a direct measurement of both the preferential orientation of the film and the mosaic spread around the preferential orientation. To overcome the problem related to the low intensity typical of X-ray characterization of thin films, quite a strong, low angle reflection was used: the [200] reflection at a Bragg angle of about 16° (Kd radiation of Co).

Anisotropy measurements were repeated along two orthogonal directions and no valuable variation of the mosaic spread have been observed. By using the $Au/Pb_xSn_{1-x}Te/Au$ (with gold contacts under the film) structure with two concentration values of x: x_1=0.20, x_2=0.16) noise measurements have been carried out, before and after annealing, close to liquid nitrogen temperature: (79±0.3)°K in two different ways. First by considering films as grown, second by using the same $Au/Pb_xSn_{1-x}Te/Au$ structure after a suitable annealing whose characteristics are the following: hold temperature close to (180±2)°K for 25 hours

and dT/dt equal to +10°C/h from and towards room temperature.

Experimental results indicate both a reduction of the spread mosaic in annealed $Pb_xSn_{1-x}Te$ films and variations of the $1/f^{\alpha}$ noise behavior.

As a matter of fact, films showed as-grown a spread mosaic of about 12, 8, 11 degrees respectively on the above mentioned substrates and, after annealing a spread mosaic of 5, 2 and 3.5 degrees.

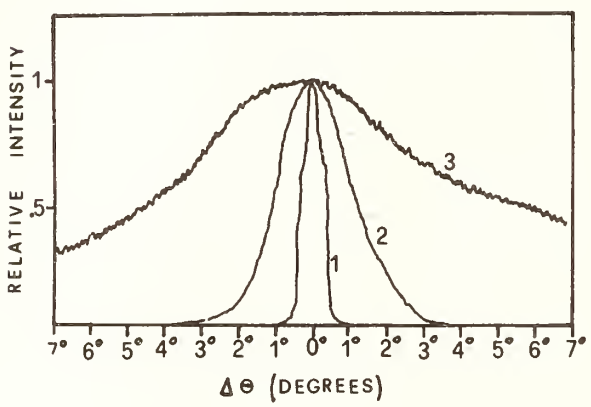

Fig. 1. Reflection intensity as function of $\Delta\Theta = \Theta\beta - \Theta$ for: (1) NaCl substrate [100], (2) $Pb_{.8}Sn_{.2}Te$ film after annealing, and (3) $Pb_{.8}Sn_{.2}Te$ film as grown.

Figure 1 shows as an example, the relative reflection intensity of X-ray as a function of $\Delta\Theta = \Theta\beta - \Theta$ for the Au/ /$Pb_xSn_{1-x}Te$/Au film as grown and after annealing on a [100] oriented NaCl substrates. Similar behavior has been observed for the other two types of substrates. Noise measurements were carried out leaving the structure in a liquid nitrogen cooled tail of a window-less cryostat in order to avoid any influence of external light. Furthermore, samples were surrounded by a copper shield whose average temperature was maintained at about 80°K. In this way the internal surface of the shield was the only source of noise radiation.

To test the linearity of our system the electronic chain has always been used after a check by a suitable calibrated low noise metal film resistor of 10.05 MΩ at 81°K.

The electronic chain used in such measurements was formed by a low noise preamplifier made up by a low noise junction field effect transistor (2N 6550) and a thermalized low drift operational amplifier, (OP05) followed by a digital signal analyzer.

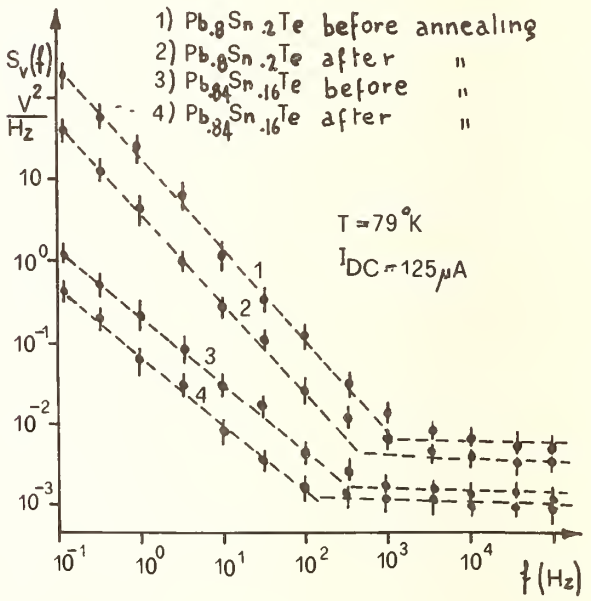

Fig. 2. Power spectral density in $Au/Pb_xSn_{1-x}Te/Au$ structures at 79°K before and after annealing.

As far as the $1/f^{\alpha}$ noise is concerned, Fig. 2 summarizes results in the case of the film grown on a NaCl substrates at 79°K with a DC polarization current of 125μA and two different concentrations of lead. As we see from Fig. 2, a lead concentration from .2 to .16 produces a lower excess $1/f^{\alpha}$ noise, and during the annealing process α ranges from 1.3 down to .9.

From Fig. 2 and from data obtained taking into considertaion the spectral noise power density vs. the DC polarization current (at a fixed frequency) we can summarize and write the following results:

$S_v(f) \propto 1/f^{1.3} \cdot I^{2.4}$ before annealing

$S_v(f) \propto 1/f^{.9} \cdot I^{2.1}$ after annealing

which confirm the flicker noise behavior and indicate a connection between the soectral noise former density and the spread mosaic variation caused by annealing processes.

Further investigations are going on to better understand a possible correlation between the $1/f^{\alpha}$ noise and the structural variations of the films under thermal conditioning.

ACNOWLEDGEMENTS

Many thanks are due to Mr.Grilli for his assistance in carrying out figures and to Dr. G. Spissu for her skilled technical assistance.

REFERENCES

[1] F.N. Hooge, Phisica, 42, 331(1969)

[2] S.T. Hsu, D.J. Fitzgerald and A.S. Grove, Appl. Phys. Lett. 12, 287 (1968)

[3] R.F. Voss and J. Clarke, Phys. Rev. B, 13 556 (1973)

[4] Noise in Physical Systems, Proceedings of the Fifth International Conference on Noise, Bad Nauheim, March 13-16, 1978

[5] A. van der Ziel "Flicker noise in semiconductors: not a true bulk effect" Appl. Phys. Lett. 33(10) 15 Nov 1978

[6] G. Balestrino, A. D'Amico, G. Petrocco and A. Grilli: Infrared Phys., 19 245 (1979)

TEMPERATURE DEPENDENCE OF 1/f NOISE IN THICK-FILM RESISTORS

Maria Prudenziati and Bruno Morten
Gruppo Nazionale Struttura della Materia
Istituto di Fisica dell'Università, Modena, Italy

Aldo Masoero
Gruppo Nazionale Struttura della Materia
Istituto Elettrotecnico Nazionale Galileo Ferraris, Torino, Italy

INTRODUCTION

Thick-film resistors (TFRs) are a particular class of cermet materials with a relevant role in microelectronics [1]. The conduction mechanisms consistent with their microstructure [2] and electrical properties have been analyzed and include different possibilities, i.e. hopping of electrons from and to conductive grains and localized states in the glassy matrix, direct tunneling of electrons between near-neighboring grains assisted by resonant centres in the intergranular material, and conduction in a narrow band of nearly delocalized states in the intergranular material [3]. In any case a relevant role in the conduction mechanisms of TFRs seems to be played by deep energy levels in the glass.

One method of investigating the nature of these energy levels and the conduction mechanism is by a study of the current noise of these materials. In this framework we have undertaken an extensive study of the noise effects in TFRs. The results of the temperature dependence of 1/f noise are here reported and discussed. Although presently limited to a narrow range of resistivities the study gives interesting results for further progress in our knowledge of electrical properties and conduction mechanisms in TFRs.

EXPERIMENTAL PROCEDURE

We included in the study three commercial ink series based on different metal-oxides and a prototype RuO_2-based ink series [4], see Table I.

Resistors were prepared with the well-known techniques [1] on 96% alumina and were provided with prefired thick-film PtAu-based terminations in order to minimize the effect of metal migration in TFRs [5]. The connections for the TFR from the metal terminations towards the measuring circuit were obtained with platinum pressure contacts, which enabled us to extend the measurements up to high temperatures. Patterns of resistors of constant width (2 mm) and variable length (from 0.5 mm to 10 mm) were prepared in order to evaluate the effect of contact (at the interface between terminations and TFR) on the detected noise [6]. Experimental procedures for characterizing the composition of the samples were described in [7].

Temperature dependence of resistance in the samples was measured with a digital multimeter with a relative accuracy of 10^{-5}. The temperature of the samples was changed from 77 to 650 K in ultrahigh vacuum (10^{-8} mbar) and was measured with a platinum sensor capable of

Table I. Data on composition and electrical properties of TFRs.

Sample	Nom. Sheet Resist. (KΩ/□)	Metal-Oxide	T_{mr} (K)
Du Pont 1741	10	IrO_2	180
Du Pont 1441	10	$Bi_2Ru_2O_7$	350
ESL 2914	10	RuO_2	303
Prototype	90	RuO_2	465

an accuracy and reproducibility of 1 K.

In order to measure the excess noise, a d.c. current was supplied to the sample through a low-pass filter from fresh dry cells. The voltage fluctuations across the sample were

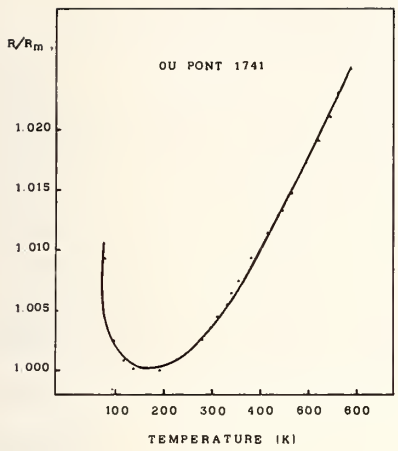

Fig.1 Normalized resistance vs temperature for Du Pont 1741 resistors.

amplified by a low noise preamplifier (PAR Mod. 113) and then fed to a spectrum analyzer to measure the spectral power density in a frequency range from 0.1 Hz to 20 KHz; spectra were measured at different fixed temperatures. In order to measure the noise integral, the amplified noise signal in the bandwidth from 2 Hz to 10 KHz was fed to a true RMS voltmeter, giving a d.c. output signal which was continuously recorded together with the temperature during its variations in the sample chamber.

The experimental results on both resistance and noise of TFRs were reproducible even after many cycles of temperature changes over the whole range investigated.

EXPERIMENTAL RESULTS AND DISCUSSION

Figure 1 shows the temperature dependence of resistance in Du Pont 1741 resistors; resistance is normalized to the value R_m at which it exhibits a minimum according to the typical behaviour of TFRs. The temperature T_{mr} corresponding to this minimum is in this case quite low. Table I reports values for T_{mr} in other samples investigated.

According to the literature [8] the excess noise in TFRs should exhibit a noise power spectral density S_v of the type:

$$S_v = \langle \Delta V^2 \rangle_{\Delta f} / \Delta f = K I^2 R^2 / f \qquad (1)$$

where $\langle \Delta V^2 \rangle_{\Delta f}$ is the mean square voltage noise found in the bandwidth Δf, I the steady state current flowing in the sample of resistance R, f the center of the bandwidth Δf and K a constant which depends on the composition of the sample and is inversely proportional to the sample volume v (v=Lwt where L is the length, w the width and t the thickness of the resistor) for TFRs having the same intrinsic resistivity.

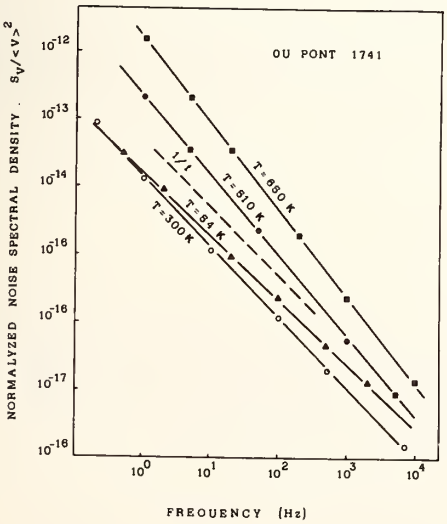

Fig.2 Normalized noise power spectral density $S_V/\langle V \rangle^2$ vs frequency in Du Pont 1741 resistors at different temperatures. The sample was 2 mm wide and 8 mm long.

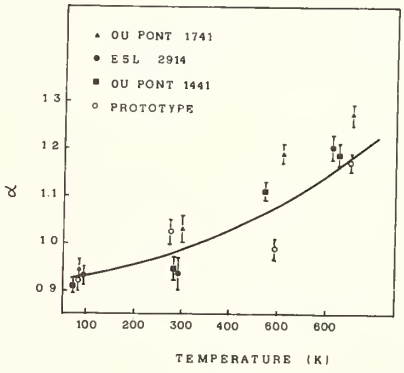

Fig.3 Frequency exponent vs temperature for the samples investigated.

Relation (1) implies that: i) a plot of S_v vs L, with the other parameters fixed, is a straightline which crosses the zero-point in absence of any contact noise [6]; ii) the quantity $S_v/\langle V\rangle^2$ is independent of the bias conditions of the resistor; iii) the noise spectral density is proportional to 1/f. These three conditions have been checked in our samples.

Measurements of S_v vs L show that the contribution due to contacts to the total noise is negligible in our samples, since S_v vs L plots cross the zero-point within the experimental errors.

We found that at a fixed temperature S_v is proportional to the square of the applied d. c. voltage used for noise measurements (up to some tens of volts).

Figure 2 shows typical noise power spectra of Du Pont 1741 (10 KΩ/□) resistors, at various temperatures. The quantity $S_v/\langle V\rangle^2$ is reported as a function of frequency; the spectra have the form of $1/f^{\alpha}$ with values of the frequency exponent α very close to the unity near room temperature, but $\alpha<1$ at lower temperatures and $\alpha>1$ at higher temperatures. This is quite general behaviour for resistors investigated, as shown by the data reported in Fig.3. It is worthnoticing that the values of α are quite similar in resistors of different composition , little differences appearing at the highest temperatures.

Since the noise spectra at both 84 and 650 K in Fig.2 are higher than that at 300 K, data in the figure support for the first time the evidence of a minimum of the power spectral density at the intermediate temperatures. The existence of this minimum is well evidenced in Fig.4 where the relative integral noise $\langle\Delta V^2\rangle/\langle V\rangle^2$ is given for different TFRs. As already reported [9] starting from liquid nitrogen temperature the noise decreases by increasing the temperature, but it reaches a minimum after which it increases again. This behaviour recalls the analogous temperature dependence of resistance of TFRs (Fig.1); on this topic it should be noted that: i) the relative change of noise can be much larger (up to some hundred times) than that of resistance in the same temperature range (compare Fig.1 with Fig.4 and note log. scale in Fig.4); ii) the temperature T_{mr} at which the minimum of resistance occurs (Tab.I) does not always coincide with the temperature T_{mn} at which the minimum of noise is observed in the same sample (Fig.4); in some cases $T_{mn}<T_{mr}$, but, at least intuitively, a correlation between these minima naturally arises.This findings could suggest a common physical origin for the temperature dependence of resistance and noise.

In conclusion we have collected new experimental evidence for the noise behaviour in different TFR systems. We observed that the exponent α characterizing the frequency dependence of excess noise is temperature dependent, making the power spectrum more white at low temperatures, in the line reported in [9]. A minimum of the noise was observed in analogy with the minimum of resistance, even if the temperatures where these minima occur are not necessarily the same in the same sample. The relative changes of noise are much larger than that of resistance in the same sample. The integral noise scales with the sample resistance and it is contained in half a decade in resistors with the same nominal resistivity but different composition.

Presently there is no comprehensive model which satisfactorily describes conductivity and current noise behaviours in TFRs.

A recently proposed model for excess noise in TFRs [9] is based on the assumption of direct electron tunneling between conductive grains. This hypothesis holds true only if resonant centres strongly enhance the tunneling probability [3,10]. In this picture the excess

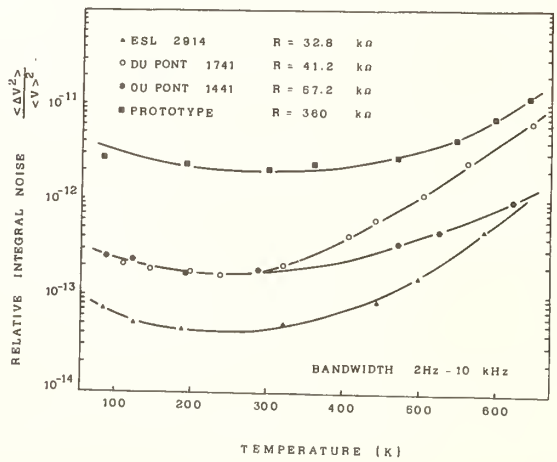

Fig.4 Relative integral noise $\langle\Delta V^2\rangle/\langle V\rangle^2$ in the bandwidth from 2 Hz to 10 KHz as a function of temperature. The samples were 2 mm wide and 8 mm long.

noise may be generated by barrier height fluctuations due to trapping-detrapping effects in the intergranular material in analogy to discontinuous metal thin films [11]. This leads to simple suggestions for frequency exponent α near to unity but does not easily predict the existence of a minimum of the noise at intermediate temperatures.

An alternative model, which can be of interest, follows the results of [12] for variable range hopping (VRH) . Also in this case $1/f^{\alpha}$ noise should be expected with exponent α around the unity and with a noise level which might be much larger than that in free electron conduction [13] as found in TFRs. Of course the original theory [12] must be further elaborated to make explicit the temperature dependence of noise in the case of VRH.

AKNOWLEDGEMENTS

This work was partially supported by Consiglio Nazionale delle Ricerche of Italy. Stimulating discussions of Prof.P.Mazzetti and Dr.L.Reggiani are aknowledged. Moreover we thank Drs. G.Aprilesi and T.Garofano for making available their electronic systems for some measurements.

REFERENCES

[1] C.A.Harper Ed.,*Handbook of thick film microelectronics*(Mc Graw Hills Inc.,New York,1977)

[2] T.V.Nordstrom and C.R.Hills, in *Proc. Int. Microelectronics Symposium*, Los Angeles (1979), p.40.

[3] M.Prudenziati, in *Proc. 3rd Europ. ISHM Conference*, Avignon (1981).

[4] M.Prudenziati, *Alta Frequenza* 46, 287 (1977); M.Prudenziati and U.Costa in *Proc. 76a Riunione Annuale AEI*, Bari (1976) n.18.

[5] A.Cattaneo,F.Forlani,M.Cocito and M.Prudenziati, *ElectroComp. Sci.Technol.*4 ,205 (1977)

[6] T.M.Chen, in *Proc. 5th Conf. on Noise in Physical Systems*,Ed.D.Wolf (Springer Verlag , New York, 1978) p.134.

[7] C.Canali, D.Malavasi, B.Morten, M.Prudenziati and A.Taroni,*J.Appl.Phys.* 51, 3282 (1980)

[8] C.Y.Kuo and H.G.Blank, in *Proc. ISHM Symposium* (1968) p.163.

[9] T.M.Chen and D.Smith, in *Proc. 2nd Symposium on 1/f Noise*, Florida (1980) p.376.

[10] G.E.Pike and C.H.Seager, *J.Appl.Phys.* 48 , 5152 (1977).

[11] M.Celasco, A.Masoero, P.Mazzetti and A.Stepanescu, *Phys.Rev.* B-17, 2553 and 2564 (1978)

[12] B.I.Shklovskii, *Solid State Comm.*, 33 , 273 (1980)

[13] F.N.Hooge ,*Phys. Letters*, 29 A , 139 (1969).

EXCESS CONDUCTANCE NOISE IN SILICON RESISTORS

B. K. Jones

Department of Physics
University of Lancaster
Lancaster LA1 4YB England

ABSTRACT

Excess noise has been measured on a number of silicon resistors over a wide range of variables such as carrier number, dimensions, surface condition and temperature. In all cases the noise has a near 1/f spectrum and can be interpreted as a number fluctuation, $\overline{n_n^2} = \overline{g_n^2}/\mu^2$, located at the boundary of the conducting channel, where μ is the carrier mobility at the boundary and $\overline{g_n^2}$ is the measured conductance noise. This number fluctuation changes little with the variables.

INTRODUCTION

The results presented here extend the interpretation of the measurements presented in full previously [1,2]. The specimens were commercial silicon field-effect transistors biased in their ohmic condition, that is with very small drain-source voltage, so that the conducting channel has uniform dimensions, and other properties, along its length. This condition was rigorously met in the experiments so that the noise was often of low intensity. The specimens were of the categories, junction fet (jfet), enhancement MOS fet (enhmost) and depletion MOS fet (deplmost). Where possible n and p-channel devices have been selected with separate contacts to the oxide gate (G) and the diffusion gate (sub) so that separate biases V_G and V_{sub} can be applied. The measurements have been carried out over a range of gate bias and temperature (100 K - 380 K).

In this way the following influences on the noise have been studied:- presence of oxide interface, number of carriers, width of channel, temperature, proportions of lattice, impurity and surface scattering, transverse quantum effects, carrier freeze-out, doping density and the presence of a space charge. Measurements have been made of the excess voltage noise, that is the increase in noise on applying a dc current, and the resistance as a function of the gate bias voltages. At room temperature additional measurements have been made of the carrier density profile (from 100 KHz C-V_G or C-V_{sub}) across the channel and the local mobility at the channel edge (from 100 KHz transconductance).

ANALYSIS

It is now well established that in homogeneous conductors the excess noise is a resistance fluctuation. To compare the results with the three basic categories of noise the reduced noise, or noisiness $\overline{r_n^2}/R^2$, has been plotted as a function of R as the resistance has been altered by the gate voltages. Simple considerations suggest that a true bulk effect should give no R-dependence, an effect based on Hooge's empirical formula in a uniform specimen should give an R-dependence and a boundary effect should give an R^2 dependence at each temperature. The results show that a near-R^2 variation is followed in all cases. This is illustrated in figure 1 for a typical enhmost. The results for deplmost and jfets are less direct but follow a general upward trend as in figures 2, 3, 4. The deviations from the exact R^2 variation are discussed later.

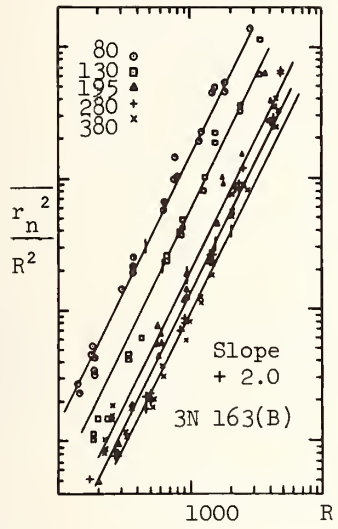

Fig.1

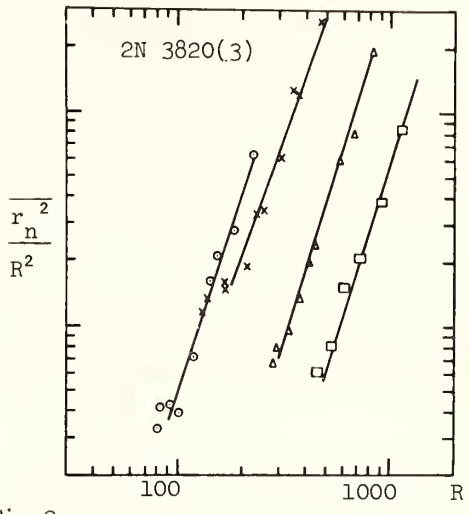

Fig.2

Figs.1 and 2 Noisiness ($\overline{r_n^2}/R^2$) against resistance (R) for the p-channel enhmost 3N 163(B). The vertical lines indicate conditions of constant inversion. Also for p-channel jfet 2N 3820(3) at temperatures 130, 190, 280, 360 K.

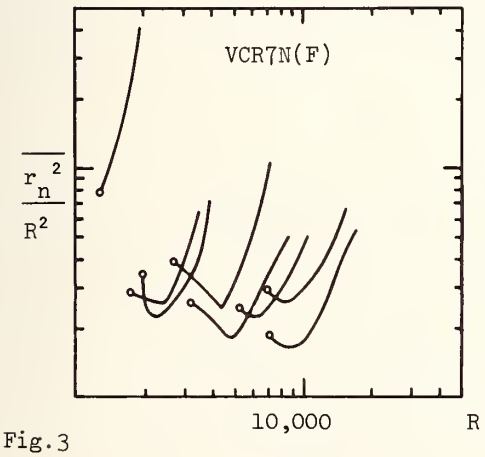

Fig.3

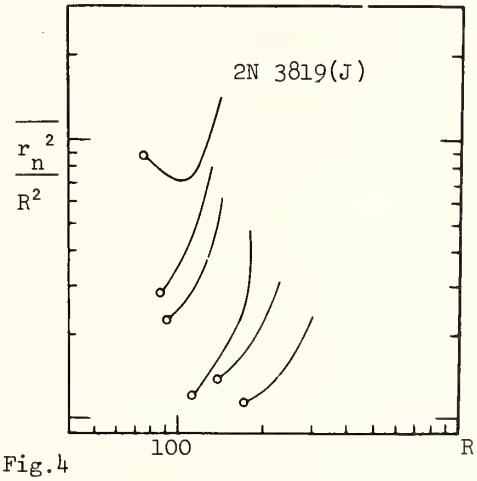

Fig.4

Figs.3 and 4 Noisiness ($\overline{r_n^2}/R^2$) against resistance (R) for the n-channel jfet VCR7N(F) at temperatures 141, 162, 194, 221, 310, 322 and 386 K and for n-channel jfet 2N 3819(J) at temperatures 187, 198, 207, 227, 262, 323 K.

Since no other model has been suggested to give such a general behaviour we assume

$$\overline{r_n^2}/R^2 = \overline{g_n^2}/G^2 = \overline{g_n^2}R^2 \qquad (1)$$

to give a constant $\overline{g_n^2}$ as the slope of the R^2 variation. A constant noise conductance as the channel is depleted suggests that it is associated with the boundary.

The temperature dependence shown in figures 1, 2, 3, 4 indicates that the curves are translated along the R axis as the average channel mobility changes. The vertical lines in figure 1 and the lowest resistance data points in figures 2, 3, 4 show conditions of constant inversion. Thus

$$\overline{r_n^2}/R^2 = f(\mu R) \tag{2a}$$

or approximately

$$\overline{r_n^2}/R^2 \alpha (\mu R)^2 \text{ or } \overline{g_n^2} \alpha \mu^2 \tag{2b}$$

A model which satisfies the data is a number fluctuation occurring at the channel boundary due to some trapping or generation-recombination process. In this case the mobility in the second part of equation 2 should be the local mobility μ_L at the carrier creation point. Then

$$\overline{n_n^2} \alpha \overline{g_n^2}/\mu_L^2 = 1/\left(\mu_L^2 R^2\right)\left(\overline{r_n^2}/R^2\right) \tag{3}$$

To investigate the validity of this assumption mobilities have been measured. For the enhmost of figure 1 the slope, or conductance noise, is almost constant. The channel is very narrow so that the local and average mobilities are similar. The mobility increases at small inversion (large R) by an amount sufficient to give a constant $\overline{n_n^2}$ at each temperature.

Using C-V_{sub}, G-V_{sub} and $g_m = dI_d/dV_{sub}$ measurements the local mobility and carrier density have been determined for the jfets at room temperature and are shown in figures 5 and 6. The carrier density increases into the channel as might be expected from a gate diffused into an epi-layer channel and hence producing compensation. The mobility also rises as the damage and impurity concentration decreases.

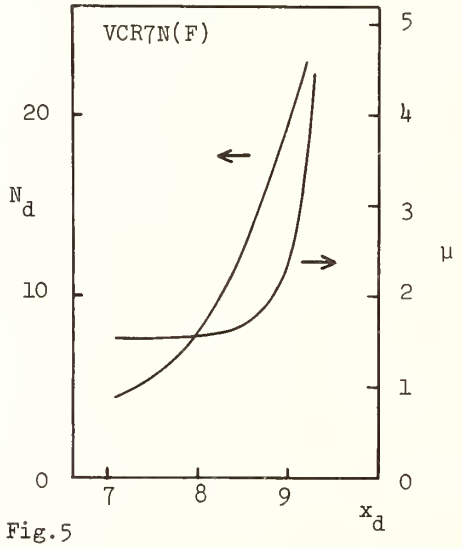

Fig.5

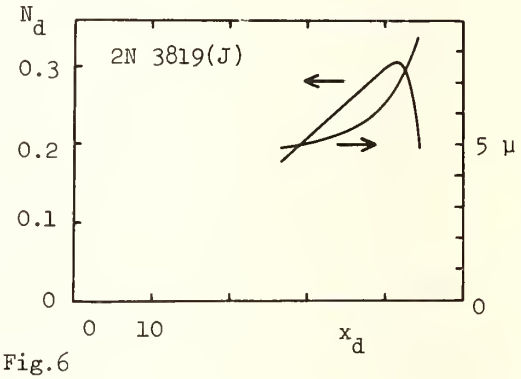

Fig.6

Figs.5 and 6 Carrier density (N_d) in units of 10^{17} cm^{-3}, and mobility (μ) in units of 10^2 cm^2/V sec against depletion layer depth (x_d) in units of μm for the n-channel jfets VCR7N(F) and 2N 3819(J).

The values of the number fluctuation, $\overline{n_n^2}$, calculated from the experimental values of eq(3) for the specimens of figures 2, 3, 4 are shown in figure 7 against d/d_o which is an approximate measure of the position of the channel boundary relative to the position at pinch-off. Figure 8 shows similar results for other jfet specimens.

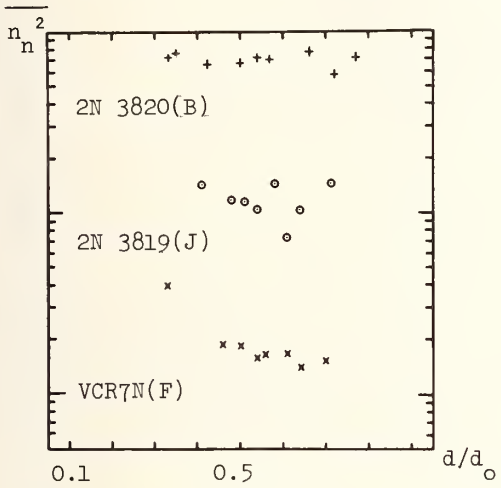

Fig.7

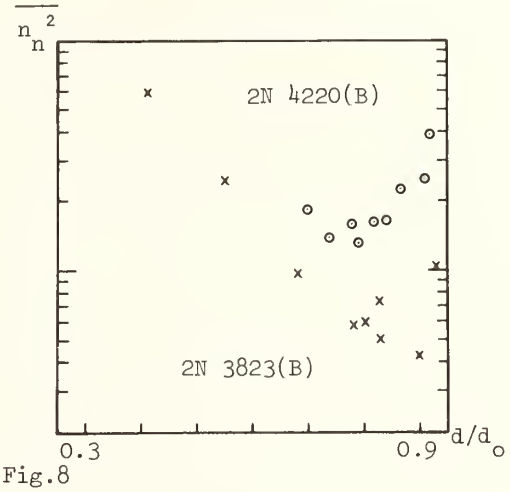

Fig.8

Figs.7 and 8 Experimental values of $(\overline{r_n^2}/R^2)/(\mu_L^2 R^2)$ proportional to $\overline{n_n^2}$ against relative position of the boundary across the channel d/d_o for jfets 2N 3820(3), 2N 3819(J), VCR7N(F); and for jfets 2N 4220(B) and 2N 3823(B).

It can be seen that whereas the value of $\overline{g_n^2}$ from the original noise measurements is not constant, the values of $\overline{n_n^2}$ are almost independent of position as might be expected for well made devices. The specimens of figure 8 show a general increase at low and high values of d. These can be interpreted as the increase in the density of g-r centres near the gate diffusion and an increase in the noise as a space charge develops in the channel.

CONCLUSION

These results suggest that the excess noise is generated by a carrier number fluctuation located at the edge of the conducting channel. This number fluctuation is relatively independent of temperature but is influenced to some extent by the quality of the specimen at the position of the boundary. Experiments on MOST suggest that the presence of an oxide interface produces a large number fluctuation as expected by a modified McWhorter model. In jfets the model of Sah [4] seems appropriate. In this traps within the gate depletion region fill and empty causing a fluctuation in the channel resistance. Since the results suggest that the effect is localised close to the channel boundary, a more detailed account of the influence of the Fermi level in the occupancy, f, and hence the efficiency of the process given by the factor f(1-f) is needed. It has been suggested by Kandiah and Whiting [3] that this results in the noise being concentrated in the transition region between the channel and the depletion region. The near-1/f spectrum probably therefore results from the distribution of the traps in space, energy and occupancy through this region to give the 1/f spectrum by a suitably weighted summation of generation-recombination processes with their individual characteristic times.

REFERENCES

[1] B K Jones, Proc Second Int Symp on 1/f Noise, Orlando 1980, p 245-50.

[2] B K Jones, J Phys D: Appl Phys 14 (1981) 471-90.

[3] K Kandiah and F B Whiting, Solid-State Electron 21 (1978) 1079-88.

[4] C T Sah, Proc IEEE 52 (1964) 795-814.

1/F NOISE IN GATE-CONTROLLED IMPLANTED RESISTORS

K. Amberiadis and A. van der Ziel

EE Dept., University of Minnesota, Minneapolis, MN 55455

L. M. Rucker

Bell Laboratories, Reading, PA

SUMMARY: We measured 1/f noise in gate-controlled p-type implanted resistors in which the surface could be brought from accumulation to strong inversion. The noise increased by a factor of 150 when the surface was brought from accumulation to strong inversion. The results indicate strongly that the noise is due to the interaction of electrons in the inversion layer with the surface oxide. This gives rise to a fluctuating surface potential, which in turn gives a 1/f modulation of the surface mobility.

There are two rival models for explaining 1/f noise in MOSFETs: 1) The number fluctuation model based on McWhorter's[1] work and 2) The mobility fluctuation model, based on the work of Hooge and his coworkers[2].

In order to discriminate between these two models, the noise equivalent current I_{eq} ($I_{eq} = \frac{S_I(f)}{2q}$, where $S_I(f)$ is the noise spectral intensity and q the electronic charge) of a gate-controlled p-type resistor was measured as a function of gate bias. The resistance R was linear and the MOS device had a transconductance of 5 μmhos. Figure 1 gives the I-V characteristics of the device for a gate bias, V_g, of 12 volts. Figure 2 gives the I versus V_g characteristic curve of the device for a constant device bias of 15 volts. The resistance of the device changes about 16% with a change of gate voltage from 0 to 16 volts.

The noise had a 1/f spectrum and, at a given frequency varied as I^2, indicating resistance fluctuation noise. In Figure 3 is shown the parameter I_{eq} as a function of the current I at a frequency of 20 Hz and at zero gate bias. Changing the gate bias from 0 to 19.5 volts and with constant current through the device of 0.5 mA, gives the curve of Fig. 4. We observe that the noise increases by about a factor of 150 when the surface is brought from accumulation to strong inversion. The onset of noise is at 6 volts where the inversion starts, as indicated by the C-V_g characteristics of the device (V_g positive only, Fig. 5).

If the 1/f noise was due to interaction of holes with the surface oxide, the noise should decrease strongly at strong inversion, since it eliminates that interaction. The increase in noise can also not be explained as bulk mobility noise, for then the noise would increase as $(R/R_o)^3$ and with $R/R_o \leq 1.2$ this would amount to an increase in noise of at most 75%. We therefore believe that the noise is due to the interaction of electrons in the inversion layer with the surface oxide. This gives rise to a fluctuating surface potential, which, in turn, gives a 1/f modulation of the surface mobility. The increase in noise is thus surface mobility noise and is not of the bulk variety.

ACKNOWLEDGEMENT

The work was supported by the National Science Foundation and the measured devices were experimental devices provided by the Bell Laboratories.

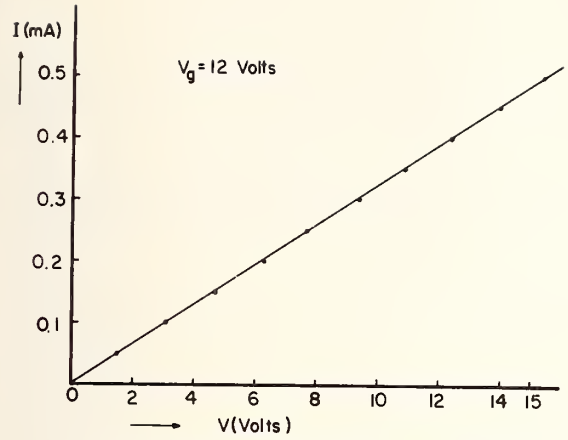

Fig. 1 I-V charactristic of the gate controlled p-type resistor at a gate bias of V_g = 12 Volts.

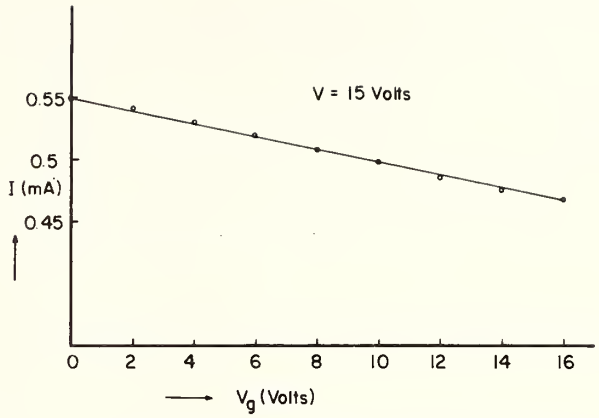

Fig. 2 Chonge of the current of the p-type resistor as a function of gate bias for a constont device bias of 15 Volts.

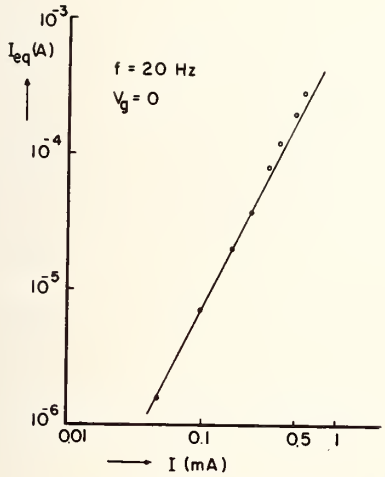

Fig. 3 Noise equivolent current ot the device os o function of current through it at f = 20 Hz.

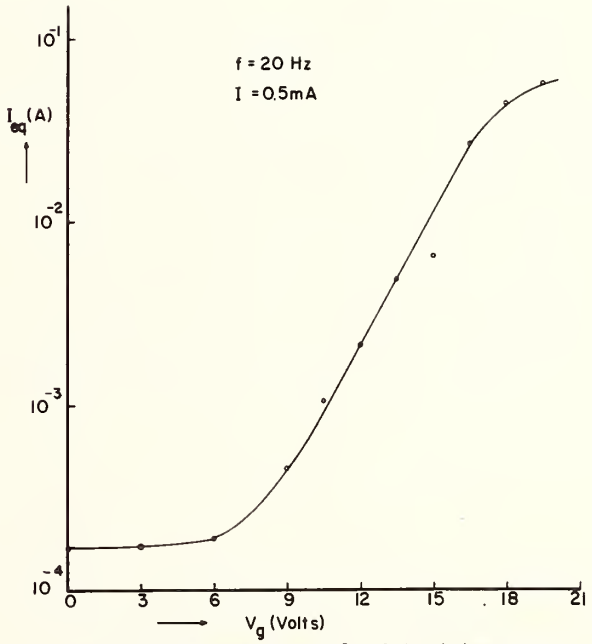

Fig. 4 Noise equivalent current I_{eq} of the device os o function of gote voltage at f = 20 Hz.

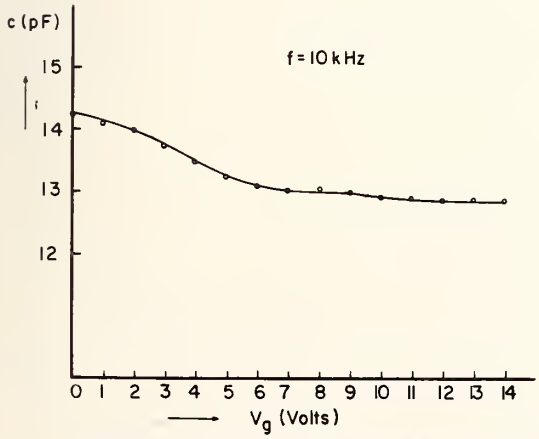

Fig. 5 Capacitance vs gate voltage of the device at 10 kHz ond positive gate voltage.

REFERENCES

1. A. L. McWhorter, "1/f Noise and Related Surface Effects in Germanium", M.I.T. Lincoln Laboratory Report, 80 (1955). Also in Semiconductor Surface Physics, U of Pennsylvania Press, (1957).

2. F. N. Hooge, Physica (Utrecht), 60, 130 (1972). - Ibid, 83B, 14 (1976).

LOW FREQUENCY VOLTAGE NOISE IN SMALL AREA JOSEPHSON JUNCTIONS

L. Krusin-Elbaum and R. F. Voss

IBM Thomas J. Watson Research Center
Yorktown Heights, NY 10598

INTRODUCTION

Recently there has been considerable interest in low frequency voltage noise in Josephson tunnel junctions. Both white [1] and 1/f [2] noise has been studied experimentally and various models have been proposed to explain the origin of the observed fluctuations. Such investigations are of importance because noise limits the performance of devices utilizing Josephson junctions such as SQUIDs (Superconducting QUantum Interference Devices). Moreover, these studies yield insight into the mechanisms responsible for 1/f noise and the manner in which quantum mechanics limits device performance at low temperatures.

The work of Clarke and Hawkins [2] on Nb-NbO_x-Pb Josephson junctions with areas $\approx 3\times10^4$ μm^2 and biased at a current I_b greater then the critical current I_0 gave strong evidence that the excess noise, $S_V(f) \propto 1/f$, arises from fluctuations in I_0 modulating the voltage across the junction. They suggested that equilibrium temperature fluctuations were responsible for the fluctuations in I_0. Their interpretation was an extension of the semiempirical approach developed by Voss and Clarke [3] for thin metal films. With the assumption that the effective volume of the junction for temperature fluctuations extended a Ginzburg-Landau coherence length into each electrode, they found good agreement between the predictions of this model and the measured $S_V(f)$. A similar agreement was found by Ketchen and Tsuei [4] in their investigation of 1/f noise in the dc SQUID. At sufficiently high frequencies $S_V(f)$ becomes white (independent of f) with a crossover frequency that depends on the experimental parameters. This white noise regime was recently investigated by Koch *et al.* [1] who suggest that it originates from equilibrium noise currents in the shunt resistor and produces $S_V \propto R_D^2$, where R_D is the dynamic resistance about the operating point.

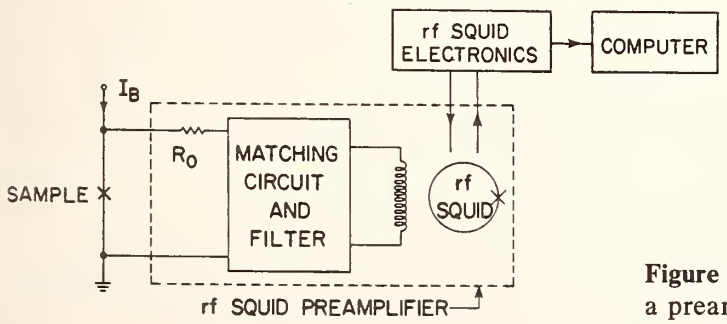

Figure 1. Measuring circuit using rf SQUID as a preamplifier with $R_0 = 25\ \Omega$.

EXPERIMENTAL PROCEDURE

We have performed a detailed investigation of the low frequency voltage noise in well characterized small-area resistively shunted Josephson junctions. The junctions were fabricated with the Pb-alloy technology developed at IBM for computer applications [5]. The junction areas were defined by 2.5 μm diameter SiO windows and were shunted with a normal resistor R $\approx$ 4-7 Ω. I_0 was typically 15-30 μA and the junction parameter $\beta_c = 2\pi I_0 R^2 C/\phi_0 \approx 0.3$ - 0.7, where C is the junction capacitance and ϕ_0 is the flux quantum. For $\beta_c \lesssim 1$ the junction I-V characteristics are non-hysteretic.

An rf SQUID with an impedance matching transformer was used as a low noise preamplifier, in a scheme similar to that used by Ketchen and Tsuei. The sensitivity of the measuring system was limited by the Johnson noise in the 10 Ω resistor in the primary of the impedance matching transformer. A simplified circuit diagram is shown in Fig. 1.

Both the junction and the rf SQUID were immersed in liquid He inside a superconducting shield. The spectral density of the voltage noise $S_V(f)$ at constant I_b and T was obtained from a Fast Fourier Transform (FFT) of the digitized rf SQUID output by an IBM Series/1 computer.

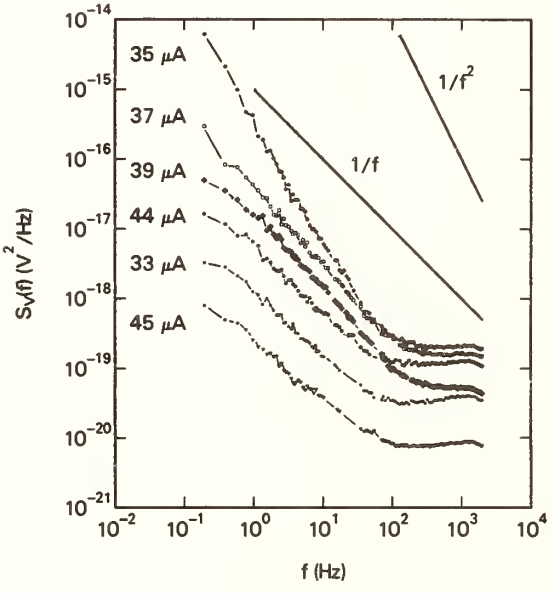

Figure 2. Spectral density of the voltage fluctuations $S_V(f)$ of a Pb-alloy shunted junction at T=3.7K for several values of bias current I_b.

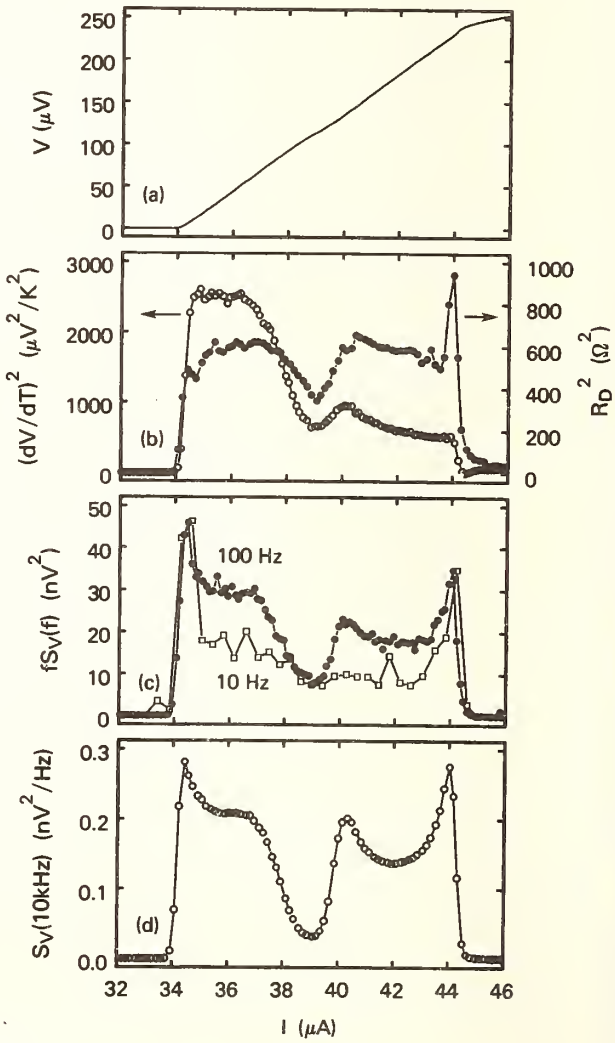

Figure 3. (a) Junction <V> vs I_b at 3.7K. (b) Temperature sensitivity $|dV/dT|^2$ and dynamic resistance R_D^2. (c) $f \times S_V(f)$ for the 1/f-like noise. (d) White noise at 10kHz.

Alternately, I_b was slowly varied by a continuous capacitor discharge while both $\langle V \rangle$ and S_V at some fixed frequency f_0 were digitally recorded. In the latter case $S_V(f_0)$ was estimated using a PAR 124A lockin amplifier with a constant Q filter in the ac voltmeter mode.

RESULTS

Typical power spectral densities for various I_b at 3.7K are shown in Fig. 2 for a junction with $I_0 \approx 34\ \mu A$. The rolloff around 2 kHz is due to the response of the measuring system. There are two distinct regimes separated by a crossover region at about 100 - 200 Hz: a white noise regime at high frequencies and a low frequency excess noise regime in which the noise can be adequately described by a power law $S_V(f) \propto 1/f^{\Delta}$. The magnitude of $S_V(f)$ in both regimes as well as the exponent Δ are strong functions of I_b.

By sweeping I_b and simultaneously measuring various junction parameters, it is possible to clarify this dependence. Figure 3(a) shows $\langle V \rangle$ across the junction as a function of I_b as measured by the rf SQUID. Fig. 3(b) shows R_D^2 from a numerical derivative of the data in Fig. 3(a). R_D exhibits structure including that corresponding to a resonance at $\approx 120\mu V$. Figure 3(b) also shows the temperature sensitivity $|dV/dT|^2$ of the junction which was measured by comparing I-V characteristics at two slightly different temperatures. As an indication of the power law behavior at low frequencies, Fig. 3(c) shows $f \times S_V(f)$ at 10 Hz and 100 Hz with background subtracted. An exact 1/f spectrum ($\Delta=1$) would correspond to coincidence of the two curves. This coincidence occurs only for a small range of I_b. Figure 3(d) shows $S_V(10kHz)$ in the white noise regime corrected for the measuring system response. The variation of Δ with bias current is shown in Fig. 4 obtained from a fit of the data in Fig. 2 to the form $1/f^{\Delta}$. Also shown is the variation in Δ with I_b at 4.2K.

DISCUSSION

As shown in Figs. 2-4, there is an obvious correlation between $S_V(f)$ and the detailed characteristics of the junction. Large increases in the noise are found as I_b is increased above I_0 until the characteristic finally becomes linear at high I_b. This is just the region in which superconducting

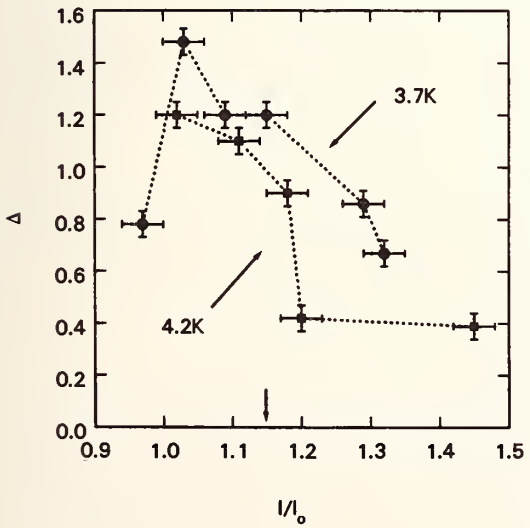

Figure 4. Power law fit of $S_V(f)$ to the form $1/f^{\Delta}$ vs I_b at 3.7K and 4.2K.

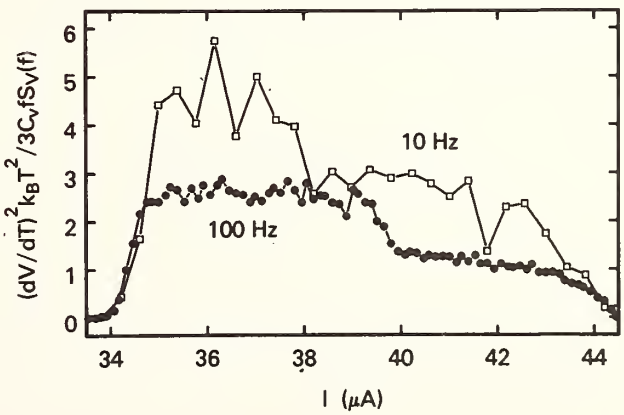

Figure 5. Comparison of $fS_V(f)$ at low f with prediction of thermal fluctuation model.

effects are important. Moreover, the influence of the junction resonance at 120 μV is clearly seen in S_V. The behavior above and below the resonance seems different. The amplitude of the 1/f-like noise is clearly related to both R_D and $|dV/dT|$ indicating a connection with the thermal properties of the junction. The fact that $|dV/dT|$ is not simply proportional to R_D indicates that the temperature sensitivity is not entirely due to changes in I_0 as assumed earlier [2]. By estimating the total heat capacity C_v ($\approx 2\times10^{-13}$J/K) of our junction area [2,4] we can make a direct comparison with the equilibrium thermal fluctuation model. Figure 5 shows the ratio of $fS_V(f)$ to that expected from equilibrium temperature fluctuations, $|dV/dT|^2 k_B T/3C_v$. The agreement in magnitude is reasonably good although the simple model of a junction voltage responding to equilibrium fluctuations cannot explain the changes in exponent Δ with I_b. Presumably, I_b cannot change the time decay of an equilibrium fluctuation although nonequilibrium thermal feedback effects might have this effect.

The magnitude of the white noise shown in Fig. 3(d) is certainly related to R_D^2 as predicted by most theories [1] but the correspondence is not exact. Increased noise appears in the regions of large $|dR_D/dI|$ where nonlinear mixing of noise at higher frequencies is expected to be important. The amplitude of the noise appears to be greater than that expected due to Johnson noise (including mixing) from the shunt [1] indicating that other noise sources may be important.

Although junctions were studied in the temperature range 1.5 - 4.2 K, the large unexplained dependences on I_b preclude any quantitative statements about the T dependence. In general, as T is lowered the structure in the I-V characteristics becomes sharper and the white noise shows significant changes in amplitude (both increases and decreases depending on I_b) while there is only a slight decrease in the 1/f-like regime. In some cases, Lorentzian-like shoulders were observed in $S_V(f)$ at specific T and I_b. Both these shoulders and the 1/f-like behavior varied with changes in the thermal coupling of the junction to the bath.

As with previous work [2,4] we find good agreement of the measured 1/f-like noise with that expected from thermal fluctuations although the detailed dependence of the exponent Δ and amplitude on I_b cannot be explained. Further investigation of both the white and 1/f regimes is needed.

ACKNOWLEDGEMENT

The authors are indebted to M. Ketchen and the Josephson fabrication group headed by J. Greiner for helpful discussions and well characterized samples.

REFERENCES

[1] R. H. Koch, D. J. van Harlingen, and J. Clarke, Phys. Rev. Lett. **45**, 2132 (1980); also R. H. Koch, D. J. van Harlingen, and J. Clarke, Bull. Am. Phys. Soc. **76**, 382 (1981).

[2] J. Clarke and G. Hawkins, Phys. Rev. **B14**, 2826 (1976).

[3] R. F. Voss and J. Clarke, Phys. Rev. **B13**, 556 (1976).

[4] M. Ketchen and C. C. Tsuei, in the Proc. of the 2nd Int. Conf. on SQUID's, Berlin, May 6-9, 1980.

[5] J. H. Greiner *et al.*, IBM J. of Res. and Dev. **24**, No. 2, (1980).

CONCENTRATION FLUCTUATIONS IN SMALL VOLUMES OF IONIC SOLUTIONS

Rutgeris J. van den Berg, Arie de Vos and Jacob de Goede

Laboratory of Physiology and Physiological Physics
Wassenaarseweg 62, 2333 AL Leiden
The Netherlands

INTRODUCTION

In small well defined volumes of ionic solutions, 1/f fluctuations in the resistance have been reported [1-4]. However the results on the intensity of this noise are controversial [1,2]. A quantitative description of 1/f noise in electrolytes is certainly a prerequisite in the search for the underlying physical mechanism. Furthermore its relative intensity plays an important role in the use of 1/f fluctuations in nerve membranes [5] and lipid bilayer membranes [6] to obtain information about ionic channels.
Therefore we reinvestigated the electrical noise in short and narrow capillaries, filled with KCl solutions. Contrary to our expectations a Lorentzian excess noise component was found instead of 1/f noise.

EXPERIMENTAL METHODS

Single capillaries were made in thin membranes (parafilm "M", American Can Company). Their lengths and diameters were about 10 μm. The membranes separated two thoroughly cleaned compartments, which were connected to a pressure source. Ultrafiltration (0.02 μm PTFE-filter, Schleicher and Schüll) and degassing of the ionic solution proved to be essential to minimize noise, induced by particulate impurities. To avoid vapour bubbles the compartments were filled under a low pressure (2 Tor). Thereafter the pressure was brought back to the atmospheric level.
The electrical measurements were made in a six or four point arrangement with Ag-AgCl electrodes (Clark). One pair was used to inject a constant current and two other pairs for measuring the voltage and the voltage fluctuations. This set-up allowed to eliminate the contribution of electrode and amplifier noise from the noise generated in the capillary by estimation of the cross spectral density. This procedure was not utilized when capillary resistances exceeded 2 MΩ. In a number of cases the current and the current fluctuations, under conditions of constant voltage, were measured.
Capillaries were accepted for fluctuation measurements whenever the electrical and flow resistances, within the experimental uncertainty, were in agreement with the theoretical values based on their dimensions.

RESULTS

The thermal noise levels of the capillaries were given by Nyquist's formula:

$$S(f) = 4\ k\ T\ \mathrm{Re}\ \{Z(f)\} \qquad (1)$$

in which Re $\{Z(f)\}$ is the real part of the membrane impedance, k the Boltzmann factor and T the absolute temperature. The d.c. measured capillary resistance was equal within 10% to the resistance $\{Z(+0)\}$ as obtained from eq (1). Current flow with or without an applied pressure ($\Delta P \leq 0.5$ mm H_2O) may raise the intensity of the noise by several orders of magnitude. The frequency dependency of the excess noise could be described by:

$$S(f) = \frac{S(+0)}{1 + (f/f_o)^x} \qquad (2)$$

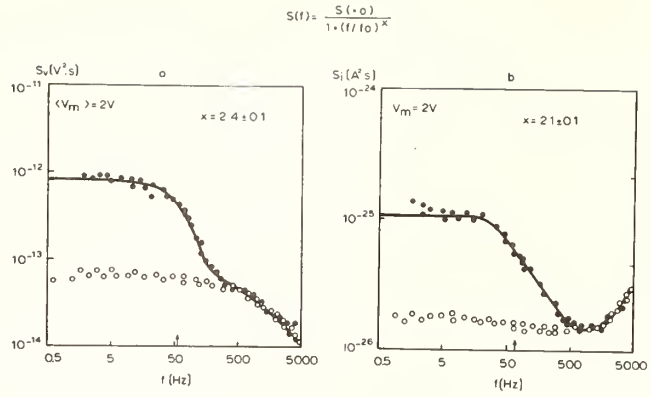

Fig. 1 The spectral density of the noise of a capillary under (a) current clamp and (b) voltage clamp conditions. The length and radius of the capillary were 6.0 μm and 3.5 μm respectively and it was filled with 10^{-2} M KCl solution. In (a) the current was 0.576 μA, producing a mean voltage $\langle V_m \rangle$ of 2.05 V. In (b) the voltage was held constant at 2.00 V. The open symbols represent the noise levels at thermodynamic equilibrium. The continuous lines are obtained by a least-squares curve fitting procedure on 300 frequency points. The arrows correspond to the corner frequencies.

where S(+0) is the low frequency asymptote, f_o represents the corner frequency and x is a constant. Since the noise generated in the capillary is filtered by the membrane impedance, the noise voltage should be multiplied by $|Z(+0)/\ Z(f)|^2$, which requires the measurement of $|Z(f)|$. To circumvent this complication, current fluctuations under the condition of constant voltage were analyzed (Fig. 1). The value of x estimated by curve fitting was found to be close to 2. The low frequency asymptote was proportional to the square of the mean voltage $\langle V \rangle$. No systematic dependence of f_o on the voltage could be found. S(+0) turned out to be inversely proportional to the ionic concentration. The corner frequency was not measurably dependent on the concentrations used.
Application of a pressure difference ($\Delta P > 0.5$ mm H_2O) caused a volume flow (Q), which is consistent with the Hagen-Poiseuille relation:

$$Q = \frac{\pi\ r^4}{8\ \eta\ l}\ \Delta P \qquad (3)$$

where r and l are the radius and length of the capillary respectively and η the viscosity of the solution. Volume flow at a certain level of applied voltage changed both S(+0) and f_o (Fig. 2). An increase in volume flow, independent of its direction, led to a decrease of S(+0) and an increase of f_o. The relative noise variance, however, was independent of ΔP.

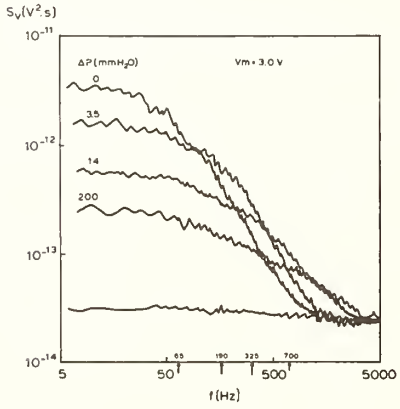

Fig. 2 The spectral density of the voltage fluctuations at various levels of an applied pressure difference, as indicated. A constant current of 1.89 μA produced a membrane voltage V_m of 3.04 V. The corner frequencies indicated by arrows from left to right, correspond to the four spectral densities from top to bottom. The lowest curve represents the thermal noise level, which is predicted by eq (1). Note that at ΔP = 200 mm H_2O where S(+0) has been decreased more than an order of magnitude with respect to its level at ΔP = 0 mm H_2O there still is no 1/f noise detectable. The capillary (6.0 μm long and a radius of 5.5 μm) was filled with 10^{-2} M KCl solution. The Q-ΔP relation was measured to be linear in a ΔP-range from 5 mm to 500 mm H_2O at a temperature of 20°C. The normalized standard error of S(f) is 0.1.

DISCUSSION AND CONCLUSIONS

It will be assumed that the voltage fluctuations are linearly related to the fluctuations in the capillary resistance. These fluctuations are likely to originate from fluctuations in the concentration, the temperature or both. Pressure fluctuations are neglected

(cf. [4]), while association - dissociation noise [7]is very unlikely to occur in diluted aqueous KCl solution. We omitted generation - recombination noise at the walls of the capillary. Since in short capillaries the electric field ($\vec{E}$) is nonuniform, the spatial variation of $\vec{E}$ must be taken into account. The correlation function of the voltage fluctuations, $\Delta V(t)$ under a constant current (I) can be written [8,9] as:

$$\langle \Delta V(0)\Delta V(\tau)\rangle = \frac{1}{\rho^4 I^2} \int_{\Omega} d\vec{r} \int_{\Omega} d\vec{r}' \langle \Delta\rho(\vec{r},0)\Delta\rho(\vec{r}',\tau)\rangle \left|\vec{E}(\vec{r})\right|^2 \left|\vec{E}(\vec{r}')\right|^2 \qquad (4)$$

In this expression $\Delta\rho(\vec{r},t)$ represents the fluctuation of the resistivity ρ. The integrations are carried out over the conducting volume (Ω) of our system. The resistivity correlation function can be calculated in terms of fluctuations of the charge carrier density $\Delta n(\vec{r},t)$ around the average density n and temperature fluctuations $\Delta T(\vec{r},t)$, viz.

$$\langle \Delta\rho(\vec{r},0)\Delta\rho(\vec{r}',\tau)\rangle = \frac{\lambda^2 \rho^2}{n^2} \langle \Delta n(\vec{r},0)\Delta n(\vec{r}',\tau)\rangle + \frac{\Theta^2 \rho^2}{T^2} \langle \Delta T(\vec{r},0)\ \Delta T(\vec{r}',\tau)\rangle \qquad (5)$$

with $\lambda = \frac{n}{\rho}\left(\frac{\partial\rho}{\partial n}\right)_{p,T}$ and $\Theta = \frac{T}{\rho}\left(\frac{\partial\rho}{\partial T}\right)_{p,n}$

It has been assumed that Δn and ΔT are not correlated. Neglecting possible contributions to the variances, due to the fact that the system is not at equilibrium, we find from thermodynamic fluctuation theory, also using electro-neutrality, for the relative variance of the voltage fluctuations

$$\frac{\langle \Delta V^2\rangle}{\langle V\rangle^2} = \left\{ \frac{\lambda^2}{n} + \frac{\Theta^2 k}{c_p} \right\} \frac{1}{V_{eff}} \qquad (6)$$

in which c_p is the heat capacity at constant pressure per unit volume and V_{eff} is an effective volume, expressed as:

$$V_{eff} = \frac{\rho^2 \langle V\rangle^2 I^2}{\int_{\Omega} d\vec{r} \left|\vec{E}(\vec{r})\right|^4} \qquad (7)$$

For the geometry of our capillaries it is reasonable to take as the effective volume (9):

$$V_{eff} = 20\pi r^3 \frac{(1+\Phi)^2}{1+20\Phi} \qquad (8)$$

where $\Phi = l/r$.

The two terms of the right hand side of eq 6 can be calculated. In the concentration range covered the relative variance of the temperature fluctuations is one to three orders of magnitude smaller than the relative variance of the concentration noise. Therefore we estimated V_{eff} from eq (6) by neglecting the contribution of the temperature fluctuations. Fig. 3 shows that the noise at different concentrations is concentrated in the same effective volume, which can be described by eq (8). This result justifies the use of eq (8) to calculate V_{eff} for different capillaries. In all capillaries studied the variance of the noise turned out to be in good agreement with the variance predicted by concentration fluctuations as the sole noise source.

In general the spectral density will be determined by the kinetics of the decay of the concentration fluctuations, which is governed by diffusion, modified by volume flow. As we could not manipulate pressure differences better than 0.5 mm H_2O, we cannot rule out that our spectral densities at no applied pressure are dominated by Poiseuille flow. This type of noise has been demonstrated in narrow, but long capillaries and was described by a Lorentzian function [7]. Volume flow, which could also originate from electro-osmosis, should lead to a spectral density proportional to $\langle V\rangle$ [4], contrary to our observations. At present it is hard to explain convincingly the Lorentzian frequency dependence of the noise. Since Poiseuille flow leads to a Lorentzian in both short and long capillaries, this sug-

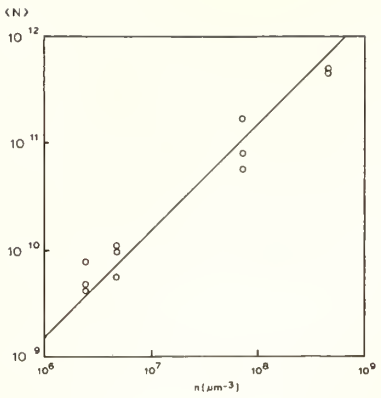

Fig. 3 For one capillary $\langle N \rangle \equiv \frac{\langle V \rangle^2}{\langle \Delta V^2 \rangle} \lambda^2$ obtained from the fluctuation measurements is plotted against the total charge carrier density n. The variance of the noise was measured under the condition of no applied pressure at voltages ranging between 0.2 to 1.0 V. The value of λ was calculated from the Debije - Hückel - Onsager parameters, using Shedlovsky's approximation method for concentrations up to 10^{-1} M. For higher concentrations λ was obtained graphically from the resistivity data given in [10]. From eq (6) it follows that for concentration fluctuations: $\langle N \rangle = V_{eff}\, n$. Drawn is the regression line: log $\langle N \rangle$ = log V_{eff} + log n, with V_{eff} estimated as 1.5×10^3 μm³. V_{eff} calculated from the capillary dimensions (eq 8) was 1.9×10^3 μm³. Since the relative error in V_{eff} may amount 0.4, due to the uncertainty in r, these values agree satisfactorily.

gests that the fringing electric field (eq 4) is not an important factor in determining the shape of the spectral density.
In all experiments we could not detect a clear 1/f noise component. Evidently, if 1/f noise exists in electrolytes it can not be explained by concentration fluctuations in a linear noise theory. In order to get a rough measure of the 1/f noise intensity possible we take as an upper limit twice the standard deviation of the low frequency asymptote. Expressing the 1/f noise intensity as [1]:

$$S(f) = \frac{\alpha}{V_{eff}\, n} \frac{\langle V \rangle^2}{f} \qquad (9)$$

we calculate as an upper limit for α:

$$\alpha \leq 4 \times 10^{-3}$$

This value approaches 2×10^{-3}, as found for homogeneous metals and semiconductors. It would be extremely interesting to determine whether the actual value of α in electrolytes indeed has this magic value.

We thank Kees Versluis for his indispensible assistance with the electronics. This research was supported by the Netherlands Organization for the Advancement of Pure Research (ZWO).

REFERENCES

[1] F.N. Hooge, and J.L.M. Gaal, Philips Res. Rep. 26, 77 (1971).
[2] D.L. Dorset, and H.M. Fishman, J. Membr. Biol. 21, 291 (1975).
[3] M.J. Strassfeld, and M.E. Green, in: Proc. Second Intern. Symp. on 1/f noise, Univ. of Florida, Gainesville (1980).
[4] M.W. Kim, Y.C. Chou, W.I. Goldburg, and A. Kumar, Phys. Rev. A. 22, 22 (1980) and references cited therein.
[5] R.J. van den Berg, Electrical fluctuations in myelinated nerve membrane. Thesis. State Univ. of Leiden (1978).
[6] S.M. Bezrukov, G.M. Drabkin, L.A. Fonina, A.I. Irkhin, E.I. Melnik, and A.I. Sibilev, Acad. Sci. USSR, Leningrad Nuclear Phys. Inst. 598 (1980).
[7] G. Feher,and M.B. Weissman, Proc. Natl. Acad. Sci. 70, 870 (1973).
[8] M.B. Weissman, Phys. Rev. Lett. 35,689 (1975).
[9] L.K.J. VanDamme, Appl. Phys. 11, 89 (1976).
[10] R.A. Robinson, and R.H. Stokes, Electrolyte Solutions, Butterworths, London (1959).

1/f NOISE IN MOS TRANSISTORS IN OHMIC REGION UNDER STRONG INVERSION

Hong S. Min

Department of Electrical Engineering
University of Minnesota
Minneapolis, MN 55455

1. INTRODUCTION

A theoretical 1/f noise model for homogeneous semiconductors given by Min [1], where 1/f noise is shown to be caused by dominance of interband scattering over intraband scattering, which gives mobility fluctuations, and where it is shown that 1/f noise in homogeneous nondegenerate semiconductors can be described by Hooge's relation [2], will be applied to 1/f noise calculation in MOS transistors. Assuming that 1/f noise occurs only in the defect-concentrated regions where interband scattering is dominant over intraband scattering, and that under strong inversion electron-electron scattering becomes an important scattering mechanism, it will be shown that the main difficulty encountered in applying Hooge's relation to a derivation of 1/f noise formulas for MOS transistors, which is that the calculated 1/f noise is 10^3 to 10^4 times as large as the experimentally determined noise [2], can be solved. It will be also shown that an introduction of a nonuniformity into the channel can explain the conflicting experimental results between n-channel and p-channel devices [3].

2. 1/f NOISE FOR MOS TRANSISTORS WITH UNIFORM CHANNELS IN THE OHMIC REGION

A diagram of an n-channel MOS transistor with uniform channel is given in Fig.1a. The channel will be divided into many sublayers parallel to the interface. We assume that in each sublayer the electron concentration profile $n(x,t)$ and the electron mobility profile $\mu(x,t)$ are homogeneous in y-z plane in the ohmic region, where x is the distance from the $Si-SiO_2$ interface, and t is time.

Now Hooge's relation will be applied to each sublayer to calculate the short-circuited 1/f noise current for each sublayer. When noise current in each sublayer is assumed to be mutually independent, the spectral intensity of the total 1/f noise current through the channel denoted by $S_{I_d}(f)$ can be written as

$$S_{I_d}(f) = \sum_i \alpha(x_i)\Delta I_{ds}(x_i)^2/[wL\Delta x n_s(x_i)f], \tag{1}$$

where the summation is taken all over the sublayers, the subscript s denotes the steady state values, $\Delta I_{ds}(x_i)$ is the dc current through the i-th sublayer, f is the frequency, and $\alpha(x_i)$ is Hooge's constant for i-th sublayer. $\alpha(x_i)$ has been believed to be a constant with a magnitude of $2X10^{-3}$, but there are many experimental evidences [4] that $\alpha(x_i)$ may vary in different samples. Min [1] has also shown that $\alpha(x_i)$ should be a function of the density of defect centers. For MOS transistors the defect-concentrated regions will be located near the $Si-SiO_2$ interface with a thickness of x_f, which will be much smaller than the channel thickness δ. So we will assume that

$$\alpha(x_i) = \alpha_H \quad \text{for } 0 \leq x_i \leq x_f, \quad \text{and} \quad \alpha(x_i) = 0 \text{ elsewhere.} \tag{2}$$

From eqs (1) and (2) we can show that

$$S_{I_d}(f)/I_{ds}^2 = (qR/L^2 f)\alpha_H \mu_{1/f}, \tag{3}$$

with (compare with $\mu_{1/f}$ in reference 5)

$$\mu_{1/f} = \int_0^{x_f} dx \mu_s(x)^2 n_s(x) / \int_0^{\delta} dx \mu_s(x) n_s(x), \tag{4}$$

where -q is the electron charge, δ is the channel thickness, R is the dc channel resistance

in ohmic region, and I_{ds} is the total dc current through the channel given by

$$I_{ds} = (qw/L)V_{ds}N_I\mu_{eff}, \tag{5}$$

with

$$N_I = \int_0^{\delta} dx n_s(x), \qquad \mu_{eff} = \int_0^{\delta} dx \mu_s(x) n_s(x) / \int_0^{\delta} dx n_s(x). \tag{6}$$

Now to evaluate eq (3), the functional form of $\mu_s(x)$ and $n_s(x)$ should be given. For $n_s(x)$ we will use an approximate quantummechanical solution of the inversion layer carrier distribution [5,6] given by

$$n_s(x) = n_o \exp(-x/h) \quad \text{for } 0 \leq x \leq 4h = \delta, \quad \text{and} \quad n_s(x) = 0 \text{ elsewhere}, \tag{7}$$

where n_o is the carrier concentration at the interface, and h is a constant.
Since it seems that there is no conclusive theoretical model for the local mobility $\mu_s(x)$, we will just assume that when the electron concentration gets larger, electron-electron scattering becomes an important scattering mechanism. If this is the case, $\mu_s(x)$ can be written as [5,7]

$$\mu_s(x) = \mu_o/(1+\sqrt{n_s(x)/n_c}), \tag{8}$$

where n_c is a critical electron concentration, μ_o is the electron mobility when $n_s(x) \ll n_c$, and in μ_o the effect on the mobility of the electric field perpendicular to the interface is assumed to be taken into account quantummechanically even though it is not known how the electric field in the x-direction reduces the mobility. Here we also assume tacitly that once the quantummechanical effect gets important, an increase of the electric field in the x-direction doesn't have much effects on reduction in μ_o.

Using eqs (3),(4),(7) and (8), it can be shown that

$$S_{I_d}(f) = I_{ds}^2(q\mu_o/fL^2)R\alpha_H x_f/h = (q\mu_o/fL^2)I_{ds}V_{ds}\alpha_H x_f/h \quad \text{for } n_o/n_c \ll 1 \text{ and } x_f/h \ll 1, \tag{9a}$$

$$S_{I_d}(f) = I_{ds}^2(q\mu_o/fL^2)R^2G_f\alpha_H = (q^2\mu_o^2 w/fL^3)V_{ds}^2\alpha_H n_c x_f \quad \text{for } n_o/n_c \gg 1 \text{ and } x_f/h \ll 1 \tag{9b}$$

with $G_f = qwx_f n_c \mu_o/L$ and V_{ds} being the dc drain voltage, where eq (9a) is same as Klaassen's formula [8] if $\alpha_H x_f/h$ is replaced by Klaassen's $\bar{\alpha}$, and eq (9b) is same as the formula for the number fluctuation model [3] if $\alpha_H n_c x_f$ can be replaced by $[N_T(E_f)]_{eff}/\varepsilon$ according to van der Ziel. The facts that x_f/h in eq (9) is believed to be much smaller than 1, and that $S_{I_d}(f)/I_{ds}^2$ is proportional to R^2 when R is small, can solve the main difficulty encountered in applying Hooge's relation to a derivation of 1/f noise formulas for MOS transistors.

To find the dependence of $S_{I_d}(f)$ on the dc gate voltage V_{gs}, and to obtain the spectral intensity of the equivalent input noise voltage at the gate defined by

$$S_{V_g}(f) = S_{I_d}(f)/g_m^2 \tag{10}$$

with g_m being the transconductance given by $g_m = \partial I_{ds}/\partial V_{gs}$, the functional dependence of N_I in eq (6) on V_{gs} should be known. Empirically we may assume the following relationship

$$qN_I \begin{cases} = k_\gamma C_{ox}(V_{gs}-V_\gamma)^\gamma & \text{with } \gamma \geq 1 \text{ and for } V_T \leq V_{gs} \leq V_{gc}, \\ = C_{ox}(V_{gs}-V_T) & \text{for } V_{gs} \geq V_{gc}, \end{cases} \tag{11}$$

where V_γ and V_{gc} are the critical gate voltages chosen empirically, k_γ and γ are constants, C_{ox} is the oxide capacitance per unit area, and V_T is the threshold voltage.
To derive the noise formulas, first we will put

$$N_I = k_\gamma C_{ox}(V_{gs}-V_\gamma)^\gamma \quad \text{for all } V_{gs} \geq V_T, \tag{12}$$

and then we will return to the case of eq (11) later. Using eqs (5),(9),(10) and (12), we can show that

$$S_{I_d}(f) \begin{cases} = (qwk_\gamma\mu_o^2/fL^3)C_{ox}V_{ds}^2(V_{gs}-V_\gamma)^\gamma \alpha_H x_f/h & \text{for } n_o/n_c \ll 1, \\ = (q^2w\mu_o^2/fL^3)V_{ds}^2\alpha_H n_c x_f & \text{for } n_o/n_c \gg 1, \end{cases} \tag{13}$$

$$S_{V_g}(f) = (q/fLwk_\gamma\gamma^2)C_{ox}^{-1}(V_{gs}-V_\gamma)^{2-\gamma}\alpha_H x_f/h \qquad \text{for all } n_o. \tag{14}$$

Curves of eqs (9),(13) and (14) for the cases of eq (12) with $\gamma=1$ and $\gamma=2$, and eq (11) with $\gamma=2$ are shown in Fig.2. Experimentally p-channel devices usually show the noise characteristics of Fig.2 [3].

3. 1/f NOISE IN MOS TRANSISTORS WITH NONUNIFORM CHANNELS IN THE OHMIC REGION

We consider an n-channel MOS transistor with a nonuniform channel with a narrow defect-concentrated region (such as misfits or interfacial dislocations [9]) lying perpendicular to the interface as shown in Fig.1b, where the region between $L_1<y<L_1+L_2$ is the newly introduced defect-concentrated region. Let R_1, R_2 and R_3 be the dc resistances for regions I, II and III, respectively (see Fig.1b). We assume that $L_2 \ll L_1+L_3$ and $R_2 \ll R_1+R_3$. We also assume that $n_s(x)$ is given by eq (7) throughout the channel, and that Hooge's constant $\alpha(x,y)$ and the mobility $\mu(x,y)$ are given by

$$\alpha(x,y) \begin{cases} =\alpha_{H1} & \text{for } 0<x<x_f \quad \text{in regions I and III,} \\ =\alpha_{H2} & \text{for } 0<x<\delta \quad \text{in region II,} \\ = 0 & \text{elsewhere,} \end{cases} \tag{15}$$

$$\mu(x,y) \begin{cases} = \mu_{o1}/(1+\sqrt{n_s(x)/n_{c1}}) & \text{for regions I and III,} \\ = \mu_{o2}/(1+\sqrt{n_s(x)/n_{c2}}) & \text{for region II,} \end{cases} \tag{16}$$

where we usually have $n_{c1}<n_{c2}$, $\mu_{o1}>\mu_{o2}$ [5], and $\alpha_{H1}<\alpha_{H2}$.
When $\mu_{1/f1}$ is $\mu_{1/f}$ for regions I and III defined by eq (4), and $\mu_{1/f2}$ is for region II given by

$$\mu_{1/f2} = \int_0^\delta dx\mu_s(x,y)^2 n_s(x,y) / \int_0^\delta dx\mu_s(x,y)n_s(x,y), \tag{17}$$

the spectral intensity of the total noise current $S_{I_d}(f)$ can be shown to be

$$S_{I_d}(f) = [qI_{ds}V_{ds}/f(L_1+L_3)^2]\{\alpha_{H1}\mu_{1/f1} + \alpha_{H2}\mu_{1/f2}[L_2/(L_1+L_3)](\mu_{eff1}/\mu_{eff2})^3\}, \tag{18}$$

where μ_{eff1} and μ_{eff2} are the effective electron mobilities for regions I and II, respectively, which are defined by eq (6).

If the first term of eq (18) is dominant, we will have the same result for $S_{I_d}(f)$ as obtained for the MOS transistors with uniform channels.

When the second term of eq (18) is dominant, to interpret eq (18) we can show that the following rough approximations can be made for μ_{eff1}, μ_{eff2}, $\mu_{1/f1}$ and $\mu_{1/f2}$ by using the exact expressions of them:

$$\mu_{eff1} = \mu_{o1}/[1+(2/3)\sqrt{n_o/n_{c1}}], \qquad \mu_{eff2} = \mu_{o2}/[1+(2/3)\sqrt{n_o/n_{c2}}], \tag{19}$$

$$\mu_{1/f1} = \mu_{o1}(x_f/h)/[1+(4/3)\sqrt{n_o/n_{c1}}], \quad \mu_{1/f2} = \mu_{o2}/[1+(2/3)\sqrt{n_o/n_{c2}}]. \tag{20}$$

When we assume eq (12) for noise calculations, we have from eqs (18)-(20)

$$S_{I_d}(f) \cong [qwL_2\mu_{o1}^4 k_\gamma \alpha_{H2}/f(L_1+L_3)^4\mu_{o2}^2]C_{ox}V_{ds}^2(V_{gs}-V_\gamma)^\gamma \times [1+\theta_2(V_{gs}-V_\gamma)^{\gamma/2}]^2/[1+\theta_1(V_{gs}-V_\gamma)^{\gamma/2}]^4, \tag{21}$$

where we usually have $\theta_1>\theta_2$, and θ_1 and θ_2 are given by

$$\theta_1 = (2/3)\sqrt{k_\gamma C_{ox}/qn_{c1}}h, \qquad \theta_2 = (2/3)\sqrt{k_\gamma C_{ox}/qn_{c2}}h. \tag{22}$$

Now from eqs (5),(10) and (21) it can be shown that
for the ranges of V_{gs} with $\theta_1(V_{gs}-V_\gamma)^{\gamma/2} \ll 1$, (denoted by region A in Fig.3)

$$S_{I_d}(f) = \frac{qwL_2\mu_{o1}{}^4 k_\gamma \alpha_{H2}}{f(L_1+L_3)^4\mu_{o2}{}^2} C_{ox}V_{ds}{}^2(V_{gs}-V_\gamma)^\gamma = \frac{qL_2\mu_{o1}{}^3\alpha_{H2}}{f(L_1+L_3)^3\mu_{o2}{}^2} I_{ds}{}^2(R_1+R_3), \quad (23)$$

$$S_{V_g}(f) = [qL_2\mu_{o1}{}^2\alpha_{H2}/f(L_1+L_3)^2 w\mu_{o2}{}^2 k_\gamma \gamma^2] C_{ox}{}^{-1}(V_{gs}-V_\gamma)^{2-\gamma}, \quad (24)$$

for the ranges of V_{gs} with $\theta_2(V_{gs}-V_\gamma)^{\gamma/2} \ll 1 \ll \theta_1(V_{gs}-V_\gamma)^{\gamma/2}$, (denoted by region B in Fig.3)

$$S_{I_d}(f) = \frac{81qwL_2\mu_{o1}{}^4(qn_{c1}h)^2\alpha_{H2}}{16f(L_1+L_3)^4\mu_{o2}{}^2 k_\gamma} C_{ox}{}^{-1}V_{ds}{}^2(V_{gs}-V_\gamma)^{-\gamma} = (\frac{27}{8})^2 \frac{qw^3L_2\mu_{o1}{}^6(qn_{c1}h)^3\alpha_{H2}}{f(L_1+L_3)^6\mu_{o2}{}^2} I_{ds}{}^2 \times (R_1+R_3)^4, \quad (25)$$

$$S_{V_g}(f) = \frac{81qL_2\mu_{o1}{}^2(qn_{c1}h)\alpha_{H2}}{16f(L_1+L_3)^2 w\mu_{o2}{}^2 k_\gamma{}^2\gamma^2} C_{ox}{}^{-2}(V_{gs}-V_\gamma)^{2\gamma-2}, \quad (26)$$

and for the ranges of V_{gs} with $\theta_2(V_{gs}-V_\gamma)^{\gamma/2} \gg 1$, (denoted by region C in Fig.3)

$$S_{I_d}(f) = \frac{9qwL_2\mu_{o1}{}^4(qn_{c1}h)n_{c1}\alpha_{H2}}{4f(L_1+L_3)^4\mu_{o2}{}^2 n_{c2}} V_{ds}{}^2 = \frac{9qwL_2\mu_{o1}{}^4(qn_{c1}h)n_{c1}\alpha_{H2}}{4f(L_1+L_3)^4\mu_{o2}{}^2 n_{c2}} I_{ds}{}^2(R_1+R_3)^2, \quad (27)$$

$$S_{V_g}(f) = (9/4)[qL_2\mu_{o1}{}^2 n_{c1}\alpha_{H2}/f(L_1+L_3)^2 w\mu_{o2}{}^2 n_{c2} k_\gamma \gamma^2] C_{ox}{}^{-1}(V_{gs}-V_\gamma)^{2-\gamma}. \quad (28)$$

Fig.3 shows the curves of eqs (23)-(28). Similar types of curves as in Fig.3a have been observed by Park [10]. Also similar curves as in Fig.3b have been observed by Vandamme et al [11] in the devices with low surface state densities, where the second term of eq (18) may easily become dominant over the first term. Since the curves in Fig.3c have been found more often in n-channel devices [3], we may say that n-channel devices have more possibilities to have nonuniform channels than p-channel devices.

4. FINAL DISCUSSION

We have derived various theoretical expressions of 1/f noise characteristics of MOS transistors. These noise characteristics depend on the dc characteristics (specially N_I vs V_{gs}, and $\mu_s(x)$ vs $n_s(x)$ characteristics) and geometries (specially uniformity of channels) of devices, and we have shown that one noise characteristic can not predict other noise characteristics without knowing the dc characteristics and geometries. It has been quite common that interpretations of experimental 1/f noise characteristics of MOS transistors are confined to one or two specific types of noise datas with assumptions of $qN_I = C_{ox}(V_{gs}-V_T)$ and uniform channels. But as we have shown above, to understand the 1/f noise characteristics of MOS transistors we must analyze all the noise characteristics discussed in this paper as well as the dc characteristics simultaneously without interpreting each noise data separately.

This work was supported by the government of R.O.K. I am grateful to Dr. A. van der Ziel for his encouragement.

REFERENCES

1. H.S. Min, J. Appl. Phys. 51, 1637 (1980), and in Proc. Symposium on 1/f Fluctuations, Orlando, Florida (1980).
2. F.N. Hooge, Physica 83B, 14 (1976).
3. A. van der Ziel, in Proc. Symposium on 1/f Fluctuations, Orlando, Florida (1980).
4. H.I. Hanafi and A. van der Ziel, in Proc. Symposium on 1/f Fluctuations, Tokyo (1977).
5. L.K.J. Vandamme, in Proc. Symposium on 1/f Fluctuations, Orlando, Florida (1980), and Solid-State Electron. 23, 317 (1980).
6. C.T. Hsing, Ph.D. Thesis, University of Florida (1977).
7. F. Dannhäuser, Solid-State Electron. 15, 1371 (1972).
8. F.M. Klaassen, IEEE Trans. Electron Devices ED-18, 887 (1971).

9. G.F. Neumark, Phys. Rev. Lett. 21, 1252 (1968).
10. H.S. Park, Ph.D. Thesis, University of Minnesota (1981).
11. L.K.J. Vandamme and A.H. de Kuijper, in Proc. Symposium on Noise in Physical Systems, Bad Nauheim, Germany (Springer-Verlag, Berlin, 1978).

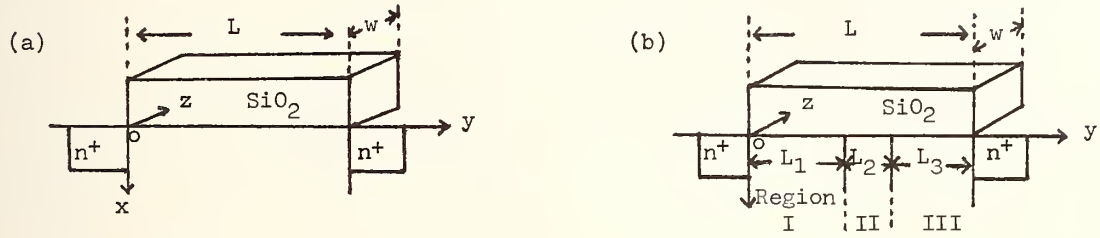

Fig. 1 Diagrams of MOS transistors with coordinates. (a) A MOS transistor with an uniform channel. (b) A MOS transistor with a nonuniform channel.

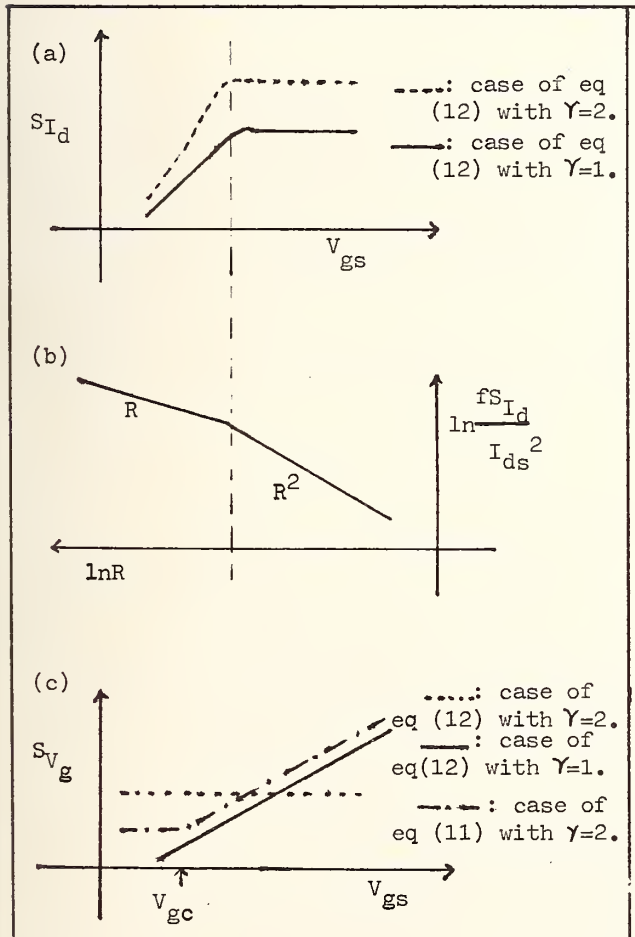

Fig. 2 Asymtotic curves of noise characteristics of MOS transistors with uniform channels. (a) $S_{I_d}(f)$ vs V_{gs}. (b) $\ln(fS_{I_d}/I_{ds}^2)$ vs $\ln R$. (c) S_{V_g} vs V_{gs}. (relative magnitudes are not important)

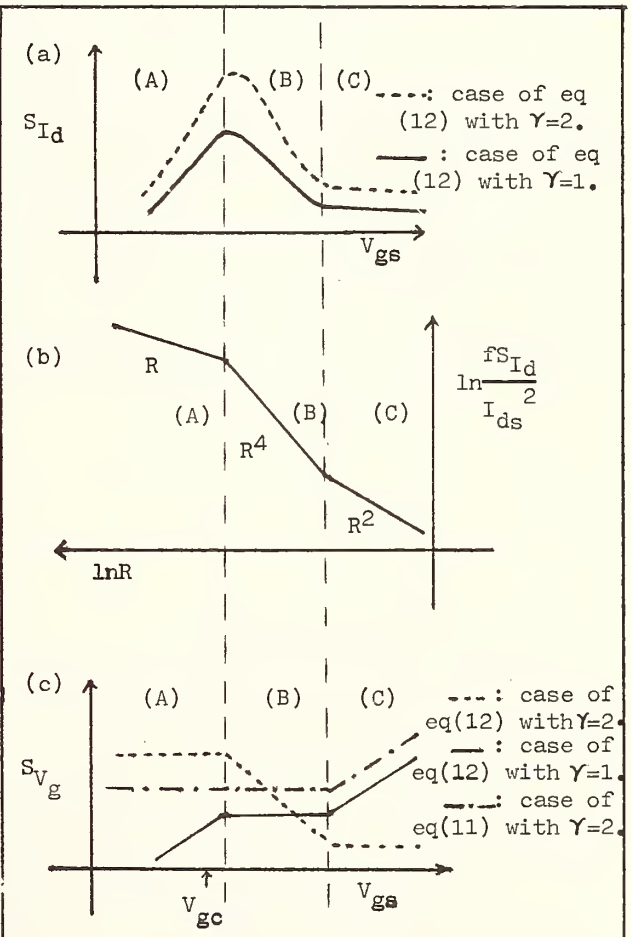

Fig. 3 Asymtotic curves of noise characteristics of MOS transistors with nonuniform channels. (a) $S_{I_d}(f)$ vs V_{gs}. (b) $\ln(fS_{I_d}/I_{ds}^2)$. (c) $S_{V_g}(f)$ vs V_{gs}. (relative magnitudes are not important)

1/f NOISE MODELS IN MOSFETs

H. S. Park and A. van der Ziel

E. E. Dept., University of Minnesota, Minneapolis, MN 55455, U.S.A.

SUMMARY

In the number fluctuation model of 1/f noise, the effective oxide trap density at Fermi level, $N_T(E_F)_{eff}$ is evaluated as a function of the gate bias voltage V_g. In the mobility fluctuation model, Hooge's parameter α is found at the same condition as in the number fluctuation model. The values for $N_T(E_F)_{eff}$ and α from the experimental results are reasonable. The $N_T(E_F)_{eff}$ is approximately proportional to the $(V_g - V_T)$ and the α is almost independent of the $(V_g - V_T)$. Where V_T is the threshold voltage of the device. But we can not discriminate between the models from the data.

To discriminate, we measure the drain current spectrum $S_{Id}(f)$ versus drain bias voltage V_d. In the number fluctuation model, $S_{Id}(f)$ increases monotonically with increasing V_d until saturation. In the mobility fluctuation model, because of the electric field dependence of α, $S_{Id}(f)$ goes through a maximum well below saturation and level off to a lower value.

Also the noise curves calculated numerically are presented for both of the models.

MEASUREMENT OF $N_T(E_F)_{eff}$ AND α

In the number fluctuation model of 1/f noise [1], the drain noise spectrum at low drain bias V_d under strong inversion is given as

$$S_{I_d}(f) = (q^2\mu^2 w\, V_d^2/fL^3)\, N_T(E_F)_{eff}\, /\epsilon \tag{1}$$

whereas for the mobility fluctuation model of 1/f noise [2],[1]

$$S_{I_d}(f) = (q\mu/fL^2)\, I_d V_d \alpha \tag{2}$$

Here w and L are the width and the length of the conducting channel, ϵ is a tunneling parameter which has a value of about 10^8 cm^{-1}, μ is the mobility of the carrier, q is the electron charge and I_d is the drain current.

To evaluate the parameters, $N_T(E_F)_{eff}$ and α, from the data, first we observe the drain conductance g_d. In the case of low V_d and under strong inversion, g_d is

$$g_d = I_d/V_d = (\mu w C_{ox}/L)(V_g - V_T) \tag{3}$$

Knowing the dimensions of the device and evaluating the threshold voltage V_T yield mobility μ as a fuction of V_g. Next from the measured value of $S_{Id}(f)$, eq (1) and eq (2), we can find the values of $N_T(E_F)_{eff}$ and α. Figure 1 shows $N_T(E_F)/\epsilon$ versus V_g for various devices. Figure 2 shows α as a function of V_g for three devices.

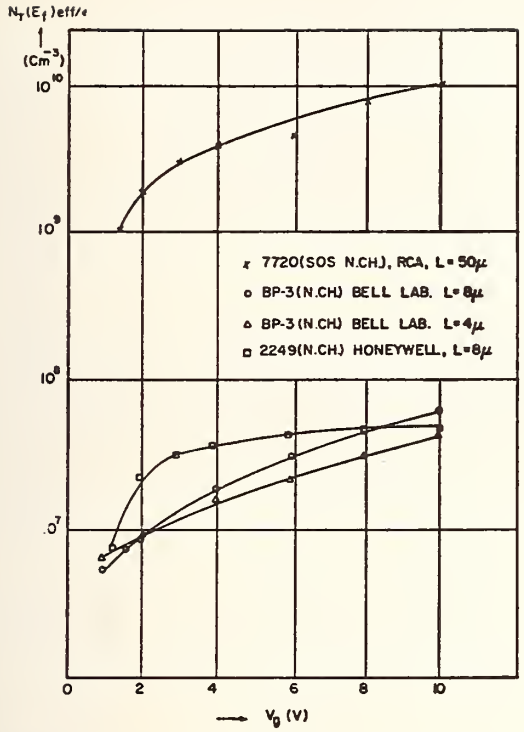

Fig. 1 $N_T(E_F)_{eff}/\epsilon$ versus the gate voltage. At larger V_g, $N_T(E_F)_{eff}$ varies almost linearly with V_g. For the silicon-on-sapphire device the parameter shows that the value is about a factor 200 larger.

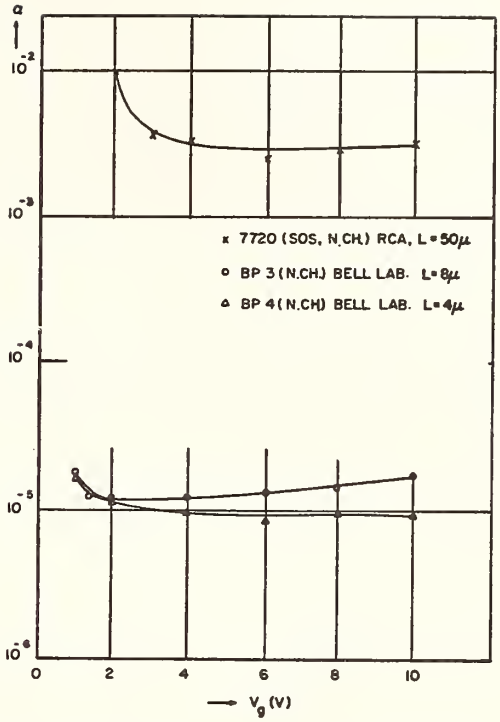

Fig. 2 Hooge's parameter α versus V_g. α is practically independent of V_g. For the SOS device the parameter shows that the value is larger than the others by factor 200.

Since the two models describe the same phenomenon , their parameters are formally related, so that

$$N_T(E_F)_{eff} = \alpha C_{ox}(V_g - V_T)/q \tag{4}$$

Here C_{ox} is the oxide capacitance per unit area.

DISCRIMINATION BETWEEN TWO NOISE MODELS

In order to discriminate between the models, we measure $S_{Id}(f)$ versus V_d from low V_d to saturation. According to van der Ziel [3] , if N(x) is the carrier concentration for unit length at arbitrary point x, then its spectrum is

$$S_N(x,f) = \frac{N_T(E_F,x)_{eff}}{f} w \tag{5}$$

Here $N_T(E_F,x)_{eff}$ is the effective trap density at Fermi level at point x.

In the mobility fluctuation model, the mobility fluctuation spectrum $S_\mu(x,f)$ for unit length was postulated such that

$$\frac{S_\mu(x,f)}{\mu^2(x)} = \frac{\alpha(x)}{f\ N(x)} \tag{6}$$

Here $\mu(x)$ is the average mobility at x, and $\alpha(x)$ is Hooge's parameter at x. If E(x) is the

electric field strength at x and the mobility μ is in the hot electron regime, such that

$$\mu = \frac{\mu_o}{1 + E/E_c} \tag{7}$$

then α must be replaced [4] by

$$\alpha = \frac{\alpha(o,x)}{(1 + E/E_c')^2} \tag{8}$$

Here μ_o is the low field mobility and E_c is a critical field strength, such that $u_c = \mu_o E_c$ is the limiting velocity of the carriers, and E_c' is another critical field strength, such that $u_s = \mu_o E_c'$ is the sound velocity in the sample. Then eq (6) and eq (8) yield

$$\frac{S_\mu(x,f)}{\mu^2(x)} = \frac{\alpha(o,x)}{f\,N(x)(1 + E/E_c')^2} \tag{9}$$

If $g(x) = q\,\mu(x)N(x)$ is conductance for unit length at x, then

$$\frac{S_g(x,f)}{g^2(x)} = \frac{S_N(x,f)}{N^2(x)} = \frac{N_T(E_F,x)_{eff}\,w}{fN^2(x)} \tag{10}$$

and

$$\frac{S_g(x,f)}{g^2(x)} = \frac{S_\mu(x,f)}{\mu^2(x)} = \frac{\alpha(o,x)}{fN(x)(1 + E/E_c')^2} \tag{11}$$

After some maniplation, one can obtain for the number fluctuation model [5] ,

$$S_{I_d}(f) = (q^2 w/fL^2)\int_o^L u_d^2(x)\left[N_T(E_F,x)_{eff}/\epsilon\right]dx \tag{12}$$

and for the mobility fluctuation model,

$$S_{I_d}(f) = (qI_d/fL^2)\int_o^L u_d^2(x)\frac{\alpha(o,x)}{(1 + E/E_c')^2}\,dx \tag{13}$$

Here $u_d(x) = \mu(x)E_o(x)$ is the drift velocity at x.

van der Ziel et al. solved the integrals eq (12) and eq (13) numerically [6] .

The Fig. 3 and Fig. 4 show the experimental results of $S_{I_d}(f)$ versus V_d in the several MOSFETs. And the Fig. 5 and Fig. 6 show the numerical results of the integrals.

CONCLUSION

In the number fluctuation model, $S_{Id}(f)$ increase monotonically with increasing V_d until saturation. In the mobility fluctuation model,because of the strong field dependence of Hooge's parameter α, $S_{Id}(f)$ goes through a maximum well before saturation and level off to a lower value. Some MOSFETs agree better with the number fluctuation model and others agree with the mobility fluctuation model.

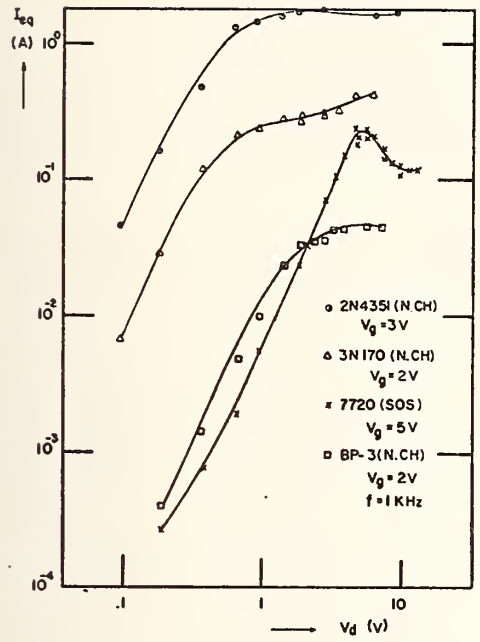

Fig. 3 Most of the devices show that a monotonic increase of $S_{I_d}(f)$ with increasing V_d until saturation sets in. They agree better with the number fluctuation model.

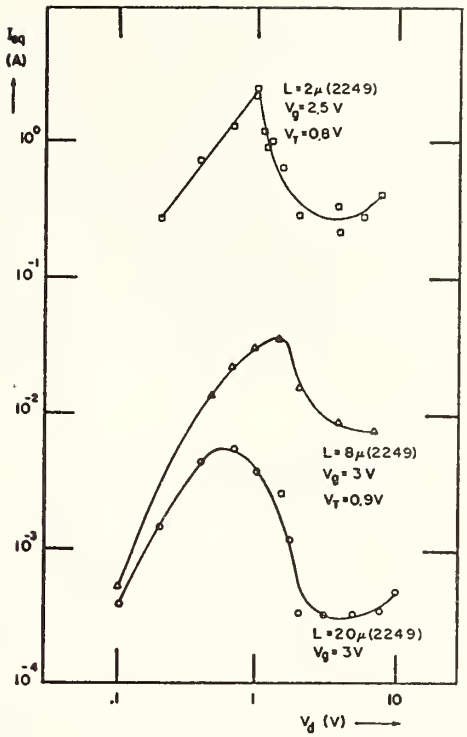

Fig. 4 A number of $S_{I_d}(f)$ vs V_d curves show a significant maximum in $S_{Id}(f)$ before saturation. Therefor these devices agree better with the mobility fluctuation model.

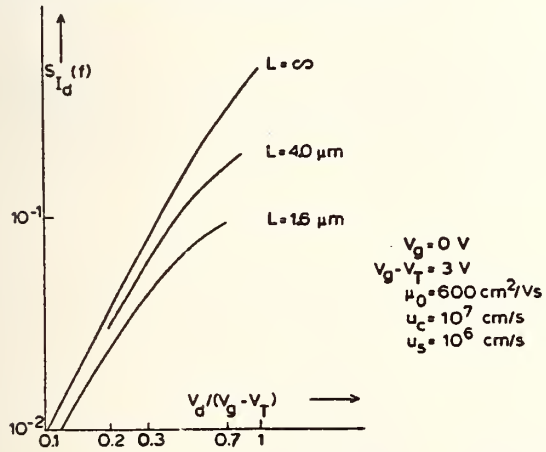

Fig. 5 The dependence of the 1/f noise in the number fluctuation model of MOSFET on the drain voltage, with L as a parameter.

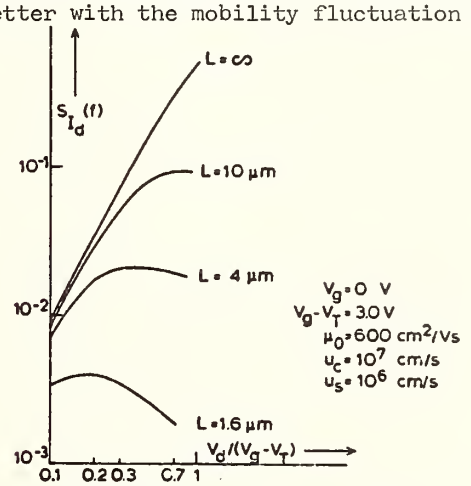

Fig. 6 The dependence of the noise in the mobility fluctuation model of MOSFET on the drain voltage, with L as a parameter.

REFERENCES

1. H.S. Park, A. van der Ziel and S.T. Liu, Solid State Electronics, in the press.
2. F.N. Hooge, Physica, 60, 130, 1972, 83B, 14, 1976.
3. A. van der Ziel, IEEE Conf. Record. Third Biennial University, Industry, Government Microelectronics Symposium, Texas Tech. U. Texas, 102-106, may 21-23, 1979.
4. G. Bosman, R.j.j. Zijlstra and A. van Rheenen, Phys. Lett. 78A, 385, 1980.
5. H.S. park, A. van der Ziel, R.J.J. Zijlstra and S.T. Liu, J. Appl. Physics, in the press.
6. A. van der Ziel, R.J.J Zijlstra and H.S. Park, J. Appl. Physics, in the press.

1/F NOISE IN SHORT CHANNEL MOSTs

Pierre Gentil and Ahmed Mounib

Laboratoire P.C.S. ERA CNRS 659
ENSERG 23 Avenue des Martyrs
38031 Grenoble Cédex FRANCE

INTRODUCTION

Short channel length MOSTs exhibit large variations of the mobility with the gate bias voltage. Consequences of this property on 1/f noise of a short channel MOST is examined below. First, we discuss whether noise physics of short channel MOSTs can be evaluated from the measured spectrum S_{Ve} of an equivalent gate fluctuation or not. Van Der Ziel and Park [1] have shown that the elementary theory of a MOST which connects S_{Ve} to the drain current spectrum S_{I_D} cannot apply in all cases. Secondly we compare experimental noise results of the devices with the surface trapping noise model and with the mobility noise model in the inverted layer closed to the Si-SiO2 interface. 1/f noise in MOSTs is explained for a long time by help of the trapping of the channel carriers by traps into the oxide near the Si-SiO2 interface. In a recent work [2], Vandamme attempts to apply the universal empirical model proposed by Hooge to the case of the MOST. The latter model considers that mobility fluctuations are the origin of flicker noise. The empirical relation of Hooge is adapted to the MOST by taking into account in the mobility, the different scattering mechanisms of the channel carriers. We apply these theories to short channel ($\#$ 1µm) MOSTs biased in the strong inversion ohmic region.

Devices were supplied by the LETI (Grenoble, France). The enhancement mode MOSTs have a 20 µm channel width (W) and an oxide thickness of 320 Å. Silicon substrate is not implanted ; doping is $10^{16}cm^{-3}$. Drain and source resistances are inferior to 20 Ω. Thermal noise and parasitic noise were subtracted from total noise when not negligible. On figures, curves are labelled by the effective channel length L (in µm) of the devices, absolute values of currents and voltages are considered.

STATIC PARAMETERS

The following current-voltage relationship of a MOST working in the strong inversion non-saturated region is used :

$$I_D = \mu_{eff} C_{ox} (W/L) (V_G - V_T - V_D/2) V_D , \quad (1)$$

where :

$$\mu_{eff} = \mu_0 [1 + \Theta(V_G - V_T)]^{-1} \quad (2)$$

Threshold voltage V_T, effective channel length L, effective mobility at small gate voltage μ_0 and the parameter Θ are carefully determined :
a- V_T is determined from the I_D v_s. V_G plot at a very low drain voltage. As shown in table 1, V_T varies with the channel length and variations agree with the theory of short channel devices [3].

L_M (µm)	2.9	3.7	4.7	5.5
V_T (V)	1.7	1.85	1.90	1.92
L (µm)	0.9	1.7	2.7	3.5
Θ (V^{-1})	0.15	0.12	0.08	0.08

Table 1 : measured parameters of short P-channel MOS transistors. The four transistors are located closed one to the other on the same chip.

b- L is determined by plotting I_D^{-1} vs. L_M. L_M is the mask channel length as measured optically $L_M = L + \Delta L$. The plot gives a straight line from which ΔL is obtained. For this experiment V_G-V_T is kept constant and sufficiently small so that $1 + \Theta(V_G-V_T)$ does not vary greatly with L. Also V_D is taken very inferior to V_G-V_T.

c- Θ and μ_0 are determined by plotting $[(V_G-V_T-V_D/2)/I_D]$ vs. V_G-V_T for each transistor. The straight lines thus obtained agree with μ_0 independent of L and allow to determine Θ for each transistor. As shown in table 1, Θ becomes important for the smallest channel length ; $\Theta(V_G-V_T)$ may become greater than unity for a few volts gate voltage. The hole mobility in the case of P channel, $\mu_0 = 150 cm^2 v^{-1} s^{-1}$ is small but agrees with the high doping of the substrate.

With the values of the parameters obtained above, good agreement is obtained between drain current model and experiments below saturation of the MOST. Uniformity of channel lengths and threshold voltages is not very good on the whole wafer so that it is necessary to determine these parameters for each transistor before applying noise models.

DRAIN CURRENT NOISE AND EQUIVALENT INPUT NOISE

N and P short channel MOSTs exhibit an experimental spectral density which varies like 1/f in all cases from 10^{-2}Hz to 10^{4}Hz. Furthermore, equivalent input noise varies about like 1/L. Noise in short channel MOSTs behave like large MOSTs do. Drain current noise S_{I_D} is more easily connected to the physics of the device, however, the equivalent gate noise S_{ve} is the usual way for evaluating noise in MOST. Figure 1 gives the ratio S_{I_D}/S_{ve} as a function of V_G-V_T for the P channel MOSTs. S_{I_D}/S_{ve} varies greatly with the gate voltage. This ratio must correspond to g_m^2 and can be evaluated from the static model described above. From (1) and (2), the transconductance g_m is given by :

$$g_m = \mu_0 C_{ox}(W/L)V_D (1 + \Theta V_D/2) [1 + \Theta(V_G-V_T)]^{-2}. \qquad (3)$$

As seen from figure 1, good agreement exists between the measured S_{I_D}/S_{ve} and the calculated g_m^2.

Consequently, on short channel MOSTs, S_{ve} cannot be a direct measure of the noise spectrum of the channel carrier density when interpreted with the help of the trapping theory. If S_{ve} is measured, relation (3) must be taken into account before interpreting data in terms of carrier trapping fluctuations.

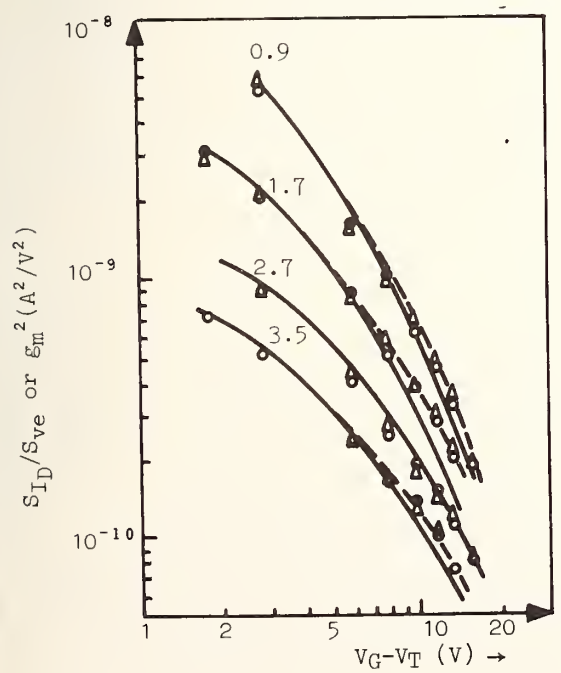

Figure 1 :

———: g_m^2 as given by (3) with the parameters determined from $I_D(V_G)$ measurements and relations (1) et (2). V_D=0.4V.

—Δ—: S_{I_D}/S_{ve} measured at F = 1kHz and V_D = 0.4V.

—o—: g_m^2 dynamically measured at F = 1 kHz and V_D = 0.4V.

TRAPPING NOISE MODEL AND MOBILITY NOISE MODEL

In the trapping model, very different variations of the noise spectrum as a function of the gate voltage can be obtained by varying the energy level of the traps, by introducing two or more discrete energy trap levels or by using different continuous energy trap distributions. The noise density level can be independently adjusted by varying the density of each type of traps.

For single energy traps distributed into the oxide, the trapping model gives the following S_{I_D} relation under small drain voltage [4] :

$$S_{I_D} = \left(\frac{I_D}{V_G - V_T}\right)^2 \frac{e^2 N_t f_{t0} (1-f_{t0}) \lambda}{WL C_{ox}^2 f} \qquad (4)$$

where : N_t is the trap level density, f_{t0} the equilibrium Fermi factor of the traps, λ the tunnel transition parameter, $\lambda = [\hbar^2/(8m^*\phi)]^{1/2}$ where ϕ is the tunnel barrier height. For I_D, relation (1) and (2) are used. For a trap below the Fermi level, $f_{t0}(1-f_{t0})$ increases with $V_G - V_T$. For a trap above the Fermi level, $f_{t0}(1-f_{t0})$ is almost independent of $V_G - V_T$. Experimentally, S_{I_D} varies slowly with $V_G - V_T$ on short channel MOSTs as shown in figure 2. However, S_{I_D} increases with $V_G - V_T$ at small and high V_G while S_{I_D} is almost constant for moderate V_G. We have used three discrete trap levels for modelling this noise as shown in table 2. The trap density near the valence band decreases when the channel length decreases. This effect could be attributed to a more important influence of the drain and source doped regions on the channel region in short channel MOSTs.

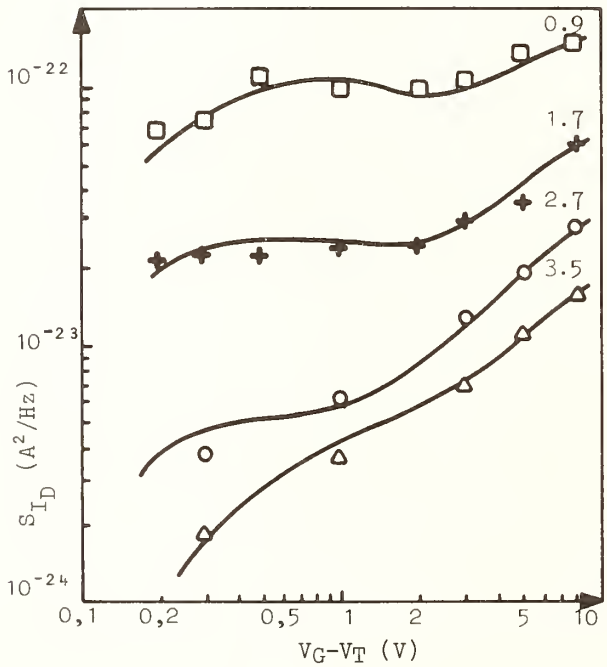

$E_i - E_t$ (eV)	0,4	0,47	0,62
L = 0,9µm ; $N_t(cm^{-3})$=	4,3 10^{15}	9 10^{15}	1,3 10^{17}
L = 1,7µm ; $N_t(cm^{-3})$=	11 10^{15}	12 10^{15}	2,3 10^{17}
L = 2,7µm ; $N_t(cm^{-3})$=	10 10^{15}	10 10^{15}	4,4 10^{17}
L = 3,5µm ; $N_t(cm^{-3})$=	5,5 10^{15}	10 10^{15}	6 10^{17}

Table 2 : trap energies and trap densities used for the model in fig.2.

Figure 2 : □□,++,○○,△△ : S_{I_D} as measured under V_D = 50mV and f = 1 KHz.
——— : theoretical curves obtained from (4), using (1) and (2) and the trap parameters given in table 2.

In order to confront trapping noise model with the mobility noise model, we have also plotted in figure 3 fS_V/V_D^2 as a function of R_c for the experimental results and the theoretical curves of the figure 2. S_V is the noise power spectrum at the drain terminal and R_c is the channel resistance. Good agreement is obtained in the whole range of investigation.

For the mobility model, we have used the theory of Vandamme [2] which proposes to take into account various scattering mechanisms of the carriers. Carrier-carrier scattering gives a direct dependence of the effective mobility on V_G . Surface scattering relation used in [2] leads to a gate voltage dependent effective mobility by considering the channel shrinkage effect. Noise models taking into account each scattering mechanism separately and the combined mechanism were compared to noise results on short channel MOSTs. The parameters were deduced by fitting conductance vs. V_G of the MOST under test with the Vandamme's model. The theoretical noise curves were then calculated using these parameters. As can be seen on figure 4, theoretical noise spectrum curves disagree with measurements. The form of the curves is not very good and theoretical noise level is too

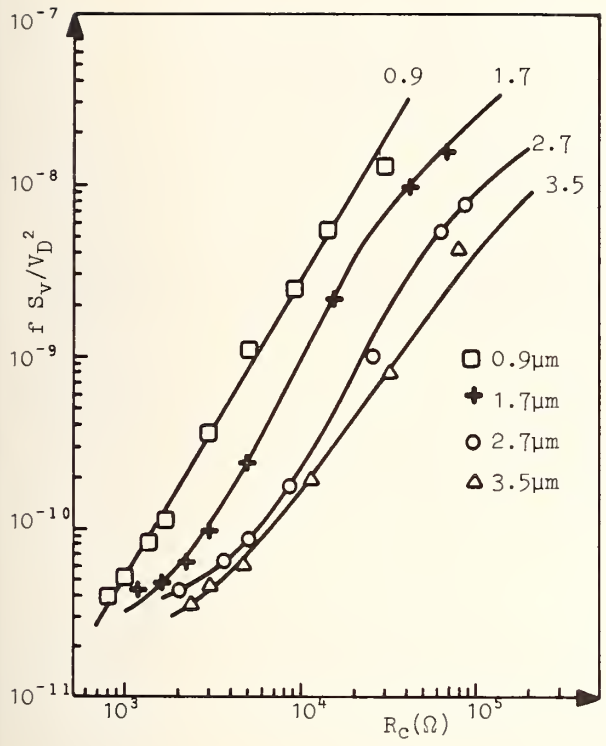

Figure 3 : trapping model. all curves are deducted from fig.2 under V_D=50mV and f=1 KHz. R_C and S_V are calculated from relations (1) to (4) for theoretical curves (———) and evaluated from measurements for experimental points (□, +, ○, △)

The same experimental points are used in fig. 3 and 4.

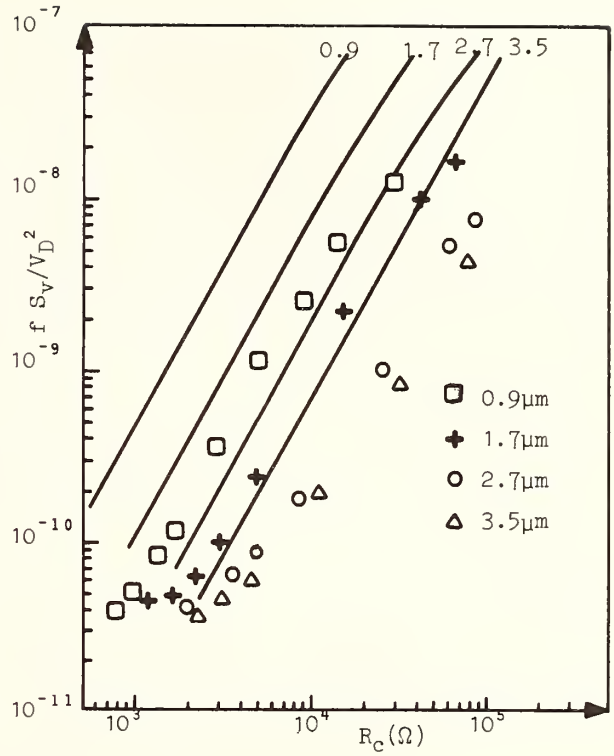

Figure 4 : Mobility model. ———: Theoretical curves which are deducted from Vandamme's model [2]. Using the carrier-carrier scattering mobility. Parameters were deducted by fits of conductance vs.(V_G-V_T). t = 100 Å ; μ_1 = 500$cm^2v^{-1}s^{-1}$;
p_e (0.9) = 4.2 $10^{16}cm^{-3}$;
p_e (1.7) = 6 $10^{16}cm^{-3}$;
p_e (2.7) = 5.$10^{16}cm^{-3}$;
p_e (3.5) = 4.3 $10^{16}cm^{-3}$.

high. The fluctuation model cannot be applied to the short channel MOST at least when using the scattering expressions of reference [2].

ACKNOWLEDGEMENTS

We wish to thank Dr Gautier and Dr de Pontcharra for supplying the devices. This work was supported in part by GCIS (LETI-CNRS) contract.

REFERENCES

[1] A. Van Der Ziel and H.S. Park, Appl. Phys. Lett., *35*, 942 (1979).

[2] L.K.J. Vandamme, Solid-State Electr., *23*, 317 (1980).

[3] L.D. Yau, Solid-State Electr., *17*, 1059 (1974).

[4] P. Gentil, Thèse d'Etat, ENSERG, GRENOBLE (1979).

THEORETICAL INTERPRETATION OF LOW 1/f NOISE IN JFETs

C. F. Hiatt*

E.E. Dept. U of Florida, Gainesville, FL 32611

A. van der Ziel

E.E. Dept. Univ. of Minnesota, Minneapolis, MN 55455

and

R. J. J. Zijlstra

Laboratory Experimental Physics, Princetonplein 5, Utrecht, The Netherlands

SUMMARY

It is shown that the absence of 1/f noise in low-noise JFETs, as found by Hiatt, can be explained by a mobility 1/f noise source as long as the low-field value of Hooge's parameter α is less than 0.4×10^{-5}.

Van der Ziel recently concluded[1] that the absence of 1/f noise in low-noise n-channel JFETs, found by Hiatt[2], could not be explained by a mobility fluctuation 1/f noise source, if the Hooge parameter[3], α, of this source had a low-field value of 2×10^{-3}. Recently, n-channel MOSFETs have been found[4] that had $\alpha \simeq 10^{-5}$ at low drain voltages. Bosman[5] found for 1/f noise in n-type space-charge-limited solid-state diodes that $\alpha \simeq 2 \times 10^{-5}$ at low fields. Hanafi and van der Ziel[6] found for HgCdTe photoresistors that α had a value of $1.5\text{-}2.0 \times 10^{-4}$ in selected units and a value as low as 10^{-6} was reported in one unit[7]. Hence much lower values for α than 2×10^{-3} are not uncommon.

Bosman et al[8] found that the high-field value of α decreased strongly with increasing field, and van der Ziel at al.[9] deduced from this that the 1/f noise in JFETs at saturation would be strongly reduced by this effect. We therefore reexamined Hiatt's data to come up with a more accurate limit for α.

The laboratory-built device used in the measurements had a 5 μ meter gate window and a 2.0 μ meter undercut on each side, so the channel length L was $5.0 + 2 \times 2.0 = 9.0$ μ meter. Van der Ziel et al.[9] found that for $L = \infty$, where the elementary theory was valid, the normalized drain 1/f noise was 0.148, whereas its value at 9.0 μ meter channel length was 0.015 , so that the α-reduction factor g(L) at saturation is $(0.015)/(0.148) = 0.10$.

Hiatt measured at $I_d = 0.62$ mA and $g_m = 6.0$ m mhos at $V_d = 0.4$; the effective gate voltage $(V_g - V_p)$ was about 0.20 V. According to Hiatt R_n was about 30 kOhm at 3 Hz, so we take for the 1/f noise at saturation (Fig. 1)

$$R_n(1/f) \leqq 2.5 \times 10^{-4}/f \text{ Ohm} \tag{1}$$

According to the elementary theory, as corrected by van der Ziel et al., the drain noise at saturation is

$$S_I(f) = 4kTR_n(1/f)\, g_m^2 = \frac{e\mu\alpha_o I_d (V_g - V_p) g(L)}{L^2 f} \tag{2}$$

---

* Now at Honeywell Solid State Electronics Division, Plymouth, MN 55441.

so that the low-field value α_o of α is

$$\alpha_o = \frac{4kTR_n(1/f)g_m^2L^2f}{e\mu I_d(V_g - V_p)g(L)} \tag{3}$$

If we substitute the numerical values just quoted we obtain $\alpha_o < 0.4 \times 10^{-5}$.

Hence a mobility fluctuation 1/f noise source with a low-field value $\alpha_o < 0.4 \times 10^{-5}$ of Hooge's parameter would not give any observable 1/f noise in Hiatt's JFET. Since this is well within the observed limits of α_o, the mobility fluctuation 1/f noise model can no longer be excluded as an explanation of Hiatt's experiments.

REFERENCES

1. A. van der Ziel, Appl. Phys. Lett., 33 (1978) 883.

2. C. F. Hiatt, Ph.D. Thesis, U of Florida (1974); C. F. Hiatt, A. van der Ziel and K. M. van Vliet, IEEE Trans. El. Devices, ED-22 (1975) 614.

3. F. N. Hooge, Phys. Lett., A-29 (1969) 139.

4. H. S. Park, A. van der Ziel and S. T. Liu, Solid State Electron. (1981) in the press.

5. G. Bosman, private communication.

6. H. I. Hanafi and A. van der Ziel, Physics, 94B (1978) 351.

7. R. N. Broudy, Honeywell Radiation Center, Lexington, Mass. Final Tech. Report Contract NASA CR-132512 (1973).

8. G. Bosman, R. J. J. Zijlstra and A. van Rheenen, Phys. Lett., 78A (1980) 385.

9. A. van der Ziel, R. J. J. Zijlstra and H. S. Park, J. Appl. Phys., June 1981, in the press.

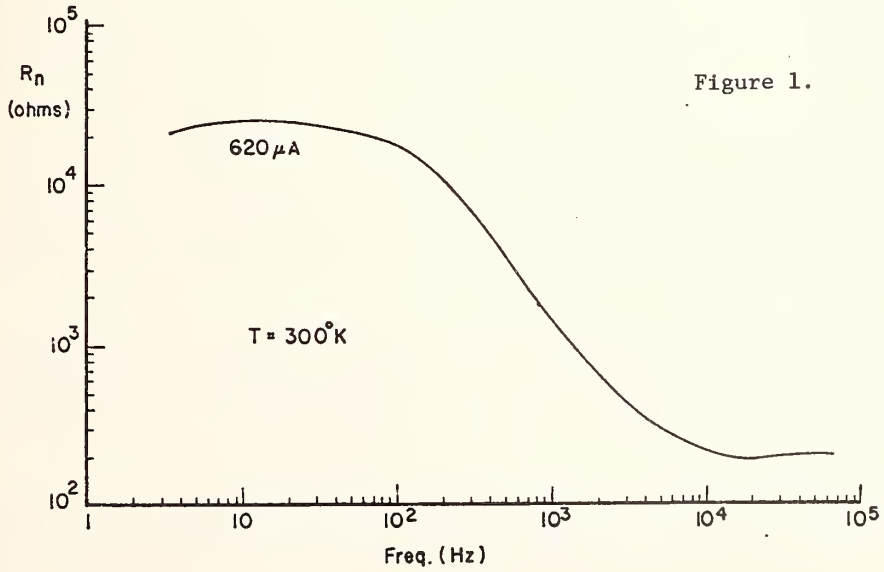

Figure 1.

1/f NOISE IN GaAs MESFETs.

C.H. Suh, A. van der Ziel and R.P. Jindal

Electrical Engineering Department

University of Minnesota

Minneapolis, Minnesota 55455

SUMMARY

Measurements on 1/f noise in GaAs MESFETs are reported. The spectra are of the form $(A/f)\left[1 - (2/\pi)\tan^{-1}(\omega\tau_o)\right]$, where A and τ_o are constants. While both the number and the mobility fluctuation models can qualitatively explain the data, the latter explanation is somewhat more likely.

We report here on 1/f noise measurements on NEC GaAs MESFETs. As shown earlier[1] these devices have spectra of the form

$$(A/f)\left[1 - (2/\pi)\tan^{-1}(\omega\tau_o)\right] \tag{1}$$

where A and τ_o are constants that depend somewhat on the gate bias. Figure 1 shows that by proper choice of A and τ_o a perfect fit can be made between curve (1) and the experimental data. A superposition of two Lorentzian spectra cannot produce such a fit.

This formula can be interpreted in terms of the following distribution of time constants

$$g(\tau)d\tau = \frac{d\tau/\tau}{\ln(\tau_1/\tau_o)} \qquad \text{for } \tau_o < \tau < \tau_1 \tag{2}$$

and zero otherwise. Such a distribution gives a spectrum of (1) for $\omega\tau_1 \gg 1$ and a 1/f spectrum for $1/\tau_1 < \omega < 1/\tau_o$. The perfect fit between the data and Eq. (1) indicates that a distribution of the form (2) is the most likely explanation of the spectra.

As a preliminary for discriminating between possible 1/f noise mechanisms, we measured the drain noise spectrum $S_I(f)$ at $V_g = -1.50$ V at very low drain bias ($V_d = 0.10$ V) and near saturation ($V_d = 1.50$V), found that the constant τ_o depended hardly on V_d whereas the parameter A did. This is shown in Fig. 2, which plots $I_{eq} = S_I(f)/2q$, the equivalent saturated diode current of the drain noise. Since τ_o does not depend on V_d, the dependence I_{eq} on V_d must come from the dependence of A upon V_d.

Figure 3 shows ln I_{eq} plotted versus ln V_d at $V_g = -1.50$ V and f = 1 kHz; this frequency was so chosen that the device operated in the 1/f part of the spectrum. At low drain bias the value of I_{eq} varies as V_d^2. At higher values of V_d the value of I_{eq} passes through maximum at $V_d = 0.65$ V, a minimum at $V_d = 1.50$ V, and levels off to a constant value above 2.0 V. This behavior will now be explained.

According to Park et al[2] the drain noise spectrum for the number fluctuation model is

$$S_I(f) = \frac{q^2 W}{\varepsilon f L^2}\int_o^L u_d^2(x)\left[N_T(E_f,x)\right]_{eff}dx \tag{3}$$

whereas for the mobility fluctuation model

$$S_I(f) = \frac{qI_d}{fL^2} \int_o^L u_d(x)\, \alpha\,(E_o,x)\, dx \tag{4}$$

Here w is the device width, L the device length, q the electron charge, f the frequency, $E_o(x)$ the d.c. field strength at x, $u_d(x)$ the drift velocity at x, and I_d the drain current at the drain voltage V_d. Furthermore $[N_T(E_f,x)]_{eff}$ is the effective trap density at the Fermi level at x, ε is a tunneling parameter and $\alpha(E_o,x)$ is Hooge's parameter at x at the field strength $E_o(x)$.

The characteristic $I_d(V_d)$ increased monotonically with increasing V_d, reaching its maximum value at saturation, as expected. Since for low drain bias V_d the drain current I_d and the drift velocity $u_d(x)$ are both proportional to V_d, whereas $[N_T(E_f,x)]_{eff}$ and $\alpha(E_o,x)$ are now constants, we see that I_{eq} should be proportional to V_d for low values of V_d, in agreement with our data.

The effective mobility μ in GaAs may be written

$$\mu = \beta\mu_1 + (1 - \beta)\mu_2 \tag{5}$$

where μ_1 and μ_2 are the mobilities in the lower and the upper valleys, respectively, and $\beta(E_o)$ is the relative occupany of the lower valley. Hence the average drift velocity is

$$u_d = \mu E_o = \beta\mu_1 E_o + (1 - \beta)\mu_2 E_o \tag{6}$$

Therefore u_d increases linearly with E_o for low E_o, passes through a maximum and then decreases when intervalley transfer of carriers becomes important; finally it increases again when most of the carriers are in the upper valley. We see from Fig. 2 that $[N_T(E_d,x)]_{eff}$ decreases with increasing $V_g - V_p$, so that $[N_T E_f,x)]_{eff}$ increases with increasing V_d at a given x and with increasing x at a given V_d. Putting it all into Eq. (3) we see that the number fluctuation model can qualitatively explain the data.

We now turn to the mobility fluctuation model. We have for fluctuations $\delta\mu_1$ and $\delta\mu_2$ in μ_1 and μ_2, respectively

$$\delta\mu = \beta\delta\mu_1 + (1 - \beta)\,\delta\mu_2 \tag{7}$$

from which follows

$$S\mu(f)/\mu^2 = \beta^2 S\mu_1(f)/\mu^2 + (1-\beta)^2 S\mu_2(f)/\mu^2 \tag{8}$$

According to Bosman et al[3] the field dependence of $S\mu(f)/\mu^2$ in silicon may be written

$$S\mu(f)/\mu^2 = \alpha(0,x)/\{fN[1 + (\mu_o E_o/u_s)^2]\} \tag{9}$$

where $\alpha(0,x)$ is the low-field value of Hooge's parameter α, μ_o he low-field mobility and u_s the velocity of sound. Hence in GaAs one would expect

$$S\mu_1(f)/\mu_1^2 = \alpha_1(0,x)/\{\beta fN[1 + (\mu_{1o} E_o/u_s)^2]\} \tag{9a}$$

$$S\mu_2(f)/\mu_2^2 = \alpha_2(0,x)/\{(1-\beta)fN\,[1 + (\mu_{2o}E_o/u_s)^2]\} \tag{9b}$$

so that

$$\alpha(E_o,x) = \alpha_1(0,x)\,\frac{\beta(\mu_1/\mu)^2}{1 + (\mu_{1o}E_o/u_s)^2} + \alpha_2(0,x)\,\frac{(1-\beta)(\mu_2/\mu)^2}{1 + (\mu_{2o}E_o/u_s)^2} \tag{10}$$

One would thus expect α to be constant for low values of E_o, followed by a decrease when $\mu_{1o}\,E_o/u_s$ becomes comparable to unity, followed by a plateau when the second term becomes significant, and finally by another decrease when $\mu_{2o}E_o/u_s$ becomes comparable to unity. It thus seems that the mobility fluctuation model can also qualitatively explain the data.

While both models seem to be able to qualitatively explain the data, the mobility fluctuation model is here more likely, since the field dependence of $\alpha(E_o,x)$ occurs at much lower fields than where the dependence of $u_d(E_o,x)$ upon E_o ceases to be linear. Hence the field dependence of $\alpha(E_o,x)$ should predominate.

ACKNOWLEDGEMENT

This work was performed under ARO and NSF contracts. Professor Suh is now back at Hong-Ik University, Seoul, Korea, and Dr. Jindal is at Bell Laboratories, Murray Hill, N.J.

REFERENCES

[1] C.H. Suh and A. van der Ziel, Appl. Phys. Lett, 37 (1980) 565.

[2] H.S. Park, A. van der Ziel, R. J. J. Zijlstra and S.T. Liu, J. Applied Physics, in the press.

[3] J. Bosman, R.J.J. Zijlstra and A. van Rheenen, Phys. Lett. 80A (1980) 57.

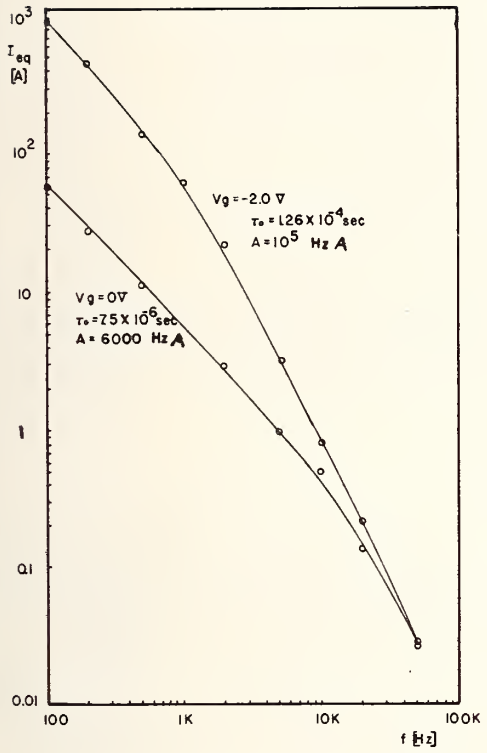

Fig. 1

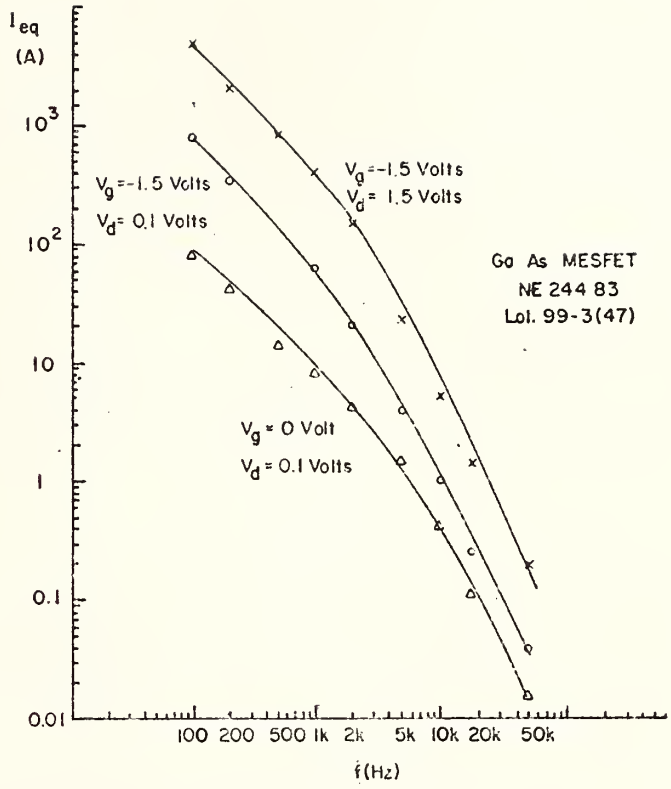

Fig. 2

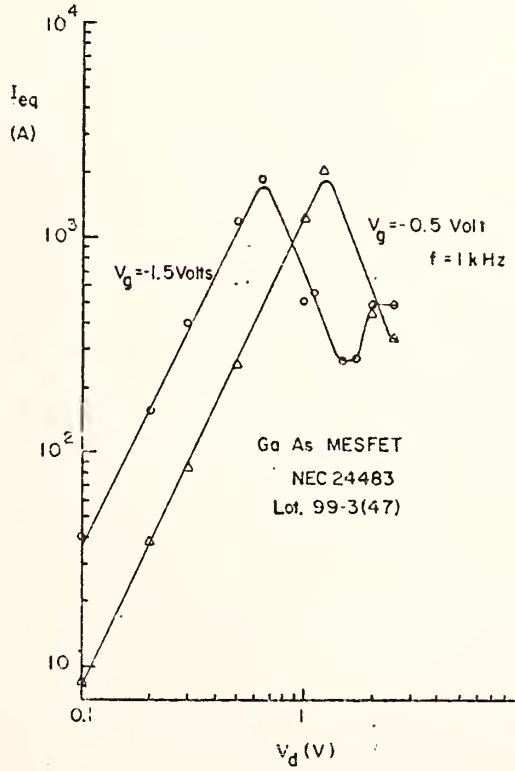

Fig. 3

1/f NOISE OF HOT CARRIERS

T.G.M. Kleinpenning

Eindhoven University of Technology
Eindhoven, Netherlands

INTRODUCTION

On the basis of experimental facts, the 1/f noise in the conductance G of homogeneous semiconductors and metals can be described by Hooge's empirical relation [1]

$$S_G = \alpha G^2/(fN) \tag{1}$$

Here, α is an empirical constant of the order of 10^{-3}, f the frequency, and N the number of free carriers. Recent investigations have proved that 1/f noise is due to mobility fluctuations [2]. Relation (1) holds for semiconductors in the case of low electric fields, where mobility is field independent. This paper presents the results of 1/f noise in semiconductors at high electric-field strengths where the mobility is field dependent.

CALCULATIONS (PLANAR GEOMETRY)

Consider an n-type semiconductor with ohmic contacts. The contact spacing is L and the cross-section is A. The current density J(t) at time t is

$$J(t) = qn\mu(x,t)E(x,t) = qn\mu\left[E(x,t),\mu_o(x,t)\right]E(x,t) \tag{2}$$

where q is the elementary charge, E(x,t) the electric-field strength at $x(0 \leq x \leq L)$. The chordal mobility $\mu = J/(qnE)$ is a function of the low-field mobility μ_o and E. At low fields we have $\mu = \mu_o$, and at high fields $\mu E = v_{sat}$, the saturation velocity [3,4]. At high fields two scattering mechanisms are simultaneously active: the low-field scattering and the scattering by the optical modes of the lattice vibrations, which are beginning to occur at high fields, where the electron energy is comparable with the optical phonon energy U_p. As the energy of an electron approaches U_p its velocity is likely to be reduced by exciting an optical phonon. In order to calculate the 1/f voltage noise we assume that μ_o fluctuates according to eq (1) and that the optical-phonon excitation process shows no 1/f noise. At constant current we have

$$\left\langle\frac{dJ}{dE}\right\rangle\Delta E(x,t) + \left\langle\frac{dJ}{d\mu_o}\right\rangle\Delta\mu_o(x,t) = 0 \quad ; \quad \Delta V(t) = \frac{\langle dJ/d\mu_o\rangle}{\langle dJ/dE\rangle}\int_o^L \Delta\mu_o(x,t)dx \tag{3}$$

With the help of the cross-correlation spectral density in the mobility [2,5]

$$S_{\mu_o}(x,x') = \frac{\alpha\mu_o^2}{fAn(x)}\,\delta(x-x') \tag{4}$$

and N = nAL, the 1/f voltage noise is found to be

$$S_V(f) = \frac{\langle dJ/d\mu_o\rangle^2}{\langle dJ/dE\rangle^2}\,\frac{\alpha\mu_o^2L^2}{fN} = \frac{\langle\mu_o dJ/d\mu_o\rangle^2}{\langle EdJ/dE\rangle^2}\,\frac{\alpha V^2}{fN} \tag{5}$$

To evaluate eq (5) we have to know the relation between μ, μ_o and E. For n-silicon this relation can be approximated by [4,5]

$$\mu(E) = \mu_o/(1+\mu_o E/v_{sat}) \tag{6}$$

Using eqs (2,6) we find $S_v(f) = \alpha V^2/fN$. The 1/f current noise is found to be

$$S_I(f) = S_V(f)\left(\frac{dI}{dV}\right)^2 = \frac{\alpha I^2}{fN}\left(\frac{VdI}{IdV}\right)^2 = \frac{\alpha I^2}{fN}\left(\frac{\mu_d(E)}{\mu(E)}\right)^2 = \frac{\alpha I^2}{fN}\left(\frac{1}{1+\mu_o E/v_{sat}}\right)^2 \tag{7}$$

where $\mu_d(E)$ is the differential mobility $d(\mu(E)E)/dE$.

If we assumed that 1/f fluctuations were caused by number fluctuations (McWhorter model), then the result would be [5] $S_I(f) = \alpha I^2/fN$.

From flicker noise measurements performed on n^+nn^+ and $p^+\pi p^+$ silicon planar devices at 78K, Bosman et al. [6,7] found experimentally

$$S_I/I^2 = \left[S_{\mu(E)}/\mu^2(E)\right]_{\Delta E=0} = \alpha(E)/fN \quad ; \quad \alpha(E) = \alpha(0)\Big/\left[1+(\mu_o E/v_s)^2\right] \tag{8}$$

where v_s is the sound velocity.

Since experiments have to be performed at high electric fields, Joule heating creates serious problems. Therefore, we investigated samples with hemispherical geometry.

CALCULATIONS AND EXPERIMENTS (HEMISPHERICAL GEOMETRY)

Consider a sample, where the radius of the point-contact a is small with respect to the other dimensions. The current through a hemispherical surface with radius r is

$$I(t) = qn\mu\left[E(r,t),\mu_o(r,t)\right]E(r,t)2\pi r^2 \tag{9}$$

With the help of eq (6) we find

$$V = \int_a^\infty E(r)dr = \int_a^\infty \frac{(\rho_o I/2\pi)dr}{r^2 - I/(2\pi qnv_{sat})} = \frac{\rho_o I}{2\pi a}\frac{z}{2}\ln\left(\frac{z+1}{z-1}\right) \tag{10}$$

where ρ_o is the low-field resistivity, $z = \sqrt{I_m/I}$, and $I_m = 2\pi a^2 qnv_{sat}$ the maximum current. At constant current, we find for low-field mobility fluctuations $\Delta\mu_o$

$$\left\langle\frac{dI}{dE}\right\rangle\Delta E(r,t) + \left\langle\frac{dI}{d\mu_o}\right\rangle\Delta\mu_o(r,t) = 0 \quad ; \quad S_V(f) = \int_a^\infty\int_a^\infty\left[\frac{dI/d\mu_o}{dI/dE}\right]^2 S_{\mu_o}(r,r')drdr' \tag{11}$$

The source term $S_{\mu_o}(r,r')$ can be obtained from (4) putting $A = 2\pi r^2$ and $x = r$, so we find

$$S_V(f) = \left(\frac{\rho_o I}{2\pi}\right)^2 \frac{\alpha z^5}{2\pi fna^5}\left[\frac{1}{z} + \frac{z}{2(z^2-1)} + \frac{3}{4}\ln\left(\frac{z-1}{z+1}\right)\right] \tag{12}$$

If we ascribed the 1/f noise to free-carrier density fluctuations, we would find [5]

$$S_V(f) = \left(\frac{\rho_o I}{2\pi}\right)^2 \frac{\alpha z^5}{2\pi fna^5}\left[\frac{z}{6(z^2-1)^3} + \frac{z}{24(z^2-1)^2} - \frac{z}{16(z^2-1)} - \frac{1}{32}\ln\left(\frac{z-1}{z+1}\right)\right] \tag{13}$$

Assuming that eq (8) is correct, we have

$$\Delta I = 0 = \left\langle \frac{dI}{dE} \right\rangle \Delta E(r,t) + \left\langle \frac{dI}{d\mu} \right\rangle \Delta\mu(r,t) = \left\langle \frac{I/E}{1+\mu_o E/v_{sat}} \right\rangle \Delta E(r,t) + \left\langle \frac{I}{\mu(E)} \right\rangle \Delta\mu(r,t) \quad . \tag{14}$$

Thus

$$S_V(f) = \int_a^\infty\int E^2(r)\left[1 + \frac{\mu_o E(r)}{v_{sat}}\right]^2 \frac{S_\mu(r,r')}{\mu^2}\, drdr' = \frac{\alpha}{2\pi fn} \int_a^\infty \frac{E^2(r)\left[1+\mu_o E(r)/v_{sat}\right]^2}{r^2\left[1+\mu_o^2 E^2(r)/v_s^2\right]}\, dr \tag{15}$$

where the source term $S_\mu(r,r')$ is obtained from (4) by putting $A = 2\pi r^2$, $x = r$, $\mu_o = \mu(E) = \mu$, and $\alpha = \alpha(E)$ given by (8). If Bosman et al. [6,7] had found $\alpha(E) = \alpha/(1+\mu_o E/v_{sat})^2$ instead of eq (8), then eq (15) would have led to the same result as eq (11).

At low fields both V/I and S_V/I^2 are current independent. At higher fields V/I increases with increasing current and S_V/I^2 also becomes current dependent. Figure 1 shows the relation between deviations from Ohm's law and deviations from the normal current dependence of the noise ($\sim I^2$). The deviations are given in normalized quantities, R_o and $(S_V/I^2)_o$ representing the low-field values. The upper curve represents the relation assuming N-fluctuations [eq (13)], the solid line that for μ_o-fluctuations [eq (12)], the broken line being based on Bosman's result [eq (15)]. The circles are experimental results obtained from n-Si samples with a $\simeq$ 15 μm at 77K. For more details see [5].

The conclusion is that 1/f noise of hot carriers must be interpreted in terms of low-field mobility fluctuations, $\Delta\mu_o$, characterized by the empirical relations (1) and (4).

MOS TRANSISTOR

Let us consider an n-channel MOST biased at a drain-source voltage V and an effective gate voltage $V_G^* = V_G - V_T$, where V_T is the threshold voltage and $V \ll V_G^*$. The distance source-drain is L. The direction source-drain is the x-axis, and the y-axis is perpendicular to the surface. Let us assume that the electric field in the y-direction E_y is approximately independent of y, at least in that part of the channel where the free electrons are located. The source-drain current is then $I = qN_1\mu(E)E_x$, with N_1 the free electron density per unit length. The open-circuit 1/f voltage fluctuations due to $\Delta\mu_o$ are given by

$$\Delta I = 0 = \langle dI/dE_x \rangle \Delta E_x(x,t) + \langle dI/d\mu_o \rangle \Delta\mu_o(x,t) \tag{16}$$

Using eqs (4,6) the 1/f voltage noise is found to be

$$S_V(f) = \frac{\langle dI/d\mu_o \rangle^2}{\langle dI/dE_x \rangle^2} \cdot \frac{\alpha\mu_o^2 L^2}{fN} = \left[1 + \frac{\mu_o E_y^2}{v_{sat}(E_x^2+E_y^2)^{\frac{1}{2}}}\right]^{-2} \cdot \frac{\alpha V^2}{fN} \tag{17}$$

At low drain-source voltages where E_x is small, eq (17) can be approximated by

$$S_V(f) = \left(\frac{1}{1+\mu_o E_y/v_{sat}}\right)^2 \frac{\alpha V^2}{fN} = \left(\frac{\mu}{\mu_o}\right)^2 \frac{\alpha V^2}{fN} \tag{18}$$

The total number of free electrons in the channel N is approximately given by [8]

$$N = C_o(V_G - V_T)/q = C_o V_G^*/q \tag{19}$$

with C_o the oxide capacitance. To find the relation between S_V and V_G^*, we have to know the relation between E_y and V_G^*. This relation can be approximated by [9]

$$E_y = E_o(1+\Theta V_G^*)^k \tag{20}$$

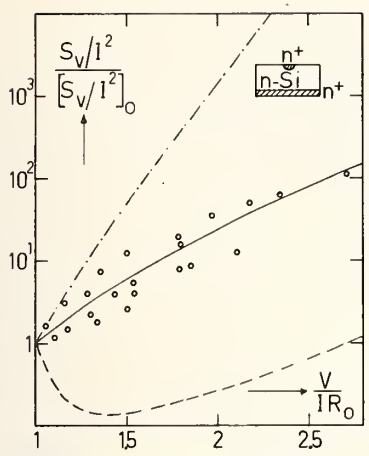

Fig. 1 Relation between deviations from the current-dependence of the 1/f noise (normally $\sim I^2$) at high electric-field strengths and deviations from Ohm's law. -,- based on eq (13); —— based on eq (12); ---- based on eq (15); o experimental results. The subscript o denotes low-field values.

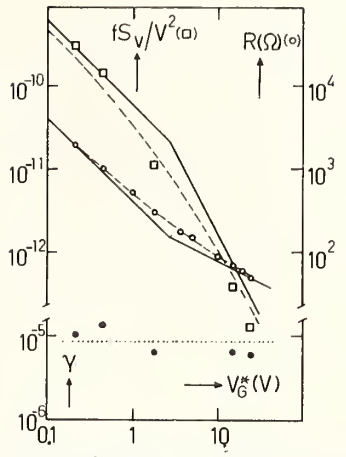

Fig. 2 Experimental data for R, S_V and γ (eq (21)) versus V_G^* of the M 100-type MOST [8]. Calculated results for the same quantities are given by solid, broken and dotted lines, respectively.

with E_o and Θ empirically fitted parameters and $0.5 \leq k \leq 1$.
Since $S_V \sim \mu^2/N$, the channel resistance $R \sim 1/(\mu N)$, and $N \sim V_G^*$, the quantity γ defined by

$$\gamma \equiv f(S_V/V^2)R^2V_G^{*3} = \alpha q L^4/(\mu_o^2 C_o^3) \qquad (21)$$

is independent of μ, N, V_G^*. In Fig. 2 are plotted the experimental results of the M 100-type MOST in Ref. [8]. The dotted line gives the calculated quantity γ using $\alpha = 2 \times 10^{-3}$. The same figure shows S_V and R versus V_G^*. The solid lines give the high and low electric-field limits, the broken lines are the best fits for k = 0.5.

From the above we conclude that the 1/f noise in MOSTs can be interpreted in terms of μ_o-fluctuations if hot carrier effects are taken into account. Furthermore, in our model we have assumed that the low-field mobility is determined by the bulk material, so inelastic surface scattering effects are neglected.

REFERENCES

1 F.N. Hooge, Physica 83B, 14 (1976).
2 T.G.M. Kleinpenning, in Proc. Second International Symposium on 1/f Noise, Univ. of Florida, Gainesville, Florida (1980), pp. 1-17.
3 R.A. Smith, Semiconductors, Cambridge Univ. Press, Cambridge (1980).
4 J.C. Jacoboni and L. Reggiani, Advances in Physics 28, 493 (1979).
5 T.G.M. Kleinpenning, Physica 103B, 340 (1981).
6 G. Bosman, R.J.J. Zijlstra and A. van Rheenen, Phys. Letters A 78, 385 (1980).
7 G. Bosman, R.J.J. Zijlstra and A. van Rheenen, Phys. Letters A 80, 57 (1980).
8 L.K.J. Vandamme, Solid-State Electron. 23, 317 (1980).
9 T.G.M. Kleinpenning and L.K.J. Vandamme, J. Appl. Phys. in press.

BIAS-TEMPERATURE TREATMENT, SURFACE STATE DENSITY, AND 1/f NOISE IN MOSTs

L.K.J. Vandamme and L.S.H. Dik,

Eindhoven University of Technology
Eindhoven, Netherlands

INTRODUCTION

There was a generally accepted relation between the surface state density N_{ss} and the equivalent input noise S_{vgs} [1,2] in MOSTs. The empirical relationship is given by

$$S_{vgs} = 10^{-25} N_{ss} [V^2 S] \tag{1}$$

at 1 kHz, 1 mA drain current and for an unspecified channel area. The proportionality $S_{vgs} \propto N_{ss}$ seems to illustrate that 1/f noise in a MOST is a surface effect. This is due to fluctuations in the occupation of interface traps and thereby in the number of free charge carriers.

There is another school of thought who believe that 1/f noise is due to mobility fluctuations [3,5]. The 1/f noise in a MOST can also be interpreted in terms of mobility fluctuations [6,7,8]. Here we report on our investigations of the effect of bias-temperature treatment on the interface state density and the equivalent input 1/f noise. This enables us to discriminate between mobility fluctuations and concentration fluctuation models.

EXPERIMENTAL PROCEDURE

The surface state density and the 1/f noise were measured prior to and after bias-temperature heat treatment. The interface state density was measured on the same MOSTs on which the 1/f noise was measured. From the shape of the I_d versus V_d curve below threshold, N_{ss} near midgap can be calculated [9]. In the subthreshold the $I_d - V_d$ relation at a constant gate voltage and temperature is given by [9]

$$I_d = I_{dmax}\left(1-e^{-\eta q V_d/kT}\right) \tag{2}$$

$$\eta = \frac{C_{ox}+C_d(V_g^*)}{C_{ox}+C_d(V_g^*)+N_{ss}q} \tag{3}$$

where q is the elementary charge, k the Boltzmann constant, and T the temperature in Kelvin. η is an ideality factor given by the oxide capacitance C_{ox}, the depletion capacitance $C_d(V_g^*)$ and the interface state capacitance per unit area qN_{ss}. The MOST is biased below threshold when a typical gate voltage V_g^* is used so that at a drain source voltage of 50 mV the drain current is 10^{-9} A. For this typical gate voltage V_g^* the series connection of the oxide capacitance and depletion capacitance is measured by a threepoint procedure [10]. N_{ss} is then given by

$$N_{ss} = \frac{1}{q}\left(C_{ox}+C_d(V_g^*)\right)\left(\frac{1}{\eta} - 1\right) \tag{4}$$

where η is obtained from the I_d versus V_d curve measured at $V_g = V_g^*$. Owing to channel lenght reduction at large V_d, problems can occur in the determination of I_{dmax}. Here we propose a

quick determination of N_{ss} by measuring the drain current at two chosen voltages: I_{d1} at V_{d1} and I_{d2} at $V_{d2} = 2\ V_{d1}$. For $\eta q/kT$ we find

$$\frac{-\ln(I_{d2}/I_{d1}-1)}{V_{d1}} = \frac{\eta q}{kT} \qquad (5)$$

We choose $V_{d1} = 30$ mV and $V_{d2} = 60$ mV. At 300 K we find

$$\eta = -0.87\ \ln(I_{d2}/I_{d1}-1) \qquad (6)$$

From eqs. (6) and (4) and observed values of I_{d2}/I_{d1}, C_{ox} and $C_d(V_G^*)$ the N_{ss} value is calculated. These results are in good agreement with computer fitting results. To avoid measuring errors due to the leakage current in the p-n junction between substrate and drain, the current I_d was measured in series with the source, the substrate being grounded.

All heat treatments were carried out on encapsulated MOSTs. The bias-temperature conditions were ½ hour at a temperature of about 600 K with $V_{gs} = V_{gb} = V_{gd}$ half the breakdown voltage, as specified by the manufacturur at 300 K. A positive bias-temperature treatment means that the gate voltage is positive with respect to the substrate. The bias voltages correspond to 15 V to 20 V per 1000 Å gate oxide thickness. After bias-temperature treatment the instabilities caused by mobile ions, were cured out during ½ hour at room temperature by biasing the MOST in saturation at a drain current of ½ I_{dmax}. The equivalent input noise voltage at the gate was measured prior to and after-bias temperature treatment using a Hewlett and Packard type 4470 A transistor noise analyzer.

RESULTS

The experimentally observed trends are: (i) bias-temperature treatment leads small increases in N_{ss} for commercial MOSTs and to larger increases in N_{ss} for a laboratory made sample, (ii) bias-temperature heat treatment with a polarity leading to strong inversion results in an increase in N_{ss} and decrease in S_{vgs}. This trend contradicts the rule $S_{vgs} \propto N_{ss}$ as proposed in surface state models [1,2], (iii) bias-temperature treatment resulting in accumulation layers lead to increases in both N_{ss} and S_{vgs} of at least a factor two, (iv) after a bias-temperature heat treatment, the dependence of S_{vgs} on V_g is reduced. A summary is presented in table 1 below.

Table 1. Change of Surface State Density and 1/f Noise in MOSTs after a Bias-Temperature Treatment.

	bias-temperature treatment polarity	N_{ss}	S_{vgs}
n-channel	+	>0	<0
	−	>0	>0
p-channel	+	>0	>0
	−	>0	<0

Ten n-channel depletion MOSTs have been investigated (M 100 and 3 N 128), 29 p-channel MOSTs (M 108 and university made samples).

The survey of our experimental results on the dependence of 1/f noise in MOSTs on N_{ss} before a bias-temperature treatment is presented in the next figure. In this survey the observed noise is expressed in a relative way in order to compare the results for different channel areas and bias conditions. When the noise is measured in the ohmic region the results are denoted by 0 and the observed relative noise is normalized as $(S_v/V^2)(fC_gV_g)/q$ where C_g is the total gate oxide capacitance. When the equivalent input noise S_{vgs} is measured under saturation conditions, then the noise results are denoted by s and normalized as $S_{vgs}x(2fC_g)/(q.V_g)$. The height of the bars have nothing to do with inaccuracies in the measurements but with the fact that the normalized noise decreases with increasing gate

voltage. This trend is in agreement with the reduction in α due to a reduction in the mobility with increasing gate voltage.

The lowest and highest values of the gate voltages V_g used are given along the bars in the figure. The numbers correspond to n-channels and the letters to p-channels.

The broken line follows $S_{vgs} \propto N_{ss}$. The experiments contradict this rule.

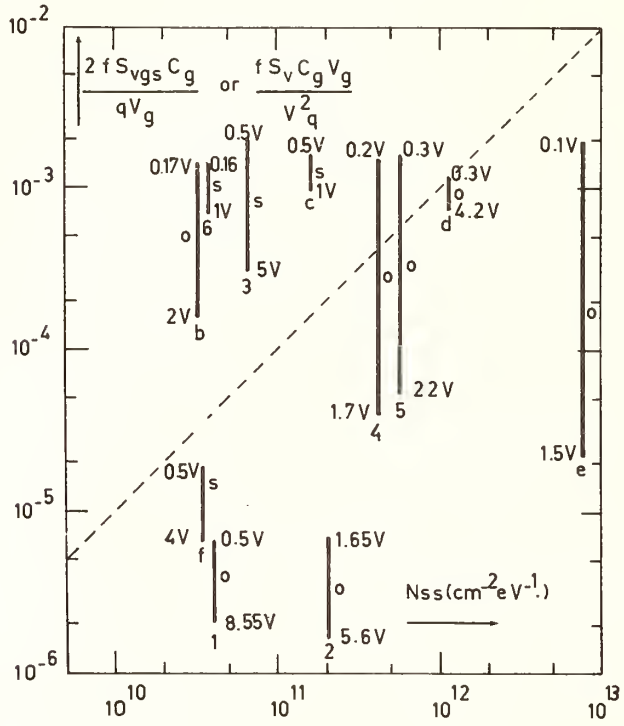

Fig. 1. Observed noise and surface state density from measurements on MOSTs.

The code used in the figure is as follows.

p-channels	n-channels	
	1. LMOA 1 before bias-temperature treatment	university made
b. 3N155 Texas Instruments	2. LMOA 1 after bias-temperature treatment	university made
c. 3N163 Siliconix	3. 3N128	R.C.A.
d. 3N174 Texas Instruments	4. 40467A	R.C.A.
e. L IV, 1 University made	5. M 100	Siliconix
f. M 108 Siliconix	6. 3N142	R.C.A.

Experimental results which can be explained by mobility fluctuation show normalized noise between 2×10^{-3} and 5×10^{-5}. There are MOSTs for which the experimental results agree with both the predictions by the trapping model and by the mobility fluctuation model. There are also MOSTs for which the noise is in agreement neither with the $\Delta\mu$ nor the Δn model. The final conclusion is that a proportionality between S_{vgs} and N_{ss} does not exist. Even after changing N_{ss} and S_{vgs} on the same sample by a bias-heat treatment the proportionality $S_{vgs} \propto N_{ss}$ is not observed.

REFERENCES

1 F.M. Klaassen, IEEE Trans. Electr. Dev. ED-18, 887 (1971).

2 G. Broux, R. van Overstraeten, G. Declerck, Electron. Lett. 11, 97 (1975).

3 F.N. Hooge, Physica 83B, 14 (1976).

4 T.G.M. Kleinpenning, Physica 77, 78 (1974).

5 F.N. Hooge, L.K.J. Vandamme, Phys. Lett. 66A, 315 (1978).

6 L.K.J. Vandamme, Solid-St. Electron 23, 317 (1980).

7 L.K.J. Vandamme, H.M.M. de Werd, Solid-St. Electron 23, 325 (1980).

8 T.G.M. Kleinpenning and L.K.J. Vandamme, J. Appl. Phys. in Press.

9 R.J. van Overstraeten, G.J. Declerck, P.A. Muls, IEE Trans. Elect. Dev. ED-22, 282 (1975)

10 I.M. Bateman, J.A. Magowan, Electron. Lett. 6, 669 (1970).

1/f NOISE IN SCHOTTKY BARRIER DIODES

J.Šikula, P.Vašina, B.Koktavý and Z.Chobola

Department of Physics
Technical University of Brno, Barvičova 85
Czechoslovakia

INTRODUCTION

The dominating component of the low-frequency noise of the Schottky barrier diodes is that of the 1/f type. The model of the 1/f noise in Schottky diodes elaborated by S.T.Hsu [1,2] assumes that the current modulation is due to the barrier height modulation which in turn is due to the fluctuation in the trap or g-r center occupation. Furthermore, it is necessary to assume the tunnelling mechanism.

T.G.M.Kleinpenning [3] elaborated another model of the noise generation. He assumes that the 1/f noise is due to the mobility fluctuation and the value of the 1/f noise spectral density S_i decreases rapidly if the ideality factor tends to unity. As the effective carrier concentration in the depletion region is inversely proportional to the current, the S_i vs. I plot in [3] follows the linear law.

EXPERIMENT

The papers hitherto published studied either the open circuit or the short circuit Schottky diode noise. In the former case the voltage spectral density S_u is measured, while in the latter one measures the current spectral density S_i. In the both cases the measuring apparatus introduces an error which can be allowed for only if the equivalent circuit of the measured diode is known.

We assume the equivalent diode circuit drawn in Fig.1. We modified the existing methods by measuring the voltage fluctuation spectral density S_{UL} across the load resistor R_L within a large range of the diode voltage or current. The spectral density S_{UL} reaches the maximum value from which we get information about the noise source resistance. At low diode voltages, when $R_d \gg R_L$, the value of the voltage fluctuation spectral density S_{UL} is proportional to the current spectral density S_i due to that the circuit is shorted and it holds $S_{UL} \doteq S_i R_L^2$. When the diode voltage is so high that $R_d \ll R_L$, then we measure the voltage fluctuation spectral density in the open circuit and $S_{UL} \doteq S_U$.

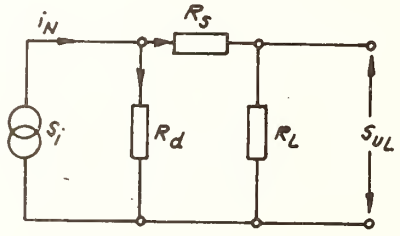

Fig.1 The equivalent diode circuit

The current spectral density S_i vs. the forward current I_F plot for GaAs Schottky diode is in Fig.2. The position of the S_i vs. U_F or I_F plot depends on the value of the load resistance R_L. Decreasing the value of R_L makes the maximum shift towards the higher currents or voltages across the diodes. The asymptote of the measured S_{iL} curves makes the short circuit spectral density S_i and it holds

$$S_i = S_{io} \cdot \exp(\beta_2 U_F) \qquad (1)$$

From our experiments on GaAs Schottky diodes we found out that $\beta_1 < \beta_2 < 2\beta_1$ where $\beta_1 = e/nkT$; n-ideality factor, e-elementary charge. Eq.(1) is in accordance with the results of other authors. Kleinpenning [3] gives for the spectral density of the current fluctuation $S_i \sim I^{\gamma}$, where $1 < \gamma < 2$; as $I = I_0 \exp(\beta_1 U_F)$, we get $S_i \sim \exp(\gamma \beta_1 U_F)$.

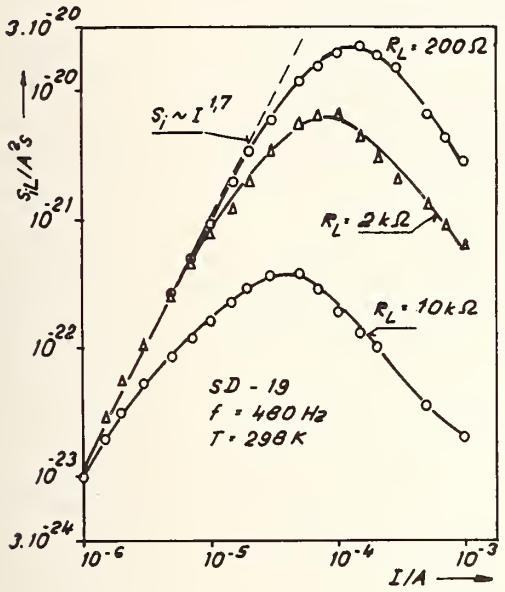

Fig.2. The current spectral density S_i and S_{iL} vs. I_F.

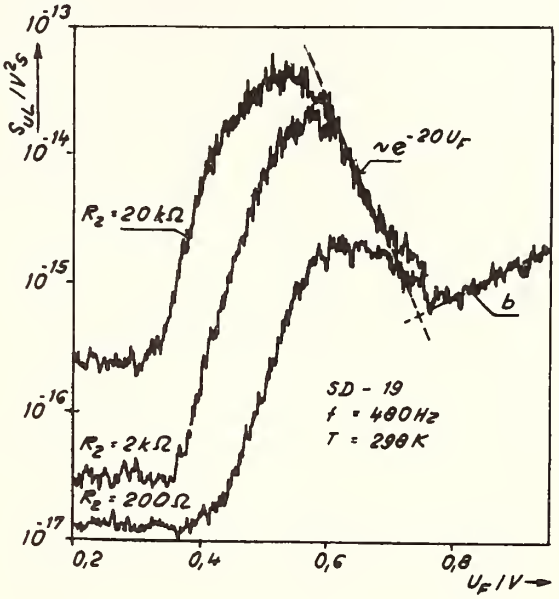

Fig.3. The voltage spectral density S_{uL} vs. U_F.

The spectral density S_{uL} vs. the forward diode voltage U_F plot is in Fig.3.

Increasing the load resistor results in shifting the maximum of the S_{uL} curves towards the lower voltages. The asymptote of the measured curves S_{ua} can be expressed in the form

$$S_{ua} = S_{uo} \exp(-\beta_3 U_F) \qquad (2)$$

where for our set of GaAs Schottky diodes it holds $0 < \beta_3 < \beta_1$. If the series diode resistance R_S is negligible with respect to the load resistance R_L, the spectral density S_{ua} follows the equation

$$S_{ua} = R_d^2 \cdot S_i \quad . \qquad (3)$$

Taking into account the dynamic diode resistance $R_d = 1/[\beta_1 I_0 \exp(\beta_1 U_F)]$ we get using (1)

$$S_{ua} = S_{io} \exp(\beta_2 U_F)/[\beta_1^2 I_0^2 \exp(2\beta_1 U_F)] \qquad (4)$$

and

$$S_{ua} = S_{uo} \exp[(\beta_2 - 2\beta_1) U_F] \qquad (5)$$

where $S_{uo} = S_{io}/\beta_1^2 I_0^2$. We find that for a Schottky diode where the current fluctuation generator is conected in parallel to the diode dynamic resistance and the load resistance it holds $\beta_3 = 2\beta_1 - \beta_2$.

Only a part of our set of Schottky diodes exhibits the noise characteristics in accordance with the suggested model. The current generator of the fluctuation is connected across the parallel combination of the dynamic diode resistance and the load resistance. The equivalent circuit is in Fig. 1. We suppose that the source of noise - in accordance with [3]- is made by the fluctuations in the space charge region of the semiconductor.

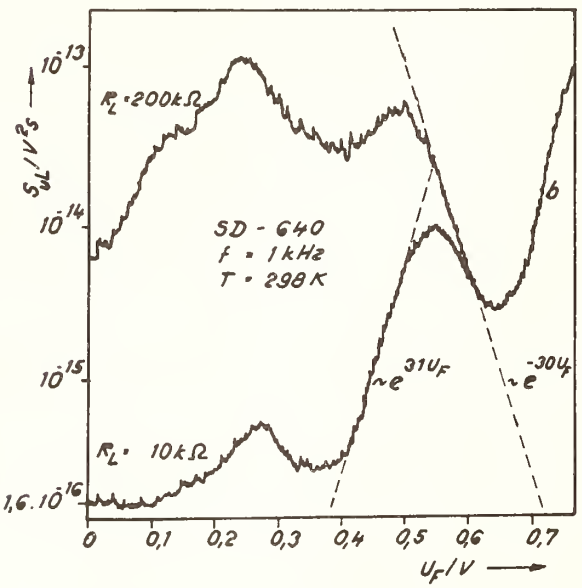

Fig.4. The voltage spectral density S_{UL} vs.U .

Table 1.

Diode N_0	U_1/V	U_2/V	U_3/V
SD-640	0,14	0,25	0,51
SD-943	0,13	0,27	0,50
SB-743	0,13	0,30	0,52

We observed that another phenomenon may be the source of the noise, namely the inhomogenities in the metal-semiconductor structure. In this group of the diodes the spectral density of the voltage fluctuation is not a monotounous function of the diode current. Fig.4 shows the voltage fluctuation spectral density S_{UL} vs. the diode voltage plot for two values of the load resistance R_L (R_L= 10 kΩ, R_L= 200 kΩ). The spectral density S_{UL} has a local maximum, the absolute value of which depends on the match of the noise generator and the load. Increasing the load resistance makes the extremum of the spectral density shift to lower values of the diode voltage. The position of local extremum of the spectral density is also slightly influenced by the value of load resistance. This fact is also due to the match of the noise generator and the load.

When taking the influence of the measuring circuit into account, we get the following extremum voltages U;for some GaAs Schottky diodes (table 1.). The predominant noise component is the 1/f noise for some samples even at a frequency of 1 kHz. Only in the proximity of the spectral density extremum we observe the burst noise.

The spectral density of the fluctuation S_{UL} reaches the minimum value at a voltage $U_F \approx 0,6$ V. At this voltage the noise spectral density of the Schottky barrier equals the spectral density of the b-type (see the b-component in Figs.3 and 4). In accordance with Kleinpenning [3]we attribute the b-component to the Schottky diode series resistance noise.

REFERENCES

[1] S. T. Hsu, IEEE ED-17, 496 (1970)

[2] S. T. Hsu, IEEE ED-18, 882 (1971)

[3] T. G. M. Kleinpenning, Sol. State Electron., 22, 121 (1979)

IV. APPLICATIONS AND MEASUREMENT TECHNIQUES

JOSEPHSON JUNCTIONS, PLASMA PHYSICS, AND ELECTRON TEMPERATURES

Bruce T. Ulrich

Max-Planck-Institute for Plasma Physics
EURATOM-Association
D-8046 Garching bei München
Federal Republic of Germany

GOALS OF FUSION PLASMA RESEARCH

Energy is set free not only by fission of heavy nuclei, but also when the lightest nuclei fuse to form heavier ones. Such fusion processes are the energy source of our sun and other stars. The goal of fusion research in many laboratories all over the world is to make this energy source available for the future energy needs of mankind. The goal is an ambitious one. To build a fusion reactor would rank as one of the great human engineering achievements of this century, or of the next. Conditions in the center of the sun in many ways are less extreme than in a fusion reactor. The sun burns hydrogen at about 15 million degrees, but the temperature in a fusion reactor which burns a deuterium-tritium fuel mixture should be about 100 million degrees. The sun confines its hot ionized gas (plasma) with its gravitational field. A fusion device confines its plasma with a magnetic field, or for a brief instant through the inertia of the plasma during implosion. The sun generates 300 Watts per cubic meter in its core; a 1 GW (1 GW = 1000 MW) tokamak fusion reactor must generate 10^4 times more power per cubic meter. The temperature in the sun decreases from its peak over a distance scale of 10^5 m, but the temperature in a magnetic confinement fusion reactor must decrease over a scale of 1 m, so the temperature gradients in the fusion reactor are 10^6 times times higher than in the sun.

A nearly limitless supply of energy on earth could be available from deuterium in water and from tritium with thermonuclear fusion via the reaction

$$D + T \longrightarrow He^4 + n + (17.6\ \text{MeV}).$$

Tritium does not occur naturally on earth, but can be formed by the neutrons in the fusion reactor via a reaction with lithium. The term "thermonuclear fusion" means that the temperature of the DT fuel mixture should be high enough that the thermal energy of the D and T is high enough for this reaction to take place. In practice, a temperature of about 10 keV (10^8 K) would be required. The goal of fusion energy research is to create this temperature at high enough density for a time long enough that a useable amount of energy is released by the DT reaction. The problem of fusion research, then, is to confine the DT fuel while heating it to ignition, in a reactor which is small enough to be built by humans. The size of fusion device experiments has changed from table top experiments in a university laboratory to international collaborations. The time scale has expanded from one year to twenty. Extrapolation from present fusion devices to a full scale reactor stretches the limits of present technology.

The problem of plasma confinement is so difficult that many methods are being tried in parallel. The two basic approaches are called magnetic confinement fusion (MCF) and inertial confinement fusion. In MCF, the electrons and ions in a plasma spiral around a line of magnetic field and can be held away from a wall. Two difficulties arise with this approach. The first arises because a charged particle experiences no force when it moves parallel to a magnetic line. Thus, the lines of magnetic field confining the plasma should

not cross a material surface. A doughnut shaped (toroidal) magnetic field satisfies this criterion. The second difficulty is that a simple toroidal magnetic field alone does not confine the plasma in equilibrium. To retain the plasma, the magnetic field should twist as it goes around the torus. One way to introduce this twist is with an additional magnetic field produced by a current circulating around the torus in the plasma itself. Such a device is called a tokamak, a word derived from the Russian word "tok" for current. The current in the toroidal shaped plasma is induced by a transformer, in which the plasma serves as a single turn secondary winding. The circulating current simultaneously produces the stabilizing twisted field, and heats the plasma ohmically through the resistance of the plasma. The tokamak suffers from the important drawback that because of the transformer, it must operate in pulses. In addition, because the resistance of the plasma drops as the temperature increases, the circulating current cannot heat the plasma enough to reach fusion temperatures, so additional heating is needed. The main technique is to inject beams of neutral atoms which can cross the magnetic field lines and deposit their energy in the plasma, heating it to temperatures high enough for fusion.

The early success of tokamaks in confining a plasma for longer times and in reaching higher temperatures than other techniques has led to a much greater investment in this fusion device. Over 100 tokamaks have been built, and the largest fusion devices presently built, and under construction are tokamaks. Tokamaks have come closer to achieving conditions for a MCF reactor than other approaches, and parameters can be extrapolated more confidently for tokamaks than for other MCF devices to the domain of reactor operation. Other approaches, called "alternative lines" are pursued because of potential advantages such as steady state, rather than pulsed operation, and in some cases, greater simplicity. Because parameters generally have improved as the size of the MCF device has increased, it is difficult to compare results of alternative lines directly with the results for present-day tokamaks, because the alternative lines are generally at a much earlier stage of development.

In addition to confining the plasma in a stable way, the MCF device also must retain the thermal energy of the plasma to maintain the plasma temperature at a high value. A plasma can cool by radiation or by conduction. Atoms of heavy impurities such as titanium, tungsten, and iron are not completely ionized at the temperature of several keV in the center of a plasma, and can radiate energy directly from the center as X-rays. Light impurities such as carbon and oxygen radiate energy from the cooler edge regions of the plasma. Radiation from impurities has such an important influence on the conditions of the plasma that the ability to control the parameters of a plasma is to a large degree the ability to control impurities. One technique to control impurities is to divert the magnetic field lines near the edge of the plasma to a cooler region. Impurities that enter from the walls are diverted by the lines to a target where they are caught before they can enter the center of the plasma. Such divertors require an expensive increase in the total volume of the magnetic field region. The divertors appear to extract heavy impurities, but not light ones. Other techniques, such as discharge cleaning, and titanium getter pumping also are effective to reduce light impurities. It appears that in present and future experiments in thermonuclear fusion, effective methods can be developed to control impurities without a divertor, but that a divertor may be required for a fusion reactor.

A plasma cools also by conducting heat. Here lies the great unsolved problem of plasma physics. The electrons in a plasma conduct heat 1000 times faster than they would if the magnetic field lines remained rigid and the electrons collided only in pairs. The ion heat conductivity seems in fair agreement with theoretical predictions. Although several mechanisms have been proposed for the high electron heat conductivity and for other anomalously high transport processes, the underlying physics is not well enough understood to calculate important parameters of a tokamak, such as the energy confinement time. In default of physical understanding, the measured confinement time is plotted versus other experimental parameters such as density, temperature, major and minor radius of different tokamak experiments in an effort to find empirical interpolation schemes. These interpolation schemes are called "scaling laws", but they do not represent physical laws in the usual meaning of the word. They are then used to extrapolate from present experiments to future ones. Different interpolation schemes extrapolate differently. An important goal is "ignition", at which the thermonuclear reaction releases enough energy to sustain itself. An example of the degree of uncertainty is indicated by the amount of additional heating required to reach ignition in the Joint European Torus now under construction. Estimates for the amount of required additional heating range from 15 MW to 100 MW, depending on the scaling law chosen.

Clearly there is a need for further physical understanding, but the pressure to make engineering choices for the next generation of devices dictates that empirical extrapolation be used in default of physical understanding.

Significant progress in alternative approaches to MCF occurred in the first true operation of a stellarator in a current-free mode. A reactor built from a stellarator could in principle operate in a steady state, rather than in a pulsed mode. A stellarator, like a tokamak, has a doughnut shaped magnetic field, but the twist in the magnetic field is obtained with additional external magnetic field coils, rather than with a circulating current as in a tokamak. Until the recent results [1] at the Wendelstein (W VII-A) Stellarator in West Germany, stellarators had achieved high temperatures and densities only through use of a circulating current to heat the plasma, so, in fact, they operated like tokamaks, although with a lower value of current circulating in the plasma. At W VII-A, the plasma was heated with 1 MW of power from neutral injectors while in the current free mode. The plasma remained stable in the current free mode, and the energy confinement time increased. This result was surprising, and very encouraging, because the magnetic field of W VII-A twists uniformly without shear, and generally, it was thought by theoreticians that shear in the magnetic field was necessary to stabilize the plasma. An additional result from W VII-A and from CLEO (England) was that the electron heat conductivity decreased in the experiments as $T^{-0.7}$, where T is the electron temperature of the plasma. This result indicates that in operation at higher temperatures in future stellarator experiments, the heat losses via electron thermal conductivity should decrease. Further important progress in the understanding of fusion plasmas can be made through better measurements of the electron temperature distributions in MCF experiments.

ELECTRON TEMPERATURES

The temperature of the electrons in a fusion plasma can be measured only indirectly. Important techniques include Thomson scattering, soft X-ray emission, and electron cyclotron emission measurements. In the first, light from a laser is scattered from the plasma, and the Doppler broadening of the scattered light by the thermal motion of the electrons is measured to determine the electron temperature. Such lasers generally provide temperature information only once during a plasma discharge, and do not give the time evolution of the temperature. In the second, the ratio of thermal X-ray radiation at different photon energies gives an effective electron temperature along the line of sight. Time resolution is high, but spatial detail difficult to resolve without a tomograph-type inversion method. The third method, electron cyclotron emission, offers the advantages of both high time and high spatial resolution.

Electrons in a plasma spiral around magnetic field lines, and radiate electromagnetic radiation at the electron cyclotron frequency

$$f_{ce} = \frac{1}{2\pi}\frac{e}{m} B = 28\, B_{Tesla} \quad GHz$$

and its harmonics. Such radiation is called "electron cyclotron emission". In toroidal plasma machines, such as stellarators and tokamaks, typical plasma conditions are such that the plasma is optically thick at the second harmonic $2f_{ce}$ so the electrons in the plasma radiate like a black body at this frequency [2,3]. Thus, the intensity of the radiation is proportional to the electron temperature T_e. In a toroidal plasma machine, the magnetic field decreases in a known way with the major radius from the inside to the outside of the torus. For temperatures below about 1 keV, the Doppler broadening of the cyclotron emission due to thermal motion is small, so the emission at a particular frequency corresponds to a particular location in the torus. This location can be determined because the magnetic field profile is known in advance. Thus, when electron cyclotron emission is observed from the plasma in the plane of the torus, the intensity of the radiation as a function of frequency determines the electron temperature as a function of position. The width of the peak in the frequency spectrum is determined by the fractional variation of the magnetic field over the torus, and in W VII-A is 10 %. Under typical conditions, the peak is 20 GHz wide, centered at 200 GHz. In other present and future plasma machines, the width of the peak ranges up to 30 or 40 %. The entire peak needs to be scanned to determine the

temperature profile. In a heterodyne receiver based on conventional microwave techniques, it is already difficult to scan the local oscillator over 10%, and nearly impossible over a wider range. In addition, it is important to make rapid observations of the temperature profile during each plasma discharge to determine the temporal structure of plasma instabilities and oscillatory modes. In the W VII-A stellarator, as observed by X-ray emission, the plasma electron temperature oscillates with a sawtooth waveform with a period ranging from one to a few milliseconds under typical conditions. The X-ray observations have not given the spatial profile of these temperature oscillations, whereas the observation of electron cyclotron emission can give this spatial dependence provided the frequency profile is scanned in less than 1 ms. A typical plasma electron temperature is 500 eV = 6 x 10^6 K, and experimental results for self-oscillating Josephson mixers have been reported [4] with mixer noise temperatures of 600 K, so a sufficiently low receiver noise temperature appears realistically obtainable. The main advantage of a Josephson effect heterodyne receiver with internal local oscillator is the ease of changing the frequency of observation rapidly. Such a receiver is under development in Garching. [5,6].

JOSEPHSON EFFECT

When two superconductors are weakly connected together, such as via a point contact a few μm in size, or via quantum mechanical tunneling through an oxide layer about 20 Å thick between the two superconductors, a supercurrent I_s, where

$$I_s = I_c \sin \phi \tag{1}$$

can flow between the two superconductors. The characteristic current I_c is proportional to the strength of the coupling between the two superconductors, and typically ranges from a few μA to a few mA. The variable ϕ is the difference between the phases of the quantum wave functions in the two superconductors on opposite sides of the contact region. The phase ϕ evolves in time according to time dependent quantum mechanics as

$$\frac{1}{2\pi} \frac{d\phi}{dt} = \frac{2e}{h} V \tag{2}$$

where V is the voltage difference across the contact. The other quantities are the fundamental constants, e, the charge of the electron, and h, Planck's constant. The ratio 2e/h = 0.483594 GHz/μV.

The phenomena which arise from (1) and (2) are collectively called the Josephson effect, and the weakly connected superconductors which exhibit them are called a Josephson junction [7]. For a constant bias voltage V, when (2) is integrated and substituted into (1) it can be seen that the supercurrent I_s oscillates at frequency

$$f_o = (2e/h)\, V_o \tag{3}$$

and can serve as the local oscillator in a mixer for a heterodyne receiver. When a signal voltage v cos $2\pi f_s t$, such as from electron cyclotron emission, adds to the constant bias voltage V_o, the total voltage across the junction is

$$V = V_o + v \cos 2\pi f_s t. \tag{4}$$

The signal voltage produces a frequency modulation of the local oscillator frequency as can be seen by substituting (4) into (2), with mixing currents at frequencies $f_o + nf_s$, where $n = \pm 1, \pm 2, \pm 3, \ldots$. The component of interest for a heterodyne receiver is that at the intermediate frequency $f_o - f_s$. When (1), (2) and (4) are combined, the current at the intermediate frequency is

$$I_{i.f.} = I_c\, J_1(2ev/hf_s) \cos 2\pi(f_o - f_s)\, t \tag{5}$$

where J_1 is the first Bessel function. For small values of its argument, $2\, ev_s/hf_s$, this Bessel function is linear in its argument, so the Josephson junction acts as a mixer with output at the i. f. linear in the input signal voltage. The above discussion illustrates the origin of mixing in a voltage biased Josephson junction. In practice, a Josephson

junction is more nearly current biased, and the analysis is somewhat more complex but the physical mechanism of mixing and the results remain essentially the same [8].

To discuss the sensitivity of a Josephson effect mixer, and the dependence of the sensitivity on frequency, we need to introduce the idea of the characteristic frequency f_c of a Josephson junction. When a voltage is applied across a Josephson junction, in addition to the supercurrent I_s, a normal current also can flow. Within the resistively shunted model [9], this current can be represented by V/R, so the total current through the junction can be represented by

$$I = I_c \sin \phi + V/R, \tag{6}$$

The normal resistance R of the junction is, for example, the resistance determined just above the superconducting transition temperature. The junction model now contains an intrinsic characteristic frequency

$$f_c = \frac{2eRI_c}{h} \tag{7}$$

which in typical junctions ranges from 100 to 500 GHz, and in especially good junctions can be above 1 THz. The characteristic frequency divides the low frequency properties of a Josephson junction from the high frequency properties as follows. For small input signals, it can be shown that the supercurrent component I_s responds to the signal voltage v as if the junction were an inductive reactance. At f_c, the impedance for the current to flow as a supercurrent is exactly R, so the current produced by the signal divides equally a supercurrent and as a normal current. Only the supercurrent component interacts nonlinearly to produce output at the intermediate frequency. At higher frequencies $f_s >> f_c$ more current flows as a normal current, and the performance of the junction as a mixer falls off. The low and high frequency limits of the mixer noise temperature (DSB, referred to the output) are [10]

$$(T_N)_{min} = \begin{cases} T, & f << f_c \\ 8T\,(f/f_c)^2, & f >> f_c \end{cases} \tag{8}$$

where T is the temperature of the Josephson junction, typically 4.2 K.

For magnetic fields of most present and planned tokamaks and stellarators, at the usual frequency of observation, 2 f_{ce}, where f_{ce} is the electron cyclotron frequency, the Josephson junction would be oeprating in the low frequency limit, and mixer noise temperatures less than 10 K are predicted. These ultimate values have never been realized in practice because of contradictory requirements on the resistance R of the junction. On one hand, R should be close to the signal source resistance R_s which typically is $R_s \gtrsim 50$ ohms. On the other hand, the line width of the internal oscillation is directly proportional to R, and is 0.5 GHz for each ohm of normal resistance at 4.2 K. It is this line width which determines the frequency resolution of the receiver. For this reason, the minimum noise temperatures of the Josephson junction oscillator-mixer which have been obtained experimentally are about two orders of magnitude higher than the predicted minimum. A Josephson junction oscillator-mixer has been operated over the frequency range of 40 to 260 GHz, with the best $T_N \approx 600$ K at 80 GHz, and values of T_N ranging up to a factor of 3 higher over the entire frequency range of 40 to 260 GHz [4]. For use as a receiver for observation of electron cyclotron emission, a receiver noise temperature T_R of 6000 K ("NEP" = $kT_R = 10^{-19}$ W/Hz) would be adequate. The method of operation is to sweep the junction bias voltage V_o over a range corresponding the frequency range of interest. For example, a 20 GHz wide peak at 200 GHz would be covered by a sweep of amplitude 41 μV centered at 414 μV. The speed at which the bias voltage, and thus the frequency can be swept is not limited by the properties of the Josephson junction, and would be determined by the required signal to noise. For example, assuming a receiver noise temperature of $T_R = 6000$ K, and a comparable source brightness temperature, a frequency resolution of 1 GHz, a 100 μs observation time for a single frequency element, the signal to noise ratio would be about 150.

EXPERIMENTAL PROGRAM

A Josephson effect heterodyne receiver has been used in the frequency scanning mode

to observe electron cyclotron emission from W VII - A. A preliminary version of this receiver, not optimized for input coupling, or for coupling to the i.f. amplifier was used. The purpose of the initial experiments was to gain information about the effects of the electrical disturbances present near the plasma device and to determine whether it was possible to shield the junction from these disturbances. Oversize circular waveguide 2.5 cm in diameter with a polarization rotator was used to transmit the radiation from one end which served as a microwave horn outside the access port of W VII-A, to the junction after a taper transition to the 5 mm dia circular waveguide leading down the neck of the helium dewar. The radiation was coupled to the junction at the bottom of a circular cone tapering from 5 mm to 1 mm diameter. The junction consisted of a Nb wire which entered the side of the cone where it was bent to contact the other superconducting electrode attached to the center conductor of the coaxial line that carried the intermediate frequency signal from the junction. The receiver operated as a double sideband receiver with an intermediate frequency amplifier of bandwidth 10 MHz to 500 MHz. The line width of the internal oscillation of the Josephson junction determined the observed resolution of 8.5 GHz (FWHM) as measured with a klystron source at 156 GHz. In laboratory experiments, frequency resolutions of 2 GHz have been obtained.

In the vicinity of the helium dewar, the magnetic field was of order 50 gauss, and the junction was surrounded by a lead supershield, but without external mu metal shielding. The bias leads from the metal dewar were carried to a shielded electronics enclosure inside a flexible 10 GHz waveguide which served as shielding. Battery powered bias electronics inside the enclosure were used to sweep the bias voltage across the junction with an offset triangle wave of 30 ms period to scan the frequency of observation. The bias voltage is shown in the middle curve of Figure 1. The lower curve shows the plasma current as a function of time. During the rising part of the plasma current, the bias voltage is strongly disturbed. It is not yet known whether the variations in the bias voltage sweep during the plasma discharge occur across the junction, or whether they are picked up in the amplifier which measures the bias voltage. The upper curve shows the output from the i.f. amplifiers. The absolute frequency scale of the receiver was calibrated by observing the signals from a 156 GHz klystron (turned off in Figure 1) to avoid uncertainties in the exact bias voltage which could be caused by thermoelectric potentials in the leads to the junction. The frequency of electron cyclotron emission at 2 f_{ce} was 169 GHz. The signals observed occur at the expected bias voltage. A signal to noise about ten times higher than that presently attained is required before the results of this technique can be used for electron temperature measurements. Through improvements in the input signal coupling, in the coupling to the i.f. amplifier, and in the noise temperature of the i.f. amplifier, it is expected that this requirement improvement in signal to noise can be achieved.

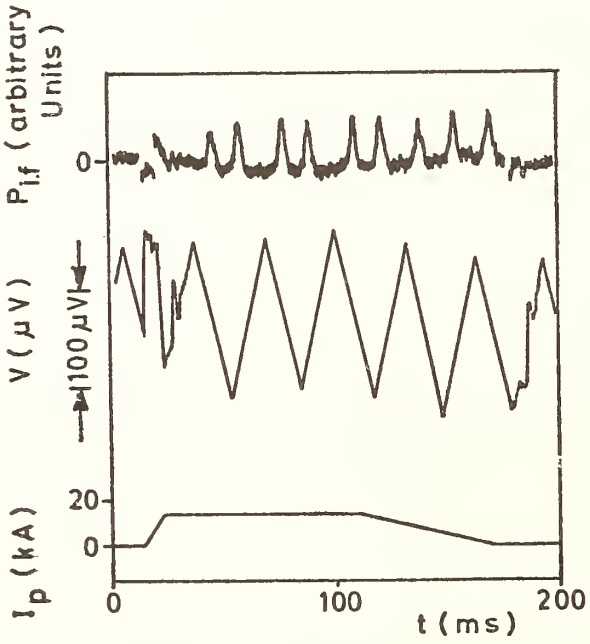

Fig. 1. Lower curve: Ring plasma current I_p during discharge in W VII-A stellarator.

Middle curve: Swept bias voltage V across Josephson junction.

Upper curve: Power output $P_{i.f.}$ at the intermediate frequency from the Josephson effect heterodyne receiver with electron cyclotron emission profiles.

DISCUSSION

The present measurements demonstrate that a Josephson junction heterodyne receiver can be used in the vicinity of a plasma machine to observe electron cyclotron emission at 2 f_{ce}. Additional work is required to improve the signal to noise by about a factor of 10 and to shield the junction and electronics more completely from electrical disturbances. The simplicity and ease in changing the frequency of observation suggest that such a Josephson receiver can be useful in electron cyclotron emission measurements. It can be used in a scanning mode to obtain spectra, or in a fixed frequency mode to obtain measurements with high time resolution.

REFERENCES

[1] W VII-A Team, Procs. of the IAEA Eighth International Conference on Plasma Physics and Controlled Nuclear Fusion Research, Brussels, July 1980.

[2] Engelmann, I., Curatolo, M., Nucl. Fusion 13, 497 (1973).

[3] Meservey, E. B., Schlesinger, S. P., Phys. of Fluids 8, 500 (1965).

[4] Avakjan, R. S., et al., IEEE Trans. Magnetics MAG-11, 838 (1975).

[5] B. T. Ulrich and M. Tutter, in Proc. of the Second International Conference on Superconducting Quantum Devices, Berlin (West), May 1980, Eds. H. D. Halbohm, et al., Walter de Gruyter, Berlin, 1980.

[6] B. T. Ulrich and M. Tutter, in Proc. of the Joint Workshop on ECE and ECRH, Oxford, July 1980, Culham Laboratory, Report No. CLM-ECR.

[7] See, for example, M. Tinkham, "Introduction to Superconductivity", McGraw-Hill, New York 1975.

[8] K. K. Likharev and B. T. Ulrich, "Systems with Josephson Junctions", Moscow University Press, Moscow 1978 (English edition to be published).

[9] L. G. Aslamasov and A. I. Larkin, JETP Letters 15, 349 (1972).

[10] V. P. Zavaleev and K. K. Likharev, Radiotechnika i Elektronika, 23, 1268 (1978).

SURVEY, APPLICATIONS, AND PROSPECTS OF JOHNSON NOISE THERMOMETRY*

T. Vaughn Blalock

Electrical Engineering Department
University of Tennessee
Knoxville, Tennessee 37916

Robert L. Shepard

Instrumentation and Controls Division
Oak Ridge National Laboratory
Oak Ridge, Tennesee 37830

INTRODUCTION

Significant progress in the field of Johnson noise thermometry has occurred since the 1971 survey of Kamper [1]. This paper will review the foundation work of Johnson noise thermometry, survey several basic methods of noise thermometry which use conventional electronic signal-processors, and present some applications of noise thermometry in temperature scale metrology and process temperature instrumentation. The important methods of cryogenic noise thermometry [1] which use quantum devices such as Josephson junctions are not included in this survey.

THEORETICAL FOUNDATION FOR JOHNSON NOISE THERMOMETRY

Johnson noise thermometry is based on the early work of Johnson [2] and Nyquist [3]. The noise-voltage power density spectrum (S_V) in positive frequency space appearing across an unloaded resistor of value R ohms was first measured by Johnson [2], and a few months later it was shown by Nyquist [3] to be given by

$$S_V = 4hfR/[\exp(hf/kT) - 1] \quad , \tag{1}$$

where S_V has units of V^2/Hz, h is Planck's constant, k is Boltzmann's constant, f is the frequency in Hz, and T is the absolute temperature in K. If the frequency is sufficiently low that $f \ll kT/h$ ($kT/h = 6.25$ GHz at $T = 300$ K), then to a very good approximation

$$S_V = 4kTR \quad . \tag{2}$$

One circuit model for Eq. (2) is a noise voltage generator in series with a resistor of value R ohms. An alternate circuit model is a resistor R in parallel with a noise current generator of power density (A^2/Hz) expressed by

$$S_I = \frac{4kT}{R} \quad . \tag{3}$$

*Research sponsored by the Division of Reactor Research and Technology, U.S. Department of Energy under contract W-7405-eng-26 with the Union Carbide Corporation.

Equations (2) and (3) suggest three methods of measuring absolute temperature. In the first method, the resistor's noise voltage over a bandwidth Δf_v is amplified by a signal processor using a high input-impedance, voltage-sensitive preamplifier to obtain an output rms voltage given by

$$\left[\overline{e_{nv}^2}\right]^{(1/2)} = K_v \, (4kT\Delta f_v R)^{1/2} \quad , \tag{4}$$

where K_v is the gain constant of the signal processor which is assumed to be ideal (noiseless). Calibration of the signal processor and an auxiliary measurement of R would allow a determination of the absolute temperature. The second method uses a low input-impedance, current-sensitive preamplifier with a gain K_i and bandwidth Δf_i, to obtain T from

$$\left[\overline{e_{ni}^2}\right]^{(1/2)} = K_i \, (4kT\Delta f_i/R)^{1/2} \quad . \tag{5}$$

The third method requires the measurement of Johnson noise power by multiplying Eqs. (4) and (5) to obtain the result

$$P_n = 4kK_vK_i(\Delta f_v \Delta f_i)^{1/2} \, T \quad , \tag{6}$$

which is independent of R. By dividing Eq. (4) by (5), the value of R can be found independently of T.

The output noise voltages of Eqs. (4) and (5) are fluctuating quantities that are subject to a fundamental statistical uncertainty. This uncertainty in the averaged signal appearing at the output of an integrator or low-pass network following a detector was given by Rice [4] for noise described by a Gaussian probability density function as

$$\sigma = 100 \, (c\Delta f_n t)^{-1/2} \quad , \tag{7}$$

where t is the integration time or a characteristic time-constant of the low-pass network, Δf_n is the noise bandwidth of the noise at the input to the detector, c is a constant that depends on the noise detector and the type of averaging, and σ is the percent standard deviation of the output signal from the integrator or low-pass network. A value of c = 1 is appropriate for narrow-band white noise and pure integration of the output signal from a quadratic detector.

Equations (4)-(7) provide the theoretical basis for Johnson noise thermometry.

BASIC METHODS OF PRACTICAL JOHNSON NOISE THERMOMETRY

The first reported practical noise thermometer, developed by Garrison and Lawson [5] for high temperature measurement (990-1340 K), employed a technique (Fig. 1) of comparing the noise voltage of a reference resistor R_1 at temperature T_1 to the noise voltage of a sensing resistor R_s at unknown temperature T_s. The two noise voltages are made equal in the low-frequency channel by adjusting R_1. The effect of capacitance across the resistors on noise bandwidths is compensated by adjusting capacitors C_s and C_1 to obtain equal noise voltages in the high-frequency channel so that $R_1C_1 = R_sC_s$. This technique eliminates errors due to signal processor nonlinearities and long-term transfer function drifts. The error caused by preamplifier noise is also reduced by the averaging provided by the low-pass filter. The unknown temperature is found from

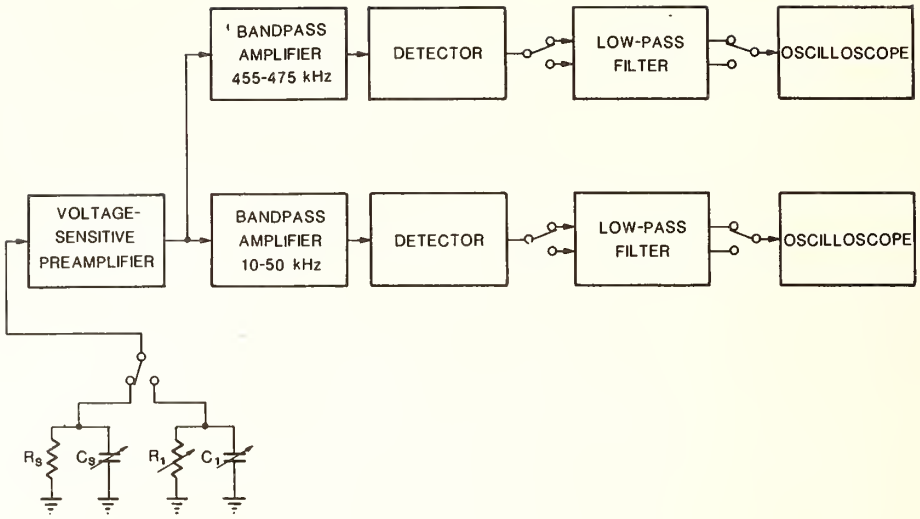

Fig. 1. Noise thermometer of Garrison and Lawson [5].

$$T_s = \frac{T_1 R_1}{R_s} \quad . \tag{8}$$

Commutation switches allow the same measurement system to interrogate both the reference and sensing resistors. To obtain the value of the temperature by this comparison technique, three quantities are measured: the reference temperature T_1, the value of the reference resistor R_1, and the value of the sensing resistor R_s. Garrison and Lawson claimed uncertainties as low as ±0.1%, but Hogue [6] estimated that their results were subject to errors up to ±0.5%. A major contribution to the error is the dependence of noise generated in the preamplifier on source impedance. Pursey and Pyatt [7] developed a new thermometer that uses reference and sensor resistors of equal impedance. In their design, balance is achieved by attenuating the noise voltage from the resistor which is at the higher temperature. The authors [7] concluded that, with further research, errors due to the preamplifier noise could be reduced to ±0.1% and, perhaps, lower.

Several other noise thermometry systems have been published [8-11], all based on the voltage comparison method. All are equipped with commutation switches, except the system developed by Fink [9]. His system (suggested by Garrison and Lawson) uses a cross-correlation scheme which incorporates a sensing resistor and its associated capacitance in an R-C, π-section, two-port network. The noise voltage at each port is measured, and, after proper adjustment of the π-section parameters, the unknown temperature is determined from the values of two reference resistors, the value of the sensing resistor and the temperatures of the reference resistors. Fink reported an uncertainty of ±1% between 1.3 and 4.2 K, and ±0.2% in the range from 77 to 90 K.

A simpler correlation scheme for noise thermometry was suggested by Shore and Williamson [12]; it uses the correlator-amplifier system (Fig. 2) of Brophy, Epstein, and Webb [13] to reduce the noise contribution of the preamplifiers, which is a major source of error in noise thermometry--especially at low temperatures. The outputs from two voltage amplification channels, driven by the noise voltage from a single sensor are multiplied and averaged (Fig. 2) to reduce the uncorrelated noise from the two channels while emphasizing the correlated noise generated by the sensing resistor. The scheme is still subject to the statistical uncertainty expressed by Eq. (7) and it requires careful matching of the transfer functions of the two channels. Practical realizations of the scheme were published by Wagner and Bertman [14], Storm [15], and Brixy [16].

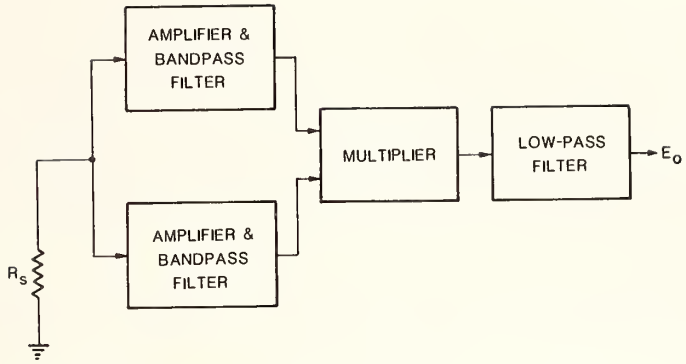

Fig. 2. Correlator-amplifier system of Brophy, Epstein, and Webb [13].

The correlator-amplifier system (Fig. 2) is most useful at low temperatures and with noise voltage preamplifiers having high equivalent noise resistance, R_n. Over the years, values of R_n have been decreased from a value of 1000 Ω in 1959 for a vacuum-tube preamplifier [8] to 44 Ω in 1974 for a junction field effect transistor (JFET) input stage [17], and to 24 Ω in 1979 for a differential preamplifier with parallel JFETs in the input [18]. The lowest published value of R_n is 10.6 Ω for a wideband, feedback, single-ended, voltage preamplifier designed by Blalock [19]. The recent availability of low-noise preamplifiers may eliminate the more complex correlation techniques in future noise thermometers, except perhaps for high-accuracy thermometers used for temperature scale metrology at low temperatures.

A different approach to noise thermometry signal processing was reported by Brodskii and Savateev [20] in 1960 and by Maninger [21] in 1961. The temperature of a resistor is measured by counting the number of times N that the noise voltage levels exceed a reference level V in a unit time. This level-crossing process is described by the equation

$$N = A \exp\left[- V^2/(B + CT)\right] \quad , \tag{9}$$

where the constants A, B, and C depend on the value of the sensing resistor, the transfer function of the signal processor, and the noise of the signal processor. The sensitivity of this method varies with the temperature T being measured, since the output N is a very nonlinear function of T; consequently, a rather complex calibration procedure is required. Although this method does not need an rms-to-dc converter with its inherent nonlinearities, it requires a special-purpose pulse height discriminator, which is no easier to implement than a high-linearity rms-to-dc converter. Unpublished work at the Oak Ridge National Laboratory (ORNL) on noise pulse counting techniques shows no improvement in accuracy over the rms-to-dc conversion technique for the same measurement time, and no significant simplification or improvement in the signal processor. However, the counting technique allows greater discrimination against some types of nonthermal noise.

All of the preceeding methods of noise thermometry involve a measurement of open-circuit noise voltage and an auxiliary measurement of resistance. The quantity defined by Eq. (6)--termed "virtual power" by Johnson in his classic paper [2]--is the product of the open-circuit noise voltage and the short-circuit noise current of a resistor and is independent of the value of the resistor. A Johnson noise power thermometer (JNPT) based on Eq. (6) was developed by Borkowski and Blalock [19] in 1974. The system (Fig. 3) uses a single resistor, a voltage preamplifier with a high input-impedance and a current preamplifier with a low input-impedance to alternately sample the resistor noise through commutating reed relays at the preamplifier inputs. A stable noise source with a level large compared to the preamplifier noise was developed [22] to facilitate calibration of the JNPT amplifiers. For field use, the JNPT (Fig. 3) is equipped to perform the sample-and-hold, multiplication, and data correction functions with a minicomputer which also controls both the switching and the automatic calibration functions.

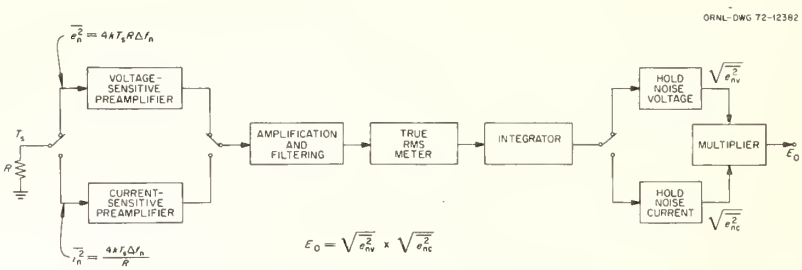

Fig. 3. Johnson noise power thermometer system of Borkowski and Blalock [19].

The JNPT was also implemented [19, 23] in pure analog form, using a probe containing two sensing resistors that maintain a constant resistance ratio as their temperature varies. The noise voltage of one resistor and the noise current of the other resistor are processed simultaneously. These signals are multiplied by an analog multiplier, and the product signal, after resistance-capacitance low-pass filtering, is displayed by a digital panel meter for direct indication of absolute temperature.

APPLICATIONS OF NOISE THERMOMETRY IN TEMPERATURE SCALE METROLOGY

Several high-accuracy noise thermometers have been reported for applications in the determination of the temperature scale.

Crovini and Actis, following extensive contributions [11, 24, 25] to noise thermometry in the temperature range above 670 K, have recently reported [26] the development and use of a noise thermometer to measure differences between the thermodynamic scale and the IPTS-68 (International Practical Temperature Scale of 1968). They carefully measured absolute temperature referenced to the ice point (273.15 K) with two different realizations of a noise voltage thermometer using a signal processor similar to the low-frequency channel of the Garrison-Lawson (GL) system (Fig. 1). In the first realization, the rms voltages of two equal resistors at different temperatures were compared (method of [7]). Balance of the two output voltages was achieved with a precision attenuator switched into the signal processing chain when the higher noise voltage was measured. In the second realization, a modified version of the classical GL system, the balance was achieved in two steps: first, the resistance ratio [Eq. (8)] was preadjusted to match the IPTS-68 kelvin temperature ratio; after which an attenuator in the higher level noise measurement was adjusted to achieve an accurate balance which is described by

$$T_s = a^2 \frac{R_1}{R_s} T_1 + (a^2 - 1) \frac{R_n}{R_1} T_1 \quad . \tag{10}$$

Since a^2, the power attenuator ratio, is in practice so near unity, a measurement of R_n to within a few percent is adequate. Resistors R_1 and R_s were alumina insulated, platinum resistance thermometers with resistance values near 600 Ω at 1230 K. In both realizations, the noise voltage measurements were made in the frequency band from 20 to 120 kHz and a low-noise ($R_n \approx 120$ Ω) preamplifier with selected JFETs was used. The average uncertainty of the experimental results of Crovini and Actis was ±0.034% (99% confidence limits). Their results showed that the IPTS-68 is lower than the thermodynamic scale between 900 and 1230 K; the maximum difference is 0.56 ± 0.20 K (99% confidence limits) near 1093 K.

A high-resolution noise thermometer for measurements in the temperature range from 90 to 100 K was reported by Pickup [27]. The measurement system employed was a modified GL system; the preamplifier input circuit consisted of a JFET cascoded with a bipolar transistor second stage, yielding an R_n of ∿300 Ω. The signal processor bandpass extends from ∿10 kHz to 200 kHz for the low-frequency channel and the sensing resistor is ∿10 kΩ. The temperature of a 3-kΩ reference resistor was ∿25°C as indicated by a platinum resistance thermometer calibrated against the triple point of water. Pickup estimates that the overall uncertainty of his results is ± 0.0078% at 90 K and ± 0.0096% at 97 K (99% confidence

limits) for 7-h integration times. His results show that the IPTS-68 is lower than the thermodynamic scale by 3 ± 6.99 mK at 90.17 K and 8 ± 9.32 mK at 97 K (99% confidence).

Another high-resolution noise thermometer for measurement of temperatures near 4 K was developed by Klein, Klempt, and Storm [18]. Their thermometer system measures noise voltage in a frequency band from 2 to 15 kHz and employs a correlator-amplifier system with a low noise (R_n = 24 Ω) differential preamplifier achieved by a parallel JFET input stage. The temperature sensing resistor is about 10 kΩ. A thorough analysis of error sources led the authors to conclude that the total uncertainty in their measurements was 0.30 mK (±0.35 mK, 99% confidence).

Some of the latest developments in precision noise thermometry for temperature scale metrology are reported in this conference by Klempt and Storm [28] and by Pickup [29].

APPLICATIONS OF NOISE THERMOMETRY IN PROCESS TEMPERATURE INSTRUMENTATION

Brixy applied the GL method, modified by using the correlator-amplifier technique [13], to measurements of temperatures in nuclear reactors [30-32]. His preamplifier has a JFET-bipolar transistor cascode input with $R_n \approx 50$ Ω. Brixy suggests some techniques [32] for solving problems arising from the use of long cables to connect the sensing resistor to the preamplifier and that it is possible to make accurate temperature measurements even with cables as long as 100 m. He reported that the measurement inaccuracy was <0.1% over a range from 300 to 1200 K under laboratory conditions, and <0.5% over a range from 300 to 500 K in high radiation fields in a nuclear reactor. Brixy concluded that noise thermometry is especially suitable for the measurement of temperature in nuclear reactors, and that no additional noise would be contributed from ionization produced in the sensing resistor by gamma rays and neutrons.

Development of the JNPT [19] at ORNL has continued since the early feasibility studies of 1971 and this work has resulted in several practical applications in process temperature measurements. Temperatures and sensor resistances are routinely measured by Johnson noise with uncertainties less than ±0.5% (99% confidence) for sensing resistors from 50 to 300 Ω, and temperature range of from 273 to 1000 K, using signal cables as long as 18 m. Calibration of the signal processor independently of the sensing resistor and connecting cable is accomplished by injection of a high-level noise signal of known spectral density directly into the inputs of the voltage and current preamplifiers [22]. The Johnson noise generated in the cable itself and the effect of the cable on the system transfer function are accounted for by applying data reduction algorithms. One algorithm, developed by Blalock [34], uses a lumped-element model for the cable and has been employed successfully for most cables <20 m in length. For longer cables, a different algorithm based on a distributed model was developed by Agouridis [34].

The JNPT was used to measure temperatures of uranium fuel during irradiation in a nuclear reactor. The JNPT sensor, made of rhenium wire with a resistance value near 80 Ω at 1670 K, was installed in the centerline of the fuel irradiated in ORNL High Flux Isotope Reactor (HFIR). After 4500 hours of high-temperature (1570-1770 K) high-radiation exposure, the decalibration of the JNPT was negligible even though 80% of the rhenium transmuted to osmium [35]. Occasional bursts of microphonic noise caused by vibrations of the loosely supported rhenium coil contaminated the JNPT output. This defect was corrected by swaging the sensor sheaths to form a more rigid containment.

Recently the ORNL group applied the JNPT to an in situ calibration of reactor power plant platinum resistance thermometers [34]. The JNPT can independently measure both the temperature and the resistance of the plant thermometers without removal of the sensor. JNPT measurements in two power plants [34] show great promise for in situ calibration where access to the sensor can be achieved through short cables (<18 m). Long cables, already installed in power plants for dc measurements, may receive large amounts of nonthermal noise from the wide variety of noise sources. The major challenge in this application appears to be the characterization of both the noise contribution and the signal attenuation produced by long, industrial signal cables using measurements made only at the accessible end of the cable.

CONCLUSIONS AND PROSPECTS

Much progress has been made in Johnson noise thermometry since the early pioneering work of Garrison and Lawson in 1949. Progress has accelerated in the last 10 years due to rapid improvements in signal processor components and the increasing availability and power of digital computation. The difficulties noted by Kamper [1] of eliminating noise of nonthermal origin still remain and provide challenging opportunities in the design of grounding and shielding systems for successful noise thermometry.

The successful applications of noise thermometry to temperature scale metrology by Crovini, Actis, Pickup, Klein, Klempt, and Storm show the advantages of using a fundamentally linear, absolute thermometer for interpolation and extrapolation of the defining fixed points of the temperature scale.

The process temperature measurements of Brixy and the ORNL group indicate encouraging prospects for such applications. Major problems are the effects of extraneous noise pickup and random noise generated in the cable, and the effect of the cable signal transfer characteristics on the overall transfer function of the signal processor. Solution of these problems will be provided by specification of special cables for noise thermometry, development of effective techniques for measuring relevant cable parameters, and design of appropriate digital computer algorithms for data reduction and correction.

REFERENCES

[1] R. A. Kamper, "Survey of Noise Thermometry," *Temperature, Its Measurement and Control in Science and Industry*, Instrument Society of America, Vol. IV (1), 349 (1972).

[2] J. B. Johnson, "Thermal Agitation of Electricity in Conductors," Phys. Rev. 32, 97 (1928).

[3] H. Nyquist, "Thermal Agitation of Electric Charge in Conductors," Phys. Rev. 32, 110 (1928).

[4] S. O. Rice, "Mathematical Analysis of Random Noise," Bell Sys. Tech. J. 23, 282 (1944).

[5] J. B. Garrison and A. W. Lawson, "An Absolute Noise Thermometer for High Temperatures and High Pressures," Rev. Sci. Instrum. 20, 785 (1949).

[6] E. W. Hogue, "Factors Affecting the Precision and Accuracy of an Absolute Noise Thermometer," NBS Report 3471 (1954).

[7] H. Pursey and E. C. Pyatt, "Measurement of Equivalent Noise Resistance of a Noise Thermometry Amplifier," J. Sci. Instrum. 36, 260 (1959).

8] E. T. Patronis, Jr., H. Marshak et al., "Low Temperature Thermal Noise Thermometer," Rev. Sci. Instrum. 30, 578 (1959).

[9] H. J. Fink, "A New Absolute Thermometer at Low Temperatures," Can. J. Phys. 37, 1397 (1959).

[10] M. H. Tillinger, "Noise Thermometer at High Pressure," Technical Report No. 1, Polytechnic Institute of Brooklyn (1965).

[11] L. Crovini, "Absolute Temperature Measurement by Means of Thermal Noise," La Ricenca Scientifica 37(12), 1238 (1967).

[12] F. J. Shore and R. S. Williamson, "Suggested Thermometer for Low Temperatures Using Nyquist Noise and Correlator-Amplifier," Rev. Sci. Instrum. 37(6), 787 (1966).

[13] J. J. Brophy, M. Epstein, and S. L. Webb, "Correlator-Amplifier for Very Low Level Signals," Rev. Sci. Instrum. 36(12), 1803 (1965).

[14] R. Wagner and B. Bertman, paper T-2, Commission 1, International Institute of Refrigeration, Tokyo (1970).

[15] L. Storm, Z. Ang. Phys. 28, 331 (1970).

[16] H. G. Brixy, "Temperature Measurement in Nuclear Reactors by Noise Thermometry," Nucl. Instrum. Methods 97, 75 (1971).

[17] P. T. Anderson and P. B. Pipes, "A Low Noise Amplifier with Application to Noise Thermometry Between 300 and 4 K," Rev. Sci. Instrum. 45(1), 42 (1974).

[18] H. Klein, G. Klempt, and L. Storm, "Measurement of ^{4}He at Various Vapour Pressures by a Noise Thermometer," Metrologia 15, 143 (1979).

[19] C. J. Borkowski and T. V. Blalock, "A New Method of Johnson Noise Thermometry," Rev. Sci. Instrum. 45(2), 151 (1974).

[20] A. D. Brodskii and A. V. Savateev, "A New Method of Absolute Temperature Measurements," Izmeritel'naya Teknika No. 5, 21 (1960).

[21] R. C. Maninger, "Thermal Noise Investigation," U.S.A. Patent 3,181,365, May 4, 1965. Filed January 9, 1961.

[22] T. V. Blalock and C. J. Borkowski, "High-Level Noise Source for the Calibration of Johnson Noise Power Thermometers," Rev. Sci. Instrum. 49(8), 1046 (1978).

[23] T. V. Blalock and R. L. Shepard, "Johnson Noise Power Thermometer," ORNL internal report (1977).

[24] A. Actis, A. Cibrario, and L. Crovini, "Methods of Noise Thermometry Above 400°C," *Temperature, Its Measurement and Control in Science and Industry*, Instrument Society of America, Vol. IV(1), 355 (1972).

[25] L. Crovini and A. Actis, "Systematic Errors in High Temperature Noise Thermometry," *Temperature Measurement* (Eds., B. F. Billings and T. J. Quinn) Inst. Phys. Cont. Ser. 26. 398 (1975).

[26] L. Crovini and A. Actis, "Noise Thermometry in the Range 630-962°C," Metrologia 14, 69 (1978).

[27] C. P. Pickup, "A High Resolution Noise Thermometer for the Temperature Range 90-100 K," Metrologia 11, 151 (1975).

[28] G. Klempt and L. Storm, "Determination of the Thermodynamic Temperature of Fixed Points by Means of a Highly Accurate Noise Thermometry," Proc. 6th Int. Symp. Noise in Physical Systems, April 1981.

[29] C. P. Pickup, "A Precision Noise Thermometry for Temperature Scale Studies," Proc. 6th Int. Symp. Noise in Physical Systems, April 1981.

[30] H. G. Brixy, "Temperature Measurement in Nuclear Reactors by Noise Thermometry," Nucl. Instrum. Methods 97, 75 (1971).

[31] H. Brixy, "Die Rauschthermometrie als Temperaturmeszmethode in Kernreaktoren," Dissertation, Jül-885-RG (1972).

[32] H. Brixy, R. Hecker, and T. Overhoff, "Development of the Noise Thermometer and Its Test as an In-Core Temperature Detector," Proc. Symp. Nuclear Power Plants Control and Instrumentation, International Atomic Energy Agency Report No. IAEA/SM-168/F-1, Vienna, 1973.

[33] H. Brixy, K. Rittinghaus, K. Gärtner, and R. Hecker, "Developments in the Area of Noise Thermometry at KFA-JÜLICH," Proc. Int. High Temperature In-Pile Thermometry Colloquium, Petten, The Netherlands, December 1974.

[34] R. L. Shepard, T. V. Blalock, J. L. Horton, and D. C. Agouridis, "In-Situ Calibration of Reactor Plant Platinum Resistance Thermometers Using Johnson Noise Methods," Final Report, EPRI Contract RP-1440-1 (1980).

[35] R. L. Shepard, C. J. Borkowski, J. K. East, R. J. Fox, J. L. Horton, and T. V. Blalock, "Ultrasonic and Johnson Noise Fuel Centerline Thermometry," Proc. Int. High Temperature In-Pile Thermometry Colloquium, Petten, Netherlands, 1974.

DETERMINATION OF THE THERMODYNAMIC TEMPERATURE OF FIXED POINTS BY MEANS OF A HIGHLY ACCURATE NOISE THERMOMETER

G. Klempt, L. Storm

Institut für Angewandte Physik der Universität Münster,
Roxeler Str. 70/72, D-4400 Münster, Fed.Rep. of Germany

The standard device for the measurement of thermodynamic temperatures in the region from 2 K up to the melting point of gold is the gas thermometer. Since several systematic errors have been discovered in the last decades, the developement of an alternative thermometer with comparable accuracy seemed to be desirable. The noise thermometer is a suitable alternative, since the thermal noise voltage U_t of an impedance Z at the temperature T is determined by a fluctuation-dissipation theorem, i.e. the Nyquist formula:

$$\langle u_t^2 \rangle = \int 4\,k\,T\,\mathrm{Re}Z\,df \qquad (1)$$

In 1976 a device was set up to measure temperatures in the liquid ^{4}He-region with an accuracy of about 10^{-4}, s. [1]. Particularly at low temperatures, the specific error sources of the noise thermometer could be investigated. A measuring proceedure was developed, which gives the thermodynamic temperature without any additional corrections. To measure the temperature of several thermometric fixed points up to the water boiling point within a few mK, an improved noise thermometer with an accuracy of about 10^{-5} has been set up during the last years.

The figure shows the block diagram of the noise thermometer, operating by a correlation method. The temperature-sensing resistor 2R, with centre point at earth potential, is connected in parallel to two identical highly linear and stable amplifier- and filter channels, using a 4-wire measurement technique. The output voltages are digitalized by 16 bit ADC's with a rate

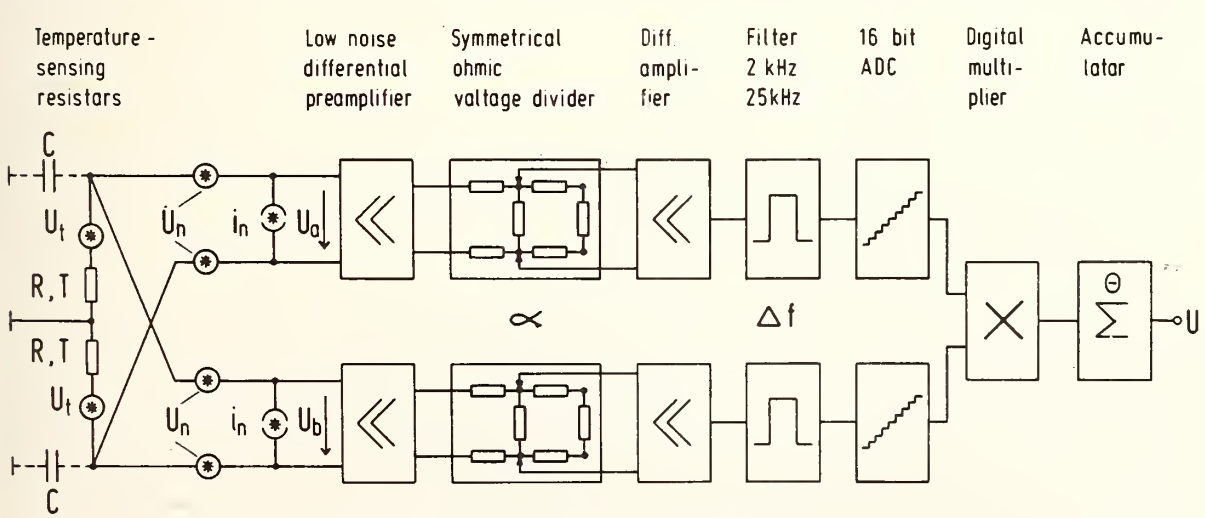

Block diagram of the noise thermometer

of 50 kHz, then multiplied and added up. The output voltage U of the cross spectrometer - averaged over a finite time Θ - represents a stochastic process. Its expectation value is given by eq (2):

$$\langle U \rangle = K \cdot \alpha_a \cdot \alpha_b \int \mathrm{Re}\{V_a^* V_b \cdot W_{uaub}\}\, df \qquad (2)$$

W_{uaub} indicates the complex cross spectrum of the preamplifier input voltages u_a and u_b. K is determined by the ADC's properties. The attenuation factor α of the resistive voltage divider is presumed to be independent of the frequency. To avoid nonlinearity errors of the ADC's, the attenuators are adjusted in such a way that the ADC's are equally modulated at the measurement of the unknown temperature T and at the calibration of the whole device at the water triple point temperature T_{tr} = 273.16 K, which defines the temperature scale. V_a and V_b are the gains of the channels a and b. V_a^* means the conjugate complex number of V_a. If both channels have an identical phase response, $V_a^* V_b$ becomes a real number and only the real part of W_{uaub} contributes to $\langle U \rangle$. A thorough theoretical analysis of the correlator input circuit leads to the following equation for the real part of W_{uaub}:

$$\mathrm{Re}W_{uaub} = 2 \cdot \frac{4kR \cdot [T + A(f,T) \cdot R]}{1 + (2\pi f RC)^2} \qquad (3)$$

$4kRT / (1 + (2\pi f RC)^2)$ means the power spectrum of the Nyquist noise of the temperature sensing resistors, filtered by the low pass consisting of R and the lead capacity C in parallel to R. The error term $A \cdot R$ is mainly caused by the current noise sources i_n including the noise current of the preamplifiers and the temperature dependent noise due to the insulating dielectric of the leads. With ultra low noise FETs in the preamplifier input stages and very low-loss dielectrics in the whole measuring input circuit, A has a value of some mK/kΩ. This error term cannot be made neglible by decreasing the value of R because of the statistical fluctuations.

In this correlation method the statistically independent noise sources u_n - including the inherent noise voltage of the preamplifiers and the temperature dependent thermal noise of the leads - contribute practically nothing towards $\langle U \rangle$. Its relative standard deviation is given by a modified Rice-formula:

$$\left(\frac{\sigma}{\langle U \rangle}\right)^2 = \frac{1}{2}\left[1 + \left(1 + \frac{W_{un}}{4kTR}\right)^2\right] \cdot \frac{1}{\Theta \cdot \Delta f} \qquad (4)$$

$$\xrightarrow{W_{un} \ll 4kTR} \frac{1}{\Theta \cdot \Delta f}$$

Even in the best case ($W_{un} \ll 4kTR$) a measuring time Θ of $5 \cdot 10^5$ s and a bandwith Δf of $2 \cdot 10^4$ Hz is needed for $\sigma(u) = 10^{-5}$, which equals an accuracy of some mK in the measurement of medium temperatures. 4kTR should not be made smaller than W_{un}, otherwise the measuring time would become inadmissibly high. This implies values of R in the order of some kΩ with conventional transistor amplifiers. Thus eq (4) determines a lower limit of R and hence of the error term AR. As the theoretical estimation is not accurate enough, AR must be eliminated by experimental means taking advantage of the fact that A is independent of R.

For the measurement of an unknown temperature T, the same sensing resistors are brought alternatingly to T and the water triple point temperature T_{tr} = 273.16 K. We measure the output voltages $\langle U \rangle$ and $\langle U_{tr} \rangle$, the resistances R and R_{tr} and the attenuation factors α_a and α_b. With the measured values for eq (2) and eq (3) for both temperatures we compute the magnitude F

$$F(R) = \frac{\langle U \rangle}{\langle U_{tR} \rangle} \cdot \frac{R_{tr}}{R} \cdot \alpha_a \alpha_b \cdot T_{tr} \cdot (1 - \gamma \cdot \Delta(RC)) \qquad (5)$$

$$= T \cdot (1 + PR)$$

which is a linear function of R. If one measures F at the same temperature T for different values of R, the unknown temperature can be obtained by extrapolation of R to 0. The variations ΔR in R and ΔC in C can be kept so small at the changeover from T to T_{tr}, that the correction term $\gamma \cdot \Delta(RC)$ is of the order of 10^{-6} with R below 5 kΩ.

The described method has the advantage that all the disturbing noise is eliminated. But for an accuracy of 10^{-5} in T one needs 10^{6} s for the measurement of $\langle U \rangle$ and $\langle U_{tr} \rangle$ and for each value of R. Therefore a long-term stability of some 10^{-6} of all electronic components and the temperature baths is demanded. The temperature sensor 2R is located together with four platinum resistance thermometers in a cylindrical block of copper. Its temperature is kept constant within some 100 μK by a heater controlled by one of the platinum resistors. The dominant error sources are the statistical error and the gain stability of the correlator.

For the momentary series of measurement the four platinum resistance temperatures have been calibrated at the Physikalisch-Technische Bundesanstalt in Braunschweig at the argon triple point temperature. At the Symposium on Noise in April 1981, we will present the value of the argon triple point temperature measured by the noise thermometer in Münster.

[1] H.-H. Klein, G. Klempt, L. Storm: Metrologia 15, 143 (1979)

A PRECISION NOISE THERMOMETER FOR TEMPERATURE SCALE STUDIES

C. P. PICKUP

CSIRO Division of Applied Physics
Sydney, Australia 2070

INTRODUCTION

Practically all of our knowledge of thermodynamic temperatures has been obtained from gas thermometry either by direct pressure versus volume measurements or more indirectly from isotherm or acoustic thermometry, all of which are difficult and tedious experiments subject to many corrections. In particular the non-ideal properties of all real gases have a serious effect which is difficult to determine accurately.

In recent years a program of high precision gas thermometry here at NBS [1] from room temperature upwards has shown a serious systematic error in the International Practical Temperature Scale, amounting to approximately 30 mK at the steam point and increasing at higher temperatures.

It is unlikely that any comparable gas thermometer experiment will be undertaken elsewhere in the near future, and noise thermometry is one of the very few alternative techniques which might be capable of yielding confirmatory data. We at the Division of Applied Physics (DAP) have accordingly constructed a noise thermometer operating in the range 100-150°C which is designed to be accurate to within a few mK.

PRINCIPLE OF THE NOISE THERMOMETER

The noise thermometer is based fairly closely on a successful earlier design [2] which operated at the oxygen boiling point using the switching principle pioneered by Garrison and Lawson [3] more than thirty years ago in which a noise measuring channel is switched alternately between two resistors at different temperatures, one of which is known. The noise of the measuring system is constant (ideally) and thus a balanced condition can be detected in which the resistors produce the same noise. An unknown temperature can then be determined from the other, which would usually be 273.15 K, and the ratio of the two resistances.

DETAILED DESCRIPTION

A block diagram of the noise thermometer is shown in figure 1. The resistor R_1 is maintained at the temperature to be measured (T_1) whilst R_2 is in an ice bath ($T_2 = 273.15$ K). Either resistor may be connected via mercury-wetted reed switches S_1 and S_2 to a fairly low noise pre-amplifier with a type BFW 11 JFET cascode input stage. This was selected mainly for high input resistance, and its equivalent noise resistance is 450 ohm.

The amplified noise signals are fed through the shield surrounding the noise thermometer by a screened transformer and split by filters into two frequency ranges, 10-100 kHz and 100-200 kHz. The mean amplitudes of each filter output are determined by linear detectors, V/F converters and frequency counters. The data are collected and processed by a micro-computer system.

A crystal-controlled clock and counter chain provides timing control signals for the system. In normal operation the switches change over each 15 s with 5 s being allowed after each switching for settling before integration begins. In addition an early stage of the pre-amplifier is gated off during the switching period. Signals for this gating and the reed switch operation are transferred through the shield by optical links with light pipes.

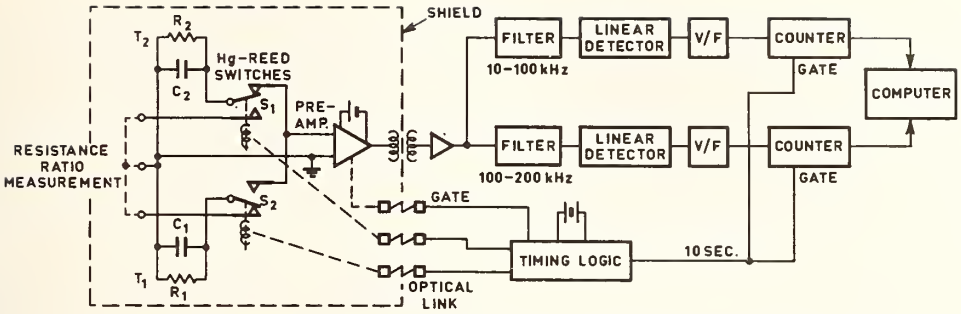

Fig. 1 Block diagram of switching noise thermometer.

The unselected noise resistor is normally short-circuited; however, with the shield raised and both switches operated, it is possible to measure the ratio R_1/R_2 at 1 kHz using a 7 decade inductive divider bridge. This is normally done at the beginning and end of each run.

The temperature of resistance R_1 is maintained by heated oil circulated from an external bath with the returning oil providing thermal shielding for an isothermal column extending into the electromagnetically shielded area. An IPTS calibrated platinum resistance thermometer is provided for both measurement and control of the oil temperature. This temperature exhibits rapid fluctuations of the order of 10 mK, due presumably to the turbulent processes in the circulating pump; however, the mean value is stable to within 1 mK indefinitely.

Resistance R_2 is surrounded by high purity ice with the melt water drained from the bottom of the container. Tests conducted with a standard platinum resistance thermometer in this ice bath showed variations generally less than 1 mK.

THERMOMETRIC RESISTANCES

Desirable properties for the thermometric resistors include

a. only thermal noise should be produced
b. the conductance should be independent of frequency to at least 200 kHz
c. the conductance should be adequately stable at temperatures approaching 150°C.

Metal film resistors (Philips MR25) were used. Any excess noise from these should be well below the 10 kHz low frequency cut-off of the system and would presumably be proportional to the dc current which is only 2 pA.

Present technology does not permit the convenient measurement of the conductance ratio with sufficient precision at frequencies as high as 200 kHz, and thus extrapolation of audio frequency measurement is necessary. The resistive film is too thin for skin effect to be significant and any change of conductance with frequency would have to be due to some effect such as loss in the substrate or protective lacquer or extreme spiral grooving.

In order to provide even greater confidence in the ratio determination it was decided to use initially groups of identical resistors (6.8 kΩ) in parallel, three for R_1 and two for R_2. This forces a 3/2 ratio of thermodynamic temperatures for balance, i.e. $T_1 \approx 135°C$.

This is a reasonably convenient temperature for the purpose of checking the scale and a few hours after each warm-up the resistance ratio becomes stable to within a few PPM although there is a small change each time the hot resistors are cycled to room temperature.

MEASUREMENT PROCEDURE

Before the series of measuring runs was commenced (and also after) calibrating tests were performed with short circuits substituted for the noise resistors. This process provides a direct measurement of the difference in noise of the reed switches and the leads to

the resistors at their normal operating temperatures. In principle it also provides reasonable corrections for any (possibly non-Gaussian) extraneous noise signals arising from mechanical vibration or inductive coupling which fall within the pass-band. When the resistors are replaced in the circuit there will be some attenuation of this measured difference due to the shunt capacitances but this is less than 1% at 200 kHz and can be neglected.

Also at this time the actual resistances of the leads at their operating temperatures can be measured. These resistances, of the order of 1 ohm, are needed to correct the measured resistance ratio which includes them.

In normal operation the bath temperature T_1 and the capacitance C_1 are varied until balance is obtained in both frequency ranges, thus ensuring that there will be no errors caused by the attenuation of the R_1C_1 and R_2C_2 time constants. The results of each 10 s integration are squared (because the detector is of the linear type) and the differences between those from R_1 and R_2 (called LOWER and UPPER respectively) are stored by a dedicated micro-computer over the period of each run which normally lasts just under 24 hours.

At the end of each run, after the correction for the noise of the leads has been subtracted, there is normally a small residual unbalance $\overline{U-L}$ in both channels and the temperature T_1 is calculated from the formula [2]

$$T_1 = \frac{R_2}{R_1} T_2 \left[1 - p\left(\frac{7}{6} \frac{\overline{U-L}}{\overline{U}}\bigg|_{LF} - \frac{1}{6} \frac{\overline{U-L}}{\overline{U}}\bigg|_{HF}\right)\right] \qquad (1)$$

Here $\overline{U}$ represents the total mean square noise from the system when switched to the UPPER resistor and the factor p, which is taken as 1.15, reflects the reduction in the relative unbalance caused by the noise of the amplifier.

ERRORS DUE TO GATE NOISE CURRENTS

Since the resistors R_1 and R_2 have different values the switching noise thermometer is subject to errors due to noise currents originating in the input circuit of the amplifier and also, of course, to any systematic dependence of gain on source impedance resulting from feedback. The latter is effectively eliminated by the cascode arrangement.

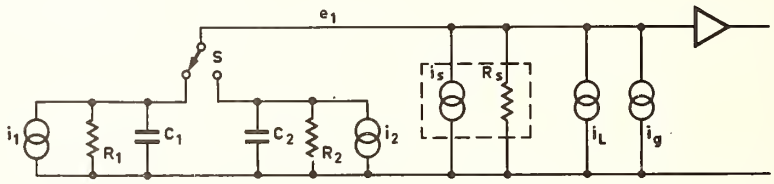

Fig. 2 Equivalent circuit in terms of noise current generators. Johnson noise in the thermometric resistances is represented by i_1 and i_2, R_s is the shunt resistance of the input circuit with noise i_s and i_L, i_g are respectively the shot noise due to the gate leakage current and the induced gate noise.

The important noise current generators are shown in figure 2. The shunt resistance R_s arising from the input conductances of the FET and the insulation losses of the circuit was measured using a special digital Q-meter at 150 kHz to be approximately 1000 MΩ. This may be considered to produce ordinary thermal noise corresponding to room temperature and causes an error in the present system of only 0.2 mK. This error would, however, be more serious in a cryogenic noise thermometer.

The gate leakage current I_g is 2 pA and its shot noise component given by $\overline{di_L^2} = 2eI_g df$ may also be shown to give a completely insignificant error in this case.

The induced gate noise current is capacitively coupled from the channel and may be represented by $di_g^2 = Bf^2 df$ where B is a constant. For the frequencies and impedances involved here the correlation with the channel noise is pure imaginary and the noise voltages at the gate may be simply added in quadrature. The effect of this additional noise current is largest for the higher value resistance R_1 in the higher frequency range when it represents an apparent temperature increase of approximately 5 mK. This would be partly off-set by a proportionately smaller increase in the apparent temperature of R_2; however, it was shown in [2] that errors due to capacitively-coupled noise currents at the gate, for the noise thermometer balanced simultaneously in two frequency ranges, cancel out completely in a second order analysis.

RESULTS

The standard deviations of the differences in both frequency ranges throughout all the runs were consistent with the integration period and pre-detection bandwidth. For a single 24 hour run, after combining the high and low frequency means, the standard deviation of the temperature should be approximately 12 mK.

For 62 runs the mean difference $T_{IPTS} - T_{NOISE}$ was 12 mK, the standard deviation 19 mK and the S.D. of the mean 2.4 mK. The largest positive and negative difference from the mean were 30 mK and -39 mK respectively with rather more than the expected number of large differences.

This result is in the same direction but otherwise not in particularly good agreement with the recent gas thermometry; however, a number of break-downs towards the end of the series of runs raises the possibility of undetected intermittent electronic problems earlier. A further series of tests are planned during the next few months after the detectors and counting systems have been re-built.

REFERENCES

[1] L. A. Guildner and R. E. Edsinger, *J. Res. NBS* 80A, 703 (1976).

[2] C. P. Pickup, *Metrologia* 11, 151 (1975).

[3] J. B. Garrison and A. W. Lawson, *Rev. Sci. Instr.* 20, 785 (1949).

ELECTRO-ACOUSTICAL NOISE

R.J.J. Zijlstra and W. Westera

Fysisch Laboratorium, Rijksuniversiteit Utrecht, The Netherlands

1. INTRODUCTION

Electro-acoustical noise is the noise associated with the interaction of free carriers with acoustic waves in piezoelectric semiconductors. Increased interest in these physical phenomena was triggered by the experimental results on acoustic amplification in CdS reported in 1961 by Hutson, McFee and White [1]. The electric field accompanying an acoustic wave, be it a bulk or a surface wave, in a piezoelectric semiconductor produces periodic variation in the electric potential. Free electrons, interacting with these waves, tend to seek the potential minima and in doing so get dragged along by the propagating wave. If the drift velocity of the carriers is smaller than the sound velocity, the acoustically trapped carriers receive a net accelerating force from the wave. Acoustic energy is thereby transferred from the wave to free electrons and the wave is attenuated. However, if an applied electric field causes the drift velocity of electrons to become larger than the sound velocity, then energy is transferred from electrons to the wave while it is travelling in the direction of the drifting carriers. As a result the acoustic waves are amplified. White [2] in 1962 gave a linear description of this electro-acoustic effect, known as the linear small signal gain theory. This effect also applies to spontaneously generated waves with thermal amplitudes. These amplified acoustic waves also interact with the free carriers. This gives rise to essentially non-linear effects, which may include parametric interaction of acoustic waves, current saturation, large current noise and domain formation [3,4]. These effects cannot be described by White's theory. Several authors [5,6] have tried to describe these phenomena. Since, however, it is very difficult to describe these non-linear effects when starting from basic principles, many of these phenomena are not yet understood quantitatively. Moore realized that the observed current saturation and current fluctuations are caused by the trapping of bunches of free charge carriers in potential troughs that are associated with acoustic waves amplified from the thermal background. Accordingly, he ascribed the observed current noise in CdS to fluctuations in the creation-annihilation processes of these potential troughs [7]. The expression for the noise spectrum thus obtained gave a reasonable explanation for Moore's experimental data. Subsequently Friedman [8] and Nakamura [9,10] using different approaches were less successful in describing these experimental data.

In our opinion Moore's model is essentially correct and scored highest in the description of experimental data. Zijlstra and Gielen [11] extended Moore's theory by accounting for transit time effects in a local description. However, they neglected the displacement and the diffusion current in the expression for the current density and assumed that the creation and annihilation of troughs are independent of electric field strength. Their calculation resulted among other things in a frequency independent impedance. Experimentally, however, the observed ac impedance of electro-acoustically active CdS crystals turned out to be frequency dependent [12]. The observed frequency dependence of the ac impedance could be explained, however, by taking into account diffusion, space charge, displacement current and the electric field dependence of the trough creation and annihilation rates [13,14].

In section 2 we present theoretical results along the lines indicated. Section 3 is concerned with experimental results on electro-acoustical noise in CdS.

2. THEORY

Essentially we shall use Moore's model but extend it as indicated in the introduction. In addition we shall use the so-called phenomenological, hydrodynamic theory of electron absorption and emission of sound in semiconductors. Usually the criterion for the validity of this approach is written as $ql << 1$ and $\omega\tau << 1$ [14], where q is wave number of acoustic waves, l is free carrier mean free path, τ is their collision time and ω is angular frequency. Gulguaev and Kozorezov [15] argue, however, that the mean free path l should be replaced by $\sqrt{D\tau_\zeta}$ and the collision time by τ_ζ, where τ_ζ is the energy relaxation time and D is the free carrier diffusion constant.

2.1. DESCRIPTION OF THE MODEL AND BASIC EQUATIONS

We consider an n-type homogeneous piezoelectric semiconducting crystal, where the electric field is applied along a symmetry axis, the x-axis. The sample is provided with two ohmic contacts with spacing L. It can be shown for this case that the formulas can be put in a one-dimensional form [14]. Therefore we shall start straightaway with a one-dimensional description.

In the analysis we use the following sign convention, $E < 0$ and $I < 0$; then $V > 0$, where E is the electric field strength, I is the electric current and V is the applied voltage.

Let n_d be the local density of the free electrons in the conduction band and n_s the density of electrons trapped in potential troughs that are associated with acoustic waves amplified from the thermal background. The total density of electrons in the conduction band is then given by $n = n_d + n_s$. Gauss's equation yields

$$\partial D/\partial x = - q(n - \bar{n}) \quad , \tag{1}$$

where D is the dielectric displacement, -q the electron charge and where steady-state values are indicated by bar; $\bar{n}$ is assumed to be equal to the thermal equilibrium density of free carriers. The total current density then is

$$j = - qn_d v_d - qn_s v_s' + qD_n(\partial n/\partial x) + \partial D/\partial t \quad , \tag{2}$$

where D_n is the diffusion constant of electrons, v_d is the drift velocity of free electrons and v_s' is the x-component of the sound velocity v_s. Since j is solenoidal, we have $\partial j/\partial x = 0$. The piezoelectric relations read

$$T = cS - eE \quad ; \qquad D = \varepsilon E + eS \quad . \tag{3}$$

According to Newton's second law

$$\partial T/\partial x = \rho(\partial^2 u/\partial t^2) \tag{4}$$

with $S = \partial u/\partial x$, where T and S are the stress and strain, whereas c, e and ε in eq (3) are the elastic, piezoelectric and dielectric constants respectively, ρ is the mass density and u the displacement. It should be borne in mind that the constants in the piezoelectric relations are related to elastic, piezoelectric and dielectric tensor elements valid for an anisotropic solid [14].

When p and b are the creation and annihilation rates of troughs per unit volume respectively, the master equation for the trough density n_t reads

$$\partial n_t/\partial t = p - b - v_s'(\partial n_t/\partial x) \quad . \tag{5}$$

In addition we assume that each trough contains N electrons, independent of position x and electric field strength E. Then the density of trapped electrons becomes $n_s = N\, n_t$.

2.2. THE STATIONARY STATE

From eq (1), (3) and (4) it follows for the steady state that $\partial \bar{D}/\partial x = (1 + K_e^2)(\partial \bar{E}/\partial x) = 0$ where $K_e = (e^2/\varepsilon c)^{\frac{1}{2}}$ is the electromechanical coupling constant, which is usually much smaller than one. Thence $\bar{E} = - \bar{V}/L$ and $\bar{v}_d = \bar{V}/L$ is independent of position. It follows from eq (3) and (4) that $v_s'(\partial \bar{n}_s/\partial x) = \bar{v}_d(\partial \bar{n}_s/\partial x)$ and since $\bar{v}_d \neq v_s'$ in the electroacoustically active regime we have $(\partial \bar{n}_s/\partial x) = (\partial \bar{n}_d/\partial x) = 0$. Finally for the current we obtain $\bar{I} = - qA\bar{n}_s v_s' - qA\bar{n}_d(\mu \bar{V}/L)$, where A is the contact area. Note that the mobility μ as well as $\bar{n}_s$ and $\bar{n}_d$ may depend on electric field strength at high applied fields.

2.3. AC BEHAVIOUR AND NOISE

In order to describe the ac behaviour and fluctuations around a steady state, we linearize the equations from section 2.1. Then the linearized current equation becomes

$$\Delta j = \sigma\,\Delta E + q(\bar{v}_d - v_s')\Delta n_s + qD_n\frac{\partial \Delta n}{\partial x} - q\bar{v}_d\Delta n + \frac{\partial \Delta D}{\partial t} \qquad (2a)$$

where $\sigma = q\mu\bar{n}_d$. The linearized rate equation for the troughs extended by a Langevin source function H, which formally describes the fluctuations in the creation and annihilation, reads:

$$\frac{\partial \Delta n_t}{\partial t} + \frac{\Delta n_t}{\tau} = \beta\Delta E - v_s'\frac{\partial \Delta n_t}{\partial x} + H \qquad (5a)$$

where $\tau^{-1} = -[\partial(p-b)/\partial n_t]_{\Delta n_t=0}$, $\beta = [\partial(p-b)/\partial E]_{\Delta E=0}$ and $H \equiv \Delta(p-b)_{\Delta E=\Delta n_t=\Delta n_s=0}$.

Note that we finally have 11 linearized equations with 14 variables. We are interested in a spectral decomposition of the fluctuations. We Fourier transform the equations with respect to time. Then 11 equations result with 13 variables. These 11 equations allow one in principle to eliminate 10 variables so that 3 remain. If we do not consider fluctuations (H = 0) 2 variables remain, say $\tilde{j}$ and $\tilde{E}$ (Fourier transforms are denoted by tilde). Thence $\tilde{j}$ can be expressed in $\tilde{E}$ and in the ac voltage $\tilde{V} = -\int_0^L \tilde{E}dx$. As a result the ac impedance can be calculated.

If one considers an ac open circuit by putting $\tilde{j} = 0$, then $\tilde{V}$ can be expressed in $\tilde{H}$ and the voltage fluctuations can be calculated in terms of Langevin source terms.

2.4. THE AC IMPEDANCE

Carrying out the programme for the calculation of the ac impedance as indicated in section 2.1 and using the boundary conditions $\tilde{T}(0) = \tilde{T}(L) = 0$, corresponding to free end surfaces one finds [13,14]

$$Z(\omega) = \frac{L}{A\left(\frac{\alpha\tau}{1+i\omega\tau} + \sigma + i\omega\varepsilon\right)}\{1 + K_e^2 f(\omega)\}\,, \qquad (6)$$

where $\alpha = q(\bar{v}_d - v_s')N\beta$ and $f(\omega)$ is a complicated function of frequency [13,14]. Substituting reasonable values for the unknowns in eq (6) we found that the second term between brackets only contributes significantly at frequencies given by

$$f = (2m+1)v_s'/2L \qquad m = 0, 1, 2, \ldots . \qquad (7)$$

Four limiting cases are of interest:
(i) If we put $\alpha = 0$ and $\sigma = q\mu\bar{n}$, in other words we neglect the presence of troughs, we have the linear small signal approximation, and eq (6) reduces to an expression derived by Greebe [17].
(ii) If $\omega \to 0$, then eq (6) reduces to the differential resistance: $Z(0) = L/A(\alpha\tau + \sigma)$.
(iii) If $\omega >> |\sigma + \alpha\tau/(1 + i\omega\tau)|/\varepsilon$, then $Z(\omega) \approx L/iA\omega\varepsilon$, corresponding to the geometrical capacitance of the device.
(iv) If $\sigma >> |i\omega\varepsilon + \alpha\tau/(1 + i\omega\tau)|$, then we find $Z(\omega) \sim L/A\sigma$.
Note that $\alpha < 0$ if the number of troughs increases with increasing applied voltage.
It follows that the low frequency plateau value of the impedance is a factor $\sigma/(\sigma + \alpha\tau)$ larger than the intermediate frequency plateau value.

In addition to the ac impedance the following expression could be found for the imaginary part of the wavenumber of waves travelling in the direction of drifting particles:

$$\alpha_e = \frac{1}{2} K_e^2 \frac{\omega_c}{v_s} \frac{\gamma^*}{\gamma^{*2} + \left(\frac{\omega}{\omega_D} + \frac{\omega_c}{\omega}\right)^2} \tag{8}$$

where v_s = sound velocity, $\omega_D = v_s^2/D_n$ and $\omega_c = (\alpha\tau + \sigma)/\varepsilon$; $\gamma^* = 1 - (\vec{v}_d \cdot \vec{v}_s)/v_s^2$. These expressions reduce to White's result for the linear attenuation coefficient if the differential conductivity is replaced by the ohmic one. The frequency of maximum amplification, ω_m, is given by

$$\omega_m^2 = \omega_c \omega_D \tag{9}$$

For a discussion of the influence of traps and magnetic fields on the electro-acoustic effect we refer to the literature [3,18].

2.5. NOISE

The noise problem has been solved only by ignoring diffusion and displacement current, by assuming space charge neutrality and by assuming that the number of electrons, N, trapped per trough is independent of position and electric field strength. By Fourier transforming eq (5a) with respect to time and using $\tilde{n}_s = N \tilde{n}_t$ one then finds

$$\frac{d\tilde{n}_s}{dx} + \frac{1}{\tau v_s'}(1 + i\omega\tau)\tilde{n}_s = \frac{\beta N}{v_s'}\tilde{E} + \frac{N}{v_s'}\tilde{H} \tag{5b}$$

The Fourier transformed eq (2a) reads

$$\tilde{j} = \sigma\tilde{E} + q(\bar{v}_d - v_s')\tilde{n}_s \tag{2b}$$

If one considers an ac open circuit by putting $\tilde{j} = 0$, $\tilde{n}_s$ can be eliminated from these equations and the following differential equation in $\tilde{E}$ results:

$$\frac{d\tilde{E}}{dx} + \Lambda\tilde{E} = -\frac{qN\eta}{\sigma}\tilde{H} \tag{10}$$

where $\Lambda = (\tau_1^{-1} + i\omega)/v_s'$, $\tau_1^{-1} = \tau^{-1} + \alpha/\sigma$ and $\eta = (\bar{v}_d - v_s')/v_s'$. If we assume that the end surfaces are kept free, then $\tilde{T}(0) = \tilde{T}(L) = 0$, which for this case also implies $\tilde{E}(0) = \tilde{E}(L)$. Using these boundary conditions and remembering that $S_v(f)$ is proportional to $\langle\tilde{V}\cdot\tilde{V}^*\rangle$, where $\tilde{V} = -\int_0^L \tilde{E}\,dx$, one finds by integrating eq (10)

$$S_V(f) = \frac{1}{\Lambda\Lambda^*}\left[\frac{qN\eta}{\sigma}\right]^2 \int_0^L\int_0^L S_H(x_1,x_2,f)\,dx_1 dx_2 \tag{11}$$

If it is assumed that creation and annihilation processes occur spontaneously and that a δ-function space correlation exists, we have $S_H(x_1,x_2,f) = (4\bar{b}/A)\delta(x_1 - x_2)$, where we used $\bar{p} = \bar{b}$. Substituting this into eq (11) yields:

$$S_V(f) = \frac{4\bar{b}Lv_s'^2\tau_1^2}{A(1 + \omega^2\tau_1^2)} \frac{q^2N^2\eta^2}{\sigma^2} \tag{12}$$

The outcome of the calculations is a Lorentzian noise spectrum. It should be remembered, however, that the outcome depends on the boundary conditions and on the rather stringent restriction on the space correlation of the fluctuations in the creation and annihilation processes. The latter condition is obviously included for mathematical convenience. It seems reasonable to assume that physically these conditions are met if $\omega << \omega_m$. If the ac impedance Z is calculated using the same conditions as for the noise calculations one finds

$$|Z| = \frac{L}{A\sigma} \frac{\tau_l}{\tau} \left(\frac{1 + \omega^2\tau^2}{1 + \omega^2\tau_l^2}\right)^{\frac{1}{2}} \tag{13}$$

If we introduce the trough transit time $\tau_t = L/v_s'$ and assume that $\bar{b} = \bar{n}_t/\tau$, then the saturation current $I_s = Aq\bar{N}\bar{b}\tau v_s'$ and then it follows from eqs (12) and (13) that

$$S_I(f) = 4NqI_s \frac{\eta^2\tau/\tau_t}{1 + \omega^2\tau^2} \tag{14}$$

3. EXPERIMENTAL RESULTS

Some experimental results obtained recently with CdS [16] crystal bars will be presented. The small faces, typically of the order of 1 mm^2, were provided with indium evaporated ohmic contacts; the lengths of the bars varied from 1.4-2.8 mm. The c-axis of the hexagonal crystals was in the length direction. In this shape the crystal bars could be used for Brillouin scattering as well as for electrical measurements. The crystals were semiconducting with resistivities of the order of 1 Ωm. The length of the bars was kept smaller than 3 mm in order to suppress travelling electro-acoustic domain formation and the accompanying oscillatory behaviour. To avoid excessive Joule heating of the samples the high voltage was applied in voltage pulses of 40 μs duration with a repetition rate of 4 Hz.

Figure 1 shows a typical current-voltage (I-V) characteristic. At low applied voltage the sample is ohmic, whereas at higher voltages non-ohmic conduction occurs because electrons are trapped in potential troughs associated with acoustic waves moving at the sound velocity. In figure 2 the spectral intensity of the ac short-circuited current noise, S_I, at 10 MHz is plotted double logarithmically versus applied voltage. One distinguishes a rise with slope 2 at low voltages due to generation-recombination noise, followed by a very sharp rise because of the occurrence of the electro-acoustic effect and finally a less sharp rise which is even followed by a decrease with increasing voltage.

The threshold voltage V_c for the occurrence of electro-acoustic current fluctuations can be determined [12] by an extrapolation of the steep curve down to the thermal current noise level. The thus obtained values for V_c invariably turned out to be somewhat lower than the knee voltage of the I-V characteristic due to the fact that in the transition region between ohmic and non-ohmic linear behaviour the density of trapped electrons is field dependent. In the past there has been a controversy about whether longitudinal or transverse waves are responsible for the onset of the electro-acoustic effect. Particularly, electrical data alone left some room for speculation. This was partly due to the wide spread in the electron mobility values reported in the literature and to the occurrence of trapping effects, which were not taken into account [7,12].

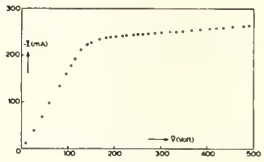

Fig. 1 Current versus applied voltage for a CdS crystal with the electric field applied along the c-axis.

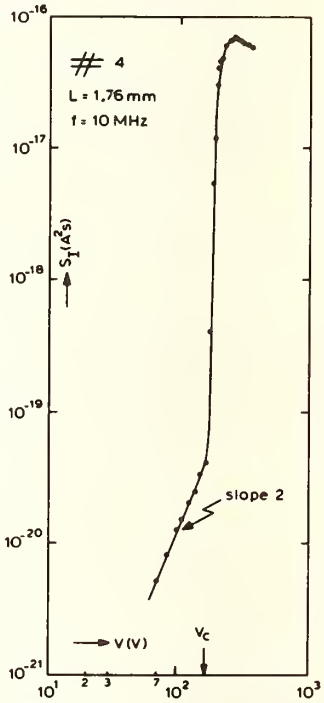

Fig. 2 The spectral current noise intensity S_I at 10 MHz versus applied voltage. The critical voltage V_c for the onset of the electro-acoustic effect is indicated by an arrow.

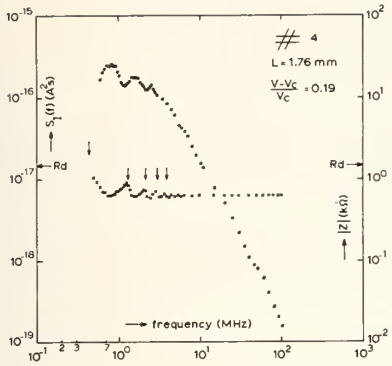

Fig. 3 The current noise intensity $S_I(f)$ and the absolute value of the ac impedance Z vs frequency. Resonances in $|Z|$ are indicated by arrows.

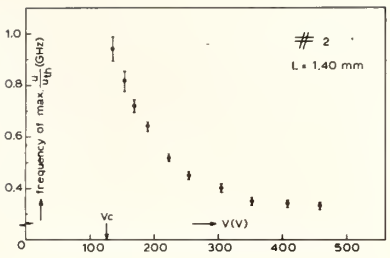

Fig. 4 The frequency where the relative acoustic energy density is at its maximum is plotted versus applied voltage. The voltage V_c marking the onset of the electro-acoustic effect is indicated by an arrow.

By combining results of electrical measurements on relatively low ohmic samples with good ohmic contacts with Brillouin scattering data on the same samples, Westera [14,16] settled the dispute by proving that transverse waves were responsible for the onset of the electro-acoustic effect. The measured threshold voltage (cf. figure 2) corresponded to a sound velocity of transversal on-axis waves of 1.77×10^3 ms^{-1} and a room temperature mobility of 2.20×10^{-2} m^{2}V^{-1}s^{-1}, in agreement with a value for the mobility reported by Spear and Mort [19]. Figure 3 shows S_I and the absolute value of the ac impedance $|Z|$ versus frequency for the same sample at $(V - V_c)/V_c = 0.19$. The spectrum has a Lorentzian frequency dependence with some modulations and can, apart from these modulations, be interpreted with eq (14). The observed cross-over frequency corresponds to an average life time for troughs of 5.3×10^{-8} s. From the low frequency plateau and a saturation current of 160 mA (deduced from the IV-characteristic) one then finds with the help of eq (14) that N is about 10^6. $|Z|$ is almost frequency independent for frequencies larger than 10 MHz, whereas with decreasing frequency it gradually rises towards the value of the differential resistance. In addition resonances are observed at the odd harmonics of 450 Hz. The impedance data can be well interpreted with eqs (6) and (13) with $\tau_1/\tau = 2.4$ and provided that the velocity occurring in eq (7) can be interpreted as the x-component of a group velocity that corresponds to a phase velocity with an off-axis angle of 25° of a transverse wave, which is in good agreement with Keller [20] and San'ya et al. [21]. The very sharp peaks predicted by eq (6) are apparently smoothed out because of the occurrence of a distribution of waves with different off-axis angles. It should be noted that minima occur in the noise spectrum at the resonance frequencies of the impedance. However, spectral noise intensities often differ markedly from a Lorentzian. This is supposedly due to the fact that the δ-function space correlation for the trough creation and annihilation fluctuations no longer holds. Finally in figure 4 the frequency f_m, where the ratio of electro-acoustic to thermal acoustic energy has a maximum, as determined from Brillouin scattering data, is plotted versus applied voltage. It was found that the behaviour of f_m is in good agreement with eq (9).

REFERENCES

[1] A.R. Hutson, J.M. McFee and D.L. White, *Phys. Rev. Lett.* 7, 237 (1961).
[2] D.L. White, *J. Appl. Phys.* 33, 2547 (1962).
[3] N.I. Meyer and M.H. Jørgensen, *Festkörperprobleme X*, Ed. O. Madelung, Pergamon Vieweg (1970) p. 21.
[4] H. Kuzmany, *Phys. Stat. Sol.* 25a, 9 (1974).
[5] G. Johri and H.N. Spector, *Phys. Rev.* B14, 4955 (1977).
[6] P.K. Tien, *Phys. Rev.* 171, 970 (1968).
[7] A.R. Moore, *J. Appl. Phys.* 38, 2327 (1967).
[8] L. Friedman, *Phys. Rev.* 174, 737 (1968).
[9] K. Nakamura, *J. Phys. Soc. Japan* 39, 860 (1975).
[10] K. Nakamura, *J. Phys. Soc. Japan* 40, 350 (1976).
[11] R.J.J. Zijlstra and P.A. Gielen, *Physica* 95B, 190 (1978).
[12] P.A. Gielen and R.J.J. Zijlstra, *Physica* 95B, 347 (1978).

[13] W. Westera, R.J.J. Zijlstra and M.A. van Dijk, *Phys. Lett.* 78A, 371 (1980).
[14] W. Westera and R.J.J. Zijlstra, *Physica* 106B, to be published June 1981.
[15] Y.V. Gulguaev and A.G. Kozorezov, *Sol. State Commun.* 27, 375 (1978).
[16] W. Westera and R.J.J. Zijlstra, *Physica*, to be published.
[17] C.A.A.J. Greebe, *Philips Res. Repts.* 20, 1 (1965).
[18] R.M. White, *High-Frequency Ultrasonic Devices, Topics in Solid State and Quantum Electronics*, Ed. W.D. Hershberger, Wiley, London, (1972).
[19] W.W. Spear and J. Mort, *Proc. Phys. Soc.* 81, 130 (1963).
[20] D. Keller, *Phys. Stat. Sol.* 16a, 87 (1973).
[21] M. San'ya, M. Yamada, C. Hamaguchi and J. Nakai, *Jap. J. Appl. Phys.* 13, 611 (1974).

EXPERIMENTAL STUDIES OF NOISE IN A CHEMICAL REACTION AND IN A FLUID FLOW

Harry L. Swinney, J. C. Roux*, and G. P. King

Department of Physics
The University of Texas
Austin, TX 78712

We are investigating noise that appears in two quite different physical nonlinear systems when they are taken away from equilibrium. In each system two types of noise can be distinguished, at least qualitatively: intrinsic noise and extrinsic noise. The noise that is a consequence of random fluctuations in the boundary conditions is termed here extrinsic noise, while intrinsic noise, which is the principal object of our studies, is fundamentally different--it is the chaotic (unpredictable) behavior that occurs in nonlinear deterministic systems.

Nearly two decades ago Lorenz [1] discovered that a simple nonlinear deterministic model system could exhibit complex behavior that was completely unpredictable. It is now realized that the Lorenz model, which consists of three coupled ordinary differential equations, is not an isolated example, but in fact nonlinear systems, which are common in all sciences, frequently have chaotic regimes [2].

We will describe briefly the two systems we have studied and will give examples of the noisy behavior that has been observed. Details of this work are described elsewhere [3-5].

NOISE IN THE BELOUSOV-ZHABOTINSKII REACTION

About twenty years ago Belousov discovered an oscillating chemical reaction that has become the prototype system for the study of oscillations and complex dynamics in chemical and biological systems. Soon thereafter another Soviet scientist, Zhabotinskii, extended Belousov's work, and subsequently the "BZ" reaction has been investigated by many workers, notably Noyes and collaborators [6].

In our experiments the four input chemicals of the BZ reaction are continuously fed into a reactor, which is vigorously stirred so the system is essentially homogeneous. The resultant reaction produces more than 30 reaction products or intermediate species [6]. The reactor has a fixed volume--the outflow rate for the reacting mixture is the same as the input flow rate. In the experiments the distance away from equilibrium is varied by varying the rate at which the chemicals are pumped through the reactor (the concentrations are held fixed).

The concentration $B(t)$ of one of the reaction products, the bromide ion, is measured as a function of time and recorded in a computer. From these digital time series records we determine (a) the power spectral density and (b) a two-dimensional phase space portrait, obtained by plotting points $[B(t), B(t + \tau)]$ for a suitably chosen time delay τ.

The time series, power spectra, and phase portraits are shown in Fig. 1 for two rates of flow of the chemicals through the reactor: in (a) - (c) the mean residence time of the chemicals in the reactor is 62 minutes, and the system is essentially

---

* Permanent Address: Centre de Recherche Paul Pascal, Domaine Universitaire, 33405 Talence Cédex, France

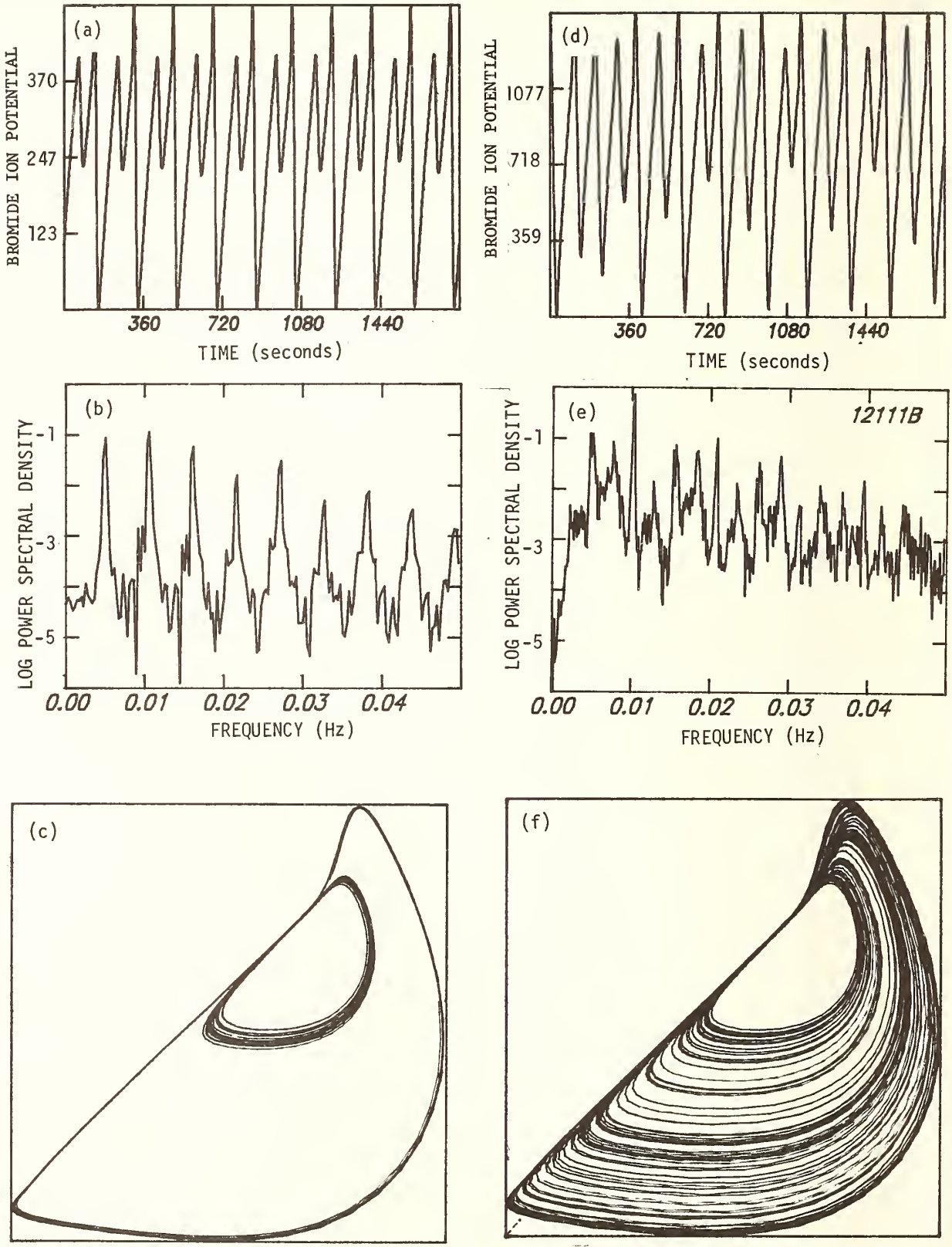

Fig. 1 The Belousov-Zhabotinskii reaction in a periodic state [(a)-(c)] and in a chaotic state [(d)-(f)]. The time dependence of the bromide ion concentration is shown in (a) and (d), the power spectral density in (b) and (e), and two-dimensional phase plots in (c) and (f).

periodic, characterized by sharp peaks in the power spectrum and a limit cycle phase space attractor.

In contrast, when the residence time is decreased to 54 minutes, the behavior is qualitatively different, as shown in Fig. 1 (d) - (f): it is characterized by a broadband spectrum and a "strange attractor" [2] in phase space. This chaotic behavior has been found by Turner [5] to be modeled accurately by a deterministic four-variable model that contains the principal chemical mechanisms.

Noise is also present in the periodic state: the amplitude of the small peak fluctuates [see the inner loop of the attractor in Fig. 1 (c)]. The small amplitude peak is sensitive to external perturbations, and in fact the small amplitude peak disappears at shorter chemical residence times (< 50 minutes); hence it seems likely that the small amount of noise observed for this state is caused by extrinsic noise.

NOISE IN CIRCULAR COUETTE FLOW

In the circular Couette system a fluid is contained between concentric cylinders. In our apparatus the inner cylinder rotates and the outer cylinder is stationary. The distance away from equilibrium is given by the Reynolds number, which is proportional to angular frequency of the inner cylinder.

At sufficiently small Reynolds number the flow is purely azimuthal, except near the ends. Experiments [4] have revealed the following transitions as the Reynolds number R is increased: (1) To Taylor vortex flow (at $R = R_c$), in which toroidal vortices encircle the inner cylinder; (2) From Taylor vortex flow to wavy vortex flow, in which there are traveling azimuthal waves on the vortices. (This flow is periodic--the velocity power spectrum consists of a single sharp frequency component and its harmonics.); (3) From wavy vortex to a doubly periodic modulated wavy vortex flow, in which the spectrum contains two sharp fundamental frequencies and their combinations; (4) From modulated wavy vortex flow to noisy modulated wavy vortex flow, in which the spectrum has a broadband component in addition to the sharp frequencies.

A velocity power spectrum for noisy modulated wavy vortex flow is shown in Fig. 2 (a), and a photograph of the flow is shown in Fig. 2 (b). This flow appears to be another example of intrinisic noise: the spectrum is not changed qualitatively by imposing small amounts of external noise, and essentially the same spectrum has been obtained in another laboratory by Walden and Donnelly [7]. Also, in a deterministic model of circular Couette flow (based on the Navier-Stokes equations), noise appears at around $22R_c$, in qualitative agreement with the observed onset at $12R_c$ [8].

The transitions in Couette flow described above were observed for a system with twenty or fewer vortices. Donnelly et al. [9] found that when the annulus length was increased beyond about 80 times the size of the gap between the cylinders, a different kind of unpredictability appeared, and this "noise" was observed in the periodic wavy vortex flow regime even at very low Reynolds number ($\simeq 2\ R_c$). This type of noise is illustrated in Fig. 2 (c) and (d), obtained in our laboratory. The spectral component ω_1 corresponding to the azimuthal traveling waves is broadened [Fig. 2(c)] and this broadening is due to wandering dislocations [Fig. 2 (d)].

Our preliminary studies of the dislocations indicate that they occur for conditions under which the system is particulary sensitive to external perturbations. At a given Reynolds number wavy vortex flows can be obtained for a wide range of axial wavelengths, but the dislocations are much more numerous for wavelengths near the extremes of the range. In fact, for wavelengths in the middle of the range, the system can be free of dislocations even when it is very tall. Thus the dislocations appear to be an example of extrinsic noise.

CONCLUSIONS

We have described preliminary results that indicate that it is possible to distinguish between two types of noise in the systems we have studied: extrinsic

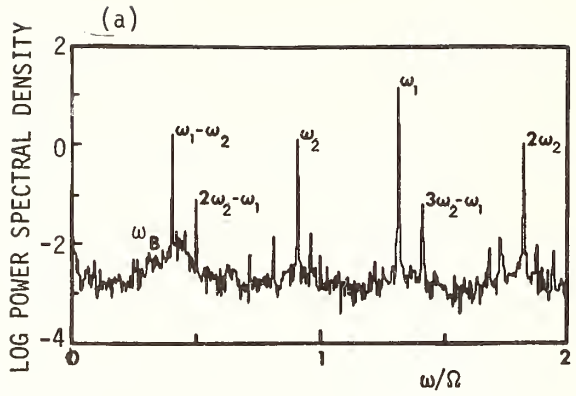

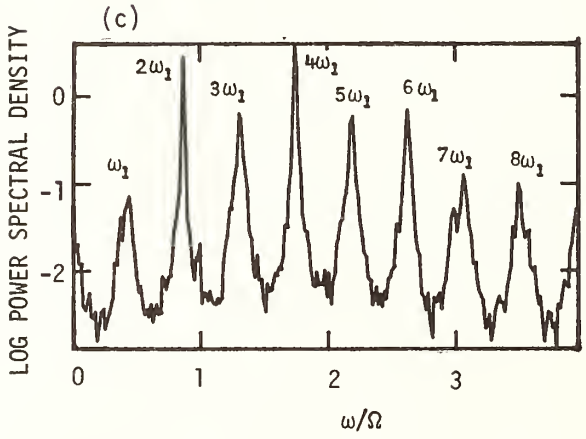

Fig. 2 Circular Couette Flow: (a) and (b)--a chaotic or turbulent flow at R/R_c = 15.1 in an annulus with a ratio of height to the gap between the cylinders equal to 20. (c) and (d)--a chaotic flow at R/R_c = 1.6 caused by vortex boundary dislocations in a tall annulus (height to gap ratio equal to 82). Power spectral density plots are shown in (a) and (c), where Ω is the frequency of rotation of the inner cylinder. The frequency component labeled ω_1 is the frequency of traveling azimuthal waves. This component is instrumentally sharp in (a) but significantly broadened in (c). The fluid motion that corresponds to the broad component ω_B in (a) is not known. Photographs of the flow corresponding to the power spectra in (a) and (c) are shown in (b) and (d). The flow pattern is made visible by seeding the flow with small platelets that align with the flow. Only the central portion of the tall annulus is shown in (d); note the dislocations in the middle of the photograph.

noise, which is caused by external stochastic driving forces, and intrinsic noise, which is the chaotic or unpredictable behavior that can occur in deterministic systems.

We should emphasize that the intrinsic noise discussed here does not arise from thermally excited fluctuations. Chaotic behavior occurs in deterministic continuum systems in the absence of fluctuations [2]. Studies of thermal noise in chemical and hydrodynamic systems have shown that thermally excited fluctuations will be difficult to observe in experiments such as ours.

How can a deterministic system exhibit apparently unpredictable behavior? It is true that if the initial conditions and boundary conditions are specified, then the behavior is determined for all times. However, in a chaotic regime, two sets of initial conditions that are only infinitesimally different can evolve quite differently at large times. Since in practice the initial conditions can never be specified with arbitrarily high accuracy, it follows that the behavior of a chaotic deterministic system cannot be predicted far into the future. This is called sensitive dependence on initial conditions.

Our distinction between intrinsic and extrinsic noise in the experiments has been a heuristic one. In the future we intend to be more quantitative. The data will be analyzed using tests that have been developed to distinguish between intrinsic and extrinsic noise processes.

The distinction between extrinsic and intrinsic noise is helpful in developing an understanding of physical phenomena, even though no absolute distinction can ever be made. That is, a given set of noisy data might be simply and elegantly described by a deterministic model, yet one could in principle always devise a stochastic process, albeit a complex one, that would fit the data.

We thank Professor Mark Kac for the discussion that led to the last paragraph. This research was conducted in collaboration with J. Turner, W. D. McCormick, M. Kilgore, D. Andereck, M. Gorman, and L. Reith. This work was supported by National Science Foundation Grants CME 79-09585 and CHE 79-23627 and by The Robert A. Welch Foundation.

REFERENCES

[1] E. Lorenz, J. Atm. Sci. 20, 130 (1963).

[2] See, e.g., proceedings of recent conferences: Nonlinear Nonequilibrium Statistical Mechanics, Supplement 64, Prog. Theor. Phys. (1978); Nonlinear Dynamics, ed. by R. G. Helleman, Vol. 357, Ann. N. Y. Acad. Sci. (1980).

[3] H. L. Swinney and J. P. Gollub, Physics Today 31 (8), 41 (1978).

[4] P. R. Fenstermacher, H. L. Swinney, and J. P. Gollub, J. Fluid Mech. 94, 103 (1979).

[5] J. C. Roux, J. Turner, W. D. McCormick, M. Kilgore, and H. L. Swinney, to be published; J. Turner, to be published.

[6] See, e.g., R. J. Field and R. M. Noyes, Accounts in Chem. Res. 10, 214, 273 (1977).

[7] R. Walden and R. J. Donnelly, Phys. Rev. Lett. 42, 301 (1979).

[8] H. Yahata, Prog. Theor. Phys. 61, 791 (1979).

[9] R. J. Donnelly, K. Park, R. Shaw, and R. Walden, Phys. Rev. Lett. 44, 987 (1980).

DYNAMICAL NOISE IN TUNNEL DIODE OSCILLATOR SYSTEMS

J.P. Gollub

Physics Department
Haverford College
Haverford, PA 19041

INTRODUCTION

Most of the noise phenomena exhibited by electronic devices have their origin in microscopic processes such as thermal fluctuations or the discrete nature of the charge carriers. It is not widely appreciated that macroscopic nonlinearity can also produce noise in an electronic circuit, and that this noise can be understood without reference to noise sources. In this paper we briefly describe laboratory experiments and models of the noisy behavior of coupled tunnel diode relaxation oscillators. This noise is far larger than that caused by shot noise in the diodes, and is not appreciably affected by microscopic processes. The noise is caused by instability of trajectories in the phase space of the system. A more extensive description has been published elsewhere [1,2].

EXPERIMENTS

The circuit we have studied experimentally is shown in Fig. 1. (For details, see Ref. 1.) It consists of two tunnel diode oscillators coupled by a resistance R_C. Because of the negative resistance of part of the current/voltage characteristic of the diodes (Fig. 1b), the diode voltages V_{D1} and V_{D2} and the corresponding currents I_{D1} and I_{D2} oscillate at frequencies determined by the inductances (and resistances). The voltage signals are pulse-like, while the current signals are composed of segments of exponentials. These signals can be either periodic or nonperiodic (noisy), depending on the way in which each oscillator influences the switching times of the other oscillator.

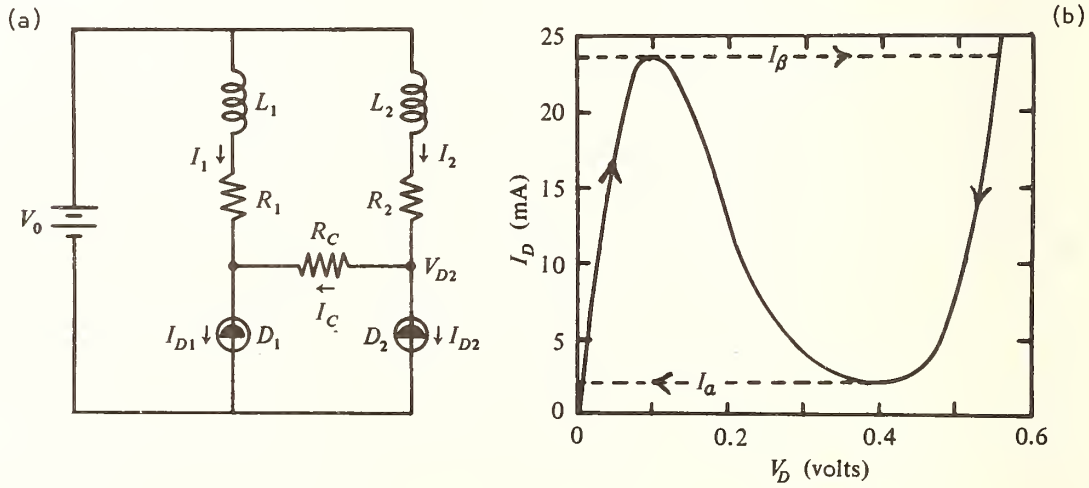

Fig. 1 (a) Tunnel diode oscillator circuit. Each oscillator consists of an inductor, a resistor, and a tunnel diode; the two oscillators are coupled by the resistor R_C. (b) Current/voltage characteristic of the tunnel diode. Arrows indicate the path of oscillation.

In order to demonstrate that this circuit exhibits broadband noise, we show power spectra of the diode voltages for two different values of the natural frequency ratio F_o of the uncoupled oscillators (Fig. 2a,b). In one case (Fig. 2a) the spectrum is composed of sharp peaks at multiples of a fundamental frequency. This complex but periodic behavior is due to the frequency modulation of one oscillator by the other. The modulation is such that the two oscillators phase lock; their frequencies are in the ratio of two integers.

This periodic spectrum is to be contrasted with that of Fig. 2b obtained by varying one of the inductances and hence changing the natural frequency ratio of the two oscillators. This spectrum contains broadband noise, and the peaks that remain are in fact broadened as well. The behavior is hence nonperiodic or noisy under these conditions. These two qualitatively different spectra, one of which is broadband, both result from a deterministic process. To prove this, we generated a discrete sequence of current values $\{(I_{D2})_n\}$ by conditional sampling whenever $V_{D1} = 0.42$ V, $I_{D1} = 5$ ma, and $V_{D2} < 0.2$ V. These conditions enable us to reduce the dynamics to a single discrete dynamical variable. We plot $(I_{D2})_{n+1}$ versus $(I_{D2})_n$ to obtain Fig. 2c,d. These diagrams are known as return maps. The use of conditional sampling to reduce the dimensionality of a dynamical system was

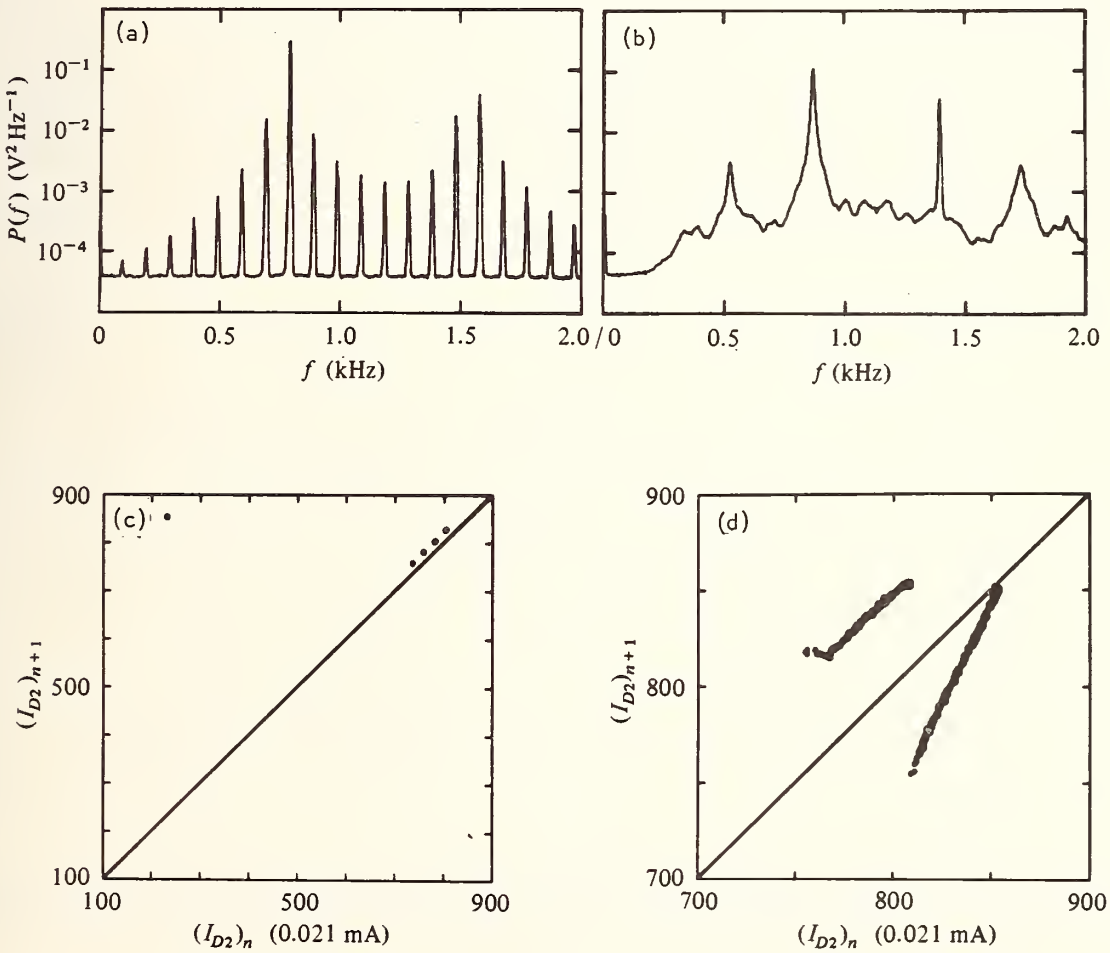

Fig. 2 (a) Power spectrum of the diode voltage V_{D2} for a phase-locked periodic state. The peaks are instrumentally sharp. (b) Power spectrum for a nonperiodic (broadband) state obtained by changing the uncoupled frequency ratio F_o. (c) and (d) Corresponding return maps obtained by conditional sampling of the current I_{D2} to reduce the dynamics to a single discrete variable. These maps demonstrate that the system is deterministic even when it is noisy.

invented by Poincaré. In the periodic case, the return map consists of a finite number of discrete points which are traversed repetitively, as one might expect. In the noisy case, the relationship between $(I_{D2})_{n+1}$ and $(I_{D2})_n$ is still one-to-one, although it is no longer a finite set of points. Thus, the process is <u>deterministic</u>, in the sense that each value is sufficient to predict the next one.

How can the process be deterministic and yet noisy? The answer lies in the steepness of the mapping of Fig. 2b. When the slope of this mapping has magnitude greater than one, then two currents $(I_{D2})_n$ which are separated by Δ_1 will be separated by $\Delta_2 > \Delta_1$ at the next sampling. More precisely, if the quantity

$$h = \lim_{N\to\infty} \frac{1}{N} \sum_{n=1}^{N} \ln\left|f'((I_{D2})_n)\right| \qquad (1)$$

is positive, where f' is the local slope of the return map, then separations are magnified by a factor e^h per iteration, on the average. In Fig. 2b, $h = 0.40 \pm 0.05$. As a result, trajectories in a phase space spanned by I_{D1}, I_{D2}, V_{D1}, and V_{D2} are unstable, and this is the fundamental cause of the noise. The instability is common in many nonlinear systems and models [3].

In order to further support the above explanation, we mapped out the behavior of the system in a parameter space composed of the coupling conductance $G_c = 1/R_c$ and the uncoupled frequency ratio F_o. Our goal was to compare the behavior of the experimental system and an appropriate numerical model. The experimental behavior is shown in Fig. 3a. The non-periodic (broadband) regions are labeled N, while periodic (phase-locked) regions are labeled by the frequency ratio, or by the letter P where the integers are large. The phase diagram is quite complex, with many different interlaced regions.

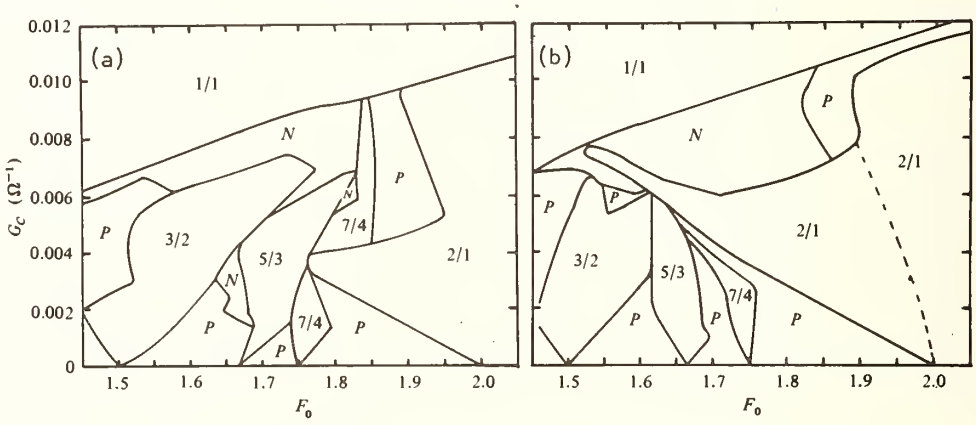

Fig. 3 Parameter space defined by the coupling conductance $G_c = 1/R_c$ and the uncoupled frequency ratio F_o of the two oscillators for (a) experiment and (b) numerical model. (See text for legend.)

NUMERICAL MODEL

In order to demonstrate that noise sources are not required to reproduce this behavior, we constructed a simple numerical model [1] using the standard circuit equations and a rectangular approximation to the I-V characteristic of the tunnel diodes. With this

approximation, the diode voltages change only in discrete steps, and the equations become linear in the intervals between the steps. The solutions can hence be obtained by computing the switching times for 1000 or more oscillations with very little cumulative error. Return maps and spectra were then used to construct a diagram of the parameter space of the model (Fig. 3b) to compare with the experimental behavior (Fig. 3a). The agreement is reasonably good. Many of the periodic regions are accurately simulated, and the model correctly reproduces the large region of nonperiodic behavior (with positive divergence rate h) near the center of the diagram. There are also some significant differences which we believe arise from the approximations of the model.

CONCLUSIONS

The fact that the numerical model correctly reproduces the noisy behavior of the circuit, and the fact that the return maps are one-to-one even in the noisy state, provide strong evidence that the observed noise is not due to thermal fluctuations or other microscopic processes. Rather, it arises solely from macroscopic nonlinearity, and the resulting nonperiodic orbits in phase space. Similar conclusions have also been reached by other investigators [3,4], and processes of this type may be responsible for the onset of turbulence in fluids [5].

Dynamical noise may occur in any system of nonlinear oscillators; the tunnel diodes may be replaced by other negative resistance devices. Furthermore, if the inductances are stray components, the noise will be at very high frequency and its source might not be easily recognized. Noise levels beyond thermal values in oscillatory systems may be due to macroscopic nonlinearity more often than is generally recognized.

The experiments were performed by J.E. Socolar and E.J. Romer. This work was supported by the National Science Foundation.

REFERENCES

[1] J.P. Gollub, E.J. Romer, and J.E. Socolar, *J. Stat. Phys.* 23, 321 (1980).

[2] J.P. Gollub, T.O. Brunner, and B.G. Danly, *Science* 200, 48 (1978).

[3] M.I. Rabinovitch, *Sov. Phys. - Usp.* 21, 443 (1978).

[4] Y. Ueda and N. Akamatsu, *IEEE Trans.* CAS-28, 217 (1981).

[5] J.P. Gollub and S.V. Benson, *J. Fluid Mech.* 100, 449 (1980).

NOISE IN RESONANT GRAVITATIONAL WAVE DETECTORS

R. P. Giffard[+], P. F. Michelson and R. C. Taber

Department of Physics and High Energy Physics Laboratory
Stanford University
Stanford, CA 94305

INTRODUCTION

A striking feature of Einstein's general theory of relativity is the predicted existence of gravitational waves which can transport energy with the velocity of light. In fact, various modes of gravitational radiation are allowed in all contemporary theories of gravitation. Gravity is a very weak force, and a significant flux of energy is only radiated by an event of astrophysical scale in which objects of near solar mass move with a significant fraction of the velocity of light. Efforts to demonstrate the existence of the radiation thus depend on extraterrestrial sources. The careful study of waves from such sources might eventually provide a unique observational probe of physical processes involving strongly non-linear gravitational interactions.

The pioneeering work of J. Weber in the sixties encouraged several groups of experimenters to build and operate sensitive gravitational wave detectors. In spite of a vigorous program, the evidence for the detection of gravitational waves is not yet conclusive. This situation is initially surprising in view of the enormous energy flux which is predicted from the strongest sources. For example, current estimates of the gravitational wave luminosity associated with the collapse of a spinning star of about 5 solar masses suggest a peak energy spectral density of 10^{45} wHz^{-1} in the range 1 to 10 kHz. Such an event, occurring once in the lifetime of a star and lasting about 1 ms, is expected to occur in a galaxy like our own between once every 10 and once every 75 years. For observations at a reasonable rate, one would need to be able to detect such events in all galaxies within about 6×10^{23}m, the distance characterizing the M101 cluster containing several hundred galaxies. These events result in about one pulse per month with a flux density of 2×10^{-4} wm^{-2} Hz^{-1} at the earth. In view of approximate sensitivity limits for astronomy in the visible -- perhaps 4×10^{-17} wm^{-2}, and for radioastronomy -- considerably less than 1 Jy or 10^{-26} wm^{-2} Hz^{-1}, it is clear that gravitational wave detection must involve special difficulties. In this paper we consider the way in which various forms of random noise limit the sensitivity of existing resonant-mass detectors. The problem is unusual in the fact that thermal noise of both electrical and mechanical origin is important. As an example to illustrate some of the unconventional technology involved in obtaining a low noise level, we describe a refrigerated 4800 kg detector now operating at Stanford.

RESONANT-MASS DETECTORS

The problem of detecting gravity waves has been the subject of several reviews.[1-5] It is well known that the signal available from an ideal electromagnetic antenna irradiated by an incident flux E is given by the product of E, the ideal antenna cross section $\lambda^2/4\pi$, and a directionality factor g_r which is equal to unity for an isotropic antenna. For detection in bandwidth B, this power must be of the order of $k_B T_N B$, where T_N is the receiver noise temperature. Although physical arguments show that this relationship is also valid for an ideal gravity wave detector, two factors reduce the performance of practical antennas dramatically. Since the lowest order mass multipole which can emit gravitational radiation is the quadrupole, the most promising receiving antenna is also a quadrupole. A typical antenna, described as a "Weber Bar", consists of a massive aluminum cylinder oscillating in its fundamental longitudinal acoustic mode, whose eigen-frequency must be within the expected signal spectrum. The antenna oscillations are monitored by a readout system sensitive to mechanical signals. The mechanical quantity analogous to the radiation resistance for such an antenna may readily be calculated by finding the gravitational radiation power emitted for a given stored energy. An idea of the magnitude of this quantity can be grasped

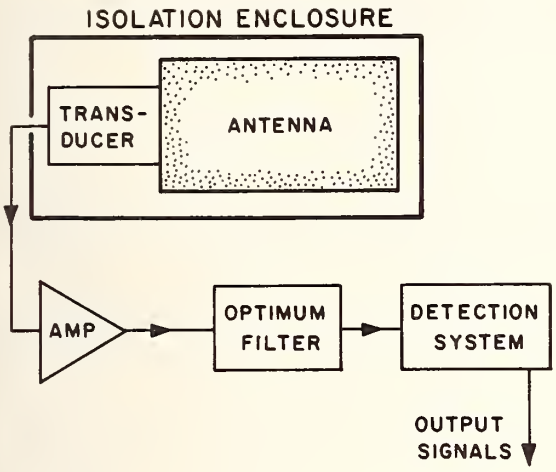

Fig. 1 Typical arrangement of a resonant-mass gravitational wave detector. The antenna motion is converted by a transducer into an electrical signal which is detected by a sensitive amplifier. The transducer may use either electric or magnetic field modulation and may be parametric. In order to obtain a suitable impedance match, resonant structures may be used in both the mechanical and electrical branches.

from the fact that if a typical resonant mass antenna such as that described in Section 4 were to lose energy only to gravitational radition, its amplitude would decay with a time constant τ_g of the order of 10^{18} times the age of the universe.

Obviously the bandwidth of a radiation-dominated gravity wave antenna would be ridiculously small. In practice, however, the antenna possesses mechanical dissipation mechanisms which limit the decay time to a value τ_d, typically of the order of 10^3 s for a low temperature antenna. Thus in the most general sense, the efficiency of a resonant mass gravitational wave antenna (equal to the ratio τ_d/τ_g) is exceedingly small, 10^{-32} in the case considered. If the overall detector noise level is dominated in bandwidth B by dissipation in the antenna, assumed to be at temperature T_a, the condition for detection of a continuous gravity wave by an isotropic antenna is given by

$$E\lambda^2/4\pi \geq k_B T_a B\ (\tau_g/\tau_d), \qquad (1)$$

where E is the signal flux in bandwidth B. For the example given, assuming T_a = 4K and B = 1 Hz, the minimum detectable flux would be about 0.8 wm^{-2}.

PRACTICAL ANTENNAS

A typical arrangement for a resonant-mass detector is shown schematically in Figure 1. The low signal level part of the detector may be exactly represented by an electrical equivalent circuit in which a shunt resonator representing the antenna is connected by a cascade of linear twoports to the amplifier. The gravitational wave signal is correctly represented by a current generator shunting the resonator. Since the signal of interest is a pulse, it is best described by its Fourier Transform $M(\omega)$. The relationship between $M(\omega)$ and the energy spectral density $E(\omega)$ in the incoming wave may be obtained by an extension of the antenna theory given in Section 2. It is easy to show that $M(\omega)$ can be expressed in the form

$$\frac{1}{2}\omega Z_0 |M(\omega)|^2 = E(\omega)\left[\lambda^2 g_r/2\pi\tau_g\right] \quad , \qquad (2)$$

where $\omega = 2\pi c/\lambda$ is the frequency, and $Z_0 = \sqrt{L/C}$ is the characteristic impedance of the equivalent resonator. Equation (2) is most easily understood in terms of the response of a noiseless antenna to a very short signal pulse. The quantity $\frac{1}{2}\omega_a Z_0 |M(\omega_a)|^2$, where ω_a is the antenna eigenfrequency, is then equal to the available signal energy induced by the pulse. The quantity multiplying $E(\omega_a)$ on the right-hand side of the equation is known as the *integrated antenna cross section* σ. In the case of the antenna discussed in section 4, σ is about 2×10^{-25} m^2Hz so that a pulse with a flux of 50 $Jm^{-2}Hz^{-1}$ gives an available signal energy of 10^{-23} J.

Each element in the equivalent circuit potentially contributes noise which can always be modelled by placing a noise generator in parallel with each port. The total system noise current referred to the input is given, as usual, by

$$S_n(\omega) = 4k_B T_a/\omega Z_0 \tau_d + \sum_j h_j(\omega)/G_j(\omega) \ , \tag{3}$$

where $h_j(\omega)$ is the spectrum of the j^{th} noise source and $G_j(\omega)$ is a transfer function connecting it with the resonator input termainals. The first term on the right of the equation represents thermal noise.

With optimum filtration the maximum signal-to-noise ratio ρ_{opt} which can be achieved is well known to be

$$\rho_{opt} = \frac{1}{2\pi} \int_{-\infty}^{\infty} \{ |M(\omega)|^2 / S_n(\omega) \} \, d\omega \ . \tag{4}$$

A practical approximation is obtained by assuming that the noise level is dominated by the antenna thermal noise over a bandwidth B_n near the antenna frequency, and is much larger elsewhere. Equations 2-4 then give the conditions for detection with unity signal-to-noise ratio

$$E(\omega_a)\left[\lambda^2 g_r / 2\pi\tau_g\right] = 4\pi k_B T_a / B_n \tau_d \ . \tag{5}$$

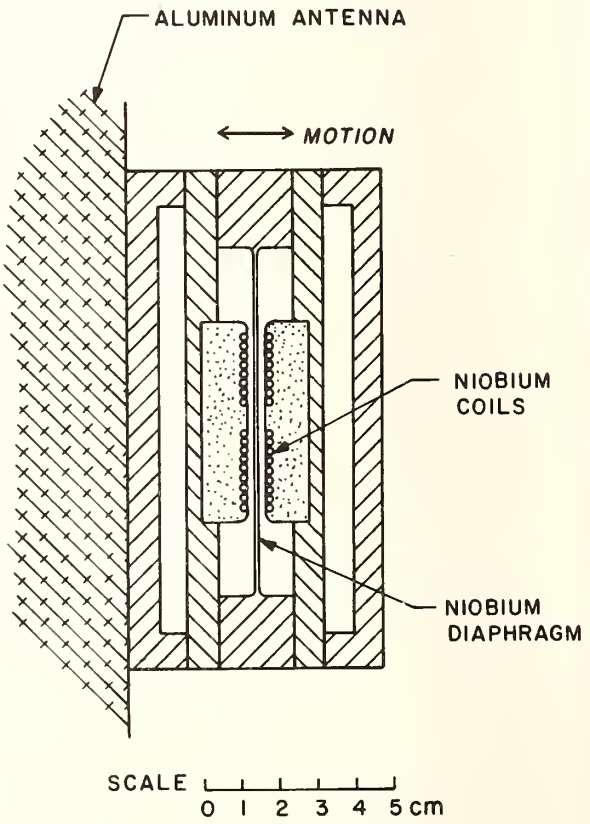

Fig. 2 Superconducting transducer. A thin circular superconducting diaphragm is clamped at its edge to one end-face of the antenna. The mechanical resonance of the diaphragm matches that of the antenna. Facing the diaphragm and separated from it by small gaps are two flat superconducting pickup coils carrying a persistent d.c. supercurrent.

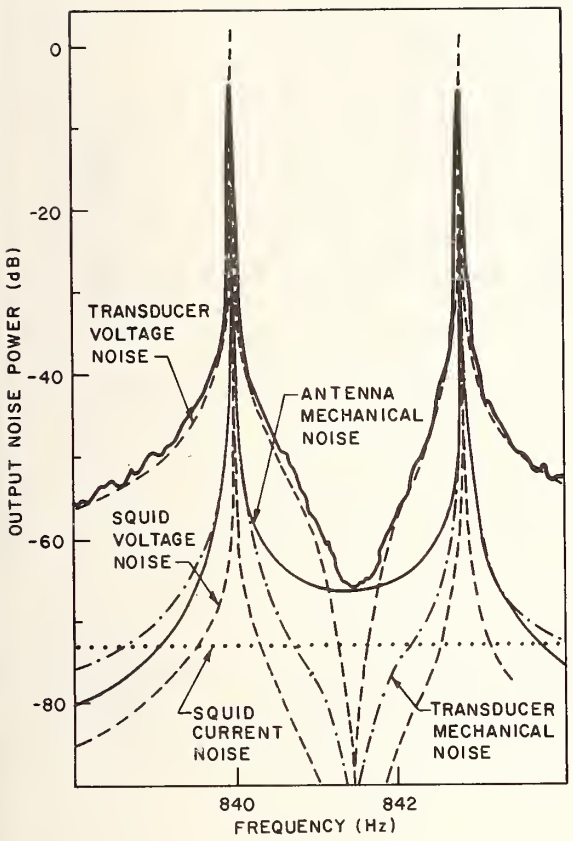

Fig. 3 Measured output spectrum of the detector. Also shown are the calculated contributions from various sources. Antenna thermal noise dominates in a region of about 0.5 Hz close to the uncoupled antenna frequency. Elsewhere transducer electrical noise is most significant. The optimization of the transducer design requires attention to all of these noise sources; with the available technology, the parameters can be adjusted to cause any one of the noise sources indicated here to dominate. The only exception to this is the SQUID voltage noise; it has the same frequency dependence as the transducer voltage noise, and for electrical Q's $< 2 \times 10^7$, the transducer voltage noise exceeds the SQUID voltage noise.

Another interesting limit obtains if the noise is entirely due to an amplifier of noise temperature T_N. The detection condition becomes

$$E(\omega_a)\left[\lambda^2 g_r / 2\pi\tau_g\right] = k_B T_N \quad , \tag{6}$$

which may be described as the amplifier limit of sensitivity.[6]

It is clear from Equations 2, 3, and 4 that one task of the antenna designer is to maximize the quantity on the right of Equation (2). The only free parameter for a given frequency is τ_g which is minimized by building the heaviest possible antenna. The second objective is to minimize the quantity $S_n(\omega)$ over the largest possible bandwidth. In practice this involves using an antenna of high Q, at a low temperature, matched over the widest possible bandwidth to a low noise amplifier. Losses in the matching structure -- the transducer -- must of course be minimized. An example of a working detector embodying these principles will now be presented.

STANFORD DETECTOR

The cryogenic resonant-mass detector now operating at Stanford follows the form shown schematically in figure 1. The cylindrical aluminum antenna weighing 4800 kg is suspended by a multi-stage vibration isolation system inside a vacuum tank cooled to 4.2 K by liquid helium. The unloaded Q of the antenna is 2×10^6.

The transducer shown in figure 2 makes use of the low mechanical and electrical losses in superconducting materials. Oscillations of the antenna end-face are coupled to the fundamental mechanical eigenmode of a superconducting diaphragm, which modulates the inductance

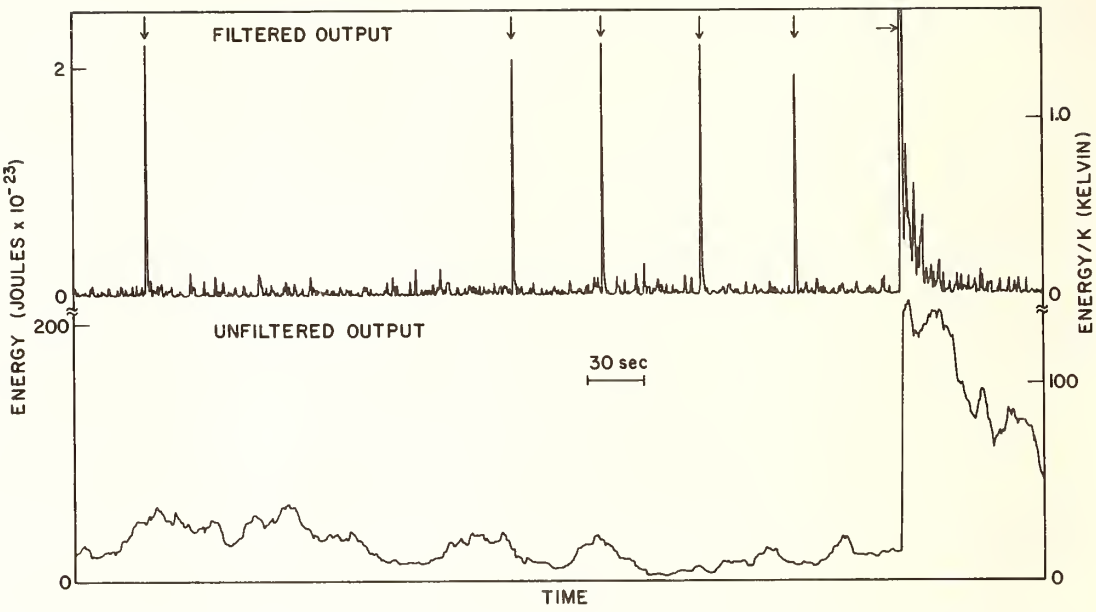

Fig. 4 Time-domain response of the detector to input pulses of known strengths applied by a piezoelectric calibrator. The upper trace shows the detector output after filtration: five calibration pulses with available signal energies of 2×10^{-23} J are easily identified. The lower trace shows the mean energy in the antenna modes: only a single large pulse of energy 2×10^{-21} J can be positively identified.

of current-carrying pick-up coils, causing an a.c. voltage proportional to the velocity of the diaphragm to appear at the output terminals.[7] The transducer output signal is fed to a Josephson junction parametric amplifier or SQUID.[8] The function of the diaphragm resonance is to provide a suitable noise match between the impedance of the antenna and the much higher impedance characterizing the electromechanical transduction process. The present transformation ratio is about 300, resulting in a useful bandwidth of about 1 Hz.

A detailed analysis of the signal-to-noise ratio of the detector will appear elsewhere.[9] The main contributions of the overall system noise presently come from mechanical dissipation in the antenna and the transducer, and from a.c. losses in the transducer output ciruit. Further contributions from the SQUID voltage and current noise are of minor significance. Figure 3 shows the output noise spectrum of the detector and the calculated contributions from the various sources. Figure 4 shows the response of the complete detector in its present form to calibration pulses. The measured noise level after signal processing corresponds to an available signal energy of 3×10^{-25} J.

CONCLUSIONS

The analysis of resonant antennas is completely supported by the measurements discussed above. The 4800 kg detector is now in almost continuous use for observations, which are being carried out in collaboration with other experimental groups.

The authors have collaborated with W. M. Fairbank, C. Chun, S. Boughn, J. Hollenhorst, E. Mapoles, M. S. McAshan, and H. J. Paik on the development and construction of the detector.

REFERENCES

[1] J. A. Tyson and R. P. Giffard, Ann. Rev. Astron. Astrophys. 16, 521 (1978).

[2] D. H. Douglass and V. B. Braginsky, in *General Relativity: An Einstein Centenary Survey*, edited by S. W. Hawking and W. Israel (Cambridge University, Cambridge, England, 1979).

[3] G. Pizzella, Rev. Nuovo Cimento 5, 369 (1975).

[4] G. Papini, Can. J. Phys. 52, 880 (1974).

[5] K. S. Thorne, Rev. Mod. Phys. 52, 285 (1980).

[6] R. P. Giffard, Phys. Rev. D. 14, 2478 (1976).

[7] H. J. Paik, J. Appl. Phys. 47, 1168 (1976).

[8] J. N. Hollenhorst and R. P. Giffard, IEEE Trans. Mag. MAG-15, 474 (1979).

[9] P. F. Michelson and R. C. Taber, to be published in J. Appl. Phys., June, 1981.

+ Present address: Hewlett-Packard Laboratories, 3500 Deer Creek Road, Palo Alto, CA

MEASUREMENT OF THE BROWNIAN NOISE OF A HARMONIC OSCILLATOR WITH MASS M=389 kg

P.Bonifazi, F.Bordoni, G.V.Pallottino, G.Pizzella

Istituto Plasma Spazio del CNR, Frascati
Istituto di Fisica dell'Università, Roma

1. INTRODUCTION

We report experimental data on the Brownian noise at the fundamental longitudinal mode (ν_R=1795 Hz) of an aluminum (6061 alloy) cylinder (M=389 kg) in a cryostat at the temperature of the liquid helium.

The cylinder is part of an antenna system [1] designed for the detection of the gravitational waves emitted by celestial bodies according to Einstein's general relativity theory [2].

The sensitivity of the antenna system is limited by the Brownian noise of the mechanical oscillator and by the electronic noise of the instrumentation.

The measurement of the Brownian motion is very important for the gravitational experiment. It must be performed with accuracy over several decades of energy in order to observe possible small disturbances due to the environment, which affect the performance of the antenna as a detector of gravitational waves.

2. THE EXPERIMENTAL APPARATUS

According to the energy equipartition principle, the Brownian energy of the oscillator is

$$M \omega_R^2 x^2/4 = kT/2 \qquad (1)$$

where M/2 is the reduced mass of the aluminum bar and x(t) the displacement of the bar ends measured relative to the center of mass. The temperature of the oscillator is increased from T to T_e by the heating effect of the current noise, with spectral density I_n^2, due to the preamplifier and to the electrical losses of the input node.

It can be shown [1] that the equivalent temperature is

$$T_e = T+\Delta T=(1+\alpha^2 Q I_n^2/2 M \omega_R^2 k) \qquad (2)$$

where Q is the merit factor of the oscillator and the response of the piezoelectric transducer is

$$v(t) = \alpha x(t) \qquad (3)$$

Our transducer consists of two Gulton G-1408 piezoelectric ceramics located in a slot cut around the median plane of the aluminum cylinder. The preamplifier [3,4] has an input stage with four FET's BF 817 connected in parallel and is followed by a selective amplifier tuned at ν_R with Q=10. The output signal is then applied to a pair of phase-sensitive detectors driven in phase and in quadrature by a synthesizer operating at ν_R, in order to extract the components p(t) and q(t) of the signal in a narrow band near ν_R.

The output signals are converted in digital form by a 12 bit analog-to-digital converter, with sampling time Δt which can be adjusted from 1 ms to 10 s, and stored on magnetic tape. The block diagram of the experimental apparatus is given in Fig. 1. We also have an electronic analog chain composed by squarers, summer and integrators (τ=1 min - 3 h), whose output is applied to a chart recorder that provides quick-look information on the status of the system.

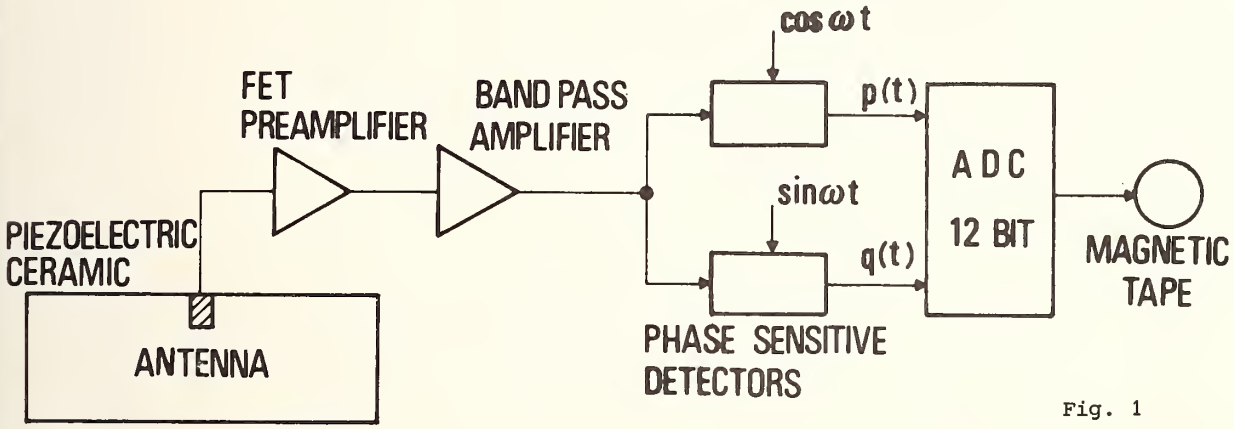

Fig. 1

The two signals p(t) and q(t) are independent and with equal variance 6^2. Therefore the probability density function of the variable

$$r^2(t) = p^2(t)+q^2(t) \tag{4}$$

is given by the Boltzmann function

$$f(r^2) = \exp\{-r^2/2\sigma^2\}/2\sigma^2. \tag{5}$$

We remark here that, since our transducer is wide-band, our antenna is a multimode detector; in fact, its vibration can be observed in the various odd longitudinal modes, that are coupled with the gravitational radiation, and also in the flexural modes.

3. EXPERIMENTAL RESULTS

We report experimental results obtained in March 1980 with the M=389 kg antenna operating in Frascati [5].

Run	T (K)	Q (10^6)	α (MV/m)	T_e (K) comp.	T_e (K) meas.	Duration of run
1	4.4±0.1	.667	57±1	5.9±.1	6.1±.1	35^h36^m
2	5.2±0.1	.621	52±1	5.5±.1	5.6±.1	5^h36^m

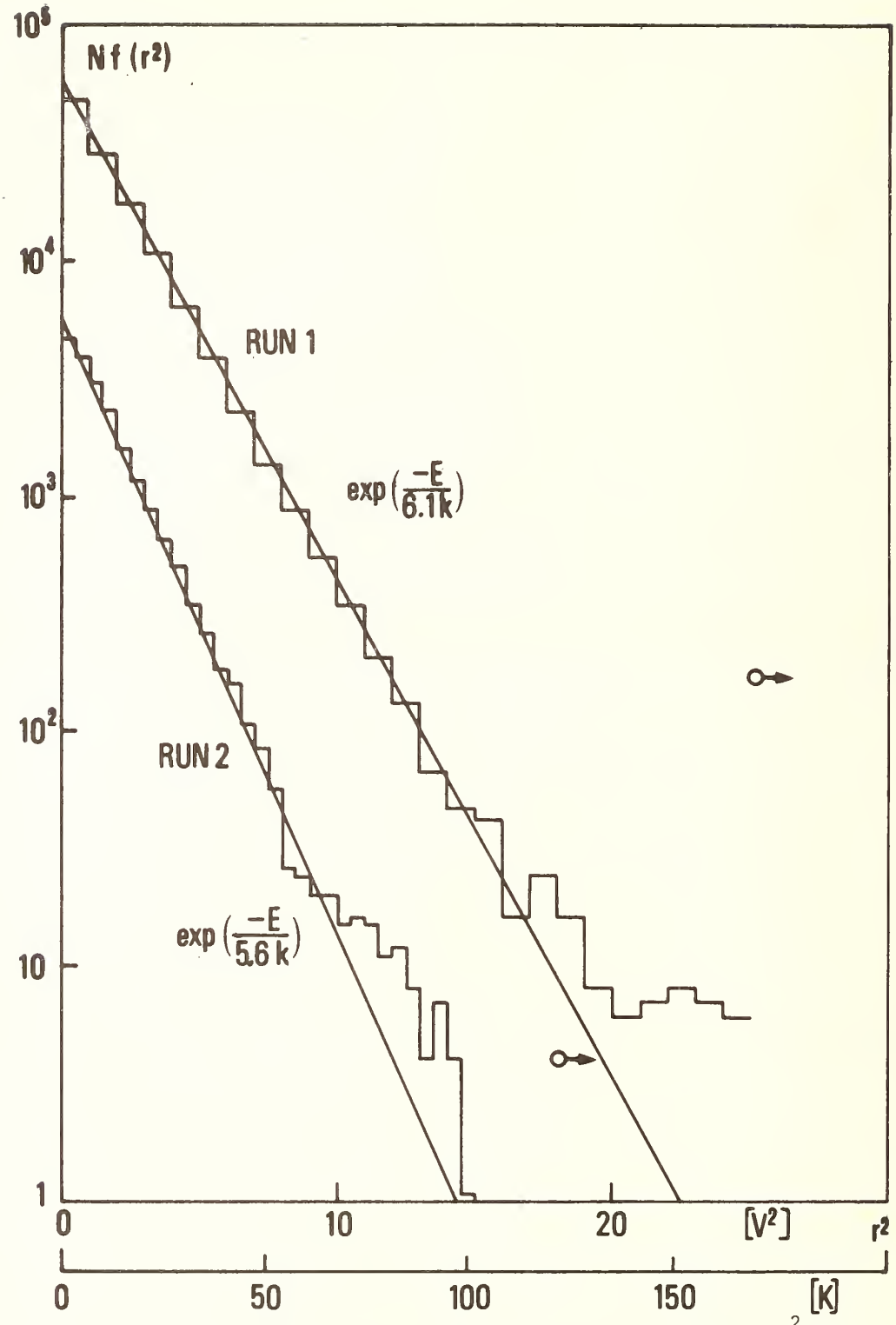

Fig. 2

Fig. 2 gives a semilog plot of the hystogram of the variable $r^2(t)$ in two different operating conditions as specified in the table; N is the number of samples, obtained with $\Delta t=1$ s.

During run 1 we used a preamplifier with $T_n=0.11$ K; during run 2 we used a preamplifier [4] with $T_n=36$ mK with input stage cooled at 140 K, but the temperature of the bar was slightly higher due to a lower level of the liquid helium in the cryostat.

The scale of Fig. 2 is given both in volt^2 and in K, as computed from the calibration of the measuring system. The calibration is based on the knowledge of the parameter and of the gain of the electronics; it has been also checked independently by means of capacitor plates which are used to inject a calculable amount of energy into the mechanical oscillator. Note that this system allows one to perform mechanical noise thermometry on objects of large size, but requires a very careful isolation from the mechanical and electrical disturbances due to the environment.

The attenuation provided by the filters used at present amounts to 240 db at 1795Hz.

As regards the operation of our system as a gravitational wave antenna, we recall here that the quantity of interest is the sensitivity, which depends on the effective temperature T_{eff} [6], rather than the equivalent temperature T_e.

The effective temperature is a measure of the detectable fluctuations at the input of the antenna, when the data analysis algorithms are applied to the data. It has been shown that when the antenna system is properly designed (optimum coupling), the effective temperature is equal to twice the noise temperature of the preamplifier [7]. In the two runs mentioned above , by using the Wiener-Kolmogoroff optimum filter, we have obtained T_{eff}=.42 K (first run) and T_{eff}=.28 K (second run). The last value can be further reduced by modifying the apparatus, which was designed for an amplifier with T_n=.11 K.

REFERENCES

[1] E. Amaldi et al. "Initial operation of the M=389 kg cryogenic gravitational wave antenna" Nuovo Cimento, Nov.-Dec. 1978, pp. 497-509.

[2] J. Weber "General Relativity and Gravitational Waves" Interscience, New York, 1961.

[3] F. Bordoni, G. V. Pallottino "Low noise amplifier for gravitational research" Rev. Sci. Instr., July 1977, pp. 757-761.

[4] F. Bordoni, G. V. Pallottino "Very low noise cooled audiofrequency amplifier for gravitational research" in press, Rev. Sci. Instr., 1981.

[5] E. Amaldi et al. "Information on the operation of the M=389 kg gravitational wave antenna of the Roma group at an effective noise temperature of T^W_{eff}=0.3 K" Lett. Nuovo Cimento, 5 July 1980, pp. 366-366.

[6] P. Bonifazi et al. "Data Analysis Algorithms for Gravitational-Wave Experiments" Nuovo Cimento, vol. 1c, nov.-dec. 1978, pp. 465-487.

[7] R. P. Giffard "Ultimate sensitivity limit of a resonant gravitational wave antenna using a linear motion detector" Phys. Rev. D, vol. 14, 15 nov. 1976, pp. 2478-2486.

TWO-PORT NOISE CHARACTERIZATION BY MEANS OF A FEEDBACK METHOD

Gabriel Blasquez

Laboratoire d'Automatique et d'Analyse des Systèmes
Centre National de la Recherche Scientifique
7 Ave. Roche, 31400 Toulouse, France

A BRIEF OUTLINE OF THE METHOD

Let us consider an operational amplifier set up as a voltage follower with non-inverting input connected to a voltage source E. It is known that the output voltage is equal to E. This circuit is similar to the one given in figure 1.

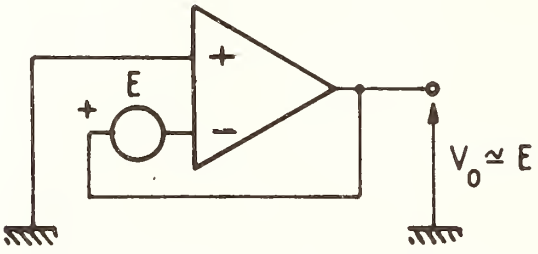

Fig. 1 Equivalent circuit of a generator E connected to the non inverting input of a voltage follower.

By applying this property, the equivalent input voltage noise generator E_{nx} of an amplifying two-port X can be simply and directly obtained. To this end, the input and the output of the two-port must be short-circuited, and the output noise voltage V_{no} measured. We then have

$$\langle |E_{nx}|^2 \rangle \simeq \langle |V_{no}|^2 \rangle \qquad (1)$$

Let us now consider an electrometer, the input of which is connected to a current source I. If R_s is the feedback resistance, the voltage output $V_o = R_s I$. By applying this property to the two-ports having a sufficient gain, the equivalent input I_{nx} current noise generator can be simply and directly obtained. To this end a resistance R_s of a high value must be placed between the input and the output of the two-port, and the output voltage noise V_{no} must be measured. We then have

$$\langle |I_{nx}|^2 \rangle \simeq \langle |V_{no}|^2 \rangle / R_s^2 \qquad (2)$$

Finally, let us consider figure 2 where a resistance R_s is connected in the way just indicated, and where E_{ns} is the equivalent noise source of R_s.

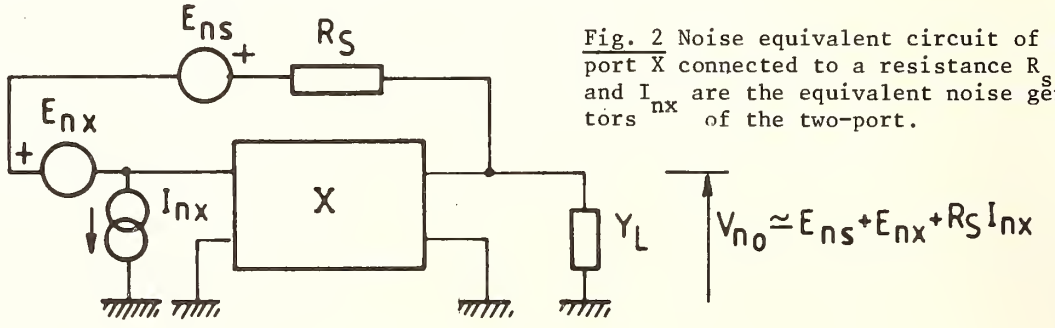

Fig. 2 Noise equivalent circuit of two-port X connected to a resistance R_s. E_{nx} and I_{nx} are the equivalent noise generators of the two-port.

It follows from the preceding that

$$\langle |V_{no}|^2 \rangle \simeq \langle |E_{ns}|^2 \rangle + \langle |E_{nx} + R_S I_{nx}|^2 \rangle \qquad (3)$$

With

$$\langle |E_{ns}|^2 \rangle \simeq 4 k T R_S \Delta f \qquad (4)$$

and where k, T, Δf have their usual meanings.

Let F be the noise factor of the two-port X connected to a resistance R_s at a temperature T. It is known that

$$F \simeq \frac{\langle |E_{ns}|^2 \rangle + \langle |E_{nx} + R_S I_{nx}|^2 \rangle}{\langle |E_{ns}|^2 \rangle} \qquad (5)$$

Substituting (3) into (5) yields

$$F \simeq \frac{\langle |V_{no}|^2 \rangle}{\langle |E_{ns}| \rangle} \qquad (6)$$

If we assume that the output of X is loaded by Y_L and that the noise of Y_L can be disregarded, the noise power P_{nL}, measurable at the output of the feedback circuit, is equal to :

$$P_{nL} \simeq \langle |V_{no}|^2 \rangle \, \mathrm{Re}(Y_L) \qquad (7)$$

where Re ( ) is used for the real part of the quantity between brackets.
Following (7) and (6) we have

$$F \simeq \frac{P_{nL}}{4 k T R_S \, \mathrm{Re}(Y_L) \, \Delta f} \qquad (8)$$

We can see that in order to obtain F of X connected to a resistance R_s it is necessary and sufficient to measure $\langle |V_{no}|^2 \rangle$ or P_{nL}. A more detailed analysis would show that relations (1), (2), (6) and (8) are only correct if the open-loop transfer function of the circuit (voltage gain) in figure 2 is high.

EXPERIMENTAL RESULTS

In order to test the validity of the method under discussion, experiments were carried out on integrated operational amplifiers, field effect transistors, and bipolar transistors. The parameters measured were $\langle |E_{nx}|^2 \rangle$, $\langle |I_{nx}|^2 \rangle$ and F. The experimental procedure consisted of estimating these parameters using a classical technique as well as using the method under discussion. For the classical technique we constituted and amplifier stage with the device

under test, its load and the source resistance R_s. The input noise was obtained from the measurement of the low frequency voltage gain ($1^{s}KH_z$). An example of the circuits used and the results obtained are given in figures 3 to 5.

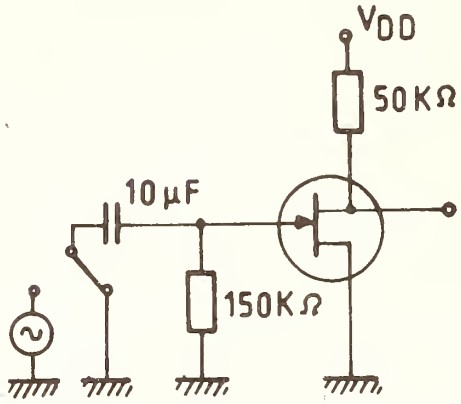

Fig. 3 Indirect noise measurement-sine wave method

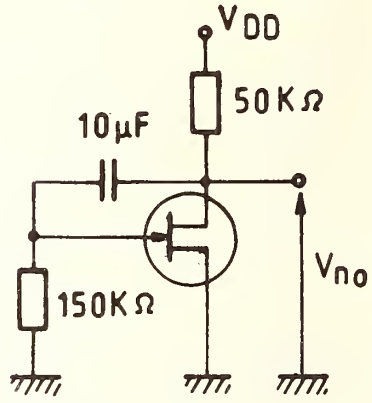

Fig. 4 Direct noise measurement-voltage follower configuration

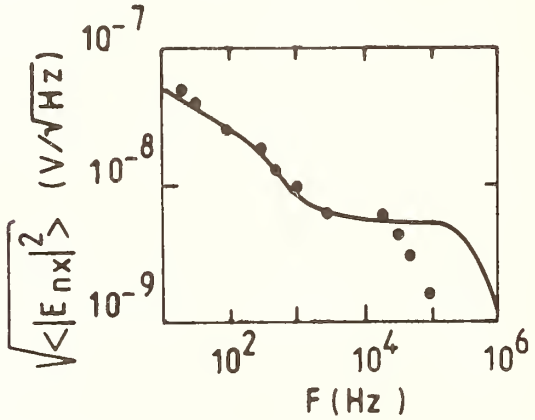

Fig. 5 Equivalent input noise generator of a JFET (BIFET technology)
—— feedback method
.....indirect method.
$V_{DS} = -7\,V$, $I_{DS} = 180\,\mu A$,
$T = 20°C$, $V_G = 0V$

A satisfactory agreement is seen up to 20 KHz. Beyond it a decrease in the noise determined by the classical technique is observed. This effect is due to two causes : (i) the decrease in voltage gain in the high frequency range which had not been taken into account, and (ii) the attenuation by the output impedance of the device under test and the preamplifier input capacitance of the measurement system. This effect appears at higher frequencies in the method under discussion because feedback decreases (a) circuit sensitivity to two-port gain variations, and (b) output impedance (as long as the open-loop gain remains high).

CONCLUSION

By using the properties of the feedback systems it is possible to directly measure the input noise of amplifying two-ports. This method has the advantage, when compared to classical techniques, of not requiring the measurement of the two-port gain. It follows that the total number of measurements to be carried out is reduced from 3 to 1, and the duration of the experiments considerably decreased. The method is considerably faster, more accurate and, in addition, is more economical to implement because it does not use sine wave or noise generators. Finally, it can easily be automated.

The author wishes to thank J. Borreil for his measurement assistance and valuable experimental contribution.

REFERENCE

[1] G. BLASQUEZ, Revue de Physique Appliquée, 15 (1980) 1007.

NEW METHOD FOR WIDE BAND MEASUREMENT OF NOISE TEMPERATURE OF ONE-PORT NETWORKS AT HIGH PULSED BIAS

D. Gasquet, J.C. Vaissière, J.P. Nougier

Université des Sciences et Techniques du Languedoc
Centre d'Etudes d'Electronique des Solides†
34060 Montpellier Cédex, France

1. INTRODUCTION

Measurement of noise temperature of non linear one-port networks under high bias conditions must be performed using pulsed techniques in order to avoid heating of the device. The usual technique [1][2] consists in comparing the output signal x_n corresponding to the studied noise temperature $T_n(V)$ of the device at the bias voltage V, to the output signals x_G and x_o corresponding to input noise temperatures T_G and T_o. T_G and T_o are known values given by a standard noise generator. These three measurements give then [1]:

$$T_n - T_o = (T_G - T_o)\ (x_n - x_o)/(x_G - x_o) \qquad (1)$$

if λ and T_A are respectively the gain and the noise temperature of the apparatus, eq. (1) follows from the fact that each noise temperature T_i gives an output signal $x_i = \lambda(T_i + T_A)$.

The above equations are valid under the conditions that λ and T_A are kept unchanged during the three measurements, which implies that the load impedance at the input of the apparatus remains constant (generally equal, for convenience, to its characteristic impedance R_o). Since the device studied may be non linear, its impedance is bias dependent, so that it must be matched to R_o, using a tuner without losses, which then keeps unchanged the noise temperature of the device [1][2]. It can be shown [1] that the finite duration t_o of the measurement during the pulsed bias results in a statistical fluctuation of the output signal of average value x, such that

$$\sigma_x / x = \sqrt{2/(N t_o\ \Delta\nu)} \qquad (2)$$

where σ_x is the r.m.s. deviation of x, $\Delta\nu$ is the bandwidth and N is the number of pulses over which the result is averaged (N t_o is the total duration of the measurement).

Since t_o must be as short as possible in order to avoid thermal heating, $\Delta\nu$ has to be increased for increasing the accuracy. Unfortunately the impedance matching is very selective, and when impedances are matched at the central frequency of the band, they are mismatched at the edges, thus producing standing waves, hence losses.

The purpose of this paper is to evaluate these losses, which will be shown to be important (section 2), then to describe a new method allowing to take these losses into account (section 3). The uncertainty on the measurement, and example of results obtained, will be given in sections 4 and 5.

2. EVALUATION OF THE LOSSES

Using a computer simulation, the losses have been determined at each frequency for a given real input impedance R matched to 50 Ω at frequency ν_o.

---

† Laboratoire associé au C.N.R.S., LA 21 et Greco Microondes. This work was partially supported by D.G.R.S.T. (France).

Figure 1, shows, for a stub stretcher tuner, the percentage of losses versus frequency ν (plotted in relative units $(\nu - \nu_o)/\nu_o$, for various values of R in the range 50 Ω- 10 kΩ.

Figure 2 shows the overall losses, integrated in the bandwidth $\Delta\nu$ centered on ν_o, plotted versus R. The curves are given for a stub stretcher. The losses were found to be much higher for a double stub tuner which is much more selective : for example the losses corresponding to $\Delta\nu \simeq 0.1\ \nu_o$ for a double stub are about the same as those corresponding to $\Delta\nu = 0.25\ \nu_o$ for a stub stretcher.

Figures 1 and 2 clearly show that the matching impedance technique requires a very narrow bandwidth and hence very long or numerous pulses (see eq. 2) : each experiment is then very long and tedious, and matching impedances at low repetition rate is much tricky.

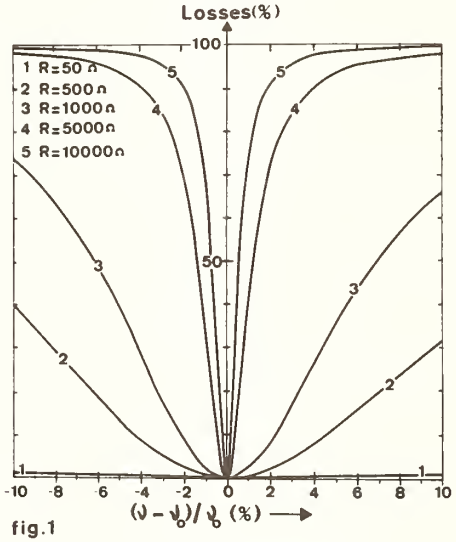

fig.1

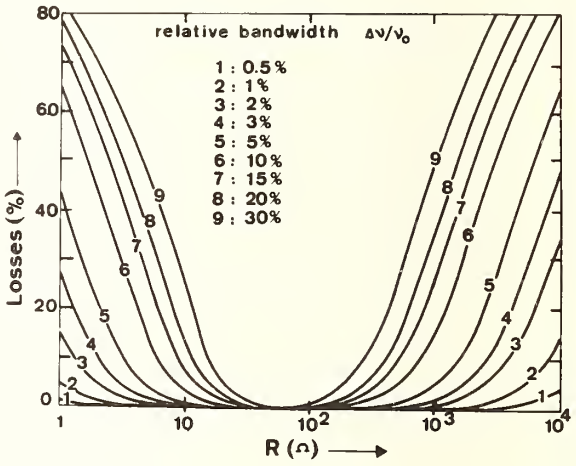

fig. 2

3. PRINCIPLE OF THE METHOD WITHOUT MATCHING IMPEDANCES :

In this method we suppress the impedance matching and we measure the losses on the whole bandwith. For this purpose we use a circulator (see figure 3). The impedance at the port 2 is always kept equal to R_o, so that the input load of the amplifier is always equal to R_o, hence λ and T_A will be constant. Now we have to determine four values T_n, λ , T_A, r, where r is the reflection coefficient of the device studied. Four measurements are performed:

1/ Port 2 : R_o at room temperature T_o. Port 1 : device of impedance Z, and noise temperature T_n we want to measure. The reflexion coefficient is r, and the signal x at the output of the apparatus is

$$x_n = \lambda\left[(1 - |r|^2)\ T_n + |r|^2\ T_o + T_A\right] \qquad (3)$$

2/ Port 2 : R_o at a temperature T_G (noise generator). Port 1 : unchanged.

$$x'_n = \lambda\left[(1 - |r|^2)\ T_n + |r|^2\ T_G + T_A\right] \qquad (4)$$

3/ Port 2 : unchanged. Port 1 : a short circuit (r = 1)

$$x_G = \lambda\ (T_G + T_A) \qquad (5)$$

4/ Port 2 : R_o at room temperature T_o. Port 1 : unchanged.

$$x_o = \lambda (T_o + T_A) \tag{6}$$

equations (3) to (6) give

$$\begin{cases} |r|^2 = (x'_n - x_n)/(x_G - x_o) & (7) \\ T_n - T_o = \left[(T_G - T_o)/(1 - |r|^2)\right] \times \left[(x_n - x_o)/(x_G - x_o)\right] & (8) \end{cases}$$

Note that eqs. (5) and (6) give λ and T_A. Eq. (1) is now the particular case of eq. (8) when impedances are matched in the whole bandwidth, since then $r = 0$.

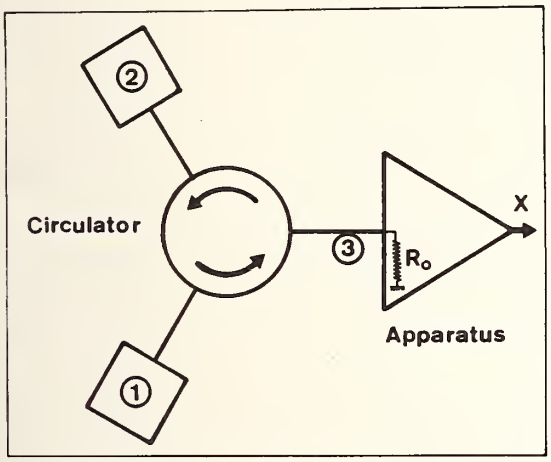

fig.3

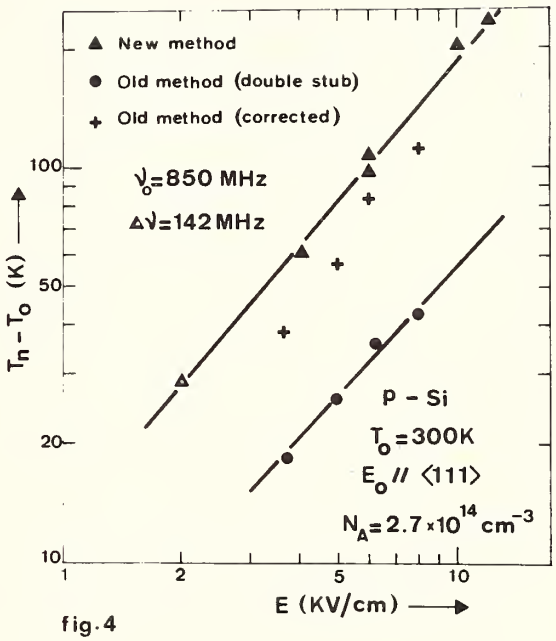

fig.4

4. UNCERTAINTY ON THE MEASUREMENT

Equations (7) and (8) give :

$$\frac{\Delta(T_n - T_o)}{T_n - T_o} = \frac{\Delta(T_G - T_o)}{T_G - T_o} + \frac{(\Delta x_n + \Delta x_o)(x_G - x'_n)}{(x_n - x_o)(x_n - x_o + x_G - x'_n)} + \frac{\Delta x'_n + \Delta x_G}{x_n - x_o + x_G - x'_n} \tag{9}$$

From eq. (2), we define the uncertainty Δx as :

$$\Delta x = \alpha \sigma_x \quad , \quad \text{with } \alpha = 1.96 \quad \text{since} \quad N > 30. \tag{10}$$

The number of measurements performed for getting x_o, x_G, x_n and x'_n will be set equal to N_o, N_o, N_n and N_n respectively. Eqs (9), (10) and (2) to (6) give :

$$\Delta(T_n - T_o) = \left[\frac{\Delta(T_G - T_o)}{T_G - T_o} + \frac{\alpha}{(1 - |r|^2)} \sqrt{\frac{2}{t_o \Delta\nu}} \left(\frac{1}{\sqrt{N_n}} + \frac{1}{\sqrt{N_o}}\right)\right] (T_n - T_o) + \frac{\alpha}{(1 - |r|^2)} \sqrt{\frac{2}{t\Delta\nu}} \left(\frac{1}{\sqrt{N_n}} + \frac{1}{\sqrt{N_o}}\right) (T_A + T_o) \tag{11}$$

We can see that the absolute uncertainty is the sum of a constant term and a term proportional to $(T_n - T_o)$. In order to increase the accuracy, one should increase N_o and N_n ,

decrease the reflection coefficient (R near R_o), increase the bandwith $\Delta\nu$, decrease T_A. If the impedance of the sample is matched, the uncertainty is given by (11) using r = 0.

5. RESULTS

We have built two apparatus, the first one works between 220 MHz and 850 MHz with five points of frequency (220 MHz, $\Delta\nu/\nu_o$ = 10 % ; 360 MHz, $\Delta\nu/\nu_o$ = 10 % ; 460 MHz, $\Delta\nu/\nu_o$ = 10 % ; 650 MHz $\Delta\nu/\nu_o$ = 5 % ; 850 MHz, $\Delta\nu/\nu_o$ = 1 %, $\Delta\nu/\nu_o$ = 5 % and $\Delta\nu/\nu_o$ = 15 %), the second one works at 10.5 GHz, $\Delta\nu/\nu_o$ = 10 %.

Figure 4 shows the excess longitudinal noise temperature $T_n(E)-T_o$ measured, ν_o = 850MHz, for p-type silicon bars ($N_A = 2.7 \times 10^{14}$ cm^{-3}, T_o = 300 K, E_o // <111> , R = 184 Ω at E_o=0) versus the electric field E_o up to E_o = 12 kV cm^{-1}. The triangles represent experimental points measured using the new technique described in the present paper, although the dots represent results obtained using the old method (impedance matching). The conditions were such that a great difference could be exhibited, as one can see on figure 4 : thus, we used a double stub tuner (which is more selective than a stub stretcher) and a relatively large bandwith of 142 MHz (≃ 0.15 ν_o). Of course, it has been verified that the noise was white at that frequency. The crosses on Fig. 4 were obtained from the dots by applying a computed correction using a simulation analogous to that mentioned earlier, but performed for a double stub tuner. The losses are thus shown to be quite important. As comes out from the theory here above, only the impedance mismatching was taken into account, the line was supposed to be perfectly non dissipative : indeed, the results represented by the crosses should be raised by the amount of the power displayed in the resistive part of the line and of the insertion losses of the connectors, which could not be evaluated : as can be shown on Fig. 4, losses a low as 1.3 dB are sufficient to take into account the difference between the triangles and the crosses.

6. CONCLUSION

The new method, presented here, needs four measurements. Its advantages are the following :

(i) All the losses (mismatching as well as insertion losses) are taken into account on the whole bandwidth.

(ii) The bandwidth may be wide, thus allowing short pulses.

(iii) The matching impedance, which is tricky and time consuming at low repetition rate pulses, is suppressed.

(iv) It allows automation of the measurements.

The mismatching must be low enough so that the losses be lower than about 90 % of the noise power, so as to reach an acceptable accuracy : this corresponds to an a.c. impedance of the device of about 2 kΩ. Note that, for such devices, the noise level is in many cases so high that the accuracy on the 10 % noise power remaining is good enough.

REFERENCES

[1] J.P. Nougier, J. Comallonga and M. Rolland, J. Phys. E 7, 287 (1974).

[2] J.P. Nougier, Proc. 5th Int. Conf. on Noise in Physical Systems, Springer Series in electrophysics 2, Springer Verlag, 1978, p. 72.

APPLICATION OF THE THEORY OF RANDOM MATRICES TO A REACTOR NOISE PROBLEM

Felix C. Difilippo

Department of Nuclear Engineering
University of Tennessee, Knoxville, TN 37916

J. J. Piñeyro

Departamento de Reactores
Comisión Nacional de Energía Atómica
Buenos Aires, Argentina

INTRODUCTION

There are neutron reacting systems where a degree of randomness exists in the spatial distribution of materials. Fluctuations in composition appear, for example, as a consequence of the operational characteristic of boiling water and pebble-bed reactors. Traditionally these type of systems have been approximated by homogenizing methods that use average values for the distribution of materials; this deterministic approach gives values of reactivities and flux distributions that do not agree with a stochastic treatment of the problem [1, 2, 3, 4]. According to ref [1] a knowledge of the statistical laws obeyed by the system are necessary in order to obtain an equivalent homogeneous system. In this context, a model has previously been developed which gives the first two moments of the reactivity distribution in an ensemble of reactors having a specified random distribution of macroscopic absorption and fission cross sections. An important result of this previous work is that the use of higher order perturbation theory gives a positive value for the average reactivity as opposed to a value of zero when calculated by ordinary perturbation theory. Recent work [3] confirms this conclusion but these same authors [4] stress that the sign of the average reactivity depends on the fluctuations in the moderation process.

In the present work we have recast the equations derived in ref [2] in a matrix form. In this way the distribution of reactivities can be described by the distribution of the highest eigenvalues of random matrices, with the result that all the mathematical techniques developed for the study of the statistical laws of excited nuclei [5] can be applied to the similar reactor physics problem. Following a presentation of the theory, a numerical example is given, for which a Monte Carlo simulation of several ensembles of reactors is made.

THEORY

Using the standard nomenclature of reactor theory, the reactivity, ρ, of each member of an ensemble of reactors is given by the highest eigenvalue of the equation

$$[C]\vec{\alpha} = \rho\vec{\alpha}, \tag{1}$$

where the matrix elements of [C] are given b

$$C_{ij} = \frac{1}{\nu\Sigma_{f_0}} \int_R \left[\nu\delta\Sigma_f(\vec{r}) - \delta\Sigma_a(\vec{r})\right] \psi_i \psi_j \, d\vec{r} + \rho_i \delta_{ij} \tag{2}$$

and the components of vector $\vec{a}$ are the coefficients of the expantion of the neutron flux in a basis ψ_i given by the Helmholtz equation. In eq (2), $\delta\Sigma_f$ and $\delta\Sigma_a$ are, respectively, the fluctuations of the macroscopic fission and absorption cross sections, ρ_i is the reactivity of the ith mode in the reference homogeneous reactor, and δ_{ij} is the Kronecker delta functions. Equations (1) and (2) were obtained with the following assumptions: (a) each member of the ensemble is a bare reactor; (b) one energy group theory applies and (c) random dispersal of materials does not affect the diffusion coefficient, which is assumed a constant throughout the reactor volume.

Due to the linear relation, eq (2), between C_{ij} and the fluctuating cross sections, the matrix element are Gaussian distributed. If, in addition, we assume that the ensemble average of $\delta\Sigma_a$ and $\delta\Sigma_f$ are zero for all $\vec{r}$, the mean value of C_{ij} is equal to $\rho_i \delta_{ij}$ and the variance is given by

$$\sigma_{ij}^2 = \frac{1}{(\nu\Sigma_{f_0})^2} \int_R \psi_i(\vec{r})\,\psi_j(\vec{r})\,f_{ij}(\vec{r})\,d\vec{r}, \tag{3}$$

where R is the reactor volume and f_{ij} is the correlation function.

$$f_{ij} = \int_R \langle \delta\Sigma(\vec{r})\,\delta\Sigma(\vec{r}')\rangle\,\psi_i(\vec{r}')\,\psi_j(\vec{r}')\,d\vec{r}', \tag{4}$$

where $\delta\Sigma = \nu\delta\Sigma_f - \delta\Sigma_a$.

If we make the additional assumptions that the fluctuations are correlated only within a distance λ and (b) the ensemble average $\langle\delta\Sigma^2\rangle$ is independent of $\vec{r}$, then the variance can be approximated, in the case of a slab reactor, by

$$\sigma_{ij}^2 = \frac{\lambda}{a}\,\frac{\langle\delta\Sigma^2\rangle}{(\nu\Sigma_{f_0})^2},\ i \neq j\ ;\quad \sigma_{ii}^2 = \frac{3}{2}\,\frac{\lambda}{a}\,\frac{\langle\delta\Sigma^2\rangle}{(\nu\Sigma_{f_0})^2} \tag{5}$$

where the thickness a is much greater than λ. Under these conditions the distribution of reactivities, $p(\rho)$, is given by the distribution of the highest eigenvalues of random matrices which have the following properties: (1) they are real and symmetric; (2) the elements are Gaussian distributed; (3) the off-diagonal elements have zero mean; (4) the diagonal elements have mean values equal to ρ_i; (5) all off-diagonal elements have the same variance, σ_{ND}^2; (6) all diagonal elements have the same variance, σ_D^2 and (7) defining $\beta^2 \equiv 2\sigma_{ND}^2/\sigma_D^2$, this parameter has a value 4/3 in our case.

The probability distributions are known for particular and restricted cases. For example, if the diagonal elements have zero mean and $\beta^2 = 1$, the probability distribution is given by the Wishart law [6], a distribution well known for its application to the analysis of level distribution in excited nuclei [7]. A relaxation of these conditions, namely diagonal elements with zero mean but $\beta^2 \neq 1$, was studied [8] in the case of 2 x 2 matrices. We will now derive a more general expression for $p(\rho)$, in the case of 2 x 2 matrices having properties 1 to 7 above. The joint distribution H of the 3 independent matrix elements of a symmetric 2 x 2 matrix is given by

$$H(C_{00}, C_{01}, C_{11}) = G(C_{00})\,G(C_{01})\,G(C_{11}), \tag{6}$$

where G is the Gauss distribution; the highest eigenvalue is given by

$$\rho = \frac{C_{00}+C_{11}}{2} + \sqrt{\left(\frac{C_{00}-C_{11}}{2}\right)^2 + C_{01}^2} \tag{7}$$

If we now select C_{00}, C_{11} and ρ as independent variables the corresponding distribution, P, is given by

$$P(C_{00}, C_{11}, \rho) = 2\, H[C_{00}, C_{11}, C_{01}(\rho)]\, \frac{\partial C_{01}}{\partial \rho}\,, \tag{8}$$

where the factor 2 appears because, given C_{00}, C_{11}, and ρ, two values of C_{01} satisfy eq (7). Integration of eq (8) with respect to C_{00} and C_{11} gives $p(\rho)$, namely

$$p(\rho) = \frac{2 \exp\left\{-\frac{2\rho^2+2|\rho_1|\rho+\rho_1^2}{2\sigma_{00}\sigma_{00}}\right\}}{\beta \sigma_{00}^3 \pi^{3/2}} \int_0^\infty z \exp\left\{-\left[\frac{z^2-2\rho z-|\rho_1|z}{\sigma_{00}^2} + \frac{z^2}{\beta^2\sigma_{00}^2}\right]\right\} I(z)\, dz \tag{9}$$

$$I(z) = \int_{-z}^{z} \frac{\exp\left\{-\left[1-\frac{1}{\beta^2}\right]\frac{u^2}{\sigma_{00}^2} + \frac{|\rho_1| u}{\sigma_{00}^2}\right\}}{\sqrt{z^2-u^2}}\, du \tag{10}$$

where we have assumed that the reference reactor is in the critical state ($\rho_0=0$). However in the case $\rho_1 \neq 0$ and $\beta^2 \neq 1$, no closed expression can be obtained for $p(\rho)$. Expanding the exponential in eq (10) as a power series and integrating term by term, we have

$$I(z) = \sqrt{\pi}\, \exp\left\{-\frac{z^2}{\sigma_{00}^2}\left[1-\frac{1}{\beta^2}\right]\right\} \sum_{m=0}^{\infty} \frac{\Gamma\left(m+\frac{1}{2}\right)}{m!} \left[\frac{2}{|\rho_1|}\left(1-\frac{1}{\beta^2}\right)\right]^m z^m I_m\left(\frac{|\rho_1| z}{\sigma_{00}^2}\right), \tag{11}$$

where I_m are the modified Bessel functions of order n.

Introducing eq (11) into eq (9), an asymptotic expression for $p(\rho)$ can be obtained when $\sigma_{00}^2 \ll |\rho_1|^2$; for values of ρ near the average $\langle \rho \rangle$, this is

$$p(\rho) = \frac{1}{\sqrt{2\pi}\,\sigma_{00}}\, e^{-\rho^2/2\sigma_{00}^2} \left[1 + \frac{\rho}{1.88|\rho_1|}\right], \tag{12}$$

where the value $\beta^2 = 4/3$ has been substituted. However, due to the approximations, $p(\rho)$ vanishes when $\rho = -1.88|\rho_1|$ whereas we should obtain a smooth behaviour for $\rho \to -\infty$. The corresponding moments are

$$(\text{even } n)\ \langle \rho^n \rangle = \sigma_{00}^n (n-1)!! \ ; \ (\text{odd } n)\ \langle \rho^n \rangle = \frac{0.532}{|\rho_1|}\, \sigma_{00}^{n+1}\, n!! \qquad (13)$$

which implies that the mean value and the skewness of the distribution are positive and that the distribution has a kurtosis less than 3.

MONTE CARLO SIMULATION

Due to the availability of diffusion theory simulations of ensembles of reactors, we chose to study the same ensembles as in ref [2]. In this way we compared our matrix simulations with simulations based on the direct solution of the diffusion equation. The properties assumed for the reference reactor and the stochastic parameters that describe each ensemble of reactors are given in Table I.

Table I. Data for the reference reactor and stochastic parameters of different ensembles of reactors

Reference reactor

Slab width (cm)	100
Σ_f (cm^{-1})	0.05
Σ_a (cm^{-1})	0.1
ν	2.01974
D(cm)	1
ρ_0	0.0
ρ_1	-0.02932

Stochastic parameters

Ensemble	λ(cm)	$\langle(\delta\Sigma_a/\Sigma_a)^2\rangle$	$\langle(\delta\Sigma_f/\Sigma_f)^2\rangle$	σ_{00}
1	4.	3.33 E-3	0	0.0140
2	4.	0	3.33 E-3	0.0141
3	4.	8.33 E-4	0	0.00700
4	4.	0	8.33 E-4	0.00707
5	10.	8.33 E-4	0	0.0111
6	10.	0	8.33 E-4	0.0112

As in ref [2] rectangular probability distributions for $\delta\Sigma_a$ and $\delta\Sigma_f$ were assumed for each ensemble without reference to any particular variation of composition. These distributions were symmetric about zero and were scaled to provide relative variations of ±10% (ensembles 1 and 2) and ±5% (ensembles 3, 4, 5 and 6). For each ensemble we ran a sampling of 1,000 reactors, in each case the order of the matrix was varied so as to see the effect of expanding the flux with a limited number of harmonics ψ_i. In all cases an symptotic behaviour was achieved, for matrix order greater than a certain minimum, the two simulations agreed, and for small perturbations (cases 3, 4, 5, and 6) even simulations based on low order matrices gave reasonable results.

Other aspects of the theory were also studied such as the Gaussian distribution of matrix elements and the distribution given by eq (12) for the highest eigenvalues of 2 x 2 matrices having the seven properties listed previously. In particular, we compared mean value, variance, skewness and kurtosis from Monte Carlo simulation with the theoretical results. In all cases the agreement was within the statistical uncertainties attributable to finite sampling. However, we found that while the shape of the distribution of reactivities from simulations with the appropriate matrix order is reproduced reasonably well by eq (12), the mean values tend to be preserved by this equation when the perturbations are small.

CONCLUSION

We have related a space-domain reactor noise problem to the theory of random matrices. Simulations based on random matrices have been shown to give good results in comparison to simulations based on numerical solution of the diffusion equation, thereby allowing us to apply mathematical techniques developed for nuclear physics problems to the calculation of the probability distribution of reactivities. This distribution is not Gaussian and illustrates the non-linear relationship between variations of reactor materials composition and reactivity. The shape of the theoretical distribution obtained compares quite well with a Monte Carlo simulation, but the theoretical averages reproduce the numerical results in cases with small perturbation.

The probability distribution of reactivities was related in an explicit way with a stochastic parameter (σ_{00}) which is determined by the random distribution of materials in a reactor. In this way it is possible to relate the probability to find the system in a given reactivity range with the degree of randomness, this relationship might be important in the safety analysis of nuclear reacting systems with inherent randomness. An important limitation of the results presented in this report is the use of one energy group approximation, further investigations are needed in order to include fluctuations effects in the moderation process in our model.

REFERENCES

[1] M. M. R. Williams, Random Processes in Nuclear Reactors (Pergamon Press, Oxford, 1974) Chapter 8.

[2] H. van Dam, in Progress in Nuclear Energy, Vol 1, Numbers 2-4, Edited by M. M. R. Williams and R. Sher (Pergemon Press, Oxford, 1977), p. 273,

[3] S. Yamada, M. Nishimura, and K. Sumita, Annals of Nuclear Energy, 7, 561(1980).

[4] S. Yamada, C. Yamagoe, and K. Sumita, Annals of Nuclear Energy, 7, 655(1980)

[5] C. E. Porter, Statistical Theories of Spectra: Fluctuations (Academic Press, New York, 1965).

[6] S. S. Wilks, Mathematical Statistics (Princeton University Press, New Jersey, 1943), Chapter XI.

[7] J. E. Lynn, Theory of Neutron Resonance Reactions, (Clarendon Press, 1968) Chapter V.

[8] C. Porter, N. Rosenzweig, Suomolaisen Tiedeakatemian Toimituksia (Ann. Acad. Sci. Fennicae) AVI, No. 44(1960).

BURST NOISE MEASUREMENTS ON OP AMP'S BY R.F. SQUID

Arnaldo D'Amico

Istituto di Elettronica dello Stato Solido del
Consiglio Nazionale delle Ricerche
Via Cineto Romano, 42
00156 Roma

During the past ten years burst noise has been extensively studied in P/N junctions [1-3], transistors [4-7] but not sufficiently in operational amplifiers which are used in many [8] fields of application such as: low noise AC preamplifier; low noise, low drift low offset DC instrumentation amplifier, etc. At both low and intermediate frequencies, they are the most important and utilized electronic devices.

Here we report preliminary burst noise measurements performed on commercially available op amp's by a new technique. The measurement technique considered makes use of a high sensitive low noise radiofrequency superconducting quantum interference device (SQUID) which has allowed both the detection and the measure of the very low magnetic field intensity due to current variations into the devices associated to the burst noise mechanisms.

A superconducting magnetometer coupled to a second derivative gradiometer used as spatial discriminating pick-up coil has been utilized. By using such a gradiometer, the SQUID system becomes practically insensitive to both spatial uniform magnetic field and gradients, and it can be used to detect the weak magnetic field of a nearby source also in the presence of a stronger but uniform field at distant sources.

The same apparatus is almost daily used for biomagnetic measurements in our Institute by the biomagnetic group and it has been extensively described in a recent paper [9].

The main performances associated to the SQUID system and related to the noise measurements are the following: the r.m.s. noise is about 40fT/$\sqrt{Hz}$, i.e. 40 x 10^{-11} gauss/$\sqrt{Hz}$ above its $1/f^{\alpha}$ corner frequency which is located at about .5 Hz (see Fig. 1).

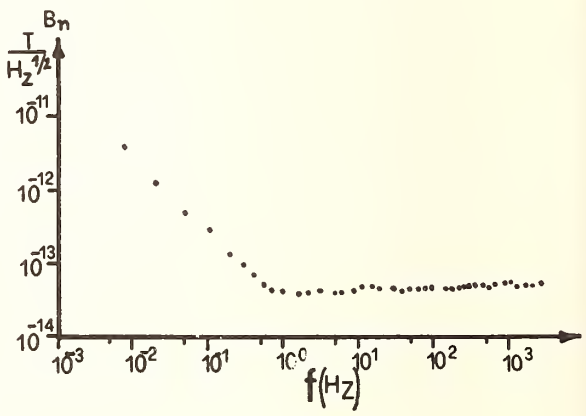

Fig. 1. Noise spectrum of the 2nd derivative gradiometer used for burst noise measurements

The overall gain is 12.5 x 10^5 V/gauss and the bandwidth used is: BW = 700 Hz (with this value the minimum detectable pulse width is about 500 μs). The SQUID system is actually limited, due to a sensible deviation from the linearity only at 8KHz. Measurements have been carried out by putting the head of different kinds of bipolar op amp's as close as possible to the pick-up coil of the SQUID

used.

The first network configuration considered round the op amp is shown in Fig. 2 where we see a noninverting unity gain configuration with a feed back low noise resistor value Rf and a load low noise resistor Rc.

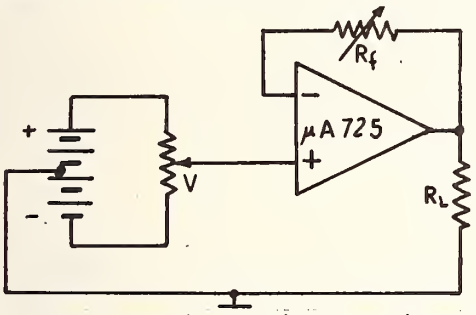

Fig. 2.The non inverting configuration

The second external network used (see Fig. 3) refers to an op amp in the differential configuration with a DC battery used to change the common mode DC input voltage.

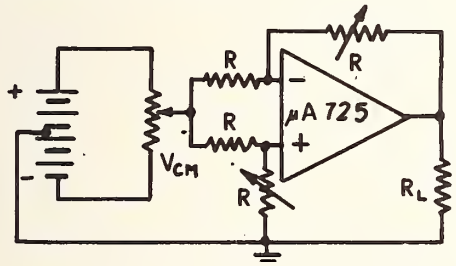

Fig. 3. The differential configuration

The two circuits have been utilized to investigate burst noise amplitude duration and rate of occurence at a nearby constant temperature and in different conditions as far as the common mode input DC voltage values are concerned.

All measurements have been done at 15°C with a tempearture stability of .5°C by using a cooling system based on the Peltier effect. This value of temperature has been selected because it is the highest (for most of our samples) which can permit a sufficient number of bursts to be statistically analyzed in a reasonable time.

In this condition, a typical burst noise amplitude measurement gave us an overall response of about 90 mV which means that the SQUID detected a magnetic field intensity of about 10^{-7} gauss. Taking into account as a crude estimation of the decoupling between the magnetometer and the op amp, a factor 10^2, current variations, due to burst noise in the output load of about 10 μA have been measured.

Photo 1 shows the burst noise in two traces: the upper one represents the output we can observe by using a low noise AC amplifier chain, with a low cut off frequency of 5 Hz, the lower one is the response (inverted) of the superconductive magnetometer chain. The good agreement suggests to continue to improve this method in order to make it more promising, although at present the high cost of the apparatus compared to the conventional one seems to be the only remarkable inconvenience.

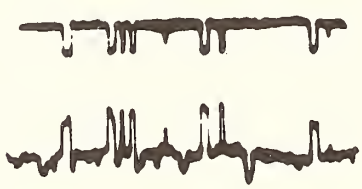

Photo 1 : upper trace is the response of the electronic chain, lower trace is the response of the SQUID

Fig. 4 shows experimental data of the burst noise amplitude behaviour obtained by considering the schematic of Fig. 3 where the common mode DC voltage has been gradually changed.

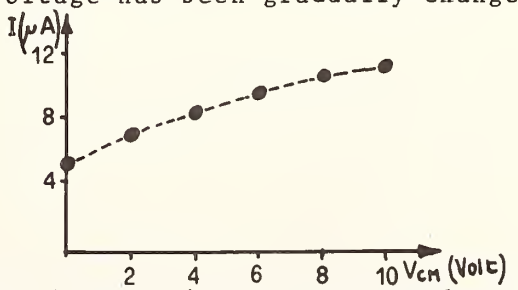

Fig. 4 Burst noise current measured by the SQUID versus the DC common voltage.

Our future developments and studies on this subject will be polarized towards the low temperature dynamic dependence of both burst noise amplitude and occurrence, for different closed loop gain values in order to collect sufficient data to validate the current interpretation on its both physic origin and location [10,11]. Finally we list some features which can be associated to this non touching techniques:

a) the posssibility to measure $1/f^{\alpha}$, g-r and burst noise because of the intrinsic $1/f^{\alpha}$ low noise of the SQUID system,
b) the possibility by a suitable pick up coil with reduced dimension coupled to the magnetometer to have "local" noise information in scanned surface investigation,
c) the possibility to measure either the excess noise or other kind of noise in very high impedence devices where the matching problem between source under investigation and conventional low noise preamplifier could be a problem,
d) the possibility to check the noise behaviour in working active and passive electronic chains.

The author wishes to thank Dr. P. Carelli, Dr. R. Leoni and Dr. G.L. Romani for their assistance and discussions. Particularly, he wishes to thank Dr. G. Spissu for her skilled technical assistance.

REFERENCES

[1] D.S. Tan, "Current pulses during breakdown in silicon p-n junctions", Proc. IEEE (Corresp.) Vol. 53, Feb. 1965, pp. 210-211

[2] J.F. Schenk, "Burst noise and walkout in degraded silicon devices", Proc. 6th. Annu. Reliability of Physics Symp., Nov. 6-8, 1967, pp. 31-35

[3] D. Wolf and E. Holber, "Bistable current fluctuations in reverse biased p-n junctions of germanium J. Appl. Phys. Vol. 38, Jan. 1967 p. 189-192

[4] S.Y. Hsu and R.J. Whitter, "Characterization of burst noise in silicon devices", Solid State Electron., Vol. 12, 1969, pp. 867 878;

[5] G. Ginalt, J.C. Martin and F.X. Maten-Paeriz, "Burst noise of silicon devices", Solid-State Electron., Vol. 12, June 1956, pp. 228-229.

[6] R. C. Jaeger and A. J. Broderson "Low-frequency noise sources in bipolar junction transistors", IEEE Trans. Electron Devices, Vol. ED-17, Feb. 1970 pp. 128-133

[7] S.T. Hsu, R.J. Whittier, and C.A. Mead, "Physical model for burst noise in semiconductor devices", Solid State Electron., Vol. 13, 1970, pp. 1055-1071

[8] Sheng. T. Hsu, "Bistable noise in operational amplifier" IEEE Journal of Solid-State circuit, Vol. SC-6, No. 6, Dec. 1971

[9] S. Barbanera, et al., "Use of superconducting instrumentation for biomagnetic measurements performed in a hospital" presented at A.S.C. Sept. 29, 1980, Santa Fé, New Mexico, USA

[10] K.F. Knott, "Anomalous 1/V and burst noise characteristics associated with surface channel in an NPN integrated transistors" Solid State Electronics, Vol. 23, pp. 727-733, Nov. 1979

[11] K.F. Knott, "Evidence of collector base junction burst noise", Electronics Lett., Vol. 15, No. 6 pp. 184-198, Mar. 15, 1979.

DOMAIN WALLS IN FERROMAGNETIC MATERIAL AND IRREVERSIBLE MAGNETIZATION PROCESSES

Wilhelm Grosse-Nobis

Institut für Angewandte Physik, Universität Münster
D-4400 Münster, Fed. Rep. Germany

INTRODUCTION

The concept of domains and displaceable domain walls had been successful in the early years to explain the macroscopic features of ferromagnetism as the magnetization curve and the Barkhausen noise. The first measurements on moving domain walls were made by Sixtus and Tonks [1] in 1931. Since then walls became by further experimental and theoretical work objects which now are fundamental in understanding the behavior of most of the varied phenomena in applied ferromagnetism and ferrimagnetism.

The wall displacement is the process which makes the easy remagnetization of both soft crystalline and amorphous solids possible. In case of large excursions, walls are mainly displaced irreversibly because of randomly distributed defects of the magnetic solid which act as pinning centers. This may result in sudden macrosopic wall displacements, the Barkhausen jumps. This report deals mainly with the space-time behavior of domain walls in soft ferromagnetic material and is confined to measurements performed by electrical methods. Regarding this subject, the monograph of Stierstadt [2] and the review article of McClure et al. [3] are to be mentioned as well as the articles by Bittel [4] and Montalenti [5]. Wiegman [6] gave a report on Barkhausen noise in thin films.

ORIGIN OF WALLS

Crystalline and amorphous solids exhibit ferromagnetism because of the exchange interaction which aligns electronic moments against thermal agitation and thus defines a direction by the macroscopic saturation polarization vector $\vec{J}_s$. The other main property is the crystal anisotropy which defines easy axes of lowest energy content for the polarization vector being parallel with them. These easy axes are well defined in an ideal crystal lattice, but exist also in a metallic glass. These two features alone may cause the solid to split into several Weiss domains magnetized each in one of the

easy directions and which are separated by the above mentioned interfaces, e. g. the Bloch walls. Their interfacial energy density of order 1 mJ/m^2 in soft magnetic material raises the energy content of the solid, and hence walls are stable under internal or external restrictions. These inhomogeneous states of finite solids are result of the other main sources which raise the total energy of the body: the stray field energy due to divergencies of the magnetic polarization, the magnetostrictive stress energy and the field energy due to an applied external field. The static micromagnetic and Maxwell's equations determine the possible states of the finite solid under given boundary conditions [7] if noise is excluded.

WALL DISPLACEMENT

Bloch walls are in most cases thick (about 100 nm) compared with the lattice constant and could easily be moved in an ideal crystal by changing the external field. But the real structure of magnetic material is given by random fluctuations of compositional and structural defects and internal stresses. These disturbances determine energetically favored positions of the walls with characteristic distances well comparable with the wall thickness and hence are very effective as pinning centers for the walls [8]. For this reason and because of the flexibility of the interfaces, which introduces a large number of internal degrees of freedom, as well as the nonlinearity of the micromagnetic equations a large set of stable solutions of the magnetic state is generated. Some of them may have a limited range of existence as function of, say, the external field. Hence, if the system of domain walls occupies a certain metastable state and the field is changed quasistatically to a certain value, the domain wall system will change discontinuously to a configuration given by another possible solution. These transitions correspond to the observed Barkhausen discontinuities. The configuration which is actually reached depends on the exact dynamics of the domain walls and in some cases of the pinning defects if they are also mobile, e. g. by thermal agitation. Moreover, just before walls are released from pinning centers, the noise in the solid is able to influence very effectively the branching into the different states and thus determines the behavior on a macroscopic scale. Lieneweg [9] found an increased Barkhausen noise spectrum below 10 kHz depending on the rate of field change for a hard-drawn 50% NiFe-wire at temperatures below 77 K which he attibuted to the lack of thermal agitation with the consequence that only large segments of the Bloch walls can move coherently. This means that large groups of Barkhausen jumps occur and determine the Barkhausen noise spectrum [10]. This grouping is of great importance in the theory of losses of magnetic material [11,12].

The thermal activation theory has been reviewed by Gaunt [13] and the book by Lambeck [14]. The influence of thermally activated unpinning of walls

from defects was recently investigated in case of thin films and massive material [15-17]. Some of the papers discuss also the possibility of quantum mechanical tunneling which could be the main process below some Kelvin. In the case of narrow domain walls degenerated to socalled monatomic walls the thermally activated wall displacement determines the available coercive field of Co-RE intermetallic compounds [18] and hence applies to hard magnetic material.

SIGNIFICANCE OF DOMAIN WALLS

The existence of displaceable domain walls is the reason that soft magnetic material is magnetized by low fields. This is due to the fact that the wall displacement process prevents the polarization vector from attaining transitory other than the easy directions in the major parts of the solid and thus from dissipating the large amount of anisotropy energy stored when the polarization passes the direction of extreme anisotropy energy. Existence of walls on the other hand means that the process of remagnetization is very inhomogeneous: the rate of polarization change is high at the interfaces and otherwise very low. This concentration of the externally impressed flux change causes near and inside the walls high dissipation by eddy current and spin relaxation damping because of the considerably high wall velocities. The internal degrees of freedom of the interfaces enhance this effect, e. g. by micro eddy currents and emission of sound waves. Hence, the existence of domain walls as the nonlinear elementary excitations of a ferromagnet with localized energy leads far away from thermodynamic equilibrium, even when we try to magnetize the solid quasistatically. On the other hand, further walls may be produced if a given sample is magnetized at high rates [19,20], and there exists a close relation between the number of walls and the magnetizing frequency [21,22]. At low rates there might be evidence that for a given 180° Bloch wall the average simultaneously moved wall area depends on the mean wall velocity [23].

The dynamics of wall displacement is thus an important contribution in understanding losses associated with the widespread applications of soft magnetic material. The method of Sixtus and Tonks [1] is nowadays still applied experimentally [24,25], and much theoretical work has been done to include the flexibility of the walls [25,26].

RANDOM MAGNETIZATION PROCESSES

The Sixtus-Tonks experiment needs the shape of the moving wall to be known and is a deterministic experiment which can only be performed under certain ideal conditions. These are not met by the usual magnetization of ferromagnets in which process mobile wall segments are generated and annihi-

lated. When slowly magnetized by an external homogeneous field the polarization change proceeds by starting the wall movement at a certain position where a wall is most probably released from pinning centers over a long enough distance so that this segment might serve as a nucleus for Barkhausen discontinuities which sometimes cover a considerable part of the sample. The nucleus grows in consideration of a sufficiently low stray field energy along the direction of the local polarization and at right angles to it. The process is modified by the random local pinning forces and the already mentioned damping mechanisms. Numerous processes of that kind form a space-time random process. We call the resulting rate $\dot{\Phi}(z,t)$ of the magnetic flux through the sample at position z (measured along the sample axis) at time t the stochastic Barkhausen field [27,28]. It is hoped that the experimental analysis of this random one-dimensional field could support the understanding of magnetization noise and power loss [11] and stimulate calculations on irreversible Bloch wall movement.

The first step could be calculations similar to those of refs. [26,29, 30] which apply to the one-dimensional wall curvature in the plane perpendicular to the polarization vector. An important contribution to these questions with full account also of bowing in the other direction was given by Hilzinger et al. [31]. But this consideration has to be worked out to yield the time development of a wall which is passing randomly distributed defects. There have been some efforts to include dynamical effects into the model of Néel [32]. This was done by adding a Rayleigh dissipation term to the generalized forces corresponding to the Fourier coefficients of the wall distortion as the generalized coordinates by Baldwin [33] which work was one of the starting considerations for his nonconservative spring model [34]. Wagner [35] used the more general interaction energy due to the perturbation of the material to derive the spectrum of the magnetic field fluctuations needed to maintain a constant wall velocity in a picture frame single crystal [36]. The equations of motion of this model clearly show at least with the simplifications to be made that it is superior to impress the average wall velocity instead of the magnetic field. One main problem which is yet unsolved is to determine the coefficients of the Rayleigh dissipation function for each of the Fourier components of the wall distortion. Concerning the measurements made with frame-type single crystals and their consequences Porteseil [37] and Vergne et al. [38] have published valuable concepts.

The stochastic Barkhausen field should be easier to be interpreted when only one wall is involved. Hence, we measured the normalized cross power spectrum of a single crystal, cf. figure 1 and [27] for the measuring method and definition. The data apply to a 180° Bloch wall running round the frame and moving with a mean wall velocity of 0.2 mm/s with excursions of ± 0.5 mm around the middle of the legs (width 2 mm). The Barkhausen jumps were observed as flux jumps with the usual spectral density [36] above the cutoff

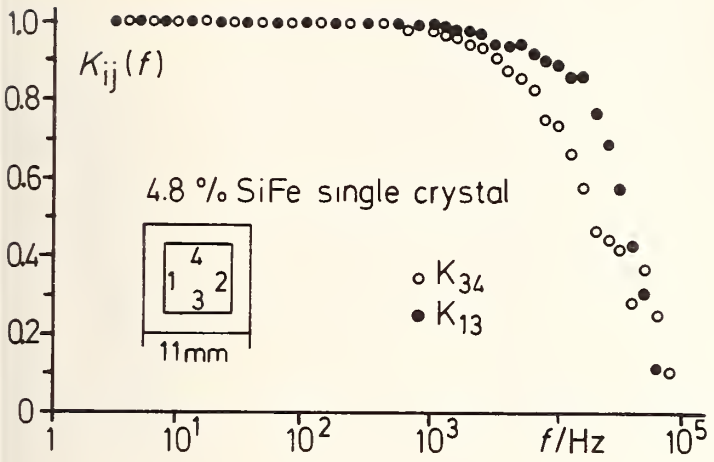

Fig. 1 Normalized cross spectrum of the Barkhausen noise due to one 180° wall around the shown single crystal frame. Thickness 0.285 mm, width of the legs 2.0 mm, specific electric resistance 0.65 μΩm, J_s = 1.92 Tesla.

frequency of the control circuit of 20 Hz. Their correlation is given by K_{ij} for different legs of the crystal as indicated in the figure. (For $K_{34} < 0.5$ this quantity is much effected by the noise of the control circuit which could not be detected with sufficient accuracy.) The wall shows a good correlation ($K_{ij} > 0.7$) in the direction parallel with the polarization (main stiffness by stray field effect) up to 11 kHz along a distance of 18 mm and up to 26 kHz along 9 mm.

Recently measurements of the cross spectra were made by Jansen [39] on long thin samples with the method of ref. [27]. The wavenumber spectrum

$$\Gamma(k,\omega) = \int_{-\infty}^{+\infty}\int_{-\infty}^{+\infty} C(\xi,\tau)\,\exp[j(k\xi - \omega\tau)]\,d\xi\,d\tau \qquad (1)$$

of the covariance

$$C(\xi,\tau) = T^{-1}\int_{t}^{t+T} \langle \dot{\Phi}(z+\xi, t'+\tau)\,\dot{\Phi}(z,t')\rangle dt' \qquad (2)$$

was determined for slowly varying external field of period T. Γ decays with increasing k and ω as is shown in [28]. The cutoff wavenumber k_g for a given angular frequency $\omega = 2\pi f$ defined by $\Gamma(k_g,\omega)/\Gamma(0,\omega) = 1/2$ is shown in figures 2 and 3 for the indicated materials. a_i^{-1} is the cutoff wavenumber for the slow irreversible processes. The range a_i (a_{irr} after [27] equals $(\sqrt{2}-1)^{1/2}a_i$) is by the factor of Λ larger than the reversible range a_r. The figures show the dispersion of the irreversible range beginning at about f = 1 to 10 Hz. Figure 2 indicates also that of the reversible propagation above $\omega = 10^4\ s^{-1}$ which had been compared [27] to linear calculations [40]. a_i = 80 mm, cf. figure 2, is determined by the finite length of the sample. An estimate of the irreversible range for an infinitely long sample is a_i = 214 mm. The full lines of the figures are determined from interpolation functions similar to those given in [27], Jansen [39]. They have not been calculated from first principles.

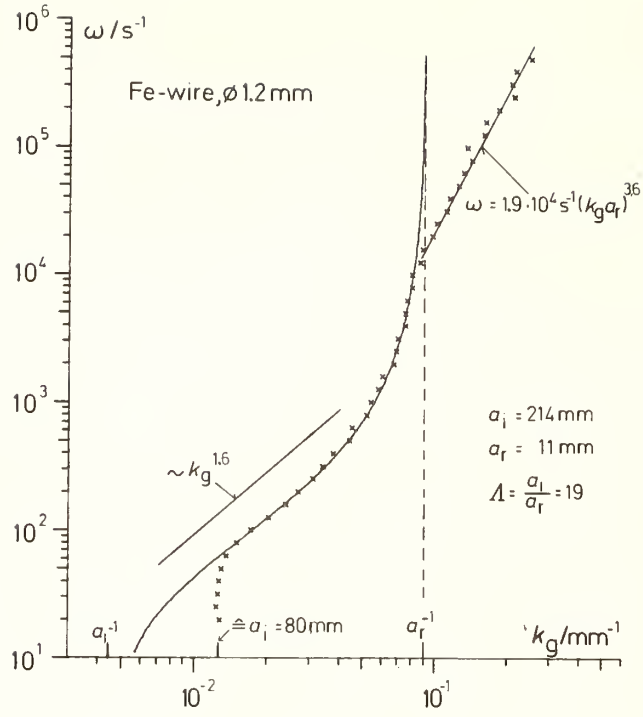

Fig. 2 Dispersion relation of the cut-off wavenumber of a harddrawn iron wire.

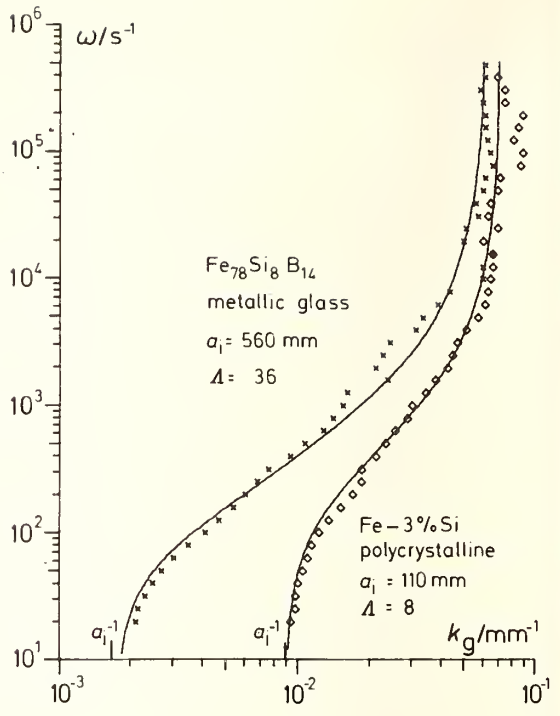

Fig. 3 Same as figure 2 for ribbons. Width/thickness 2.0/0.10 mm (FeSi, Goss texture); 0.95/0.033 mm (metallic glass as quenched).

We are indebted to Fried. Krupp GmbH, Forschungsinstitut, D-4300 Essen for providing the sample material of the metallic glass. The author thanks K. Jansen and N. Hangmann for experimental work.

REFERENCES

[1] K. J. Sixtus and L. Tonks, Phys. Rev. 42, 419 (1932).
[2] K. Stierstadt, Der Magnetische Barkhausen-Effekt, Springer Tracts Modern Physics 40, 1 (1966).
[3] J. C. McClure, Jr. and K. Schröder, CRC Crit.Rev.Sol.St.Sc. 6, 45 (1976).
[4] H. Bittel, IEEE Trans. Magn. MAG-5, 359 (1969).
[5] G. Montalenti, Z. angew. Phys. 28, 295 (1970).
[6] N. J. Wiegman, Appl. Phys. 12, 157 (1977).
[7] W. F. Brown, Jr., Micromagnetics (Wiley, New York, 1963).
[8] H. Träuble, in Moderne Probleme der Metallphysik, vol. 2, Ed. A. Seeger (Springer, Berlin, Heidelberg, New York, 1966) p. 157.
[9] U. Lieneweg, J. Mag. Magn. Mat. 4, 242 (1977).
[10] P. Mazzetti and C. Oldano, J. Appl. Phys. 49, 5351 and 5357 (1978).

[11] P. Mazzetti, in Noise in Physical Systems, Springer Ser. Electrophys., vol. 2, Ed. D. Wolf (Springer, Berlin, Heidelberg, New York, 1978) and IEEE Trans. Magn. MAG-14, 758 (1978).
[12] P. Mazzetti, A. Ferro and G. Montalenti, IEEE Trans. Magn. MAG-13, 1514 (1977).
[13] P. Gaunt, J. Appl. Phys. 48, 3470 (1977).
[14] M. Lambeck, Barkhausen-Effekt und Nachwirkung in Ferromagnetika (de Gruyter, Berlin, 1971).
[15] J. A. Baldwin, Jr. and St. L. Senesac, IEEE Trans. Magn. MAG-15, 999 (1979).
[16] O. Bostanjoglo and H. P. Gemünd, phys. stat. sol. (a) 48, 481 (1978).
[17] D. Siemers and E. Nembach, J. Appl. Phys. 50, 4895 (1979).
[18] M. Fähnle, B. Barbara and H. Kronmüller, phys. stat. sol. (b) 96, 343 (1979).
[19] T. R. Haller and J. J. Kramer, J. Appl. Phys. 41, 1036 (1970).
[20] G. Hellmiss, Wiss. Ber. AEG-Telefunken 43, 77 (1970).
[21] A. Feu, phys. stat. sol. (a) 41, 361 (1977).
[22] Y. Sakaki, IEEE Trans. Magn. MAG-16, 569 (1980).
[23] W. Grosse-Nobis and G. Rauscher, NTG-Fachber. 76, 233 (1980).
[24] R. C. O'Handley, J. Appl. Phys. 46, 4996 (1975).
[25] P. Williams and J. E. L. Bishop, J. Mag. Magn. Mat. 20, 245 (1980).
[26] W. J. Carr, Jr., J. Appl. Phys. 47, 4176 (1976).
[27] W. Grosse-Nobis and K. Jansen, in Noise in Physical Systems, Ed. D. Wolf (Springer, Berlin, Heidelberg, New York, 1978), p. 204.
[28] W. Grosse-Nobis, K. Jansen and J. Tolkmitt-Pudlich, J. Mag. Magn. Mat. 19, 380 (1980).
[29] J. E. L. Bishop, phys. stat. sol. (a) 11, K75 (1972).
[30] E. Schlömann, IEEE Trans. Magn. MAG-10, 11 (1974).
[31] H.-R. Hilzinger and H. Kronmüller, J. Mag. Magn. Mat. 2, 11 (1976).
[32] L. Néel, Ann. Univ. Grenoble 22, 299 (1946).
[33] J. A. Baldwin, Jr., J. Appl. Phys. 39, 5982 (1968).
[34] J. A. Baldwin, Jr. and G. J. Culler, J. Appl. Phys. 40, 2828 (1969).
[35] W. Wagner, Diploma work, Univ. Münster 1977, unpublished.
[36] W. Grosse-Nobis, 4th Int. Conf. Phys. Aspects of Noise in Sol. St. Dev., Noordwijkerhout 1975 and J. Mag. Magn. Mat. 4, 247 (1977).
[37] J. L. Porteseil, Physica 93B, 201 (1978).
[38] R. Vergne, J. L. Porteseil and J. C. Cotillard, J. Mag. Magn. Mat. 15, 1470 (1980).
[39] K. Jansen, unpublished.
[40] H. Eifrig, W. Grosse-Nobis and F. Schulz, J. Mag. Magn. Mat. 19, 383 (1980).

BARKHAUSEN NOISE AND DOMAIN STRUCTURE DYNAMICS IN 3% SiFe SINGLE CRYSTALS

Giorgio Bertotti, Fausto Fiorillo, and Maria Paola Sassi

Istituto Elettrotecnico Nazionale Galileo Ferraris
Gruppo Nazionale Struttura della Materia del C. N. R.
I-10125 Torino, Italy

INTRODUCTION

The magnetization process in ferromagnetic materials is stochastic in nature. The domain walls overcome, under the action of the applied field, the random hindering forces of lattice defects through a sequence of jumps, which can be sensed upon a pick-up coil as induced voltage fluctuations (Barkhausen noise). Barkhausen (B.) noise experiments put in evidence the tendency of the domain wall jumps to cluster into large avalanches, under the action of internal coupling fields. The statistical investigation of such a correlation effect gives information on the dynamics of the domain walls at a microscopic level.

In a recent paper [1] it has been shown that the microscopic behavior of the domain walls is strictly related to the macroscopic magnetic properties of the material (e. g. the shape of the magnetization curve), as well as to the evolution of the domain structure as a whole during the magnetization process. This has been clearly put in evidence by means of a new experimental procedure, whose main features are: a) cyclic magnetization of the sample at a constant rate of induction variation; b) analysis of the statistical properties of the B. noise corresponding to different points of the magnetization curve. Actually, owing to the strong non-stationarity of the noise along the magnetization curve, this is the proper method of investigation, if one aims at a clear picture of the domain wall dynamic behavior along the hysteresis half-loop.

In the present work the above method has been used in the study of a (110) [001] 3% SiFe single crystal, characterized by a system of longitudinal antiparallel magnetic domains. In this case, due to the simple domain structure involved, the search for a connection: B. noise - domain structure evolution - macroscopic magnetic behavior, is of great interest from a fundamental point of view. The investigation has been made in different conditions of applied stress. The modifications of the magnetization curve and of the domain structure as a function of the stress are reflected in a predictable way into changes of the B. noise features. It is found in fact that the behavior of the noise power $\langle P \rangle$ along the hysteresis half-loop is in all cases consistent with a law of the type: $\langle P \rangle = a\mu + b\left|d\mu/dB\right|$, where μ and $d\mu/dB$ are the irreversible permeability and its derivative with respect to the induction respectively, with a and b constants. The predicted contribution of $d\mu/dB$ to the noise power is a most interesting feature of the law, not yet put in evidence so far. The term $\left|d\mu/dB\right|$ is related to the processes of enucleation and annihilation of the longitudinal domains, which take place about the knees of the magnetization curve. Here the permeability derivative exhibits sharp peaks and the same occurs to the noise power intensity. The term $a\mu$ in the law is related to the simple motion of the domain walls and predominates near the coercive field, where a stable domain structure exists. This is the term usually taken into account in the experiments reported in the literature [2, 3].

RESULTS AND DISCUSSION

A (110) [001] 3% SiFe single crystal, 150 mm long, 5 mm wide and 0.29 mm thick was investigated. Through the use of a feedback technique, a cyclic suitably shaped field waveform was applied to the sample, in order to obtain a constant rate of magnetization. The actual rate was $dB/dt = 0.14\ Ts^{-1}$, along the whole investigated induction interval ± 1.75 T. A detailed discussion of the experimental procedure is given in paper [1]. In figure 1 the measured behavior of the noise power <P> is shown, compared with the behavior of the irreversible permeability μ, for different values of the applied tensile stress σ (the magnetization is assumed to proceed from -1.75 T to + 1.75 T). A striking correspondence between the <P> and μ curves can be noticed. In fact, the noise peaks at high induction levels always take place where μ changes steeply, that is at the knees of the magnetization curve. More quantitatively, the noise intensity behavior is found to be always consistent with the law:

$$<P> = a\mu + b\left|d\mu/dB\right| \qquad (1)$$

where $d\mu/dB$ is the derivative of permeability with respect to the induction B. a and b are constant along the magnetization half-loop. This is a quite general law, which has been found to hold also for polycrystalline samples [1]. A typical fitting of the <P> curve through eq (1) is shown in figure 1a (dashed line). What turns out particularly new and

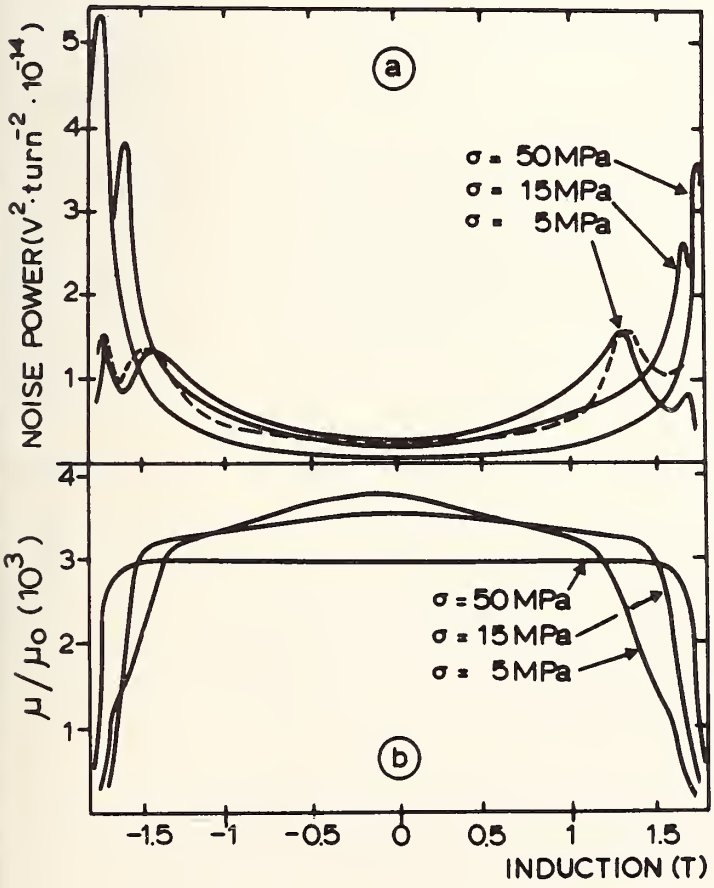

Fig. 1

a) Behavior of the noise power <P> measured at different values of the applied stress σ in a (110) [001] 3% SiFe single crystal during magnetization at a constant rate $dB/dt = 0.14\ Ts^{-1}$ ($B_{max} = \pm 1.75$ T). Fitting of <P> through the law (1) in the case $\sigma = 5$ MPa is shown by the dashed line.

b) Corresponding behavior of the irreversible permeability μ (μ_0 vacuum permeability). It can be noticed the correspondence between the drop of permeability at the knees of the magnetization curve, increasingly steep with increasing stress, and the peaks of the noise intensity.

interesting from eq (1) is the contribution $b|d\mu/dB|$ to the noise power, which accounts for the peaks occurring at the knees of the magnetization curve. Actually, early results obtained in 3% SiFe polycrystalline samples [2, 3], approximately agree with a law of the type : $\langle P \rangle \propto \mu$

Insight in the physical meaning of eq (1) can be obtained through direct domain observation, by using the magneto-optical Kerr effect technique [4]. One can see that the domain structure evolution along the magnetization curve is characterized by two types of phenomena. First, in the central portion of the curve, where the permeability is approximately constant, a well defined system of antiparallel domains is observed, which evolves through simple motion of the walls. Correspondingly, the noise power $\langle P \rangle$ is low and depends weakly on B. On the contrary, strong domain rearrangements take place about the knees of the magnetization curve. They are related to the enucleation and annihilation of the longitudinal domains. In this region the permeability changes very rapidly. $d\mu/dB$ is strongly peaked and the same occurs to $\langle P \rangle$.

Having traced a phenomenological correspondence between noise intensity behavior, shape of the magnetization curve and domain structure, one can try, through the help of the statistical theory of the B. noise [5, 6, 1], to seek an explanation in terms of microscopic dynamic properties of the domain walls. The theory, which takes into account the tendency of domain wall jumps to correlate in large clusters, predicts that $\langle P \rangle = \dot{\Phi} (\hat{\rho}/\hat{\rho}\langle\hat{\tau}_0\rangle) = \dot{\Phi} \cdot \dot{\Phi}_0$, being $\dot{\Phi}$ the flux rate upon the sample cross-section, $\hat{\rho}$ and $\hat{\rho}\langle\hat{\tau}_0\rangle$ the average flux variation and the average duration of a B. cluster respectively and $\dot{\Phi}_0$ the average flux rate associated to a cluster. Since $\dot{\Phi}$ is kept constant in the present measurements, we obtain that the processes associated to domain creation and annihilation are characterized by B. clusters carrying out on the average a much greater flux rate $\dot{\Phi}_0$ than processes occur-

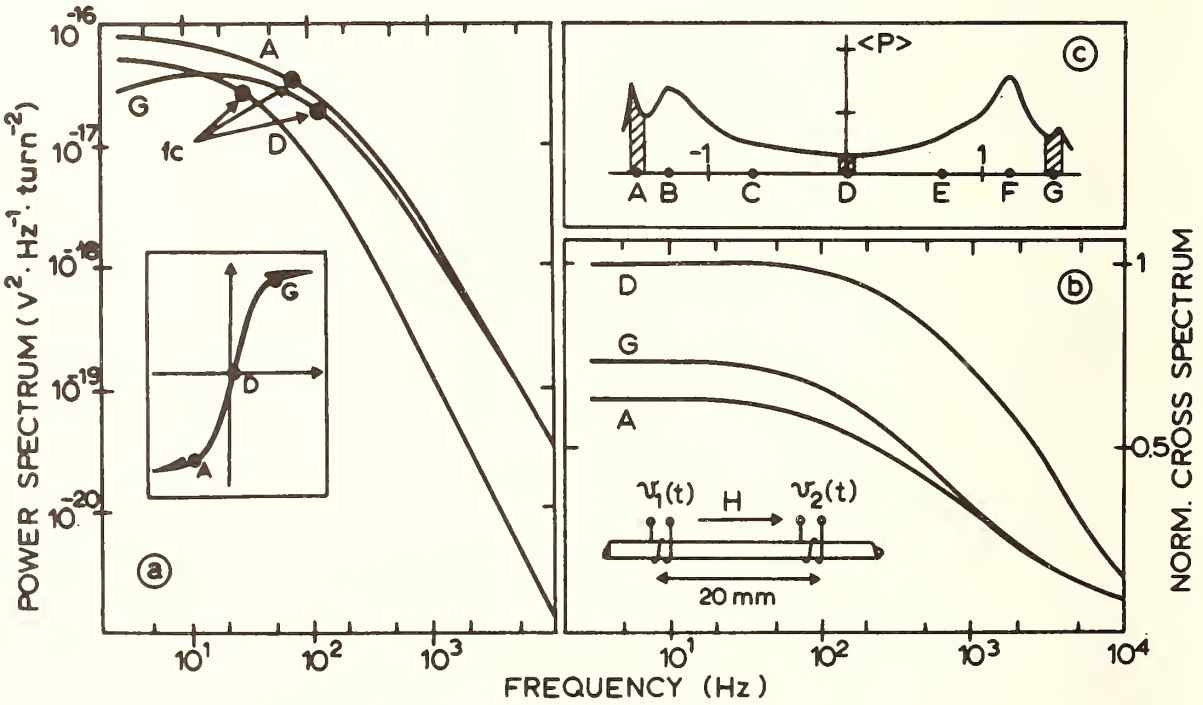

Fig. 2 a) Noise power spectra measured upon three representative points of the magnetization curve in the case σ = 5 MPa; b) Normalized cross spectra measured at the same points, upon windings 20 mm apart.

ring in the region B~0, where simple domain wall motion takes place. This means that much stronger internal coupling fields act on the domain walls in the regions where $d\mu/dB$ is high. Further insight can be obtained by analysing the spectral properties of the noise at different induction levels (points A, B, . . . , G in figure 2). Typically found power spectra S(f) and normalized cross-spectra K(f) [2], related to a couple of narrow windings placed 20 mm apart, are shown in figure 2. Two main results arise from spectra inspection. First, if we consider K(f) in the limit $f \to 0$, which represents the flux fraction propagating on the average during a B. reversal upon the coil distance, we obtain that in the region B~0 correlation on such a sample length is complete. This must be obviously connected to the presence of a well defined longitudinal domain pattern. On the contrary, one can see that a short correlation range is associated to domain enucleation and annihilation processes (K(0)~0. 6). For what concerns S(f), we get immediately that the cut-off frequency f_c, proportional to $1/\hat{\rho}<\hat{\tau}_o>$, is higher at the knees of the magnetization curve. In such regions the time needed for a B. cluster to fully develop is then the shortest.

When the applied stress is increased, the noise non-stationarity at the knees of the magnetization curve becomes nearly catastrophic, according to the approximately rectangular shape assumed by the permeability curve. Such a trend can be qualitatively explained by considering the role played by the flux-closure domains present at the sample edges and surface. Let us consider, for instance, the domain structure in the material when, starting from the nearly saturated state, magnetization begins to reverse. One has to deal with a flux-closing domain structure (spike domains [4]), which can evolve through two basic mechanisms: a) growth of the existing spikes and formation of new ones, b) transformation of the spikes into longitudinal domains. Process b) in particular is expected to require higher effective driving fields, compared to the case of growth through wall motion of a definite domain structure. This is also what is strongly suggested by the noise results, where peaks of <P> (that is of $\dot{\Phi}_o$) are found to be associated with the domain structure rearrangements. It has been in fact previously remarked that the intensity of the noise is directly related to the strength of the internal coupling fields. At low stress levels, mechanisms a) and b) mix up along a substantial induction interval. The ordered longitudinal domain structure forms at a low pace and, as figure 1 shows, the rise of permeability is slow. Correspondingly, the noise intensity maximum is wide. When the tensile stress is increased, the formation and growth of spike domains, which would imply an increasingly high magnetoelastic energy contribution, are progressively inhibited. Thus, the longitudinal domain formation, originating at the few remaining heavily pinned spikes, takes place at the very early stages of the magnetization reversal, associated with a very steep rise of the permeability. The fact that the noise peaks become increasingly sharp, gives an indication on how strongly the local driving field has to rise in order to accomplish the transformation from the spike to the longitudinal domain structure.

REFERENCES

[1] G. Bertotti, F. Fiorillo, and M. P. Sassi, J. Magn. Magn. Mat. 23 (1981), in press.

[2] L. Storm, C. Heiden, and W. Grosse-Nobis, IEEE Trans. Mag. MAG-2, 434 (1966).

[3] H. Bittel, IEEE Trans. Mag. MAG-5, 359 (1969).

[4] J.W. Shilling and G. L. Houze, Jr., IEEE Trans. Mag. MAG-10, 195 (1974).

[5] P. Mazzetti and G. Montalenti, in Proc. International Conference on Magnetism, Nottingham (1964), p. 701.

[6] M. Celasco, F. Fiorillo, and P. Mazzetti, Nuovo Cimento 23B, 376 (1974).

NOISE IN ELECTROCHEMICAL SYSTEMS

U. Bertocci

Center for Materials Science
National Bureau of Standards
Washington, D.C. 20234

INTRODUCTION

The analysis of electrochemical noise, that is, of the fluctuations of the current and potential of an electrochemical cell, can give useful information about the rate and the nature of the chemical processes taking place at the electrodes. This technique has been used to study the equilibrium properties of redox reactions [1] and homogeneous processes in solution [2]; recent work has centered on electrocrystallization [3] and on corrosion [4,5,6], particularly localized corrosion and the properties of passive films.

There are two applications of noise measurements of interest in electrochemistry. The first and more conventional consists of applying a broadband noise signal to an electrochemical cell, and in recording its current output [7]. In this way the electrode impedance as a function of frequency is obtained, which gives important kinetic information. A second and less common way of employing noise measurements consists in detecting and analyzing the fluctuations of the steady state voltage and current of an electrochemical cell.

This paper will survey the experimental techniques used in electrochemical noise studies, discussing some of the problems encountered and ways to overcome them. Finally, some recent experimental results will be presented as an example of application of these techniques to corrosion science.

MEASUREMENT TECHNIQUES

a) Galvanostatic measurements

One approach to noise measurements in electrochemistry is that of recording the spectrum of the voltage fluctuations at the open circuit potential. Some early work was done by observing the total noise power by means of an ac amplifier connected to a loudspeaker or a recorder [8], studying the effect of adding corrosion inhibitors to the solution upon the amplitude of the signals. In recent work, however, the time records are transformed in the frequency domain using either a spectrum analyzer [9] or a correlator [10].

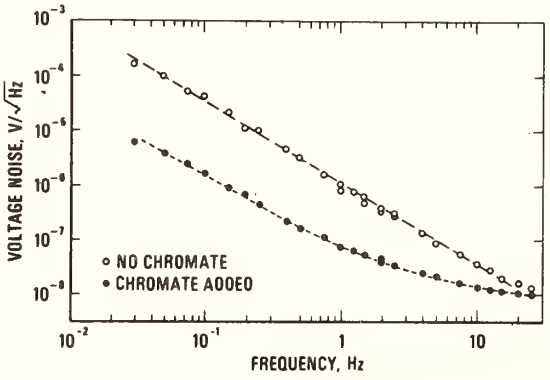

Fig. 1 Noise spectrum at open circuit of Al in borate buffer with and without corrosion inhibitor.

An example of the use of this measurement method is shown in Fig. 1, for aluminum in a chloride solution. A qualitative correlation can be observed between corrosion rate and noise amplitude: the noise decreases when a corrosion inhibitor, sodium chromate, is added to the solution.

b) Potentiostatic measurements

A more refined method consists of controlling the electrode potential by means of a potentiostat and observing the spectrum

of the current fluctuations. In this way, it was found, for aluminum in a neutral solution, that relatively little change in the noise spectrum occurred over a fairly large potential span if chlorides were not present in solution. However, if 0.01 M NaCl was added and the potential was moved from a value at which the protective film is stable, to the pitting potential, at which the oxide film breaks down the noise increased by two or three orders of magnitude [6,11], marking quite clearly the onset of pitting before it could be detected with other methods.

With the potentiostatic method, however, a problem arises because instrumental noise is being injected into the electrochemical cell by the potentiostat, and its level can interfere with the measurements. In order to obviate this problem, a low-noise potentiostat has been developed and built at NBS [12], and care is being taken to minimize the instrumental noise, as well as external interference, electrical or mechanical.

The interpretation of the experimental data, in spite of the low level of noise in the input, may become difficult because, in many instances, it is impossible to know whether the spectrum is mainly the response to the input noise or is an indication of the random fluctuations of the electrode characteristics, and only in clear-cut cases can it be attributed unequivocally to one or the other of its possible causes. On the other hand, since both parts contain useful information, it would be desirable to be able to separate them so that both can be measured at the same time.

c) Measurement of the cross-power spectrum

The use of a two-channel spectrum analyzer allows one to obtain the cross-power spectrum of the two signals, providing the means to establish the origin of the noise observed. When the potentiostat is connected to the cell, the cross-power spectrum of the input noise contained in the control voltage and of the current fluctuations gives an indication of the degree of causality between input and output.

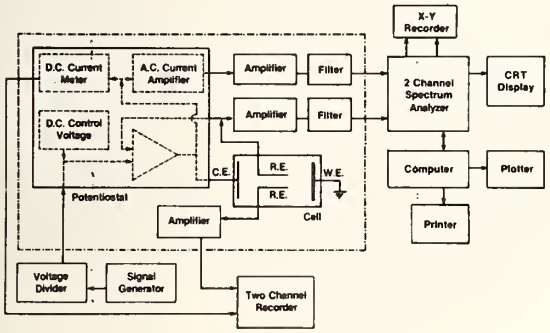

Fig. 2 Block diagram of instrumentation for electrochemical noise measurements.

Instrumental noise still plays a role and limits the overall sensitivity of the system, but if the cross-power spectrum is measured, a scheme for the separation of the deterministic and stochastic part of the current noise can be developed [13]. As far as the deterministic part is concerned, which yields the electrode impedance, the very low level of the input and output (typically less than 1 $\mu V/\sqrt{Hz}$, and less than 1 $nV/\sqrt{Hz}$) is quite desirable, since electrochemical systems are non-linear, and only when the signals are so small the deviations from linearity are negligible.

The layout of the instrumentation for potentiostatic noise measurements in use at NBS is shown in Fig. 2. A two-channel spectrum analyzer is used to measure the noise spectrum of the input (voltage) and of the output (current) as well as the cross-power spectrum. The auxiliary equipment shown in the figure records the d.c. values of the electrode potential and of the cell current. The signal generator can be used if one desires to modulate the control voltage.

The acquisition of the cross-power spectrum can be very useful also in the galvanostatic case: if two reference electrodes are employed in measuring the potential fluctuations of an electrode, the coherence function can be employed to estimate what fraction of the observed signal originates from the only common part of the two measuring circuits, so that one can discriminate between the electrode fluctuations and the noise produced by the reference electrodes and by the amplifying circuitry. This method is being tested in our laboratory for the monitoring of the corrosion of underground electrical cables.

SOME RECENT RESULTS

An important instance of the application of the analysis of noise to corrosion science is the study of the stability of passive films. Some authors have suggested that passive films are in a condition of dynamic equilibrium, so that breakdown and repair occur continuously [14]. If this is the case, such a condition could lead to observable fluctuations of the passive current, whose amplitude and frequency may depend on the degree of uniformity of the film and the time necessary for repairing the breaks, as well as on the potential applied. In our laboratory a study has been made of the passive current noise of a ternary amorphous alloy Fe-Cr-Ni alloy.

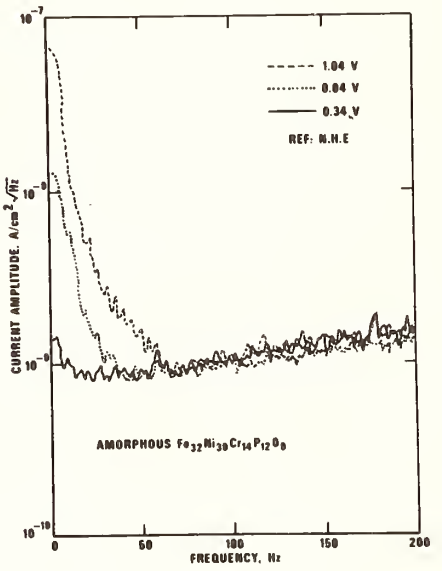

Fig. 3 Spectrum of current noise of amorphous alloy in 1 mol/L H_2SO_4 at various potentials.

The spectra of Fig. 3, taken with a single channel spectrum analyzer, show a gradual increase in noise by increasing anodic polarization, limited, however, to the low frequencies, suggesting a long relaxation time for the repair process. In order to confirm this interpretation, it was important to separate the stochastic part of the signal, generated by the breakdown-repair mechanism, from the effect of the change in electrode impedance caused by anodic polarization.

The results of the separation carried out with a two-channel analyzer are reported in Figs. 4 and 5. The electrode impedance, shown in Fig. 4, can be understood as being constituted by a capacitance, which varies little with potential, in parallel with a reaction resistance which decreases with increasing anodic polarization. The power spectrum of the random noise, shown in Fig. 5, however, indicates that a substantial increase in noise with anodic potential occurs at higher frequencies than could be inferred from the single channel data of Fig. 3, being

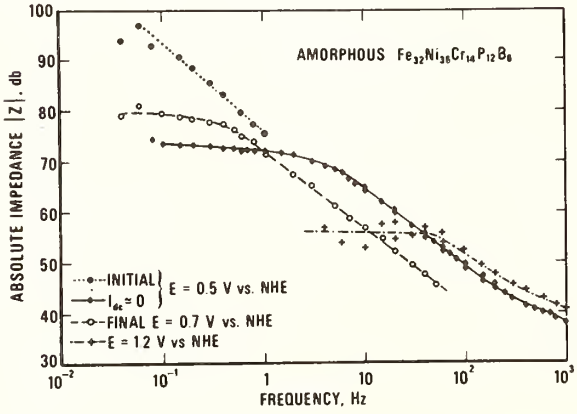

Fig. 4 Absolute value of impedance vs. frequency for amorphous alloy in 1 mol/L H_2SO_4.

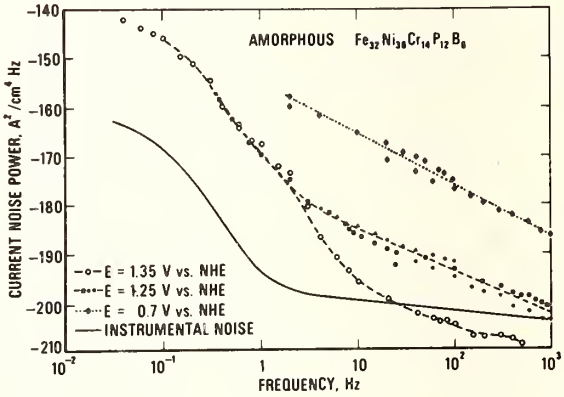

Fig. 5 Power spectrum of random current fluctuations for amorphous alloy in 1 mol/L H_2SO_4.

more prominent above one Hz. The frequency range of the noise is similar to that found in studies of the passive behavior of stainless steel [4].

REFERENCES

[1] V. A. Tyagai, N. B. Lukyanchikova, Electrokhim., 3, 316 (1967).
V. A. Tyagai, ibid., 3, 1331 (1967).
G. C. Barker, J. Electroanal. Chem., 82, 145 (1977).

[2] M. Fleischmann, J. W. Oldfield, J. Electroanal. Chem., 27, 207 (1970).

[3] C. Gabrielli, M. Ksouri, R. Wiart, J. Electroanal. Chem., 86, 223 (1978).
G. Blanc, C. Gabrielli, M. Ksouri, R. Wiart, Electrochim. Acta, 23, 337 (1978).

[4] G. Okamoto, T. Sugita, S. Nishiyama, K. Tachibana, Boshoku Gijutsu, 23, 439, 445 (1974).

[5] G. Blanc, I. Epelboin, C. Gabrielli, M. Keddam, J. Electroanal. Chem., 75, 97 (1977).
G. Blanc, C. Gabrielli, M. Keddam, C. R. Acad. Sci., Paris, 283, Serie C, 107 (1976).

[6] U. Bertocci, Seventh International Congress on Metallic Corrosion, Rio de Janiero 1978, p. 2010, ABRACO (1979).

[7] G. Blanc, I. Epelboin, C. Gabrielli, M. Keddam, Electrochim. Acta, 20, 599 (1975).
S. K. Rangarajan, J. Electroanal. Chem., 62, 43 (1975).

[8] W. P. Iverson, J. Electrochem. Soc., 115, 617 (1968).

[9] U. Bertocci, J. Kruger, Surf. Sci., 101, 608 (1980).

[10] G. Blanc, C. Gabrielli, M. Keddam, Electrochim. Acta, 20, 687 (1975).
G. Blanc, I. Epelboin, C. Gabrielli, M. Keddam, J. Electroanal. Chem., 62, 59 (1975).

[11] U. Bertocci, J. Electrochem. Soc., 127, 1931 (1980).

[12] R. W. Shideler, U. Bertocci, NBS J. Res., 85, 211 (1980).

[13] U. Bertocci, J. Electrochem. Soc., 128, 520 (1981).

[14] K. Videm, Kjeller Report Dr-149. Institutt for Atomenergi, Kjeller, Norway (1974).
J. Kruger, in "Passivity and its Breakdown on Iron and Iron-Base Alloys," p. 94, R. W. Staehle, Ed., NACE, Houston (1976).

Ion Noise in ISFETs

André Haemmerli, Jiří Janata, and James J. Brophy

University of Utah
Salt Lake City, Utah 84112

Ion fluctuations associated with the ion-sensitive membranes of ISFET sensors are observed experimentally by measuring short-circuit channel noise currents. The ISFET is a MOSFET in which the metal gate is replaced by an electrochemical structure consisting of a reference electrode, electrolyte solution, and the ion-sensitive membrane [1]. Changes in the chemical environment of the membrane induce corresponding changes in the electrical potential at the membrane/semiconductor interface which are observed as changes in the channel current. The favorable geometry of an ISFET permits detection of ion fluctuations which are not possible with conventional ion-sensitive electrodes [2].

These ISFET sensors studied are fabricated by integrated circuit techniques and consist of two ISFET devices and two conventional MOSFETs on the same p-type silicon chip. This configuration is designed to facilitate balanced circuitry and to provide an electrical reference capability. All four devices have the same geometry with channels 20 μm long by 400 μm wide. The gate area of the ISFET devices is covered by a silicon nitride layer (a so-called pH ISFET) or by calcium or sodium ion-selective polymeric membranes. The transconductance of the MOSFET units is 1.2×10^{-3}mho at standard operating potentials, V_{gs}=2V, V_{ds}=3V. A silver/silver chloride reference electrode was used for all ISFET measurements.

Channel current noise in all devices is determined by measuring voltage fluctuations across a 10^4ohm resistor in series with the source using a conventional amplifier in conjunction with a General Radio Model 1900A wave analyzer. In the absence of current, the system accurately measures the Nyquist noise spectrum of the series resistor over a frequency interval from 100Hz to 50kHz. The MOSFET noise spectra are consistent from unit to unit and agree with results reported in the literature [3]. For all measurements, the channel current was set at 0.1 mA by adjusting the gate bias or the reference electrode potential.

The current noise spectra of pH ISFETs, shown in Fig. 1, have noise levels greater than MOSFETs which are independent of pH over the range examined, pH4 to pH10. The spectral noise power varies as $f^{-3/2}$, and there is a suggestion of a low frequency plateau below 150Hz. Conversely, Ca^{2+} ISFETs do exhibit a pH effect and have a markedly weaker frequency dependence. There is, however, little variation of noise magnitude with concentration, even though the noise is two orders of magnitude greater than that of the MOSFETs. The sodium devices appear to show 1/f noise over the upper frequency range.

A simple model for noise in a pH ISFET arising from adsorption/desorption of ions on the gate insulator characterized by a single time constant τ gives for the spectral density [4]

$$S_I = \frac{4I^2}{N_o} \frac{\tau}{1+\omega^2\tau^2}$$

where I is the channel current and N_o is the average number of adsorbed ions. According to Fig. 1, the low frequency value of S_I, 4×10^{-20} A^2/Hz, and τ, 8×10^{-4}s, suggests a value for N_o of about 10^9 ions, independent of pH. Furthermore, if N_o/τ is treated as a generation rate, the equivalent exchange current density calculated from the observed noise and the ISFET geometry is 1mA/cm2, in agreement with accepted values. The comparable value for the Wasserman membrane is about $10^{-6}A/cm^2$, which has not previously been measured.

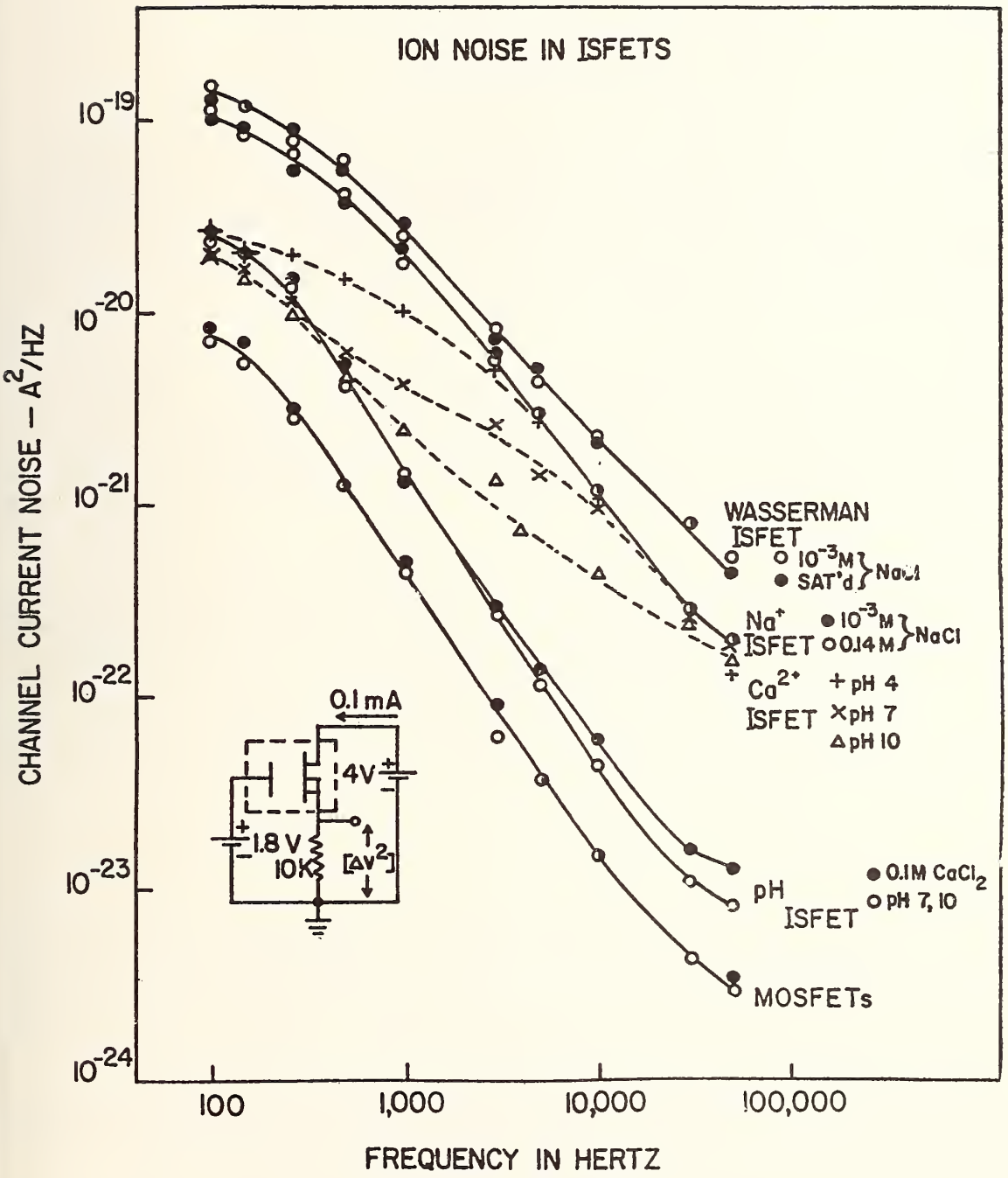

Figure 1. Channel current noise spectra of pH ISFETs and ISFETs with Na^+ and Ca^{2+} membranes compared to MOSFET with some geometry.

The absence of an ion concentration effect can be accounted for by the adjustment of the reference electrode potential for constant channel current, although this is not anticipated on the basis of the reactions at the electrolyte/membrane interface. In any event, these preliminary results illustrate a variety of noise effects in ion-selective sensors, further experiments to characterize the noise mechanisms are currently underway.

REFERENCES

[1] J. Janata and R. J. Huber, Ion-Sel-Electrode Rev., 1, 31 (1979).

[2] L. J. DeFelice and D. R. Firth, IEEE Trans. Bio-Med. Engr., BME-18, 339 (1971).

[3] A. van der Ziel and E. R. Chenett, Adv. Elect. and Electron Phys., 46, 313 (1978).

[4] A. van der Ziel, "Fluctuation Phenomena in Semiconductors", Academic Press, Inc., New York, (1959) p. 24.

QUASIELASTIC LIGHT SCATTERING FROM MACROMOLECULES AND MICELLES

Mario Corti

CISE S.p.A.
P.O.B.12081, 20100 Milano, Italy

The advent of lasers has greatly stimulated the study of matter by the scattering of light. Laser light, powerful, highly monocromatic and amplitude stabilized, is the ideal radiation source to probe properties of liquids and solutions of macromolecules by Rayleigh scattering. Spectral measurements are often simplified by modern techniques of intensity fluctuations and heterodyne analysis, which are easier to use and allow higher resolution than conventional interferometric methods. A number of excellent reviews and some books [1-8] now exist dealing with many applications in physics, physical chemistry, biology, biochemistry, and engineering.

The physical origin of the scattered light is the spatial inhomogeneity of the optical polarizability (i.e. the dielectric constant or the refractive index) of the medium. In a pure fluid in thermodynamic equilibrium at a temperature T, local fluctuations in polarizability are caused by fluctuations in the thermodynamic parameters describing the state of the system. In a macromolecular solution there is an extra contribution to the fluctuations in polarizability, due to the fluctuations in concentration of the macromolecules inside the scattering volume.

The energy transfer in the Rayleigh scattering process is quite small; hence its denomination is quasi elastic light scattering. In practical situations the Rayleigh linewidth is indeed never larger than $10^{-9}\ \nu_o$ where ν_o is the optical frequency of the incident field. The scattered field E_s is linearly related to the incident light field E_o through a scattering amplitude which is a random function of space and time. Therefore E_s is a random process. By measuring the statistical properties of E_s and knowing E_o, it is possible to characterize the statistical properties of the scattering medium.

It is well known that a complete description of the process is given by an infinite set of field correlation functions, which for a given point in space can be written as

$$G_m(t_1, \ldots, t_{2m}) = \langle E_s(t_1) \ldots E_s(t_m)\, E_s^*(t_{m+1}) \ldots E_s^*(t_{2m}) \rangle$$

where m runs from 1 to infinity. An infinite number of increasingly complex measurements is therefore needed. Fortunately great simplification occurs in the large majority of practical situations where the scattered electric field follows Gaussian statistics. In this case the field statistics is described in terms of a single quantity, the first order (m=1) correlation function $G_1(t_1,t_2) = \langle E_s(t_1)E_s^*(t_2)\rangle$ which for $t_1=t_2$ reduces to the average scattered intensity.

Gaussian statistics is found whenever the scattering volume contains a large number of independent scatterers. The field correlation function is then related to the intensity correlation function $G_2(t_1,t_2) = \langle I_s(t_1)I_s(t_2)\rangle$ by the relation $G_2(t_1,t_2) = \langle I_s\rangle^2 + |G_1(t_1,t_2)|^2$.

This relation has a great practical importance. It is in fact much easier to measure the correlation function of the intensity output from a photodetector, than a field correlation function by optical techniques. For a given scattering field the task is to measure the scattered intensity as a function of time to form the intensity correlation function. Then from the above relation it is simple to evaluate the first order field correlation function which is just the Fourier Transform of the optical spectrum.

Non Gaussian statistics may be found in experiments where the scattering particles are large, like bacteria or long viruses, and there are few of them in the scattering volume. Number fluctuation effects will arise besides the usual Gaussian fluctuations (see the articles by P.Pusey in Refs.7 and 8).

Laser light scattering has been successfully applied to a large variety of problems including the study of pure fluids, liquid mixtures, viscous liquids, liquid crystals, macromolecules in solution and motility of microorganisms.

For each problem the average scattered intensity gives a measure of the static properties of the system, while the time behaviour of the correlation function reflects the dynamics of the spatial inhomogeneities which are responsible of the scattering process. For example, in a pure fluid in thermodynamical equilibrium density fluctuations, due to entropy fluctuations, decay with a characteristic time determined by the thermal diffusivity of the fluid, while the intensity of the scattered light is proportional to the isothermal compressibility of the fluid. For a macromolecular solution the intensity of the scattered light gives the molecular weight. The temporal fluctuations in the scattered light intensity contain detailed information about the Brownian movement of the macromolecules. Hence the mutual translational diffusion coefficient can be measured.

Let us summarize the information obtainable by a laser light scattering experiment from a solution of macromolecules, whose linear dimension is smaller than the wavelength of light [7,8].

From the average intensity $\langle I_s \rangle$ we obtain:

Molecular weight of small non interacting particles,

$$\langle I_s \rangle \propto c\, M\, P(q)$$

where c is the solute concentration and M the molecular weight in Daltons. The function $P(q) = 1$ in the limit $qL \ll 1$, where $q = (4\pi/\lambda)\ \mathrm{sen}\ (\theta/2)$ is the modulus of the scattering vector, L the linear dimension of the particle, λ the wavelength of light and θ the observation angle.

Gyration radius of particles by intensity measurements at different angles. The small q expansion of P(q) depends on the gyration radius R_G

$$P(q) = 1 - \frac{q^2 R_G^2}{3} + \cdots$$

Interparticle interactions, by the nonlinear dependence of the average intensity versus concentration

$$\langle I_s \rangle \propto c \left[1/M + 2 B c + 3 C c^2 + \ldots \right]^{-1}$$

where B,C,.... are the coefficients of the virial expansion of the excess chemical potential of the solution with solute concentration c. The coefficients B,C,... are zero for non interacting particles.

From the intensity correlation function $G_2(\tau)$, with $\tau = t_2 - t_1$, we obtain:

Translational diffusion coefficient of particles.

$$G_2(\tau) = \langle I_s \rangle^2 \left(1 + [f(\tau)]^2 \right)$$

with $f(\tau) = \exp\left[- q^2 D \tau \right]$ for a monodisperse solution of small particles. The diffusion coefficient D is then related to the particle hydrodynamic radius R_H by

$$D = \frac{k_B T}{6\pi\eta R_H}$$

with k_B the Boltzmann constant, T the absolute temperature and η the solvent viscosity. This formula is valid for non interacting particles.

Polydispersity of the solute particles.

A polynomial fit of the logarithm of $f(\tau)$ determines the deviation from the single exponential benhaviour of $f(\tau)$ and hence gives information on the particle size distribution function.

Interparticle interactions from the diffusion coefficient dependence on solute concentration [11].

Combination of intensity and correlation function data gives also information on the shape, hydration and the interaction potential (eventually the macromolecular charge).

As an interesting example of application of light scattering techniques, we shall discuss the aggregation phenomena of amphiphilic molecules in solution which leads to formation of aggregates, named micelles [9] . Aggregation of amphiphilic molecules is an important subject of research since it is one of the basic aspects of living matter. Amphiphilic molecules, like detergents, are made of an hydrophobic portion, normally an hydrocarbon chain, and an hydrophilic group either polar or ionic. Above a certain critical concentration, globular aggregates are formed in water with an hydrocarbon core and a polar or ionic surface which shields the core from the surrounding water. An optimum size is reached by a self aggregation process, since the hydrophobic attraction is contrasted by the electrostatic repulsion among the polar or ionic groups on the micelle surface. Typical aggregation numbers are of the order of one hundred and the micelle radius of 20-30 Å. Rather interesting physical problems can be studied in micellar water solutions. Let us consider a representative phase diagram

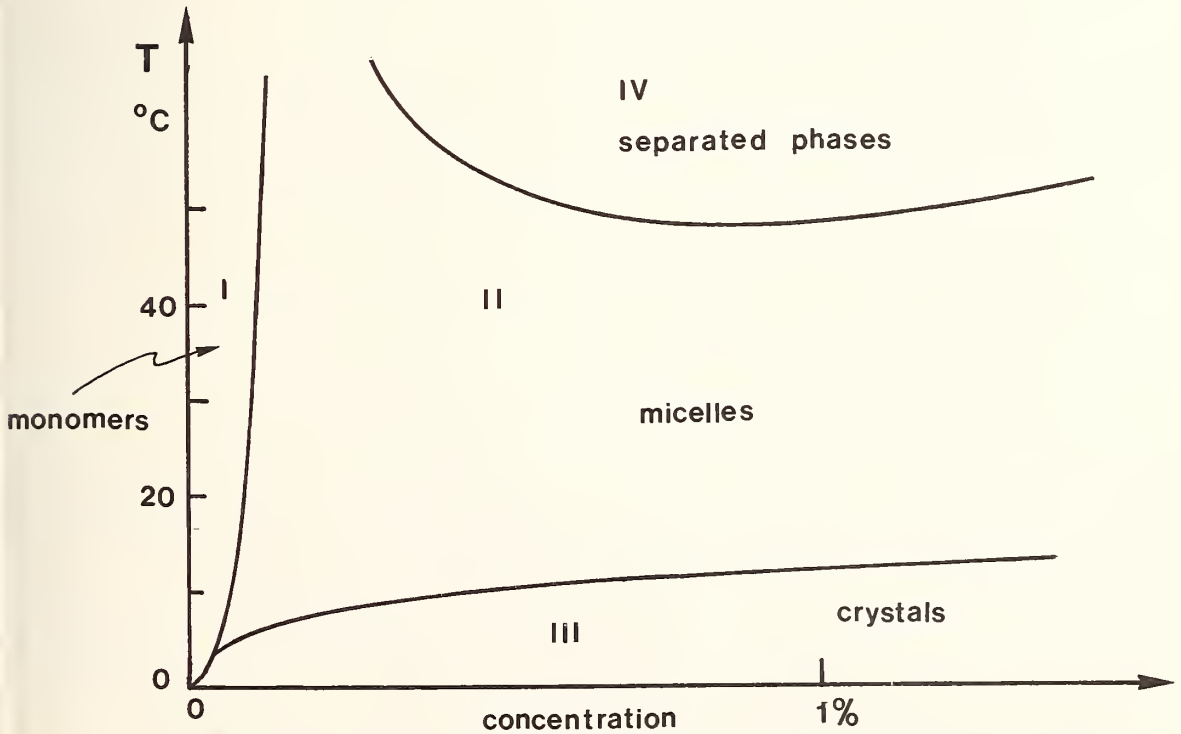

Phase I. The concentration is so low that detergent amphiphilic molecules are in solution as monomers.

Phase II. In a narrow concentration region, called critical micelle concentration, at the boundary I-II molecules aggregates to form micelles. Light scattering gives here information about aggregation number, molecular weight, diffusion coefficient (hence hydrodynamic radius) and shape of micelles at their formation [10] . Then inside phase II it is quite interesting to study micelle-micelle interactions [11] . The interaction potential can be charged by acting on the ionic strength of the solution with some added salt (micelles may be changed) and by varying the type of detergent. So micelles may offer a simple and flexible model to study interaction effects in solution like those found for proteins.

Phase III. Detergent precipitates to form very hydrated crystals. At the boundary II-III a first order melting transition can be observed.

Phase IV. A peculiar transition, mostly for non-ionic detergents, occurs at the boundary III-IV. The homogeneous micelle phase breaks into separate phases. There is a lower critical consolution point, called cloud point, and the transition is of the second order type like in binary mixtures. Approaching the transition from the homogeneous phase one finds critical exponents predicted by the mean field theory [12].

At large concentrations, not shown in the figure, other interesting transitions may be found, like transitions to gels or to liquid crystal type phases.

REFERENCES

|1| G.B.Benedek, in *Polarization, Matière et Rayonnement,* (Presses Universitaires de France, 1969) p.49.

|2| H.Z.Cummins, and H.L.Swinney, in *Progress in Optics,* Ed.E.Wolf,1970, Vol.8,p.133.

|3| P.A.Fleury, and J.P.Boon, in *Advances in Chemical Physics,*Ed.I.Prigogine and S.A.Rice (Wiley Interscience,New York,1973) Vol.24, p.1.

|4| *Photon Correlation and Light Beating Spectroscopy,* Ed.H.Z.Cummins and R.E.Pike (Plenum Press,New York,1974).

|5| B.Chu, in *Laser Light Scattering,* (Academic Press, New York,1974).

|6| B.J.Berne,and R.Pecora,in *Dynamic Light Scattering,* (John Wiley,New York,1976).

|7| *Photon Correlation Spectroscopy and Velocimetry,* Ed.H.Z.Cummins and R.E.Pike (Plenum Press,New York,1977).

|8| *Light Scattering in Liquids and Macromolecular Solutions,* Ed.V.Degiorgio,M.Corti and M.Giglio (Plenum Press,New York,1980).

|9| C.Tanford, in *The Hydrophobic Effect,* (John Wiley,New York,1980).

|10| M.Corti,and V.Degiorgio, *Chem.Phys.Lett.*53, 232 (1978).

|11| M.Corti,and V.Degiorgio, *J.Phys.Chem.* 85, 711 (1981).

|12| M.Corti,and V.Degiorgio, *Phys.Rev.Lett.* 45, 1045 (1980).

FRANK ELASTIC CONSTANT RATIOS EVALUATION IN MBBA BY INTENSITY MEASUREMENT OF THE SCATTERED LIGHT

E.Miraldi, L.Trossi and P.Taverna Valabrega

Istituto di Fisica Sperimentale
Politecnico - Torino

C.Oldano

Istituto di Fisica Sperimentale
Politecnico - Torino
Gruppo Nazionale Struttura della Materia
del C.N.R., U.R. 24

The predominant contribution to the light scattering in nematics comes from the thermally excited orientation fluctuations of the director $\vec{n}$. To each $\vec{q}$-component of the fluctuation there are two uncoupled modes, whose mean amplitudes, in the presence of a magnetic field $\vec{H} \,//\, \vec{n}$, are respectively given by [1] :

$$\langle (\delta n_\gamma)^2 \rangle = \frac{\Omega k_B T}{(K_{\gamma\gamma} \sin^2\theta + K_{33} \cos^2\theta) q^2 + \chi_a H^2} \qquad [\gamma = 1, 2] \tag{1}$$

where:
δn_1, δn_2 are the components of $\delta \vec{n}$ respectively parallel and normal to the $(\vec{n}, \vec{q})$ plane, $\langle\ \rangle$ means thermal average, Ω is the sample volume, k_B the Boltzmann constant, T the absolute temperature, θ the $(\vec{q}, \vec{n})$ angle, $\chi_a = \chi_{//} - \chi_\perp$ the diamagnetic anisotropy and K_{11}, K_{22}, K_{33} are the Frank elastic constants corresponding to splay, twist and bend deformation respectively. Both modes are purely relaxational, with a relaxation time [2], [3]:

$$\tau_\gamma = \frac{\nu_\gamma(\theta)}{(K_{\gamma\gamma} \sin^2\theta + K_{33} \cos^2\theta) q^2 + \chi_a H^2} \tag{2}$$

where $\nu_\gamma(\theta)$ is a viscosity coefficient.

The intensity of the light scattered by each mode is proportional to $\langle (\delta n_\gamma)^2 \rangle$ through a known coefficient $C_{\alpha\beta\gamma}$ which depends on the optical geometry and on the polarization states α and β of the incident and scattered beams; the spectral line-width is proportional to $1/\tau_\gamma$ [2] . By light scattering experiments one can measure in principle all the constants which determine the hydrodinamic behaviour of the nematic, i.e. K_{jj}, χ_a and the five independent viscosity parameters. More precisely the intensity of the scattered light can give the constants K_{jj} and χ_a, its line-width can give the ratio between any pair of constants.

Actually, while on line-width measurements several papers are found in literature, in-

tensity measurements aiming to the determination of K_{ii}/K_{jj} ratios are reported only in two recent papers [4, 5] . Indeed these experiments are rather difficult for the following reasons:

a) The intensity measurements are always affected by many errors, due to multiple scattering and to the scattering from crystal defects. Particularly important is the scattering due to the distorsion of the director field near the crystal surfaces.

b) In general a small error in the intensity measurements gives a very large error in the K_{ii}/K_{jj} ratios evaluation. For instance in paper [4] a standard deviation of 0.2% of the experimental points from the best fitting curve gives an error of about 5% in the K_{ii}/K_{jj} ratios.

For what concerns point a), an optimal sample thickness must be chosen. Besides the use of homeotropically aligned samples has some advantages with respect to the planar ones. The most important improvement, however, concerns point b), with the choice of suitable geometric conditions. One must select the incidence and scattering angles θ_i , θ_f which allow the best separation of the scattering effect of pure splay, twist and bend fluctuations. This cannot be obtained with the normally used scattering geometries, i.e. with the incident beam parallel or perpendicular to the director. Oblique incidence gives the further advantage of reducing the background due to diffuse multiple scattering, as discussed in a previous paper [5].

In the present note we report some results concerning the K_{ii}/K_{jj} ratios evaluation, carried out in the following conditions.

The sample is a mono-domain cell of nematic MBBA, homeotropically aligned between glass plates. Its thickness is 50 μm, such that the double scattering never exceedes 2% of the single scattering, and that the higher order effects are negligible. In order to reduce the forward scattering the sample is kept in a magnetic field of 3000 gauss. The shape of the magnet is such as to allow a large variation of both the incidence and scattering angles. The light source is a 3 mW He-Ne laser. The irradiated area is about 2 mm in diameter. A fraction of the incident beam is sent to a photodiode, and the scattered light to a single-photon photomultiplier, whose effective area is seen from the sample under an angle of 2 mrad. The ratio between the measured intensities is done by using an electronic analogic divider.

The intensities have been corrected taking into account:

- the attenuation of the incident and scattered beams inside the nematic;
- the double scattering contribution;
- the transmission factors at nematic-glass and glass-air surfaces;
- the solid angle change of the scattered beam when it goes from inside the crystal out. The correction factors are given in ref. [5] .

All measurements are carried out with the director lying in the scattering plane, because in this condition the light scattered by the two independent distortion modes can be separated by simply selecting the polarization states of the incident and scattered beams. When both beams are polarized in the scattering plane [E - E geometry], one selects the splay + bend mode; with crossed polarizers [E - O or O - E geometry] one selects the twist + bend mode.

In fig. 1 are reported the intensities measured at 22 °C for an incident external angle $\theta_i^{(e)} = 45°$ and for different scattering angles and polarization states. The experimental points are divided in three separated sets which correspond respectively to:

a) nearly pure splay ($\sim$90% splay and $\sim$10% bend), E - E geometry;

b) nearly pure twist (90 ÷ 100 % twist and 0 ÷ 10% bend), E - O geometry;

c) predominantly bend mode (55 ÷ 75% bend and 25 ÷ 45% twist), E - O geometry.

The full lines are the best fitting curves for E - E and E - O geometries, and have been obtained with refractive indices $n_o = 1.544$ and $n_e = 1.758$ [6], and with $K_{11}: K_{22}: K_{33} = 5/ 4/ 7.5$.

The standard deviation of the experimental points from the best fitting curves is ~3%, corresponding to a standard deviation of ~5% for the K_{11}/K_{22} ratio and of ~6% for the K_{22}/K_{33} ratio.

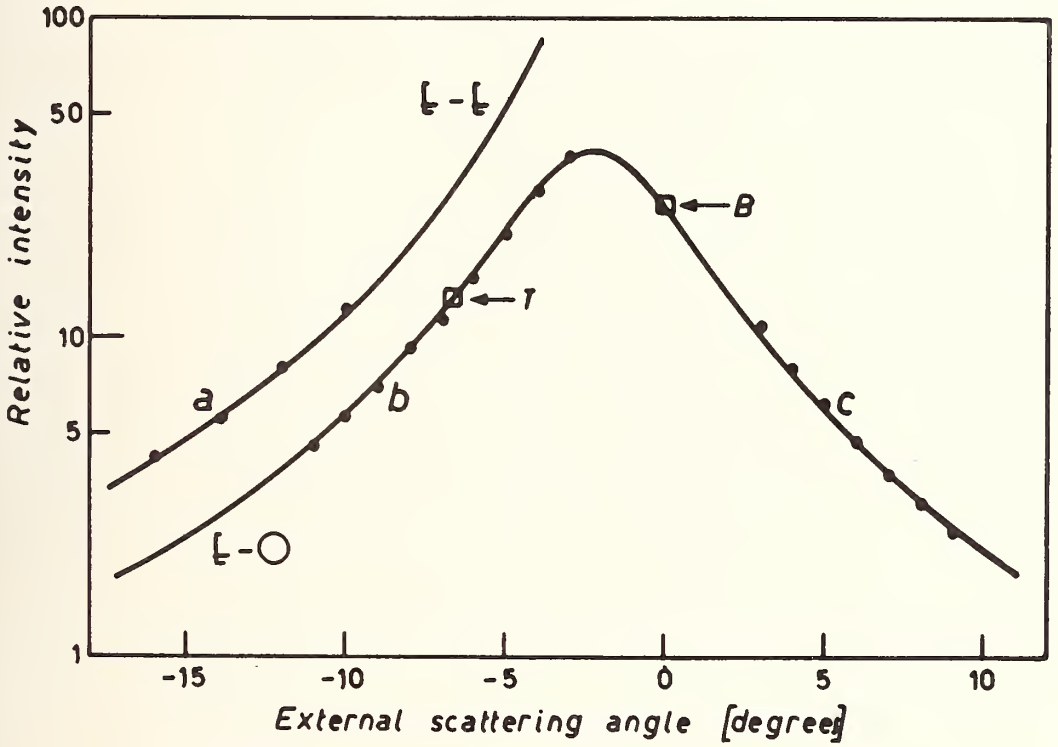

Fig. 1 Experimental points of the relative intensity of scattered light versus external scattering angle for an external incidence angle of 45°, and theoretical best fitting curves for E - E (a), E - O (b and c) geometries. Points labelled T and B correspond to pure Twist and pure Bend respectively.

We are indebted to Prof. P.Mazzetti for many stimulating and helpful discussions.

REFERENCES

[1] P.G. de Gennes, The Physics of liquid crystals, Claredon Press, Oxford.

[2] Group d'Etude des Cristaux Liquides (Orsay), J.Chem. Phys. 51 816 (1969).

[3] D.Forster, T.C. Lubensky, P.C. Martin, J.Swift and P.S. Pershan, Phys. Rev. Lett. 26, 1016 (1971).

[4] H.Usui, H.Takezoe, A.Fukuda and E. Kuze, Jpn. J. Appl. Phys. 18 1599 (1979).

[5] E.Miraldi, C.Oldano, L.Trossi and P.Taverna Valabrega, Nuovo Cimento 60B, 165 (1980).

[6] E.B.Priestley et al., Introduction to Liquid Crystal, Plenum Press, New York, London, 1975.

THE DETERMINATION OF ELASTIC CONSTANTS OF NEMATIC LIQUID CRYSTALS FROM NOISE MEASUREMENTS OF SCATTERED LASER LIGHT

Jitze P. van der Meulen, Rijke J.J. Zijlstra and Jaap J. van Kooten

Fysisch Laboratorium, Rijksuniversiteit, Princetonplein 5,
3584 CC Utrecht, The Netherlands

ABSTRACT

A new optical technique is introduced for determining the elastic constants of nematic liquid crystals by measuring the spectral noise intensity of scattered laser light.

I. INTRODUCTION

In a nematic liquid crystal three types of distortion can be distinguished, each of which is characterized by a specific elastic constant [1]. These static quantities can be determined via light scattering experiments by measuring the angular dependence of the total cross section [2]. However, experimental problems will arise because of refraction phenomena at the walls of the sample. These problems are caused mainly by poorly defined angular dependent reflection, interference phenomena and a change in the subtended solid angle [3]. In addition the measurements may be impaired by the occurrence of stray light.

In a liquid crystal the elongated molecules fluctuate around a mean direction called the director. It is because of these orientation fluctuations that light is strongly scattered. Relaxation effects that are coupled with the three types of distortion give rise to Lorentzian line broadening of the scattered light, from which a relaxation time can be determined. This relaxation time provides us with direct information about the dynamics of the nematics, namely the distortion viscosity constants [4].

The experimental problems that one normally associates with total cross section measurements are of little consequence in measurements of the spectral linewidth of the scattered light. Because of the three types of distortion one generally measures a spectrum of a sum of Lorentzian broadened lines each with an intensity that is weighted by functions depending on optical parameters and on the elastic constants. The linewidth as determined from noise data has been published earlier [5, 6].

As this paper will show we can obtain the three bandwidths separately and the ratio of the elastic constants by making a computer analysis of noise data obtained as a function of the scattering angle.

We shall demonstrate this for the case of an optical configuration in which only the splay and twist deformation phenomena are observed.

II. THEORY

The expression for the noise intensity spectrum of scattered laser light is given by [5, 6]:

$$S_{\Delta I}(\omega) = M^2 \left\{ \sum_{\alpha=1,2} \Gamma_\alpha^{\,2} \frac{2u_{s_\alpha}}{[\omega^2 + (2u_{s_\alpha})^2]} + 2\Gamma_1\Gamma_2 \frac{(u_{s_1} + u_{s_2})}{[\omega^2 + (u_{s_1} + u_{s_2})^2]} \right\} , \qquad (1)$$

where $\Gamma_\alpha \equiv G_\alpha^{\,2}/\kappa_\alpha(\vec{q})$, with $G_\alpha \equiv (f_\alpha i_3 + f_3 i_\alpha)$; M is a constant.

The vectors $\vec{i}$ and $\vec{f}$ are the polarization vectors of the incoming and scattered light respectively. The vector components are considered with respect to an orthonormal coordinate system defined by the following base vectors $\hat{e}_3 \equiv \vec{n}_0$, $\hat{e}_2 \equiv (\vec{n}_0 \times \vec{q})/|\vec{n}_0 \times \vec{q}|$, $\hat{e}_1 \equiv \hat{e}_2 \times \hat{e}_3$,

where $\vec{q}$ is the scattering wave vector and $\vec{n}_0$ represents the director. The function $\kappa_\alpha(\vec{q})$ is equal to $K_\alpha q_\perp^2 + K_3 q_{//}^2$ (α = 1, 2), where K_1, K_2 and K_3 represent the splay, twist and bend elastic constants respectively [2]. The components $q_{//}$ and $q_\perp$ of the scattering wave vector are parallel and normal to the director. In our case we took the polarization of the incoming light to be $\vec{i}$ = [0 1 0]; therefore $q_{//} = 0$ and $\kappa_\alpha = K_\alpha q_\perp^2$. Hence denoting splay and twist by α = 1, 2 respectively we observe that the spectral intensity $S_{\Delta I}$ can be considered to be a sum of three Lorentzians, associated with *pure* splay, *pure* twist and a splay/twist cross term, the half-bandwidths of which are related to the viscoelastic properties [5], i.e. $(\omega_{\frac{1}{2}})_\alpha = 2u_{s_\alpha} = 2\kappa_\alpha/\eta_\alpha$. In our configuration it holds that $u_{s_\alpha} = (K_\alpha/\eta_\alpha)q_\perp^2$.
Although the measured noise spectrum itself is not a pure Lorentzian, but is a sum of three Lorentzians, it is still possible to determine its half-width.

This result depends on the well-known optical parameters G_α and $q_\perp$ as well as on three unknown ratios, i.e. η_1/K_1, η_2/K_2 and K_1/K_2, which are constants (see eq (1)).

By measuring the noise spectrum at several different scattering angles, the half-bandwidths can be found as a function of G_α and $q_\perp$, because the latter parameters are functions of the scattering angle. With the help of a computer one can obtain a best fit to these data by using the following ratios as fitting parameters: η_1/K_1, η_2/K_2 and K_1/K_2.
Therefore not only one can obtain the viscoelastic ratios from noise measurements [5] but one can also find the ratio of the elastic constants.

III. EXPERIMENTAL RESULTS

In figure 1 results are shown for OHMBBA (O-hydroxy-p-methoxybenzylidene-p'-butylaniline) at a temperature t = 60.00°C. In the figure the experimental data for $u_s \equiv \frac{1}{2}(\omega_{\frac{1}{2}})_{exp.}$ are plotted on a log-log scale versus $q_\perp^2$. The solid line is the best fit to the experimental data. This best fit is obtained with the help of a least squares method on a log-log scale. The fitted values for the viscoelastic and elastic ratios are indicated in figure 1. Figure 2 shows results for K_1/K_2 at different temperatures. In addition we present the results obtained from measurements of scattered light intensity distributions [7] and from measurements of Freedericksz transitions [8].

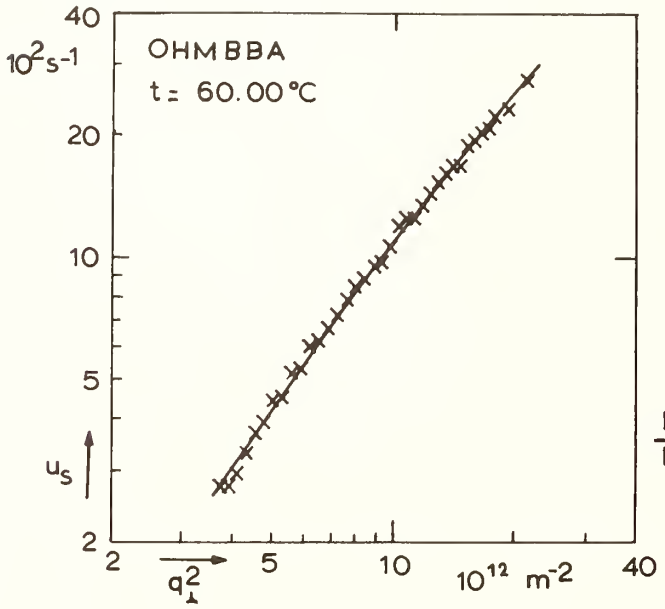

Fig. 1 An example of u_s versus $q_\perp^2$. The crosses represent the experimental data; the straight curve is the best fit with $\eta_1/K_1 = 7.2 \cdot 10^9$ sm^{-2}, $\eta_2/K_2 = 1.45 \cdot 10^{10}$ sm^{-2} and $K_1/K_2 = 1.8$.

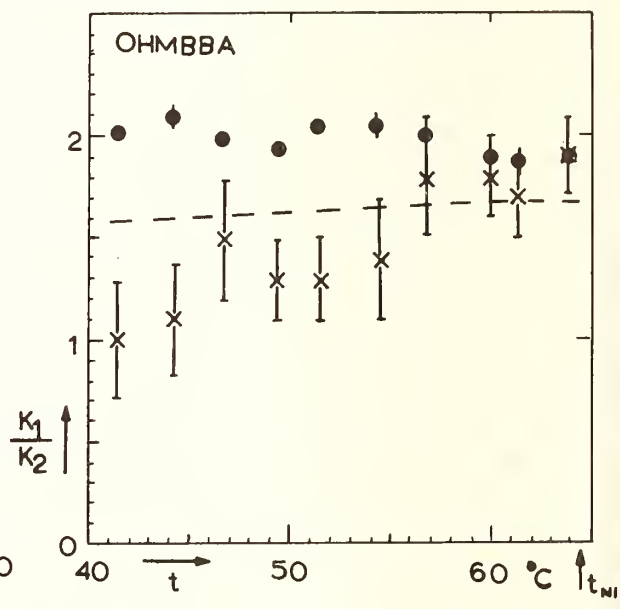

Fig. 2 Results of K_1/K_2 versus temperature. The crosses are from the fitting procedure; the dots are from light intensity distributions [7]; the dashed curve is the best fit for data obtained from Freedericksz transitions [8].

IV. CONCLUSION

It has been shown that spectral noise intensity measurements not only give us information about dynamical quantities but they also tell us about static quantities such as the splay/twist elastic ratio, K_1/K_2. The error in K_1/K_2 is mainly caused by experimental errors in $(\omega_{\frac{1}{2}})_{exp.}$. As is shown in figure 2, this statistical error is rather large compared to the statistical errors associated with the other two methods. It should be noted, however, that the different methods yield results which differ by more than can be accounted for by statistical errors. Apparently the errors involved are of a systematic nature.

We thank Sheila McNab for indicating and correcting the grammatical mistakes and Greetje Hollander for typing this manuscript.
This work was performed as a part of the research program of the "Stichting voor Fundamenteel Onderzoek der Materie" (FOM) with financial support from the "Nederlandse Organisatie voor Zuiver Wetenschappelijk Onderzoek" (ZWO).

REFERENCES

[1] M.J. Stephen, and J.P. Straley, *Rev. Mod. Phys.* 46, 617 (1974).

[2] P.G. de Gennes, *The Physics of Liquid Crystals* (Clarendon Press, Oxford, 1974).

[3] M. Lax, and D.F. Nelson, in *Coherence and Quantum Optics*, Ed. L. Mandel and E. Wolf (Plenum Press, New York, 1973) p. 415.

[4] D.C. van Eck, and R.J.J. Zijlstra, *J. Physique* 41, 351 (1980).

[5] D.C. van Eck, and R.J.J. Zijlstra, in *Noise in Physical Systems*, Ed. D. Wolf (Springer Verlag, Berlin, 1978) p. 270.

[6] D.C. van Eck, and W. Westera, *Mol. Cryst. Liq. Cryst.* 38, 319 (1977).

[7] J.P. van der Meulen, and R.J.J. Zijlstra, to be published.

[8] F. Leenhouts, H.J. Roebers, A.J. Dekker, and J.J. Jonker, *J. Physique* 40. C3-291 (1979).

V. QUANTUM NOISE

QUANTUM NOISE LIMITED DETECTION IN TUNNELING DEVICES AT MILLIMETER WAVELENGTHS

John R. Tucker

Department of Electrical Engineering
and Coordinated Science Laboratory
1406 West Green Street
University of Illinois
Urbana, Illinois 61801

INTRODUCTION

Detectors and heterodyne receivers designed to approach quantum limited sensitivity in the millimeter wave spectral region are currently being developed. This new class of quasiparticle mixer utilizes the extraordinary nonlinearities that occur in single-particle tunneling of electrons into a superconductor on one or both sides of a tunnel junction. These nonlinear devices perform the same detector functions as standard Schottky diodes and other resistive mixers, but with an important physical difference. At frequencies where the photon energy exceeds the voltage scale of the dc nonlinearity, a single-particle tunnel junction ceases to respond classically and becomes capable of detecting individual quanta. The results of this transformation are very dramatic, and appear certain to revolutionize low noise receiver technology in the millimeter wave region.

The phenomenon of photon-assisted tunneling was first observed almost twenty years ago by Dayem and Martin [1]. A theoretical interpretation proposed shortly thereafter by Tien and Gordon [2] correctly described the basic effect illustrated in figure 1a. Microwave power applied to a superconductor-insulating oxide-superconductor (SIS) tunnel barrier results in the appearance of well-defined step structures on the quasiparticle portion of the dc I-V curve. This type of SIS diode is actually a form of Josephson junction in which the capacitance is large enough to effectively shunt the oscillating pair current at frequencies $\omega = 2eV_0/\hbar$ near the gap voltage $V_0 = 2\Delta/e$. Under these conditions, the tunneling of single electron quasiparticles will determine the shape of the dc I-V curve over a substantial range of bias voltage. The sharp onset of quasiparticle current at $V_0 = 2\Delta/e$ is a direct reflection of the gap opened up in the single-particle excitation spectrum for identical superconductors on opposite sides of the barrier, as schematically illustrated in figure 1b. At the bias voltage in this diagram, the absorption of a single millimeter wave quantum $\hbar\omega$

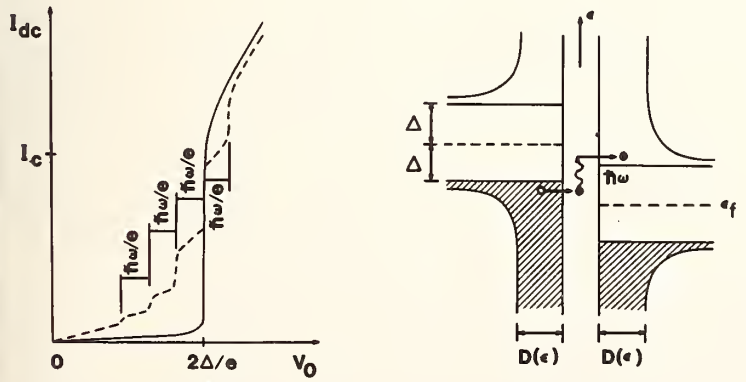

Fig. 1 (a) Photon-assisted tunneling steps (dashed curve) induced by an applied microwave field on the dc I-V characteristic (solid curve) of an SIS tunnel junction. (b) Densities of states vs. energy of single-particle excitations for identical superconductors on either side of a tunnel barrier.

can supply the energy required to tunnel from occupied single-particle states on the left into unoccupied states above the energy gap on the right. The sequence of steps below the gap voltage on the driven I-V curve in figure 1a reflects the series of bias thresholds for which the absorption of at least n = 1,2,3 ... photons is required to provide sufficient energy for single-particle tunneling. The amplitudes of these steps are directly related to the magnitude of the applied ac field.

Although this effect has been known for many years, the relationship between photon-assisted tunneling and the potential for quantum limited detection has been understood and applied only recently. The first device to utilize the extreme single-particle nonlinearity of a superconductive tunnel junction as a detector was the superconductor-semiconductor or super-Schottky diode [3]. The super-Schottky demonstrated extraordinary sensitivity as both a direct detector and heterodyne mixer at 10 GHz [4], and subsequently at 31 GHz [5]. It also stimulated a substantial body of theoretical work aimed at characterizing the potential impact of photon-assisted tunneling on the detection process [6,7,8]. Quantum effects in this type of resistive mixer were predicted at frequencies where the photon energy $\hbar\omega/e$ is large compared to the voltage scale of the dc nonlinearity, as in figure 1a. The nonlinearity of the super-Schottky diode is less spectacular than that of an SIS junction, however, and parasitic effects have thus far prevented its operation at frequencies high enough to induce significant quantum effects. In the spring of 1979, three groups reported successful mixing experiments using the sharp quasiparticle nonlinearity in small area SIS tunnel junctions [9,10,11]. Since that time, substantial progress has been made toward utilizing photon-assisted tunneling as a technique for approaching quantum noise limited detection in the millimeter wave region.

THEORY

A physical feeling for photon-assisted tunneling and its impact on detection may be obtained by considering the response to an applied sinusoidal potential:

$$V(t) = V_0 + V_1 \cos\omega t \tag{1}$$

The result derived by Tien and Gordon [2] for the dc component of the tunneling current is then given by:

$$I_{dc} = \sum_{n=-\infty}^{\infty} J_n^2(eV_1/\hbar\omega)\, I_{dc}(V_0 + n\hbar\omega/e) \tag{2}$$

Here the dc current in the presence of applied radiation is expressed in terms of the static dc I-V characteristic evaluated at a series of bias voltages reflecting the absorption or emission of integral numbers of quanta in the tunneling process. Equation (2) provides a quantitative account of the step structure observed in figure 1a.

In small ac fields, the following result for incremental change in the dc current is obtained by expanding these Bessel functions to lowest order:

$$\Delta I_{dc} = \frac{1}{4} V_1^2 \left\{ \frac{I_{dc}(V_0 + \hbar\omega/e) - 2I_{dc}(V_0) + I_{dc}(V_0 - \hbar\omega/e)}{(\hbar\omega/e)^2} \right\} \tag{3}$$

The expression in brackets is a second difference which reduces to the second derivative of the I-V curve in the classical limit. The dissipative component of current induced at the applied frequency is similarly found to be [7,8]:

$$I_\omega = V_1 \left\{ \frac{I_{dc}(V_0 + \hbar\omega/e) - I_{dc}(V_0 - \hbar\omega/e)}{2\hbar\omega/e} \right\} \tag{4}$$

The conductance of the junction at high frequencies is thus determined by a first difference form representing the absorption or emission of a single photon. The current responsivity

of the tunnel junction, defined as the change in dc current per unit power absorbed, may be obtained from eqs. (3) and (4) in the form:

$$R_i = \Delta I_{dc}/\tfrac{1}{2}V_1 I_\omega$$

$$= \frac{e}{\hbar\omega}\left\{\frac{I_{dc}(V_0 + \hbar\omega/e) - 2I_{dc}(V_0) + I_{dc}(V_0 - \hbar\omega/e)}{I_{dc}(V_0 + \hbar\omega/e) - I_{dc}(V_0 - \hbar\omega/e)}\right\} \qquad (5)$$

$$= \frac{1}{2}\,\frac{d^2I_{dc}/dV_0^2}{dI_{dc}/dV_0}, \quad \text{Classical limit}$$

$$= \frac{e}{\hbar\omega}, \quad \text{Quantum limit}$$

The standard classical result is recovered when the slope of the dc I-V curve changes slowly on a voltage scale $\hbar\omega/e$. The quantum limit, on the other hand, is realized at high frequencies where the nonlinear conductance varies rapidly on the photon energy scale. This limit would be approached in figure 1a, for example, at values of dc bias voltage lying in the region of the first step below the gap. The basic process in this case is illustrated in figure 1b. The quantum limit for current responsivity, $e/\hbar\omega$, represents the tunneling of one additional electron for each signal photon absorbed.

The transition to quantum limited response in a single-particle tunnel junction produces a variety of new phenomena which can be utilized to achieve low noise detection. The complete theoretical framework developed in Ref. [8] characterizes all properties of such devices in terms of their static dc I-V characteristic. The resistive portion of the response is directly related to the dc current at voltages corresponding to the absorption or emission of specific number of photons, as in eq. (2). At high frequencies, additional quantum reactances appear which are expressed in terms of the Kramers-Kronig transform of the dc I-V curve. The noise properties of these tunnel junctions may also be related to the dc current through a fluctuation-dissipation theorem. In the direct detection mode described above, the noise equivalent power will be limited by shot noise due to the bias current. Heterodyne detection may be utilized, however, to approach quantum noise limited sensitivity. Photon-assisted tunneling theory makes the following major predictions for such heterodyne mixers under appropriate operating conditions [12]:

(1). Quantum noise limited mixer temperatures: $T_M \approx \hbar\omega/k$.

(2). Conversion gain: simultaneous amplification accompanying frequency down-conversion of the incoming signal.

The potential for conversion gain is a matter of crucial practical importance. Since photon energies correspond to only a few degrees Kelvin in the millimeter wave region, noise from amplifiers following the mixer would otherwise dominate the total receiver temperature. Modest amounts of conversion gain, however, will reduce these amplifier noise contributions sufficiently that quantum noise limited performance may be approached in practical receivers. The theory also predicts that very large conversion gain associated with a negative output impedance may be obtained under certain conditions.

EXPERIMENT

The initial experiments on SIS quasiparticle mixers [9,10,11] all reported very low mixer noise temperatures, but with conversion losses in the range $L_c \approx$ 6-10 db. These results were comparable to those previously achieved with the super-Schottky diodes, except that distinct evidence of quantum effects due to photon-assisted tunneling were observed [9,10]. The direct detection properties of SIS junctions were also measured at 36 GHz, yielding an NEP $\approx 2.6\times10^{-16}$ W/Hz$^{\frac{1}{2}}$ and a current responsivity in virtually exact agreement with eq. (5) [13].

Subsequent work on SIS heterodyne mixers has produced dramatic improvements. The Caltech-Bell Labs group has constructed complete 115 GHz astronomical receivers that are already competitive with the best available cooled Schottky diode instruments [14]. Conversion efficiencies in excess of the theoretical maximum for classical resistive mixers were first demonstrated by the Berkeley group [15]. A single-sideband (SSB) conversion efficiency of 0.90, and a double-sideband gain of 1.40 were reported using Pb(Bi) alloy junctions whose mixer noise temperatures $T_M \gtrsim 1.5K$ equaled the quantum noise limit within experimental accuracy at 36 GHz. Their measurement is shown in figure 2. The peaks in mixer output correspond to the positions of the photon steps on the driven dc I-V curve, and are separated by $\hbar\omega/e \approx 0.15$ mV. The theoretical prediction indicates that even greater conversion efficiencies could be realized on steps closer to the gap voltage $2\Delta/e \approx 3$ mV if higher harmonics, not included in the calculation, were suppressed by a larger junction capacitance. Below about 2 mV, Josephson pair tunneling currents disrupt the low-noise quasiparticle mixer performance. This effect may be partially suppressed by application of a constant dc magnetic field.

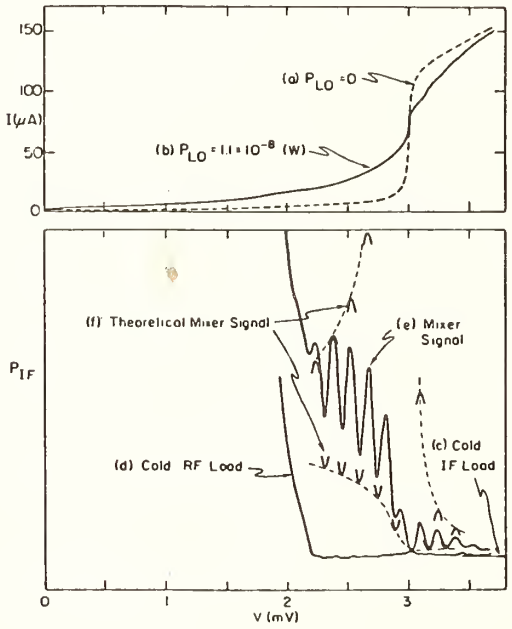

Fig. 2 I-V curves at T = 1.5K for a Pb(Bi) alloy junction (a) without and (b) with applied 36 GHz local oscillator power. Plots of IF mixer output power are shown in the lower portion of the figure as a function of bias voltage. Point (c) and curve (d) represent thermal sources, and are used to deduce mixer noise temperature. Curve (e) is the mixer signal obtained from a calibrated 36 GHz source, and measures conversion efficiency. The dashed curve (f) is the prediction of 3-port quantum mixer theory with no adjustable parameters [15].

The group at Chalmers University in Sweden recently reported excellent results using six-junction Pb(In) series arrays at 73 GHz [16]. Their maximum SSB conversion efficiency was approximately 0.65 (L_C = 2.0 db) as illustrated in figure 3, again with mixer noise temperatures near the quantum limit. Note that optimum efficiency occurs for dc bias voltages near the middle of the first and second photon steps below the gap. Because this is a six-junction array, the width of these steps and the spacing between conversion peaks becomes $6\hbar\omega/e$. The entire voltage scale is thus enlarged by a factor of six, because six times as many photons must be absorbed in passing a single electron through the array compared with a single junction. The use of arrays, particularly for high frequency applications, appears very promising based on these experiments. Larger area junctions can be combined in series to achieve a total impedance appropriate to meet circuit matching requirements, and these larger areas alleviate constraints on both fabrication requirements and the magnetic field strengths required to suppress Josephson effects. Dynamic range will be increased for an array, although the quantum limited mixer noise temperature will also increase to $T_M \approx N\hbar\omega/e$ for N junctions in series.

Very recently, the Berkeley group has achieved quite large SSB conversion gains of approximately 5.7 db at 36 GHz using Sn junctions with very sharp I-V curves [17]. Infinite available conversion gain has been observed by Kerr, et al. [18] at 115 GHz, and the predicted negative differential output impedance seen for the first time. The

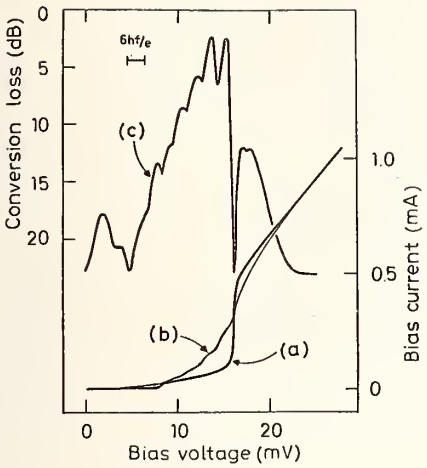

Fig. 3 I-V curve (a) without and (b) with applied local oscillator power at 73.5 GHz, and (c) mixer conversion loss for a six element series array of Pb(In) alloy junctions at T = 1.5K [16].

development of these SIS quasiparticle mixers is proceeding very rapidly, and practical millimeter wave receivers with system noise temperatures approaching the quantum limit should be realized in the near future.

This work was supported in part by the Joint Services Electronics Program (U.S. Army, U.S. Navy, U.S. Air Force) under contract number N00014-C-79-0424.

REFERENCES

[1] A. H. Dayem and R. J. Martin, *Phys. Rev. Lett.* 8, 246 (1962).

[2] P. K. Tien and J. P. Gordon, *Phys. Rev.* 129, 647 (1963).

[3] M. McColl, M. F. Millea, and A. H. Silver, *Appl. Phys. Lett.* 23, 263 (1973).

[4] M. McColl, M. F. Millea, A. H. Silver, M. F. Bottjer, R. J. Pedersen, and F. L. Vernon, Jr., *IEEE Trans. Magn.* MAG-13, 221 (1977).

[5] A. H. Silver, R. J. Pedersen, M. McColl, R. L. Dickman, and W. J. Wilson, *IEEE Trans. Magn.* MAG-17, 698 (1981).

[6] J. R. Tucker, in *Proc. 14th Int. Conf. on Low Temperature Physics LT-14,* Eds. M. Krusius and M. Vuorio (North Holland, Amsterdam, 1975), vol. 4, p. 180.

[7] J. R. Tucker and M. F. Millea, *Appl. Phys. Lett.* 33, 611 (1978).

[8] J. R. Tucker, *IEEE J. Quantum Electron.* QE-15, 1234 (1979).

[9] P. L. Richards, T. M. Shen, R. E. Harris, and F. L. Lloyd, *Appl. Phys. Lett.* 34, 345 (1979).

[10] G. J. Dolan, T. G. Phillips, and D. P. Woody, *Appl. Phys. Lett.* 34, 347 (1979).

[11] S. Rudner and T. Claeson, *Appl. Phys. Lett.* 34, 711 (1979).

[12] J. R. Tucker, *Appl. Phys. Lett.* 36, 477 (1980).

[13] P. L. Richards, T. M. Shen, R. E. Harris, and F. L. Lloyd, *Appl. Phys. Lett.* 36, 480 (1980).

[14] T. G. Phillips, D. P. Woody, G. J. Dolan, R. E. Miller, and R. A. Linke, *IEEE Trans. Magn.* MAG-17, 684 (1981).

[15] T. M. Shen, P. L. Richards, R. E. Harris, and F. L. Lloyd, *Appl. Phys. Lett.* 36, 777 (1980).

[16] S. Rudner, M. J. Feldman, E. Kollberg, and T. Claeson, *IEEE Trans. Magn.* MAG-17, 690 (1981).

[17] W. R. McGrath, P. L. Richards, A. D. Smith, H. Van Kempen, D. E. Prober, and P. Santhanan, *Bul. Am. Phys. Soc.* 26, 307 (1981).

[18] A. R. Kerr, S. K. Pan, M. J. Feldman, and A. Davidson, paper submitted to *16th Int. Conf. on Low Temperature Physics LT-16,* Los Angeles, August 1981.

QUANTUM TUNNELLING AND NOISE IN SQUIDS

A.J. Leggett

School of Mathematical and Physical Sciences,
University of Sussex, Falmer, Brighton, BN1 9QH,
Sussex, U.K.

The dynamics of the flux ϕ threading a SQUID ring is usually described by the so-called RSJC ("resistively shunted junction with capacitance") model (see e.g. ref [1]) which leads to the following classical equation of motion:

$$C\ddot{\phi} + \dot{\phi}/R + \delta U/\delta\phi = 0 \tag{1}$$

$$U(\phi:\phi_x) \equiv \frac{(\phi - \phi_x)^2}{2L} + \frac{I_c\phi_o}{2\pi}\left(1 - \cos\left(\frac{2\pi\phi}{\phi_o}\right)\right) \tag{2}$$

Here C is the effective capacitance of the Josephson junction (cf. below) and R the resistance shunting it, which under the assumptions of the model can be inferred [2] from the asynptote of the experimental I-V characteristic. ϕ_x is the externally imposed flux threading the ring, which in the present context will be taken as a c-number parameter controlled by the experimenter, I_c the junction critical current, L the self-inductance of the ring and $\phi_o \equiv h/2e$ the flux quantum. I shall be concerned in this paper exclusively with "hysteretic" SQUIDS ($2\pi LI_c/\phi_o > 1$) for which the "potential" $U(\phi)$ may have one of more metastable minima; I shall refer to a well (minimum) as "deep" if the energy barriers separating it from the neighbouring wells are approximately $I_c\phi_o/\pi$ (a necessary, but not sufficient, condition for this is evidently that $LI_c/\phi_o >> 1$).

If the flux is trapped in a well which is metastable with respect to its neighbours, thermal noise may drive it over the energy barrier; this process is of particular practical significance when it occurs near the classical "break point" of a SQUID operated in the rf mode, since it will then limit the accuracy with which the external flux ϕ_x can be measured. The standard theory of this process is due to Kurkijärvi [1], and for present purposes it is useful to note how the main factors in his expression arise. As is well known, for any classical nucleation process, the rate can be expressed, apart from a prefactor of order unity, in the form

$$P_{cl} = \omega_o \exp - \Delta U/k_B T \tag{3}$$

where ω_o is the frequency of small oscillations around the metastable equilibrium (but see below) and ΔU is the height of the free energy barrier. Note that the (dominant) exponent is independent of both the capacitance C and the resistance R of the junction (The prefactor depends on both, and in fact for the highly damped case is proportional to $\omega_o^2/2\pi\gamma$ rather than ω_o, where $\gamma \equiv 1/CR$: thus in this limit it is proportional to R and independent of C). The order of magnitude of the rms fluctuation, σ_{cl} of the value of external flux at which the transition to the neighbouring well occurs can be obtained by setting σ_{cl} equal to the value of $\delta\phi_x \equiv \phi_{xc} - \phi_x$ at which the P_{cl} is of the order of τ^{-1}; here τ is the time available for the transition to occur ($\sim$ rf period) and ϕ_{xc} is the values of ϕ_x at the classical break point (i.e. $\Delta U(\phi_{xc}) = 0$). In the case of a strongly hysteretic SQUID ($LI_c/\phi_o >> 1$) we have [1]. $\Delta U(\delta\phi_x) = \frac{2\sqrt{2}}{3\pi}\frac{\phi_o^2}{L}\cdot\left(\frac{\phi_o}{LI_c}\right)^{1/2}\left(\frac{\delta\phi_x}{\phi_o}\right)^{3/2}$ (4)

and also (for future reference)

$$\omega_o(\delta\phi_x) = \left(\frac{1}{LC}\right)^{1/2} (2\pi\sqrt{2})^{1/2} (LI_c/\phi_o)^{1/4}\left(\frac{\delta\phi_x}{\phi_o}\right)^{1/4} \tag{5}$$

Note that ω_o as well as ΔU tends to zero as we approach the classical break point. From (4) we obtain the result [1]

$$\sigma_{c1} = \text{const.} \left[\frac{3\pi}{2\sqrt{2}} \left(\frac{k_B T}{\phi_o^2/L}\right)^{2/3} \left(\frac{LI_c}{\phi_o}\right)^{1/3} \phi_o \right] \tag{6}$$

where the constant depends logarithmically on the sweep rate and is of order 1. The formula (6) agrees well with the published data [3].

It was long ago suggested [4] that at sufficently low temperature the dominant flux transition mechanism in a SQUID should be not thermal fluctuations but quantum tunnelling through the energy barrier. Such a possibility is of interest not merely in the context of the ultimate attainable sensitivity of SQUID magnetometers but also because, since the tunnelling variable (the flux) is recognizably macroscopic, the observation of this phenomenon would constitute circumstantial evidence for the hypothesis that the linear laws of quantum mechanics can be extrapolated to arbitrarily complex systems [5,6] - an assumption which, while often made in the context of discussions of the quantum theory of measurement, has at present no experimental basis (see ref. [6]). In the remainder of this paper I review the theoretical and experimental status of this problem. Although similar considerations can be given for the case of a single current-biased Josephson junction [7], I shall confine the explicit discussion to the case of SQUID rings, where the tunnelling process is in some ways conceptually simpler and also more unarguably "macroscopic". (though see below).

If we for the moment forget about the dissipative terms in eqn.(1), this equation can be derived from a Hamiltonian consisting of the "potential" energy $U(\phi)$ (eqn. (2)) plus a "kinetic" energy $p_\phi^2/2C = \frac{1}{2}C\dot{\phi}^2$, where the junction capacitance C plays the role of the particle mass in a mechanical problem. Application of the standard WKB techniques to the problem of tunnelling between neighbouring minima of $U(\phi)$ (at zero temperature) then leads to the result

$$P_{QM} = \text{const. } \omega_o \exp - \alpha\Delta U/\hbar\omega_o \tag{7}$$

when the dimensionless constant α depends on the shape (but not the scale) of the energy barrier: we note that α is 36/5 for a cubic potential [8] (appropriate to tunnelling near the break point) and $8\sqrt{2}$ for a pure cosine potential (roughly appropriate to tunnelling between "deep" wells). Comparing eqn. (7) with eqn. (2) we see that for a fixed potential shape quantum tunnelling is likely to overtake thermal fluctuation as the dominant flux transition mechanism when $k_B T \lesssim \alpha^{-1} \hbar\omega_o$; however, by this time both processes will have negligible probability in a laboratory time-scale unless $\alpha\Delta U/\hbar\omega_o$ is less than about 30. In particular, the observation of tunnelling between "deep" wells would appear to require $CI_c \lesssim 10^{-21}$ in SI units.

For transitions occuring near the break point of a strongly hysteretic SQUID we use the same order-of-magnitude argument as above to estimate the rms uncertainty σ_{QM} in the value of ϕ_x at the transition which is due to quantum tunnelling (at zero temperature). This gives

$$\sigma_{QM} = \text{const.} \left(\frac{5}{24}\right)^{1/5} \pi \left[\frac{\hbar\omega_{LC}.\hbar\omega_J}{(\phi_o^2/L)^2} \frac{LI_c}{\phi_o}\right]^{2/5} \phi_o \tag{8}$$

where $\omega_{LC} \equiv (LC)^{-1/2}$ and $\omega_J \equiv (2\pi I_c/C\phi_o)^{1/2}$ (ω_J is the Josephson plasma frequency of the isolated junction at zero current bias). More quantitative treatments of this problem are given in refs. [8] and [9]. Comparing (8) with (6) we would conclude that tunnelling is likely to become the dominant mechanism at temperatures well below a characteristic temperature T_o given by

$$k_B T_o \simeq 0.15c\,\hbar\omega_J, \quad c \equiv (\hbar\omega_J/I_c\phi_o)^{0.2} \tag{9}$$

The factor c is fairly insensitive to the parameters and is generally of order 0.2. Thus for $\omega_J \sim 10^{12}$ we would expect tunnelling to be dominant at temperatures well below 100 mK.

However, the above results are all based on a simple WKB approach in which the

dissipative term in the equation of motion (1) is completely neglected. Since practical SQUIDS are often quite heavily overdamped, it is of crucial importance to know how the dissipation will affect the quantum tunnelling probability. This is a special case of a general problem considered recently by Caldeira and the author [8,10]; transposing our results to the SQUID case, we find that if the motion in the classically accessible region is well described by eqn. (1), then the tunnelling probability P_{QM} is suppressed relative to the value $P_{QM}^{(0)}$ calculated in the simple WKB approximation by an exponential factor:

$$P_{QM}/P_{QM}^{(0)} \sim \exp - f.(\Delta\phi)^2/R\hbar \qquad (10)$$

Here $\Delta\phi$ is the distance in flux space that must be traversed "under the barrier", and f is a numerical factor which must be found from the solution of a nonlinear integrodifferential equation and depends on the shape of the barrier and, weakly, the degree of damping. Without obtaining an exact solution, it can be shown [8] that f is in general of order unity and for heavy damping is bounded by the inequalities $\beta_1 > f > \beta_2/\ell n\ (\gamma/\omega_o)$ where $\gamma \equiv 1/RC$ is the damping coefficient and the numbers β_1, β_2 depend on the shape of the potential barrier. In this limit, therefore, the "effective WKB exponent" is dominated by the shunting resistance R and is almost independent of the junction capacitance.

Two consequences are immediately evident. First, tunnelling between "deep" wells (for which $\Delta\phi \sim \phi_o$) should be essentially forbidden, whatever the value of capacitance, if the order of magnitude of the shunting resistance is much less than the characteristic value $\phi_o^2/\hbar \sim 40\ k\Omega$. Secondly, the uncertainty σ_{QM} in tha value of ϕ_x at which the transition occurs in an rf SQUID should be changed from eqn (8) to an expression which in the overdamped limit varies approximately as RLI_c, with only a very weak dependence on C. For reasonable values of the parameters σ_{QM} can be very small indeed, and Kurkijärvi [9] has argued on this basis that it is not relevant to the ultimate flux sensitivity of a realistic rf SQUID (cf also ref. [11]).

Let us now turm to the experimental situation. We note, first, that two experiments have so far looked for the related phenomenon of quantum tunnelling of the phase in a simple current-biassed Josephson junction; one,several years ago by Fulton and Dunkleberger [12], observed some suggestive departures at low temperatures from the classically predicted behaviour which they thought might have been due to quantum effects, while a similar very recent experiment by Jackel and co-workers [13] found no deviation from the classical predictions down to temperatures of the order of $0.25\ \hbar\omega_o/k_B$. In the case of SQUID rings proper, a rather direct experiment was carried out by den Boer and de Bruyn Ouboter [5] in Leiden, using Nb point contact SQUIDS for which the parameter LI_c/ϕ_o was not large compared to 1 (and to which, therefore, not all the above formulae would be expected to apply quantitatively); they varied the externally imposed flux ϕ_x and monitored the trapped flux ϕ as it jumped between the two available minima. At ambient temperatures of the order of 1K the rate of jumping was several orders of magnitude faster than the classical fluctuation theory would allow, and they show that it is compatible with the quantum tunnelling rate as given by the simple WKB calculation without damping if one assumes a capacitance of the order of 10^{-15}F. (cf below). A second, rather less direct, experiment was carried out by T.D. Clark and co-workers at Sussex, who measured the current-voltage characteristic of a low-noise 430 MHz rf SQUID down to 1.8K; at this temperature they observed a number of intriguing departures from the conventionally expected I-V characteristic which they believe "are caused by the onset of QE behaviour (i.e. flux tunnelling) in the SQUID ring". It should be observed that the interpretation of the data given in ref. [14] appears to require an appreciable probability of tunnelling between "deep" wells.

Two questions obviously arise: first, how far are these two experiments actually evidence for quantum tunnelling of the flux, and secondly, if such tunnelling is indeed occurring, how far is this compatible with the theoretical framework outlined above? I shall not discuss the first question here, since while in the Leiden experiments the only obvious question concerns the possible presence and effect of non-thermal external noise (cf below), a proper discussion of the Sussex data would require a detailed analysis of the dynamics of the tank circuit for this somewhat novel situation. Turning to the second question, it is clear that a great deal hinges on what we take to be the effective junction capacitance C. In the Sussex experiments the above WKB type considerations, even without account of damping, would predict negligible tunnelling unless C is less than 10^{-18}F (The theory actually used in ref. [14] to interpret the Sussex data, which would allow tunnelling for values of C several orders of magnitude larger, appears not to be equivalent to any simple version of the WKB theory). For

such ultra-small values of C it is not clear that the model used here would be even a good zeroth-order description. (since, inter alia, the capacatitive energy of a single pair, $2e^2/C$, is larger than both $\hbar\omega_J$ and the bulk energy gap). In the Leiden experiments compatibility with the WKB predictions ignoring damping [5] requires that we assign to C not its bulk"geometrical"value C_b (presumably $\sim 10^{-13}$F) but a smaller value, say $\sim 10^{-15}$F. It is argued in ref [5] that this is plausible since the capacitance of the junction itself may be effectively in series with a rather large inductance L', say $\sim 10^{-10}$H, the whole being presumably shunted by the much larger geometrical capacitance C_b; the absence of hysteresis in the junction I-V characteristic is used to put an upper limit on C which is indeed of order 10^{-15}F (cf also ref. [14]). A preliminary study of the "undamped" WKB prediction for this effectively two-dimensional model seems to indicate that tunnelling is indeed possible provided that L' is large enough, but that the tunnelling event itself is localized in the region very close to the junction and the flux change then propagates through the macroscopic ring by a purely classical process. It is however less clear that such a mechanism would necessarily give the observed lack of hysteresis. The effect of damping also needs a detailed study, since the junction resistances in this experiment are sufficiently large that a crude order-of-magnitude estimate leaves it unclear whether it would suppress the tunnelling sufficiently to render it unobservable. Clearly, in the light of the above, it would be highly desirable in principle to do tunnelling experiments in SQUIDS using junctions whose capacitance can be independently measured, e.g. by observing the Josephson plasma resonance.

In conclusion I note that if the RSJ description is indeed applicable and the theory developed in ref [10] to take account of damping is correct, then it should be relatively easy to discriminate genuine quantum tunnelling in SQUIDS from extrinsic noise effects by investigating the effect of varying the shunting resistnace: the very strong suppression predicted by eqn [10] should be an unambiguous signature of quantum tunnelling.

I am grateful to A.O. Caldeira, T.D. Clark, J. Clarke, R. de Bruyn Ouboter, T.A. Fulton, J. Kurkijärvi and L.D. Jackel for helpful discussions on these topics and for various preprints.

References

[1] J. Kurkijärvi, Phys. Rev. B6, 832 (1972).

[2] D.E. McCumber, J. Appl. Phys. 39, 3113 (1968)

[3] L.D. Jackel, W.W. Webb, J.E. Lukens and S.S. Pei, Phys. Rev. B9, 115 (1974)

[4] D.J. Scalapino, in Tunnelling Phenomena in Solids, ed. E. Burstein and S. Lundqvist (Plenum, New York, 1969), p. 477.

[5] W. den Boer and R. de Bruyn Ouboter, Physica 98 B+C, 185 (1980)

[6] A.J. Leggett, Progress of Theoretical Physics, special issue in honour of R. Kubo, 1981 (in press)

[7] Yu M. Ivanchenko and L.A. Sil'bersman, Sov. Phys. JETP 28, 1272 (1969)

[8] A.O. Caldeira, Ph. D. Thesis, University of Sussex, 1980 (unpublished).

[9] J. Kurkijärvi, submitted to J. Low Temp. Phys.

[10] A.L. Caldeira and A.J. Leggett, Phys. Rev. Letters 46, 211 (1981)

[11] R.H. Koch, D.J. van Harlingen and J. Clarke, Phys. Rev. Letters 45, 2132 (1980)

[12] T.A. Fulton and L.N. Dunkleberger, Bull. Am. Phys. Soc. 19, 205 (1975): cf Phys. Rev. B9, 4760 (1974)

[13] L.D. Jackel et al, abstract submitted for March 1981 APS meeting.

[14] R.J. Prance et al, Nature 289, 542 (1981)

QUANTUM NOISE IN JOSEPHSON JUNCTIONS AND SQUIDS

Roger H. Koch, D. J. Van Harlingen and John Clarke

Department of Physics, University of California, and
Materials and Molecular Research Division, Lawrence
Berkeley Laboratory, Berkeley, California 94720

INTRODUCTION

The effects of thermal noise on a current-biased resistively shunted Josephson junction (RSJ) have been extensively studied. The noise source is assumed to be the Nyquist noise with spectral density $4k_BT/R$ developed in the shunt resistor R at a temperature T. This noise has two effects. First, it induces transitions from the zero voltage state to the non-zero voltage state at bias currents below the thermodynamic critical current, I_o, thereby inducing "noise rounding" of the current-voltage (I-V) characteristic [1]. Second, the Nyquist noise generates a voltage noise across the junction that, according to the theory of Likharev and Semenov [2], has a spectral density

$$S_v(0) = \frac{4k_BTR_D^2}{R}\left[1 + \frac{1}{2}\left(\frac{I_o}{I}\right)^2\right] \qquad (1)$$

at frequencies much less than the Josephson frequency. In Eq. (1), $R_D \equiv \partial V/\partial I$ is the dynamic resistance of the junction.

The results of the theory have been well established experimentally [3,4]. One application of the theory is to predict the sensitivity of the dc SQUID [5] for a given set of experimental parameters. The predictions have been in quite good agreement with results obtained experimentally [6]. As the sensitivity of these devices is improved, however, the theory will eventually break down as quantum processes become important and set a limit on the performance. In this paper, we briefly outline a theory for noise in the RSJ in the quantum limit [7], and extend it to the dc SQUID [8]. Experimental results for both the single junction and the SQUID are reported.

QUANTUM NOISE THEORY FOR A RESISTIVELY SHUNTED JUNCTION

We consider a Josephson tunnel junction with critical current I_o and capacitance C shunted with a resistance R. We assume that the voltage is less than $2\Delta/e$, where Δ is the energy gap, and that T is well below the transition temperature, so that the quasiparticle tunneling conductance is small compared with the shunt conductance. Our central assumption is that the current noise in the shunt resistor has a spectral density

$$S_I(\nu) = \frac{2h\nu}{R}\coth\left(\frac{h\nu}{2k_BT}\right) \equiv \frac{4h\nu}{R}\left(\frac{1}{2} + \frac{1}{e^{h\nu/k_BT}-1}\right) \qquad (2)$$

at frequency ν. The equation of motion of the junction can be written in the form

$$\frac{\hbar C}{2e}\ddot{\delta} + \frac{\hbar}{2eR}\dot{\delta} + I_o \sin\delta = I + I_N(t) \qquad (3)$$

where δ is the phase difference across the junction, and $I_N(t)$ has the spectral density of Eq. (2).

We first assume that the capacitance is small ($\beta_c \equiv 2\pi I_o R^2 C/\Phi_o << 1$, where $\Phi_o \equiv h/2e$ is the flux quantum), and that the noise is small so that noise-rounding can be neglected. The I-V characteristic is then [9] $V = R(I^2-I_o^2)^{\frac{1}{2}}$, and Eq. (3) may be solved analytically using the techniques of Likharev and Semenov [2]. For frequencies much less than the Josephson frequency 2eV/h one finds

$$S_v(0) = R_D^2 \left[\frac{4k_B T}{R} + \frac{2eV}{R} \left(\frac{I_o}{I} \right)^2 \coth\left(\frac{eV}{k_B T} \right) \right] \tag{4}$$

In the limit $eV << k_B T$, the hyperbolic cotangent may be expanded and one recovers the thermal noise limit, Eq. (1). The first term on the right hand side of Eq. (4) represents noise generated in the shunt at the measurement frequency, while the second term arises from noise generated at frequencies near the Josephson frequency that is mixed down by the non-linearity of the junction. Equation (4) is plotted in Fig. 1 for 5 values of the parameter $\kappa \equiv eI_o R/k_B T$. When $\kappa << 1$, the curve becomes indistinguishable from that of the thermal limit, but as κ increases, the voltage noise is significantly enhanced above the thermal result. In the extreme quantum limit (T=0), one finds

$$S_v(0) = 2eV(I_o/I)^2 R_D^2/R = 2eI_o^2 R^3/V. \tag{5}$$

The physical interpretation of the noise is as follows. Equation (3) also describes the motion of a particle on a tilted washboard. Then, C represents the mass of the particle, 1/R the viscous damping, and I_o the amplitude of the oscillating potential. The average slope of the washboard is proportional to I. At bias currents above the critical current, the effect of $I_N(t)$ is to induce random variations in the slope, and thus produce random noise in the velocity of the mass, $\dot{\delta}$, that represents the voltage in the case of the junction. If the current is reduced to a value below I_o, in the absence of noise the ball no longer runs freely, but remains trapped in one of the potential wells. However, if I is sufficiently close to I_o, the noise may instantaneously tilt the washboard sufficiently so that the particle rolls into the next well. This effect produces noise rounding of the I-V characteristic. In our model, this effect occurs even at T=0, where the noise current is due to the zero point fluctuations in the large collection of harmonic oscillators representing the resistor. Alternatively, one may view the current fluctuations as supplying pulses of energy that "activate" the particle over a stationary potential barrier. These fluctuations are virtual: The energy in the pulse, ΔE, and the length of the pulse, Δt, satisfy $\Delta E \Delta t \lesssim \hbar$. The dissipation that occurs when the phase changes by 2π is supplied by the bias current, not by the noise current. (On the other hand, in the thermal limit in which the noise currents have a spectral density $4k_B T/R$, $\Delta E \Delta t \sim k_B T \Delta t$, and the fluctuations are real).

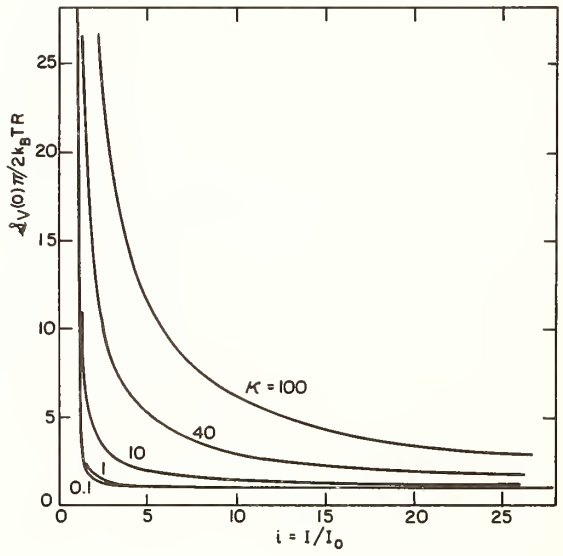

Fig. 1 Low-frequency spectral density $S_v(0)$ of the voltage noise vs current for 5 values of $\kappa \equiv eI_o R/k_B T$ with $\beta_c << 1$.

We emphasize that the description of the junction by a Langevin equation assumes that the wave packet representing the phase of the junction is highly localized so that a particle-like representation is appropriate. When the wave packet representing the phase is significantly broadened, a full quantum mechanical description is essential, and use of the Langevin equation may lead to unphysical results. Furthermore, we have neglected the effects of macroscopic quantum tunneling [10] which we believe are relatively unimportant for overdamped junctions.

EXPERIMENTS ON SINGLE JUNCTIONS

To observe quantum effects we require a junction with $\kappa \equiv eI_oR/k_BT = (e/k_BT)(\beta_c\Phi_o j_1/2\pi c)^{\frac{1}{2}} >> 1$, where j_1 is the critical current density and c is the capacitance per unit area. At 1K with $j_1 = 10^4$ Acm^{-2}, c = 0.04 pF μm^{-2} and $\beta_c = 0.1$ we find $\kappa \approx 3$, a value at which quantum corrections should be readily observable.

The PbIn-Ox-Pb junctions were fabricated using photolithographic techniques. The junction area was about 6 μm^2, and the critical currents ranged from 0.1 to 15 mA (0.2 to 30x10^4 Acm^{-2}). The CuAl shunt resistance was typically 0.1Ω, and had an inductance of about 0.2 pH. The low frequency voltage noise of each junction was amplified with a cooled 30- or 100-kHz LC-circuit coupled to a room-temperature low-noise preamplifier. The noise was mixed down to frequencies below 100 Hz, and its power spectrum was measured with a computer. Any 1/f noise contribution was estimated from the measurements at 30 and 100 kHz, and, when significant, was subtracted from the 100 kHz-measurement.

We first investigated junctions with $\kappa << 1$, and found excellent agreement with Eq. (1). These results demonstrate the accuracy of our measuring techniques, and give some assurance that we have taken adequate precautions to eliminate external noise. We then investigated junctions with $\kappa > 1$, and discovered the resonant structure illustrated in Fig. 2. The

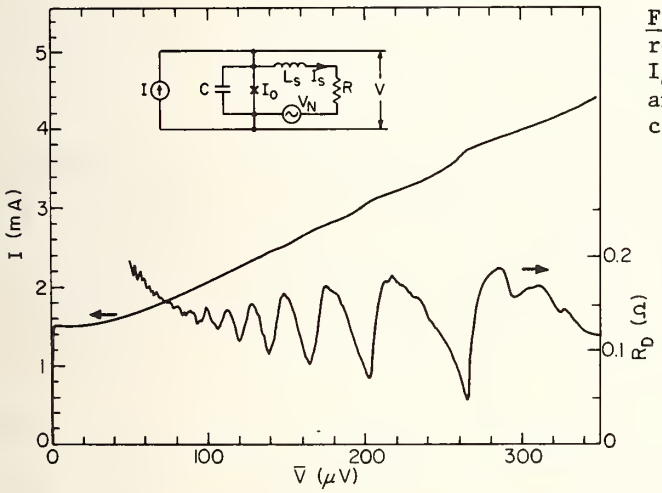

Fig. 2 I-V characteristics and dynamic resistance R_D for a junction at 1.4K with I_o = 1.53 mA, R = 0.092Ω, κ = 1.15, β_c = 0.03, and $2\pi L_s I_o/\Phi_o$ = 1.0. Inset shows equivalent circuit of junction.

resonances occur when the Josephson frequency is near a subharmonic of the resonant circuit formed by the shunt inductance L_s and the junction capacitance; the equivalent circuit is shown inset in Fig. 2. In addition to modifying the I-V characteristic, the increased nonlinearity of the phase evolution enhances the mixing down of noise from multiples of the Josephson frequency. The spectral density of the noise measured on one junction is shown in Fig. 3. The correction due to amplifier voltage and current noise is negligible. The 1/f noise was at most 20% of the total noise and was subtracted out. If we assume that the error due to an inadequate knowledge of the exact spectral density of the flicker noise is ±25%, the overall error resulting is ±5% of the total measured noise. We have subtracted the noise from the resistor at the measurement frequency, $4k_BTR_D^2/R$, from the total noise to determine the mixed down noise; the latter is also plotted in Fig. 3.

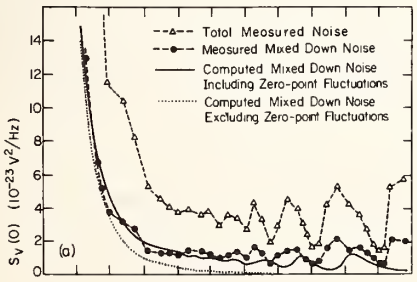

Fig. 3 Measured and computed spectral densities of the voltage noise at 1.4K for the junction in Fig. 2.

We have computed the noise expected from the circuit shown in Fig. 2 using the equations of motion

$$I = I_o \sin\delta + C\dot{V} + I_s, \tag{6}$$

and $$V = I_s R + \dot{I}_s L_s + V_N. \tag{7}$$

Here I_s is the current through the shunt inductance, L_s, and V_N has a spectral density $2h\nu R\coth(h\nu/2k_BT)$ at frequency ν. The computed mixed-down noise is plotted in Fig. 3. For comparison, the computed mixed-down noise using a noise spectral density for the resistor without the zero point term, $4h\nu R/[\exp(h\nu/k_BT)-1]$, is also shown. The latter result clearly underestimates the measured noise. The agreement between the computed and measured noise is quite good below about 120 μV, but at higher voltages the measured noise lies somewhat above the predicted value. We believe this discrepancy arises from self-heating in the junction, which increases the magnitude of the noise at the measurement frequency. Furthermore, the measured and predicted resonances are misaligned, indicating that our choices of L_s and C were slightly incorrect.

These results suggest strongly that zero point fluctuations in the shunt resistor are the source of the limiting noise in a resistively shunted Josephson junction in the quantum limit.

QUANTUM NOISE IN THE dc SQUID

The dc SQUID consists of two Josephson junctions in a superconducting loop of inductance L. The critical current of the SQUID oscillates as a function of the applied magnetic flux Φ threading the loop with a period Φ_o. Thus, when the SQUID is current-biased in the non-zero voltage regime, the voltage also oscillates as a function of the applied flux. A small change $\delta\Phi$ ($<<\Phi_o$) produces a corresponding change in voltage $\delta V = (\partial V/\partial\Phi)\delta\Phi$. The smallest detectable change in flux that can be detected is determined by the voltage noise across the SQUID. To characterize the performance, it is convenient to define the noise energy per Hz

$$\frac{\varepsilon}{1\text{Hz}} = \frac{S_\Phi}{2L} = \frac{S_V}{2(\partial V/\partial\Phi)^2 L}, \tag{8}$$

where S_V is the spectral density of the voltage noise, and S_Φ is the spectral density of the equivalent flux noise in the SQUID.

Tesche and Clarke [5] computed the noise energy assuming that the Nyquist noises in the two resistive shunts were the only sources of noise. They found that the SQUID was optimized when $\beta_c \lesssim 1$ and $\beta = 2LI_o/\Phi_o \approx 1$, and that the optimum noise energy was given by

$$\frac{\varepsilon}{1\text{Hz}} \approx 10 k_B T\,(LC)^{1/2}. \tag{9}$$

This result adequately predicts the measured performance of SQUIDs over a wide range of values of L and C. The most sensitive devices reported to date have noise energies of $\sim 6\hbar$ [11, 12, 13], in reasonable agreement with Eq. (9). When T, L, and/or C are lowered sufficiently, quantum corrections to the noise become important. The theory described earlier in this paper can be extended to the case of the SQUID, and one finds that at T=0 for an optimized device

$$\frac{\varepsilon}{1\text{Hz}} \approx \hbar. \tag{10}$$

At higher temperatures the performance is degraded: At 4K, one expects $\varepsilon/1\text{Hz} \approx 3\hbar$.

We have made SQUIDs that should approach the quantum limit in the He^4 temperature range. The fabrication procedures were similar to those used for the single junction, and the following values are typical: $L \approx 2$ pH, $C \approx 0.5$ pF, $I_o \approx 0.5$ mA, $R \approx 1\Omega$. Thus $\beta_c \approx 0.8$ and $\beta \approx 1$. The SQUID was connected across the cooled LC resonant circuits (typically 30, 100, 300 kHz) and the noise measured as for the single junction as a function of bias current and applied flux. The transfer function $\partial V/\partial \Phi$ was also measured by modulating the flux through the SQUID and lock-in detecting the resulting voltage. The best result so far was obtained at 3.4K, where the measured noise at 118 kHz was $3.8\hbar$. By measuring the noise at higher and lower frequencies, however, we estimated that approximately one-half of this noise was 1/f noise, so that the white noise contribution was approximately $2\hbar$, in rather good agreement with the predictions of the model.

CONCLUDING REMARKS

The predictions of the theory for the noise in a single junction are in good agreement with experiment when the effects of resonances are taken into account. The measured noise in dc SQUIDs also agrees well with the predictions of the theory at 3.4K, although it should be realized that the quantum corrections to the noise are small at this temperature for the parameters used. Finally, a more detailed investigation of the theory is necessary to establish the limits of validity of the Langevin approach.

This work was supported by the Director, Office of Energy Research, Office of Basic Energy Sciences, Materials Science Division, U. S. Department of Energy under contract No. W-7405-ENG-48.

REFERENCES

[1] V. Ambegaokar and B. I. Halperin, *Phys. Rev. Lett.* 22, 1364 (1969).

[2] K. K. Likharev and V. K. Semenov, *Pis'ma Zh. Eksp. Teor. Fiz.* 15, 625 (1972) [*JETP Lett.* 15, 442 (1972)].

[3] C. M. Falco, W. H. Parker, S. E. Trullinger, and P. K. Hansma, *Phys. Rev.* B10, 1865 (1974).

[4] R. P. Giffard, P. F. Michelson, and R. J. Soulen, Jr., *IEEE Trans. Mag.* MAG-15, 276 (1979).

[5] C. D. Tesche and J. Clarke, *J. Low Temp. Phys.* 29, 301 (1977).

[6] J. Clarke, *IEEE Trans. Electron Devices* ED-27, 1896 (1980).

[7] R. H. Koch, D. J. Van Harlingen, and J. Clarke, *Phys. Rev. Lett.* 45, 2132 (1980).

[8] R. H. Koch, D. J. Van Harlingen, and J. Clarke, *Appl. Phys. Lett.* 38, 380 (1981).

[9] D. E. McCumber, *J. Appl. Phys.* 39, 3113 (1968); W. C. Stewart, *Appl. Phys. Lett.* 12, 277 (1968).

[10] A. O. Caldeira and A. J. Leggett, *Phys. Rev. Lett.* 46, 211 (1980).

[11] R. F. Voss, R. B. Laibowitz, A. N. Broers, S. I. Raider, C. M. Knoedler, and J. M. Viggiano, *IEEE Trans. Mag.* MAG-17, 395 (1981).

[12] P. Carelli and M. W. Cromar, 1980 Applied Superconductivity Conference, Santa Fe, New Mexico (unpublished).

[13] R. H. Koch, D. J. Van Harlingen, and J. Clarke, 1980 Applied Superconductivity Conference, Santa Fe, New Mexico (unpublished).

QUANTUM NOISE EFFECTS AT HIGH FREQUENCIES AND LOW TEMPERATURES

A. van der Ziel

Electrical Engineering Department
University of Minnesota
Minneapolis, MN 55455

SUMMARY

It is shown how noise measurements at 100 GHz can discriminate between the various thermal noise expressions found in the literature. It is indicated how the noise in tunnel junctions transforms from thermal noise at zero bias to shot noise at sufficiently forward bias; this leads to measurable effects at 100 GHz and 2°K in the 0-1 mV bias range, both for the metal-oxide-metal (MOM) diode and for the Josephson junction. An improved version of the maser noise theory is presented that takes the zero point energy noise term in the thermal noise seriously; omission of this term would result in an earlier, erroneous expression for the maser noise.

1. THERMAL NOISE

According to Nyquist [1] the high-frequency noise os a resistance R kept at the temperature T can be represented by a series emf$[S_E(f)\Delta f]^{1/2}$ in a frequency interval Δf, where

$$S_E(f) = 4R\,\bar{E} \tag{1}$$

and $\bar{E}$ is the average energy of an harmonic oscillator of frequency f kept at the temperature T. At low frequencies $\bar{E} = kT$ and (1) reduces to the well-known expression

$$S_E(f) = 4kTR \tag{2}$$

(Nyquist's low-frequency theorem). At high frequencies quantum effects occur and

$$\bar{E} = 1/2\ hf + hf/[\exp(hf/kT) - 1] \tag{3}$$

where 1/2 hf is the zero point energy term. Nyquist omitted this term and thus obtained

$$S_E(f) = 4hfR/[\exp(hf/kT) - 1]\ . \tag{4}$$

When it is taken into account, however, one has instead

$$S_E(f) = 2hfR + 4hfR/[\exp(hf/kT) - 1] = 2hfR\ \coth(hf/2kT)\ . \tag{5}$$

It is interesting to note that the latter expression may be derived by considering emission and absorption of quanta hf by the electrons of the resistor without any reference to zero point energy considerations [2]. The name "zero point energy noise" for the term 2hfR is thus a misnomer.

At sufficiently high frequencies deviations between Eqs. (2), (4) and (5) occur, and it becomes interesting to determine experimentally which of these expressions is correct.

Efforts are on the way at the University of Florida at 100 GHz, using a Hanbury Brown-Twiss type microwave circuit being developed under the direction of A. D. Sutherland.

To discuss the measurement in more detail, we equate

$$S_E(f) = 4kT_nR \tag{6}$$

and so define an "equivalent noise temperature" T_n. If Eq. (2) is correct we have

$$T_n = T_{n1} = T \tag{6a}$$

at all frequencies; if Eq. (5) is correct we have

$$T_n = T_{n2} = 1/2\ hf/k + (hf/k)/[\exp(hf/kT) - 1] \tag{7}$$

whereas if Eq. (4) is correct

$$T_n = T_{n3} = (hf/k)/[\exp(hf/kT) - 1] = T_{n2} - hf/2k\ . \tag{8}$$

It is now easily shown that $T_{n2} - T_{n1}$ is negligible if $hf/kT \ll 1$. But at 100 GHz we have $hf/2k = 2.40°K$ and with Hanbury Brown-Twiss type circuits one can measure T_n with an accuracy of 0.10°K. Hence at 100 GHz and T = 77°K and 300°K one can discriminate between (6a) and (7) on the one hand and (8) on the other hand. By going down to T = 2.00°K and f = 100 GHz, one has $T_{n2} = 2.88°K$; so the difference $T_{n2}-T_{n1} = 0.88°K$, which can again be measured.

2. NOISE IN TUNNEL JUNCTIONS

According to Tucker [3] the h.f. conductance and the shot noise spectrum $S_I(f)$ of a tunnel junction are given by

$$g(f) = [I(V_o + hf/e) - I(V_o - hf/e)]/(2hf/e) \tag{9}$$

$$S_I(f) = e\{\coth[(eV_o+hf)/2kT]I(V_o+hf/e) + \coth[(eV_o-hf)/2kT]I(V_o-hf/e)\} \tag{10}$$

where I(V) is the current at the bias $V = V_o \pm hf/e$.

At zero bias ($V_o = 0$) this reduces to

$$g(f) = g_o(f) = [I(hf/e) - I(-hf/e)]/(2hf/e) \tag{9a}$$

$$S_I(f) = e\coth(hf/2kT)[I(hf/e) - I(-hf/e)] = 2hfg\coth(hf/2kT) \tag{10a}$$

as expected for thermal noise. For $(eV_o-hf)/2kT > 2.5$ the hyperbolic tangents are unity and the noise is

$$S_I(f) = 2eI(V_o)\,\frac{I(V_o+hf/e) + I(V_o-hf/e)}{2I(V_o)} = 2eI(V_o)\Gamma(V_o) \qquad (11)$$

corresponding to shot noise with a quantum correction factor $\Gamma(V_o)$; the factor differs from unity if the characteristic is strongly curved.

In metal-oxide metal (MOM) diodes near zero bias the characteristic is linear, $I = g_o V$, where $g_o = (dI/dV)_o$ is the 1.f. conductance at zero bias. Hence $g(f) = g_o$ and

$$S_I(f) = g_o\{(eV_o+hf)\coth[(eV_o+hf)/2kT] + (eV_o-hf)\coth[(eV_o-hf)/2kT]\} \qquad (12)$$

so that the available power per unit bandwidth is

$$P_{av}(f) = S_I(f)/4g_o = 1/2\ kT[1/2(x+y)\coth 1/2(x+y) + 1/2(x-y)\coth 1/2(x-y)] \qquad (13)$$

where $x = eV_o/kT$ and $y = hf/kT$. For low frequencies $y = 0$ and

$$P_{av}(0) = kT(1/2\ x \coth 1/2\ x) \qquad (13a)$$

as expected for shot noise. For zero bias $x = 0$ and

$$P_{av}(f) = kT(1/2\ y \coth 1/2\ y) \qquad (13b)$$

as expected for thermal noise, whereas for $1/2(x-y) > 2.5$

$$P_{av}(f) = kT(1/2\ x) \qquad (13c)$$

as again expected for shot noise. At 100 GHz and T = 2.00°K the transition from thermal noise to shot noise lies in the 0-1 mV bias range. We plan to measure it with an MOM diode having a contact diameter of 1 μ meter matched to the waveguide and feeding into a Hanbury Brown-Twiss microwave circuit.

3. NOISE IN JOSEPHSON JUNCTIONS

The Josephson junction is a much more complex device, since it is also an oscillator that produces complicated mixing effects when terminated into a non-zero load. If I(V) is the d.c. short-circuit current at the bias V, then

$$I(V) = I_n(V) + I_p(V) \qquad (14)$$

where $I_n(V)$ and $I_p(V)$ are the currents caused by single electrons and by Cooper pairs, respectively. If $S_{In}(f)$ and $S_{Ip}(f)$ are the corresponding spectra, then the total noise spectrum is

$$S_I(f) = S_{In}(f) + S_{Ip}(f)\ . \qquad (14a)$$

According to Rogovin and Scalapino [4], for a junction driven by a constant voltage source V_o,

$$S_{In}(f) = e\{\coth[(eV_o+hf)/2kT]I_n(V_o+hf/e) + \coth[(eV_o-hf)/2kT]I_n(V_o-hf/e)\} \quad (15)$$

$$S_{Ip}(f) = 2e\{\coth[(2eV_o+hf)/2kT]I_p(V_o+hf/2e) + \coth[(2eV_o-hf/2kT]I_p(V_o-hf/2e)\} \quad (16)$$

which is an extension of Tucker's expression (10).

It is interesting to note that $S_{In}(f)$ behaves normally at the bias $V_o = hf/e$. But $S_{Ip}(f)$ blows up at the bias $V_o = hf/2e$, since $I_p(V_o-hf/2e)$ does not approach zero when V_o approaches hf/2e from the upper side. Since this is also the bias at which the Josephson pair current oscillates at the frequency f, complicated mixing processes will occur when the junction is matched to a waveguide. At 100 GHz the required bias is 0.207 mV. Interesting noise effects should occur and they should be measurable.

4. MASER NOISE

In the early theory of maser noise [5] an error was made, in that Nyquist's expression (4) for the thermal noise was used. We shall now correct this error for a cavity maser and shall show that the resulting expression is more easily understood. The traveling wave maser can be treated similarly.

Let the maser be a two-level system with energies E_1 and E_2 and populations N_1 and N_2. The emitted and absorbed quanta are then $hf = E_2-E_1$, and the conductance of the maser system is

$$g = C(N_1 - N_2) \quad (17)$$

where C is a coupling factor.

With zero pump signal the noise is thermal noise of g, or

$$\overline{i_d^2} = 2ghf\ \Delta f + 4ghf\ \Delta f/[\exp(hf/kT) - 1]\ . \quad (18)$$

But in equilibrium

$$N_1/N_2 = \exp[(E_2 - E_1)/kT] = \exp(hf/kT)\ . \quad (19)$$

Substituting for g and for exp(hf/kT) yields

$$\overline{i_d^2} = 2Chf\ \Delta f(N_1 - N_2) + 4Chf\ \Delta f N_2\ . \quad (20)$$

The first term is due to the zero point energy noise term in (18). It was missing in the earlier theory, so that in that case

$$\overline{i_d^2} = 4Chf\ \Delta f N_2 \quad (20a)$$

Equation (20) may be rewritten as

$$\overline{i_d^2} = 2Chf\ \Delta f(N_1 + N_2) = 2Chf\ \Delta f\ N \qquad (20b)$$

where $N = N_1 + N_2$ is the total number of active atoms. Since this is independent of N_1 and N_2, Eq. (20b) should be valid for arbitrary pump signals.

When the total noise power of the system is evaluated, it is found to be the same for the new and the old theories. But the distribution between the source noise and the device noise is different and hence the two theories give different noise figures and different system noise temperatures.

The first half of Eq. (20b) has a very simple interpretation in that $2Chf\ \Delta fN_2$ is the true spontaneous emission noise and $2Chf\ \Delta fN_1$ is the true absorption noise. They are poissonian noise terms that come about because the elementary emission and absorption events occur independently and at random. Since Eq. (20a) has no such simple interpretation, it should be obvious that Eq. (20b) is correct.

This has ramifications for the thermal noise expression. Since the correct expression for the maser noise came about by taking the zero point energy noise term in the thermal noise expression seriously, it follows that the term actually belongs in the thermal noise expression. Eliminating it would give the wrong maser noise.

This work was done in preparation for a quantum noise project initiated at the University of Florida. The author is indebted to Professors A. D. Sutherland, E. R. Chenette and K. M. van Vliet for their interest and support. For a list of papers see references [6] - [10].

REFERENCES

[1] H. Nyquist, Phys. Rev., 32 (1928) 110.

[2] H. B. Callen and T. E. Welton, Phys. Rev., 83 (1951) 34.

[3] J. R. Tucker, IEEE J. Quantum Electron., 11 (1979) 1234.

[4] D. Rogovin and D. J. Scalapino, Ann. Physics, 86 (1974) 1.

[5] See, e.g., N. Bloembergen, Solid State Masers, in "Progress in Low Temperature Physics", North Holland, Amsterdam, Vol. 3 (1961) 396-429.

[6] A. van der Ziel, J. Gong, W. A. Krull, H. Metha, R. R. Schmidt and M. W. Trippe, Physics, 100B (1980) 97.

[7] A. van der Ziel, J. Appl. Phys., 51 (1980) 2292.

[8] A. van der Ziel, J. Appl. Phys., 51 (1980) 4329.

[9] A. van der Ziel, Physica, 101B (1980) 107.

[10] A. van der Ziel, Physica, 96B (1979) 325; A. van der Ziel, submitted to J. Applied Physics.

A THERMAL ACTIVATION MODEL FOR THE DC-SQUID

Claudia D. Tesche

LuTech, Inc.
P.O. Box 1263
Berkeley, CA 94701

A thermal activation model is described for the dc-SQUID. The device characteristics are derived directly from the features of a two dimensional potential field analogous to the washboard potential for a single current biased junction.

We describe a simple model for the dc-SQUID analogous to the thermal activation models for single junction devices. The dc-SQUID consists of a superconducting loop of inductance L interrupted by two Josephson junctions. The junction parameters are critical current I_o, capacitance C and shunt resistance R. The voltage developed across the junctions, $V = vI_oR$, is a function of the dc bias current $I = iI_o$ and the applied flux $\Phi_a = \phi_a\Phi_o$. The equations of motion can be written in the form [1], [2]

$$\beta_c \frac{d^2\delta_k}{dt^2} + \frac{d\delta_k}{dt} = -\frac{\partial u}{\partial \delta_k} + i_k \qquad k = 1, 2 \tag{1}$$

where the dimensionless time t is in units of $\phi_o/2\pi I_oR$ and the potential satisfies

$$u(\delta_1,\delta_2) = -\cos\delta_1 - \cos\delta_2 - (\delta_1+\delta_2)\, i/2 + \pi\beta j^2/2 \tag{2}$$

and

$$j = (\delta_1 - \delta_2 - 2\pi\phi_a)/\pi\beta. \tag{3}$$

In these equations, $\beta = 2LI_o/\Phi_o$ and $\beta_c = 2\pi I_oR^2C/\Phi_o$. The random currents i_k are generated by the Johnson noise in the shunt resistances.

Equations (1-3) are a set of classical equations of motion for the macroscopic variables δ_1 and δ_2. The form of the potential $U(\delta_1,\delta_2)$ is determined by the macroscopic quantum effects of superconductivity. The phase differences δ_1 and δ_2 are classical variables analogous to the coordinates of a particle moving in a two dimensional potential field. This description is adequate provided the wave function for the position/phase difference is well localized ($\Delta\delta_i \ll 2\pi$).

An example of the potential is plotted in Figure 1 for $i = 0$, $\phi_a = 0.5$ and $\beta = 1.0$.

The potential consists of a chain of wells (L) separated by saddle points (S), all situated within a low potential trough. In the thermal limit ($k_BT \gg 2eI_oR$) the random forces i_k cause the particle to oscillate within the well. Occasionally, the particle makes a classical transition over the saddle point to an adjacent well [3]. The probability P of making a single transition is

$$p = \frac{1}{2\pi}\frac{C_{w1}C_{w2}C_{s1}}{|C_{s2}|}\exp\left(-\frac{\Delta u}{\Gamma}\right) \tag{4}$$

where C_{w1}, C_{w2}, and C_{s1}, $|C_{s2}|$ are the curvatures of the well and saddle expressed in normal coordinates. The factor Δu is the barrier height and $\Gamma = 2\pi k_B T/I_o\Phi_o$.

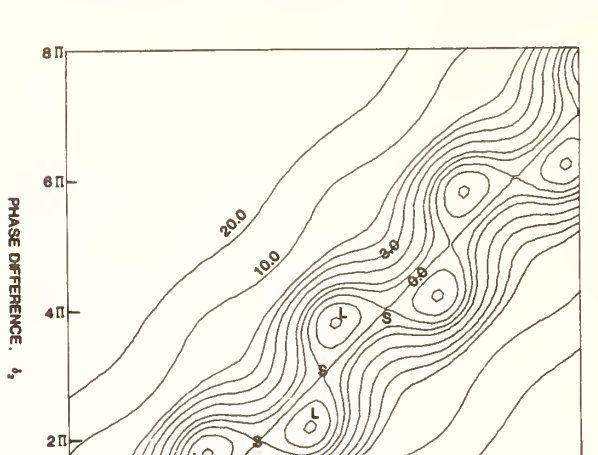

Fig. 1 Contour plot of potential energy u as a function of δ_1 and δ_2 for i = 0, ϕ_a = 0.5 and β = 1.0.

The escape of the particle from one well to the next corresponds to the generation of both a voltage pulse across the SQUID, and a circulating current pulse around the SQUID loop. In the limit $\beta_c << 1$, only one barrier is transversed with transit time τ. As a result, the motion of the particle in the periodic potential is analogous to a renewal counting process for a non-paralyzable counter. For a chain of identical wells, the average voltage $\overline{V} = (I_o R)\ \overline{v}$, where

$$\overline{v} = \frac{2\pi p}{(1+p\tau)} . \tag{5}$$

Fluctuations in the number of pulses produce a voltage noise with low frequency spectral density $S_V^o = S_v^o(k_B TR/\Gamma)$ where

$$S_v^o = 2\,\frac{(2\pi)^2 p}{(1+p\tau)^3} . \tag{6}$$

The circulating current noise, S_J, arises from two sources. A current pulse, j_p, is generated during the transition from one well to the next. Fluctuations in the number of pulses per unit time produce a current noise

$$S_{jp}^o = \frac{2\langle j_p\rangle^2 p}{(1+p\tau)^3} . \tag{7}$$

This contribution to the total current noise is strongly correlated with the voltage noise generated by the voltage pulses. In addition, motion within the well generates a contribution to the current noise which can be readily calculated from the first order correlation theory [4]. The low frequency component is

$$S_w^o = \frac{4\Gamma(a^2+b^2)}{(a+b+\pi\beta ab)^2} \quad \text{where } a = \cos\delta_{1L},\ b = \cos\delta_{2L}. \tag{8}$$

Note that this contribution is appreciable even at low bias currents, where the pulse rate p is very small (Figure 2).

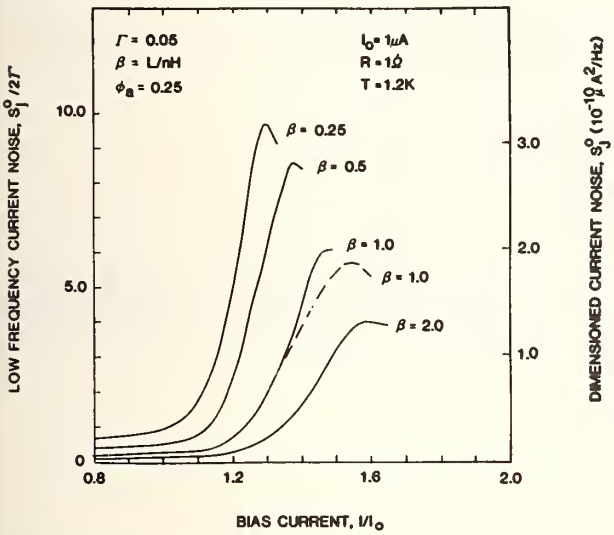

Fig. 2 Low Frequency noise spectral density S_j^o as a function of loop inductance L. The dashed curve is from a numerical simulation [5]. The smooth curves are from the thermal activation model.

If the potential consists of a chain of dissimilar wells, the analysis is more involved. In particular, if the circulating current in successive wells varies (see Figure 1), the low frequency current noise may increase dramatically [5]. If the circulating current in the wells alternates between values j_1 and j_2, switching noise will be observed. For escape probabilities p_1 and p_2, the current noise at frequency f is

$$S_j(f) = \frac{4j_s^2 p_1 p_2}{(p_1+p_2)} \frac{1}{(4\pi^2 f^2+\mu^2)} \tag{9}$$

where $j_s = (j_1 - j_2)$ and $\mu = p_1 + p_2$. At frequencies $f \ll \mu$, the spectral density is white,

$$S_j^o = \frac{4j_s^2 p_1 p_2}{(p_1+p_2)^3} . \tag{10}$$

Near zero bias current, p_1 and p_2 are small. Thus the switching noise dominates the well and pulse noise sources. As an example, we plot S_j^o as a function of applied flux in Figure 3 for $i = 0$, $\phi_a = 0.5$. Note that the current noise scales with the shunt resistance, $S_J \propto 1/R$. The critical current asymmetry parameter $\alpha = (I_{01} - I_{02})/2I_o$.

The results quoted above have been derived for a dc SQUID with junctions in the thermal limit. In general, for a lumped circuit element model, the Johnson noise currents are generated by fluctuations in the voltage across the shunt resistances. These fluctuations in the electromagnetic field are in thermal equilibrium with the resistors at temperature T. The power spectral density in this case is white. However, for junction parameters $k_B T \lesssim 2eI_oR$, the power spectral density of the thermal fluctuations near the junction resonances will roll off like $S_E \sim \hbar\omega \exp(-\hbar\omega/k_BT)$ [6]. As a result, the formalism developed by Kramers (Eqn. 4) cannot be used. In this regime, the interaction between the electromagnetic field ("zero point term") and the junction currents must be treated with care. It is not obvious that the purely classical expression for the junction phase differences (Eqs. 1-3) are adequate in this case. Furthermore, the assumption that the wave functions for δ_1 and δ_2 are well localized may break down, and macroscopic tunneling effects may be observed.

REFERENCES

[1] Claudia D. Tesche, Ph.D. Thesis, University of California, Berkeley (1978).

[2] C.D. Tesche and J. Clarke, J. Low Temp. Phys. 29, 301 (1977).

[3] H.A. Kramers, Physica 7, 284 (1940).

[4] C.D. Tesche, A Thermal Activation Model for the DC SQUID, accepted for publication in J. Low Temp. Phys.

[5] C.D. Tesche and J. Clarke, J. Low Temp. Phys. 37, 397, (1979).

[6] Herbert B. Callen and Theodore A. Welton, Phys. Rev. 83, 34 (1951).

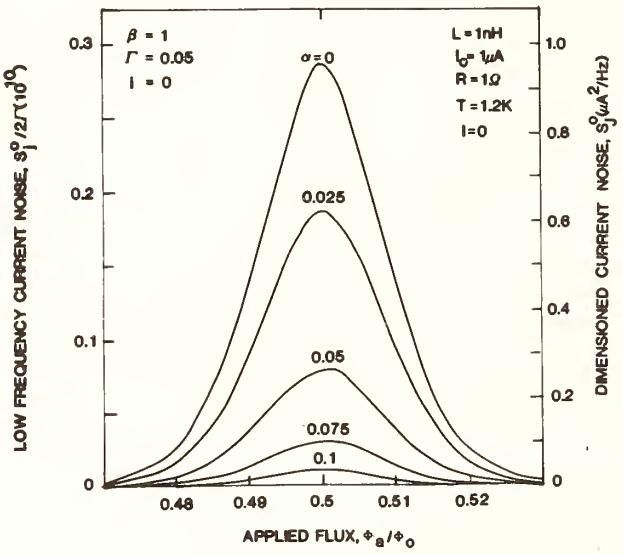

Fig. 3 Current switching noise spectral density S_j^o as a function of critical current asymmetry α and applied flux ϕ_a for i = 0 and β = 1.0.

The corresponding characteristic frequency is plotted in Figure 4. Note F_μ α R.

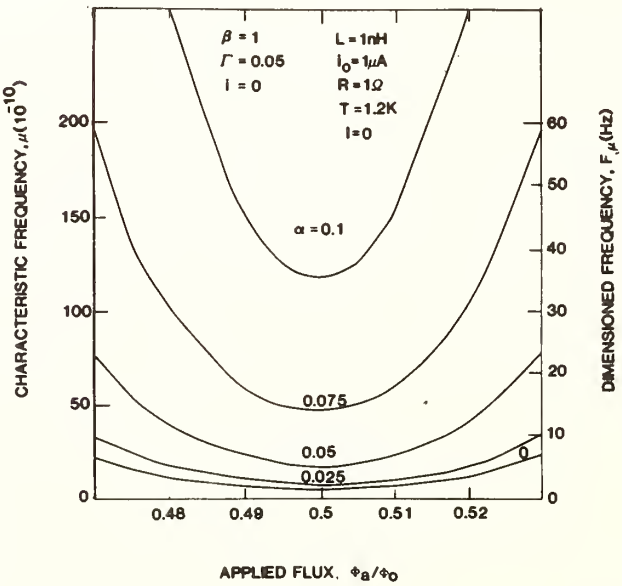

Fig. 4 Characteristic frequency μ for current switching noise as a function of critical current asymmetry α and applied flux ϕ_a.

ULTIMATE SENSITIVITY OF AN AC-SQUID

Juhani Kurkijärvi

School of Mathematical and Physical Sciences
University of Sussex
Brighton BN1 9QH
Sussex UK

If one could cool an ac-SQUID to the temperature T = 0, it still would not become a perfect magnetometer. There is an absolute limit on the noise flux of the instrument, the superconducting condensation energy lost in excluding the flux, which cannot be measured better than within the limits of the uncertainty principle

$$\frac{\delta\phi_x^2}{2L}\tau \geq \frac{\hbar}{2} \tag{1}$$

where L is the inductance of the SQUID ring, ϕ_x the external flux to be measured, and τ the time used for the measurement or the inverse frequency band width. It is suggested in this paper that a limit of a similar form

$$\frac{\delta\phi_x^2}{2L}\tau \geq \hbar\pi\sqrt{\frac{L}{C}}\frac{C}{RC} \tag{2}$$

arises from the zero point uncertainty of the flux admitted through the ring in conjunction with a construction requirement of the instrument, the necessity of making the SQUID ring Josephson junction "overdamped". Here C is the capacitance of the junction and R the normal current resistance across the junction, which is assumed to make sense even at T = 0.

There is the possibility, in principle, that collective quantum tunneling of the flux variable through a potential barrier [1] could play a role in this context, but this seems improbable [2] after the recent work on the effect of friction on quantum tunneling [3] .

The sensitivity of the ac-SQUID is determined by the accuracy with which the hysteresis loop in the external flux ϕ_x versus admitted flux ϕ plane is always triggered at the same value of ϕ_x, or at higher frequencies, how precisely the somewhat deformed loop is reproduced at each ac cycle of the instrument. The flux moves, at a given ϕ_x, in the potential

$$V(\phi) = \frac{1}{2L}(\phi - \phi_x)^2 - i_c\frac{\phi_o}{2\pi}\cos\frac{2\pi\phi}{\phi_o} \tag{3}$$

which has a hollow with a minimum at a very small value of ϕ till ϕ_x reaches a critical value ϕ_{xc} at which the hollow disappears. Here i_c is the critical current of the junction and ϕ_o the flux quantum. When ϕ_x is swept sinusoidally, ϕ either always stays in the (metastable) hollow and remains small or rolls down into a deeper minimum triggering a hysteresis loop if the amplitude of ϕ_x is large enough. It is the uncertainty in the triggering amplitude of ϕ_x which determines the intrinsic noise of the SQUID. At high temperatures chance scaling of the barrier with the aid of thermal fluctuations leads to an uncertainty in the measured flux [4] . In this paper we are interested in the uncertainty coming from the fact that the value of ϕ at the bottom of the hollow is uncertain by roughly the width of its harmonic oscillator ground state. We assume that there is no tunneling or thermal barrier penetration.

Then clearly a small uncertainty arises simply from the possibility that the flux may return into the metastable valley upon reduction of ϕ_x although it could have escaped but happened to be "on the wrong side" and did not have time to take advantage of the momentarily vanishing barrier at the peak value of ϕ_x. One understands immediately that such a process is influenced by the frequency of the sinusoidally driven ϕ_x. A scaling argument is given at the end of this paper showing that the increasing uncertainty from this source at higher frequencies is exactly cancelled by the statistical factor $(f\tau)^{1/2}$, the square root of the frequency multiplied by the measuring time, ie the number of measurements performed. Thus the maximum flux sensitivity implied by the uncertainty in ϕ is independent of the rf-frequency of the SQUID.

Why should the flux be uncertain at the bottom of the potential trough? If one writes down the well known resistively shunted junction differential equation for ϕ in a SQUID ring, linearises the potential term (ie considers the harmonic motion at the bottom of a potential valley) and imagines the system driven by the noise current at T = 0

$$I_n^2(\omega) = \frac{\hbar\omega}{\pi R} \coth \frac{\hbar\omega}{2k_B T} = \frac{\hbar\omega}{\pi R} \tag{4}$$

one can solve for $\phi^2(\omega)$ and integrate this quantity over ω to get the mean square spread of the flux. The result is exactly the harmonic oscillator ground state width $\hbar/(2C\omega_o)$ if the damping term is small and a narrower peak by the factor

$$\frac{1}{\pi} \frac{\omega_o}{\eta} \log \frac{1}{\beta}$$

in the case of large damping

$$\beta = {}^{\omega_o}/_{\eta} = RC\omega_o << 1,$$

ω_o being the oscillation frequency in the trough. Caldeira [6] has investigated an explicit model of friction for the harmonic oscillator with identical results.

One can now use the independence on the frequency of the noise considered in this paper to estimate this noise at a particular frequency where it is best known. Such a frequency is ${\omega_o}^2/_{\eta}$ at which one expects the uncertainty in ϕ_x to be roughly the same as the uncertainty of ϕ. ${\omega_o}^2/_{\eta}$ is the frequency at which the damped flux (classically) in the trough can just follow the external frequency leading to parallel trajectories of ϕ in the (ϕ_x, ϕ) plane under the sinusoidal drive of ϕ_x. Estimating the harmonic ground state spread of ϕ as

$$\frac{\hbar}{2C} \sqrt{LC}$$

a somewhat pessimistic assumption in the overdamped case, one gets eq (2) for the ultimate energy sensitivity of a SQUID. At frequencies where the parameter [4]

$$X = 0.1 \frac{R}{\omega_{rf} L} \left(\frac{2k_B TL}{\phi_o^2} \right) \left(\frac{i_c \phi_o}{2\pi k_B T} \right)^{1/3}$$

becomes comparable to unity or smaller, the present argument can be used at finite temperature as well, with the result

$$\frac{d\phi_x^2}{2L} \tau \geq 2\pi \frac{L}{R} k_B T \tag{5}$$

where $k_B T$ has been substituted for zero point energy. An experimental value at this limit has been claimed [7] but judged controversial [8]. Theoretical estimates similar to the present results have been given for the dc-SQUID [9].

We now return to the scaling argument which establishes that the noise originating in the uncertainty of ϕ is independent of the rf-frequency of the SQUID. The argument rests on the observation that the equilibrium ϕ versus ϕ_x curve of the SQUID ring

$$\phi = \phi_x - L_{ic} \sin \frac{2\pi\phi}{\phi_o} \tag{6}$$

looks like $\phi_c - \phi = \sqrt{\phi_{xc} - \phi_x}$ in the vicinity of ϕ_{xc}. If instead of a given range of ϕ_x we observe a larger range $k^\alpha \phi_x$, ie. instead of the point ϕ_x pick the point $k^\alpha \phi_x$, and scale ϕ by the factor $k^{\alpha/2}$, the shape of the trajectory remains the same. When ϕ_x is driven sinusoidally ϕ follows roughly the curve (6) but tends to have difficulties in the ever sharper and sharper turn before ϕ_{xc}. The deviation occasioned by the "centrifugal force" must be compensated by the balancing harmonic force in the potential trough. The corresponding equation of motion reads

$$\frac{d^2\phi}{d\phi_x^2}\left[2(\Delta\phi_x + \Delta)\phi_A\omega_{rf}^2\right] - \frac{d\phi}{d\phi_x}(\phi_A\omega_{rf}^2) = \omega_o^2\Delta\phi \tag{7}$$

where $\Delta\phi_x = \phi_{xc} - \phi_x$ and Δ is the overshoot of the drive amplitude ϕ_A beyond the point ϕ_{xc}, $\Delta = \phi_A - \phi_{xc}$ and $\Delta\phi$ is the deviation of ϕ from the equilibrium position. The quantity ω_o is proportional to $(\Delta\phi_x)^{1/4}$. The scaling suggested above together with scaling ω_{rf} by k leaves the equation of motion unchanged if $\alpha = 4/3$. Therefore, after this scaling, the trajectories in the (ϕ_x, ϕ)-plane are similar at different frequencies. In the particular expanded frame at each frequency we can safely assume that the uncertainty of ϕ_x, $\delta\tilde{\phi}_x$, is proportional to the uncertainty $\delta\phi$ in ϕ as observed in that frame. Then the harmonic oscillator ground state width of ϕ scales like $k^{\alpha/2}/k^{\alpha/8} = k^{3\alpha/8}$ and $\delta\tilde{\phi}_x \sim \delta\phi \sim k^{1/2}$ where the tilda on ϕ_x underlines that the statistical factor $(f\tau)^{-1/2}$ has not been included yet. After dividing with $(f\tau)^{1/2}$ we have $\delta\phi_x \sim k^0$.

REFERENCES

[1] A J Leggett, Journal de Physique Colloque C6 (1978)

[2] J Kurkijärvi, submitted to JLTP

[3] A O Caldeira and A J Leggett, Phys Rev Lett 46, 211 (1981)

[4] J Kurkijärvi and W W Webb, Proceeding of the 1972 Applied Superconductivity Conference, Annapolis, IEEE Conf Rec No 72CHo282-5TABSC

[5] E E H Shin and B B Schwartz, Phys Rev 152, 207 (1966)

[6] A O Caldeira, PhD thesis, University of Sussex, unpublished

[7] A P Long, T D Clark and R J Prance, Rev Sci Instrum 51, 8 (1980)

[8] J Clarke in SQUID '80, Proceedings of the Second International Conference on Superconducting Devices, de Gruyter, Berlin, New York 1980

[9] C D Tesche and J Clarke, J Low Temp Phys 29, 301 (1977)

The Mean Lifetimes of the Meta-Stable States of the DC-SQUID and its I-V Characteristics

Eshel Ben-Jacob*

Department of Physics and Astronomy, Tel Aviv University 69978 Tel Aviv Israel

Zeev Schuss**

Department of Applied Mathematics, School of Mathematics, Tel Aviv University

69978 Tel Aviv Israel

1. Introduction

The DC-SQUID with small coupling ($LI_J > h/2e$, where L is the self inductance and I_J is the junctions critical current) has several types of meta-stable states[1,2] and therefore it can be used as a logic element. At a finite temperature the thermal noise causes spontaneous transitions between the various states. Hence, the meta-stable states have finite mean lifetimes. It is of interest to know the dependence of these lifetimes on the DC-SQUID parameters, on the external driving current I and on the external magnetic flux ϕ_{ex}.

Here we find this dependence for the shunted DC-SQUID ($\beta_c < 1$). In this case we use the Smoluchowski approximation of the Fokker-Planck equation.[3] The resulting problem is equivalent to the exit problem of particle out of two dimensional potential well, a case for which Kramers' results[4] can not be used and have to be extended. Such an extension was done by Landauer and Swanson.[5] Here, however, we present a new method based on the results of Matkowsky and Schuss.[3,6] Using this method we compute the mean lifetime in a two dimensional potential well with several saddle points on its boundary and the relative probability of exit through each saddle point. We use these results to construct the I-V characteristics of the DC-SQUID. We find satisfactory agreement between our analytical results and the numerical simulations of Teshe and Clarke.[7] We note that the method we present can be applied to elements containing more than two coupled Josephson junctions.

2. The Meta-Stable States

We consider DC-SQUID which consists of two identical Josephson junction and which is driven by an external current source I and an external magnetic flux ϕ_{ex}, as shown in fig. 1. Assuming the RSJ model[8,9] for the junctions we obtain the following equations of motion for θ_i's, the phase differences across the junctions[2]:

$$\begin{aligned} \ddot{\theta}_1 + G\dot{\theta}_1 + \sin\theta_1 &= \frac{I}{2I_J} - K(\theta_1-\theta_2+\theta_{ex}) \\ \ddot{\theta}_2 + G\dot{\theta}_2 + \sin\theta_2 &= \frac{I}{2I_J} + K(\theta_1-\theta_2+\theta_{ex}) \end{aligned} \qquad (2\text{-}1)$$

where

$$G \equiv (\omega_J RC)^{-1} \equiv \beta_c^{-\frac{1}{2}} \; ; \; \omega_J^2 \equiv \frac{2eI_J}{\hbar C}$$
$$K \equiv \frac{\phi_0}{2\pi LI_J} \; ; \; \theta_{ex} \equiv \frac{2\pi\phi_{ex}}{\phi_0} \; ; \; \phi_0 \equiv \frac{h}{2e} \qquad (2\text{-}2)$$

R and C are the resistance and capacitance of the junctions and time is measured in units of ω_J^{-1}. Assuming the ring is made of a superconductor whose thickness is bigger than the London penetration depth, we have

$$\theta_2 - \theta_1 = \frac{2\pi\phi}{\phi_0} \qquad (2\text{-}3)$$

where ϕ is the total magnetic flux through the ring.

Equations (2-1) can be interpreted as the equations of motion of a particle with unit mass and dissipation G in a two dimensional field derived from the potential $U(\theta_1,\theta_2)$ given by

$$U(\theta_1,\theta_2) = \tfrac{1}{2}K(\theta_1-\theta_2+\theta_{ex})^2 - \cos\theta_1 - \cos\theta_2 - \frac{I}{2I_J}(\theta_1+\theta_2) \qquad (2\text{-}4)$$

Note that the energy is measured in units of $\phi_0 I_J/2\pi$.

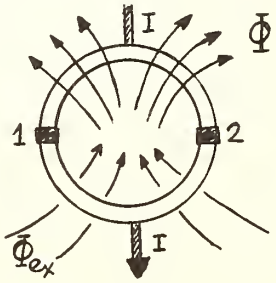

Fig. 1. The DC-SQUID model.

For a sufficiently small external current I there exist meta-stable states which are the static solutions $\dot{\theta}_i = 0$, corresponding to those values of θ_1, θ_2 where the potential has local minima. The meta-stable states are located on lines parallel to the main diagonal $\theta_1 = \theta_2$. Such lines are characterized by the integer number of fluxons passing through the ring, when the ring is at one of the meta-stable states located on a particular line. For example, at the meta-stable states along lines a in fig. 2, no fluxons pass through the ring. At points of local minimum along lines b in that figure one fluxon passes through the ring in the direction of ϕ in fig. 1 (thus the integer value of ϕ/ϕ_0 is +1). Along lines c the value is -1 and along line d in fig. 2b - +2. The number of lines of meta-stable states increases as K decreases and for $K \lesssim 1/2\pi$ there are no lines outside the main diagonal (fig. 2a). For $\phi_{ex} = 0$ and $K < 1/2\pi$ for values of I in the range

$$\frac{I}{2I_J} \gtrsim 1 - 2\pi K \qquad (2\text{-}5)$$

there are no meta-stable states outside the main diagonal. For any $K \lesssim 1/2\pi$ and any $\frac{I}{2I_J} \lesssim 1-2\pi K$ there are no lines of $\phi/\phi_0 = \pm 1$ if θ_{ex} is

$$K|\theta_{ex}| \gtrsim 1 - \frac{I}{2I_J} - 2\pi K \qquad (2\text{-}6)$$

respectively. From the foregoing description it can be seen that the DC-SQUID can be used as a logic element whose values are the different meta-stable states and the control variables are I and ϕ_{ex}.

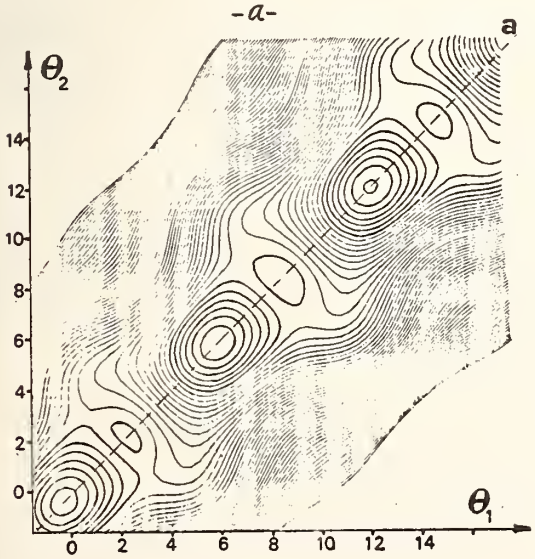

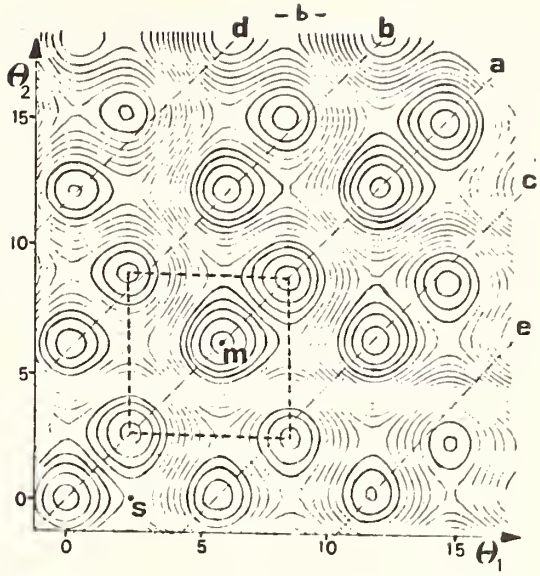

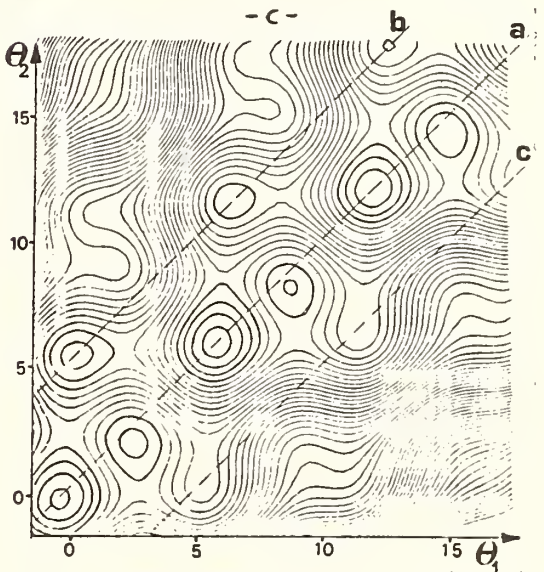

Fig. 2. Equipotential curves for $U(\theta_1, \theta_2)$ for $I/I_J = 0.5$ (a) $K = 1/\pi$, $\theta_{ex} = 0$, no meta-stable states outside the main diagonal line a. (b) $K = 0.02$, $\theta_{ex} = 0$, meta-stable states appear on diagonal lines b,c etc., see discussion in text. The domain D enclosed by the dashed line is the domain of attraction of the point M, which is the minimum of $U(\theta_1, \theta_2)$ in D. The point S is a sadlde point connecting two adjacent domains of attraction. (c) $K = 0.1$, $\theta_{ex} = \pi/2$. No metastable states on line c.

3. Thermal Noise and the Smoluchowski Equation

At finite temperature, spontaneous transitions between the meta-stable states will occur, thus these states will have finite lifetimes. Our purpose is to study the dependence of the expected lifetimes on the DC-SQUID parameters and I and ϕ_{ex}. We start by assuming that the

thermal fluctuations can be described by an additive Langevin noise term in the equations of motion[2,7] (eq. (2-1))

$$\ddot{\theta}_1 + G\dot{\theta}_1 + \sin\theta_1 = \frac{I}{2I_J} - K(\theta_1-\theta_2+\theta_{ex}) + j_1(t)$$

$$\ddot{\theta}_2 + G\dot{\theta}_2 + \sin\theta_2 = \frac{I}{2I_J} + K(\theta_1-\theta_2+\theta_{ex}) + j_2(t) \qquad (3\text{-}1)$$

where $j_i(t)$ represent independent Gaussian white noises,

$$\langle j_i(t)\rangle = \langle j_1(t)j_2(t)\rangle = 0$$

$$\langle j_i(t)j_i(t')\rangle = 2G\Gamma\,\delta(t-t') \qquad (3\text{-}2)$$

$$\Gamma \equiv K_B T \Big/ \frac{\phi_0 I_J}{2\pi}$$

The lifetimes as well as the I-V characteristics can be calculated by numerical simulations of equations (3-1). Such an approach for the calculation of the I-V characteristics is presented in ref. 7. However, in this reference the case $K > \frac{1}{2\pi}$ (no meta-stable states outside the main diagonal) was considered.

In order to calculate the lifetime analytically we would like to write an equation for the distribution function. Since we consider the case of large dissipation (shunted junctions, G>>1) we can use the Smoluchowski approximation[3] to write the following equation for the probability density $\rho(\theta_1,\theta_2,t)$

$$\frac{\partial\rho}{\partial t} = \hat{S}\cdot\rho \equiv -\mathrm{div}\,\vec{J}$$

$$\hat{S} \equiv \frac{\Gamma}{G}\frac{\partial^2}{\partial\theta_i^2} + \frac{1}{G}\frac{\partial^2 U}{\partial\theta_i^2} - \frac{1}{G}\frac{\partial U}{\partial\theta_i}\frac{\partial}{\partial\theta_i} \qquad i = 1,2$$

$$J_i \equiv -\frac{1}{G}\frac{\partial U}{\partial\theta_i}\rho - \frac{\Gamma}{G}\frac{\partial\rho}{\partial\theta_i} \qquad (3\text{-}3)$$

Kramer's approach for calculating the exit time from the Smoluchowski equation was applied in ref. 10 to the case of overdamped single junction. However, this approach fails in two dimensions as $\frac{\partial\rho}{\partial t} = -\mathrm{div}\,\vec{J} = 0$ does not imply $\vec{J} = \mathrm{const}$. The first result in higher dimensions for the mean life time in a potential well with single saddle point was given in ref. 5. Here we shall use the method of ref. 6 which will enable us to calculate the mean lifetime of potential well with number of saddle points and the relative exit probability through each of these points.

4. Exit Probabilities and Mean Lifetime of Two Dimensional Potential Well.

One of our purposes is to calculate the exit probability density through the boundary ∂D of D, the domain of attraction of some meta-stable point (see fig. 2). It can be proved that this probability P is the Green's function solution of the following boundary value problem[3]

$$\hat{S}^*P = 0 \quad \text{in} \quad D$$

$$P = \delta(\vec{\theta}-\vec{\theta}_0) \quad \text{on} \quad \partial D \qquad (4\text{-}1)$$

where $\vec{\theta}$ indicates a point θ_1,θ_2, and $\hat{S}^*$ is the operator conjugate to $\hat{S}$.

The other purpose is to calculate the mean first passage time to the boundary $\bar{\tau}$ of a particle which starts inside the domain D. It can be proved that $\bar{\tau}$ is the solution of the following boundary problem[3]

$$\hat{S}^*\bar{\tau} = -1 \quad \text{in} \quad D$$

$$\bar{\tau} = 0 \quad \text{on} \quad \partial D \qquad (4\text{-}2)$$

First we consider eq. (4-1), and use the following observation. If u satisfies

$$\hat{S}^*u = 0 \quad \text{in} \quad D$$

$$u = f \quad \text{on} \quad \partial D \qquad (4\text{-}3)$$

then

$$u = \oint_{\partial D} f\cdot p\, d\vec{\theta} \qquad (4\text{-}4)$$

Thus, we shall construct an asymptotic solution to (4-3) and recover P from (4-4).

The solution is based on the observation that u is approximately constant inside D and changes rapidly near the boundary to satisfy the boundary condition. This observation can be understood as follows: Using a power series expansion in the temperature Γ we see that the leading term u_0 which is the solution of eq. (4-3) for zero temperature has to be a constant along the characteristics of the equation. Now, since all characteristics converge to the meta-stable state in D (the minimum of the potential in the domain) u_0 should have the same value throughout D.[6] At finite small temperature there must be a boundary layer to connect u_0 with the boundary value f. Using local coordinates near the boundary we obtain

$$u(\vec{\theta}) \underset{\sim}{=} u_0 + (f(\theta')-u_0)\left[1-\mathrm{ERF}\left(y\left(\frac{2\omega_N^2}{\Gamma}\right)^{1/2}\right)\right] \qquad (4\text{-}5)$$

where $\vec{\theta}'$ is the boundary point closest to $\vec{\theta}$, y is the distance $|\vec{\theta}-\vec{\theta}'|$ and $-\omega_N^2$ is the sec-

ond normal derivative of the potential at $\vec{\theta}'$. (ERF indicates error function.) To determine u_0 we use the quasi-equilibrium distribution $\rho = \rho_0 \exp(-U/\Gamma)$ inside D to write eq. (4-3) in the form

$$\nabla\rho\nabla u = 0 \qquad (4\text{-}6)$$

Note that in the one dimensional case eq. (4-6) yields $\rho\nabla u = \text{const.}$ so that u_0 can be easily determined. In the two dimensional case we integrate eq. (4-6) over D and using the divergence theorem we obtain

$$\oint_{\partial D} \rho \frac{\partial u}{\partial n} d\vec{\theta} = 0 \qquad (4\text{-}7)$$

Evaluating the normal derivative $\partial u/\partial n$ with eq. (4-5) we obtain

$$u_0 \tilde{=} \oint_{\partial D} e^{-\frac{U}{\Gamma}} \omega_N \, f \, d\vec{\theta} \Big/ \int_{\partial D} e^{-\frac{U}{\Gamma}} \omega_N d\vec{\theta} \qquad (4\text{-}8)$$

Hence using eq. (4-4) we have

$$p = e^{-U/\Gamma} \Big/ \oint_{\partial D} \omega_N e^{-U/\Gamma} d\vec{\theta} \qquad (4\text{-}9)$$

We see that the exit probability density is concentrated about the lowest saddle points on the boundary ∂D and have a Gaussian shape of width $(\sqrt{\Gamma}/\omega_T)$ where ω_T is the frequency of vibration in the saddle point in the direction tangent to ∂D.

Next we compute the mean lifetime by considering eq. (4-2). Since $\bar{\tau}$ grows exponentially in $1/\Gamma$ for small temperature we rescale by setting $\bar{\tau} = c_1 u e^{c_2/\Gamma}$ where $\max(u) = 1$ and c_1 and c_2 are constants to be determined. Constructing a boundary layer for u as above (i.e. c_1=1 and f=0 in (4-5) we immediately obtain

$$\bar{\tau} = c_1 e^{c_2/\Gamma} \, \mathrm{ERF}\left[y\left(\frac{2\omega_N^2}{\Gamma}\right)^{1/2}\right] \qquad (4\text{-}10)$$

In order to determine c_1, c_2 we multiply eq. (4-2) by the quasi-equilibrium distribution ρ and integrate over D. proceeding as above we obtain

$$1/\bar{\tau} = \frac{\sum \omega_N/\omega_T \, e^{-\Delta U_{min}/\Gamma}}{2\pi \, \omega_1 \omega_2} \qquad (4\text{-}11)$$

where $\Delta U_{min} = U_{sad} - U_{min}$, U_{sad} and U_{min} are the values of U at the lowest saddle point and at the minimum respectively. ω_1 and ω_2 are the resonant frequencies at the minimum and the summation is over all lowest saddle points. The contribution of the higher saddle points can be incorporated into (4-11) by adding exponentials with the appropriate values of ΔU and ω. However for $\Delta U - \Delta U_{min} \gg \Gamma$ the contribution of such a saddle point is negligible.

5. Computations of the Mean Lifetimes and the I-V Characteristics

We use eq. (4-11) for the computation of the mean lifetime of the meta-stable states described in section 2. The saddle points ΔU, ω_N, ω_T, ω_1 and ω_2 were evaluated numerically from the potential equation (2-4). The dependence of $\bar{\tau}$ on I, thus obtained, is shown in fig. 3. for various values of K and θ_{ex} and for temperature $\Gamma = 0.05$. For other values of the temperature the corresponding graph can be obtained from fig. 3. since $\ell n(1/\bar{\tau})$ is linear in $1/\Gamma$.

We see in fig. 3. that for smaller values of the coupling constant K the mean lifetime of the meta-stable states on the main diagonal (lines a in fig. 2) becomes shorter (see the dotted curve 0 relative to the solid curve 0). On the other hand the mean lifetime of the meta-stable states on the diagonal $\phi/\phi_0 = \pm 1$ (lines b, c in fig. 2) becomes much longer (See the dotted curve 1 relative to the solide curve 1). For $\theta_{ex} > 0$ the mean lifetime on the diagonal $\phi/\phi_0 = -1$ is shorter than the mean lifetime on the diagonal $\phi/\phi_0 = +1$. If θ_{ex} is sufficiently large (fig. 2c) the

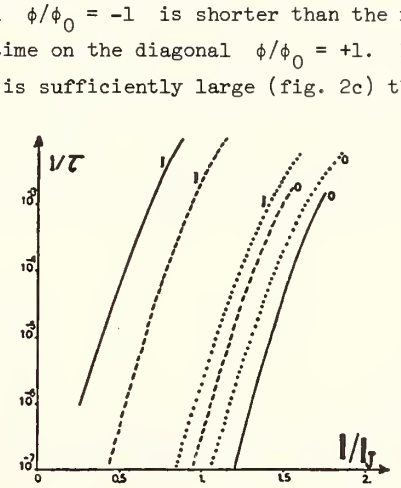

Fig. 3. $1/\bar{\tau}$ vs I/I_J, $\Gamma = 0.05$. The curves 0 correspond to metastable states on the main diagonal a of fig. 2. Curves 1 correspond to the diagonal $\phi/\phi_0 = 1$ (lines b in Fig. 2). The solid curves correspond to K = 0.1, $\theta_{ex} = 0$. The dashed curves correspond to K = 0.1, $\theta_{ex} = \pi/2$. The dotted curves correspond to K = 0.02, $\theta_{ex} = 0$.

meta-stable states on the line $\phi/\phi_0 = -1$ disappear altogether. In this case fig. 3 also shows the dependence of the mean life-time of the meta-stable states $\phi/\phi_0 = +1$ and $\phi/\phi_0 = 0$ on θ_{ex} (see the dashed curves 1 and 0 relative to the solid curves 1 and 0).

For convenient comparison with experiments or with existing numerical simulations of eq. (3-1), we have constructed the I-V characteristics. This was done with the aid of the relative probabilities of exit through the various saddle points (eq. (4-9)). The I-V characteristics for three cases is shown in fig. 4. It can be seen that our analytical results are in good quantitative agreement with the numerical simulations of ref. 7.

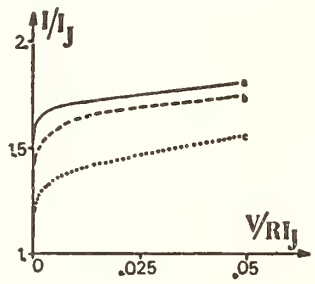

Fig. 4. The I-V characteristics in presence of thermal noise $\Gamma = 0.05$. (a) $K = 1/\pi$, $\theta_{ex} = 0$ (b) $K = 0.1$, $\theta_{ex} = 0$ (c) $K = 0.1$, $\theta_{ex} = \pi/2$.

The authors wish to express their gratitude to Ms. R. Shainsky for carrying out the numerical computations.

References

* Partially supported by Grant from the US-ISRAEL Binational Science Foundation BSF.
** Partially supported by Grant from the A.F.O.S.R.

[1] T.A. Fulton, L.N. Dunkleberger, R.C. Dynes, Phys. Rev. B-6 855 (1972).
[2] E. Ben-Jacob, Y. Imry, Submitted to J. Appl. Phys.
[3] "Theory and Applications of Stochastic Differential Equations" by Z. Schuss, John Wiley and Sons, N.Y. (1980).
[4] H.A. Kramers, Physica 7 284 (1940)
[5] R. Landauer, J.A. Swanson, Phys. Rev. 121 1668 (1961).
[6] B. Matkowsky, Z. Schuss, SIAM J. Appl. Math. 33 230 (1977).
[7] C.D. Tesche, J. Clarke, J. Low Temp. Phys. 29 301 (1977).
[8] W.G. Stewart, Appl. Phys. Lett. 12 277 (1968).
[9] D.E. McCumber, J. Appl. Phys. 32 3113 (1968).
[10] V. Ambegaokar, B.I. Halperin, Phys. Rev. Lett 22 1364 (1969).

EXTERNAL FIELD EFFECT ON PARTICLE DIFFUSION ABOVE A POTENTIAL BARRIER*

Eshel Ben-Jacob and David Bergman

Department of Physics and Astronomy, Tel Aviv University, Tel Aviv, 69978, Israel.

Benny Carmeli and Abraham Nitzan

Department of Chemistry, Tel Aviv University, Tel Aviv, 69978, Israel.

INTRODUCTION

Kramers' treatment of chemical reactions as a diffusion of a brownian particle above a potential barrier[1,2] has long become a starting point for many studies of thermally activated processes. Chemical reactions[1,3], surface desorption[4], diffusion of atoms in solids and on solid surfaces[5] and transition between the equilibrium states of a hysteretic Josephson junction[6] are but a few examples for the applicability of this model.

While Kramers' treatement focuses on thermal activation alone, recent experimental developments have made it increasingly desirable to consider this model in the presence of an external periodic force. Thus multiphoton dissociation and isomerization of molecules in high pressure gas or in condensed phases[7], the possibility of laser assisted desorption[8] and transitions in current driven Josephson junctions under the influence of microwaves[9] can all be modelled as a diffusion of a particle above a potential barrier under the influence of an externally induced oscillating force. In the present work, we solve this problem for the model depicted in Fig.1: a particle of mass m moving in a one dimensional harmonic potential well (characterized by the frequency ω_0) with a given transition threshold ($E_{th}=\frac{1}{2}m\omega_0^2 x_{th}^2$) under the influence of an oscillating force $a(t)=A\sin\omega t$ and of thermal dissipation and noise. Our aim is to derive an expression for the steady state rate of transition out of the well.

The equation of motion is

$$\ddot{X} + G\dot{X} + \omega_0^2 X = \bar{A}\sin\omega t + R(t) \qquad (1)$$
$$(x < x_{th})$$

where (k_B being the Boltzmann constant and T the temperature)

$$\langle R(t_1)R(t_2)\rangle = 2G\Gamma\delta(t_1 - t_2);\ \Gamma = k_B T/m \qquad (2)$$

In the absence of noise (T=0) the steady state solution of Eq.(1) is

$$X(t) = \bar{X}(t) \equiv \frac{\omega_0^2 - \omega^2}{\Omega}\bar{A}\sin\omega t - \frac{G\omega}{\Omega}\bar{A}\cos\omega t \qquad (3a)$$

where

$$\Omega = (\omega_0^2 - \omega^2)^2 + G^2\omega^2 \qquad (3b)$$

when noise is present the distribution $P(x,\dot{x},t)$ may be obtained exactly by standard mentods. The result is:

$$P(x,\dot{x},t) = \frac{\omega_0}{2\pi\Gamma}\exp\{-[\omega_0^2\,(x - \bar{x}(t))^2 + (\dot{x} - \dot{\bar{x}}(t))^2]/2\Gamma\} \qquad (4)$$

where $\dot{\bar{x}}(t) = d\bar{x}/dt$. At log time $\bar{x}$ and $\dot{\bar{x}}$ are given by Eq.(3) and the distribution is independent of the initial condition. (The result (4) is valid at all times where $\bar{x}$ and $\dot{\bar{x}}$ correspond to the motion in the absence of noise). We shall be interested in the low viscosity (slow damping, $G \ll \omega, \omega_0$) limit. In this limit Eq.(4) may be simplified by transforming x and $\dot{x}$ into action angle variables

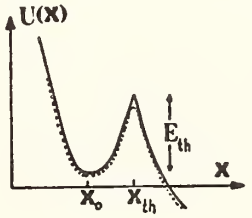

-1-

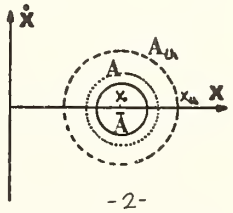

-2-

Figure 1 A potential surface with a realistic barrier and its truncated harmonic approximations.

Figure 2 Steady state trajectories in phase space. Shown are the trajectories corresponding to $\bar{A}$, $A = \bar{A} + \Delta A$, and A_{th}. Note that every point $(x,\dot{x})$ lies upon a unique trajectory characterized by a definite value of A.

$$x = (2J/m\omega_0)^{\frac{1}{2}} \cos\phi$$
$$x = (2J\omega_0/m)^{\frac{1}{2}} \sin\phi \qquad (5)$$

and integrating over the phase ϕ. This leads to a time independent probability distribution for the action J

$$P(J) = \frac{\omega_0}{k_B T} I_0\left(\frac{2\omega_0\sqrt{J\bar{J}}}{k_B T}\right) \exp\left[-\frac{\omega_0(J-\bar{J})}{k_B T}\right] \qquad (6)$$

where I_0 is the modified Bessel function of order zero and where

$$\bar{J} = \tfrac{1}{2} m(\omega_0^2 \langle \bar{x}^2 \rangle + \langle \bar{v}^2 \rangle)/\omega_0 = \frac{m(\omega_0^2+\omega^2)}{4\Omega\omega_0}\bar{A}^2 \qquad (7)$$

is the time averaged steady state action of the particle in the absence of random noise. The result (6) is obtained for $|(\omega^2-\omega_0^2)/\omega^2| \ll 1$. For $2\omega_0\sqrt{J\bar{J}} \gg k_B T$ Eq.(6) becomes (using $I_0(x) \xrightarrow{x\to\infty} \frac{\exp(x)}{\sqrt{2\pi x}}$)

$$P(E) \to \left(\frac{1}{4\pi k_B T}\right)^{\frac{1}{2}} \frac{\omega_0}{\sqrt[4]{E\bar{E}}} \exp\left[-\frac{(\sqrt{E}-\sqrt{\bar{E}})^2}{k_B T}\right] \qquad (8)$$

Here we substituted $E=\omega_0 J$ and $\bar{E}=\omega_0\bar{J}$.

Eq.(4) contains in principle all the needed information on the processes. However, for the purpose of obtaining the transition rate it is easier to take a different route. To this end, we proceed in the spirit of Kramers by first identifying the slow variable of the system and then deriving a Smoluchowski type equation for its probability distribution.[9]

The Fokker-Planck equation corresponding to Eq.(1) is

$$\frac{\partial P(x,\dot{x},t)}{\partial t} = -\frac{\partial}{\partial x}(\dot{x}P) - \frac{\partial}{\partial \dot{x}}\left[\left((\bar{A}+\Delta A)\sin\omega t - \omega_0^2 x - G\dot{x}\right)P\right] + \frac{\partial}{\partial \dot{x}}(\Delta A \sin\omega t\, P) + G\Gamma\frac{\partial^2 P}{\partial \dot{x}^2}. \qquad (9)$$

We have added and substructed a term $(\partial/\partial\dot{x})(\Delta A \sin\omega t\, P)$. ΔA may be chosen at will. A convenient choice is suggested by the observation that a stationary orbit (in phase space $(x,\dot{x})$) in the absence of noise is determined by $\bar{A}$. Indeed Eq.(3a) implies

$$\bar{x}^2 + \dot{\bar{x}}^2/\omega^2 = \bar{A}^2\Omega \qquad (10)$$

This equation describes a closed trajectory in phase space $(x,\dot{x})$ as shown in Fig.2. In this noiseless case, the stationary probability distribution satisfies

$$-\frac{\partial}{\partial x}(\dot{x}P) - \frac{\partial}{\partial \dot{x}}\left[\left((\bar{A}\sin\omega t) - \omega_0^2 x - G\dot{x}\right)P\right]\Big|_{(x,\dot{x})=(\bar{x},\dot{\bar{x}})} = 0 \qquad (11)$$

which expresses the fact that the probability current remains on the stationary orbit. The thermal noise causes fluctuations so that at a given instant $x=\bar{x}+\Delta x$ and $\dot{x}=\dot{\bar{x}}+\Delta x$. ΔA is defined such that the point $(x,\dot{x})$ lies on a stationary orbit corresponding to $A=\bar{A}+\Delta A$ (i.e. satisfies Eq.(14d) below; see Fig.2). The phase defining the position of this point along this orbit is (in the low viscosity limit) a rapidly evolving variable while A may be taken (in this limit) as the slowly changing variable. This definition of A implies that the first two terms on the r.h.s. of Eq.(9) have the form of the divergence of a current in phase space such that at every point $x,\dot{x}$ this current is tangent to the stationary orbit through that point.

Up to this point no approximation has been made. We next change variables from $(x,\dot{x})$ to (A,ϕ) where ϕ denotes the phase angle along the closed stationary trajectory in the $(x,\dot{x})$ plane. We further assume that on the interesting time-scale P is independent of ϕ. (More rigorously, this is expected to hold after coarse grained averaging over time intervals large compared with ω^{-1} or ω_0^{-1} but small compared with G^{-1}.) We then integrate Eq.(9) over ϕ for a fixed value of A. This has the effect of making the divergence term vanish, and we get a nonzero contribution only from the last two terms on the r.h.s. of Eq.(9). We thus obtain a Smoluchowski-type equation for

$$P(A,t) = 2\pi A \int d\phi\, P(x,\dot{x},t) \qquad (A=\bar{A}+\Delta A) \qquad (12)$$

i.e.,

$$\frac{\partial P(A,t)}{\partial t} = \tfrac{1}{2} G \frac{\partial}{\partial A}\left[(A-\bar{A})P + \frac{\Gamma\Omega A}{\omega^2}\frac{\partial (P/A)}{\partial A}\right] \qquad (13)$$

In performing the integration of Eq.(9) the following relations were used

$$\sin(\omega t) = \frac{1}{A}\left(G\dot{x} + (\omega_0^2-\omega^2)x\right) \qquad (14a)$$

$$\langle \dot{x}^2 \rangle / A^2 = \omega^2/2\Omega \qquad (14b)$$

$$\langle x\dot{x} \rangle = 0 \qquad (14c)$$

$$x^2 + \dot{x}^2/\omega^2 = A^2/\Omega \qquad (14d)$$

$$\left(\frac{\partial}{\partial x}\right)_{\dot{x}} = \frac{\Omega}{\omega^2}\frac{\dot{x}}{A}\frac{\partial}{\partial A} \qquad (14e)$$

where $\langle\ \rangle$ denotes time (phase) average. Eq.(13) yields the steady state probability distribution

$$P_{ss}(A) = N_A A \exp\left(-\frac{(A-\bar{A})^2\omega^2}{2\Gamma\Omega}\right) \qquad (15)$$

where N_A is the approriate normalization constant. The result(15) may be rewritten in terms of the average energy $E=\omega_0 J = \frac{m(\omega_0^2+\omega^2)}{4\Omega} A^2$ (c.f. eq.(4). This leads to

$$P_{ss}(E) = N_E \exp\left[-\frac{2\omega^2}{\omega_0^2+\omega^2}\frac{(\sqrt{E}-\sqrt{\bar{E}})^2}{k_BT}\right] \qquad (16)$$

which agrees with the result(8) obtained for $\sqrt{E\bar{E}} >> k_BT$ and for $\omega \simeq \omega_0$. (the presence of $E^{1/4}$ in the preexponential term of (8) is numerically insignificant).

It is worthwhile to mention that the same result may be obtained in a seemingly more direct fashion by making an appropriate transformation on the Langevin equation(1). Introducing the transformation $(x,\dot{x}) \longrightarrow (A,\phi)$

$$x = \frac{A}{\Omega}\left[(\omega_0^2-\omega^2)\sin\phi - G\omega\cos\phi\right] \qquad (17)$$

$$\dot{x} = \frac{A\omega}{\Omega}\left[G\omega\sin\phi + (\omega_0^2-\omega^2)\cos\phi\right],$$

we can derive a pair of Langevin equations for A and ϕ from which a Fokker-Planck equation can be obtained using the standard procedure. By assuming that $P(A,\phi)$ is independent of ϕ and by averaging over the fast time scale (e.g. replacing $\sin^2\phi$ by ½, etc.) we may again derive Eq.(13).

Eq.(13) may now be used to derive the transition rate using an approximate procedure similar to Kramers'. The threshold value of A is found from Eq.(12d) to be

$$A_{th} = \sqrt{\Omega}\, x_{th} \qquad (18)$$

The transition rate, which is the inverse mean first passage time τ^{-1} for A to attain the value A_{th} when the initial probability distribution is given by (13), is found to be

$$\tau^{-1} = \frac{G\omega}{4(2\pi k_BT\Omega)^{1/2}}\frac{A_{th}(A_{th}-\bar{A})}{\bar{A}}\exp\left[-\frac{\omega^2}{2k_BT\Omega}(A_{th}-\bar{A})^2\right] \qquad (19)$$

In terms of the average energy we obtain(putting $2\omega^2/(\omega^2+\omega_0^2) \simeq 1$)

$$\tau^{-1} = \frac{G}{4\sqrt{\pi k_BT}}\frac{E_{th}(E_{th}-\bar{E})}{\bar{E}}\exp\left[-\frac{(\sqrt{E_{th}}-\sqrt{\bar{E}})^2}{k_BT}\right] \qquad (20)$$

It should be kept in mind that this result is valid only provided that $(\sqrt{E_{th}}-\sqrt{\bar{E}})^2 >> k_BT$. A more rigorous treatment yields

$$\tau^{-1} = \frac{G}{k_BT}\left[\int_{\bar{E}}^{E_{th}}\frac{dY}{Y}\, e^{\frac{(\sqrt{Y}-\sqrt{\bar{E}})^2}{k_BT}}\int_0^{Y} e^{-\frac{(\sqrt{Z}-\sqrt{\bar{E}})^2}{k_BT}}dZ\right]^{-1} \qquad (21)$$

which is valid for all values of $\bar{E} < E_{th}$. However, when $\bar{E}$ is close to E_{th} our model, which replaces a physical barrier by the model of Fig.1, breakes down.

Eqs.(18),(20) or (21) provide our final expression for the transition rate out of a harmonic potential well in the low viscosity limit under the influence of an oscillating external field. Significantly, the activation energy E_{th} which appears in the expressions for the rate in the absence of the external force is replaced by $(\sqrt{E_{th}}-\sqrt{\bar{E}})^2$ and not by $E_{th} - \bar{E}$ as could have been naively expected. The dependence on the strength and frequency of the external force enters through the value of $\bar{E}=\omega_0\bar{J}$ as given by Eq.(7).

In the above treatment we have focused on Kramers low viscosity limit. It should be kept in mind that for real potential barriers (the dashed line of Fig.1) the low viscosity picture breaks down close to the threshold and a different procedure(e.g., transition state theory)may have to be invoked. If the difference between the two curves of Fig.1 is significant only in an energy range smaller than k_BT, the correction is expected to be small.

Finally, we note that for the high viscosity limit where $G >> \omega_0$, an external force with $\omega << G$ corresponds to an adiabatic change of the potential surface. In this case the transition rate is time dependent and is given by the usual Kramers' result for this limit with time dependent activation energy and force constants.

REFERENCES

* Partially supported by the U.S.-Israel Binational Science Foundation (BSF).

[1] H. A. Kramers, Physica 7 284 (1940)

[2] S. Chandrasekhar, Rev. Mod. Phys. 15 1 (1943)

[3] D. Chandler, J. Chem. Phys. 68 2959 (1978); J. A. Montgomery, D. Chandler and B. J. Berne, J. Chem. Phys. 70 4056 (1970); J. L. Skinner and P. G. Wolliner, J. Chem. Phys. 69 2143 (1978) and 72 4913 (1980).

[4] G. Iche and Ph. Nozieres, J. de Physique 37 85 (1976).

[5] Physics of Superiounic Conductors, Edited by M. B. Salamon, Springer, Berlin (1979)

[6] V. Ambegaokar and B. I. Halperin, Phys. Rev. Lett. 22 1364 (1969).

[7] V. N. Sazonov and S. V. Zatzepin, Chem. Phys. 52 305 (1980).

[8] K. F. Freed and A. Metiu, to be published.

[9] E. Ben-Jacob and D. J. Bergman to be presented at the LT-16 LA (1980).

[10] D. J. Bergman, E. Ben-Jacob and Z. Schuss this proceedings.

FLUX FLOW NOISE DURING INHOMOGENEOUS VORTEX-MOTION. DEPENDENCE ON DC-VELOCITY FIELD*

Heinrich M. Dirks**, Klaus F. Beckstette, C. Heiden

Institut für Angewandte Physik der Justus-Liebig-Universität Giessen, Heinrich-Buff-Ring 16, D-6300 Giessen, Germany.

INTRODUCTION

The ac-component of flux flow voltage in type-II-superconductors often is observed as a random noise signal δV [1]. A convenient setup for the investigation of flux flow noise uses thin films or foils as samples in a magnetic field perpendicular to the large surface of the specimen. (see fig. 1)

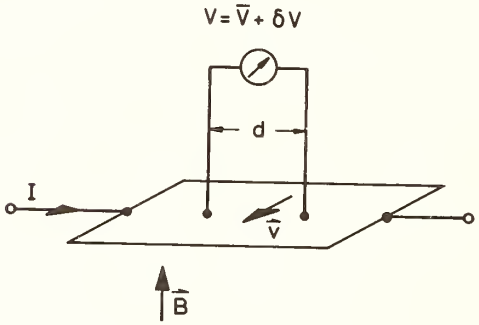

Fig. 1 Experimental setup for flux flow measurements.

Vortices are moved via the Lorentz force exerted by a sufficiently large transport current. The resulting electric field, which corresponds to the vortex velocity field is analyzed by a pair of movable voltage probes.

Local investigations performed in this way showed that flux flow noise originates at or near pinning sites, such as grain boundaries [2]. A stop and go mechanism has been proposed [3] to explain the underlying fluctuations of flux flow. Vortices come to a halt in front of a pinning site until due to the collective pressure of many flux lines the barrier can be overcome, resulting in a sudden rush of vortices, the whole process repeating in a more or less random way.

Whereas this mechanism involves a direct interaction of vortices with pinning sites, there appears to be also another possibility, in which the action of pinning with respect to flux flow noise is a more indirect one.

NOISE GENERATION DUE TO INHOMOGENEOUS VORTEX MOTION

Let us consider a sample with inhomogeneous pinning, in which domains of high critical current density without flux flow are separated by other regions with negligible pinning, where vortex motion takes place. The associated velocity field in general will not be homogeneous. Therefore the motion of a perfect vortex lattice is not possible. Local rearrangements in the relative position of vortices instead will take place. Due to the elastic properties of the flux line lattice, these rearrangement processes should be associated with a change of elastic energy, and this change may take place in a relaxation process involving plastic deformation of the vortex lattice, triggered by the randomly changing pattern of vortex positions.

---

* Supported by the Deutsche Forschungsgemeinschaft.
** This work represents parts of a Ph.D. thesis of one of the authors (HMD).

EXPERIMENTAL

To test this possibility of noise generation, a special technique was developed allowing [4] to prepare single crystalline niobium foils with very low intrinsic volume pinning. Typical values of critical current density j_c are below 100A/cm² at B=0.1T. Nb_3Sn-pinning structures of well defined geometry then were deposited on such foils by means of a photoplithographic lift-off-technique. Pinning structures realized in this way, together with their typical microstructure are shown in fig. 2.

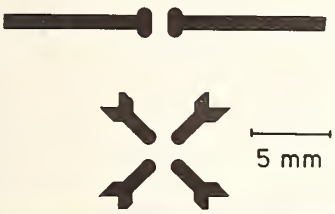

Fig. 2

a) Dipole ("twin club") and quadrupole geometry

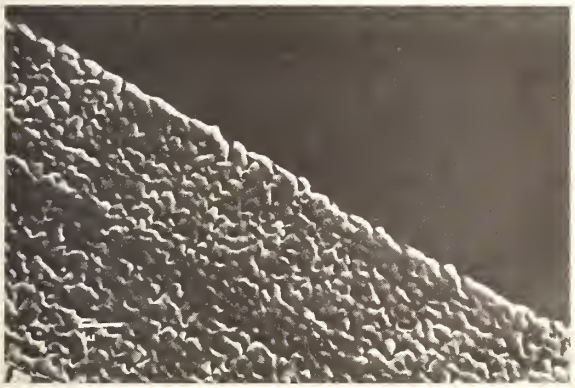

b) SEM micrograph of the border between Nb_3Sn layer (lower part) and niobium surface (upper part)

RESULTS

The mean square flux flow noise voltage $\overline{\delta V^2}$, obtained in a sufficiently wide frequency band (typically 0.1 ... 10^5 Hz), and the dc-flux flow voltage for a sample with "twin club" structure are shown in fig. 3. The data is taken for positions of the contact pair along the dashed line. Before entering and again after leaving the channel between the clubs, vortices pass a zone of convergent or divergent dc-velocity field, respectively. Since our samples have a demagnetization factor near one, local deviations from mean vortex density $n=B/\Phi_o$ are small. The two zones of divergent dc-velocity field therefore are associated with a vortex rearrangement, which may lead to flux flow noise as outlined above.

Such a feature can indeed be seen from the local behavior of $\overline{\delta V^2}$ shown in fig. 3. There are two separate regions of maximum noise, which correspond to locations of maximum divergence in the dc-flow. The channel region exhibits less noise, the minimum value of $\overline{\delta V^2}$ however being noticeably higher (more than an order of magnitude) than for the niobium sample without Nb_3Sn-structure.

These results however are not quite unambiguous. Measurements along a line in x-direction show that considerable noise is seen for all positions, for which one voltage probe comes close to the border of the pinning structure. The observed noise in fig. 3 therefore could at least in part result from contributions of the border zone along the Nb_3Sn-structure. To remove this ambiguity, a pinning structure is needed, for which the location of maximum noise also has maximum distance from all Nb_3Sn-domains.

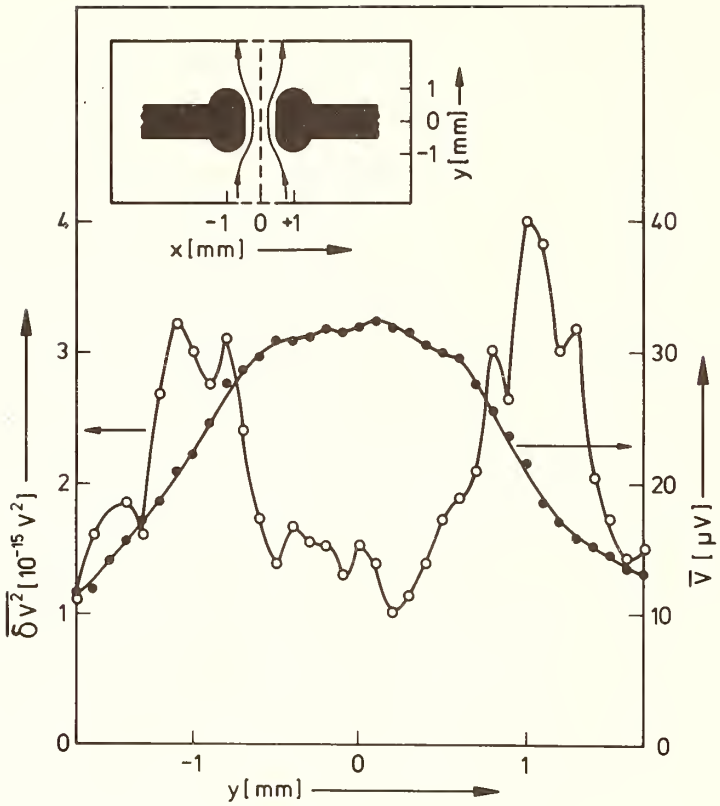

Fig. 3

Total noise power $\overline{\delta V^2}$ and dc-flux flow voltage $\overline{V}$ for different y-positions of midpoint between the voltage probes (separation 0.4 mm), which are aligned in x-direction. The gradient in the DC-velocity field corresponds to the slope of the $\overline{V}(y)$-profile. Inset: Nb_3Sn structure as black area. Vortex flow indicated by two equipotential lines. Field: 0.175T, temperature: 4.2K, transport current 4A.

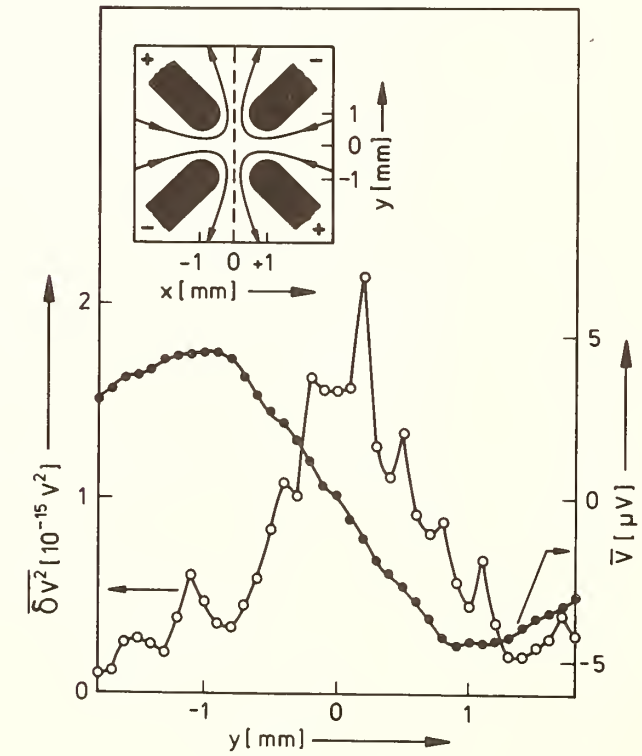

Fig. 4

$\overline{V}$ and $\overline{\delta V^2}$ measured at the quadrupole structure along the dashed line (see inset). Voltage probes aligned in y-direction for measurement of $\overline{\delta V^2}$, in x-direction for $\overline{V}$- measurement. B=.15T, T=4.2K, total transport current I=4A.

As a suitable geometry we prepared the quadrupole-arrangement of Nb_3Sn areas shown in the inset of fig. 4. At the center between the electrodes there is zero net flux flow but maximum noise, as can be seen from a comparison of the $\overline{V}$ and $\overline{\delta V^2}$ characteristics in fig. 4. Switching the polarity of two of the electrodes changes the velocity field as depicted in fig. 5.

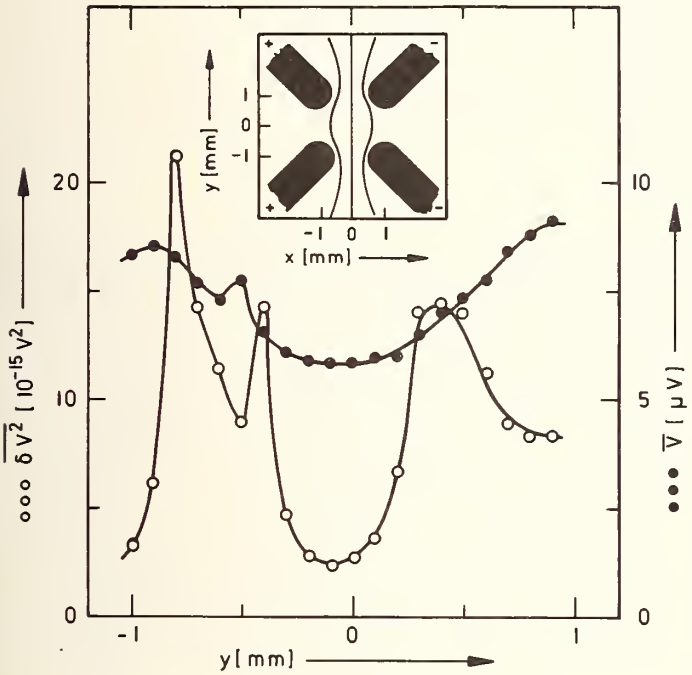

Fig. 5 Same measurement as in fig. 4, but with reversed polarity of two of the electrodes.

Local pinning properties of the sample are not affected by this procedure, of course. If however the observed noise is due to plastic deformation of the flux line lattice, the local dependence of $\overline{\delta V^2}$ should be changed drastically. Indeed, a minimum of $\overline{\delta V^2}$ is now observed at the center between the electrodes, instead of the maximum in fig. 4. Also, as expected, there are two zones with enhanced noise adjacent to the minimum of $\overline{\delta V^2}$ [5].

Concluding, we see strong evidence for a noise generation mechanism involving random plastic deformation of the vortex lattice [6]. This result is further supported by investigating the dependence of $\overline{\delta V^2}$ on magnetic field and temperature [7].

REFERENCES

[1] A good review of recent theoretical and experimental work on flux flow noise can be found in J.R. Clem. Proc. 5th Intern.Conf. on Noise (Bad Nauheim, Germany) Springer, Berlin, (1978) p. 214.

[2] D. Kohake and C. Heiden, J.Low Temp. Physics 40, 531 (1980)

[3] J.D. Thompson and W.C.H. Joiner, Phys. Rev. B20, 91 (1979)

[4] H.M.Dirks, Ph.D.thesis, Univ. of Giessen, Germany (1981)

[5] The residual resitivity of the sample changed somewhere in the time interval between the measurements of figs. 4 and 5, although no variation in the volume pinning of the niobium foil was observed. This may be the cause for the overall higher noise intensity seen in fig. 5 (c.F. Ph. D. thesis of K.F. Beckstette, Univ. of Giessen, Germany (1981).

[6] A more detailed report will be published elsewhere.

[7] See following paper, this conference.

FLUX FLOW NOISE DURING INHOMOGENEOUS VORTEX-MOTION. MAGNETIC FIELD AND TEMPERATURE DEPENDENCE*

Klaus F. Beckstette**, Heinrich M. Dirks, C. Heiden

Institut für Angewandte Physik der Justus-Liebig-Universität Giessen, Heinrich-Buff-Ring 16, D-6300 Giessen, Germany.

INTRODUCTION

Results presented in the preceeding paper [1] suggest that one rôle of pinning concerning the generation of flux flow noise is to provide guided inhomogeneous vortex motion such that plastic deformation of the flux line lattice will take place [2] . The geometrical arrangement of pinning sites and their individual pinning strength therefore should be important factors for the observed noise. This may be one reason for the lack of reproducibility in the magnetic field dependence of flux flow noise which is encountered for different polycrystalline samples with average grain diameters comparable to or larger than the distance between the voltage probes. This also provides an explanation for the fact that reproducibility in these investigations becomes better, and a smoother field dependence of the mean square noise voltage δV^2 is obtained, if the grain size is reduced such that the voltage probes see noise contributions from many grains in their neighbourhood [3] . Good reproducibility on the other hand is observed for carefully prepared single crystalline samples with isolated pinning sites of defined geometry as used in the preceeding paper. In the following we present measurements of the dependence of δV^2 on flux density B and temperature T.

EXPERIMENTAL

The sample used is a single crystalline niobium foil with "twin club" shaped dipole structure of a high pinning Nb_3 Sn-layer. All data reported here is taken for a fixed position of the voltage probes as depicted in fig. 1. Broad band measurements again are performed with the same frequency band as in the previous paper. The sample is submerged in a liquid helium bath, whose temperature can be varied by pumping. The magnetic field is supplied by a superconducting magnet. The sample is doped with nitrogen in order to increase sufficiently the normal state resistivity such that flux flow voltages of measurable magnitude are obtained. This doping is carried out in such a way that it does not increase the volume pinning force of the niobium foil from its very low value, it had before doping except for the occurence of peak effect in the critical current at a field B_{cp} just below the upper critical field B_{c_2} .

RESULTS

Fig. 1 shows the typical behaviour of the field dependence of $\overline{\delta V^2}$ and the volume pinning force $F_p = j_c \cdot B$ of the niobium foil (not of the Nb_3 Sn-structure) obtained at T=4,2 K. F_p turns out to be almost independent of B whereas $\overline{\delta V^2}$ goes through a maximum. This may be taken again as a sign that

---

* Supported by the Deutsche Forschungsgemeinschaft

** This work represents parts of a Ph.D. thesis of one of the authors (KFB).

there is no direct connection between pinning and flux flow noise.

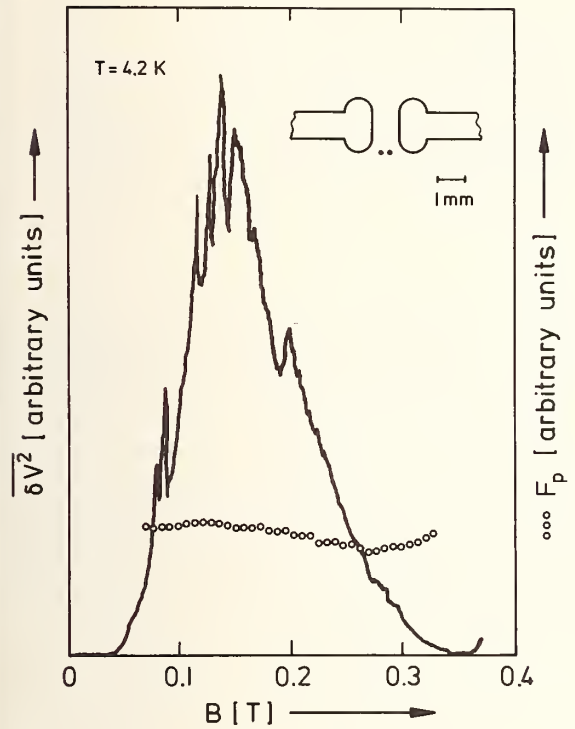

Fig.1 Typical field dependence of mean square flux flow noise voltage for low pinning single crystalline niobium foil with high pinning twin club Nb_3Sn-layer deposited on it. Contact positions as indicated by two dots. Transport current is I = 2A. Also shown is the field dependence of the volume pinning force.

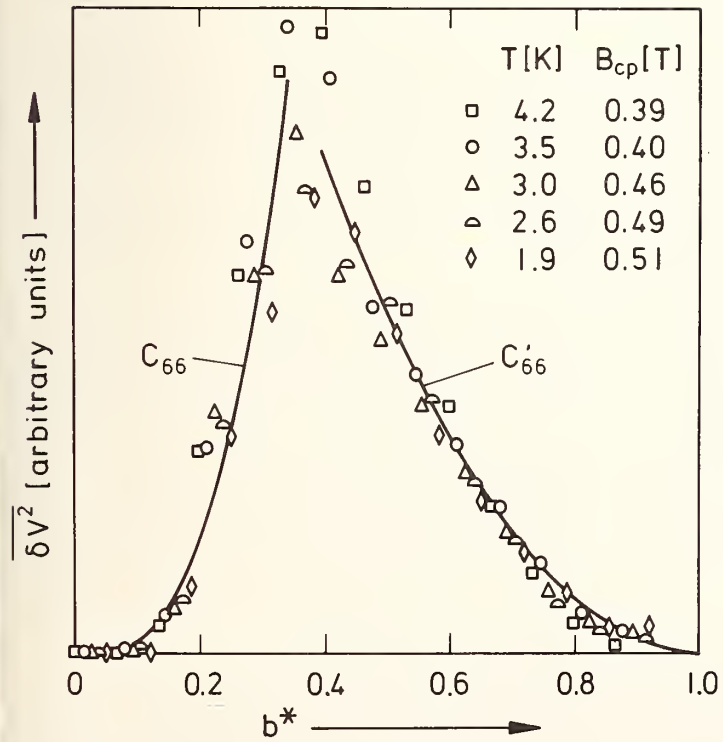

Fig.2 Dependence of mean square noise voltage on reduced field $b^*=B/B_{cp}$ obtained at five different temperatures under the same measuring conditions as in fig.1. Solid line: field dependence of the shear modulus.

Measurements at other temperatures yield analogous results. Fig. 2 shows data obtained at five different temperatures, plotted as function of the reduced field $b^*=B/B_{cp}$ [4]. Obviously, the data can be represented well by a scaling law of the form

$$\overline{\delta V^2} = f(T) \cdot h(b^*)$$

where f(T) is nearly constant for our sample. Measurements at other positions of the voltage probes in the region of inhomogeneous flux flow yield similar results, such that a function of position g(r) may be separated:

$$\overline{\delta V^2} = f(T) \cdot h(b^*) \cdot g(r).$$

DISCUSSION

The equation of motion for the vortices contains as essential parameters the driving Lorentz force determined by the transport current density, the pinning force, given by material inhomogeneities, a viscous force, which is proportional to a viscosity coefficient $\eta=B_{c2}\phi_0/\rho_n$, where ϕ_0 is the flux quantum, and ρ_n the normal state resistivity and interaction forces between the flux lines, which are controlled by the elastic moduli C_{ij} of the flux line lattice. Intrinsic volume pinning force, and viscous friction are essentially independent of magnetic field for our sample. This suggests to relate the behaviour of $\overline{\delta V^2}(B)$ to the field dependence of the elastic moduli. A major contribution during the plastic deformations of the vortex lattice certainly will arise from shear-effects. We therefore consider the shear modulus C_{66}, whose field dependence is given by [5]

$$C_{66} = \frac{1}{2}\int_0^B B^2 \frac{d^2H}{dB^2}\, dB \qquad H \geq H_{c1}$$

$$C_{66}' = 0{,}48\, \frac{\mu_0 H_c^2 \kappa_2^2 (2\kappa_2^2 - 1)}{[1+\beta_A(2\kappa_2^2-1)]^{\frac{1}{2}}} \left(1 - \frac{B}{B_{c2}}\right)^2 \qquad H \leq H_{c2}$$

The behaviour of $C_{66}(b^*)$ and $C_{66}'(b^*)$, calculated for our sample, also is shown in fig. 2. Fitted only in magnitude, these curves describe rather well the field dependence of $\overline{\delta V^2}$. These results again give strong support for noise generation by plastic deformation of the flux line lattice.

REFERENCES

[1] H.M. Dirks, K.F. Beckstette and C. Heiden, preceeding paper, this conference

[2] K.F. Beckstette, H.M. Dirks and C. Heiden, Phys. Letters 81A, 351(1981)

[3] see for instance: C. Heiden, D. Kohake, W. Krings and L. Ratke, Journal Low Temp. Phys. 27, 1 (1977)

[4] B_{cp} is used instead of B_{c_2}, since the latter could not be measured as accurate as B_{cp}.

[5] R. Labusch, Phys. Stat. Sol. 19, 715 (1967), Phys. Stat. Sol. 32, 439 (1969)

VORTEX NOISE IN TWO DIMENSIONAL SUPERCONDUCTING FILMS

C.M.Knoedler, R.F.Voss, and P.M.Horn
IBM T.J.Watson Research Center, Yorktown Heights, N.Y. 10598

INTRODUCTION

In 1969 Maul, Strandberg, and Kyhl [1] observed a large excess of noise in the power spectrum of a thin film tin bolometer. While they were unable to draw any conclusions as to its origin they noted that the noise was only observed in the transition region of the film and speculated that it might have a connection with the superconducting to normal phase transition. It is well known [2] that free vortices (or flux bundles) induced in superconductors by a magnetic field cause phase slips which result in finite electrical resistance and flux flow noise. Recent theories [3,4,5] postulate that equal numbers of positive and negative vortices exist in thin superconducting films in the absence of an applied magnetic field. Below some characteristic temperature T_{KT} they exist only as bound pairs. Above T_{KT} the pairs unbind to form a plasma of free vortices that is responsible for the resistive transition. In order to probe the nature of such superconducting-normal transitions we have systematically studied the voltage noise and I-V characteristics of granular superconducting films. In this case the noise measurements provide a unique probe of the properties of thermally excited vortices in the vicinity of the transition.

EXPERIMENTAL PROCEDURES

The aluminum and tin samples were flash evaporated in an oxygen atmosphere onto glass substrates using procedures described by Abeles, Cohen, and Cullen [6]. This technique produces films with small grains and high sheet resistances $R_{\square} \approx 30\text{-}5000\Omega/\square$. The aluminum films typically had 50Å grains and thicknesses less than 100Å while the tin films had grain sizes greater than 1500Å and thicknesses on the order of 400Å.

Individually shielded, twisted pair leads were connected to the sample in a four probe configuration. The samples were immersed in liquid helium in a cryostat surrounded by a double mu-metal shield with an ambient magnetic field of less than $1.7\text{x}10^{-4}$Oe. The leads from the sample were connected to a special low noise field-effect-transistor preamplifier and to external current and voltage connections. The preamplifier output was connected to a bandpass filter and an ac voltmeter to allow estimation of the voltage noise spectral density in the frequency range 10-100kHz. A dc current $I_b \approx (0.25\text{-}200\mu A)$ was supplied to the sample and the dc voltage V_{dc} as well as the rms noise voltage were digitally recorded and averaged.

EXPERIMENTAL RESULTS

Typical results for a $380\Omega/\square$ Al sample are shown in figure 1. The resistive transition as well as the noise spectral density at 100kHz, $S_V(100\text{kHz})$ (with the preamplifier background of $2.5\text{x}10^{-18}V^2/\text{Hz}$ subtracted from S_V) are plotted versus T. The curve with $I_b=0$ depicts the decrease in the Johnson (thermal) noise as the sample becomes superconducting. With increasing

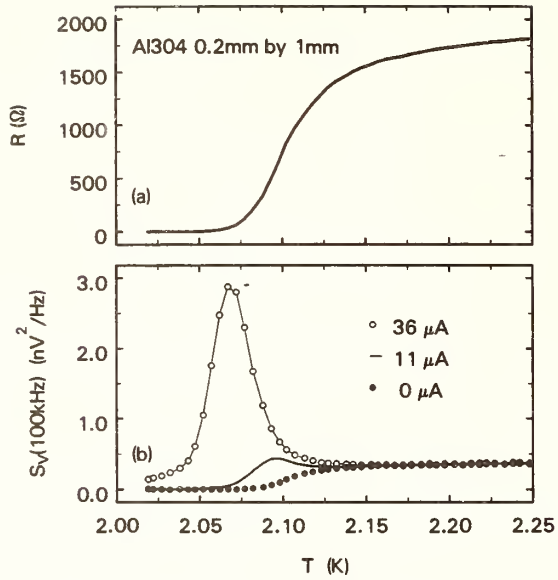

Fig. 1 (a) Resistive transition for a 380Ω/□ Al film. (b) Noise spectral density S_V(100kHz) vs. T for various I_b

I_b an increase in the magnitude of the noise is seen at the low T end of the transition. Both the transition and the noise were found to be functions of $R_\square$, with the broader noise "peaks" and transitions occuring for large $R_\square$. In the frequency range investigated (10-100kHz) the noise spectral density was independent of frequency, indicating that the characteristic times of these processes were <0.1 msec. The application of a perpendicular magnetic field was found to strongly suppress S_V, similiar to the results seen by Maul, Strandberg, and Kyhl [1].

The voltage and current dependence of the noise is better illustrated in figure 2 where the excess noise spectral density is plotted versus V_{dc} for samples of Al and Sn at various I_b. This excess noise was obtained by subtracting both the preamplifier background and the calculated Johnson noise from S_V. V_{dc} was varied by changing T and thus R at constant I_b. For low I_b and low V_{dc} the noise is proportional to V_{dc}, with the proportionality constant independent of I_b. At sufficiently large I_b the magnitude of S_V increases at low V_{dc} possibly indicating a different type of noise process. The linear relation between S_V and V_{dc} strongly indicates that S_V is a voltage shot noise arising from independent voltage pulses. Traditional noise sources such as equilibrium resistance fluctuations [7] would lead to $S_V \propto V_{dc}^2$.

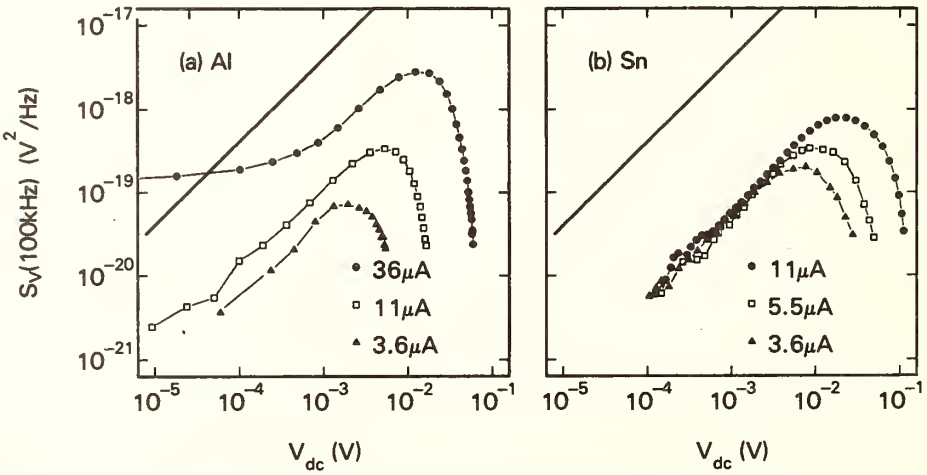

Fig. 2 (a) S_V vs V_{dc} for the Al film in Figure 1. (b) S_V vs V_{dc} for a 4000Ω/□ Sn film. Both show the dependence of S_V on I_b.

Van Ooijen and Van Gurp [8] showed that the motion of flux across a sample causes a change in the voltage at the sample electrodes. If the jumps $\Delta\phi$ in the superconducting phase occur independently at a rate r then, $V_{dc}=\phi_0 r\Delta\phi/2\pi$, where ϕ_0 is the flux quantum and

$$S_v(f) = 2\phi_0(\Delta\phi/2\pi)V_{dc} \qquad (1)$$

at frequencies $f<<\tau^{-1}$, where τ is the characteristic frequency for these phase jumps. Similar results are expected for one dimensional (weak link) superconductors and Josephson junctions with $\Delta\phi=2\pi$ as the phase jump due to vortex motion across the entire sample [9]. This 1-D prediction of eq (1) is plotted as a solid line in figure 2. S_V is seen to parallel this prediction for low I_b and low V_{dc} but with $\Delta\phi<<2\pi$.

Figure 3 depicts data for a narrow 350Ω/□ Al film with a width of 27μm, at various I_b, and with an applied magnetic field. As the width of the sample decreases the magnitude of S_V is larger than that shown in figure 2 for similar I_b and approaches the 1-D prediction of eq (1). At the same I_b the magnetic field tends to suppress the noise at low V_{dc}.

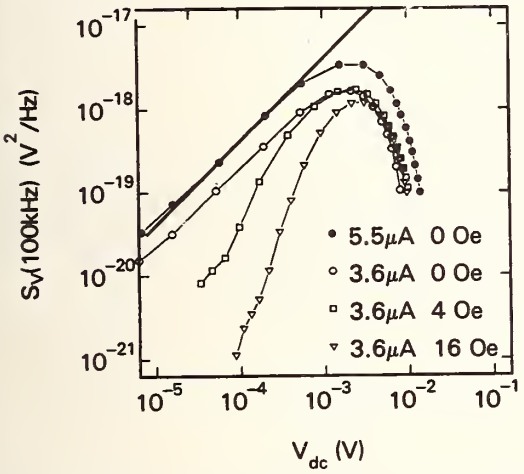

Fig. 3 S_V vs V_{dc} for a narrow (275μm by 27μm) 350Ω/□ Al sample showing the dependence of S_V on both bias current and magnetic field.

In figure 4 we display data derived from measurements on tin films in which the temperature in the cryostat was held constant to 1 mK. The current through the sample was slowly ramped using a capacitive discharge technique while V_{dc} and S_V(100kHz) were recorded. The data for several T is displayed. As expected near the transition at T≈3.81K S_V is linear with respect to V_{dc} at low voltages. As the temperature is lowered the magnitude of S_V tends to increase and approach the 1-D prediction of eq (1).

Fig. 4 S_V vs V_{dc} for a 30Ω/□ Sn sample at various temperatures. As T is lowered the magnitude of the noise increases and approaches the eq (1) prediction.

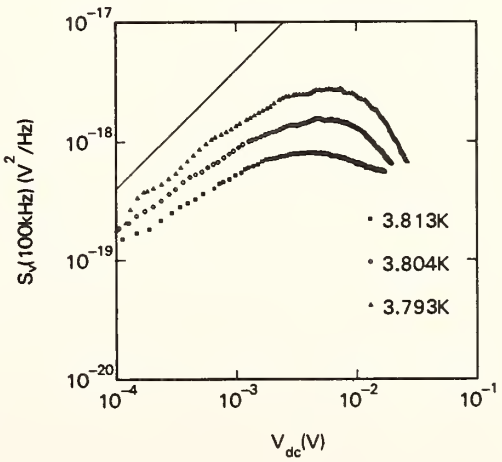

DISCUSSION

We have observed a white noise spectrum in the range of frequencies monitored, with S_V varying as V_{dc} at the onset of the resistive transition. The noise is current induced and is inversely dependent on the width of the film. These findings suggest that we are observing voltage (phase slip) shot noise in analogy with electrical shot noise. In this case the charge carrier corresponds to a flux quantum moving a distance ℓ across the film producing a phase slip $\Delta\phi = 2\pi\ell/w$ where w is the film width. In addition it should be noted that as the voltage (temperature) is increased the excess noise tends to level off and then decrease. This effect can be explained by analogy to electrical shot noise. As the temperature (and voltage) increase the vortices interact more strongly and their motion is no longer independent. Thus, the phase slips become correlated and the noise is reduced similar to shot noise in space-charge limited diodes [10]. The imposed magnetic field produces a similar result (reduction of S_V) with large numbers of field induced vortices causing a correlation in the vortex motion. It should be emphasized that these results are quite different from the usual flux flow noise in type II superconductors [8] where $\approx 10^5$ flux quanta are in motion, B=1000Oe, J≈500A/cm., and $\tau \approx 5$msec. In these experiments B≈0, J≈0.05A/cm, $\tau < 0.1$msec and we are observing the motion of individual quanta moving a fraction of the distance across the sample.

SUMMARY

We have used noise measurements in conjunction with standard electrical measurements to yield information about the nature and dynamics of the two dimensional superconducting transition. The excess current induced noise at the onset of resistance in granular Al and Sn samples can be explained as a phase slip shot noise arising from the independent motion of vortices. The amplitude of the noise provides a measure of the mean free path of the vortices.

REFERENCES

[1] M.K. Maul, M. Strandberg, and R. Kyhl, *Phys. Rev.* 182, 522 (1969).

[2] Y.B. Kim and M.J. Stephen, in *Superconductivity*, R.D. Parks, ed. (Marcel Dekker, New York, 1969) Chapter 19.

[3] J.M. Kosterlitz and D.J. Thouless, *Jour. Phys. C.* 6, 1181 (1973).

[4] M.R. Beasley, J. Mooij, and T. Orlando, *Phys. Rev. Lett.* 42, 1165 (1979).

[5] B.J. Halperin and D.R. Nelson, *Jour. of Low Temp. Phys.* 36, 599 (1979).

[6] B.A. Abeles, R.W. Cohen, and G.W.Cullen, *Phys. Rev. Lett.* 17, 632 (1966).

[7] R.F. Voss and J. Clarke, *Phys. Rev. B* 13, 556 (1976)

[8] D.J. Van Ooijen and G.J. Van Gurp, *Phys. Lett.* 17, 230 (1965).

[9] J.E. Lukens, R.J. Warburton, and W.W. Webb, *Phys. Rev. Lett.* 25, 1180 (1970).

[10] J.B. Johnson, *IEEE Spectrum* 8, 42 (1971).

VI. HOT CARRIER NOISE

MODELING NOISE OF DEVICES WORKING UNDER HOT CARRIER CONDITIONS

J.P. Nougier

Université des Sciences et Techniques du Languedoc
Centre d'Etudes d'Electronique des Solides†
34060 Montpellier Cédex, France

1. INTRODUCTION

Let us consider a device (Fig. 1), with a d.c. bias V_{oMN} between the electrodes M and N. The measurements are performed at the probes M' and N', which may be identical with or different from the bias electrodes M and N. Let $V_{oM'N'}$ be the d.c. voltage between the probes. A d.c. current I_{oMN} flows through the device, corresponding to an average flow of electrons. In fact the electrons move randomly around their average trajectory, thus producing at each point of the device a random current superimposed to the d.c. current, which results in a random voltage superimposed to the d.c. voltage between every couple of points. Of course, the local noise source at every point gives a contribution to the noise measured between M' and N', the total noise being the sum of the contributions of each local noise source.

This device can be schematically represented by a pool of water, crossed by a creek arriving at point N and going out at point M. When one drops a bunch of stones somewhere in the pool, a local noise source is created, producing noise at the terminals M' and N'. Obviously this noise depends both on the local noise source (studied in section 2) and on the way in which its effect is transmitted to the probes M' and N' : one way for studying this effect is to consider the noise source as a random signal and to study the signal resulting between the probes : such are the macroscopic models : Langevin (section 3), impedance field (section 4) and salami (section 5) methods. The other way is to consider the noise as a random motion of each particle and to derive it from the fluctuations of their velocities, known at every time (microscopic models, section 6). All these theories are linear around the bias point, and therefore apply either to large or small random signals of linear devices, or to small random signals of non linear devices.

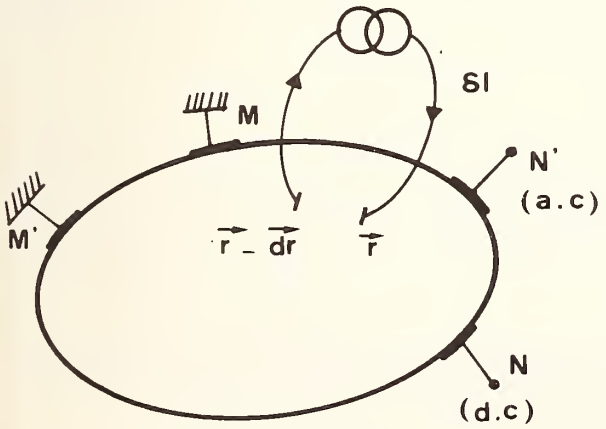

Fig. 1 : Device showing the d.c. (MN) and a.c. (M'N') electrodes.

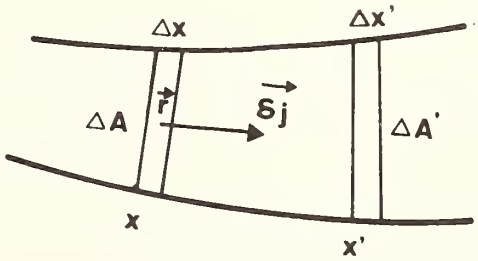

Fig. 2 : Slice of a current tube. x is the abscissa of the slice Δx along an a.c. current path.

† Laboratoire associé au Centre National de la Recherche Scientifique, LA 21 et Gréco Microondes.

2. LOCAL NOISE SOURCES OF HOT CARRIERS

2.1. Definition

Let us label $\vec{j}(\vec{r},t)$ the instantaneous local current density, of d.c. value $\vec{j}_o(\vec{r})$:

$$\Delta\vec{j}(\vec{r},t) = \vec{j}(\vec{r},t) - \vec{j}_o(\vec{r}) \tag{1}$$

$\Delta\vec{j}(\vec{r},t)$ is randomly distributed; if $\Delta j_{N\alpha}(\vec{r},f)$ denotes the current density noise source along the direction α, i.e. the component of $\Delta j_\alpha(\vec{r},t)$ at frequency f within the bandwidth Δf, one defines the noise source term $K_{\alpha\beta}(\vec{r},f)$ as [1] :

$$S_{\Delta j\alpha\beta}(\vec{r},\vec{r}',f)\Delta f = \overline{\Delta j_{N\alpha}(\vec{r},f)\ \Delta j^{*}_{N\beta}(\vec{r}',f)} = K_{\alpha\beta}(\vec{r},f)\delta(\vec{r}-\vec{r}')\ \Delta f \tag{2}$$

where * means the complex conjugate, the bar means average value over the time. Indeed, the spectral density (s.d.) $S_{\Delta j\alpha\beta}$ of Δj is the Fourier transfrom of eq. (1). Eq. (2) means that the noise sources at two different points are uncorrelated. Integration of eq. (2) over the cross section $\Delta A(x')$ of a slice $\Delta x'$ located at abscissa x' along an a.c. current path (see Fig. 2) gives, if ΔI_N denotes the noise current through the slice :

$$\overline{\Delta I_N(x,f)\ \Delta I^{*}_N(x',f)} = \Delta A(x)\ K_x(\vec{r},f)\ \delta(x-x')\ \Delta f \quad . \tag{3}$$

This relation had already been given for particular types of noise sources [2][3]. Integrating eq. (3) once more over the domain $x' \in \Delta x$ gives the relation between the local noise source $K_x(\vec{r})$ and the s.d. of the noise current $S_{\Delta I\,x}(\vec{r},f)$:

$$K_x(\vec{r},f) = S_{\Delta Ix}(\vec{r},f)\ \Delta x/\Delta A(x) \quad . \tag{4}$$

2.2. Experimental determination of the noise source term : the experimental way for determining the noise source term obviously follows from eq. (4) : one has only to determine the s.d. of the noise current of an homogeneous bar in a uniform field, from which one gets $K_x(\vec{E},f)$, and then in a non homogeneous device with the same impurity concentration, orientation, etc..., one has $K_x(\vec{r},f) = K_x[\vec{E}(\vec{r}),f]$. However, hot carrier experiments require short pulses in order to avoid thermal heating of the semiconductors, and thus high frequency analysis : at those frequencies, because of matching impedance problems, the experimental parameter which can be measured is the noise temperature T_n (an extended bibliography will be found in refs. [4][5][6]). Since T_n can be related to $S_{\Delta I}$, K can be related to T_n [7]. Let ΔY_x be the differential admittance of the slice Δx. One has [4][5]:

$$\begin{cases} S_{\Delta Ix}(\vec{r},f) = 4\ k_B\ T_{n\,x}(\vec{r},f)\ \mathrm{Re}\ \{\Delta Y_x\} & (5) \\ \Delta Y_x = \Delta A\ \delta j_x(\vec{r})/[\Delta x\ \delta E_x(\vec{r})] & (6) \end{cases}$$

when k_B is the Boltzmann constant. Eqs. (5) and (6), carried into eq. (4), give :

$$K_\alpha(\vec{r},f) = 4\ k_B\ T_{n\alpha}(\vec{r},f)\ \mathrm{Re}\{\sigma_{\alpha\alpha}(\vec{r},f)\} \tag{7}$$

where $\vec{\vec{\sigma}}(\vec{r},f)$ is the a.c. conductivity tensor : $\delta\vec{j} = \vec{\vec{\sigma}}\,\delta\vec{E}$. Eq. (7) shows that the noise source can be determined experimentally by measuring the noise temperature and the conductivity, without needing any knowledge on the physical nature of the noise (an example is given in ref. [7]). Note that the direction α may take different values for a given direction of the d.c. field [7].

2.3. Expression of the noise sources for various physical mechanisms : For deriving the expression of the local noise sources of hot carriers, one starts with the expression of the current through the slice Δx (ΔN is the average total number of carriers in the slice, n the carrier density, v their average velocity) :

$$I(x) = q\ n(x)\ v(x)\ \Delta A(x) = q\ v(x)\ \frac{\Delta N(x)}{\Delta x} \quad . \tag{8}$$

a) Diffusion noise : one assumes that the contribution to the noise is mainly due to the fluctuations of the velocities of the carriers, the fluctuations of n being negligible. Eq. (8) gives then :

$$S_{\Delta I}(x,f)=q^2n^2(x)\ \Delta A^2(x)S_{\Delta v}(x,f) = q^2n^2(x)\Delta A^2(x)\left[S_{\Delta v_i}(x,f)/n(x)\Delta A(x)\ \Delta x\right] \qquad (9)$$

where $S_{\Delta v_i}(x,f)$ describes the fluctuations of the velocity of one given carrier, although $S_{\Delta v}$ is related to the fluctuation of the average velocity of the carriers in the slice Δx. Since, by definition [4] [5], $S_{\Delta v_i}(x,f) = 4\ D\ (x,f)$ when D is the diffusion coefficient, eqs. (9) and (4) give :

$$\vec{\vec{K}}_{diff}(\vec{r},f) = 4\ q^2\ n(\vec{r})\ \vec{\vec{D}}\ (\vec{r},f)\ . \qquad (10)$$

This result was already given in Refs. [1] to [3]. Comparison of eqs. (7) and (10) give the relation [8] between the noise temperature and the diffusion coefficient :

$$k_B\ T_{n\alpha}(\vec{r},f)/q = q\ n(\vec{r})\ D_\alpha\ (\vec{r},f)/Re\ \{\sigma_{\alpha\alpha}(\vec{r},f)\}\ . \qquad (11)$$

This relation should replace in space charge regimes of hot carriers, the one previously obtained [4] [5] for homogeneous bars.

b) Generation-recombination (G.R) noise : in that case, the noise is mainly produced by the fluctuations of the number ΔN of the carriers in the slice. Eq. (8) gives then

$$S_{\Delta I} = q^2v^2(x)\ S_{\Delta N}/(\Delta x)^2 = j^2(x)\Delta A^2\ S_{\Delta N}/\Delta N^2\ . \qquad (12)$$

For G.R noise involving only two levels [9] $S_{\Delta N} = \alpha\tau(\text{var}\ \Delta N)/(1+\omega^2\tau^2)$, and due to the quasi Poissonian character of the fluctuations, $\text{var}\ \Delta N = \alpha N$; this gives for eq. (12) carried into eq. (4) :

$$K_{\alpha GR}(\vec{r},f) = \frac{j_\alpha^2\ (\vec{r})\ \alpha(\vec{r})\ \tau(\vec{r})}{n(\vec{r})\left[1+4\pi^2f^2\tau^2(\vec{r})\right]}\ . \qquad (13)$$

One thus gets an expression analogous to that obtained for thermal G-R noise [9], except that j is not linear with respect to the d.c. electric field, and that $\alpha(\vec{r})$ and $\tau(\vec{r})$ may depend on the local d.c. field. Such a situation occurs for example in n-Si at 77 K : then, at thermal equilibrium, only part of the donor impurities are ionized : when a high d.c. field is applied, a fraction of the neutral impurities is ionized, due to Poole Frenkel and/or impact ionization effect, thus leading to hot carrier G-R noise, since this fraction depends on the d.c. field, so as α and τ [10].

c) 1/f noise : The 1/f noise can be represented as if it were the sum or G-R noises on a subband of impurities with a continuous distribution of relaxation times. As a consequence, it may be inferred from eq. (13) that the bulk 1/f noise source is of the form :

$$K_{\alpha\ 1/f\ bulk}(\vec{r},f) = j_\alpha^2\ (\vec{r})\ \alpha_H(\vec{r})/[n(\vec{r})\ f^\gamma] \qquad (14)$$

where α_H tends towards the Hooge's constant [11] at low field. In the same way, the 1/f noise arising at an interface at abscissa x_o may be described by a noise source term :

$$K_{\alpha 1/f\ contact}(\vec{r},f) = \lambda\ j_\alpha^2\ (x_o)\ \delta(x-x_o)/(n(x_o)f^\gamma)\ . \qquad (15)$$

3. THE LANGEVIN METHOD

This method [12] has been extensively described in a review paper of Nicolet et al. [13] and applied to single and double injection diodes. According to this theory :

(i) one first writes the usual equations (conduction eqs., continuity eqs, Poisson eq.). For example, for a one dimensional device $j = j_n + j_p + \varepsilon\partial E/\partial t$; $j_p = q\ p\ v_p - q\ D_p\ \partial p/\partial x$; $\partial p/\partial t = -\ r_p + g_p - q^{-1}\partial j_p/\partial x$; etc...

(ii) Every variable Y involved is then set equal to $Y = Y_o + \delta Y \exp i\omega t$. The zero order terms give the static characteristics. The first order terms give the a.c. equations (i.e. linear variations around the bias point).

(iii) to each a.c. equation one adds the appropriate noise source. One then gets a set of linear equations. For example : $\delta j = \delta j_n + \delta j_p + \varepsilon\, i\omega\, \delta E$; $\delta j_p = qv_{po}\delta p + qp_o(dv_p/dE)_o\delta E - q\ D_p\partial\delta p/\partial x + \delta H_p(x)$; $i\omega\delta p = -\ \delta r_p + \delta g_p - q^{-1}(\partial\delta j_p/\partial x) + \delta H_{GR,p}(x)$; etc... Here δH_p is a

diffusion noise source term for the holes, δH_{GRp} is a G-R noise source term for the holes, etc...

(iv) the auxiliary variables are eliminated so as to get a relation between δI and δE, of the form $\delta I = \hat{\mathcal{L}}[\delta E, \delta H_p, \delta H_{GRp}, ...]$ where $\hat{\mathcal{L}}$ is a linear operator and $\delta I = A\delta j$. This eq. is solved, which gives δE as a function of δI, δH_p, δH_{GRp}, ... Then, integrating over the length L of the device, one gets the voltage at is terminals

$$\delta V = \int_o^L \hat{\mathcal{L}}'[\delta I(x'), \delta H_p(x'), \delta H_{GR}(x'), ...]\, dx' \qquad (16)$$

where $\hat{\mathcal{L}}'$ is a linear operator. When the noise sources δH_p, δH_{GRp}, ..., are set equal to zero, eq. (16) gives the a.c. impedance. When $\delta I = 0$, multiplying eq. (16) by δV^* gives the open circuit noise voltage around the bias point. For further details, see [13]. This method was applied to single injection diodes [14] [15] [16].

Obviously, an alternate possibility would be to write the usual eqs., then to set $Y = Y_o + \delta Y$, then to take the first order linear eqs. as previously. But, instead of writing the noise sources, one could first eliminate the auxiliary variables so as to get the equation $\delta I = \hat{\mathcal{L}}\,\delta E$. The local noise sources could be introduced only now, leading to an eq. of the form $\delta I = \hat{\mathcal{L}}\delta E - \sum_i \Delta I_{Ni}$ where the subscripts i stands for the various noise sources. When $\delta I = 0$, the solution of this eq., after integration over x, gives

$$\delta V = \int_o^L \psi(x',f) \sum_i \Delta I_{Ni}(x')\, dx' \qquad (17)$$

where $\psi(x')$ is some function of x', depending on which operator $\hat{\mathcal{L}}$ is involved. Multiplying eq. (17) by its complex conjugate, and taking into account eq. (3) gives :

$$S_{\Delta V}(f) = A \int_o^L |\psi(x',f)|^2 \sum_i K_i(x',f)\, dx' \qquad (18)$$

the K_i are the noise sources studied in section 2 above.

4. THE IMPEDANCE FIELD METHOD :

The impedance field method was originated on one dimensional devices for diffusion noise by Shockley et al [17], and was later on also applied to G-R noise [18]. Its purpose is to relate the local noise sources to the effect they produce at the terminals M' and N', through the "impedance field".

4.1. Expression for the noise : A three dimensional statement will be given here. Let us introduce a small a.c. current $\delta I \exp i\omega t$ at point $\vec{r}$ (see Fig. 1), superimposed to the d.c. current. The a.c. voltage appearing between M' and N' is $\delta V(M'\,N',\vec{r}) = Z(N',\vec{r},f)\delta I$ where $Z(N',\vec{r},f)$ is the a.c. impedance between $\vec{r}$ and N'. If this current is taken out at $\vec{r}-d\vec{r}$, it produces an a.c. voltage $\delta V(M',N',\vec{r}-d\vec{r}) = Z(N',\vec{r}-d\vec{r},f)\delta I$. The overal voltage is thus :

$$\delta V(M'\,N',\vec{r}) = \delta I\ \widetilde{\vec{\nabla}} Z\,(N',\vec{r},f).d\vec{r} \quad . \qquad (19)$$

Here a matrix notation has been adopted, in which the tilde means "transposed" : hence a vector such as $d\vec{r}$ is represented by a column matrix, and $\widetilde{d\vec{r}}$ by a row matrix. $\vec{\nabla} Z(N',\vec{r},f)$ is the impedance field. If $\delta\vec{j}(\vec{r})$ is the current density at $\vec{r}$, one has : $\delta I\, d\vec{r} = \delta\vec{j}\, d^3r$ so that eq. (19) after integration over the volume of the device, gives the a.c. voltage between M' and N', labelled $\delta V(N')$:

$$\delta V(N') = \iiint \widetilde{\vec{\nabla}} Z(N',\vec{r},f).\ \delta\vec{j}(\vec{r})\, d^3r \quad . \qquad (20)$$

Let us label α the component along every direction x, y or z : eq. (20) writes :

$$\delta V(N') = \sum_\alpha \iiint d^3r\ \delta j_\alpha(\vec{r})[\partial Z(N',\vec{r},f)/\partial\alpha] \quad . \qquad (21)$$

For getting the noise, one multiplies $\delta V(N')$ by $\delta V^*(N')$, which gives, using eq. (2) :

$$S_{\Delta V} = \sum_{\alpha}\sum_{\beta}\iiint \left[\partial Z(N',\vec{r},f)/\partial\alpha\right] \left[\partial Z^{*}(N',\vec{r},f)/\partial\beta\right] K_{\alpha\beta}(\vec{r})\, d^3r \quad . \tag{22}$$

This eq. can be written using a matrix notation :

$$S_{\Delta V} = \iiint d^3r\, \vec{\vec{\nabla}} Z(N',\vec{r},f)\, \vec{\vec{K}}(\vec{r})\, \vec{\nabla Z}^{*}(N',\vec{r},f) \quad . \tag{23}$$

For one dimensional devices, every quantity is a scalar and depends on only one variable labelled x, so that eq. (23) gives eq. (24), which reduces to the formula of Shockley et al [17] for diffusion noise (see eq. (10)) :

$$S_{\Delta V}(f) = \int_0^L A(x)\, K(x,f)\, \left|\nabla Z(x,f)\right|^2 dx \quad . \tag{24}$$

As one can see, by comparing eqs. (18) and (24), the impedance field method and the Langevin method are formally identical, as was previously pointed out [19] [20]. The noise voltage can also be expressed as a function of the local noise temperature by replacing K(r,f) by its value [eq. (7)]. For one dimensional devices, one gets :

$$S_{\Delta V}(f) = 4\, k_B \int_0^L T_n(x,f)\, \mathrm{Re}\{\delta I/\delta E\}\, \left|\nabla Z(x,f)\right|^2 dx \quad . \tag{25}$$

The noise sources being supposed to be known, one then needs to determine $\vec{\nabla Z}$. This will be studied in subsections 4.2 and 4.3 below.

4.2. Green function of the electric field : transfer impedance method : this method was developed by Van Vliet et al. [1] and applies easily when the fundamental electric variable is the local electric field $\vec{E}(\vec{r})$. Let us apply an a.c. voltage at the terminals M' and N'. This results in a local a.c. field and in a local current density of complex values $\delta\vec{E}(\vec{r})$ and $\delta\vec{j}(\vec{r})$, superimposed to the d.c. values $\vec{E}_o(\vec{r})$ and $\vec{j}_o(\vec{r})$. The master equations are written, the auxiliary variables are eleminated so as to get a relation between $\vec{E}(\vec{r})$ and $\vec{j}(\vec{r})$. One then sets $\vec{E}(\vec{r}) = \vec{E}_o(\vec{r}) + \delta\vec{E}(r)\exp i\omega t$ and $\vec{j}(\vec{r}) = \vec{j}_o(\vec{r}) + \delta\vec{j}(\vec{r})\exp i\omega t$. The zero order terms give the d.c. characteristics linking $\vec{E}_o(\vec{r})$ and $\vec{j}_o(\vec{r})$. The first order terms give an equation of the form :

$$\hat{L}\, \delta\vec{E}(\vec{r}) = \delta\vec{j}(\vec{r}) \tag{26}$$

where $\hat{L}$ is a linear operator. The Green matrix $\vec{\vec{z}}(\vec{r},\vec{r}',f)$ of the operator $\hat{L}$ is defined as (here $\hat{I}$ means the unitary matrix and $\delta(\vec{r}-\vec{r}')$ the Dirac function) :

$$\hat{L}\, \vec{\vec{z}}(\vec{r},\vec{r}',f) = \hat{I}\, \delta(\vec{r} - \vec{r}') \tag{27}$$

eq. (26) and (27) give then, integrating over the whole volume of the device :

$$\delta\vec{E}(\vec{r}) = \iiint d^3r'\, \vec{\vec{z}}(\vec{r},\vec{r}',f)\, \delta\vec{j}(\vec{r}',f) \quad . \tag{28}$$

Integrating on a line (generally a current line) of length L from M' to N', on gets the a.c. voltage at the terminals :

$$\delta V(N') = -\int_0^L \vec{\vec{dr}}\, \delta\vec{E}(\vec{r}) = -\int_0^L \iiint d^3r'\, \vec{\vec{dr}}\, \vec{\vec{z}}(\vec{r},\vec{r}',f)\, \delta\vec{j}(\vec{r}',f) \quad . \tag{29}$$

Comparison between eqs. (20) and (29) shows that :

$$\vec{\vec{\nabla}} Z(N',\vec{r}') = -\int_0^L \vec{\vec{dr}}\, \vec{\vec{z}}(\vec{r},\vec{r}',f) \quad . \tag{30}$$

For one dimensional devices, z(x,x',f) is the Green function of the equation linking $\delta E(x)$ and $\delta I(x)$ (and not $\delta j(x)$), as follows from eq. (28). Eq. (30) writes then :

$$\nabla Z(x') = -\int_0^L dx\, z(x,x',f) \quad . \tag{31}$$

This method was used for various modelling, among them single injection diodes [1] and FET's at low drain bias [21].

4.3. Green function of the voltage : This method [22][23] applies easily when the fundamental electrical variable is the voltage. As previously, an a.c. voltage is applied to the terminals M' and N', superimposed to the d.c. voltage between M and N. This results in a set of orthogonal equipotential surfaces and current lines. Let $\delta V(x)$ be the a.c. voltage of the equipotential surface crossing a given current line, of length L, at abscissa x, and let $\delta I(x)$ be the a.c. current through this equipotential surface. As previously, δV and δI are obtained by writing the usual eqs., which give :

$$\hat{\mathcal{L}}\,\delta V(x) = \delta I(x) \tag{32}$$

where $\hat{\mathcal{L}}$ is a linear operator. The Green function $\mathcal{Z}(x,x',f)$ of eq. (32) is a solution of :

$$\hat{\mathcal{L}}\,\mathcal{Z}(x,x',f) = \delta(x - x') \tag{33}$$

and gives

$$\delta V(x) = \int_0^L \mathcal{Z}(x,x',f)\,\delta I(x')\,dx' \quad . \tag{34}$$

By setting x=L one gets the a.c. voltage $\delta V(L) = \delta V(N')$ at the terminals. When ΔI is introduced at x and withdrawn at x + dx, being null elsewhere, eq. (34) leads to $\delta V(L) = \mathcal{Z}(L,x)\Delta I(x)dx$ which gives the impedance field initially defined by Shockley et al. [17], which in this formulation thus takes the form (see eq. (19)) :

$$\nabla Z\,(N,x') = \mathcal{Z}(L,x') \quad . \tag{35}$$

When $\vec{K}(\vec{r},f)$ only depends on x, that is does not vary on an equipotential surface, the device is then one dimensional, and the noise can be expressed using eq. (24) or (25). This method was successfully applied for deriving quite general behaviour of the noise produced at the drain [22] and at the gate [23] of FETs resulting from noise sources in the channel.

4.4. Numerical solutions : very often, the expressions of $\vec{\vec{K}}(\vec{r},f)$ and $\vec{\nabla} Z(\vec{r},f)$ are so complicated that one is unable to carry out the calculations so as to get analytical results. Then the calculation has to be performed numerically [15] [16]. Furthermore $\vec{\vec{K}}(\vec{r},f)$ and $\vec{\nabla} Z(\vec{r},f)$ may even have no analytical expression, and in that case, the entire calculation has to be performed on a computer. For example, it is possible to determine numerically the voltage produced by the introduction of a current at a mesh point, and by withdrawning it at an other mesh point : this gives a numerical value of ∇Z which is then used for getting numerically the noise [24]. The impedance field method can even be applied without writing the master eqs. : this was done in FETs [25], where the transistor was considered as an active line, being made of a chain of elementary FETs, with progressively varying bias conditions, each one representing a slice of the actual FET. The noise is then considered as the sum of the effects, at the drain and at the gate, of the noises produced by the various slices, which is the basic idea of the impedance field method, applied to a representation using circuits instead of master eqs.

5. THE SALAMI METHOD

In the salami method, the device is devided into slices supposed to be uncorrelated, so that the total noise voltage $S_{\Delta V}$ of the device is taken as being the sum of those of the slices $d\,S_{\Delta V}$. As was mentioned by Thornber [26] and later on by Van Vliet et al. [1], this method fails because, although the noise sources of two different slices are indeed uncorrelated (see eq. (2)), the noises are correlated since the noise of the slice x depends on the noise induced in it by all the other slices through the transfer impedance between slices. However, this method gave satisfactory or even exact results when applied to single or double injection diodes (see refs. [9] and [67] to [73] of the review paper [13] of Nicolet et al.), and was also applied to FETs [27].

The conditions under which the Salami method gives correct results have been recently studied [7]. From eqs. (5) and (6) one gets the noise voltage $dS_{\Delta V}$ of the slice dx :

$$dS_{\Delta V}(x) = 4\, k_B\, T_n(x)\, \mathrm{Re}\left\{\frac{\delta E(x)}{\delta I}\right\} dx \quad .$$

so that the noise voltage $S_{\Delta V}$ of the whole device is, according to the salami hypothesis :

$$S_{\Delta V} = 4\, k_B \int_o^L T_n(x)\, \mathrm{Re}\left\{\frac{\delta E}{\delta I}\right\} dx \quad . \tag{35}$$

This is to be compared with the correct result given by eq. (25). Comparison of these two expressions allows us to determine the conditions under which the salami approximation works. In particular, eqs. (25) and (35) give identical results when the integrals are equal, that is when

$$\left| \delta E/\delta I \right| = \left| \nabla Z(x) \right| \quad . \tag{36}$$

This gives, according to eqs. (31)(where ∇Z should be taken at point x and not x') and (28).

$$\left| \int_o^L z(x,x')\, dx' \right| = \left| \int_o^L z(x',x)\, dx' \right| \quad . \tag{37}$$

For bars in a uniform (even high) field, $z(x,x') = z(x',x)$ and eq. (31) is valid : the salami method gives rigourous results in that particular case.

6. MICROSCOPIC MODELS

In the microscopic models (or particle models), the current is not considered as a signal, but rather as a motion of carriers : this is a mechanical point of view instead of an electrical point of view. In these models, the trajectories of N particles inside the device are studied as a function of time, so that at each time (more exactly at multiples $n\,\Delta t$, of a time step $\Delta(t)$, the position and the velocity of each particle is known. Since the actual number of carriers in a device is very large, each particle indeed represents a number of carriers.

The basic method is the Monte Carlo technique (see for example [28][29][30]. Since this method is much time consuming, simplified models are now being studied [31] . Although the Monte Carlo technique is well suited for studying local noise [32] and diffusion, even transient [33] , the application of particle models for studying noise in devices is not well established. The only one efficient tentative, up to my knowledge, has been performed by J. Zimmermann [34], who solves the problem in the following way : the current conservation in a one dimensional device of uniform cross section writes :

$$I(t) = q\, n(x,t)\, v(x,t)\, A + \varepsilon A\ \partial E(x,t)/\partial t \quad . \tag{38}$$

After integration from x=0 to x=L of eq. (38), one gets :

$$-\partial V(t)/\partial t = \varepsilon^{-1} \left[A^{-1} L\, I(t) - q \int_o^L n(x,t)\, v(x,t)\, dx \right] \quad . \tag{39}$$

Now let us consider the $\delta N(t)$ particles located in the slice dx at time t. One has :

$n(x,t) = \delta N(t)/A\, dx$ and $v(x,t) = (\delta N)^{-1} \sum_{i=1}^{\delta N} v_i(x,t)$ where $v_i(x,t)$ is the velocity of the i th carrier in the slice. Thus, eq. (39) writes :

$$-\partial V(t)/\partial t = (\varepsilon A)^{-1} \left[L I(t) - q \sum_{i=1}^{N} v_i(x,t) \right] \tag{40}$$

where N is the total number of particles. Substracting to eq. (39) its average value gives the instantaneous deviations :

$$-\partial \delta V(t)/\partial t = (\varepsilon A)^{-1} \left\{ L \delta I(t) - q \sum_{i=1}^{N} \left[v_i(x,t) - v(x) \right] \right\} \tag{41}$$

where v(x) is the average velocity of the carriers in the slice dx. Two situations can then be investigated [34]:

a) Noise voltage of an a.c. open circuit : $\delta I(t) = 0$ in eq. (41), gives :

$$\delta V(t) = \frac{q}{\varepsilon A} \sum_{i=1}^{N} \int_a^t \left[v_i(x,t) - v(x) \right] dt \quad . \tag{42}$$

Since the velocity of each particle is known as a function of time, $\delta V(t)$ can easily been computed, so as $\delta V(t+\tau)$, and hence the noise voltage

$$S_{\delta V}(f) = 4 \int_o^\infty \overline{\delta V(t)\ \delta V(t+\tau)}^t \cos 2\pi f\tau\ d\tau$$

b) Noise current of an a.c. short circuit : $\delta V(t) = 0$ in eq. (41) gives

$$\delta I(t) = \frac{q}{L} \sum_{i=1}^{N} \left[v_i(x,t) - v(x) \right] \quad . \tag{43}$$

In the same way as previously, this allows determining the noise current $S_{\delta I}(f) = 4 \int_o^\infty \overline{\delta I(t)\ \delta I(t+\tau)}^t \cos 2\pi f\tau\ d\tau$.

Once the noise $S_{\delta V}$ or $S_{\delta I}$ of the particles has been obtained, the noise of the carriers is deduced by dividing the result by the number of carriers represented by each particle.

In spite of its simplicity, this model is questionnable. Eq. (38) is valid only for average values, since it is deduced from the Boltzmann eq. which involves probabilities, that is average number of particules in each state. Thus, using eq. (38), when describing the noise, is probably erroneous, since obviously, due to the local fluctuations, I should depend on x, being randomly distributed around its x independent value : in the Langevin formulation for example, this is taken into account by the addition of the x dependent noise term.

7. CONCLUSION

In the last few years, powerful methods for modelling the noise of devices have been built (Langevin, impedance field), providing formulations which can be applied to a great variety of situations, and to analytical as well as to numerical models.

However these methods are valid for usual situations, where the noise is considered as a signal, that is for devices long enough, such that each carrier inside is in a steady state. For devices short enough (submicron devices) such that the distance between the electrodes is of the order of magnitude of the mean free path, the carriers have no time to undergo enough collisions so as to reach their steady state : even in the steady state regime, each carrier is in a transient state. A microscopic model is then required, and the applicability of the previous methods for modelling noise then becomes questionnable. An important effort should be devoted in thee next years in the formulation of methods suited to such situations.

REFERENCES

[1] K.M. Van Vliet, A. Friedmann, R.J.J. Zijlstra, A. Gisolf and A. Van der Ziel, J. Appl. Phys. 46, 1804 (1975) and J. Appl. Phys. 46, 1814 (1975).

[2] A. Van der Ziel and K.M. Van Vliet, Solid St. Electron. 11, 508 (1968).

[3] K.M. Van Vliet, Solid St. Electron. 13, 649 (1970).

[4] J.P. Nougier, Proc. 5th Int. Conf. on Noise in Physical Systems (Bad-Nauheim, FRG, 1978), Springer Series in Electrophysics 2, Springer Verlag ed., p.72 (1978).

[5] J.P. Nougier, in Physics of Non Linear Transport in Semiconductors, ed. by D.K.Ferry, J.R. Barker and C. Jacoboni, Plenum Publ. Corp. p. 415 (1980).

[6] Y. Pozhela, hot electron diffusion coefficient, to be published.

[7] J.P. Nougier, J.C. Vaissière, D. Gasquet and A. Moatadid, to be published, J. Appl. Phys.

[8] J.P. Nougier, J.C. Vaissière, D. Gasquet, to be published.

[9] A. Van der Ziel, "Noise : Sources, Characterization, Measurement", Prentice Hall ed., Englewood Cliffs, New Jersey, 1970.

[10] A. Van der Ziel, R. Jindal, S.K. Kim, H. Park and J.P. Nougier, Solid St. Electron. 22, 177 (1979).

[11] F.N. Hooge, Phys. Lett. 29 A, 139 (1969).

[12] P. Langevin, Comptes Rend. Ac. Sc. Paris 146, 530 (1908).

[13] M.A. Nicolet, H.R. Bilger and R.J.J. Zijlstra, Phys. Stat. Sol. b 70, 9 and 415 (1975).

[14] A. Gisolf and R.J.J. Zijlstra, Solid. St. Electron. 17, 839 (1974).

[15] G. Bosman and R.J.J. Zijlstra, Phys. Lett. 71A, 464 (1979).

[16] J.P. Nougier, D. Gasquet, J.C. Vaissière and H.R. Bilger, Proc. 5th Int. Conf. Noise in Phys. Systems, Springer Series in Electrophysics 2, Springer Verlag ed., p. 110 (1978).

[17] W. Shockley, J.A. Copeland and R.R. James, in "Quantum Theory of Atoms, Molecules and the Solid State, P. Lowdin ed.,Acad. Press, New York, 1966.

[18] A. Rigaud, M.A. Nicolet and M. Savelli, Phys. Stat. Sol. a 18, 531 (1973).

[19] T.C. Mc Gill, M.A. Nicolet and K.K. Thornber, Solid St. Electron. 17, 107 (1974)

[20] K.K. Thornber, T.C. Mc Gill and M.A. Nicolet, Solid St. Electron. 17, 587 (1974)

[21] K.M. Van Vliet, Solid St. Electron. 22, 233 (1979)

[22] J.P. Nougier, J.C. Vaissière and D. Gasquet, Proc. 6th Int. Conf. on Noise in Physical Systems, Washington (USA), 6-10 April 1981.

[23] P. Hesto, J.C. Vaissière, D. Gasquet, R. Castagné and J.P. Nougier, to be published.

[24] C.R. Brewitt-Taylor, P.N. Robson and J.E. Sitch, Proc. 8th Europ. Microwave Conf., Paris, 1978, p. 415.

[25] D. Sodini, D. Rigaud, Proc. 6th Int. Conf. on Noise in Physical Systems, Washington (USA), 6-10 April 1981.

[26] K.K. Thornber, Solid St. Electron. 17, 95 (1973).

[27] J.P. Nougier, D. Sodini, M. Rolland, D. Gasquet and G. Lecoy, Solid St. Electron. 21, 133 (1978).

[28] C. Moglestue, Solid. St. El. Dev. 3, 133 (1979)

[29] J. Zimmermann, R. Fauquembergue, M. Charef and E. Constant, Electron. Lett. 16, 664 (1980).

[30] B. Carnez, A. Cappy, A. Kaszynski, E. Constant and G. Salmer, J. Appl. Phys. 51, 784 (1980).

[31] P. Bonjour, R. Castagné, J.P. Pone, J.P. Courat, G. Bert, G. Nuzillat and M. Peltier, IEEE Trans. El. Dev. ED27, 1019 (1980).

[32] C. Moglestue, Computer simulated noise current in semiconducting material, to be published.

[33] R. Fauquembergue, J. Zimmermann, A. Kaszynski and E. Constant, J. Appl. Phys. 51, 1065 (1980).

[34] J. Zimmermann, Thèse de Doctorat ès Sciences, Université des Sciences et Techniques de Lille, 59655 Villeneuve d'Ascq Cédex-France (available on request)(1980).

NOISE OF HOT HOLES IN Ge DUE TO PREDOMINANT INELASTIC SCATTERING

V. Bareikis, A. Galdikas, R. Miliušytė, V. Viktoravičius

Institute of Semiconductor Physics of the Academy of Sciences of the Lithuanian SSR, K. Pozhelos 52, 232600 Vilnius. USSR

INTRODUCTION

It is well established that the spectral density of current noise in isotropic semiconductors is anisotropic in respect to the direction of high electric field $\vec{E}$ [1,2].

Two limiting cases in the study of hot current carrier fluctuations are of particular interest. The first one, when the scattering is quasielastic and the second one, when the scattering is strongly inelastic.

For the quasielastic scattering theory predicts [1] that along the electric field direction in adition to the thermal noise, the convective noise due to energy fluctuations exists. For this reason in the case of sublinear current-voltage dependence transverse ($\perp$) spectral density of current noise exceeds the longitudinal ($\parallel$) one ($S(\omega)_\perp > S(\omega)_\parallel$).

The theory for highly inelastic scattering by optical phonons gives that $S(\omega)_\parallel$ has peaks at frequencies equal to the multiple reciprocal time necessary to accelerate the current carriers from energy $\varepsilon = 0$ to the energy of optical phonon ε_0 [4]. $S(\omega)_\perp$ for such scattering mechanism is not investigated yet.

RESULTS

So far, the available experimental investigations on hot current carrier noise [2] and closely related phenomenon-diffusion [3] have confirmed the main conclusions of the theory for quasielastic scattering mechanisms.

The purpose of this work is to study experimentally the anisotropy of fluctuations for predominant inelastic scattering. For this the noise temperature T_n and small signal conductivity $\sigma(\omega)$ were measured in microwave range (9,8 GHz) in p-type Ge with concentration of holes $n_{300K} = 8.7 \cdot 10^{13}$ cm^{-3} at the lattice temperature 10 K. At low temperatures in Ge in high electric field the inelastic scattering of holes by optical phonons becomes predominant [5]. The technique used for T_n and $\sigma(\omega)$ measurement have been described elsewhere [6]. The electric field was applied along <110> direction. Noise in transverse <110> and longitudinal direction was investigated.

The data of T_n, d.c. conductivity σ, differential conductivity $\tilde{\sigma}$ and $\sigma(\omega)$ for longitudinal and transverse direction are plotted in Fig. 1. It was found that at low temperatures as well as at 80 K and 300 K $T_{n\parallel} > T_{n\perp}$ but anisotropy of T_n at 10 K is stronger.

At electric fields $E < 180$ V/cm the difference between $\sigma(\omega)_\perp$ and σ as well as of $\sigma(\omega)_\parallel$ and $\tilde{\sigma}$ is observed. This effect is caused by the inertia of the heating process of holes.

$S(\omega)_\alpha$ along α direction was determined from $T_{n\alpha}$ and $\sigma(\omega)_\alpha$ measurements using the relation

$$S(\omega)_\alpha = 4kT_{n\alpha}\,\sigma(\omega)_\alpha ,$$

where k - is the Boltzmann constant.

$S(\omega)_\alpha$ are plotted as a functions E in Fig. 2a. The results indicate that in the electric field region up to ~ 140 V/cm $S(\omega)_\parallel > S(\omega)_\perp$. Consequently, the sign of anisotropy of $S(\omega)_\alpha$ is opposite to that obtained for quasielastic scattering mechanisms. At higher electric fields ($E > 140$ V/cm) $S(\omega)_\parallel < S(\omega)_\perp$.

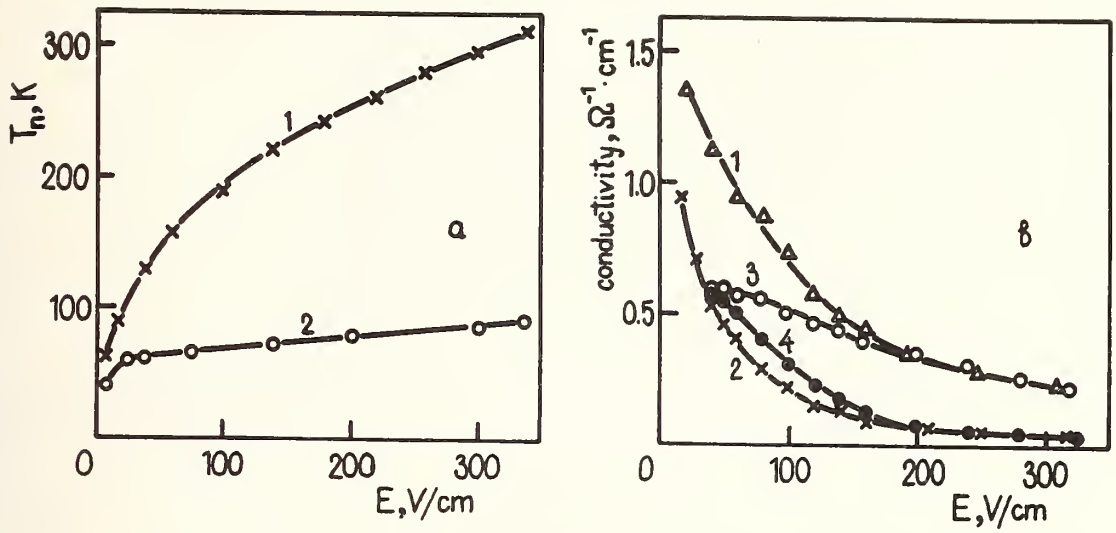

Fig. 1. (a) Experimental T_n vs E: 1 - longitudinal; 2 - transverse. (b) Conductivity vs E: 1 - direct-current σ ; 2 - differential $\tilde{\sigma}$; 3,4 - small signal transverse $\sigma(\omega)_\perp$ and longitudinal $\sigma(\omega)_\parallel$.

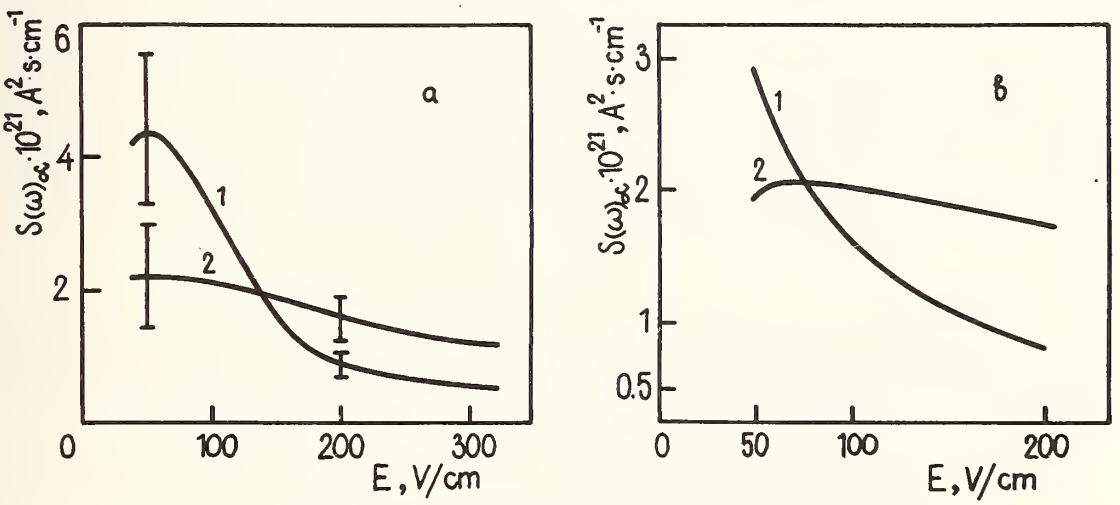

Fig. 2. $S(\omega)_\alpha$ vs E. (a) experimental. (b) calculated. 1 - longitudinal; 2 - transverse.

DISCUSSION

Calculations on $S(\omega)_\alpha$ were carried out by Monte Carlo technique for the simple model of p-Ge including only isotropic and parabolic heavy hole band, acoustic and nonpolar optical scattering. Calculated $S(\omega)_\alpha$ vs E are plotted in Fig. 2b. Fig. 3 reports the dependence of $S(\omega)_\alpha$ on the frequency as well as autocorrelation function of hole velocity $\psi(\tau)_\alpha$ vs time. It is seen that at certain resonant frequency $S(\omega)_\parallel$ has a maximum. This frequency corresponds to the reciprocal time necessary for a hole with $\varepsilon = 0$ to get the energy equal to that

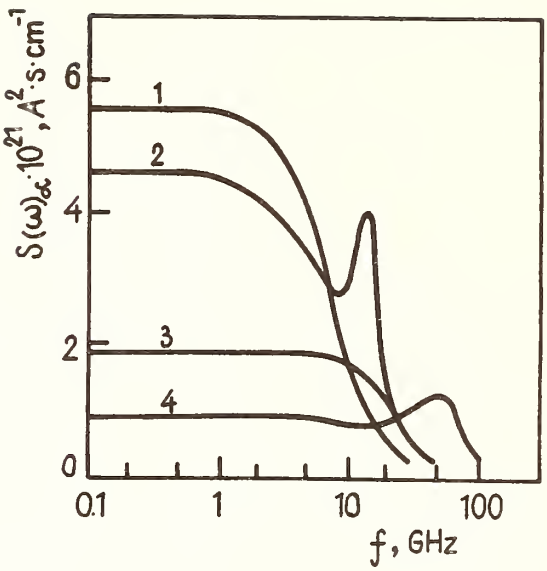

Fig. 3. Calculated $S(\omega)_\alpha$ vs frequence 1,3 - transverse, 2,4 - longitudinal; 1,2 - E = 50 V/cm; 3,4 - E = 200 V/cm; 1 - longitudinal, 2 - transverse.

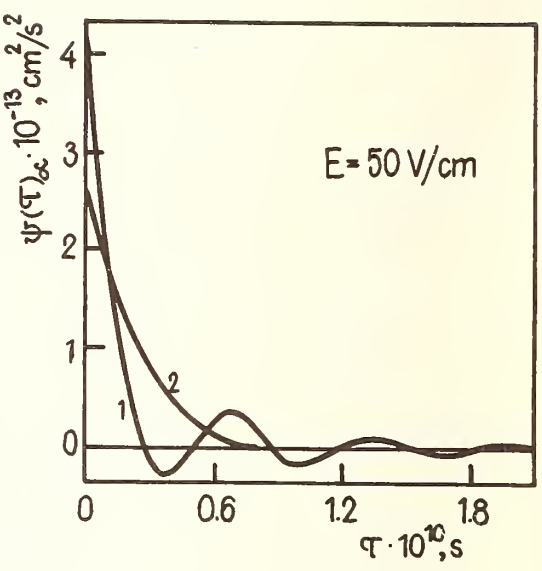

Fig. 4. Calculated autocorrelation function $\psi(\tau)_\alpha$ vs time. 1 - longitudinal; 2 - transverse.

of optical phonon. In the range of high frequencies at the vicinity of this maximum $S(\omega)_\parallel > S(\omega)_\perp$. This effect suggests the existance of the excess noise caused by the hole transit resonance due to predominant inelastic scattering by optical phonons. The resonant character of $S(\omega)_\parallel$ and oscillations of $\psi(\tau)_\parallel$ shows the regular motion of holes in the longitudinal direction. While increasing E the maximum of $S(\omega)_\parallel$ shifts to the higher frequencies. For this reason anisotropy of $S(\omega)_\alpha$ depends on the frequency used in measurement. For the fixed frequency (9,8 GHz) for E = 50 V/cm $S(\omega)_\parallel > S(\omega)_\perp$ while for E = 200 V/cm $S(\omega)_\parallel < S(\omega)_\perp$ These results agree with experimental data.

REFERENCES

1 J.P. Price, in Fluctuation Phenomena in Solids, Ed. R.E. Burgess (Academic Press, New York, 1965), p. 355; S.V. Gantsevich, V.L. Gurevich and R. Katilius, Rivista del Nouvo Cimento 2, 1 (1979).

2 V. Bareikis, J. Pozhela, I. Matulionene, in Proc. International Conference on the Physics in Semiconductors, Moscow (1968), p. 760; J.P. Nougier and M. Rolland, Phys. Rev. B 8, 5728 (1973).

3 C. Canali, G. Gavioli, F. Nava, G. Ottaviani, L. Reggiani, in Proc. International Conherence on the Physics in Semiconductors, Rome (1976), p. 1231.

4 I.B. Levinson, A.J. Matulis, Zurn. Exp. Teor. Fiz. 54, 1466 (1968).

5 T. Kurosawa and H. Maeda, Journ. of the Phys. Soc. of Japan, 31, 668 (1971).

6 V. Bareikis, R. Šaltis, J. Pozhela, Lietuvos fizikos rinkinys, 6, 99 (1966); J. Vindervoghel, Y. Leroy, C. Bruneel and J. Zimmermann, Rev. Sci. Instr. 45, 920 (1974).

HOT CARRIER TRANSPORT NOISE IN p-TYPE SILICON

G. Bosman, R.J.J. Zijlstra and A. van Rheenen

Fysisch Laboratorium, Rijksuniversiteit Utrecht, The Netherlands

ABSTRACT

The electric field dependence of the longitudinal diffusion coefficient D, the Hooge parameter α and the mobility μ were determined from thermal noise, 1/f noise, and d.c. current measurements respectively on $p^+\pi\ p^+$ planar silicon devices. Generation-recombination noise measurements revealed the presence and the properties of four different deep-level impurities.

1. INTRODUCTION

In this paper we report on the electric transport noise of $p^+\pi\ p^+$ planar silicon devices operating at low bias voltages in the ohmic regime and at sufficiently high bias voltages in a regime where space charge injection and carrier heating occur. Three types of noise could be distinguished in the measured voltage noise spectra ($1 < f < 10^8$ Hz):
(i) 1/f noise at low frequencies;
(ii) frequency independent diffusion noise caused by charge carrier velocity fluctuations at high frequencies ($f > 10^6$ Hz);
(iii) generation-recombination (g-r) noise caused by the trapping of charge carriers by deep-level impurities at intermediate frequencies.
From diffusion noise measurements versus bias voltage, we calculated the longitudinal diffusion coefficient D of holes as a function of the electric field strength. The field dependence of the Hooge parameter α was derived from 1/f noise measurements versus bias voltage and the field dependence of the mobility followed from d.c. current measurements versus bias voltage. From g-r noise measurements (in the ohmic regime) versus temperature we were able to determine the properties of four deep-level impurities.

2. THEORY

2.1. THERMAL AND 1/f NOISE

Neglecting the displacement- and the diffusion-current, Zijlstra derived the following expression for the spectral intensity of the a.c. open-circuited voltage fluctuations of a planar semiconductor device operating in a regime where space charge injection and carrier heating occur [1]

$$S_{\Delta V}(f) = \frac{4\varepsilon qA}{I_0^2} \int_0^{E_L} \frac{D(E)(E_L - E)^2 dE}{(1 - qAp_a E\mu(E)/I_0)^3} + \frac{\varepsilon qA}{fI_0^2} \int_0^{E_L} \frac{\alpha(E)(E_L - E)^2 dE}{(1 - qAp_a E\mu(E)/I_0)^3} \quad . \qquad (1)$$

In eq (1) p_a = density of ionized acceptors, I = current, L = contact spacing, E_L = electric field at the collecting contact at x = L, A = cross-sectional area, ε = permittivity of the material, -q = electron charge. Steady-state values are denoted by subscript 0.
Note that D, μ and α may depend on the electric field strength. In addition, Zijlstra derived for the current-voltage characteristic [1]

$$V_0 = \frac{\varepsilon A}{I_0} \int_0^{E_L} \frac{E^2\mu(E)dE}{(1 - qAp_a E\mu(E)/I_0)} \quad \text{and} \quad L = \frac{\varepsilon A}{I_0} \int_0^{E_L} \frac{E\mu(E)dE}{(1 - qAp_a E\mu(E)/I_0)} \quad . \qquad (2)$$

In eqs (1) and (2) the following sign convention holds: $I_0, V_0, E > 0$. On the assumption that α, μ and D do not change appreciably within a small electric field interval ΔE, eqs (1) and (2) were used to calculate α, μ and D as a function of E, with the help of a numerical decomposition procedure [2].

2.2. GENERATION-RECOMBINATION (g-r) NOISE

We consider a semiconductor at thermal equilibrium with s discrete energy levels i at energies ε_i; where i = 1 refers to the bottom of the conduction band at $\varepsilon_1 = 0$ eV, i = 2 refers to the top of the valence band at $\varepsilon_2 = \varepsilon_g$; $-\varepsilon_g$ is the band gap energy. The number of available states at level i which are occupied by one electron is N_i, whereas the number of vacant states is P_i. In thermal equilibrium N_i and P_i follow from Fermi-Dirac statistics. The rate of the electron transitions from level i to level j is given by: $p_{ij} = \alpha_{ij} N_i P_j$, where α_{ij} = transition parameter. Note that $\alpha_{i2} \cdot vol = v_p \delta_i$, which is the hole capture coefficient of the impurities at level i. In this expression vol = sample volume, v_p = average thermal velocity of the holes and δ_i = hole capture cross section of the impurities at level i. Due to electron transitions between levels the number of electrons occupying a level becomes time dependent. The rate equation for N_i becomes

$$\frac{d}{dt} N_i = \sum_{l=1}^{s} p_{li} - p_{il} \tag{3}$$

where $p_{ii} = 0$. In our g-r noise measurements we consider a time scale that is large with respect to the dielectric relaxation time. Then space charge fluctuations may be neglected and consequently it holds that $\sum_{i=1}^{s} \Delta N_i = 0$. This indicates that in the case of a system with s energy levels we are dealing with (s - 1) independent variables N_i. We linearize eq (3) with respect to these independent variables and obtain

$$\frac{d}{dt} \Delta N_i = - \sum_{j=1}^{s-1} M_{ij} \Delta N_j \tag{4}$$

where $M_{ij} = \sum_{l=1}^{s} \left(\frac{\partial p_{il}}{N_j} - \frac{\partial p_{li}}{N_j} \right)^0$ is an element of the so-called relaxation matrix M. The superscript 0 denotes thermal equilibrium values. Assuming that the electron transitions occur at random and are uncorrelated Klaassen [3] and van Vliet and Fassett [4] found the following expression for the spectral cross intensity

$$S_{\Delta N_l \Delta N_m}(f) = 4 \sum_{k=1}^{s-1} \sum_{i=1}^{s} \frac{C_{lk}^{-1} (p_{im})^0 (C_{km} - C_{ki}) \tau_k^2}{(1 + (2\pi f \tau_k)^2)} \tag{5}$$

where the τ_k's are the reciprocal eigenvalues of M and C_{ij}'s are elements of matrix C which transforms M into a diagonal matrix M' with elements $M'_{ij} = \tau_i^{-1} \delta_{ij}$: $M' = CMC^{-1}$.
Note that $S_{\Delta N_l \Delta N_m}(f)$ consists of a sum of (s - 1) Lorentzian-shaped spectra, each of which is characterized by a time τ_k and a low-frequency plateau level.

For the spectral intensity of the a.c. open-circuited voltage fluctuations in the ohmic regime we obtain with the help of eq (5)

$$S_{\Delta V}(f)/V_0^2 = \{\mu_n^2 S_{\Delta N_1 \Delta N_1}(f) + \mu_p^2 S_{\Delta N_2 \Delta N_2}(f) - 2\mu_n \mu_p S_{\Delta N_1 \Delta N_2}(f)\} / \{\mu_n N_1 + \mu_p P_2\}^2 \tag{6}$$

where μ_n and μ_p are the electron and hole mobility respectively.

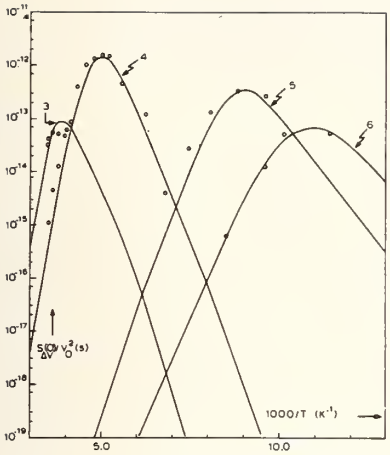

Fig. 1 The low frequency g-r noise plateau values divided by V_0^2 versus 1000/T. The open circles represent the measured values. The solid curves show the results of the computer calculation. The labels 3-6 refer to the impurity level mainly responsible for the maximum.

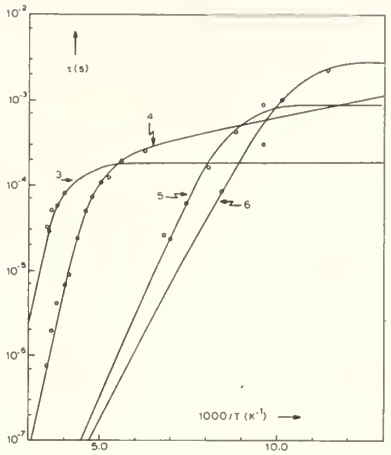

Fig. 2 The characteristic times of the different g-r noise components versus 1000/T. The open circles represent the measured values. The solid curves show the results of the computer calculation. The labels 3-6 refer to the impurity level mainly responsible for the curve.

3. MEASUREMENTS

We used $p^+\pi\ p^+$ (Boron-doped) planar silicon devices which were provided with plane parallel contacts having a cross-sectional area of $1.0 \cdot 10^{-6}$ m^2. The contact spacing was 40 μm and the room-temperature resistivity of the π region was 100 Ωm. The electric field could be applied along the <100> crystallographic direction.

The experimental set-up permitted spectral noise analysis to be carried out at frequencies between 2 and 10^8 Hz and at temperatures between 78 and 300 K [5]. Thermal noise and I_0 were measured as a function of V_0 by Gisolf [5] at T = 100, 145 and 210 K under pulsed bias conditions. Using d.c. bias we measured 1/f noise and I_0 as a function of V_0 at T = 78 K [6]. The 1/f frequency dependence was observed for at least two decades of frequency, depending on the voltage applied. The frequency exponent was -1 within the accuracy of our measurements (10%). We checked that no excessive Joule heating occurred.

We found that in the ohmic regime the magnitude of the 1/f noise was proportional to V_0^2. However, at bias voltages where carrier heating occurred substantial deviations from this proportionality became apparent.

Generation-recombination noise was measured as a function of temperature in the ohmic range. We observed that the number of g-r noise components, their low frequency plateau level and their characteristic time all varied with temperature. In figure 1 we have plotted the values of the low frequency plateau levels of the various g-r noise components divided by V_0^2 versus 1000/T for $78 \leqq T \leqq 300$ K. The corresponding characteristic times are shown in figure 2.

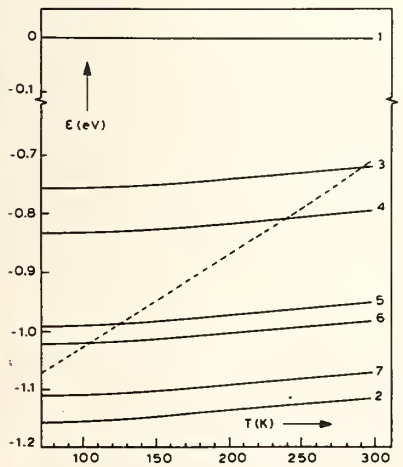

Fig. 3 The energy level positions of our model for p-type silicon versus the temperature. The solid lines represent the energy level positions. The dashed line represents the position of the Fermi level. Levels 1 and 2 represent the bottom of the conduction band and the top of the valence band respectively. The levels labelled 3-7 are associated with impurities.

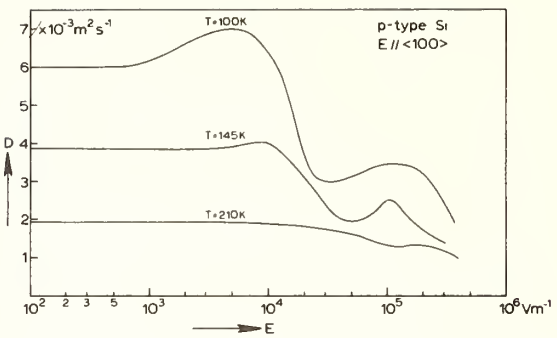

Fig. 4 The longitudinal diffusion coefficient of holes versus E for different temperatures.

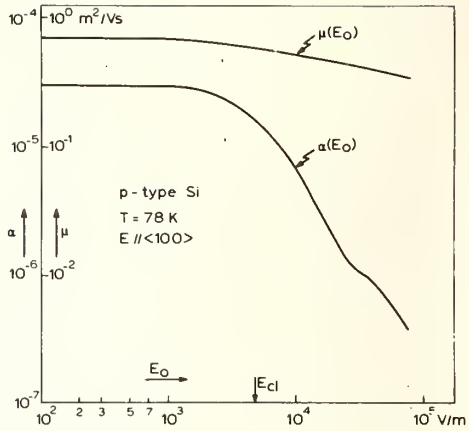

Fig. 5 The Hooge parameter and the mobility of holes versus E.

The relative error in the experimental data is about 20%. We observe four maxima in the noise (cf. figure 1) located at T = 270, 200, 113 and 91 K, respectively.

4. DISCUSSION AND INTERPRETATION

The solid lines in figure 1 and 2 show the results of computer calculations [9] based on the theory given in section 2.2 and applied to the seven-level model depicted in figure 3. In this figure the energy positions of the different levels and the Fermi level are given as a function of temperature. Note that levels 3-6, which are responsible for the measured g-r noise, are traversed by the Fermi level at different temperatures. In table 1 we have listed the trap parameters which followed from the computer calculations and have compared them with literature values. We assumed that the spin degeneracy of the impurity levels equals four.

Table 1. Calculated impurity parameters and values collected from the literature.

Level	Energy position (eV)		Hole capture coefficient (m^3s^{-1})		Concentration (m^{-3})
Lit.	Exp.	Lit.	Exp.	Lit.	Lit.
3 Fe [11]	ε_g+0.40	ε_g+0.40	$9.0\cdot10^{-15}$	5 $\cdot10^{-15}$	$8.0\cdot10^{16}$
4 Pt [12]	ε_g+0.325	ε_g+0.32	$2.3\cdot10^{-14}(T/300)^2$	$9.1\cdot10^{-15}$ at T=135 K	$4.9\cdot10^{17}$
5 Mn [13]	ε_g+0.165	ε_g+0.17	$1.9\cdot10^{-15}$	2 $\cdot10^{-15}$	$8.6\cdot10^{15}$
6 Cr [14]	ε_g+0.13	ε_g+0.11	6 $\cdot10^{-16}$	—	$6.7\cdot10^{14}$

From the thermal noise data we calculated μ and D as a function of E_0. The mobility results are in very good agreement with those obtained by Ottaviani et al. [7], who used the Time of Flight technique. The results for D are plotted in figure 4 for different temperatures. The curves at T = 100 and 145 K show a pronounced structure which we ascribe to the effect of light and heavy holes. A more quantitative explanation of this structure is given elsewhere [2]. In figure 5 we show μ and α as a function of E_0 at T = 78 K. We found that α can be described by $\alpha(E_0) = \alpha(0)/(1 + (E/E_{c1})^2)$, where E_{c1} is the field where the drift velocity of the light holes equals the sound velocity.

5. CONCLUSIONS

(1) It is clear from D(E) curves that light as well as heavy holes contribute to charge transport.
(2) Light and heavy holes become hot when their respective drift velocities are equal to the sound velocity.
(3) At T = 78 K α(E) can be described for $E \leqq 10^5$ V/m by $\alpha(E) = \alpha(0)/(1 + E(E_{c1})^2)$, where $E_{c1} = v_s/\mu_1(0)$. This indicates that there is a connection between 1/f noise and the scattering of light holes by acoustic phonons.

(4) Our experimental results for 1/f noise at T = 78 K are at variance with the expression for hot carrier 1/f noise derived by Kleinpenning [10] $S_{\Delta V}/v_0^2 = \alpha(0)/fN_0$.
(5) The g-r noise measurement technique is a powerful tool for the spectroscopic study of deep-level impurities even in multi-level systems.

REFERENCES

[1] R.J.J. Zijlstra, in *Noise in Physical Systems*, Ed. D. Wolf (Springer-Verlag, Berlin, 1978) Chapter II, p. 90.
[2] G. Bosman and R.J.J. Zijlstra, *Phys. Lett.* 71A, 464 (1979).
[3] F.M. Klaassen, thesis, Free University of Amsterdam, The Netherlands (1961).
[4] K.M. van Vliet and J.R. Fassett, in *Fluctuation Phenomena in Solids*, Ed. R.E. Burgess (Academic Press, New York, 1965).
[5] A. Gisolf and R.J.J. Zijlstra, *J. Appl. Phys.* 47, 2727 (1976).
[6] G. Bosman, R.J.J. Zijlstra and A. van Rheenen, *Phys. Lett.* 80A, 57 (1980).
[7] G. Ottaviani, L. Reggiani, C. Canali, F. Nava and A. Alberigi Quaranta, *Phys. Rev. B* 12, 3318 (1975).
[8] P.J. Price, *J. Appl. Phys.* 31, 949 (1960).
[9] G. Bosman, R.J.J. Zijlstra, to be published.
[10] T.G.M. Kleinpenning, *Physica* 103B, 340 (1981).
[11] C.B. Collins, R.O. Carlson, *Phys. Rev.* 108, 1409 (1957).
[12] J.A. Pals, *Solid-State Electron.* 17, 1139 (1974).
[13] A.O. Evwaraye, *J. Appl. Phys.* 48, 3813 (1977).
[14] H.H. Woodburg and G.W. Ludwig, *Phys. Rev.* 117, 102 (1960).

MONTE CARLO CALCULATION OF HOT-ELECTRON NOISE IN SI AT 77 K

Lino Reggiani, Rossella Brunetti and Carlo Jacoboni

Gruppo Nazionale di Struttura della Materia, Istituto di Fisica
Università di Modena, Via Campi 213/A, 41100 Modena, Italy.

INTRODUCTION

This paper reports on a Monte Carlo calculation of the hot-electron noise temperature associated with velocity fluctuations for the case of electrons in Si at 77 K. The main objective is to present a microscopic theory which interprets three main aspects of transport phenomena, namely: drift, diffusion and white-noise. Furthermore, results will throw light on a recently controversial interpretation of noise-temperature measurements [1,2] about the importance of the most relevant sources of noise (i.e. velocity fluctuations and generation recombination processes).

THEORY AND RESULTS

The transport approach follows a Monte Carlo procedure of standard type [3,4]. The parameters modelling the Si band structure and scattering mechanisms were obtained by fitting existing drift and diffusion data in a wide range of field strengths and temperatures [5] and are summarized in Table 1.

Table 1 - Physical parameters used in calculations.

Longitudinal effective mass $m_\ell = 0.916$

Transverse effective mass $m_t = 0.190$

Sound velocity $v_s = 9.04\ 10^5$ cm/sec

Crystal density $\rho = 2.33$ gr/cm^3

Non-parabolicity parameter $\alpha = 0.5$ eV^{-1}

Acoustic deformation potential $E_1 = 9.0$ eV

Type of intervalley scattering	Phonon mode	Eq. Temp. (K)	Coup. Cons. (10^8 eV/cm)
f_1	(TA)	220	0.3
f_2	(LA)	550	2.0
f_3	(TO)	685	2.0
g_1	(TA)	140	0.5
g_2	(LA)	215	0.8
g_3	(LO)	720	11.0

The theoretical longitudinal noise temperature $T_{n\ell}$ is obtained by substituting computed values of the longitudinal diffusion coefficient D_ℓ and of the differential longitudinal mobility μ'_ℓ, numerically interpolated from results of drift velocity versus field, through the formula [6]

$$T_{n_\ell} = \frac{e}{K_B} \frac{D_\ell(E)}{\mu'_\ell(E)} \qquad (1)$$

e being the unit charge and K_B the Boltzmann constant.

Fig. 1 reports the results at 77 K for the two directions ⟨100⟩ and ⟨111⟩ : (a) refers to the drift velocity, (b) to the longitudinal

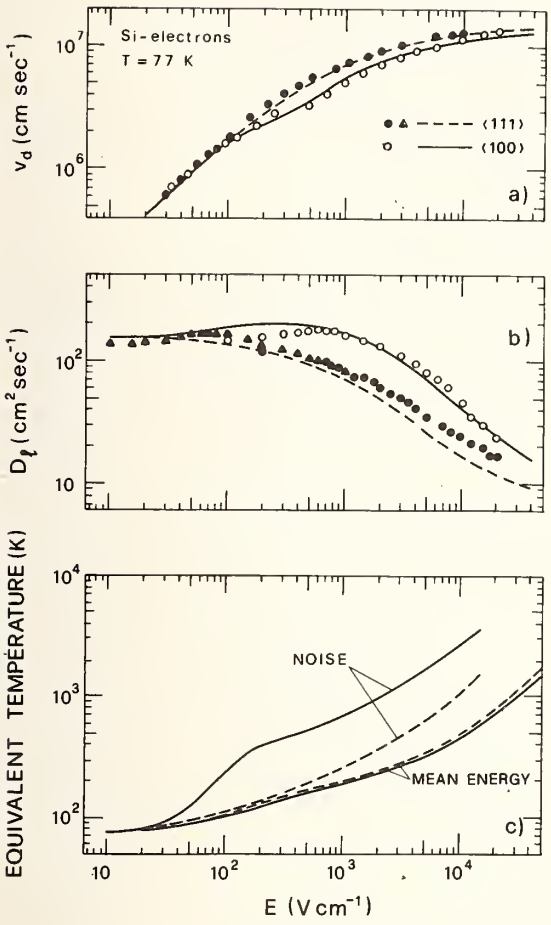

Fig. 1 Drift velocity (a), longitudinal diffusion coefficient (b), mean energy and longitudinal noise (c) in Si as a function of field strength at 77 K. Circles indicate time-of-flight data, triangles noise-conductivity data, lines the results of Monte Carlo calculations.

diffusion coefficient, (c) to the mean carrier energy and longitudinal noise both measured in equivalent temperature units. Drift and diffusion results are compared with available experimental data obtained with two complementary techniques (time-of-flight and noise-conductivity) and the agreement, which is found to be within experimental and theoretical uncertainties, guarantees the reliability of the microscopic model.

Concerning the longitudinal noise temperature, values calculated with an uncertainty of about 15% are reported up to about 15 kV/cm; in fact the saturation tendency of the drift velocity above about these field strengths, leading to a zero value of u'_ℓ, sets a physical and a numerical limit to the application of Eq.(1). From Fig. 1(c) it is seen that: i) noise values systematically exceed those of the mean energy; ii) a strong anisotropy shows up, with values along ⟨100⟩ direction higher than along ⟨111⟩ by about a factor three. This latter fact is known to be due to the presence of intervalley noise resulting from different drift velocities in different valleys when the field is along a ⟨100⟩ direction [5,7].

Fig. 2 shows the comparison between theory and available experiments on the noise temperature.

Data of Bareikis et al [8] obtained for 30Ω cm samples at a frequency of 10 GHz confirm the anisotropy effects, and are found to agree with theory within about 40%. In view of an experimental uncertainty estimated around 20% [9] this result has to be considered acceptable. Thus, the above agreement supports that the noise measured in Ref.(8) is due to velocity fluctuations source.

Data of Nougier et al [1] obtained for 15Ω cm and 6Ω cm samples in a frequency range 250 - 950 MHz disagree with present calculations; in particular, they are higher by more than a factor three with respect to the theory at the highest field strengths. Furthermore, by decreasing the sample resistivity from 15 to 6 and 2Ω cm the noise temperature was found to increase systematically. Consequently other sources of noise, in addition to the velocity fluctuations one, should be taken into account for the microscopic interpretation. A plausible source of additional noise which has been suggested [2] is generation recombination due to traps, and a calculation performed in the 1 - 3 kV/cm region succeds in totally attributing the noise measured to this mechanism [2]. From present results it is found that in the 1 - 3 kV/cm region and for 6Ω cm samples, the contribution to the noise measurements of

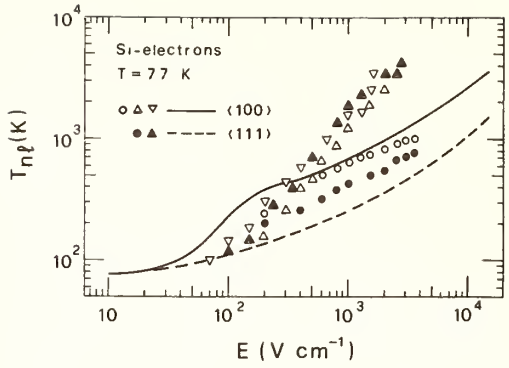

Fig. 2 Comparison between theoretical and experimental longitudinal noise temperature of electrons in Si at 77 K. Triangles (△ and ▽ refer to 15 and 6 Ω cm sample resistivity, respectively) indicate data of Ref. (1). Circles indicate data of Ref.(2).

Ref.(1) due to velocity fluctuations is negligible only when $\vec{E}$ is along a ⟨111⟩ direction, while when $\vec{E}$ is along a ⟨100⟩ direction the contribution is about 35% at 1 kV/cm and reduces to about 20% at 3 kV/cm.

CONCLUSIONS

Hot-electron noise due to velocity fluctuations in Si at 77 K is calculated on the basis of a reliable microscopic model. Results show that for a perfect crystal, hot-electron effects become evident at field strengths above about 50 V/cm. Furthermore, the noise temperature exhibits a strong anisotropy with respect to the field direction with values along a ⟨100⟩ direction higher by about a factor three than those along a ⟨111⟩ direction. Comparison with experiments confirms theoretical expectations in the most favourable case of Ref.(8) (i.e. higher resistivity samples, measurements performed at 10 GHz). Thus present calculations provide useful information for a discussion on the relative importance of other sources of noise, such as generation recombination [2] .

ACKNOWLEDGMENTS

We are grateful to the Computer Center of the Modena University for providing computer facilities. One of the authors (L.R.) wishes to thank the European Research Office for providing a travel grant to the U.S.A..

REFERENCES

[1] J.P. Nougier, D. Sodini, M. Rolland, D. Gasquet and G. Lecoy, Solid-St. Electron., 21, 133 (1978).
[2] A. van der Ziel, R. Jindal, S.K. Kim, H. Park and J.P. Nougier, Solid-St. Electron., 22, 177 (1979).
[3] C. Canali, C. Jacoboni, F. Nava, G. Ottaviani and A. Alberigi-Quaranta, Phys. Rev. B12, 2265 (1975).
[4] C. Canali, C. Jacoboni, G. Ottaviani and A. Alberigi-Quaranta, Appl. Phys. Lett., 27, 278 (1975).
[5] R. Brunetti, C. Jacoboni, F. Nava, L. Reggiani, G. Bosman and R.J.J. Zijlstra, to be published.
[6] J.P. Nougier in "Physics of Nonlinear Transport in Semiconductors", Eds. D.K. Ferry, J. R. Barker and C. Jacoboni: Plenum Press (New York, 1980).
[7] P.J. Price, J. Appl. Phys., 31, 124 (1960).
[8] V. Bareikis, V. Viktoravichyus, A. Gal'dikas and R. Milyushite, Sov. Phys. Sol. State 20, 85 (1978).
[9] V. Bareikis, V. Viktoravichyus, A. Gal'dikas and R. Milyushite, Sov. Phys. Semicon., 14, 847 (1980).

NBS-114A (REV. 2-8C)

U.S. DEPT. OF COMM. BIBLIOGRAPHIC DATA SHEET (See instructions)	1. PUBLICATION OR REPORT NO. NBS SP 614	2. Performing Organ. Report No.	3. Publication Date September 1981

4. TITLE AND SUBTITLE

Sixth International Conference on Noise in Physical Systems
Proceedings of a conference held at the National Bureau of Standards, Gaithersburg, MD, April 6-10, 1981

5. AUTHOR(S)

P. H. E. Meijer, R. D. Mountain, and R. J. Soulen, Jr., Editors

6. PERFORMING ORGANIZATION (If joint or other than NBS, see instructions)

NATIONAL BUREAU OF STANDARDS
DEPARTMENT OF COMMERCE
WASHINGTON, D C 20234

7. Contract/Grant No.

8. Type of Report & Period Covered

Final

9. SPONSORING ORGANIZATION NAME AND COMPLETE ADDRESS (Street, City, State, ZIP)

The Catholic University of America
Washington, DC 20064

and

National Science Foundation
Washington, DC 20550

10. SUPPLEMENTARY NOTES

Library of Congress Catalog Card Number: 81-600084

☐ Document describes a computer program; SF-185, FIPS Software Summary, is attached.

11. ABSTRACT (A 200-word or less factual summary of most significant information. If document includes a significant bibliography or literature survey, mention it here)

This document contains the full text of papers submitted to the Sixth International Conference on Noise in Physical Systems. There are six categories of papers: THEORY; DEVICES; 1/f NOISE; APPLICATIONS AND MEASUREMENT TECHNIQUES; QUANTUM NOISE; HOT CARRIER NOISE.

12. KEY WORDS (Six to twelve entries; alphabetical order; capitalize only proper names; and separate key words by semicolons)

Hot carrier noise; noise; noise in devices; noise measurement; quantum noise; 1/f noise

13. AVAILABILITY

☒ Unlimited

☐ For Official Distribution. Do Not Release to NTIS

☒ Order From Superintendent of Documents, U.S. Government Printing Office, Washington, D C 20402.

☐ Order From National Technical Information Service (NTIS), Springfield, VA. 22161

14. NO. OF PRINTED PAGES

419

15. Price

$8.50

USCOMM-DC 6043-P80

☆U.S. GOVERNMENT PRINTING OFFICE: 1981-340-997/1780

NBS TECHNICAL PUBLICATIONS

PERIODICALS

JOURNAL OF RESEARCH—The Journal of Research of the National Bureau of Standards reports NBS research and development in those disciplines of the physical and engineering sciences in which the Bureau is active. These include physics, chemistry, engineering, mathematics, and computer sciences. Papers cover a broad range of subjects, with major emphasis on measurement methodology and the basic technology underlying standardization. Also included from time to time are survey articles on topics closely related to the Bureau's technical and scientific programs. As a special service to subscribers each issue contains complete citations to all recent Bureau publications in both NBS and non-NBS media. Issued six times a year. Annual subscription: domestic $13; foreign $16.25. Single copy, $3 domestic; $3.75 foreign.

NOTE: The Journal was formerly published in two sections: Section A "Physics and Chemistry" and Section B "Mathematical Sciences."

DIMENSIONS/NBS—This monthly magazine is published to inform scientists, engineers, business and industry leaders, teachers, students, and consumers of the latest advances in science and technology, with primary emphasis on work at NBS. The magazine highlights and reviews such issues as energy research, fire protection, building technology, metric conversion, pollution abatement, health and safety, and consumer product performance. In addition, it reports the results of Bureau programs in measurement standards and techniques, properties of matter and materials, engineering standards and services, instrumentation, and automatic data processing. Annual subscription: domestic $11; foreign $13.75.

NONPERIODICALS

Monographs—Major contributions to the technical literature on various subjects related to the Bureau's scientific and technical activities.

Handbooks—Recommended codes of engineering and industrial practice (including safety codes) developed in cooperation with interested industries, professional organizations, and regulatory bodies.

Special Publications—Include proceedings of conferences sponsored by NBS, NBS annual reports, and other special publications appropriate to this grouping such as wall charts, pocket cards, and bibliographies.

Applied Mathematics Series—Mathematical tables, manuals, and studies of special interest to physicists, engineers, chemists, biologists, mathematicians, computer programmers, and others engaged in scientific and technical work.

National Standard Reference Data Series—Provides quantitative data on the physical and chemical properties of materials, compiled from the world's literature and critically evaluated. Developed under a worldwide program coordinated by NBS under the authority of the National Standard Data Act (Public Law 90-396).

NOTE: The principal publication outlet for the foregoing data is the Journal of Physical and Chemical Reference Data (JPCRD) published quarterly for NBS by the American Chemical Society (ACS) and the American Institute of Physics (AIP). Subscriptions, reprints, and supplements available from ACS, 1155 Sixteenth St., NW, Washington, DC 20056.

Building Science Series—Disseminates technical information developed at the Bureau on building materials, components, systems, and whole structures. The series presents research results, test methods, and performance criteria related to the structural and environmental functions and the durability and safety characteristics of building elements and systems.

Technical Notes—Studies or reports which are complete in themselves but restrictive in their treatment of a subject. Analogous to monographs but not so comprehensive in scope or definitive in treatment of the subject area. Often serve as a vehicle for final reports of work performed at NBS under the sponsorship of other government agencies.

Voluntary Product Standards—Developed under procedures published by the Department of Commerce in Part 10, Title 15, of the Code of Federal Regulations. The standards establish nationally recognized requirements for products, and provide all concerned interests with a basis for common understanding of the characteristics of the products. NBS administers this program as a supplement to the activities of the private sector standardizing organizations.

Consumer Information Series—Practical information, based on NBS research and experience, covering areas of interest to the consumer. Easily understandable language and illustrations provide useful background knowledge for shopping in today's technological marketplace.

Order the **above** *NBS publications from: Superintendent of Documents, Government Printing Office, Washington, DC 20402.*

Order the **following** *NBS publications—FIPS and NBSIR's—from the National Technical Information Services, Springfield, VA 22161.*

Federal Information Processing Standards Publications (FIPS PUB)—Publications in this series collectively constitute the Federal Information Processing Standards Register. The Register serves as the official source of information in the Federal Government regarding standards issued by NBS pursuant to the Federal Property and Administrative Services Act of 1949 as amended, Public Law 89-306 (79 Stat. 1127), and as implemented by Executive Order 11717 (38 FR 12315, dated May 11, 1973) and Part 6 of Title 15 CFR (Code of Federal Regulations).

NBS Interagency Reports (NBSIR)—A special series of interim or final reports on work performed by NBS for outside sponsors (both government and non-government). In general, initial distribution is handled by the sponsor; public distribution is by the National Technical Information Services, Springfield, VA 22161, in paper copy or microfiche form.

U.S. DEPARTMENT OF COMMERCE
National Bureau of Standards
Washington, D.C. 20234

OFFICIAL BUSINESS

Penalty for Private Use, $300

POSTAGE AND FEES PAID
U.S. DEPARTMENT OF COMMERCE
COM-215

U.S.MAIL

SPECIAL FOURTH-CLASS RATE
BOOK